frontiers | Research Topics

Immunometabolism and metabolic reprogramming of immune cells in human physiology and disease

Edited by
Soumya R. Mohapatra and Christiane A. Opitz

Published in
Frontiers in Immunology

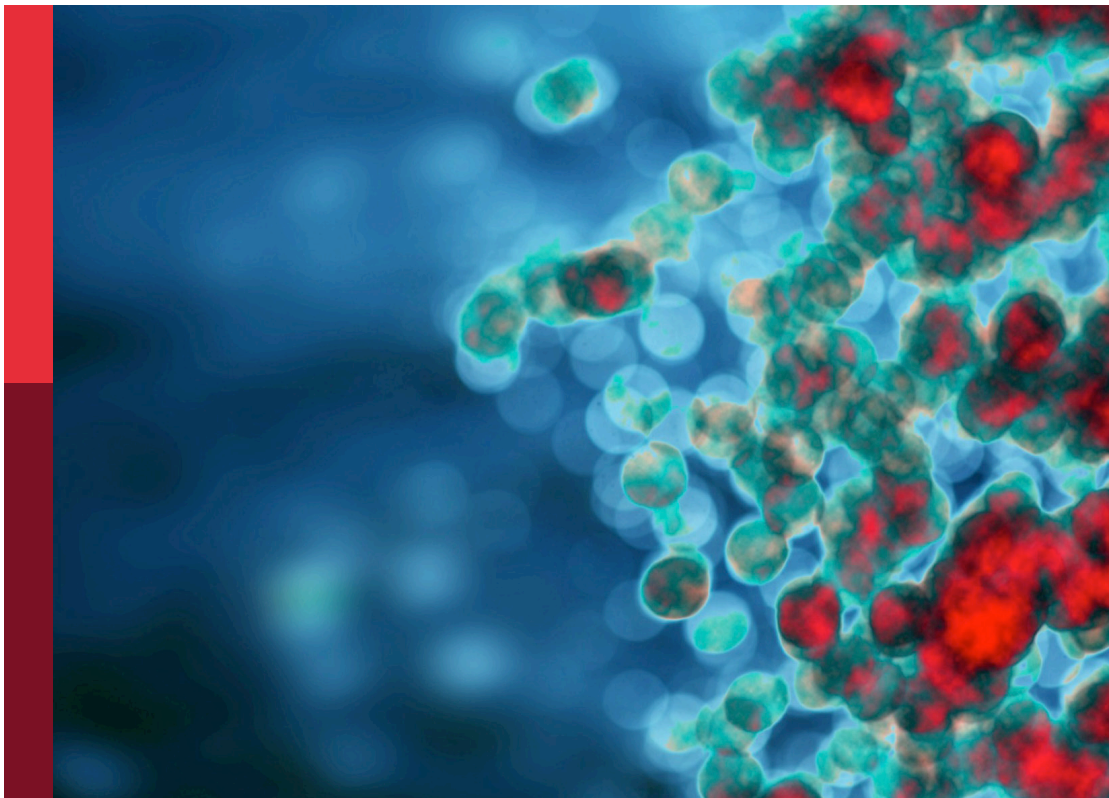

ISSN 1664-8714
ISBN 978-2-8325-3399-4
DOI 10.3389/978-2-8325-3399-4

About Frontiers

Frontiers is more than just an open access publisher of scholarly articles: it is a pioneering approach to the world of academia, radically improving the way scholarly research is managed. The grand vision of Frontiers is a world where all people have an equal opportunity to seek, share and generate knowledge. Frontiers provides immediate and permanent online open access to all its publications, but this alone is not enough to realize our grand goals.

Frontiers journal series

The Frontiers journal series is a multi-tier and interdisciplinary set of open-access, online journals, promising a paradigm shift from the current review, selection and dissemination processes in academic publishing. All Frontiers journals are driven by researchers for researchers; therefore, they constitute a service to the scholarly community. At the same time, the *Frontiers journal series* operates on a revolutionary invention, the tiered publishing system, initially addressing specific communities of scholars, and gradually climbing up to broader public understanding, thus serving the interests of the lay society, too.

Dedication to quality

Each Frontiers article is a landmark of the highest quality, thanks to genuinely collaborative interactions between authors and review editors, who include some of the world's best academicians. Research must be certified by peers before entering a stream of knowledge that may eventually reach the public - and shape society; therefore, Frontiers only applies the most rigorous and unbiased reviews. Frontiers revolutionizes research publishing by freely delivering the most outstanding research, evaluated with no bias from both the academic and social point of view. By applying the most advanced information technologies, Frontiers is catapulting scholarly publishing into a new generation.

What are Frontiers Research Topics?

Frontiers Research Topics are very popular trademarks of the *Frontiers journals series*: they are collections of at least ten articles, all centered on a particular subject. With their unique mix of varied contributions from Original Research to Review Articles, Frontiers Research Topics unify the most influential researchers, the latest key findings and historical advances in a hot research area.

Find out more on how to host your own Frontiers Research Topic or contribute to one as an author by contacting the Frontiers editorial office: frontiersin.org/about/contact

Immunometabolism and metabolic reprogramming of immune cells in human physiology and disease

Topic editors

Soumya R. Mohapatra — KIIT University, India

Christiane A. Opitz — German Cancer Consortium, German Cancer Research Center (DKFZ), Germany

Citation

Mohapatra, S. R., Opitz, C. A., eds. (2023). *Immunometabolism and metabolic reprogramming of immune cells in human physiology and disease*. Lausanne: Frontiers Media SA. doi: 10.3389/978-2-8325-3399-4

Table of contents

frontiers in Immunology

REVIEW
published: 17 May 2021
doi: 10.3389/fimmu.2021.657293

Immunometabolism at the Nexus of Cancer Therapeutic Efficacy and Resistance

Javier Traba[1]*, *Michael N. Sack*[2], *Thomas A. Waldmann*[3] and *Olga M. Anton*[3]*

[1] Departamento de Biología Molecular, Centro de Biología Molecular Severo Ochoa, Consejo Superior de Investigaciones Científicas-Universidad Autónoma de Madrid (CSIC-UAM), Madrid, Spain, [2] Cardiovascular Branch, National Heart, Lung and Blood Institute, NIH, Bethesda, MD, United States, [3] Lymphoid Malignancies Branch, Center for Cancer Research, National Cancer Institute, NIH, Bethesda, MD, United States

Constitutive activity of the immune surveillance system detects and kills cancerous cells, although many cancers have developed strategies to avoid detection and to resist their destruction. Cancer immunotherapy entails the manipulation of components of the endogenous immune system as targeted approaches to control and destroy cancer cells. Since one of the major limitations for the antitumor activity of immune cells is the immunosuppressive tumor microenvironment (TME), boosting the immune system to overcome the inhibition provided by the TME is a critical component of oncotherapeutics. In this article, we discuss the main effects of the TME on the metabolism and function of immune cells, and review emerging strategies to potentiate immune cell metabolism to promote antitumor effects either as monotherapeutics or in combination with conventional chemotherapy to optimize cancer management.

Keywords: immunometabolism, cancer, immune cells, T cells, NK cells, macrophages, immunosuppression, metabolites

OPEN ACCESS

Edited by:
Ignacio Melero,
University of Navarra, Spain

Reviewed by:
Alessandro Poggi,
San Martino Hospital (IRCCS), Italy
Robert J. Canter,
University of California, Davis, United States

***Correspondence:**
Javier Traba
jtraba@cbm.csic.es
Olga M. Anton
olga.antonhurtado@nih.gov

Specialty section:
This article was submitted to Cancer Immunity and Immunotherapy, a section of the journal Frontiers in Immunology

Received: *22 January 2021*
Accepted: *29 April 2021*
Published: *17 May 2021*

Citation:
Traba J, Sack MN, Waldmann TA and Anton OM (2021) Immunometabolism at the Nexus of Cancer Therapeutic Efficacy and Resistance. Front. Immunol. 12:657293. doi: 10.3389/fimmu.2021.657293

INTRODUCTION

Cancer is a highly heterogeneous disease that constitutes a major worldwide health problem. Cancer cell presents the following main hallmarks: self-sufficiency in growth signals, insensitivity to anti-growth signals, evading apoptosis, limitless replicative potential, sustained angiogenesis, reprogramming of energy metabolism, evading immune destruction and tissue invasion and metastasis (1). An additional and important characteristic of cancer cells is that they recruit a repertoire of healthy cells that contribute to tumorigenesis, such as fibroblasts (the predominant cell type), pericytes, endothelial cells, mesenchymal stem cells, macrophages and lymphocytes (2). This review deals with two of those important hallmarks: reprogramming of energy metabolism and evasion of immune destruction.

Quiescent cells in the human body typically display a catabolic metabolism that mainly relies on oxidative phosphorylation, utilizing glucose, fatty acids or amino acids as substrates. In contrast, proliferating cells, such as rapidly dividing immune cells, switch to an anabolic metabolism, rely on glycolysis for energy generation and utilize large amounts of glucose and glutamine as building blocks for lipids, nucleic acids and amino acids for proliferation. Immunometabolism is an emerging concept that studies metabolic changes that occur in immune cells to support their functions. These changes are critical for the appropriate immune response, as they control

downstream transcriptional and posttranscriptional events, and their dysregulation may compromise growth, proliferation and effector functions. As a general overview, in an inflammatory context immune cells will upregulate aerobic glycolysis (such is the case in B cells, effector Th1 and Th17 T cells, M1 macrophages, dendritic cells and Natural Killer cells), while a metabolism relying more on the oxidative phosphorylation usually supports an anti-inflammatory phenotype (as is the case in M2 macrophages and regulatory T (T_{reg}) cells).

Cancer cells also undergo changes in metabolism that are required to support their bioenergetic needs and biosynthesis requirements for fast growth and invasiveness, and in fact, metabolic reprogramming is now considered one of the hallmarks of the cancer cell (3). Metabolic changes in pro-inflammatory immune and cancer cells mirror each other, which leads to competition for nutrients and oxygen in the tumor microenvironment (TME). In addition, cancer cells and other cells embedded in the tumor secrete metabolites and inhibitory cytokines that interfere with the targeting of immune cells to eliminate tumor cells. These characteristics represent the way tumoral cells have evolved to create a favorable environment for their growth and development while evading and suppressing the immune response. The aim of immunotherapy is to modulate the host immune system to attack cancer cells with tools such as immune checkpoint blockade, T cell therapy or cancer vaccines, and it has been shown to be effective (4). The alteration of metabolic pathways involved in cancer-induced immune failure seem to be a suitable target to enhance existing immunotherapies.

OVERVIEW OF CELLULAR METABOLISM AND CANCER CELL METABOLISM

Cells utilize a number of substrates, including glucose, fatty acids and amino acids (such as glutamine), to obtain energy in the form of adenosine triphosphate (ATP), precursors for biosynthesis and redox equivalents. A key pathway is glycolysis, which consists on the catabolism of glucose to generate pyruvate and 2 molecules of ATP. Pyruvate can in turn be transformed into lactate (anaerobic glycolysis) or preferentially (under normoxic conditions) transferred to the mitochondria where it is transformed into acetyl coenzyme A (acetyl-CoA), which is then metabolized by the tricarboxylic acid (TCA) cycle to produce ATP, CO_2 and reduced nicotinamide adenine dinucleotide (NADH). NADH is oxidized by the electron transport chain (ETC) of the inner mitochondrial membrane, which transfers its electrons sequentially *via* redox reactions to several respiratory complexes (I, III and IV), and finally to O_2 as final acceptor. Electron transport is an exergonic process and is coupled to the pumping of protons (H^+) by those complexes to the intermembrane space, generating an electrochemical gradient that is used by the ATP synthase to generate ATP, a process called oxidative phosphorylation (OxPhos). Cells can also burn fatty acids in the mitochondria in a process called fatty acid β-oxidation (FAO). This process yields large amounts of acetyl-CoA and redox equivalents that can be oxidized by the ETC.

The main metabolic differences between normal cells and cancer cells are described in **Figure 1**. Cancer cells display a metabolic switch that supports their rapid proliferation. In these cells, even in the presence of oxygen, pyruvate is not used by the TCA cycle, but instead converted to lactate by lactate dehydrogenase A (LDHA). This phenomenon is called Warburg effect or aerobic glycolysis (5). The excess lactate produced by the proliferating cancer cells is exported by monocarboxylate transporters (MCTs) and increases the acidity of the TME. Cancer cells also divert significant amounts of glycolytic intermediates into the pentose phosphate pathway (PPP) to generate NADPH (used for reductive anabolism and to reduce the disulfide form of glutathione, GSSG, to the sulfhydryl form, GSH, which is an antioxidant) and pentoses, including ribose-5-phosphate (for nucleic acid synthesis). Glutamine is also a major nutrient in cancer cells, which in fact display glutamine addiction, and is utilized as a source of nitrogen for biosynthetic pathways, including the synthesis of non-essential amino acids and nucleotides (by participating in nitrogen-donating reactions), and to replenish the TCA cycle (anaplerosis) which is used to synthesize large amounts of lipids from citrate (6). Glutamine is initially converted to glutamate by the enzyme Glutaminase, and then to alpha-ketoglutarate, by Glutamate Dehydrogenase (GDH), which fuels the TCA cycle. Cancer cells also display a lipogenic phenotype, showing increased *de novo* synthesis of fatty acids. Remarkably, the highly active metabolic activity of the tumor cell depletes nutrients and O_2 in the TME and renders it hostile to immune cells.

Cellular metabolism has been proved a key factor to regulate cellular responses. In the field of immune cells, immunometabolism has become a new target to control and modulate immune responses, with special relevance in the fields of immunotherapy and cancer.

OVERVIEW OF IMMUNOMETABOLISM

Most resting immune cells are relatively metabolically inactive. The concept of immunometabolism illustrates the changes in metabolism and special needs that immune cells undergo to be able to fulfill their specific functions. Immunometabolism has been most extensively studied in the modulation of macrophage polarization and of $CD4^+$ T cell activation. The metabolic changes that occur in macrophages, $CD4^+$ T cells and Natural Killer (NK) cells after activation are schematized in **Figure 2**. The characterization of immunometabolism is being extended to other immune cells such as dendritic cells (7, 8), neutrophils, myeloid-derived suppressor cells (MDSC), innate lymphoid cells (ILC) (9), B cells (10) and plasma cells (11).

Immunometabolism of Macrophages

Macrophages are a multifunctional type of leukocyte that plays a role in innate immunity, but also collaborate in the initiation of

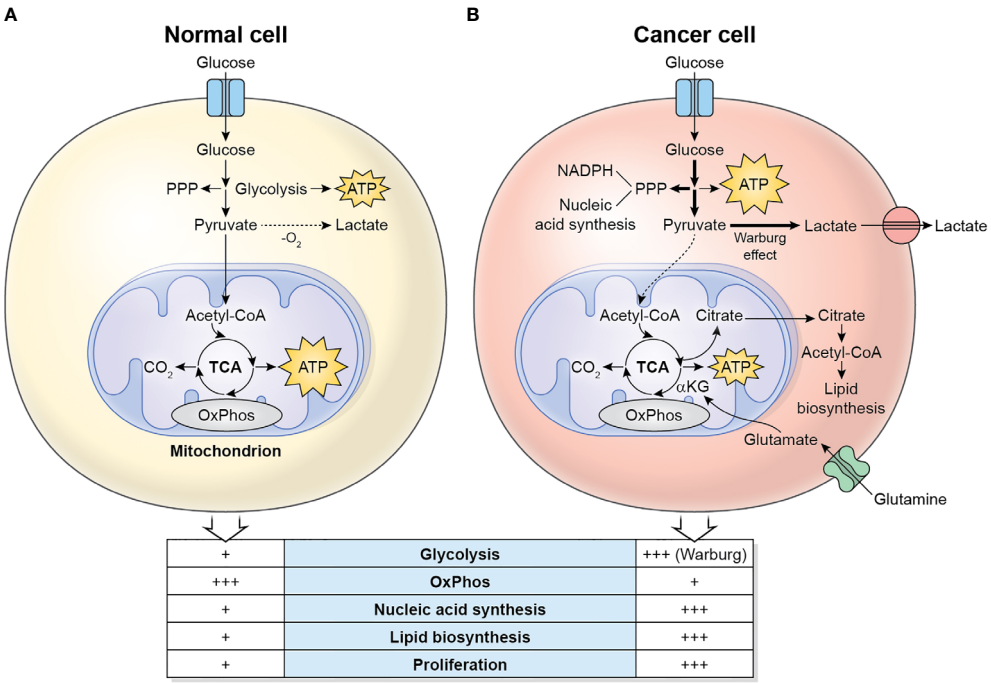

FIGURE 1 | Metabolic differences between normal cells **(A)** and cancer cells **(B)**. Normal/quiescent cells in aerobiosis metabolize glucose mainly to pyruvate, which is then oxidized in the mitochondria to CO_2 using the TCA cycle and OxPhos for the generation of ATP. ATP synthesis takes places preferentially in the mitochondria. In anaerobiosis, pyruvate is metabolized to lactate instead. Cancer cells in aerobiosis or anaerobiosis convert most glucose to lactate (which is exported to the TME), while diverting some glycolytic intermediates to the PPP, which generates NADPH and pentoses for the synthesis of nucleic acids. ATP synthesis is largely cytosolic. Glutaminolysis generates glutamate, which is converted to α-ketoglutarate, a major substrate to refuel the TCA cycle. The TCA cycle intermediate citrate is exported to the cytosol, where it is converted to acetyl-CoA, used for the synthesis of lipids.

adaptive immunity, as they are antigen presenting cells (APCs) to helper T cells. They are terminally differentiated cells and perform functions related to tissue homeostasis, repair, phagocytosis and development.

There are distinct varieties of macrophages in several tissues, including Kupffer cells, alveolar macrophages, osteoclasts, peritoneal macrophages, microglia, and others. Macrophages either derive from circulating monocytes or are established in tissues before birth and then maintained during adult life independently of monocytes (12).

After activation using *in vitro* stimuli, macrophages can be broadly divided into two subgroups: M1, classically activated or proinflammatory macrophages, generated *in vitro* by incubation with bacterial-derived products such as lipopolysaccharide (LPS) that bind to Toll-like receptors (TLRs), and signals associated with infection such as interferon γ (IFN-γ); and M2, alternatively activated or reparative macrophages, generated *in vitro* by incubation with interleukin (IL)-4, IL-10 or IL-13. It is probable that macrophage polarity *in vivo* is much more complex and cells display a spectrum of functional phenotypes between M1 and M2 subtypes.

In solid tumors there is a population of macrophages called tumor-associated macrophages (TAMs) that typically resembles M2 macrophages and exert immunosuppressive and pro-tumorigenic functions (13), including stimulation of angiogenesis, which contributes to nutritional support of the tumor, and remodeling of the extracellular matrix. TAMs constitute the largest population of myeloid cells that infiltrate solid tumors.

M1 Macrophages

M1 macrophage secrete proinflammatory cytokines such as IL-1β, tumor necrosis factor (TNF-α), IL-6 or IL-12 that initiate the immune response, perform phagocytosis of microbes and generate reactive oxygen species (ROS), and metabolize arginine using inducible nitric oxide synthase (iNOS) to generate nitric oxide (NO).

Early Metabolic Changes in M1 Activation

During early activation of the M1 phenotype, the Toll-like receptor 4 (TLR4) agonist LPS induces a rapid induction in both glycolysis and mitochondrial oxygen consumption, as well as an increases in glucose uptake and the levels of TCA cycle metabolic intermediates (14). Metabolites typical of M1 macrophages such as lactate, itaconate or succinate do not reach high levels until after 24 hours. Glucose-derived pyruvate is taken up by the mitochondria and oxidized. Increased citrate is exported to the cytosol through the mitochondrial citrate carrier (CIC) and converted to acetyl-CoA by the ATP-citrate lyase enzyme (ACLY), which is then utilized not only for fatty acid and

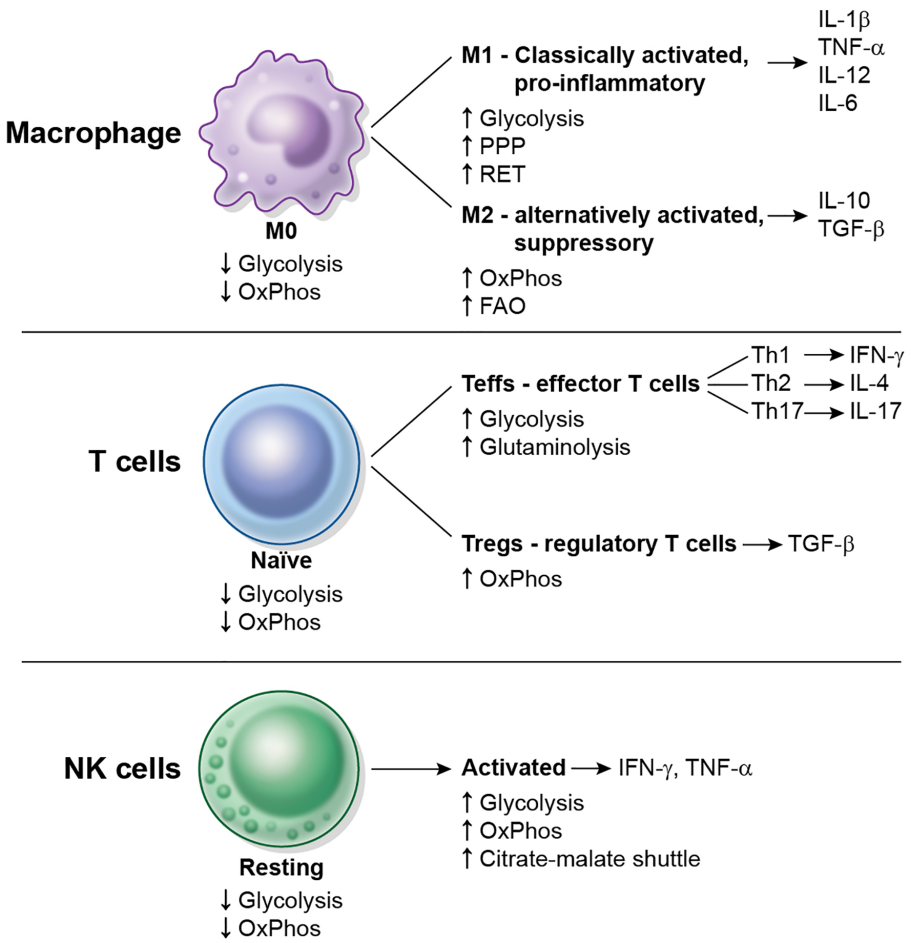

FIGURE 2 | Overview of metabolic changes in some immune cell types upon activation. Macrophages, $CD4^+$ T cells and NK cells are shown. Resting or naïve cells typically display a low metabolic rate (low glycolysis, low OxPhos). M0 macrophages differentiate into M1 and M2 macrophages, naïve CD4+ T cells differentiate into Teffs or Tregs, and resting NK cells become activated. Each cell subtype displays different metabolic requirements and repertoire of cytokines to function.

cholesterol synthesis, but also for acetylation reactions. Thus, LPS stimulates glucose-dependent histone acetylation and pro-inflammatory gene expression at early time points after M1 activation.

Late Changes in M1 Activation

The late metabolism of the M1 cell is mainly glycolytic, and they also display increased fatty acid synthesis and increased flux though the PPP, involved in the synthesis of NADPH which is in turn required for fatty acid synthesis, ROS generation (by NADPH oxidase), and NO synthesis. The TCA cycle becomes incomplete, as two breaks occur (15), which leads to the accumulation of specific metabolites: the first break is caused by a decrease in the expression of isocitrate dehydrogenase (IDH), and leads to citrate accumulation, which is required for lipids, prostaglandins and itaconate synthesis. Itaconic acid is formed from cis-aconitate by the inducible Immune-Responsive Gene 1 (IRG1), and is an anti-microbial compound. Because of the first brake in the cycle, alpha-ketoglutarate in M1 macrophages is derived from glutamine rather than from glucose. The second break occurs at succinate dehydrogenase, with accumulation of succinate, required for hypoxia-inducible factor 1 alpha (HIF-1α) stabilization, a key transcription factor for pro-inflammatory genes such as IL-1β (16). Because of the second break in the cycle, malate in M1 cells is thus generated *via* the arginosuccinate shunt. The increased generation of ATP by glycolysis in the cytosol of M1 cells decreases significantly the requirement for mitochondrial OxPhos to supply ATP to the cell. As a consequence, M1 cells do not synthesize significant amounts of ATP in the mitochondria, and perform instead reverse electron transport (RET), which is the flow of electrons from ubiquinol back to respiratory complex I for the generation of ROS in the mitochondrial matrix (17, 18). These electrons typically come from succinate oxidation by respiratory complex II, succinate dehydrogenase.

Other late metabolic changes in M1 cells include: increased expression of acetyl-CoA carboxylase (ACC), which leads to increased levels of malonyl-Coenzyme A in the cytosol and

increased protein malonylation (19). One of the substrates of this modification is the glycolytic enzyme glyceraldehyde 3-phosphate dehydrogenase (GAPDH), which converts glyceraldehyde 3-phosphate into 1,3-bisphosphoglycerate. GAPDH binds to the 3' UTR region of the mRNA of TNF-α and blocks its translation. After its malonylation, GAPDH detaches from the mRNA and allows the synthesis of TNF-α protein. M1 differentiation also leads to an increase in succinylation of proteins (16), possibly because of elevated succinate levels, although its consequences have not been explored in detail.

M1 polarization is irreversible (20), as subsequent incubation of M1 cells with IL-4 or IL-10 does not turn the cells into M2. The main reason for this is that the mitochondrial respiratory chain is permanently damaged by NO after M1 differentiation, and accordingly, inducible NO synthase (iNOS) inhibition allows M1 cells to repolarize to M2.

Regulation of Cytokine Production by Glycolysis

In macrophages and monocytes glucose availability controls the expression of proinflammatory cytokines by several mechanisms. The first involves regulation of mRNA translation: in situations of low glycolysis the glycolytic enzyme GAPDH binds, as explained above, to the TNF-α mRNAs and blocks its translation (21). However, during active glycolysis GAPDH detaches from the mRNA which allows high production of the cytokine. A second mechanisms deal with the transcription of the mRNA for IL-1β. After activation of the macrophage, glycolysis drives an increase in the levels of succinate (derived from glutamine) (16), which in turn control the stability of HIF-1α. Under basal conditions, HIF-1α is hydroxylated by prolyl-hydroxylases (PDHs) and targeted for degradation by the proteasome. However, under limited oxygen or under high ROS levels, the activity of PHD is impaired and this leads to HIF-1α accumulation. The model that emerges from these studies is that glycolytic ATP drives M1 macrophage activation by providing an increase in mitochondrial membrane potential that is absolutely required for succinate oxidation-dependent RET to occur, leading to a large increase in mitochondrial ROS levels that facilitate HIF-1α accumulation, which binds directly to the promoter of the IL1B gene and favors expression of pro-inflammatory genes (17). This process reciprocally decreases anti-inflammatory cytokines, such as IL-10.

M2 Macrophages

Alternatively-activated macrophages do not secrete pro-inflammatory cytokines and are involved in tissue recovery, remodeling of the extracellular matrix or immunosupression. Another signature of these cells is highly N-glycosylated lectin and mannose receptors and thus there is an increase in the metabolism of nucleotide sugars such as uridine diphosphate N-acetylglucosamine (UDP-GlcNAc), UDP-glucose, and UDP-glucuronate (15). They are also characterized by utilization of arginine *via* Arginase 1 (Arg1), which catalyzes its conversion to L-ornithine, and by the secretion of TFG-β and IL-10.

In contrast to M1 cells, M2 cells use OxPhos (including FAO) to support ATP synthesis. Strikingly, high glycolysis is also required for M2 polarization, since its blockade blunts expression of M2 markers such as Arg1 or resistin-like molecule alpha (Retnla) (22, 23), which suggests that glycolysis probably provides pyruvate for the TCA cycle, and recent studies suggest that FAO is largely not essential for M2 polarization (23, 24). Knockdown of pyruvate dehydrogenase kinase 1 (PDK1), an enzyme that drives inhibitory phosphorylation on the pyruvate dehydrogenase complex, increases conversion of glucose-derived pyruvate to acetyl-CoA and enhances M2 differentiation while preventing M1 differentiation (23).

IL-4 addition to macrophages increased glucose uptake and oxygen consumption, and this depended on Akt and mTOR1, which regulate ACLY phosphorylation to control cytosolic/nuclear acetyl-CoA levels for acetylation of histones on some M2 genes (22). IL-4 also induces phosphorylation and activation of the transcription factor signal transducer and activator of transcription 6 (STAT6), which induces expression of protein peroxisome proliferator-activated receptor gamma (PPARγ) coactivator-1β (PGC-1β), which in turn stimulates mitochondrial biogenesis and OxPhos (25). PGC-1β also coactivates STAT6-responsive genes, such as Arg1. Interestingly, overexpression of PGC-1β strongly stimulates FAO and potentiates M2 differentiation without altering STAT6 phosphorylation, while it prevents M1 differentiation (25). Similarly to PGC-1β, PPARγ is required for M2 activation, mitochondrial biogenesis and stimulation of fatty acid metabolism as well (26).

Immunometabolism of T Cells

T cells are leukocytes involved in adaptive immunity. T cells are largely divided into two subtypes: T helper (Th) cells, also known as $CD4^+$ cells, that participate in the activation of other immune cell types (B cells, cytotoxic cells and macrophages) by the release of cytokines; and T cytotoxic (Tc) cells, also known as $CD8^+$ cells or cytotoxic T lymphocytes (CTLs), that kill cancer and virus-infected cells.

$CD4^+$ T Cells

Naïve $CD4^+$ T cells have a very low metabolic rate that depends mainly on OxPhos using pyruvate and FAO. Stimulated $CD4^+$ T cells can differentiate into effector T cells (Teff), including T helper 1 (Th1), T helper 2 (Th2) and T helper 17 (Th17) subsets, which switch to an anabolic state that is orchestrated by mTOR, and inducible regulatory T cells (Treg), which do not depend on mTOR, but on 5' adenosine monophosphate-activated protein kinase (AMPK). Th1 cells are involved in Type 1 or cell-mediated immunity, which includes neutrophils, natural killer cells, $CD8^+$ cytotoxic T cells and classically activated macrophages (M1), and responds to intracellular pathogens, bacteria and viruses (27). Th2 cells are involved in Type 2 immunity, which includes eosinophils, mast cells, basophils and alternatively activated macrophages (M2), and typically regulates tissue repair and regeneration, but also responds to extracellular parasites and helminths (28). Th17 are involved in Type 3 immunity, which responds to extracellular bacteria and fungi, and are characterized by the capacity to release IL-17 (and IL-22). Other minor subsets of T helper cells include T helper 9 (Th9) cells, which secrete IL-9. Type 1 and 3 immunity largely mediate autoimmune diseases, with Th17 cells playing an

important role in the pathogenesis of diseases such as psoriasis, rheumatoid arthritis or asthma (27), whereas type 2 immunity can cause allergic diseases. All 3 types of immune responses display substantial cross–regulation.

Effector T Cells

Upon *in vitro* activation of the T cell receptor (TCR) with anti-CD3 and -CD28 antibodies, there is a dramatic increase in glycolysis and OxPhos in order to support their proliferation and biosynthesis, and the oxygen consumption/glycolysis ratio greatly decreases. Fatty acid and pyruvate oxidation decrease compared to resting T cells, while the increase in OxPhos is likely fueled by glutamine oxidation in the TCA cycle (29). Interestingly, OxPhos, but not glycolysis, is required during the initial activation of the cell that is accompanied by cell growth but not proliferation (29, 30). However, once the T cell has been activated for at least 48 hours, either glycolysis or OxPhos are enough to sustain survival or proliferation (30), while glycolysis remains essential for some effector functions (see below).

The increase in glycolysis is mainly driven by an increase in the glucose transporter GLUT1 and the glycolytic enzymes hexokinase 2 (HK2), pyruvate kinase M2 (PKM2) and LDHA (29), while the increase in OxPhos comes from a large activation of mitochondrial biogenesis, with increasing levels of mitochondrial DNA and mitochondrial proteins (31). Interestingly, while there is a gradual increase in GLUT1 along several days after activation, mitochondrial biogenesis largely occurs during the first 24 hours (31). There is a concomitant elevation in ROS levels, which is important as a second signal (32). Additionally, the expression of glutaminolysis-associated genes such as glutaminase 2 (GLS2) is upregulated, including transporters of glutamine and amino acids, and there is an increase in the flux though the PPP, involved in the biosynthesis of ribose-5-phosphate for nucleic acids and NADPH, required for lipid synthesis. This extensive metabolic remodeling requires mTOR and NO (31), and is accompanied by upregulation of transcription factors and signaling pathways, including the proto-oncogene Myc that regulates and supports the anabolic needs of proliferating T cells. Deletion of Myc prevents activation-induced increases in glycolysis and glutaminolysis in T cells (29). Th17 cells also utilize the transcription factor HIF-1α, which binds to the promoter of retinoid-related orphan receptor-γ (RORγt), a lineage-specific marker of Th17 cells (33).

The energy sensor 5' adenosine monophosphate-activated protein kinase (AMPK), which is activated by an increased ratio of AMP to ATP, is required for metabolic adaptation and flexibility under conditions of limited nutrient availability. Indeed, energy depletion by reduced glucose concentration or nutrient limitation is sensed by AMPK, which is phosphorylated in threonine 172 of its alpha subunit, and drives the expression of genes involved in glutamine metabolism such as glutamine transporters or glutaminase (34), which fuel mitochondrial metabolism under these conditions. This leads to a decrease in glycolysis, while oxygen consumption and cellular ATP levels are largely maintained.

Regulation of Cytokine Production by Glycolysis

T cell activation leads to an increase in IFN-γ production by at least three mechanisms: the first mechanism is epigenetic and involves increased expression LDHA by Myc and HIF-1α, which promotes aerobic glycolysis and generation of ATP in the cytosol. As a result, in the presence of glucose, citrate is not required by the TCA for mitochondrial ATP generation and can rather be exported to the cytosol and converted to acetyl-CoA by ACLY, where it is used as a substrate by histone acetyltransferases for regulation of gene expression, including IFN-γ gene transcription (35). The second mechanism is similar to the regulation of TNF-α expression in macrophages and involves regulation of mRNA translation: in situations of low glycolysis the glycolytic enzyme GAPDH binds to the 3' UTR regions of IL-2 and IFN-γ mRNAs and blocks their translation. On the other hand, during active glycolysis GAPDH detaches from mRNAs which allows high production of cytokines (30). AMPK seems to be involved in this translational mechanism of regulation as well: AMPK activators such as 5-aminoimidazole-4-carboxamide ribonucleotide (AICAR) decrease IFN-γ production (34), possibly by inhibition of mTOR. AMPKα-1 deficiency leads to increase production of IFN-γ, which becomes resistant to AICAR inhibition (34), and to increased translation of the IFN-γ mRNA. The third mechanism involves regulation of Ca^{2+} signaling by the glycolytic metabolite phosphoenolpyruvate (PEP), which accumulates in activated T cells, as they express the M2 isoform of pyruvate kinase (PKM2) (29, 36) which is preferentially a dimer and enzymatically less active in the conversion of PEP to pyruvate than the tetrameric PKM1 isoform. PEP accumulates in the presence of glucose and inhibits the sarco/endoplasmic reticulum Ca^{2+} (SERCA)-ATPase (a P-type ATPase whose function is to pump and sequester Ca^{2+} into the endoplasmic reticulum), thus increasing cytosolic Ca^{2+} transients after TCR signaling and activation of the nuclear factor of activated T cells (NFAT) transcription factor (37). Accordingly, glucose depletion in T cells prevents accumulation of PEP after TCR signaling, and active SERCA limits cytosolic Ca^{2+} transients, which leads to cytoplasmatic localization of NFAT and decreased expression of IFN-γ.

Regulatory T Cells

In contrast to effector cells, Tregs express low levels of GLUT1, utilize mainly FAO and depend on the expression of the transcription factor Forkhead box P3 (Foxp3). Tregs do not use mTOR or HIF-1α, but constitutively show high levels of phosphorylated AMPK, which positively regulates FAO and blocks mTORC1 activity.

Consistent with their dependence on FAO rather than glycolysis, the deletion of HIF-1α promotes rather than inhibits Treg differentiation, likely due to the ability of HIF-1α to bind to and degrade Foxp3. Rather, Tregs shows high levels of phosphorylated AMP-activated protein kinase (AMPK), which regulates FAO by phosphorylating and inhibiting acetyl-CoA carboxylase (ACC) thereby activating carnitine palmitoyl transferase 1a (CPT1a), the rate-limiting step in FAO (38).

Interestingly, glycolysis and mTORC1 are essential to support the migration of Tregs (38). Tumor-infiltrating Tregs, which may constitute up to 20–30% of the total $CD4^+$ population of the tumor (39), are strongly associated with advanced cancer stage and poor prognosis.

CD8$^+$ T Cells

Naïve CD8$^+$ T cells have a similar metabolism to naïve CD4$^+$ T cells. Stimulated CD8$^+$ T cells differentiate into effector cells. The best characterized effector CD8$^+$ T cell subpopulation are Tc1 cells, which are promoted by IL-12 and IFN-γ, secrete cytokines such as IFN-γ and TNF-α and have high cytolytic potential against cells infected with intracellular pathogens by releasing cytotoxic molecules, such as granzymes and perforin. In contrast, Tc2 cells secrete IL-4, IL-5 and IL-13, but not IFN-γ, and display reduced cytotoxic activity compared to Tc1 cells. Other subsets of effector CD8$^+$ T cells include Tc9 and Tc17. Activation of CD8$^+$ T, as in CD4$^+$ T cells, also induces cell growth and proliferation, and a metabolic switch to aerobic glycolysis that depends on Glut1, mTOR and Myc.

During resolution of an immune response, surviving T cells convert to memory T cells. Interestingly, while effector CD8$^+$ T cells are highly glycolytic, CD8$^+$ T memory cells rely on OxPhos again. OxPhos and FAO are essential for these cells to respond upon re-exposure to the antigen and for longevity.

Immunometabolism of NK Cells

NK cells are cytotoxic lymphocytes involved in anti-tumor and anti-viral innate immunity. NK cells do not express polymorphic germline-encoded receptors, such as TCR or BCR, nor require prior sensitization (40), and the activation of their cytolytic functions is prompted by the engagement of receptors that recognize invariable ligands on the surface of a target cell (41, 42). The balance of the signal coming from activating and inhibitory receptors will dictate the activating or inhibitory fate of the NK cell response. If they get activated, NK cells will kill target cells by releasing lytic granules (which contain perforin and granzyme) or activating cell death receptors on their targets. NK cell activation response also induces secretion of cytokines, such as IFNγ or TNFα.

Resting NK cells have very low basal metabolic rates and utilize OxPhos primarily. While short times of cytokine stimulation or receptor signaling does not alter metabolic parameters significantly (43), overnight incubations with IL-2 or IL-15 induce an increase in OxPhos and especially glycolysis (44, 45). Activated NK cells metabolize pyruvate into acetyl-CoA and then engage the citrate–malate shuttle, which consists of the export of citrate (generated by condensation of acetyl-CoA and oxaloacetate by citrate synthase) into the cytosol *via* CIC in exchange for malate, its breakdown by Acly into acetyl-CoA and oxaloacetate, which is metabolized by malate dehydrogenase 1 (MDH1), consuming cytosolic NADH and yielding cytosolic malate that is exchanged for citrate though CIC, and then oxidized in the mitochondria to oxaloacetate by malate dehydrogenase 2 (MDH2) with the generation of NADH. Thus, this process bypasses the TCA cycle, and generates both mitochondrial NADH to support OxPhos and cytosolic acetyl-CoA to support acetylation reactions and fatty acid synthesis (46). NK cell activation is also associated with increased mitochondrial mass (46) and increased mitochondrial membrane potential (47). Interestingly, unlike in other types of lymphocytes, glutamine is not metabolized through glutaminolysis or the TCA cycle in activated NK cells (48).

There are different pathologies that can alter NK cells metabolism, including cancer (49), obesity (50) and viral infections (51). As many other immune cells, NK cell metabolism regulation depends on mTORC1 (52). Upon cytokine stimulation, mTORC1 activity increases and enhances glycolysis rate. mTORC1 inhibitors, such as rapamycin, results in inhibition of glycolysis but not OxPhos (52, 53). mTORC2 is closely related to mTORC1, and they share the kinase core subunit, but differ in some specific subunits (which makes mTORC2 insensitive to inhibition with rapamycin). mTORC2 inhibits mTORC1 activity, which results in an inhibition of NK cell functions (54).

Other regulators of NK cells metabolism are transcriptional factor cMyc, controlled by the availability of glutamine and other amino acids (55), and the sterol regulatory element binding protein (SREBP), driven by mTORC1 signaling, essential for glycolysis and OxPhos regulation (46).

Fibroblasts

Fibroblasts are not immune cells, but cells that have a role in synthesizing extracellular matrix proteins. They are however the predominant cell type in some tumors and contribute to tumorigenesis. Interestingly, transplantation of tumor cells together with cancer-associated fibroblast (CAFs) leads to more malignant cancers compared to tumor cells alone or with normal fibroblasts. From the immunometabolic perspective, oxygen depletion in the TME promotes, *via* epigenetic reprogramming, a metabolic switch in CAFs leading to a glycolytic metabolism that fuels biosynthetic pathways of cancer cells, including the PPP and nucleic acid metabolism (56, 57). Metabolites secreted by CAFs and taken up by tumors include lactate (58), glutamine (59, 60) and lipids (61), among others. CAFs also promote the recruitment of monocytes towards a tumor, their differentiation into macrophages, and their polarization to an M2 phenotype (62, 63). Interestingly, there is reciprocal crosstalk between CAFs and TAMs (64), as TAMs are able to activate normal fibroblasts into CAFs (62).

TUMOR MICROENVIRONMENT (TME) AND METABOLIC REPROGRAMING OF IMMUNE CELLS

The cancer metabolic phenotype generates a milieu that is hostile to proinflammatory immune cells. This TME exerts immunosuppressive effects in immune cells by several mechanisms, including competition for nutrients, and secretion of metabolites and cytokines (**Figure 3**). In addition, the TME may alter dysfunctional immune cells to make them transition into tumor-supporting cells. These effects on macrophages, T cells and NK cells are reviewed below.

Metabolic Competition for Nutrients

Tumor cells are known to be highly glycolytic and solid tumors consume large amounts of glucose and other nutrients, which results in low extracellular levels of glucose, glutamine and other

amino acids, including arginine and tryptophan (65), and this blunts antitumor responses through multiple mechanisms.

A mouse sarcoma model shows that tumor-mediated glucose depletion in the TME skews the differentiation of macrophages toward the M2 phenotype (66). Unlike M1 macrophages, M2 macrophages do not compete for glucose with the tumor cells, as they preferentially employ OxPhos.

Intratumoral $CD4^+$ T cells in Braf/Pten melanoma-bearing mice express a glucose-deprivation transcriptional signature, suggesting that they experience glucose deprivation *in vivo* and that their glycolysis is indeed restricted (37). Although glucose depletion does not lead to defects in proliferation or survival in T cells, it leads to decreased synthesis of cytokines, suppresses activation and may limit antitumor responses. Inhibition of glycolysis also decreases the expression of perforin and granzymes, and blocks cytolytic activity in $CD8^+$ cells (67). Indeed, it has been shown in a mouse sarcoma model that tumor-mediated glucose depletion in the TME inhibits mTOR activity and glycolysis in $CD8^+$ T cells and dampens their ability to produce cytokines (66). Glutamine depletion leads to defects in T cell proliferation and synthesis of IL-2 and IFN-γ (68).

In NK cells, limited glucose directly reduces glycolysis and OxPhos, but will also affect the activity of regulators of the activation such as mTORC1 (44). Consequently, glucose depletion significantly impairs IFN-γ production (69), proliferation and cytotoxicity (51). NK cells express several glucose transporters (GLUT1, GLUT3 and GLUT4) and it has been shown that cytokine stimulation increases expression of GLUT1, needed to increase the uptake of glucose essential to fuel the augmented glycolysis rate that will support the activating functions of NK cells. Interestingly, glutaminolysis does not sustain OxPhos in activated NK cells, that rely on the citrate–malate shuttle instead of a full TCA cycle, but supports cMyc expression (48). Accordingly, glutamine depletion leads to a rapid loss of c-myc protein and loss of effector functions.

Hypoxia

Due to their high metabolic profile and sometimes poor vascularization, tumors also contain areas of hypoxia.

During hypoxia, NK cells upregulate HIF-1α, but lose their ability to upregulate the surface expression activating receptors in response to IL-2 or IL-15, including NKp46, NKp30, NKp44, and NKG2D, as well as their capacity to kill target cells (70). It has also been shown that hypoxia modifies the NK cell transcriptome and reduces release of some cytokines including IFN-γ and TNF-α in response to several stimuli or soluble cytokines, although it sustains the expression of chemokine receptors, including CCR7 and CXCR4 (71).

TAMs in oxygen-rich regions of the tumor, such as those close to blood vessels, display features of M1 macrophages, whereas TAMs in hypoxic regions of the tumor display M2-like features (72). Hypoxia stimulates the expression of HIF-1α in TAMs, which controls the levels of proteins involved in angiogenesis, such as vascular endothelial growth factor (VEGF), or metastasis, such

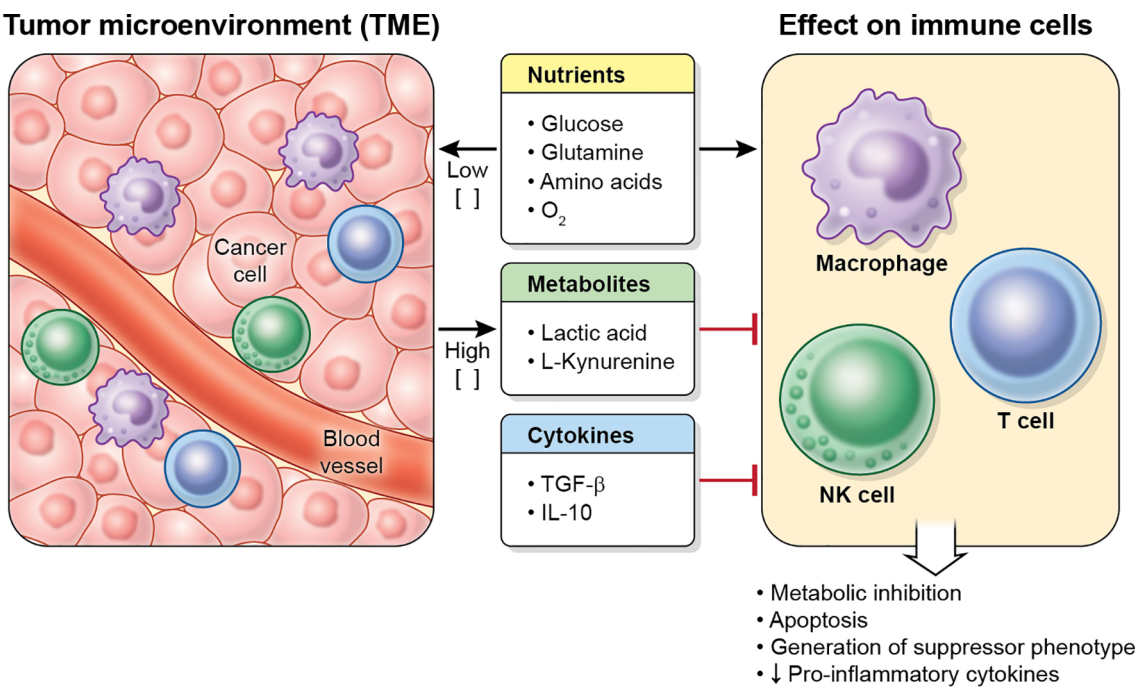

FIGURE 3 | Characteristics of the TME. Tumor cells (and other cells in the tumor) deplete nutrient levels (glucose, glutamine, amino acids, O_2, etc.) in the TME, increase the levels of some metabolites, such as lactic acid or L-kynurenine, and secrete cytokines (including TGF-β and IL-10), which inhibit the metabolism, effector function and proliferation in immune cell, and may cause apoptosis.

as regulated in development and DNA damage response 1 (REDD1) (72, 73). Interestingly, REDD1 is an mTOR inhibitor, which decreases glycolysis in the hypoxic TAM, leading to more glucose available for endothelial cells and an excessive angiogenic response, which in turn leads to aberrant and dysfunctional blood vessel formation and increased metastasis. When REDD1 is depleted, an mTOR-mediated glycolytic enhancement in the TAM leads to glucose competition with blood vessels and their normalization (73).

Metabolites Secreted by Tumor Cells

Lactic Acid

Due to their glycolytic metabolism, tumor cells secrete large amounts of lactic acid that can reach up to 30–40 mM, which generates regions of high acidity in the TME. In fact, a negative correlation between tumor LDHA expression and patient survival has been found in melanoma (74). In $CD8^+$ T cells lactic acid, but not its sodium salt, inhibits the expression of IFN-γ and IL-2, suppresses proliferation and cytotoxic activity, and may induced cell death (74, 75).

In NK cells, lactic acid also inhibits the expression of IFN-γ and induces apoptosis in a mitochondrial ROS-dependent fashion (74, 76, 77). Interestingly, lactate suppresses IFN-γ expression even at physiologic pH in NK cells (77).

Lactate also inhibits the release of proinflammatory cytokines in macrophages (78) and induces M2 macrophage polarization (79). Conditioned medium from lactate-treated macrophages stimulates angiogenesis, and proliferation and migration of cancer cells *in vitro (*79). Lactic acid induces expression of VEGF, Arg1 and other M2 genes in TAMs *via* HIF-1α stabilization, and this is critical for tumor growth, as Arg1-deficient macrophages impair tumor progression *in vivo* in a mouse model (80).

l-kynurenine

l-kynurenine, a tryptophan-derived catabolite resulting from the activity of indoleamine 2,3-dioxygenase (IDO), an enzyme that is often expressed in tumor cells or tumor-associated cells (TAMs, dendritic cells, etc.) (81, 82), interferes with NK cells by regulating the surface expression of activating receptors and thus their antitumor function (83). In additional studies, IDO is also shown to inhibit NK cell proliferation *via* l-kynurenine (84, 85).

l-kynurenine also inhibits proliferation of $CD4^+$ and $CD8^+$ T effector cells (86) and induces the generation of Tregs by interacting with the aryl hydrocarbon receptor (AHR) (87). Furthermore, a blockade of IDO leads to conversion of Tregs to T_h17 cells (88), which highlights the role of IDO in the choice between immunosuppression and immune activation. Importantly, increased IDO expression correlates with poor prognosis in some cancers (89). IDO causes inhibition of effector T cells also by an additional mechanisms: it leads to tryptophan depletion in the TME, which activates the protein general control nonderepressible 2 (GCN2) in T cells, a stress-response kinase that is activated by elevations in uncharged tRNA. GCN2 function is to phosphorylate eukaryotic Initiation Factor 2 alpha (eIF2α) to activate the integrated stress response, which leads to a decrease in global protein synthesis and the induction of selected genes, which leads to $CD8^+$ T cell anergy (90). Strikingly, in a mouse model of skin carcinogenesis, the absence of GCN2 does not phenocopy the absence of IDO, which promotes resistance against tumor development, suggesting the existence of additional pathways that operate downstream of IDO (91). This additional pathway is mTOR, which senses tryptophan depletion.

Cytokines Present in the TME

TGF-β

TGF-β inhibits cytokine-induced metabolic changes and effector functions in NK cells, including expression of CD71 (transferrin receptor), granzyme B, IFN-γ and the stimulatory receptor CD69, *via* mTORC1-dependent and independent pathways (92, 93). It has been suggested that upregulation of the gluconeogenic enzyme Fructose-1,6-bisphosphatase 1 (FBP1) in NK cells of lung cancer, which inhibits their glycolytic metabolism, is caused by high levels of TGF-β in the TME (94). TGF-β also supports the induction of Tregs in tumors (95).

IL-10

This cytokine is frequently upregulated in cancers and has been shown to directly affect the function of APCs by inhibiting the expression of major histocompatibility complex (MHC) class II and costimulatory molecules CD80/B7-1 and CD86/B7.2, which in turn induces immune suppression or tolerance (96). The role IL-10 in macrophage immunometabolism is well stablished. This cytokine opposes the switch to the M1 metabolic program in macrophages by inducing mitochondrial oxygen consumption and increasing mitochondrial integrity *via* mTOR, by decreasing mitochondrial ROS levels, by decreasing the cell surface expression of GLUT1 and thus by inhibiting glycolysis (97).

On the other hand, IL-10 downregulates the expression of Th1 cytokines (TNF-α, IFN-γ), inhibits $CD4^+$ and $CD8^+$ T cell proliferation and production of IFN-γ and IL-2 (98), and induces T-regulatory responses. IL-10 deficiency also impairs Treg function and enhances Th1 and Th17 immunity to inhibit tumor growth (99).

Finally, IL-10 suppresses production of IFN-γ by NK cells without altering cytotoxicity (100).

TARGETING IMMUNOMETABOLISM FOR IMMUNOTHERAPY

Immunotherapy involves the use of the immune system as therapy to treat cancer. Current therapies include blockade of immune checkpoint receptors (which maintain self-tolerance and prevent uncontrolled inflammation) and adoptive cell transfer. However, these techniques have their limitations, including T and NK cell exhaustion, possibly because of the effects of the TME. This section describes some immunotherapies in T cells, NK cells and macrophages and briefly describes some strategies used to modulate the metabolism of the tumor cell or the immune cell that can be combined with other therapies to boost the immune response to cancer.

Targeting T Cells

T cells have been successfully used for immunotherapy in a number of ways, including immune checkpoint blockade, which uses monoclonal antibodies to bind and inactivate inhibitory receptors such as cytotoxic T-lymphocyte-associated protein 4 (CTLA-4) and programmed cell death-1 (PD-1) or its ligand programmed cell death ligand 1 (PD-L1) (101), or adoptive cell transfer, which involves the isolation of T cells, improving their anti-tumor capacity *in vitro*, expanding them in culture, and transferring them back to the patient (102). Adoptive cell transfer was improved by generation of T cells that express engineered TCRs that target a specific antigen and lately by the generation of chimeric antigen receptor (CAR) T cells, which express an artificial chimeric antigen-binding receptor that combines both antigen-binding and T-cell activating functions into a single molecule (103). Some strategies to indirectly or directly target the metabolism of T cells and improve immunotherapy are described here.

Pharmacological inhibition of the lactate transporters MCT1 and MCT4 using diclofenac restores T cell function, slows tumor growth and improves the efficacy of checkpoint inhibition therapies (104). Knockdown of LDHA in tumor cells using RNAi nanoparticles neutralized the pH of the TME, increased infiltration with $CD8^+$ T and NK cells, decreased the number of Tregs, significantly inhibited the growth of tumors and potentiated checkpoint inhibition therapy (105).

Removal of extracellular kynurenine in the TME by administration of bacterial kynureninase linked to polyethylene glycol (for prolonged systemic retention) increases the frequency of effector $CD8^+$ T cells in the tumor (but not in the periphery), reduces tumor growth, increases survival in a $CD8^+$ cell-dependent manner and potentiates checkpoint inhibition therapy (106). In a mouse model of melanoma, the combination of the tryptophan analog 1-methyl-D-tryptophan plus an antitumor vaccine caused conversion of Tregs to the Th17, with marked enhancement of $CD8^+$ T cell activation and antitumor efficacy (88). It is interesting to remark that the IDO inhibitor 1-methyl-tryptophan exists in two stereoisomers, and it has been shown that the L isomer (1-methyl-L-tryptophan) is the more potent inhibitor of IDO activity. Remarkably, the D isomer (Indoximod), although it does not bind to, or biochemically inhibit IDO, nor prevents the production of kynurenine, is much more effective in reversing the suppression of T cells and has stronger therapeutic effects (107). This probably happens *via* direct restoration of mTOR activity, which is suppressed due to tryptophan deprivation (91, 108). Several small-molecule IDO inhibitors, including Indoximod, Navoximod, Epacadostat or BMS-986205, are currently being used in several clinical trials (108)

JHU083, a pro-drug of 6-diazo-5-oxo-L-norleucine (DON), a glutamine antagonist which inhibits glutaminase and other glutamine-requiring enzymes, impairs tumor cell metabolism, which in turn increases the availability of nutrients and oxygen in the TME. Remarkably, in the presence of JHU083, tumor infiltrating $CD8^+$ T cells display increased glycolysis and mitochondrial oxygen consumption and regain their effector functions and proliferation. This is probably because of the plasticity of T cells, which in the absence of glutamine metabolism undergo a metabolic reprogram and are able to replenish the TCA using glucose anaplerosis *via* pyruvate carboxylase and acetate metabolism, while tumor cells do not possess that plasticity (109).

Overexpression of phosphoenolpyruvate carboxykinase 1 (PCK1), which converts oxaloacetate into PEP and CO_2, increases PEP levels in T cells even in glucose depleted conditions and consequently restores cytosolic Ca^{2+} transients, nuclear localization of NFAT and IFN-γ expression (37). Furthermore, after adoptive transfer of PCK1-overexpressing $CD4^+$ or $CD8^+$ T cells into a melanoma-bearing mice, there was a decrease in tumor growth which prolonged survival of the mice (37).

Targeting NK Cells

NK cells are also being used for immune checkpoint blockade therapies: blocking of NKG2A, an inhibitory receptor, by the use of antibodies improves NK-mediated cytotoxicity and this is currently being used in ongoing clinical trials (110). Adoptive cell transfer with NK cells is also a promising therapy: NK cells may be treated with IL-15, other cytokines or drugs prior to their transfer back to the patient (111). Antibody blockade of PD-1 or CTLA-4 in combination with IL-15 has also been used (112) Some strategies to target the metabolism of NK cells and improve immunotherapy are described here.

Adoptive transfer of NK cells treated with MB05032, an FBP1 inhibitor that restores NK cell glycolysis and effector functions, slows tumor growth in a lung cancer model in mouse (94).

In mice, systemic pH buffering of the tissue milieu by supplementing drinking water with sodium bicarbonate normalizes IFN-γ expression but not cytotoxic capacity in NK cells, and delays tumor growth (77).

Blockade of glutaminase should not affect NK cells effector functions, since they do not metabolize glutamine to glutamate, but use it for the import of other amino acids in order to sustain mTOR function and cMyc expression (48). Since MYC in NK cells is degraded by glycogen synthase kinase 3 (GSK3), inhibitors of this enzyme should also activate effector functions in these cells. Indeed, increased antitumor activity in NK cells has been shown after *ex vivo* pharmacologic inhibition of GSK with CHIR99021 or other compounds followed by adoptive transfer (113, 114), although it appears that GSK3 inhibition leads to activation of the NF-αB pathway and increased expression of TNF-α, and only to a modest increase in IFN-γ, and whether the metabolism of the NK cells or MYC levels were altered was not explored in those studies.

Targeting Macrophages

Therapies that deal with macrophages mainly consists of two approaches, those that deplete TAMs in an effort to prevent their tumor supporting functions (chemokine (C-C motif) ligand 2 (CCL2) or CC-chemokine receptor 2 (CCR2) blockade, which prevents their recruitment into tumors, for example), and those that try to repolarize them towards an M1-like antitumor

phenotype (115). Some strategies to target the metabolism of macrophages and improve immunotherapy are described here.

Pharmacologic or genetic blockade of glutamine synthetase, the enzyme that converts glutamate into glutamine, alters the metabolism of macrophages and skews their differentiation from the M2 phenotype to M1 in an HIF-1α-dependent fashion, which leads to decreased T cell suppression, decreased angiogenesis and prevention of metastasis in a Lewis lung carcinoma mouse model (116).

TAMs express high levels of the T cell checkpoint receptor PD1, and these PD1-containing TAMs are preferentially M2 macrophages (117). Strikingly, the frequency of M2 PD-1 containing TAMs increased with disease stage in human cancer patients. PD-1 expression in TAMs correlates negatively with phagocytic potency against tumor cells, and blockade of PD-1 or PD-L1 *in vivo* increases macrophage phagocytosis, reduces tumor growth and increases the survival of mice in mouse models of cancer in a macrophage-dependent fashion, as depletion of TAMs abrogates these effects (117). Remarkably, TAMs (and even mouse bone marrow-derived macrophages or human monocyte-derived macrophages) express PD-L1 as well (118). Blockade of PD-L1 with antibodies induces macrophage activation, release of proinflammatory cytokines and an activation of mTOR, suggesting that PD-L1 constitutively provides a negative signal to these macrophages (118). In addition, blockade of PD-L1 in macrophages alters the transcriptome to resemble that of M1 proinflammatory cells (118). In a mouse model of melanoma, *in vivo* treatment of $RAG^{-/-}$ mice (which lack functional T cells) with PD-L1 antibodies triggers TAM activation to a proinflammatory state and a significant slowing of tumor growth which is independent of T cells, the main target for immune checkpoint blockers (118).

Respiratory complex I inhibitor metformin (an anti-diabetic drug) inhibits M2 polarization of macrophages and blocks the migration-promoting and angiogenesis-promoting properties of conditioned media from M2 cells (119). Metformin also inhibits metastasis in a Lewis lung carcinoma model, and this effect is abolished when TAMs are depleted, which suggests that metformin indeed targets macrophages in this model (119).

Nutrient Restriction as Therapy

Because of a strong competition at the TME, it might be argued that dietary interventions that limit nutrient availability in an attempt to prevent the growth of cancer cells may also deprive immune cells of those very same nutrients, thus raising concerns about the possible detrimental effect of suppressing anti-cancer immunity. Despite this, fasting, long-term fasting, fasting-mimicking diets, and ketogenic diets are currently under investigation in trials for several cancer types. Fasting has been shown not only to be useful as therapy against cancer by several mechanisms, but also to increase tolerance to chemotherapy, with reduction of many side effects (120), as it protects normal cells, but not cancer cells, from high doses of chemotherapy by a mechanism that involves a reduction in the levels of circulating insulin-like growth factor-I (121, 122).

From the immunometabolic perspective, fasting suppresses the polarization of TAMs towards the M2 phenotype, possibly because of decreased presence of adenosine in the TME (123), a metabolite that directly restricts antitumor responses by activating the adenosine A2A receptor (A2AR) in T-cells (124). Low-protein diet also shifts the polarization of TAMs toward the inflammatory M1 phenotype and increases the response to immunotherapies (125). Nutrient restriction is also able to increase mitochondrial ROS, including superoxide levels, in several cancer cell types, which increases the efficacy of chemotherapy (126, 127). However, since fasting and caloric restriction are hard to implement in the clinical setting, especially in cancer patients that are struggling with cachexia or loss of appetite, the use of caloric restriction mimetics such as resveratrol or anti-hyperglycemic agents such as metformin, which might provide the same effect without the need to fast, is increasingly being used in the field (128). In fact, the caloric restriction mimetic hydroxycitrate improves antitumor immunity by depleting Tregs in the tumor, and enhances immunotherapy (129).

OTHER FACTORS THAT INFLUENCE CANCER IMMUNOMETABOLISM AND IMMUNOTHERAPY

Obesity

Obesity is a disease characterized by the excessive accumulation of fat tissue and lipids along the body. The accumulation of lipids occurs inside immune cells as well, reprograming their metabolism and affecting their function. Obesity is characterized by the activation of mTOR signaling because of nutrients excess. The contribution of obesity to cancer is two-fold: it drives a low-grade sistemic chronic inflammatory state but it also blocks cancer immune surveillance by metabolically reprogramming immune cells and affecting their function (130).

In NK cells, obesity downregulates the transcription of genes involved in NK-cell mediated cytotoxicity, resulting in an impairment of killing function and less production of IFN- γ. NK cells from obese individuals display an impaired ability to increase glycolysis and OXPHOS after stimulation with cytokines, and this effect depends on PPARα/δ (50). The number of circulating NK cells is reduced in obese people compared to control individuals and lipid treated NK cells fail to control tumor growth *in vivo*.

In the case of T cells, lipid accumulation supports Treg function, which relies on FAO to fuel OxPhos (131). On the other hand, the chronic inflammatory environment present in obesity suppresses Teff, which show an exhausted phenotype with impaired cytokine secretion (132, 133). Consistent with this, high fat diet in mice accelerates tumor growth, and the mechanism involves depletion of intratumoral T cells and an increase in MDSCs and TAMs (134). Interestingly, tumor cells and T cells adapt differently to lipid accumulation and undergo opposing metabolic changes: while tumor cells increase fatty acid utilization, $CD8^+$ T cells do not (134). The increase in TAMs is consistent with lipid accumulation, since FAO is associated with the M2 suppressor phenotype (25, 135).

Regarding immunotherapy, and taking into account the multiple suppressor effects of obesity in the immune system, it could be assumed that obesity might contribute negatively to the efficacy of immunotherapies, but this is not always the case. In obese individuals there is an increased expression of PD-1, an inhibitory checkpoint molecule, likely due to increased levels of leptin, an hormone produced by adipose tissue. High expression of PD-1 has been generally linked to T-cell exhaustion, but it also means that therapies targeting PD-1 might have more efficacy (136, 137). When PD-1 is upregulated in T cells, the interaction with its ligand PD-L1 (on tumor cells) will inhibit the anti-tumor T-cell activity. Anti PD-1-PD-1L therapy will block this interaction and allow T cells to better fulfill their tumor killing function. Some studies show and association between obesity and immune checkpoint blockade immunotherapy, being this therapy more successful in patients with higher expression of PD-L1 (138).

Sex-Related Differences

There are fundamental metabolic aspects that are different between males and females. For instance, sex differences are apparent in adipose tissue distribution and, as discussed previously, fat tissue and lipids may influence immune cells and metabolism. Also, there are sex differences in immune responses: males are more prone to developing certain infections and cancer types whereas females experience higher risk to developing autoimmune diseases (139). Factors that could potentially contribute to these differences are steroid hormones, sex chromosomes (overall the genes that escape to X-chromosome inactivation), mitochondrial function and environmental factors (139).

As adult females display stronger innate and adaptive immune responses than males, they present increased susceptibility to inflammatory and autoimmune diseases, but lower risk for cancer. Interestingly, neutrophils in females display an activated neutrophil profile characterized by an upregulation of the pathway for type I interferons, enhanced proinflammatory responses, and distinct bioenergetics, which are driven by the sex hormone estradiol (140). We have not covered neutrophils in this review, but there is growing evidence that suggests an important role of this leukocytes, especially tumor-associated neutrophils (TANs), in cancer progression (141). There is currently a debate and conflicting results on whether there are differences in the efficacy of immunotherapy between men and women (142), and this is probably because of sampling bias in clinical trials.

Aging

Age is a risk factor a number of pathologies. It is associated with metabolic disease, autoimmunity, higher risk of infections, and cancer. There are plenty of metabolic changes associated with aging: a decline in mitochondrial activity (143), decreases in NAD levels (144) and low grade chronic inflammation (145).

Aging is a strong risk factor for cancer. In fact, subcutaneously injected tumors grow faster in old mice compared to young mice (146). It is known that Treg cells accumulate in spleens and lymph nodes of old mice, and depletion of those cells induces a strong cytotoxic response and protects old mice against some tumors (147). M2 macrophages are also increased in tissues of old mice, and these macrophages appear to be hypersensitive to tumor-derived stimuli, as they secrete higher amounts of immunosuppressive cytokines, including IL-4 and TGF-β (148). Interestingly, several immunotherapies are less effective in aged animals, while others such as immune checkpoint blockade remain useful (149). Older human adults are under-represented in clinical trials in general, although they seem to benefit similarly to younger patients from checkpoint blockade (150).

CONCLUDING REMARKS

Immunotherapy is becoming increasingly successful for many cancers, especially against hematological malignancies. However, immunotherapy still fails for a substantial numbers of patients, especially in those with solid tumors, and one of the reasons for that failure is that the TME limits the killing capacity of these cells and makes the patients refractory to such therapy. Strategies to bypass the inhibitory effect of the TME in proinflammatory cells are currently being developed. They are key for the success of immunotherapies, and the study of immunometabolism is thus a critical field for cancer research. Targeting immunometabolism during immunotherapy is proving to be challenging, as tumor cells and inflammatory immune cells utilize similar metabolic pathways, and thus targeting a given pathway, such as tumor glucose metabolism to reverse the Warburg phenotype by use of glycolysis inhibitors, may concurrently disrupt the tumor lytic effect of immune cells. Subtle differences between the cancer cell and the immune cell and or TME and/or immune cell targeted metabolic modulation strategies should be investigated as alternate strategies to enhance the cancer disease spectrum for immunotherapy.

AUTHOR CONTRIBUTIONS

JT and OA conceived the work. JT, MS, TW and OA wrote the manuscript. All authors contributed to the article and approved the submitted version.

FUNDING

This work was supported by the Intramural Research Programs of the National Institutes of Health, National Cancer Institute and National Heart, Lung, and Blood Institute. JT is supported by the Ministry of Science and Innovation (MICINN) of Spain (grants RYC2018-026050-I and PID2019-105665RA-I00).

REFERENCES

1. Hanahan D, Weinberg RA. Hallmarks of Cancer: The Next Generation. *Cell* (2011) 144(5):646–74. doi: 10.1016/j.cell.2011.02.013
2. Guo S, Deng CX. Effect of Stromal Cells in Tumor Microenvironment on Metastasis Initiation. *Int J Biol Sci* (2018) 14(14):2083–93. doi: 10.7150/ijbs.25720
3. Cuezva JM, Ortega AD, Willers I, Sanchez-Cenizo L, Aldea M, Sanchez-Arago M. The Tumor Suppressor Function of Mitochondria: Translation Into the Clinics. *Biochim Biophys Acta* (2009) 1792(12):1145–58. doi: 10.1016/j.bbadis.2009.01.006
4. Rosenberg SA. Il-2: The First Effective Immunotherapy for Human Cancer. *J Immunol* (2014) 192(12):5451–8. doi: 10.4049/jimmunol.1490019
5. Ortega AD, Sanchez-Arago M, Giner-Sanchez D, Sanchez-Cenizo L, Willers I, Cuezva JM. Glucose Avidity of Carcinomas. *Cancer Lett* (2009) 276 (2):125–35. doi: 10.1016/j.canlet.2008.08.007
6. Choi YK, Park KG. Targeting Glutamine Metabolism for Cancer Treatment. *Biomol Ther (Seoul)* (2018) 26(1):19–28. doi: 10.4062/biomolther.2017.178
7. Everts B, Amiel E, van der Windt GJ, Freitas TC, Chott R, Yarasheski KE, et al. Commitment to Glycolysis Sustains Survival of NO-producing Inflammatory Dendritic Cells. *Blood* (2012) 120(7):1422–31. doi: 10.1182/blood-2012-03-419747
8. Malinarich F, Duan K, Hamid RA, Bijin A, Lin WX, Poidinger M, et al. High Mitochondrial Respiration and Glycolytic Capacity Represent a Metabolic Phenotype of Human Tolerogenic Dendritic Cells. *J Immunol* (2015) 194 (11):5174–86. doi: 10.4049/jimmunol.1303316
9. Rolot M, O'Sullivan TE. Living With Yourself: Innate Lymphoid Cell Immunometabolism. *Cells* (2020) 9(2):334. doi: 10.3390/cells9020334
10. Akkaya M, Traba J, Roesler AS, Miozzo P, Akkaya B, Theall BP, et al. Second Signals Rescue B Cells From Activation-Induced Mitochondrial Dysfunction and Death. *Nat Immunol* (2018) 19(8):871–84. doi: 10.1038/s41590-018-0156-5
11. Wang H, Gonzalez-Garcia I, Traba J, Jain S, Conteh S, Shin DM, et al. ATP-Degrading ENPP1 is Required for Survival (or Persistence) of Long-Lived Plasma Cells. *Sci Rep* (2017) 7(1):17867. doi: 10.1038/s41598-017-18028-z
12. Kierdorf K, Prinz M, Geissmann F, Gomez Perdiguero E. Development and Function of Tissue Resident Macrophages in Mice. *Semin Immunol* (2015) 27(6):369–78. doi: 10.1016/j.smim.2016.03.017
13. Pathria P, Louis TL, Varner JA. Targeting Tumor-Associated Macrophages in Cancer. *Trends Immunol* (2019) 40(4):310–27. doi: 10.1016/j.it.2019.02.003
14. Lauterbach MA, Hanke JE, Serefidou M, Mangan MSJ, Kolbe CC, Hess T, et al. Toll-Like Receptor Signaling Rewires Macrophage Metabolism and Promotes Histone Acetylation Via ATP-Citrate Lyase. *Immunity* (2019) 51 (6):997–1011 e7. doi: 10.1016/j.immuni.2019.11.009
15. Jha AK, Huang SC, Sergushichev A, Lampropoulou V, Ivanova Y, Loginicheva E, et al. Network Integration of Parallel Metabolic and Transcriptional Data Reveals Metabolic Modules That Regulate Macrophage Polarization. *Immunity* (2015) 42(3):419–30. doi: 10.1016/j.immuni.2015.02.005
16. Tannahill GM, Curtis AM, Adamik J, Palsson-McDermott EM, McGettrick AF, Goel G, et al. Succinate is an Inflammatory Signal That Induces IL-1beta Through HIF-1alpha. *Nature* (2013) 496(7444):238–42. doi: 10.1038/nature11986
17. Mills EL, Kelly B, Logan A, Costa ASH, Varma M, Bryant CE, et al. Succinate Dehydrogenase Supports Metabolic Repurposing of Mitochondria to Drive Inflammatory Macrophages. *Cell* (2016) 167(2):457–70 e13. doi: 10.1016/j.cell.2016.08.064
18. Robb EL, Hall AR, Prime TA, Eaton S, Szibor M, Viscomi C, et al. Control of Mitochondrial Superoxide Production by Reverse Electron Transport at Complex I. *J Biol Chem* (2018) 293(25):9869–79. doi: 10.1074/jbc.RA118.003647
19. Galvan-Pena S, Carroll RG, Newman C, Hinchy EC, Palsson-McDermott E, Robinson EK, et al. Malonylation of GAPDH is an Inflammatory Signal in Macrophages. *Nat Commun* (2019) 10(1):338. doi: 10.1038/s41467-018-08187-6
20. Van den Bossche J, Baardman J, Otto NA, van der Velden S, Neele AE, van den Berg SM, et al. Mitochondrial Dysfunction Prevents Repolarization of Inflammatory Macrophages. *Cell Rep* (2016) 17(3):684–96. doi: 10.1016/j.celrep.2016.09.008
21. Millet P, Vachharajani V, McPhail L, Yoza B, McCall CE. Gapdh Binding to TNF-alpha Mrna Contributes to Posttranscriptional Repression in Monocytes: A Novel Mechanism of Communication Between Inflammation and Metabolism. *J Immunol* (2016) 196(6):2541–51. doi: 10.4049/jimmunol.1501345
22. Covarrubias AJ, Aksoylar HI, Yu J, Snyder NW, Worth AJ, Iyer SS, et al. Akt-mTORC1 Signaling Regulates Acly to Integrate Metabolic Input to Control of Macrophage Activation. *Elife* (2016) 5:e11612. doi: 10.7554/eLife.11612
23. Tan Z, Xie N, Cui H, Moellering DR, Abraham E, Thannickal VJ, et al. Pyruvate Dehydrogenase Kinase 1 Participates in Macrophage Polarization Via Regulating Glucose Metabolism. *J Immunol* (2015) 194(12):6082–9. doi: 10.4049/jimmunol.1402469
24. Nomura M, Liu J, Rovira II, Gonzalez-Hurtado E, Lee J, Wolfgang MJ, et al. Fatty Acid Oxidation in Macrophage Polarization. *Nat Immunol* (2016) 17 (3):216–7. doi: 10.1038/ni.3366
25. Vats D, Mukundan L, Odegaard JI, Zhang L, Smith KL, Morel CR, et al. Oxidative Metabolism and PGC-1beta Attenuate Macrophage-Mediated Inflammation. *Cell Metab* (2006) 4(1):13–24. doi: 10.1016/j.cmet.2006.05.011
26. Odegaard JI, Ricardo-Gonzalez RR, Goforth MH, Morel CR, Subramanian V, Mukundan L, et al. Macrophage-Specific PPARgamma Controls Alternative Activation and Improves Insulin Resistance. *Nature* (2007) 447(7148):1116–20. doi: 10.1038/nature05894
27. Annunziato F, Romagnani C, Romagnani S. The 3 Major Types of Innate and Adaptive Cell-Mediated Effector Immunity. *J Allergy Clin Immunol* (2015) 135(3):626–35. doi: 10.1016/j.jaci.2014.11.001
28. Gieseck RL, Wilson MS, Wynn TA. Type 2 Immunity in Tissue Repair and Fibrosis. *Nat Rev Immunol* (2018) 18(1):62–76. doi: 10.1038/nri.2017.90
29. Wang R, Dillon CP, Shi LZ, Milasta S, Carter R, Finkelstein D, et al. The Transcription Factor Myc Controls Metabolic Reprogramming Upon T Lymphocyte Activation. *Immunity* (2011) 35(6):871–82. doi: 10.1016/j.immuni.2011.09.021
30. Chang CH, Curtis JD, Maggi LB, Jr., Faubert B, Villarino AV, O'Sullivan D, et al. Posttranscriptional Control of T Cell Effector Function by Aerobic Glycolysis. *Cell* (2013) 153(6):1239–51. doi: 10.1016/j.cell.2013.05.016
31. Akkaya B, Roesler AS, Miozzo P, Theall BP, Al Souz J, Smelkinson MG, et al. Increased Mitochondrial Biogenesis and Reactive Oxygen Species Production Accompany Prolonged Cd4(+) T Cell Activation. *J Immunol* (2018) 201(11):3294–306. doi: 10.4049/jimmunol.1800753
32. Murphy MP, Siegel RM. Mitochondrial ROS Fire Up T Cell Activation. *Immunity* (2013) 38(2):201–2. doi: 10.1016/j.immuni.2013.02.005
33. Dang EV, Barbi J, Yang HY, Jinasena D, Yu H, Zheng Y, et al. Control of T (H)17/T(reg) Balance by Hypoxia-Inducible Factor 1. *Cell* (2011) 146 (5):772–84. doi: 10.1016/j.cell.2011.07.033
34. Blagih J, Coulombe F, Vincent EE, Dupuy F, Galicia-Vazquez G, Yurchenko E, et al. The Energy Sensor AMPK Regulates T Cell Metabolic Adaptation and Effector Responses In Vivo. *Immunity* (2015) 42(1):41–54. doi: 10.1016/j.immuni.2014.12.030
35. Peng M, Yin N, Chhangawala S, Xu K, Leslie CS, Li MO. Aerobic Glycolysis Promotes T Helper 1 Cell Differentiation Through an Epigenetic Mechanism. *Science* (2016) 354(6311):481–4. doi: 10.1126/science.aaf6284
36. Angiari S, Runtsch MC, Sutton CE, Palsson-McDermott EM, Kelly B, Rana N, et al. Pharmacological Activation of Pyruvate Kinase M2 Inhibits Cd4(+) T Cell Pathogenicity and Suppresses Autoimmunity. *Cell Metab* (2020) 31 (2):391–405 e8. doi: 10.1016/j.cmet.2019.10.015
37. Ho PC, Bihuniak JD, Macintyre AN, Staron M, Liu X, Amezquita R, et al. Phosphoenolpyruvate Is a Metabolic Checkpoint of Anti-Tumor T Cell Responses. *Cell* (2015) 162(6):1217–28. doi: 10.1016/j.cell.2015.08.012
38. Kempkes RWM, Joosten I, Koenen H, He X. Metabolic Pathways Involved in Regulatory T Cell Functionality. *Front Immunol* (2019) 10:2839. doi: 10.3389/fimmu.2019.02839
39. Oleinika K, Nibbs RJ, Graham GJ, Fraser AR. Suppression, Subversion and Escape: The Role of Regulatory T Cells in Cancer Progression. *Clin Exp Immunol* (2013) 171(1):36–45. doi: 10.1111/j.1365-2249.2012.04657.x
40. Herberman RB, Nunn ME, Holden HT, Lavrin DH. Natural Cytotoxic Reactivity of Mouse Lymphoid Cells Against Syngeneic and Allogeneic

Tumors. II. Characterization of Effector Cells. *Int J Cancer* (1975) 16(2):230–9. doi: 10.1002/ijc.2910160205
41. Long EO, Kim HS, Liu D, Peterson ME, Rajagopalan S. Controlling Natural Killer Cell Responses: Integration of Signals for Activation and Inhibition. *Annu Rev Immunol* (2013) 31:227–58. doi: 10.1146/annurev-immunol-020711-075005
42. Caligiuri MA. Human Natural Killer Cells. *Blood* (2008) 112(3):461–9. doi: 10.1182/blood-2007-09-077438
43. Keppel MP, Saucier N, Mah AY, Vogel TP, Cooper MA. Activation-Specific Metabolic Requirements for NK Cell IFN-gamma Production. *J Immunol* (2015) 194(4):1954–62. doi: 10.4049/jimmunol.1402099
44. O'Brien KL, Finlay DK. Immunometabolism and Natural Killer Cell Responses. *Nat Rev Immunol* (2019) 19(5):282–90. doi: 10.1038/s41577-019-0139-2
45. Traba J, Waldmann TA, Anton OM. Analysis of Human Natural Killer Cell Metabolism. *J Vis Exp* (2020) (160). doi: 10.3791/61466
46. Assmann N, O'Brien KL, Donnelly RP, Dyck L, Zaiatz-Bittencourt V, Loftus RM, et al. Srebp-Controlled Glucose Metabolism is Essential for NK Cell Functional Responses. *Nat Immunol* (2017) 18(11):1197–206. doi: 10.1038/ni.3838
47. Miranda D, Jara C, Ibanez J, Ahumada V, Acuna-Castillo C, Martin A, et al. PGC-1alpha-Dependent Mitochondrial Adaptation Is Necessary to Sustain Il-2-Induced Activities in Human Nk Cells. *Mediators Inflammation* (2016) 2016:9605253. doi: 10.1155/2016/9605253
48. Loftus RM, Assmann N, Kedia-Mehta N, O'Brien KL, Garcia A, Gillespie C, et al. Amino Acid-Dependent cMyc Expression is Essential for NK Cell Metabolic and Functional Responses in Mice. *Nat Commun* (2018) 9 (1):2341. doi: 10.1038/s41467-018-04719-2
49. Zheng X, Qian Y, Fu B, Jiao D, Jiang Y, Chen P, et al. Mitochondrial Fragmentation Limits NK Cell-Based Tumor Immunosurveillance. *Nat Immunol* (2019) 20(12):1656–67. doi: 10.1038/s41590-019-0511-1
50. Michelet X, Dyck L, Hogan A, Loftus RM, Duquette D, Wei K, et al. Metabolic Reprogramming of Natural Killer Cells in Obesity Limits Antitumor Responses. *Nat Immunol* (2018) 19(12):1330–40. doi: 10.1038/s41590-018-0251-7
51. Mah AY, Rashidi A, Keppel MP, Saucier N, Moore EK, Alinger JB, et al. Glycolytic Requirement for NK Cell Cytotoxicity and Cytomegalovirus Control. *JCI Insight* (2017) 2(23):e95128. doi: 10.1172/jci.insight.95128
52. Donnelly RP, Loftus RM, Keating SE, Liou KT, Biron CA, Gardiner CM, et al. mTORC1-dependent Metabolic Reprogramming is a Prerequisite for NK Cell Effector Function. *J Immunol* (2014) 193(9):4477–84. doi: 10.4049/jimmunol.1401558
53. Marcais A, Cherfils-Vicini J, Viant C, Degouve S, Viel S, Fenis A, et al. The Metabolic Checkpoint Kinase mTOR is Essential for IL-15 Signaling During the Development and Activation of NK Cells. *Nat Immunol* (2014) 15 (8):749–57. doi: 10.1038/ni.2936
54. Wang F, Meng M, Mo B, Yang Y, Ji Y, Huang P, et al. Crosstalks Between mTORC1 and mTORC2 Variagate Cytokine Signaling to Control NK Maturation and Effector Function. *Nat Commun* (2018) 9(1):4874. doi: 10.1038/s41467-018-07277-9
55. Dong H, Adams NM, Xu Y, Cao J, Allan DSJ, Carlyle JR, et al. The IRE1 Endoplasmic Reticulum Stress Sensor Activates Natural Killer Cell Immunity in Part by Regulating C-Myc. *Nat Immunol* (2019) 20(7):865–78. doi: 10.1038/s41590-019-0388-z
56. Aghakhani S, Zerrouk N, Niarakis A. Metabolic Reprogramming of Fibroblasts as Therapeutic Target in Rheumatoid Arthritis and Cancer: Deciphering Key Mechanisms Using Computational Systems Biology Approaches. *Cancers (Basel)* (2020) 13(1):35. doi: 10.3390/cancers13010035
57. Becker LM, O'Connell JT, Vo AP, Cain MP, Tampe D, Bizarro L, et al. Epigenetic Reprogramming of Cancer-Associated Fibroblasts Deregulates Glucose Metabolism and Facilitates Progression of Breast Cancer. *Cell Rep* (2020) 31(9):107701. doi: 10.1016/j.celrep.2020.107701
58. Fiaschi T, Marini A, Giannoni E, Taddei ML, Gandellini P, De Donatis A, et al. Reciprocal Metabolic Reprogramming Through Lactate Shuttle Coordinately Influences Tumor-Stroma Interplay. *Cancer Res* (2012) 72 (19):5130–40. doi: 10.1158/0008-5472.CAN-12-1949
59. Francescone R, Barbosa Vendramini-Costa D, Franco-Barraza J, Wagner J, Muir A, Lau AN, et al. Netrin G1 Promotes Pancreatic Tumorigenesis Through Cancer-Associated Fibroblast-Driven Nutritional Support and Immunosuppression. *Cancer Discovery* (2021) 11(2):446–79. doi: 10.1158/2159-8290.CD-20-0775
60. Yang L, Achreja A, Yeung TL, Mangala LS, Jiang D, Han C, et al. Targeting Stromal Glutamine Synthetase in Tumors Disrupts Tumor Microenvironment-Regulated Cancer Cell Growth. *Cell Metab* (2016) 24 (5):685–700. doi: 10.1016/j.cmet.2016.10.011
61. Gong J, Lin Y, Zhang H, Liu C, Cheng Z, Yang X, et al. Reprogramming of Lipid Metabolism in Cancer-Associated Fibroblasts Potentiates Migration of Colorectal Cancer Cells. *Cell Death Dis* (2020) 11(4):267. doi: 10.1038/s41419-020-2434-z
62. Comito G, Giannoni E, Segura CP, Barcellos-de-Souza P, Raspollini MR, Baroni G, et al. Cancer-Associated Fibroblasts and M2-polarized Macrophages Synergize During Prostate Carcinoma Progression. *Oncogene* (2014) 33(19):2423–31. doi: 10.1038/onc.2013.191
63. Zhang R, Qi F, Zhao F, Li G, Shao S, Zhang X, et al. Cancer-Associated Fibroblasts Enhance Tumor-Associated Macrophages Enrichment and Suppress NK Cells Function in Colorectal Cancer. *Cell Death Dis* (2019) 10(4):273. doi: 10.1038/s41419-019-1435-2
64. Komohara Y, Takeya M. Cafs and TAMs: Maestros of the Tumour Microenvironment. *J Pathol* (2017) 241(3):313–5. doi: 10.1002/path.4824
65. Hirayama A, Kami K, Sugimoto M, Sugawara M, Toki N, Onozuka H, et al. Quantitative Metabolome Profiling of Colon and Stomach Cancer Microenvironment by Capillary Electrophoresis Time-of-Flight Mass Spectrometry. *Cancer Res* (2009) 69(11):4918–25. doi: 10.1158/0008-5472.CAN-08-4806
66. Chang CH, Qiu J, O'Sullivan D, Buck MD, Noguchi T, Curtis JD, et al. Metabolic Competition in the Tumor Microenvironment Is a Driver of Cancer Progression. *Cell* (2015) 162(6):1229–41. doi: 10.1016/j.cell.2015.08.016
67. Cham CM, Driessens G, O'Keefe JP, Gajewski TF. Glucose Deprivation Inhibits Multiple Key Gene Expression Events and Effector Functions in CD8+ T Cells. *Eur J Immunol* (2008) 38(9):2438–50. doi: 10.1002/eji.200838289
68. Carr EL, Kelman A, Wu GS, Gopaul R, Senkevitch E, Aghvanyan A, et al. Glutamine Uptake and Metabolism are Coordinately Regulated by ERK/MAPK During T Lymphocyte Activation. *J Immunol* (2010) 185(2):1037–44. doi: 10.4049/jimmunol.0903586
69. Keating SE, Zaiatz-Bittencourt V, Loftus RM, Keane C, Brennan K, Finlay DK, et al. Metabolic Reprogramming Supports IFN-gamma Production by CD56bright Nk Cells. *J Immunol* (2016) 196(6):2552–60. doi: 10.4049/jimmunol.1501783
70. Balsamo M, Manzini C, Pietra G, Raggi F, Blengio F, Mingari MC, et al. Hypoxia Downregulates the Expression of Activating Receptors Involved in NK-cell-mediated Target Cell Killing Without Affecting ADCC. *Eur J Immunol* (2013) 43(10):2756–64. doi: 10.1002/eji.201343448
71. Parodi M, Raggi F, Cangelosi D, Manzini C, Balsamo M, Blengio F, et al. Hypoxia Modifies the Transcriptome of Human Nk Cells, Modulates Their Immunoregulatory Profile, and Influences Nk Cell Subset Migration. *Front Immunol* (2018) 9:2358. doi: 10.3389/fimmu.2018.02358
72. Laoui D, Van Overmeire E, Di Conza G, Aldeni C, Keirsse J, Morias Y, et al. Tumor Hypoxia Does Not Drive Differentiation of Tumor-Associated Macrophages But Rather Fine-Tunes the M2-like Macrophage Population. *Cancer Res* (2014) 74(1):24–30. doi: 10.1158/0008-5472.CAN-13-1196
73. Wenes M, Shang M, Di Matteo M, Goveia J, Martin-Perez R, Serneels J, et al. Macrophage Metabolism Controls Tumor Blood Vessel Morphogenesis and Metastasis. *Cell Metab* (2016) 24(5):701–15. doi: 10.1016/j.cmet.2016.09.008
74. Brand A, Singer K, Koehl GE, Kolitzus M, Schoenhammer G, Thiel A, et al. Ldha-Associated Lactic Acid Production Blunts Tumor Immunosurveillance by T and NK Cells. *Cell Metab* (2016) 24(5):657–71. doi: 10.1016/j.cmet.2016.08.011
75. Fischer K, Hoffmann P, Voelkl S, Meidenbauer N, Ammer J, Edinger M, et al. Inhibitory Effect of Tumor Cell-Derived Lactic Acid on Human T Cells. *Blood* (2007) 109(9):3812–9. doi: 10.1182/blood-2006-07-035972
76. Harmon C, Robinson MW, Hand F, Almuaili D, Mentor K, Houlihan DD, et al. Lactate-Mediated Acidification of Tumor Microenvironment Induces Apoptosis of Liver-Resident Nk Cells in Colorectal Liver Metastasis. *Cancer Immunol Res* (2019) 7(2):335–46. doi: 10.1158/2326-6066.CIR-18-0481

77. Potzl J, Roser D, Bankel L, Homberg N, Geishauser A, Brenner CD, et al. Reversal of Tumor Acidosis by Systemic Buffering Reactivates NK Cells to Express IFN-gamma and Induces NK Cell-Dependent Lymphoma Control Without Other Immunotherapies. *Int J Cancer* (2017) 140(9):2125–33. doi: 10.1002/ijc.30646
78. Errea A, Cayet D, Marchetti P, Tang C, Kluza J, Offermanns S, et al. Lactate Inhibits the Pro-Inflammatory Response and Metabolic Reprogramming in Murine Macrophages in a GPR81-Independent Manner. *PloS One* (2016) 11 (11):e0163694. doi: 10.1371/journal.pone.0163694
79. Mu X, Shi W, Xu Y, Xu C, Zhao T, Geng B, et al. Tumor-Derived Lactate Induces M2 Macrophage Polarization Via the Activation of the ERK/STAT3 Signaling Pathway in Breast Cancer. *Cell Cycle* (2018) 17(4):428–38. doi: 10.1080/15384101.2018.1444305
80. Colegio OR, Chu NQ, Szabo AL, Chu T, Rhebergen AM, Jairam V, et al. Functional Polarization of Tumour-Associated Macrophages by Tumour-Derived Lactic Acid. *Nature* (2014) 513(7519):559–63. doi: 10.1038/nature13490
81. Munn DH, Mellor AL. IDO in the Tumor Microenvironment: Inflammation, Counter-Regulation, and Tolerance. *Trends Immunol* (2016) 37(3):193–207. doi: 10.1016/j.it.2016.01.002
82. Mondanelli G, Ugel S, Grohmann U, Bronte V. The Immune Regulation in Cancer by the Amino Acid Metabolizing Enzymes ARG and IDO. *Curr Opin Pharmacol* (2017) 35:30–9. doi: 10.1016/j.coph.2017.05.002
83. Della Chiesa M, Carlomagno S, Frumento G, Balsamo M, Cantoni C, Conte R, et al. The Tryptophan Catabolite L-kynurenine Inhibits the Surface Expression of NKp46- and NKG2D-activating Receptors and Regulates NK-cell Function. *Blood* (2006) 108(13):4118–25. doi: 10.1182/blood-2006-03-006700
84. Liu X, Shin N, Koblish HK, Yang G, Wang Q, Wang K, et al. Selective Inhibition of IDO1 Effectively Regulates Mediators of Antitumor Immunity. *Blood* (2010) 115(17):3520–30. doi: 10.1182/blood-2009-09-246124
85. Frumento G, Rotondo R, Tonetti M, Damonte G, Benatti U, Ferrara GB. Tryptophan-Derived Catabolites are Responsible for Inhibition of T and Natural Killer Cell Proliferation Induced by Indoleamine 2,3-Dioxygenase. *J Exp Med* (2002) 196(4):459–68. doi: 10.1084/jem.20020121
86. Opitz CA, Litzenburger UM, Sahm F, Ott M, Tritschler I, Trump S, et al. An Endogenous Tumour-Promoting Ligand of the Human Aryl Hydrocarbon Receptor. *Nature* (2011) 478(7368):197–203. doi: 10.1038/nature10491
87. Mezrich JD, Fechner JH, Zhang X, Johnson BP, Burlingham WJ, Bradfield CA. An Interaction Between Kynurenine and the Aryl Hydrocarbon Receptor can Generate Regulatory T Cells. *J Immunol* (2010) 185(6):3190–8. doi: 10.4049/jimmunol.0903670
88. Sharma MD, Hou DY, Liu Y, Koni PA, Metz R, Chandler P, et al. Indoleamine 2,3-Dioxygenase Controls Conversion of Foxp3+ Tregs to TH17-like Cells in Tumor-Draining Lymph Nodes. *Blood* (2009) 113 (24):6102–11. doi: 10.1182/blood-2008-12-195354
89. Liu H, Shen Z, Wang Z, Wang X, Zhang H, Qin J, et al. Increased Expression of IDO Associates With Poor Postoperative Clinical Outcome of Patients With Gastric Adenocarcinoma. *Sci Rep* (2016) 6:21319. doi: 10.1038/srep21319
90. Munn DH, Sharma MD, Baban B, Harding HP, Zhang Y, Ron D, et al. GCN2 Kinase in T Cells Mediates Proliferative Arrest and Anergy Induction in Response to Indoleamine 2,3-Dioxygenase. *Immunity* (2005) 22(5):633–42. doi: 10.1016/j.immuni.2005.03.013
91. Metz R, Rust S, Duhadaway JB, Mautino MR, Munn DH, Vahanian NN, et al. IDO Inhibits a Tryptophan Sufficiency Signal That Stimulates Mtor: A Novel IDO Effector Pathway Targeted by D-1-Methyl-Tryptophan. *Oncoimmunology* (2012) 1(9):1460–8. doi: 10.4161/onci.21716
92. Zaiatz-Bittencourt V, Finlay DK, Gardiner CM. Canonical TGF-beta Signaling Pathway Represses Human Nk Cell Metabolism. *J Immunol* (2018) 200(12):3934–41. doi: 10.4049/jimmunol.1701461
93. Viel S, Marcais A, Guimaraes FS, Loftus R, Rabilloud J, Grau M, et al. TGF-Beta Inhibits the Activation and Functions of NK Cells by Repressing the mTOR Pathway. *Sci Signal* (2016) 9(415):ra19. doi: 10.1126/scisignal.aad1884
94. Cong J, Wang X, Zheng X, Wang D, Fu B, Sun R, et al. Dysfunction of Natural Killer Cells by FBP1-Induced Inhibition of Glycolysis During Lung Cancer Progression. *Cell Metab* (2018) 28(2):243–255 e5. doi: 10.1016/j.cmet.2018.06.021
95. Moo-Young TA, Larson JW, Belt BA, Tan MC, Hawkins WG, Eberlein TJ, et al. Tumor-Derived TGF-beta Mediates Conversion of CD4+Foxp3+ Regulatory T Cells in a Murine Model of Pancreas Cancer. *J Immunother* (2009) 32(1):12–21. doi: 10.1097/CJI.0b013e318189f13c
96. Sato T, Terai M, Tamura Y, Alexeev V, Mastrangelo MJ, Selvan SR. Interleukin 10 in the Tumor Microenvironment: A Target for Anticancer Immunotherapy. *Immunol Res* (2011) 51(2-3):170–82. doi: 10.1007/s12026-011-8262-6
97. Ip WKE, Hoshi N, Shouval DS, Snapper S, Medzhitov R. Anti-Inflammatory Effect of IL-10 Mediated by Metabolic Reprogramming of Macrophages. *Science* (2017) 356(6337):513–9. doi: 10.1126/science.aal3535
98. Taga K, Tosato G. Il-10 Inhibits Human T Cell Proliferation and IL-2 Production. *J Immunol* (1992) 148(4):1143–8.
99. Wang S, Gao X, Shen G, Wang W, Li J, Zhao J, et al. Interleukin-10 Deficiency Impairs Regulatory T Cell-Derived Neuropilin-1 Functions and Promotes Th1 and Th17 Immunity. *Sci Rep* (2016) 6:24249. doi: 10.1038/srep24249
100. Peppa D, Micco L, Javaid A, Kennedy PT, Schurich A, Dunn C, et al. Blockade of Immunosuppressive Cytokines Restores NK Cell Antiviral Function in Chronic Hepatitis B Virus Infection. *PloS Pathog* (2010) 6(12): e1001227. doi: 10.1371/journal.ppat.1001227
101. Robert C. A Decade of Immune-Checkpoint Inhibitors in Cancer Therapy. *Nat Commun* (2020) 11(1):3801. doi: 10.1038/s41467-020-17670-y
102. Rosenberg SA, Restifo NP, Yang JC, Morgan RA, Dudley ME. Adoptive Cell Transfer: A Clinical Path to Effective Cancer Immunotherapy. *Nat Rev Cancer* (2008) 8(4):299–308. doi: 10.1038/nrc2355
103. Tokarew N, Ogonek J, Endres S, von Bergwelt-Baildon M, Kobold S. Teaching an Old Dog New Tricks: Next-Generation CAR T Cells. *Br J Cancer* (2019) 120(1):26–37. doi: 10.1038/s41416-018-0325-1
104. Renner K, Bruss C, Schnell A, Koehl G, Becker HM, Fante M, et al. Restricting Glycolysis Preserves T Cell Effector Functions and Augments Checkpoint Therapy. *Cell Rep* (2019) 29(1):135–150 e9. doi: 10.1016/j.celrep.2019.08.068
105. Zhang YX, Zhao YY, Shen J, Sun X, Liu Y, Liu H, et al. Nanoenabled Modulation of Acidic Tumor Microenvironment Reverses Anergy of Infiltrating T Cells and Potentiates Anti-PD-1 Therapy. *Nano Lett* (2019) 19(5):2774–83. doi: 10.1021/acs.nanolett.8b04296
106. Triplett TA, Garrison KC, Marshall N, Donkor M, Blazeck J, Lamb C, et al. Reversal of Indoleamine 2,3-Dioxygenase-Mediated Cancer Immune Suppression by Systemic Kynurenine Depletion With a Therapeutic Enzyme. *Nat Biotechnol* (2018) 36(8):758–64. doi: 10.1038/nbt.4180
107. Hou DY, Muller AJ, Sharma MD, DuHadaway J, Banerjee T, Johnson M, et al. Inhibition of Indoleamine 2,3-Dioxygenase in Dendritic Cells by Stereoisomers of 1-Methyl-Tryptophan Correlates With Antitumor Responses. *Cancer Res* (2007) 67(2):792–801. doi: 10.1158/0008-5472.CAN-06-2925
108. Prendergast GC, Malachowski WP, DuHadaway JB, Muller AJ. Discovery of IDO1 Inhibitors: From Bench to Bedside. *Cancer Res* (2017) 77(24):6795–811. doi: 10.1158/0008-5472.CAN-17-2285
109. Leone RD, Zhao L, Englert JM, Sun IM, Oh MH, Sun IH, et al. Glutamine Blockade Induces Divergent Metabolic Programs to Overcome Tumor Immune Evasion. *Science* (2019) 366(6468):1013–21. doi: 10.1126/science.aav2588
110. van Hall T, Andre P, Horowitz A, Ruan DF, Borst L, Zerbib R, et al. Monalizumab: Inhibiting the Novel Immune Checkpoint NKG2A. *J Immunother Cancer* (2019) 7(1):263. doi: 10.1186/s40425-019-0761-3
111. Davis ZB, Felices M, Verneris MR, Miller JS. *Natural Killer Cell Adoptive Transfer Therapy: Exploiting the First Line of Defense Against Cancer*. *Cancer J* (2015) 21(6):486–91. doi: 10.1097/PPO.0000000000000156
112. Waldmann TA, Dubois S, Miljkovic MD, Conlon KC. Il-15 in the Combination Immunotherapy of Cancer. *Front Immunol* (2020) 11:868. doi: 10.3389/fimmu.2020.00868
113. Cichocki F, Valamehr B, Bjordahl R, Zhang B, Rezner B, Rogers P, et al. Gsk3 Inhibition Drives Maturation of NK Cells and Enhances Their Antitumor Activity. *Cancer Res* (2017) 77(20):5664–75. doi: 10.1158/0008-5472.CAN-17-0799
114. Parameswaran R, Ramakrishnan P, Moreton SA, Xia Z, Hou Y, Lee DA, et al. Repression of GSK3 Restores NK Cell Cytotoxicity in AML Patients. *Nat Commun* (2016) 7:11154. doi: 10.1038/ncomms11154
115. DeNardo DG, Ruffell B. Macrophages as Regulators of Tumour Immunity and Immunotherapy. *Nat Rev Immunol* (2019) 19(6):369–82. doi: 10.1038/s41577-019-0127-6

116. Palmieri EM, Menga A, Martin-Perez R, Quinto A, Riera-Domingo C, De Tullio G, et al. Pharmacologic or Genetic Targeting of Glutamine Synthetase Skews Macrophages Toward an M1-like Phenotype and Inhibits Tumor Metastasis. *Cell Rep* (2017) 20(7):1654–66. doi: 10.1016/j.celrep.2017.07.054
117. Gordon SR, Maute RL, Dulken BW, Hutter G, George BM, McCracken MN, et al. PD-1 Expression by Tumour-Associated Macrophages Inhibits Phagocytosis and Tumour Immunity. *Nature* (2017) 545(7655):495–9. doi: 10.1038/nature22396
118. Hartley GP, Chow L, Ammons DT, Wheat WH, Dow SW. Programmed Cell Death Ligand 1 (Pd-L1) Signaling Regulates Macrophage Proliferation and Activation. *Cancer Immunol Res* (2018) 6(10):1260–73. doi: 10.1158/2326-6066.CIR-17-0537
119. Ding L, Liang G, Yao Z, Zhang J, Liu R, Chen H, et al. Metformin Prevents Cancer Metastasis by Inhibiting M2-like Polarization of Tumor Associated Macrophages. *Oncotarget* (2015) 6(34):36441–55. doi: 10.18632/oncotarget.5541
120. Safdie FM, Dorff T, Quinn D, Fontana L, Wei M, Lee C, et al. Fasting and Cancer Treatment in Humans: A Case Series Report. *Aging (Albany NY)* (2009) 1(12):988–1007. doi: 10.18632/aging.100114
121. Raffaghello L, Lee C, Safdie FM, Wei M, Madia F, Bianchi G, et al. *Starvation-Dependent Differential Stress Resistance Protects Normal But Not Cancer Cells Against High-Dose Chemotherapy. Proc Natl Acad Sci USA* (2008) 105 (24):8215–20. doi: 10.1073/pnas.0708100105
122. Lee C, Safdie FM, Raffaghello L, Wei M, Madia F, Parrella E, et al. Reduced Levels of IGF-I Mediate Differential Protection of Normal and Cancer Cells in Response to Fasting and Improve Chemotherapeutic Index. *Cancer Res* (2010) 70(4):1564–72. doi: 10.1158/0008-5472.CAN-09-3228
123. Sun P, Wang H, He Z, Chen X, Wu Q, Chen W, et al. Fasting Inhibits Colorectal Cancer Growth by Reducing M2 Polarization of Tumor-Associated Macrophages. *Oncotarget* (2017) 8(43):74649–60. doi: 10.18632/oncotarget.20301
124. Ohta A. A Metabolic Immune Checkpoint: Adenosine in Tumor Micro environment. *Front Immunol* (2016) 7:109. doi: 10.3389/fimmu.2016.00109
125. Orillion A, Damayanti NP, Shen L, Adelaiye-Ogala R, Affronti H, Elbanna M, et al. Dietary Protein Restriction Reprograms Tumor-Associated Macrophages and Enhances Immunotherapy. *Clin Cancer Res* (2018) 24 (24):6383–95. doi: 10.1158/1078-0432.CCR-18-0980
126. Antunes F, Pereira GJ, Jasiulionis MG, Bincoletto C, Smaili SS. Nutritional Shortage Augments Cisplatin-Effects on Murine Melanoma Cells. *Chem Biol Interact* (2018) 281:89–97. doi: 10.1016/j.cbi.2017.12.027
127. Bianchi G, Martella R, Ravera S, Marini C, Capitanio S, Orengo A, et al. Fasting Induces anti-Warburg Effect That Increases Respiration But Reduces ATP-synthesis to Promote Apoptosis in Colon Cancer Models. *Oncotarget* (2015) 6(14):11806–19. doi: 10.18632/oncotarget.3688
128. Turbitt WJ, Demark-Wahnefried W, Peterson CM, Norian LA. Targeting Glucose Metabolism to Enhance Immunotherapy: Emerging Evidence on Intermittent Fasting and Calorie Restriction Mimetics. *Front Immunol* (2019) 10:1402. doi: 10.3389/fimmu.2019.01402
129. Pietrocola F, Pol J, Vacchelli E, Rao S, Enot DP, Baracco EE, et al. Caloric Restriction Mimetics Enhance Anticancer Immunosurveillance. *Cancer Cell* (2016) 30(1):147–60. doi: 10.1016/j.ccell.2016.05.016
130. Dyck L, Lynch L. Cancer, Obesity and Immunometabolism - Connecting the Dots. *Cancer Lett* (2018) 417:11–20. doi: 10.1016/j.canlet.2017.12.019
131. Michalek RD, Gerriets VA, Jacobs SR, Macintyre AN, MacIver NJ, Mason EF, et al. Cutting Edge: Distinct Glycolytic and Lipid Oxidative Metabolic Programs are Essential for Effector and Regulatory CD4+ T Cell Subsets. *J Immunol* (2011) 186(6):3299–303. doi: 10.4049/jimmunol.1003613
132. Aguilar EG, Murphy WJ. Obesity Induced T Cell Dysfunction and Implications for Cancer Immunotherapy. *Curr Opin Immunol* (2018) 51:181–6. doi: 10.1016/j.coi.2018.03.012
133. Manzo T, Prentice BM, Anderson KG, Raman A, Schalck A, Codreanu GS, et al. Accumulation of Long-Chain Fatty Acids in the Tumor Microenvironment Drives Dysfunction in Intrapancreatic CD8+ T Cells. *J Exp Med* (2020) 217(8):e20191920. doi: 10.1084/jem.20191920
134. Ringel AE, Drijvers JM, Baker GJ, Catozzi A, Garcia-Canaveras JC, Gassaway BM, et al. Obesity Shapes Metabolism in the Tumor Microenvironment to Suppress Anti-Tumor Immunity. *Cell* (2020) 183(7):1848–1866 e26. doi: 10.1016/j.cell.2020.11.009
135. Huang SC, Everts B, Ivanova Y, O'Sullivan D, Nascimento M, Smith AM, et al. Cell-Intrinsic Lysosomal Lipolysis is Essential for Alternative Activation of Macrophages. *Nat Immunol* (2014) 15(9):846–55. doi: 10.1038/ni.2956
136. Sanchez-Jimenez F, Perez-Perez A, de la Cruz-Merino L, Sanchez-Margalet V. Obesity and Breast Cancer: Role of Leptin. *Front Oncol* (2019) 9:596. doi: 10.3389/fonc.2019.00596
137. Cortellini A, Bersanelli M, Buti S, Cannita K, Santini D, Perrone F, et al. A Multicenter Study of Body Mass Index in Cancer Patients Treated With anti-PD-1/PD-L1 Immune Checkpoint Inhibitors: When Overweight Becomes Favorable. *J Immunother Cancer* (2019) 7(1):57. doi: 10.1186/s40425-019-0527-y
138. Kichenadasse G, Miners JO, Mangoni AA, Rowland A, Hopkins AM, Sorich MJ. Association Between Body Mass Index and Overall Survival With Immune Checkpoint Inhibitor Therapy for Advanced non-Small Cell Lung Cancer. *JAMA Oncol* (2020) 6(4):512–8. doi: 10.1001/jamaoncol.2019.5241
139. Markle JG, Fish EN. SeXX Matters in Immunity. *Trends Immunol* (2014) 35 (3):97–104. doi: 10.1016/j.it.2013.10.006
140. Gupta S, Nakabo S, Blanco LP, O'Neil LJ, Wigerblad G, Goel RR, et al. *Sex Differences in Neutrophil Biology Modulate Response to Type I Interferons and Immunometabolism. Proc Natl Acad Sci USA* (2020) 117(28):16481–91. doi: 10.1073/pnas.2003603117
141. Lecot P, Sarabi M, Pereira Abrantes M, Mussard J, Koenderman L, Caux C, et al. Neutrophil Heterogeneity in Cancer: From Biology to Therapies. *Front Immunol* (2019) 10:2155. doi: 10.3389/fimmu.2019.02155
142. Ye Y, Jing Y, Li L, Mills GB, Diao L, Liu H, et al. Sex-Associated Molecular Differences for Cancer Immunotherapy. *Nat Commun* (2020) 11(1):1779. doi: 10.1038/s41467-020-15679-x
143. Catic A. Cellular Metabolism and Aging. *Prog Mol Biol Transl Sci* (2018) 155:85–107. doi: 10.1016/bs.pmbts.2017.12.003
144. Covarrubias AJ, Perrone R, Grozio A, Verdin E. NAD(+) Metabolism and its Roles in Cellular Processes During Ageing. *Nat Rev Mol Cell Biol* (2021) 22 (2):119–41. doi: 10.1038/s41580-020-00313-x
145. Chung HY, Kim DH, Lee EK, Chung KW, Chung S, Lee B, et al. Redefining Chronic Inflammation in Aging and Age-Related Diseases: Proposal of the Senoinflammation Concept. *Aging Dis* (2019) 10(2):367–82. doi: 10.14336/AD.2018.0324
146. Sekido K, Tomihara K, Tachinami H, Heshiki W, Sakurai K, Moniruzzaman R, et al. Alterations in Composition of Immune Cells and Impairment of Anti-Tumor Immune Response in Aged Oral Cancer-Bearing Mice. *Oral Oncol* (2019) 99:104462. doi: 10.1016/j.oraloncology.2019.104462
147. Sharma S, Dominguez AL, Lustgarten J. High Accumulation of T Regulatory Cells Prevents the Activation of Immune Responses in Aged Animals. *J Immunol* (2006) 177(12):8348–55. doi: 10.4049/jimmunol.177.12.8348
148. Jackaman C, Radley-Crabb HG, Soffe Z, Shavlakadze T, Grounds MD, Nelson DJ. Targeting Macrophages Rescues Age-Related Immune Deficiencies in C57BL/6J Geriatric Mice. *Aging Cell* (2013) 12(3):345–57. doi: 10.1111/acel.12062
149. Drijvers JM, Sharpe AH, Haigis MC. The Effects of Age and Systemic Metabolism on Anti-Tumor T Cell Responses. *Elife* (2020) 9:e62420. doi: 10.7554/eLife.62420
150. Kanesvaran R, Cordoba R, Maggiore R. Immunotherapy in Older Adults With Advanced Cancers: Implications for Clinical Decision-Making and Future Research. *Am Soc Clin Oncol Educ Book* (2018) 38:400–14. doi: 10.1200/EDBK_201435

Conflict of Interest: The authors declare that the research was conducted in the absence of any commercial or financial relationships that could be construed as a potential conflict of interest.

frontiers | Frontiers in Immunology

TYPE Original Research
PUBLISHED 22 July 2022
DOI 10.3389/fimmu.2022.946468

OPEN ACCESS

EDITED BY
Antonio Curti,
University of Bologna, Italy

REVIEWED BY
Nan Wang,
First Affiliated Hospital of Zhengzhou University, China
Jinhui Liu,
Nanjing Medical University, China
Lingming Kong,
The First Affiliated Hospital of University of Science and Technology of China Anhui Provincial Hospital, China

*CORRESPONDENCE
Yongmei Yin
ymyin@njmu.edu.cn
Jinhai Tang
jhtang@njmu.edu.cn

†These authors have contributed equally to this work

SPECIALTY SECTION
This article was submitted to Cancer Immunity and Immunotherapy, a section of the journal Frontiers in Immunology

RECEIVED 17 May 2022
ACCEPTED 27 June 2022
PUBLISHED 22 July 2022

CITATION
Jiang M, Wu X, Bao S, Wang X, Qu F, Liu Q, Huang X, Li W, Tang J and Yin Y (2022) Immunometabolism characteristics and a potential prognostic risk model associated with TP53 mutations in breast cancer. *Front. Immunol.* 13:946468. doi: 10.3389/fimmu.2022.946468

Immunometabolism characteristics and a potential prognostic risk model associated with TP53 mutations in breast cancer

Mengping Jiang[1,2†], Xiangyan Wu[3†], Shengnan Bao[1,2†], Xi Wang[1,2], Fei Qu[1,2], Qian Liu[1,2], Xiang Huang[1,2], Wei Li[1,2], Jinhai Tang[4*] and Yongmei Yin[1,5*]

[1]Department of Oncology, The First Affiliated Hospital of Nanjing Medical University, Nanjing, China, [2]The First Clinical College of Nanjing Medical University, Nanjing, China, [3]School of Electro-mechanical Engineering, Guangdong University of Technology, Guangzhou, China, [4]Department of General Surgery, The First Affiliated Hospital of Nanjing Medical University, Nanjing, China, [5]Jiangsu Key Lab of Cancer Biomarkers, Prevention and Treatment, Collaborative Innovation Center for Personalized Cancer Medicine, Nanjing Medical University, Nanjing, China

TP53, a gene with high-frequency mutations, plays an important role in breast cancer (BC) development through metabolic regulation, but the relationship between TP53 mutation and metabolism in BC remains to be explored. Our study included 1,066 BC samples from The Cancer Genome Atlas (TCGA) database, 415 BC cases from the Gene Expression Omnibus (GEO) database, and two immunotherapy cohorts. We identified 92 metabolic genes associated with TP53 mutations by differential expression analysis between TP53 mutant and wild-type groups. Univariate Cox analysis was performed to evaluate the prognostic effects of 24 TP53 mutation-related metabolic genes. By unsupervised clustering and other bioinformatics methods, the survival differences and immunometabolism characteristics of the distinct clusters were illustrated. In a training set from TCGA cohort, we employed the least absolute shrinkage and selection operator (LASSO) regression method to construct a metabolic gene prognostic model associated with TP53 mutations, and the GEO cohort served as an external validation set. Based on bioinformatics, the connections between risk score and survival prognosis, tumor microenvironment (TME), immunotherapy response, metabolic activity, clinical characteristics, and gene characteristics were further analyzed. It is imperative to note that our model is a powerful and robust prognosis factor in comparison to other traditional clinical features and also has high accuracy and

clinical usefulness validated by receiver operating characteristic (ROC) and decision curve analysis (DCA). Our findings deepen our understanding of the immune and metabolic characteristics underlying the TP53 mutant metabolic gene profile in BC, laying a foundation for the exploration of potential therapies targeting metabolic pathways. In addition, our model has promising predictive value in the prognosis of BC.

KEYWORDS

TP53, prognostic model, immune heterogeneity, metabolic heterogeneity, breast cancer

Introduction

Breast cancer (BC) is the most common cancer that threatens women's health around the world (1). Thanks to the spread of early diagnosis based on advanced medical technology and comprehensive and precise treatment, the survival of early BC patients has greatly improved (2, 3). However, a certain number of BC patients relapse following therapy or develop metastatic cancer within a short period, with unsatisfactory treatment efficacy and only a 30% 5-year survival rate, which has become a clinical challenge nowadays (4). Several lines of evidence have shown that BC progression is associated with changes in cellular metabolism, and a high level of metabolic heterogeneity within breast tumors is one of the main causes of these changes (5–8). Over the past decades, burgeoning studies have focused on the metabolic heterogeneity of BC, due to its tumor-promoting function and important impact on prognosis and therapeutic response, and attempted to overcome it to develop novel approaches, including genomic profiling, the development of biomarkers, and targeted metabolic therapies (9, 10). Nevertheless, there are few types of research on the detailed elaboration of the association between metabolic phenotypes and BC prognosis.

TP53 (P53) gene, widely regarded as a tumor suppressor gene, is the most frequently mutated gene in cancer (11). Protein p53 encoded by human gene *TP53* has diverse biological functions, primarily acting as a transcription factor to initiate gene transcription and participate in cell cycle arrest, metabolism, DNA repair, cell senescence, apoptosis, and ferroptosis (12, 13). The majority of TP53 mutations in human cancer are missense mutations in its DNA-binding domain that generate mutant p53 protein, thus affecting its transcriptional ability and abnormal downstream signaling pathway (14). Numerous studies have revealed that mutant p53 can lose their tumor-suppressive function and obtain dominant–negative activities that are independent of wild –type p53, which may confer them oncogenic functions to participate in cancer development (15, 16). Although the clinical relevance of TP53 mutation status in BC has been recently debated, it is also worth noting that TP53 mutations are linked with worse survival in BC, supported by credible results from several large samples of clinical data (17–19). Therefore, more efforts to further discover the roles of TP53 in BC progression are warranted.

As observed in multiple studies, mutant p53 may exert its oncogenic functions primarily by regulating cancer metabolism (20, 21). Thus, we speculate that the prognosis of BC patients with TP53 mutations may be related to cancer metabolism regulation mediated by mutant p53. In our research, a comprehensive analysis of TP53 gene status in BC was conducted to reveal the relationship between TP53 mutations and metabolic phenotypes. Furthermore, a TP53-related metabolic gene profile containing 24 metabolic genes was identified and characterized by a high degree of metabolic and immune microenvironmental heterogeneity according to differential gene expression analysis in patients with TP53 mutations and TP53 wild type. Importantly, we developed a prognostic risk score model based on TP53-associated metabolic gene profiles that could contribute to risk stratification in BC patients and guidance of clinical decision making. The validation of The Cancer Genome Atlas (TCGA) and Gene Expression Omnibus (GEO) data proves the excellent predictive value of this model for BC prognosis.

Materials and methods

Sources of breast cancer datasets and preprocessing

The RNA sequencing data (HTSeq-Counts) and copy number variation (CNV) data of BC were retrieved from TCGA website (https://portal.gdc.cancer.gov/) and the University of California, Santa Cruz (UCSC) Xena website,

respectively. In addition, Breast Invasive Carcinoma TCGA PanCancer data of 1,084 samples containing somatic mutation data, especially *TP53* gene condition, and the matched clinical information were downloaded from cBio Cancer Genomics Portal (http://cbioportal.org/), which collected a large number of comprehensive multidimensional cancer genome databases (22, 23). Patients without survival data were removed from further analysis. To facilitate comparability among samples, HTSeq-Counts data were normalized to transcripts per kilobase million (TPM) values and transformed to log2TPM for the following analysis (24).

For microarray data from the GEO database (https://www.ncbi.nlm.nih.gov/geo/), we downloaded GSE20685 (n = 327) and GSE20711 (n = 90) datasets with the matrix files of the gene expression profile and full clinical information based on the same platform GPL570 and developed a GEO cohort of 415 BC cases. Gene expression data of the GEO cohort were log2-transformed. Batch effects from non-biological technical biases were corrected by using the "ComBat" algorithm of the "SVA" package.

To validate the ability of our model to predict response to anti-PD-1/L1 therapy, we adopted two immunotherapeutic cohorts after a series of searches: IMvigor210 cohort (advanced urothelial cancer treated with atezolizumab) (25) and GSE78220 (metastatic melanoma with the intervention of pembrolizumab (26). The count data of IMvigor210 and microarray data of GSE78220 were converted to log2TPM and log2-transformed as described above, respectively.

Generally, the average expression value of genes was used in the present study if gene duplication was detected. Data used in this study are publicly available from TCGA and GEO databases.

Gene set variation analysis

We performed gene set variation analysis (GSVA) enrichment analysis among different groups or patterns to reveal metabolic heterogeneity in BC by the "GSVA" R packages, as visualized in the heatmap (27). The file of "c2.cp.kegg.v7.4.symbols" was obtained from the MSigDB database for GSVA. We screened for statistically significant pathways between different clusters depending on the adjusted $p < 0.05$.

Estimation of tumor microenvironment cell infiltration

To describe meaningful variations among distinct groups or clusters in tumor microenvironment (TME) cell infiltration, a single-sample gene set enrichment analysis (ssGSEA) algorithm was employed to quantify the relative abundance of 28 subpopulations of tumor-infiltrating lymphocytes (TILs) in the BC TME for differential analysis. The natural killer T cells, activated CD8+ T cells, activated CD4+ T cells, activated dendritic cells, macrophages, and other representative human immune cell subtypes are included in this study (28, 29).

Differentially expressed genes associated with TP53 condition

We classified 1,003 BC patients with gene expression data and TP53 mutation information from TCGA cohort into TP53 wild-type (n = 659) and TP53 mutant (n = 344) groups. The "edgeR" package was conducted on the real count data of BC samples to identify differentially expressed genes (DEGs) between the two groups in BC ($|logFC|>1$ and adjusted $p < 0.05$). The results were visualized in volcano plots and heatmap.

Metabolic gene source and functional analysis

With the use of the Kyoto Encyclopedia of Genes and Genomes (KEGG) metabolic pathway-related gene sets on the KEGG website (https://www.kegg.jp/), a total of 3,067 metabolic genes were extracted from 86 KEGG metabolic pathways and collected (Supplementary Table 1) (30). The intersection of the DEGs and metabolic genes were selected as metabolism-related genes (MRGs) associated with the TP53 condition for subsequent analysis. By using the "clusterProfiler" R package, the analysis of KEGG pathways was utilized to explore the significant pathways associated with TP53-related MRGs, highlighting the biological implications of the prognostic model (31). The notable pathways were shown in the bar plot using "ggplot2" R packages.

Consensus clustering

Consensus clustering was performed to identify distinct TP53-related metabolic patterns based on the expression of 24 TP53-associated MRGs by the k-means method. Notably, the optimal cluster number of clusters depended on the consensus clustering algorithm by applying the "ConsensusClusterPlus" package. We carried out 1,000 repetitions to further verify the robustness of our classification (32).

Gene set enrichment analysis

Based on the gene set database of "c2.cp.kegg.v7.5.1.symbols," GSEA version 4.2.2 (33) was used to discover different underlying mechanisms of enrichment in the high- and low-risk groups, with a particular focus on MRG sets. In terms of key parameter

setting, "high risk versus low risk" was assigned the phenotypic label, and the number of random sample permutations was set at 1,000.

Development of the risk score model based on TP53-related metabolism-related genes

We selected a total of 1,039 BC cases with gene expression data and survival information from TCGA database as the training cohort and 415 BC patients from the GEO cohort as the testing cohort. Before subsequent analysis, the gene expression data of two cohorts were corrected by the "scale" method. In the training cohort, we performed the prognostic analysis for TP53-related MRGs with an application of the univariate Cox regression model. Those TP53-related MRGs with p-values <0.05 were regarded as significant in statistics and then enrolled into the least absolute shrinkage and selection operator (LASSO) regression analysis for the foundation of the prognostic risk score model.

$$Risk \quad Score = \sum_{i=1}^{n} KiXi$$

where n, Ki, and Xi represent the number of included genes, the coefficient index, and the gene expression, respectively. With median risk score as a cutoff point, the patients in the training cohort were stratified into low- and high-risk subgroups. We attempted to evaluate the predictive accuracy of the model *via* time receiver operating characteristic (ROC) analysis.

Statistical analysis

All statistical tests and drawings were conducted using R statistical software (version 4.1.2). Two-group comparisons were carried out using Student's t-test and Wilcoxon's test, and the Kruskal–Wallis tests for comparisons of three or more groups. The overall survival (OS) differences among diverse groups were analyzed by the Kaplan–Meier method, and the statistical significance of differences was identified using the log-rank test. Univariate Cox regression analysis was performed to assess the prognostic value of genes and visualized with forest plots by "Survival" R packages. The measure of the correlation between 24 metabolic genes was implemented using "psych" R packages. The waterfall plots for the mutation landscape of patients with or without TP53 mutations in TCGA cohort were generated *via* the function of the "maftools" R package. Univariate and multivariate Cox regression analyses were executed to assess whether the risk score in combination with clinical characteristics had independent prognostic power. A $p < 0.05$ was considered statistically significant.

Results

Functional changes associated with TP53 mutations in breast cancer

In TCGA cohort, TP53 mutation frequency was up to 35%, among which missense mutations accounted for the largest proportion, as shown in Figure 1A. Analysis of p53 protein mutation sites displayed the most mutation sites in the DNA-binding domain that initiated their principal functions, indicating that the functional changes of mutant p53 were affected by DNA-binding ability (Figure 1B). In our research, no remarkable variable in OS for BC patients was observed between the TP53 mutated and unmutated groups (log-rank $p > 0.05$, Supplementary Figure 1). To identify differences in the biological pathway activities of the two groups, we employed GSVA to determine that BC cases with TP53 mutation exhibit enrichment of energy metabolism (galactose metabolism, and pentose phosphate pathway), amino acid metabolism (methionine and cysteine), and immunologic function (natural killer cell-mediated cytotoxicity), as compared to those without TP53 mutation (Figure 1D, Supplementary Table 2). In addition, we found a high degree of immune cell infiltration in the TP53 mutation group by ssGSEA (Figure 1C). In brief, our results confirmed that TP53 mutations led to changes in metabolic and immune characteristics in BC, which may be biological hallmarks of malignancy.

The identification of metabolism-related differentially expressed genes based on TP53 status

DEG analysis was performed between the TP53 mutant group and TP53 wild-type group using the "edgeR" package among a total of 1,003 samples with complete data on gene expression and TP53 status, and we finally identified 1,271 DEGs related to the TP53 condition (false discovery rate (FDR) < 0.05 and $|\log2\ FC| > 1.0$, Figures 2A, B). To further analyze the relationship between TP53 mutations and metabolism in BC, 3,067 MRGs assigned to metabolic pathways were obtained from the official website of the KEGG database, and then 92 TP53-related DEGs relevant to metabolic regulation were ultimately ascertained (Figure 2C). Among them, 47 genes were upregulated (FDR < 0.05 and log2 FC > 1.0), and 45 genes were downregulated (FDR < 0.05 and log2 FC < 1.0). In addition, KEGG pathway analysis revealed that 92 metabolism-related DEGs (MRDEGs) were mainly involved in 20 metabolic pathways, including amino acid metabolism (tryptophan, tyrosine, cysteine, methionine, glutathione, glutamate, serine, threonine, and arginine metabolism), glucose metabolism (glycolysis, gluconeogenesis, galactose,

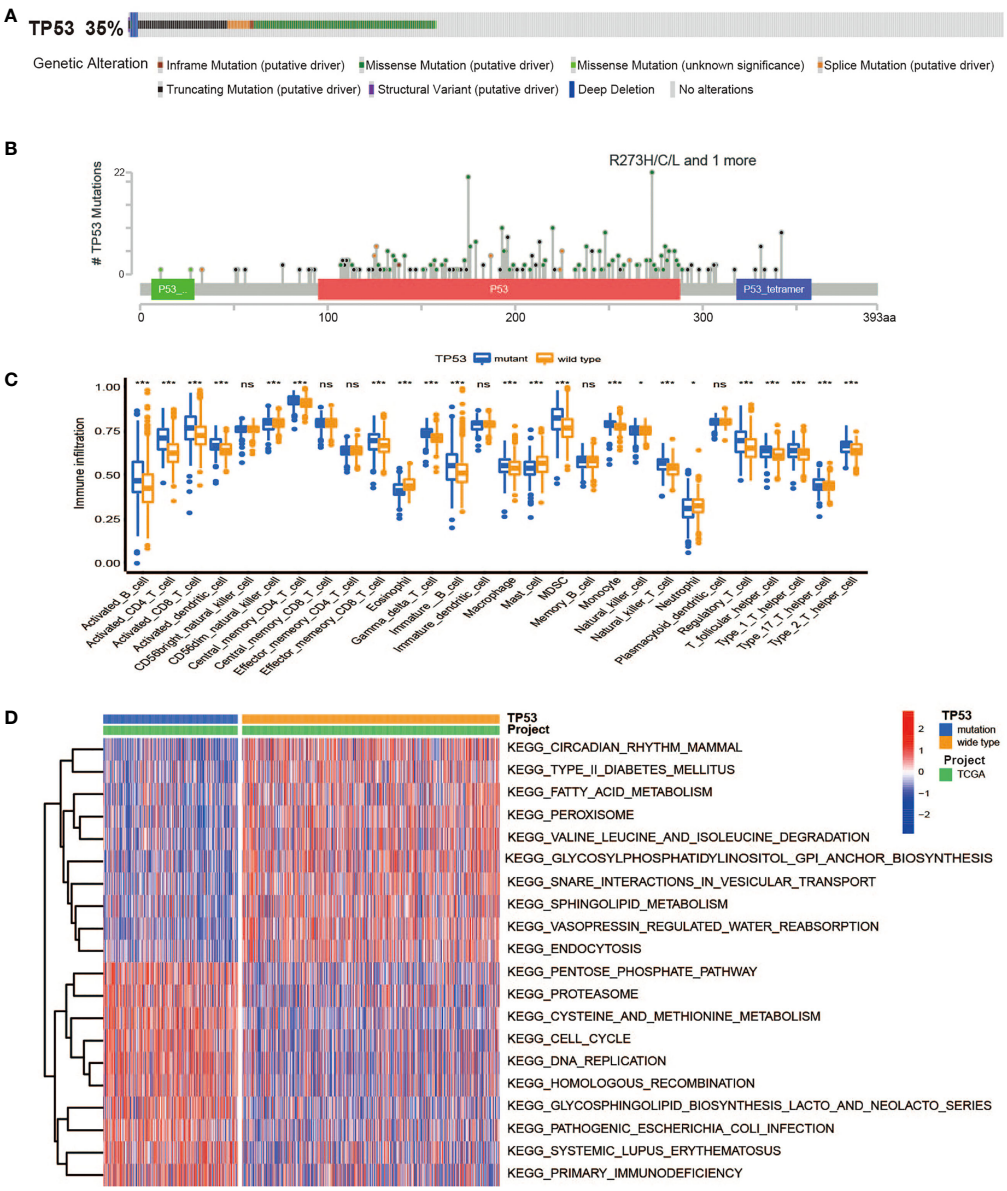

FIGURE 1
The overall characteristics of TP53 mutations in breast cancer. **(A)** Frequency and types of *TP53* gene alterations in TCGA Breast Invasive Carcinoma samples from cBioPortal. **(B)** The distribution of amino acids in TP53 protein in TCGA Breast Invasive Carcinoma samples from cBioPortal. **(C)** The abundance of each TME infiltrating cell between TP53 mutant and wild-type groups (ns, no significance; *p < 0.05; ***p < 0.001). **(D)** Heatmap for GSVA enrichment analysis showing the activation states of biological pathways between TP53 mutant and wild-type groups. TCGA, The Cancer Genome Atlas; TME, tumor microenvironment; GSVA, gene set variation analysis.

fructose, and mannose metabolism), and tricarboxylic acid (TCA) cycle and followed by oxidative phosphorylation, lipid metabolism (biosynthesis of unsaturated fatty acids), and drug metabolism (Figure 2D, Supplementary Table 3). Similar to those of other studies, these results demonstrated the pivotal role of TP53 status in metabolic regulation for BC patients.

The features of metabolic genes profile with TP53 mutations

First, we used univariate Cox analysis to estimate the survival prognostic value of 92 MRDEGs, and eventually, 24 prognostic genes were determined and regarded as the metabolic genes profile with TP53 mutation (Figure 2E). The network

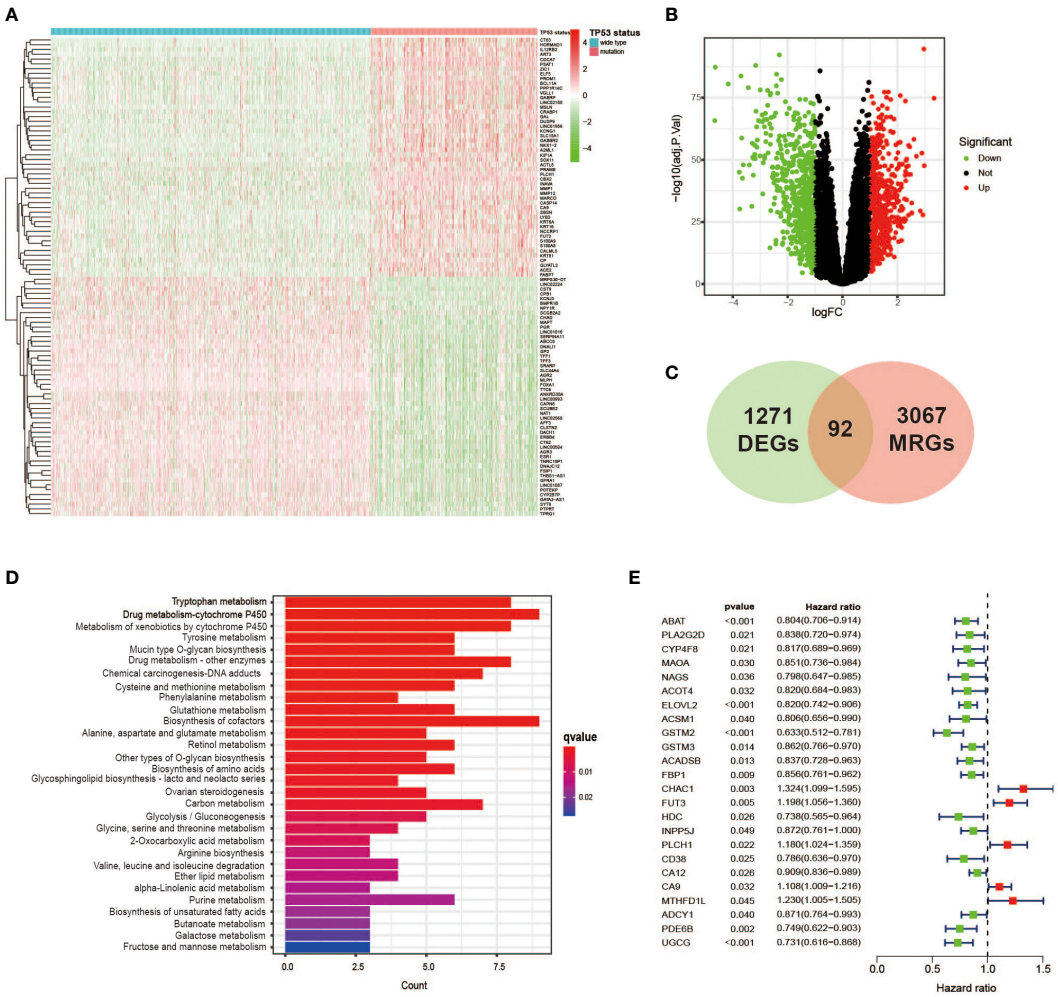

FIGURE 2
Identification of TP53 mutation-related metabolic gene profile. **(A)** Heatmap of the DEGs between TP53 mutant and wild-type groups in breast cancer cases. **(B)** A volcano plot exhibiting the identified DEGs including upregulated (red) and downregulated (green) genes. **(C)** Venn diagram summarizes the TP53-related metabolic genes intersected by 3,067 MRGs and 1,271 DEGs. **(D)** KEGG analysis of 92 metabolic genes related to TP53 showing the main significantly enriched pathways. **(E)** Overall survival in univariate Cox regression of TP53-related metabolic genes. DEGs, differentially expressed genes; MRGs, metabolism-related genes; KEGG, Kyoto Encyclopedia of Genes and Genomes.

diagram depicts the intricate but close correlations and their prognostic significance for BC patients among 24 prognostic genes (Figure 3A). Of them, we found 5 prognostic risk factors, as follows: CA9, CHAC1, FUT3, MTHFD1L, and PLCH1. As shown in the heatmap (Figure 3B), these 5 risk genes were highly expressed in the mutant TP53 group, and survival analysis indicated that BC cases with elevated expression of these genes were more likely to have a poor survival outcome (Figure 3C). Furthermore, Gene Ontology (GO) and KEGG enrichment analyses of the metabolic genes profile were conducted to discover enriched biological processes and activities. We found that they were mainly involved in the regulation of various substances' metabolism that promoted tumor growth, including amino acids, lipids, and nucleic acids (Figure 3D, Supplementary Table 4).

We further studied the genomic alterations of 24 key metabolic genes associated with TP53 mutations, thereby deepening our understanding of the metabolic gene profile based on TP53 status. Combined with the copy number information of 1,002 samples and corresponding TP53 status information, 343 patients in the TP53 mutant group and 659 patients in the TP53 wild-type group were used to analyze copy number gain and loss frequencies, respectively. The findings showed that the TP53 mutant group tended to have higher copy number gain or loss frequencies than the TP53 wild-type group (Figures 3E, F). Next, we also explore 24 metabolic genes

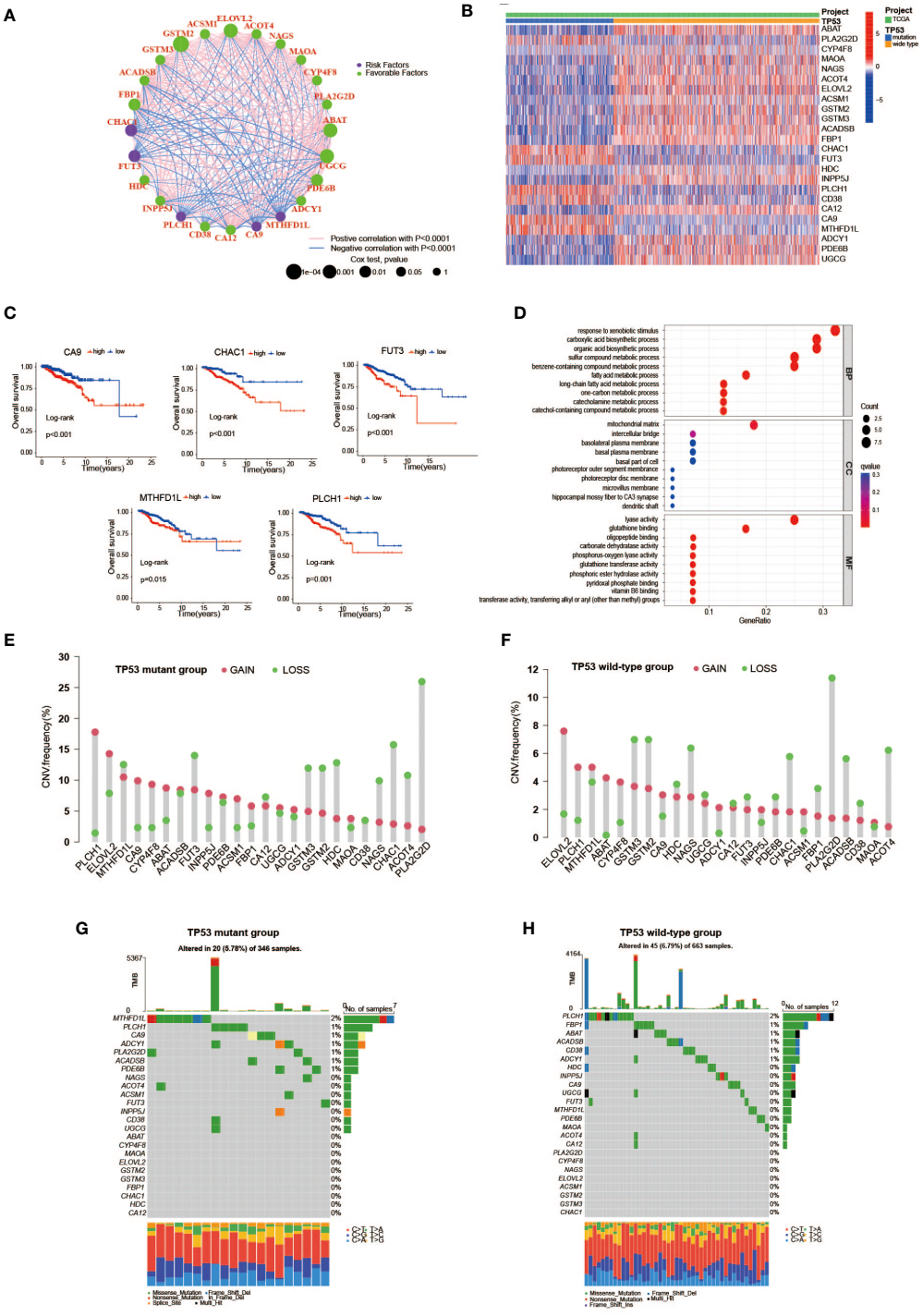

FIGURE 3
The features of TP53 mutation-related metabolic gene profile. **(A)** A network of the interactions among the 24 metabolic genes associated with TP53 mutations. **(B)** Heatmap of TP53 mutation-related metabolic gene expression profile between TP53 mutant and wild-type groups. Seven upregulated genes including *CA9*, *PLCH1*, *FUT3*, *CHAC1*, *CD38*, *MTHFD1L*, and *PLA2G2D* in the TP53 mutant group. **(C)** Kaplan–Meier survival analysis of breast cancer patients with high and low gene expression of 5 prognostic risk genes (*CA9*, *CHAC1*, *FUT3*, *MTHFD1L*, and *PLCH1*). **(D)** GO enrichment analysis of TP53 mutation-related metabolic gene profile in cellular component terms, biological process terms, and molecular function terms. **(E, F)** Lollipop charts depict the CNV frequency of TP53 mutation-related metabolic gene profiles in TP53 mutant **(E)** and wild-type groups **(F)**. **(G, H)** The waterfall plot of tumor somatic mutation in TP53 mutant **(G)** and wild-type groups **(H)**. GO, Gene Ontology; CNV, copy number variation.

mutation between two groups, with detailed TP53 mutation data. As displayed in Figures 3G, H, the mutation rate of the 24 genes did not differ apparently between the two groups, as well as the overall mutation rate.

The heterogeneity of TP53 mutation-related metabolic gene profile

To investigate the metabolic heterogeneity of 92 MRDEGs in BC, 24 prognostic genes were under intensive study. The unsupervised clustering method was utilized to classify patients with qualitatively different metabolic regulation patterns based on the expression of 24 prognostic genes. Considering the principle of high intragroup correlation and low intergroup correlation, we finally determined that the optimal cluster number was three (Figures 4A, B). We termed these clusters as Clusters A–C: 363 cases in Cluster A, 448 cases in Cluster B, and 228 cases in Cluster C. Furthermore, the Kaplan–Meier survival analysis exhibited striking differences in OS among the three clusters, notably showing a conspicuous survival disadvantage in Cluster A compared with the other two clusters (log-rank p = 0.002, Figure 4C). To explore the distinctions in biological processes of the three clusters, we subsequently performed a GSVA enrichment analysis. Obviously, from the perspective of metabolic regulation,

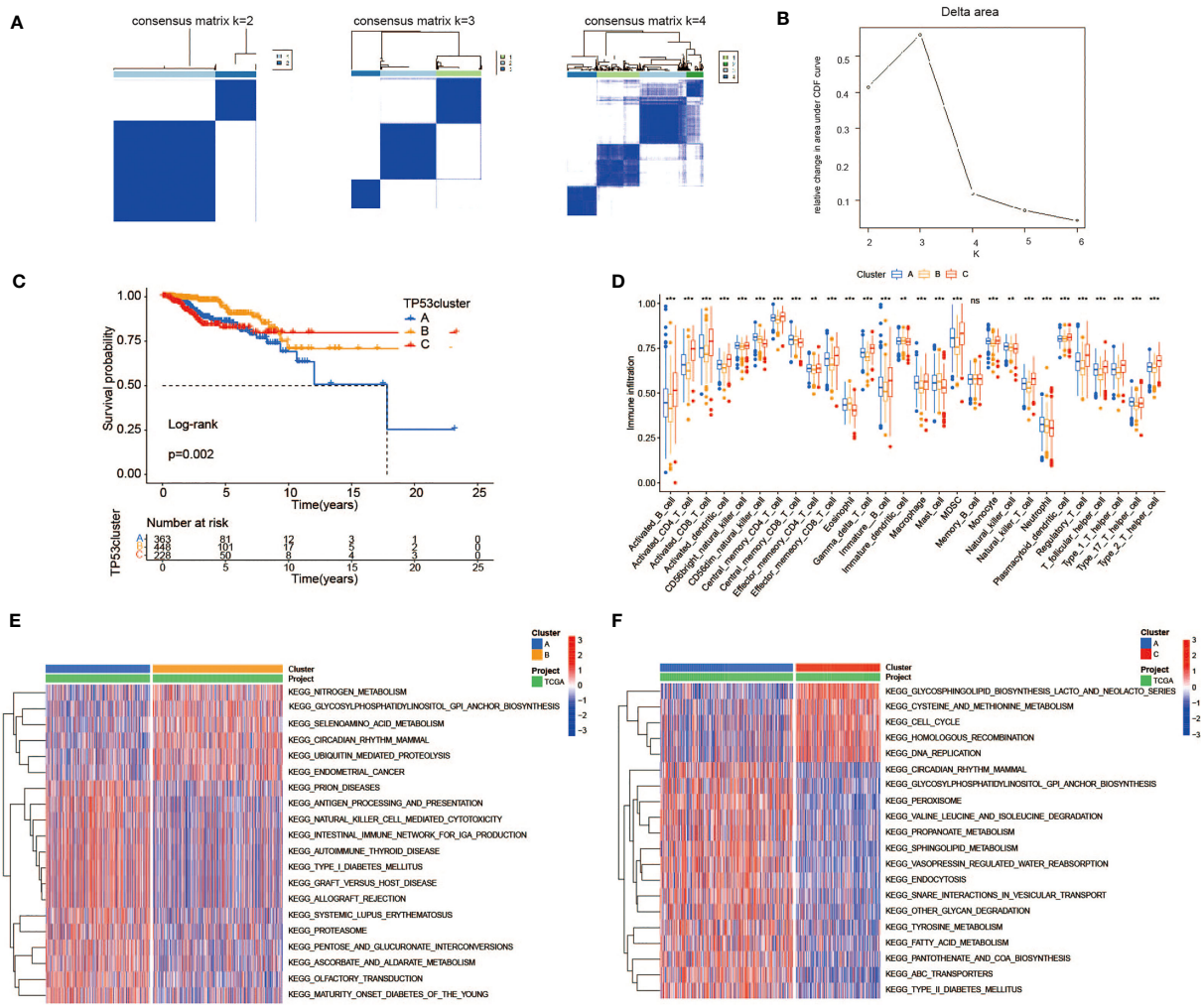

FIGURE 4
Heterogeneity of TP53 mutation-related metabolic gene profile. **(A)** Consensus clustering matrix of 1,039 TCGA samples for k = 2, k = 3, and k = 4. **(B)** Relative change in area under CDF curve according to various k values. **(C)** Kaplan–Meier survival analysis of three clusters in TCGA samples. **(D)** The abundance of each TME infiltrating cell among three clusters (ns, no significance; **p < 0.01; ***p < 0.001). **(E, F)** Heatmap for GSVA enrichment analysis showing the activation states of biological pathways between Clusters A and B **(E)** and between Clusters A and C **(F)**. TCGA, The Cancer Genome Atlas; CDF, cumulative distribution function; TME, tumor microenvironment; GSVA, gene set variation analysis.

Cluster A was mainly enriched in tyrosine metabolism and fatty acid metabolism pathways, Cluster B was closely related to nitrogen metabolism and selenoamino acid metabolism pathways, and Cluster C was intimately associated with pathways that regulate the metabolism of cysteine, methionine, and galactose (Figures 4E, F, Supplementary Table 5). Meanwhile, we sought to further distinguish the three clusters in TME cell infiltration *via* the ssGSEA method. It was worth noting that multiple subpopulations of TILs, presented in Figure 4D, were significantly different among the three clusters, revealing immune heterogeneity of TP53 mutation-associated metabolic gene profile in BC patients. Taken together, the discovery of metabolic and immune heterogeneity among the three clusters enabled us to speculate that there may be a complicated pattern of immune metabolic cross-talk regulation in BCs with TP53 mutations.

Construction of a prognostic risk score model based on metabolic genes (The cancer genome atlas)

To better quantify the metabolic features and prognosis of each individual, the expression data of 24 metabolic genes associated with TP53 mutations that had been proved above the significance in differentiating BC patients were used to establish a scoring model. Under the application of the LASSO regression model that effectively avoids overfitting conditions, 9

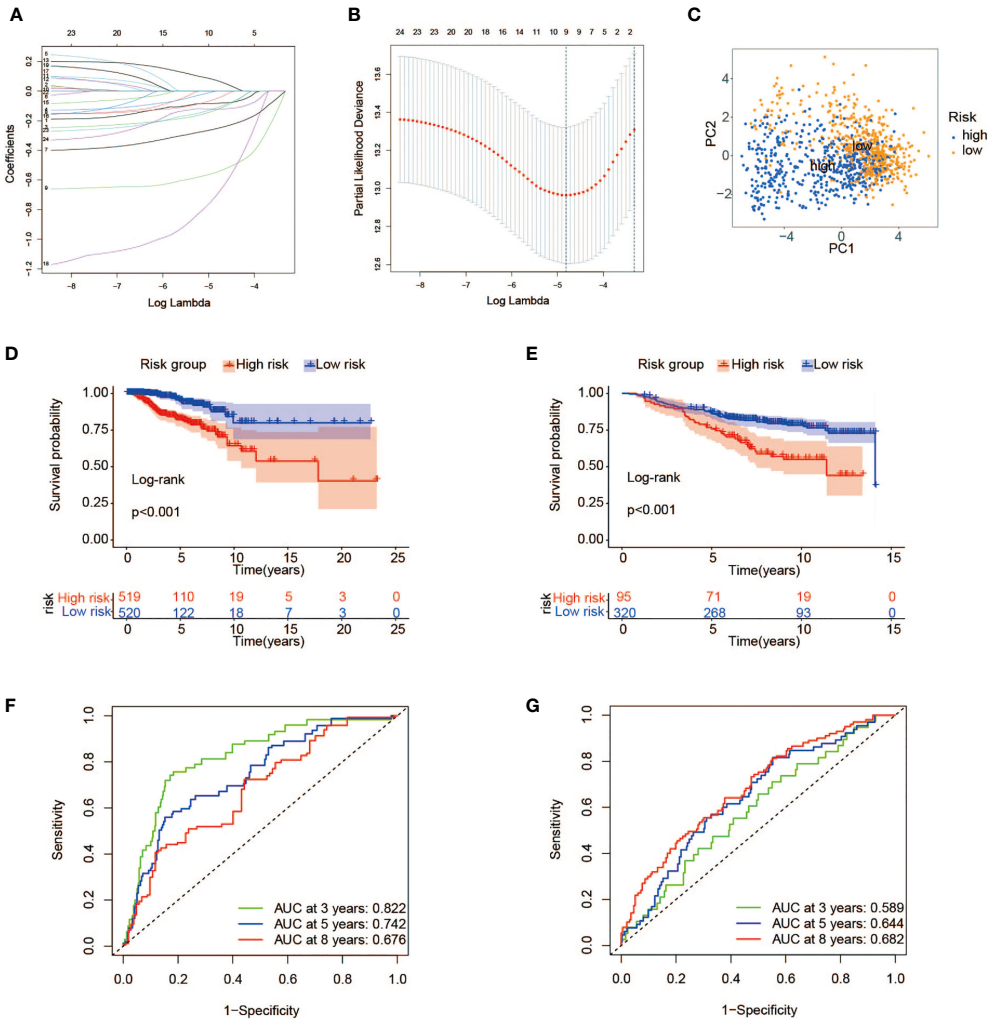

FIGURE 5
Construction of a prognostic risk model associated with TP53 mutations. **(A, B)** LASSO regression analysis of the 24 metabolic genes associated with TP53 mutations. **(C)** PCA of breast cancer patients with high- and low-risk scores in TCGA. **(D, E)** Kaplan–Meier survival analysis of high- and low-risk groups in TCGA **(D)** and GEO cohorts **(E)**. **(F, G)** ROC curves indicating the sensitivity and specificity of predicting 3-, 5-, and 8-year survival with the TP53 mutation-related signature in TCGA **(F)** and GEO cohorts **(G)**. LASSO, least absolute shrinkage and selection operator; PCA, principal component analysis; TCGA, The Cancer Genome Atlas; GEO, Gene Expression Omnibus; ROC, receiver operating characteristic.

of 24 metabolic genes were retained for the construction of risk scoring formulas with a minimum of λ (Figures 5A, B). The specific risk scoring formula is defined as a linear combination of included gene variables weighted by their respective Cox regression coefficients (Table 1). Next, we attempted to further probe the clinical implication of this scoring model. In the training cohort, 1,039 samples from TCGA database, with risk scores calculated using the risk scoring formula, were then divided into high- and low-risk groups according to the median score. The risk scatter plot described that BC patients with high-risk scores also have a high risk of death (Supplementary Figure 2A). We can see from Figure 5D that BC cases at low risk showed a remarkable survival advantage as compared with the high-risk group (log-rank $p < 0.001$). Furthermore, principal component analysis (PCA) results showed a high degree of differentiation between the high- and low-risk groups (Figure 5C). To verify the predictive power of this model, a time-dependent ROC analysis was performed to chart the corresponding ROC curves, and the area under the curve (AUC) was 0.822 for 3-year survival, 0.742 for 5-year survival, and 0.676 for 8-year survival (Figure 5F), exhibiting a good predictive accuracy. These findings pointed out that the risk score was expected to be a promising predictor for the prognosis of BC patients.

Validation of the prognostic risk score model

To certify the universal applicability of the scoring model, a testing cohort consisting of 415 BC samples from GSE20685 and GSE20711 in the GEO database has been analyzed. First of all, GEO gene expression data were integrated after removing the batch effect and finally standardized by the "scale" method. A total of 415 BC patients were separated into high-risk (n = 95) and low-risk (n = 320) groups with the same cutoff from the training set (Supplementary Figure 2B). As depicted in the Kaplan–Meier curve, a prominent difference in OS did exist between the two groups, and cases at high risk had a worse clinical outcome than those with low-risk scores (Figure 5E). Furthermore, ROC curve analysis confirmed the high predictive ability of our model, and the AUC values for 3, 5, and 8 years were 0.589, 0.644, and 0.682, respectively (Figure 5G).

TABLE 1 Gene variables and their respective coefficients in the risk scoring formula.

Gene	Coefficient
ABAT	−0.082288109
CYP4F8	−0.124018768
ELOVL2	−0.252333184
ACSM1	−0.048626551
GSTM2	−0.546619727
CHAC1	0.070470329
CD38	−0.696837951
PDE6B	−0.111403019
UGCG	−0.1220607

Metabolic characteristics of the high- and low-risk groups

To map metabolic alterations between the high- and low-risk groups, we employed a GSEA on 1,039 BC samples from both groups. In the high-risk group, we observed that 17 gene sets representing functions or pathways were significantly upregulated in the KEGG signatures ($p < 0.05$), among which the main metabolic pathways included glucose metabolism (galactose metabolism, fructose/mannose metabolism, glycolysis/gluconeogenesis, and starch/sucrose metabolism) as well as redox pathways (the pentose phosphate pathway and cysteine/methionine metabolism) (Figure 6A, Supplementary Table 6). Remarkably, some pathways have been proven to be associated with tumor development and poor prognosis (34–36). In contrast, in the low-risk group, 34 KEGG gene sets were significantly enriched ($p < 0.05$), with lipid metabolism as the dominant metabolic pathway, typically comprising arachidonic acid metabolism, glycerophospholipid metabolism, alpha-linolenic acid/linoleic acid metabolism, and JAK_STAT signaling pathway (Figure 6A). It may reflect that activation of lipid metabolism-related pathways plays a dominant role in tumorigenesis and progression in BC patients with low-risk scores. Finally, there is a bold idea that BC patients in the high-risk group may benefit from therapy targeting glucose MRGs, such as HK3 (37) and PFKP (38). Meanwhile, the novel therapy targeting genes associated with lipid metabolisms, such as HMGCR (39) and FASN (40), may be effective in those at low risk. Before that, further research is indispensable.

The immune landscape of the high- and low-risk groups

To describe the immune characteristics between low- and high-risk groups, we first calculated the immune infiltrate scores of 28 subpopulations of TILs across TCGA BC samples using the ssGSEA method, and then we performed a differential analysis. Compared with patients in the high-risk group, multiple subpopulations of TILs, such as CD8+ T cells, macrophages, mast cells, natural killer cells, and Type 1 T helper cells (Th1 cells), exhibited enrichment in those with low-risk scores (Figure 6B). It was revealed that the low-risk group had an abundance of immune cell infiltration, speculating that patients with low-risk scores may possess more antitumor immunity, such as that mediated by CD8+ T cell. Moreover, we further sought to investigate the correlation between risk scores and important immune checkpoint molecules

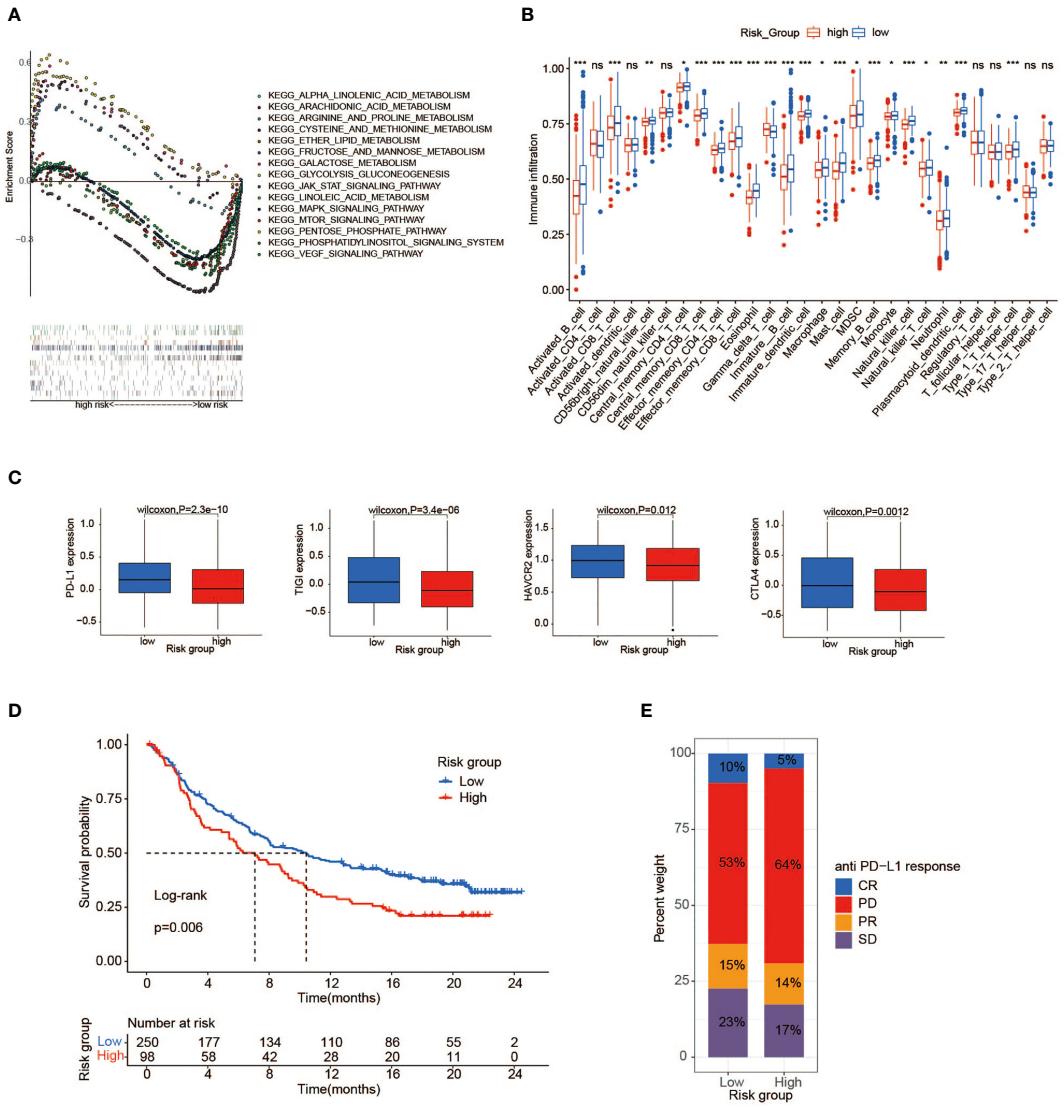

FIGURE 6
Immune and metabolic differences between high- and low-risk groups. **(A)** GSEA shows a significant enrichment of biological processes in BC patients with low-risk scores compared to those with high-risk scores. **(B)** The abundance of each TME infiltrating cell between high- and low-risk groups (ns, no significance; *p < 0.05; **p < 0.01; ***p < 0.001). **(C)** PD-L1, CTLA4, HAVCR2, and TIGIT gene expression differences between high- and low-risk groups. **(D)** Kaplan–Meier survival analysis of high-risk and low-risk groups in immune cohort IMvigor210. **(E)** The proportion of anti-PD-L1 response in the high- and low-risk groups of the immune cohort IMvigor210. GSEA, gene set enrichment analysis; BC, breast cancer; TME, tumor microenvironment.

in TCGA cohorts. As illustrated in Figure 6C, the expression of a series of potentially targetable immune checkpoints (PD-L1, CTLA4, HAVCR2, and TIGIT) all tended to be higher in the low-risk group than the high-risk group, implying that low-risk patients may easily benefit from immunotherapy and achieve an improved survival.

To advance this research, we made a meaningful comparison between risk score and 6 immune subtypes (C1–C6) identified by previous researchers based on 30 tumor types (41) (Supplementary Table 7). The features of the TME varied substantially across 6 immune subtypes, where C1 was characterized by an increased expression of angiogenic genes, abundant Th2 cell infiltrates, and an elevated proliferation rate, while C2 showed the highest M1/M2 macrophage polarization, a strong CD8 signal, and the greatest T-cell receptor (TCR) diversity. Next, particular immune features of the two groups were then further analyzed (Figures 7B–D). We observed that Th1 cells and leukocyte fractions were enriched in cases within the low-risk group, which had a high proportion of immune subtype C2, making a major involvement in cell-mediated

immunity possible (Figures 7A, B). In contrast, patients with high-risk scores, consisting mostly of immune subtype C1, showed a high proliferation rate, intratumoral heterogeneity (ITH), and aneuploidy score, which may account for the poor prognosis of cases with high-risk scores.

The risk score model in the role of anti-PD-1/L1 immunotherapy

We attempted to verify the value of the risk score model to predict the efficacy of anti-PD-1/L1 immunotherapy in other independent cancer cohorts (IMvigor210, GSE78220). The median risk score was selected as the cutoff value to stratify cases into low- and high-risk groups in both cohorts. It was shown that patients with low-risk scores are correlated to a satisfactory prognosis in the IMvigor210 cohort, which was consistent with the previous results (Figure 6D). In both cohorts, additional consequences indicated that most cases in the high-risk group displayed discouraging responses to immunotherapy, whereas the low-risk patients showed the opposite (Figure 6E, Supplementary Figure 3B). Although the exploration and analysis of the relationship between risk score and clinical efficacy did not show a marked difference, they still

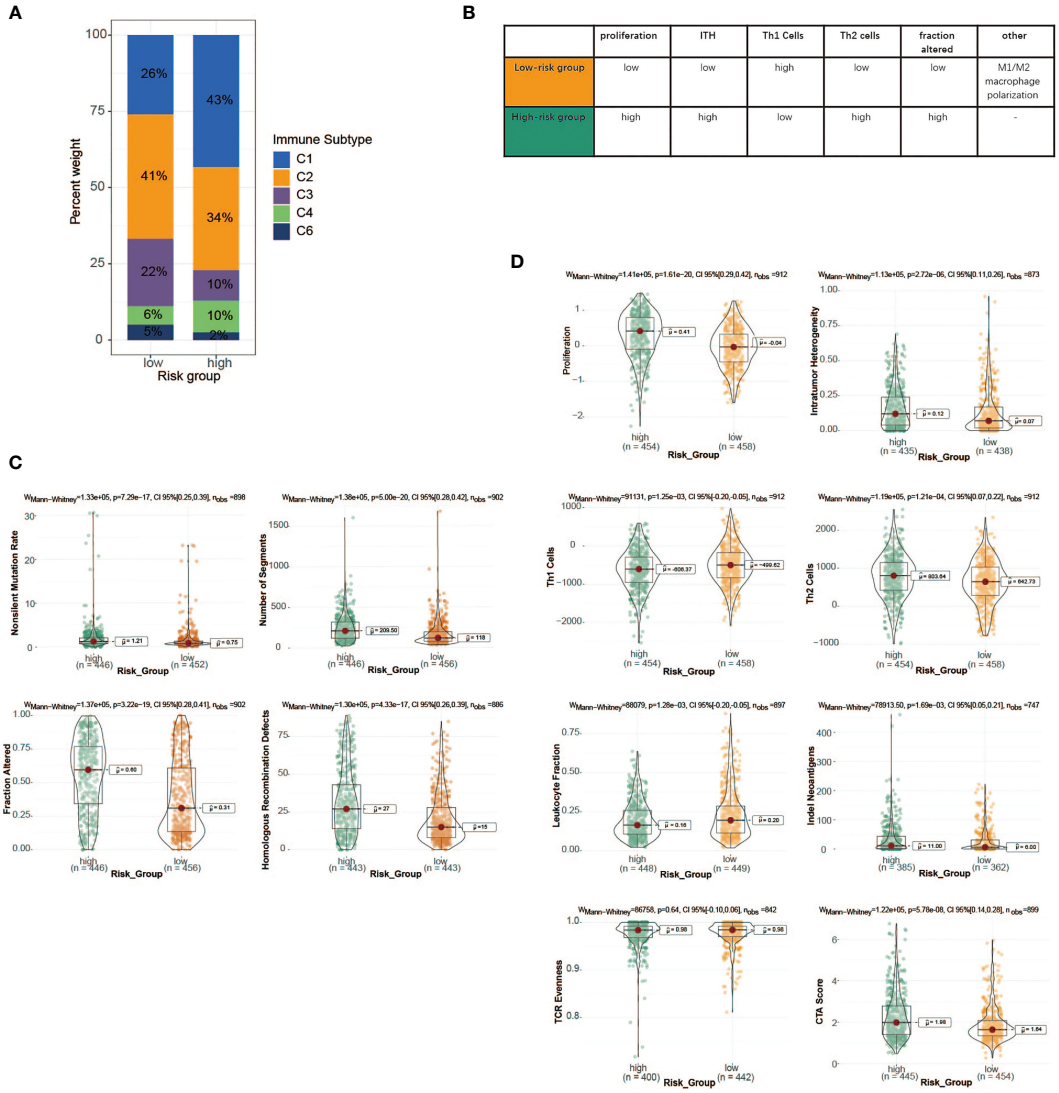

FIGURE 7
Immune characteristics of the high- and low-risk groups in TCGA cohort. **(A)** The proportion of distinct immune subtypes in the high- and low-risk groups. **(B)** Key characteristics of high- and low-risk groups. **(C)** DNA damage measures of high- and low-risk groups, including non-silent mutation rate, copy number burden scores (number of segments and fraction of genome alterations), and homologous recombination deficiency. **(D)** Values of key immune characteristics between high- and low-risk groups. TCGA, The Cancer Genome Atlas.

displayed a trend of poor responses in high-risk cases (Supplementary Figures 3C, E). Intriguingly, in comparison with the high-risk group, the elevated expression of the PD-L1 gene as a pivotal target for immunotherapy was observed in the low-risk group, possibly contributing to favorable responses to anti-PD-1/L1 therapy (Supplementary Figures 3D, F).

Independence evaluation of risk score model

A total of 934 BC samples with detailed clinical features were obtained from TCGA and summarized in Table 2. A univariate Cox regression model was performed to seek the prognostic connection between OS time for BC cases and several special characteristics, including age, clinical stage, T classification, N classification, molecular subtype, TP53 condition, and risk score.

TABLE 2 Baseline characteristics of breast cancer cases in TCGA cohort.

Characteristics	TCGA
Patients (n)	934
Mean follow-up time (months, range)	27.0 (0, 282.9)
Age (years)	
<65	647
≥65	287
Stage	
I–II	716
III–IV	218
AJCC pathologic T	
T1–2	797
T3–4	137
AJCC pathologic N	
N0	463
N1–3	471
AJCC pathologic M	
M0	794
M1	15
Mx	124
Risk group	
Low	472
High	462
TP53	
Wild type	604
Mutant	330
Subtype	
BRCA_Normal	34
BRCA_LumA	477
BRCA_LumB	186
BRCA_Her2	72
BRCA_Basal	165

TCGA, The Cancer Genome Atlas; AJCC, American Joint Committee on Cancer.

Among them, only 4 significant factors with a p-value <0.001 were closely related to OS and subsequently incorporated into the multivariate Cox analysis (Figures 8A, B). Collectively, the result in Figures 8C–E underlined the stronger role of risk score based on our model as an independent prognostic factor for BC patients.

To further evaluate the predictive sensitivity of the risk score in distinct stratified subgroups, the differences in OS between the high- and low-risk subgroups were compared by using the Kaplan–Meier survival analysis in TCGA cohort. In most subgroups, it was well demonstrated that BC cases with high-risk scores were linked to worse prognosis, especially in the <65 years, Luminal A, Luminal B, T3–4, N1–3, stage III–IV, and TP53 wild-type subgroups (Figure 8F).

The following analyses were also presented for the correlation between risk scores and various clinicopathological features (Supplementary Figure 4). As a result, patients in the TP53 mutant subgroup were indicative of a higher risk score in comparison to those without mutated TP53, which reflected poorer survival outcomes as well. In terms of molecular subtype, patients with basal-like subtype and her2-enriched subtype were close related to high-risk scores. Moreover, we found that several known risk factors, such as larger tumor size, lymph node metastasis, and advanced clinical stage, were accompanied by superior risk scores.

Discussion

Considering the high heterogeneity of BC, clinicians are confronted with great challenges in the improvement of the survival rate for BC patients who exhibit poor responses to treatment (11, 42). With the advances in medicine, multiple novel approaches have emerged as indispensable tools in patient classification, disease status monitoring, and personalized treatment regimens, including molecular biomarkers, prognosis, and diagnostic gene signatures (43, 44). Therefore, it is necessary to explore the promising genetic signatures to better predict the prognosis of BC patients and assist in making individualized treatment options.

Currently, many researchers have proved that the status of *TP53* gene is closely related to the prognosis of BC (45, 46), but it could not improve the prognostic accuracy in the absence of comprehensive bioinformatics and clinicopathological factors analysis. In this study, we are the first to identify a metabolic gene profile associated with TP53 mutations using a large cohort of TCGA BC patients and, further, reveal its underlying immunological and metabolic heterogeneity. Furthermore, a powerful TP53 mutation-related prognostic model was figured out *via* the LASSO regression methods and validated in two GEO datasets. Meanwhile, through various bioinformatics methods, we summarized that patients with different risk scores varied in the immune microenvironment, metabolic

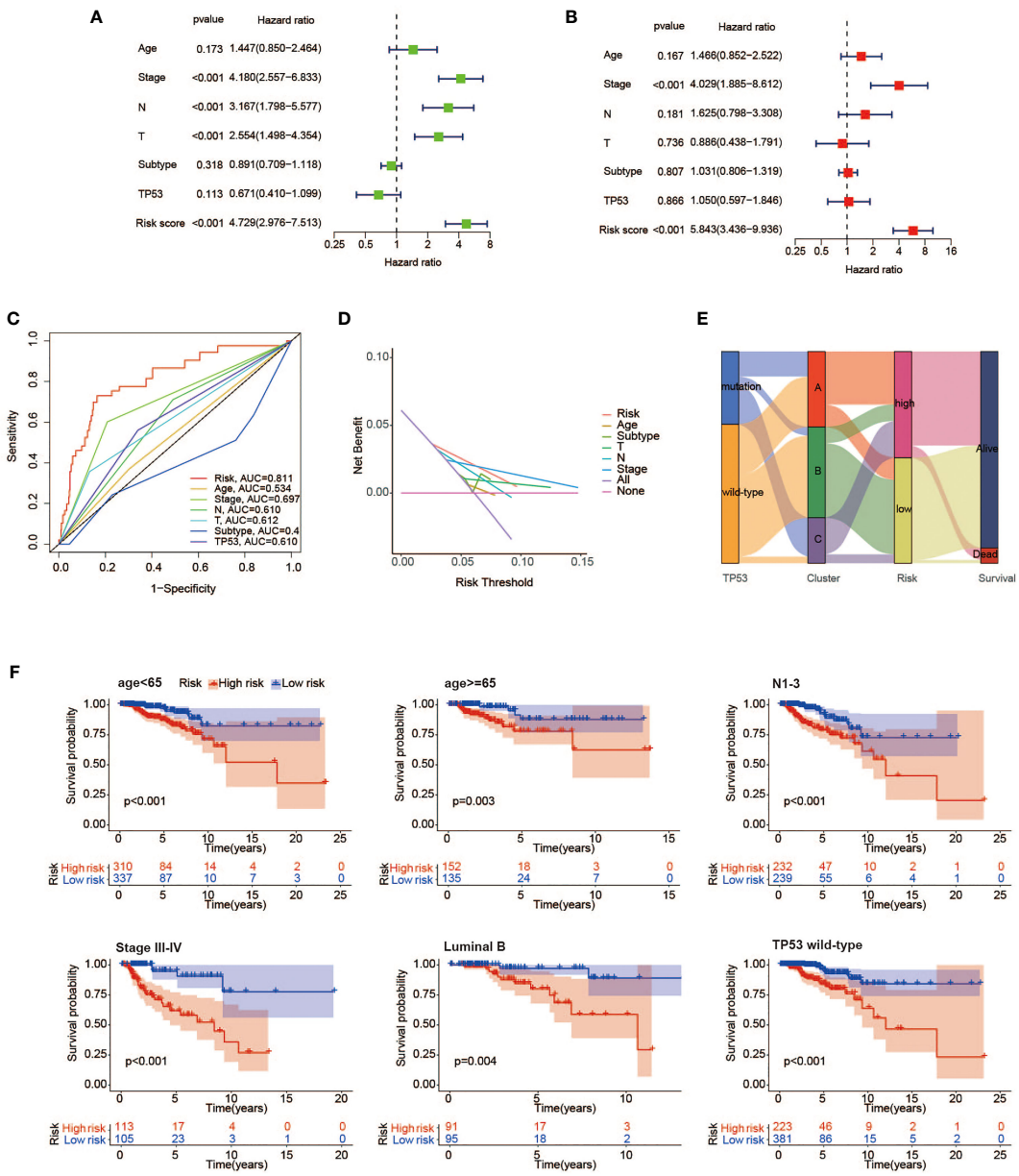

FIGURE 8
Independence evaluation of the prognostic risk model. Univariate **(A)** and multivariate **(B)** analyses of traditional clinical features and the prognostic risk model. **(C)** ROC curves indicating the sensitivity and specificity of predicting 3-year survival with traditional clinical features and the prognostic risk model in TCGA cohort. **(D)** Decision curves for traditional clinical features and the prognostic risk model to predict 3-year survival probability. **(E)** Alluvial diagram showing the changes of TP53 condition, molecular clusters, risk group, and survival status. **(F)** Kaplan–Meier survival analysis of high- and low-risk groups in the <65 years, Luminal B, N1–3, stage III–IV, TP53 mutant, and wild-type subgroups. ROC, receiver operating characteristic; TCGA, The Cancer Genome Atlas.

activities, and responses to immunotherapy, providing a guide for targeted metabolic therapy of BC. This is also a prognostic model that goes beyond traditional clinical features and a single gene to accurately identify those patients with poor survival and better guide clinical therapy.

Mutant TP53 has attracted much attention in tumorigenesis and development since its first description in 1989 (47). Clinically, patients with mutant TP53 have been associated with a discouraging prognosis in various cancers, but the results remain controversial (48). In a study of 859 BC patients, the researchers determined that patients with mutant TP53 had worse BC-specific and all-cause mortality than those with wild-type TP53, which is consistent with other studies (17–19). In our study, we finally illustrated no statistically significant

difference in survival between the TP53 mutant and wild-type groups from TCGA cohort of 1,003 BC patients. Currently, many researchers have proved that the status of *TP53* gene is closely related to the prognosis of BC (45, 46), but it could not improve prognostic accuracy in the absence of comprehensive bioinformatics and clinicopathological factors analysis. In this study, we are the first to identify a metabolic gene profile associated with TP53 mutations using a large cohort of TCGA BC patients and, further, reveal its underlying immunological and metabolic heterogeneity. Furthermore, a powerful TP53 mutation-related prognostic model was figured out *via* the LASSO regression methods and validated in two GEO datasets. Meanwhile, through various bioinformatics methods, we summarized that patients with different risk scores varied in the immune microenvironment, metabolic activities, and responses to immunotherapy, providing a guide for targeted metabolic therapy of BC. This is also a prognostic model that goes beyond traditional clinical features and a single gene to accurately identify those patients with poor survival and better guide clinical therapy. In this regard, it may be caused by differences in clinical characteristics or treatment options that affect prognostic determinations. Of note, a large study of the METABRIC dataset (n = 1,979) elucidated the clear relationship between TP53 mutation status and survival in different therapy regimens. Consequently, in patients treated with hormone replacement therapy (HRT) only, those without TP53 mutation had a survival advantage. Conversely, the TP53 mutant patients obtained a superior rate of pathologic complete response (pCR) when chemotherapy was only administrated (45, 49, 50). In brief, the profound impact of TP53 on the prognosis of BC is indisputable.

Accumulating evidence suggests that *TP53* gene is essential for cancer initiation and progression by reprogramming cancer cell metabolism in addition to p53-mediated classical regulatory mechanisms (51). In our research, we identified 92 metabolic genes related to TP53 mutation, and results of KEGG analysis showed that mutated TP53 principally participated in glycolysis/gluconeogenesis, tryptophan metabolism, glutathione metabolism, glycosphingolipid biosynthesis, and purine metabolism, which may promote tumor progression *via* meeting increased demands for energy, biomass, and nutrients. Some mechanistic research revealing detailed mutant p53-mediated metabolic regulatory pathways has been reported. A study in 2013 demonstrated that mutated p53 protein assisted GLUT1 transport to the plasma membrane and enhanced glycolysis and tumorigenesis *via* a RhoA/ROCK/GLUT1 signaling pathway (52). Additionally, it has been revealed that mutated p53 tended to bind with the AMP-activated protein kinase (AMPK) α subunit and then restrained its activation, resulting in increased lipid production and tumor growth in the head and neck cancer cells (53). Although there are more and more in-depth mechanistic studies mentioned above, which provide a theoretical basis for targeted metabolic therapy, metabolic flexibility that enables cancer cells to adapt to the microenvironmental perturbations and metabolic heterogeneity are regarded as critical barriers to targeting cancer metabolic profiles (54, 55). Our subsequent research results referring to TP53 mutation-related metabolic gene profiles showed that enrichment of metabolic pathways varied in three clusters, which embodied metabolic heterogeneity. Cluster A was enriched in fatty acid metabolism and tyrosine metabolism, but it had the worst prognosis among the three clusters. This can be explained by some standpoints in several studies that aberrantly activated fatty acid metabolism, including synthesis, lengthening, and desaturation can facilitate tumor proliferation (56, 57). However, our findings indicated that Cluster A was expected to benefit from targeted therapy of fatty acid metabolism.

Using TCGA cohort data as a training set, we constructed a prognostic risk scoring model based on 9 metabolic genes associated with TP53 to quantitatively score the risk of an individual BC patient, so as to improve individualized cancer treatment and monitoring. GEO data of 415 BC cases were used as a validation set, which well verified the good accuracy of our model. We then used the median risk score to classify patients into the high- and low-risk groups. It has been revealed that various metabolic mechanisms have an intricate relationship with the behavior of immune cells and antitumor immune response and are involved in the process of tumor genesis and development (58). Therefore, we sought to uncover the distinct immunological landscape and heterogeneity of metabolic profiles between the high- and low-risk groups. First, our results showed that compared with the high-risk prognosis group, higher abundance of most immune cells, whether immunosuppressive cells (such as Tregs, tumor-associated macrophages (TAMs), and myeloid-derived suppressor cells (MDSCs)) or immune effector cells, was observed in the low-risk prognosis group, highlighting the existence of a complex internal immune microenvironment. Further studies indicated that IFN-γ signaling was dominant in the low-risk group, with high M1/M2 macrophage polarization and strong CD8 signaling. Meanwhile, CD8+ T cell was accepted as a crucial determinant of favorable clinical prognosis in patients with BC (59). Of interest, our study found that cases in the low-risk prognosis group had elevated expression of PD-L1, CTLA4, HAVCR2, and TIGIT and were more sensitive to anti-PD1 treatment than those with high-risk scores. Taken together, these results suggest that good outcomes in the low-risk group may be associated with immune effector cell-dominated antitumor immunity and those patients may benefit from immunotherapy. For metabolic activities, significant enrichment of lipid-related metabolism was found in the low-risk group, with compelling evidence from other literature showing abnormally activated lipid metabolism in BC. Previous studies have demonstrated that JAK/STAT signaling pathway is closely related to BC stem cells and chemotherapy

resistance, mainly by inhibiting fatty acid β-oxidation (FAO) (60). Moreover, arachidonic acid is an important component of phospholipids in cell membranes, and its metabolism is critical for the migration of BC cells induced by oleic acid (61). At present, metabolic-targeting therapy strategies have been put into practice, with many drugs targeting metabolic enzymes in clinical trials, so our results provide a precise direction on lipid metabolism for BC. It is interesting to note that other literature has reported that activated T cells can upregulate lipid synthesis and cholesterol uptake to reprogram lipid metabolism (61, 62). Thus, we hypothesized that the complicated pattern of immunometabolic intermodulation played an irreplaceable role in BC survival.

According to the Cox proportional hazards model, univariate and multivariate analyses were utilized to identify clinical stage and risk sore as independent prognostic factors for BC survivors. This result also indicates that the excellent prognostic ability of our risk scoring model for BC is comparable to the clinical stage and even better than age and molecular subtypes. In terms of predicting the 3-year survival of BC patients, ROC curve results intuitively suggested that our model had higher accuracy than traditional clinical features. Subsequently, we performed decision curve analysis (DCA) to show the superior clinical utility of the risk model, which was supported by our discovery that our model can be widely applied to different clinical subgroups.

Certainly, there are some shortcomings that arise in the present study. First, the data of our study cohort are all obtained from public databases, which may be incapable of representing the entire population of BC patients due to large heterogeneity. Another limitation is that our study could not thoroughly explore the relationship between the TP53 condition and different treatment options for BC survivors because of incomplete data on treatment regimens. Finally, our nomogram and risk scoring system are limited by the retrospective nature of data collection, so it is necessary to develop further prospective studies to validate our findings.

In conclusion, we identified 24 metabolic genes associated with TP53 mutations and defined them as metabolic gene profiles, which are conducive to a deeper understanding of metabolic pathway changes caused by TP53 mutations and provide therapeutic targets for targeted metabolic pathways for BC patients with TP3 mutations. Second, five risk metabolism genes (*CA9*, *CHAC1*, *FUT3*, *MTHFD1L*, and *PLCH1*) were found to confer potential for targeted therapy. In addition, the risk score model based on TP53-related metabolic genes was constructed and verified for the first time, providing a new prediction method for the prognosis of BC and contributing to the clinical decision making and dynamic monitoring of individuals.

Data availability statement

The datasets analyzed for this study can be found in the online repositories. The names of the repository/repositories and accession number(s) can be found in the article.

Author contributions

MJ, XW (2nd Author), and SB contributed to the conception and design of the study. MJ and XW (2nd Author) obtained the online datasets. MJ and SB performed the statistical analysis. MJ wrote the first draft of the manuscript. SB, FQ, QL, XW (4th Author), XH, WL, JT, and YY contributed to the revision of the manuscript. All authors contributed to the article and approved the submitted version.

Funding

This work was financially supported by the National Key Research and Development Program of China (ZDZX2017ZL-01), High-level Innovation Team of Nanjing Medical University (JX102GSP201727), Wu Jieping Foundation (320.6750.17006), Key Medical Talents (ZDRCA2016023), 333 Project of Jiangsu Province (BRA2017534 and BRA2015470), The Collaborative Innovation Center for Tumor Individualization Focuses on Open Topics (JX21817902/008), and Project of China Key Research and Development Program Precision Medicine Research (2016YFC0905901).

Conflict of interest

The authors declare that the research was conducted in the absence of any commercial or financial relationships that could be construed as a potential conflict of interest.

The reviewer JL declared a shared affiliation with the authors MJ, SB, XW, FQ, QL, XH, WL, JT and YN, to the handling editor at time of review.

Publisher's note

Supplementary material

The Supplementary Material for this article can be found online at: https://www.frontiersin.org/articles/10.3389/fimmu.2022.946468/full#supplementary-material

References

1. DeSantis CE, Ma J, Gaudet MM, Newman LA, Miller KD, Goding Sauer A, et al. Breast cancer statistics, 2019. *CA: Cancer J Clin* (2019) 69(6):438–51. doi: 10.3322/caac.21583

2. Berry DA, Cronin KA, Plevritis SK, Fryback DG, Clarke L, Zelen M, et al. Effect of screening and adjuvant therapy on mortality from breast cancer. *N Engl J Med* (2005) 353(17):1784–92. doi: 10.1056/NEJMoa050518

3. Wang SY, Dang W, Richman I, Mougalian SS, Evans SB, Gross CP. Cost-effectiveness analyses of the 21-gene assay in breast cancer: Systematic review and critical appraisal. *J Clin Oncol Off J Am Soc Clin Oncol* (2018) 36(16):1619–27. doi: 10.1200/jco.2017.76.5941

4. Riggio AI, Varley KE, Welm AL. The lingering mysteries of metastatic recurrence in breast cancer. *Br J Cancer* (2021) 124(1):13–26. doi: 10.1038/s41416-020-01161-4

5. DeBerardinis RJ, Chandel NS. Fundamentals of cancer metabolism. *Sci Adv* (2016) 2(5):e1600200. doi: 10.1126/sciadv.1600200

6. Pavlova NN, Thompson CB. The emerging hallmarks of cancer metabolism. *Cell Metab* (2016) 23(1):27–47. doi: 10.1016/j.cmet.2015.12.006

7. Hanahan D, Weinberg RA. Hallmarks of cancer: The next generation. *Cell* (2011) 144(5):646–74. doi: 10.1016/j.cell.2011.02.013

8. Mishra P, Ambs S. Metabolic signatures of human breast cancer. *Mol Cell Oncol* (2015) 2(3):e992217. doi: 10.4161/23723556.2014.992217

9. Fukano M, Park M, Deblois G. Metabolic flexibility is a determinant of breast cancer heterogeneity and progression. *Cancers* (2021) 13(18):4699. doi: 10.3390/cancers13184699

10. Long JP, Li XN, Zhang F. Targeting metabolism in breast cancer: How far we can go? *World J Clin Oncol* (2016) 7(1):122–30. doi: 10.5306/wjco.v7.i1.122

11. Comprehensive molecular portraits of human breast tumours. *Nature* (2012) 490(7418):61–70. doi: 10.1038/nature11412

12. Kruse JP, Gu W. Modes of P53 regulation. *Cell* (2009) 137(4):609–22. doi: 10.1016/j.cell.2009.04.050

13. Liu J, Zhang C, Wang J, Hu W, Feng Z. The regulation of ferroptosis by tumor suppressor P53 and its pathway. *Int J Mol Sci* (2020) 21(21):8387. doi: 10.3390/ijms21218387

14. Kato S, Han SY, Liu W, Otsuka K, Shibata H, Kanamaru R, et al. Understanding the function-structure and function-mutation relationships of P53 tumor suppressor protein by high-resolution missense mutation analysis. *Proc Natl Acad Sci USA* (2003) 100(14):8424–9. doi: 10.1073/pnas.1431692100

15. Baugh EH, Ke H, Levine AJ, Bonneau RA, Chan CS. Why are there hotspot mutations in the Tp53 gene in human cancers? *Cell Death Differ* (2018) 25(1):154–60. doi: 10.1038/cdd.2017.180

16. Olivier M, Hollstein M, Hainaut P. Tp53 mutations in human cancers: Origins, consequences, and clinical use. *Cold Spring Harbor Perspect Biol* (2010) 2 (1):a001008. doi: 10.1101/cshperspect.a001008

17. Andersson J, Larsson L, Klaar S, Holmberg L, Nilsson J, Inganäs M, et al. Worse survival for Tp53 (P53)-mutated breast cancer patients receiving adjuvant cmf. *Ann Oncol Off J Eur Soc Med Oncol* (2005) 16(5):743–8. doi: 10.1093/annonc/mdi150

18. Rossner PJr., Gammon MD, Zhang YJ, Terry MB, Hibshoosh H, Memeo L, et al. Mutations in P53, P53 protein overexpression and breast cancer survival. *J Cell Mol Med* (2009) 13(9b):3847–57. doi: 10.1111/j.1582-4934.2008.00553.x

19. Olivier M, Langerød A, Carrieri P, Bergh J, Klaar S, Eyfjord J, et al. The clinical value of somatic Tp53 gene mutations in 1,794 patients with breast cancer. *Clin Cancer Res Off J Am Assoc Cancer Res* (2006) 12(4):1157–67. doi: 10.1158/1078-0432.Ccr-05-1029

20. Stein Y, Rotter V, Aloni-Grinstein R. Gain-of-Function mutant P53: All the roads lead to tumorigenesis. *Int J Mol Sci* (2019) 20(24):6197. doi: 10.3390/ijms20246197

21. Mantovani F, Collavin L, Del Sal G. Mutant P53 as a guardian of the cancer cell. *Cell Death Differ* (2019) 26(2):199–212. doi: 10.1038/s41418-018-0246-9

22. Gao J, Aksoy BA, Dogrusoz U, Dresdner G, Gross B, Sumer SO, et al. Integrative analysis of complex cancer genomics and clinical profiles using the cbioportal. *Sci Signaling* (2013) 6(269):pl1. doi: 10.1126/scisignal.2004088

23. Cerami E, Gao J, Dogrusoz U, Gross BE, Sumer SO, Aksoy BA, et al. The cbio cancer genomics portal: An open platform for exploring multidimensional cancer genomics data. *Cancer Discov* (2012) 2(5):401–4. doi: 10.1158/2159-8290.Cd-12-0095

24. Wagner GP, Kin K, Lynch VJ. Measurement of mrna abundance using rna-seq data: Rpkm measure is inconsistent among samples. *Theory Biosci = Theor Biowissenschaften* (2012) 131(4):281–5. doi: 10.1007/s12064-012-0162-3

25. Mariathasan S, Turley SJ, Nickles D, Castiglioni A, Yuen K, Wang Y, et al. Tgfβ attenuates tumour response to pd-L1 blockade by contributing to exclusion of T cells. *Nature* (2018) 554(7693):544–8. doi: 10.1038/nature25501

26. Hugo W, Zaretsky JM, Sun L, Song C, Moreno BH, Hu-Lieskovan S, et al. Genomic and transcriptomic features of response to anti-Pd-1 therapy in metastatic melanoma. *Cell* (2016) 165(1):35–44. doi: 10.1016/j.cell.2016.02.065

27. Hänzelmann S, Castelo R, Guinney J. Gsva: Gene set variation analysis for microarray and rna-seq data. *BMC Bioinf* (2013) 14:7. doi: 10.1186/1471-2105-14-7

28. Barbie DA, Tamayo P, Boehm JS, Kim SY, Moody SE, Dunn IF, et al. Systematic rna interference reveals that oncogenic kras-driven cancers require Tbk1. *Nature* (2009) 462(7269):108–12. doi: 10.1038/nature08460

29. Charoentong P, Finotello F, Angelova M, Mayer C, Efremova M, Rieder D, et al. Pan-cancer immunogenomic analyses reveal genotype-immunophenotype relationships and predictors of response to checkpoint blockade. *Cell Rep* (2017) 18 (1):248–62. doi: 10.1016/j.celrep.2016.12.019

30. Gong Y, Ji P, Yang YS, Xie S, Yu TJ, Xiao Y, et al. Metabolic-Pathway-Based subtyping of triple-negative breast cancer reveals potential therapeutic targets. *Cell Metab* (2021) 33(1):51–64.e9. doi: 10.1016/j.cmet.2020.10.012

31. Yu G, Wang LG, Han Y, He QY. Clusterprofiler: An r package for comparing biological themes among gene clusters. *Omics J Integr Biol* (2012) 16 (5):284–7. doi: 10.1089/omi.2011.0118

32. Wilkerson MD, Hayes DN. Consensusclusterplus: A class discovery tool with confidence assessments and item tracking. *Bioinf (Oxford England)* (2010) 26 (12):1572–3. doi: 10.1093/bioinformatics/btq170

33. Subramanian A, Tamayo P, Mootha VK, Mukherjee S, Ebert BL, Gillette MA, et al. Gene set enrichment analysis: A knowledge-based approach for interpreting genome-wide expression profiles. *Proc Natl Acad Sci USA* (2005) 102(43):15545–50. doi: 10.1073/pnas.0506580102

34. Warburg O. On the origin of cancer cells. *Sci (New York NY)* (1956) 123 (3191):309–14. doi: 10.1126/science.123.3191.309

35. Alberghina L, Gaglio D. Redox control of glutamine utilization in cancer. *Cell Death Dis* (2014) 5(12):e1561. doi: 10.1038/cddis.2014.513

36. Hensley CT, Wasti AT, DeBerardinis RJ. Glutamine and cancer: Cell biology, physiology, and clinical opportunities. *J Clin Invest* (2013) 123(9):3678–84. doi: 10.1172/jci69600

37. Wu X, Qian S, Zhang J, Feng J, Luo K, Sun L, et al. Lipopolysaccharide promotes metastasis *via* acceleration of glycolysis by the nuclear factor-Kb/Snail/Hexokinase3 signaling axis in colorectal cancer. *Cancer Metab* (2021) 9(1):23. doi: 10.1186/s40170-021-00260-x

38. Fan Y, Wang J, Xu Y, Wang Y, Song T, Liang X, et al. Anti-warburg effect by targeting Hrd1-pfkp pathway may inhibit breast cancer progression. *Cell Commun Signaling CCS* (2021) 19(1):18. doi: 10.1186/s12964-020-00679-7

39. Jiang W, Hu JW, He XR, Jin WL, He XY. Statins: A repurposed drug to fight cancer. *J Exp Clin Cancer Res CR* (2021) 40(1):241. doi: 10.1186/s13046-021-02041-2

40. Hu Y, He W, Huang Y, Xiang H, Guo J, Che Y, et al. Fatty acid synthase-suppressor screening identifies sorting nexin 8 as a therapeutic target for nafld. *Hepatol (Baltimore Md)* (2021) 74(5):2508–25. doi: 10.1002/hep.32045

41. Thorsson V, Gibbs DL, Brown SD, Wolf D, Bortone DS, Ou Yang TH, et al. The immune landscape of cancer. *Immunity* (2018) 48(4):812–30.e14. doi: 10.1016/j.immuni.2018.03.023

42. Valastyan S, Weinberg RA. Tumor metastasis: Molecular insights and evolving paradigms. *Cell* (2011) 147(2):275–92. doi: 10.1016/j.cell.2011.09.024

43. Harbeck N, Sotlar K, Wuerstlein R, Doisneau-Sixou S. Molecular and protein markers for clinical decision making in breast cancer: Today and tomorrow. *Cancer Treat Rev* (2014) 40(3):434–44. doi: 10.1016/j.ctrv.2013.09.014

44. Symmans WF, Hatzis C, Sotiriou C, Andre F, Peintinger F, Regitnig P, et al. Genomic index of sensitivity to endocrine therapy for breast cancer. *J Clin Oncol Off J Am Soc Clin Oncol* (2010) 28(27):4111–9. doi: 10.1200/jco.2010.28.4273

45. Shahbandi A, Nguyen HD, Jackson JG. Tp53 mutations and outcomes in breast cancer: Reading beyond the headlines. *Trends Cancer* (2020) 6(2):98–110. doi: 10.1016/j.trecan.2020.01.007

46. Zhao S, Liu XY, Jin X, Ma D, Xiao Y, Shao ZM, et al. Molecular portraits and trastuzumab responsiveness of estrogen receptor-positive, progesterone receptor-positive, and Her2-positive breast cancer. *Theranostics* (2019) 9(17):4935–45. doi: 10.7150/thno.35730

47. Baker SJ, Fearon ER, Nigro JM, Hamilton SR, Preisinger AC, Jessup JM, et al. Chromosome 17 deletions and P53 gene mutations in colorectal carcinomas. *Sci (New York NY)* (1989) 244(4901):217–21. doi: 10.1126/science.2649981

48. Robles AI, Harris CC. Clinical outcomes and correlates of Tp53 mutations and cancer. *Cold Spring Harbor Perspect Biol* (2010) 2(3):a001016. doi: 10.1101/cshperspect.a001016

49. Ungerleider NA, Rao SG, Shahbandi A, Yee D, Niu T, Frey WD, et al. Breast cancer survival predicted by Tp53 mutation status differs markedly depending on treatment. *Breast Cancer Res BCR* (2018) 20(1):115. doi: 10.1186/s13058-018-1044-5

50. Curtis C, Shah SP, Chin SF, Turashvili G, Rueda OM, Dunning MJ, et al. The genomic and transcriptomic architecture of 2,000 breast tumours reveals novel subgroups. *Nature* (2012) 486(7403):346–52. doi: 10.1038/nature10983

51. Li T, Kon N, Jiang L, Tan M, Ludwig T, Zhao Y, et al. Tumor suppression in the absence of P53-mediated cell-cycle arrest, apoptosis, and senescence. *Cell* (2012) 149(6):1269–83. doi: 10.1016/j.cell.2012.04.026

52. Zhang C, Liu J, Liang Y, Wu R, Zhao Y, Hong X, et al. Tumour-associated mutant P53 drives the warburg effect. *Nat Commun* (2013) 4:2935. doi: 10.1038/ncomms3935

53. Zhou G, Wang J, Zhao M, Xie TX, Tanaka N, Sano D, et al. Gain-of-Function mutant P53 promotes cell growth and cancer cell metabolism *via* inhibition of ampk activation. *Mol Cell* (2014) 54(6):960–74. doi: 10.1016/j.molcel.2014.04.024

54. Pisarsky L, Bill R, Fagiani E, Dimeloe S, Goosen RW, Hagmann J, et al. Targeting metabolic symbiosis to overcome resistance to anti-angiogenic therapy. *Cell Rep* (2016) 15(6):1161–74. doi: 10.1016/j.celrep.2016.04.028

55. Allen E, Miéville P, Warren CM, Saghafinia S, Li L, Peng MW, et al. Metabolic symbiosis enables adaptive resistance to anti-angiogenic therapy that is dependent on mtor signaling. *Cell Rep* (2016) 15(6):1144–60. doi: 10.1016/j.celrep.2016.04.029

56. Vriens K, Christen S, Parik S, Broekaert D, Yoshinaga K, Talebi A, et al. Evidence for an alternative fatty acid desaturation pathway increasing cancer plasticity. *Nature* (2019) 566(7744):403–6. doi: 10.1038/s41586-019-0904-1

57. Röhrig F, Schulze A. The multifaceted roles of fatty acid synthesis in cancer. *Nat Rev Cancer* (2016) 16(11):732–49. doi: 10.1038/nrc.2016.89

58. Xia L, Oyang L, Lin J, Tan S, Han Y, Wu N, et al. The cancer metabolic reprogramming and immune response. *Mol Cancer* (2021) 20(1):28. doi: 10.1186/s12943-021-01316-8

59. Byrne A, Savas P, Sant S, Li R, Virassamy B, Luen SJ, et al. Tissue-resident memory T cells in breast cancer control and immunotherapy responses. *Nat Rev Clin Oncol* (2020) 17(6):341–8. doi: 10.1038/s41571-020-0333-y

60. Wang T, Fahrmann JF, Lee H, Li YJ, Tripathi SC, Yue C, et al. Jak/Stat3-regulated fatty acid B-oxidation is critical for breast cancer stem cell self-renewal and chemoresistance. *Cell Metab* (2018) 27(1):136–50.e5. doi: 10.1016/j.cmet.2017.11.001

61. Soto-Guzman A, Villegas-Comonfort S, Cortes-Reynosa P, Perez Salazar E. Role of arachidonic acid metabolism in Stat5 activation induced by oleic acid in mda-Mb-231 breast cancer cells. *Prostaglandins Leukot Essent Fatty Acids* (2013) 88(3):243–9. doi: 10.1016/j.plefa.2012.12.003

62. Kidani Y, Elsaesser H, Hock MB, Vergnes L, Williams KJ, Argus JP, et al. Sterol regulatory element-binding proteins are essential for the metabolic programming of effector T cells and adaptive immunity. *Nat Immunol* (2013) 14(5):489–99. doi: 10.1038/ni.2570

frontiers | Frontiers in Immunology

TYPE Review
PUBLISHED 05 September 2022
DOI 10.3389/fimmu.2022.937406

OPEN ACCESS

EDITED BY
Xue-Zhong Yu,
Medical University of South Carolina, United States

REVIEWED BY
Xia Liu,
Saint Louis University, United States
Xiao Chen,
Medical College of Wisconsin, United States

*CORRESPONDENCE
Danfeng Guo
guodanfeng0617@163.com

†These authors have contributed equally to this work and share first authorship

SPECIALTY SECTION
This article was submitted to Cancer Immunity and Immunotherapy, a section of the journal Frontiers in Immunology

RECEIVED 06 May 2022
ACCEPTED 12 August 2022
PUBLISHED 05 September 2022

CITATION
Zhang M, Wei T, Zhang X and Guo D (2022) Targeting lipid metabolism reprogramming of immunocytes in response to the tumor microenvironment stressor: A potential approach for tumor therapy. *Front. Immunol.* 13:937406. doi: 10.3389/fimmu.2022.937406

Targeting lipid metabolism reprogramming of immunocytes in response to the tumor microenvironment stressor: A potential approach for tumor therapy

Ming Zhang[1,2†], Tingju Wei[3†], Xiaodan Zhang[1,2] and Danfeng Guo[1,2*]

[1]Department of Hepatobiliary and Pancreatic Surgery, the First Affiliated Hospital of Zhengzhou University, Zhengzhou, China, [2]Henan Key Laboratory for Digestive Organ Transplantation, Zhengzhou, China, [3]Department of Cardiac Surgery, The First Affiliated Hospital of Zhengzhou University, Zhengzhou, China

The tumor microenvironment (TME) has become a major research focus in recent years. The TME differs from the normal extracellular environment in parameters such as nutrient supply, pH value, oxygen content, and metabolite abundance. Such changes may promote the initiation, growth, invasion, and metastasis of tumor cells, in addition to causing the malfunction of tumor-infiltrating immunocytes. As the neoplasm develops and nutrients become scarce, tumor cells transform their metabolic patterns by reprogramming glucose, lipid, and amino acid metabolism in response to various environmental stressors. Research on carcinoma metabolism reprogramming suggests that like tumor cells, immunocytes also switch their metabolic pathways, named "immunometabolism", a phenomenon that has drawn increasing attention in the academic community. In this review, we focus on the recent progress in the study of lipid metabolism reprogramming in immunocytes within the TME and highlight the potential target molecules, pathways, and genes implicated. In addition, we discuss hypoxia, one of the vital altered components of the TME that partially contribute to the initiation of abnormal lipid metabolism in immune cells. Finally, we present the current immunotherapies that orchestrate a potent antitumor immune response by mediating the lipid metabolism of immunocytes, highlight the lipid metabolism reprogramming capacity of various immunocytes in the TME, and propose promising new strategies for use in cancer therapy.

KEYWORDS

tumor microenvironment, lipid metabolism reprogramming, immunocyte, immunotherapy, immunometabolism

1 Introduction

Worldwide, an estimated 19.3 million new cancer cases (18.1 million excluding non-melanoma skin cancer) and almost 10.0 million cancer deaths (9.9 million excluding non-melanoma skin cancer) occurred in 2020. The global cancer burden is expected to be 28.4 million cases in 2040, a 47% rise from 2020, with a larger increase in transitioning (64% to 95%) versus transitioned (32% to 56%) countries due to demographic changes, although this may be further exacerbated by increasing risk factors associated with globalization and a growing economy (1). Hence, finding a valid and highly effective therapeutic method for cancer is the primary task for the contemporary medical community.

The tumor microenvironment (TME) has gained recent attention in the field of cancer research, as a complex localized tissue state that comprises various cellular and non-cellular components and soluble molecules (2). Although various diverging neoplasms have been described, the TME is generally characterized by hypoxia, low nutrient levels, and a low pH (3); such changes have been shown to play significant roles in carcinogenesis and tumor progression. Mounting evidence has shown that the TME is correlated with tumor initiation, progression, invasion, metastasis, tumor recurrence, and immune evasion (4). The uncontrolled proliferation of tumor cells depletes blood nutrient and oxygen stores. Such resources are required by the surrounding cells for their normal activity. Additionally, tumor cells also secrete specific effector mediators that construct suitable conditions for their survival.

Immunocytes are pivotal regulators of tumor activity; thus, their normal function directly affects cancer prognosis. The maintenance of normal metabolism is of utmost importance to immunocytes, as their activation, differentiation, and function are dependent on a constant energy supply and metabolic transformation (5). However, due to changes in the availability of fuel and other resources within the TME, immunocytes undergo metabolic pattern alterations that have a profound influence on their immune function. Mounting evidence suggests that immunocytes within the TME exist in an altered metabolic state to survive in such a tough environment (6–8).

Lipids play critical roles in cell function. In addition to being used as an alternative fuel source and resolving energy shortages for cells residing in the TME, lipids also participate in the synthesis of biological membranes, provide substrates for biomass production, and activate complex signaling pathways related to the normal cellular activity (9). Therefore, it is inevitable that cellular function becomes impaired due to aberrant lipid metabolisms, such as the change in cytoplasmic lipid content, fatty acid (FA) oxidation (FAO) and FA synthesis (FAS) levels, and patterns of cholesterol, phospholipid, and lipid droplet (LD) metabolism. The altered lipid metabolism of immunocytes within the TME has raised concerns among the scientific community. Furthermore, a recent study has reported that lipid metabolic alterations in immune cells were commonly associated with the TME and immune dysfunction (6).

The purpose of this review is to provide an overview of recent research progress in the study of lipid metabolism reprogramming of immunocytes within the TME. Specifically, we discuss topics such as the potential markers that may predict the prognosis of patients with cancers and the influence of hypoxia, an oncogenic factor, contributing to the phenomenon of lipid metabolism transition in immunocytes within the TME. The field of cancer immunotherapy has experienced a period of rapid development, with encouraging clinical results and prolonged patient survival, compared with conventional treatment approaches (10). Encouragingly, some forms of immunotherapy have successfully enhanced the antitumor potency of immune cells by regulating their lipid metabolism. These findings support our viewpoint that modulating lipid metabolism in immunocytes is crucial for tumor eradication. Herein, we provide prospective therapeutic strategies by aiming at changes in immunocyte lipid metabolism, which occur as a result of the TME.

2 Lipid metabolism reprogramming of various immunocytes in the tumor microenvironment and the associated targets and pathways

The TME is a flexible tissue state comprising a heterogeneous cell population and non-cellular components. TME-associated cell types include precancerous and cancerous cells; more specifically, stromal cells such as epithelial cells, fibroblasts, endothelial cells, and hematopoietically derived immune cells (11). The TME is enriched for the following types of immunocytes: macrophages, T lymphocytes, dendritic cells (DCs), natural killer (NK) cells, myeloid-derived suppressor cells (MDSCs), and neutrophils, among others. Due to the harsh conditions within the TME, these immunocytes are forced to transform their normal metabolic states (regardless of whether they reside within or are recruited to the tumor tissue) to adapt and survive, a process called metabolic reprogramming. Metabolic reprogramming is known to occur in cancer cells and has been suggested as a major sign of cancer progression. In contrast, the metabolic reprogramming of immune cells in the TME has only been recently observed. In the past decade, immunometabolism has progressively become a vibrant area of immunology because of its importance in immunotherapy (12). Nonetheless, we are still some distance from understanding the underlying mechanisms of metabolic changes affecting immunocytes residing in the TME.

In general, lipid metabolism involves three major steps: 1) FAS and FAO, 2) steroid metabolism, and 3) compound lipid metabolism. Ever-increasing evidence has shown that the lipid

metabolism of tumor-infiltrating immune cells is associated with an immunosuppressive TME and tumor progression (13). We therefore dedicate the following sections of the review to describing the latest research on the signaling axes, proteins, and genes that are associated with lipid metabolism alterations in each type of tumor-infiltrating immunocyte within the TME. Furthermore, we also summarize potential therapeutic targets that are worthy to be considered in this context (Figure 1).

2.1 Macrophages in the tumor microenvironment

Macrophages carry out multiple critical innate immunity functions. They are essential in immune defense, the inflammatory response, tissue remodeling, and homeostasis. Each of these processes is orchestrated by different macrophage subsets, which display remarkable heterogeneity (14). Macrophages have considerable plasticity and can adopt different activation states in response to changes in their tissue microenvironment (15, 16). They differentiate into distinct phenotypes following stimulation with various factors. These phenotypes exhibit different characteristics and biological functions, thus exerting different regulatory functions for physiological and pathological activities in the body, a phenomenon known as the "polarizing effect" (16). Typically, polarized macrophages could be divided into the classically activated M1 and the alternatively activated M2 phenotypes (17). M1 macrophages are predominantly responsible for antigen presentation, pro-inflammatory, scavenger, and antitumor effects, while M2 macrophages have the biological capacity to inhibit inflammation, promote tissue remodeling, and prevent parasitic infection. In addition, the M2 subtype is implicated in angiogenesis, immune regulation, and tumor progression (18).

Tumor-associated macrophages (TAMs) exhibit significant immunosuppressive effects and belong predominantly to the M2 phenotype of macrophages. M2 executes the pro-tumoral function by promoting tumor growth, immune evasion, angiogenesis, invasion, and metastasis (19, 20). The peroxisome proliferator-activated receptor (PPAR) pathway is a well-known signaling pathway involved in FA metabolism (21). Wu et al. reported that the receptor-interacting protein kinase 3 (RIPK3), a central factor in necroptosis, was downregulated in hepatocellular carcinoma (HCC)-associated macrophages. This increased the accumulation and polarization of M2 TAMs by significantly inhibiting caspase1-mediated cleavage of PPAR and facilitating FA metabolism (e.g., *via* FAO), ultimately leading to accelerated HCC growth (22). Zhang et al. utilized an *in vitro* model to mimic the TAM–HCC interaction in the TME. They found that M2 monocyte-derived macrophages (MDMs) promoted HCC cell migration in an FAO-dependent manner by enhancing interleukin (IL)-1β secretion (23). Sterol regulatory element-binding proteins (SREBPs), a family of membrane-bound transcription factors located in the endoplasmic reticulum (ER), play a central role in regulating lipid metabolism. Liu et al. reported that regulatory T cells (Tregs) suppressed the secretion of interferon (IFN)-γ by $CD8^+$ T cells, which would otherwise block the activation of SREBP1-mediated FAS in M2 TAMs. Moreover, SREBP1 inhibition augmented the efficacy of immune checkpoint blockade, suggesting that the combination of targeting Tregs and the lipid metabolism of M2 TAMs could improve the efficacy of cancer immunotherapy (24). Another study revealed that the activity of the mammalian target of rapamycin (mTOR) pathway was elevated in TAMs. Enhanced

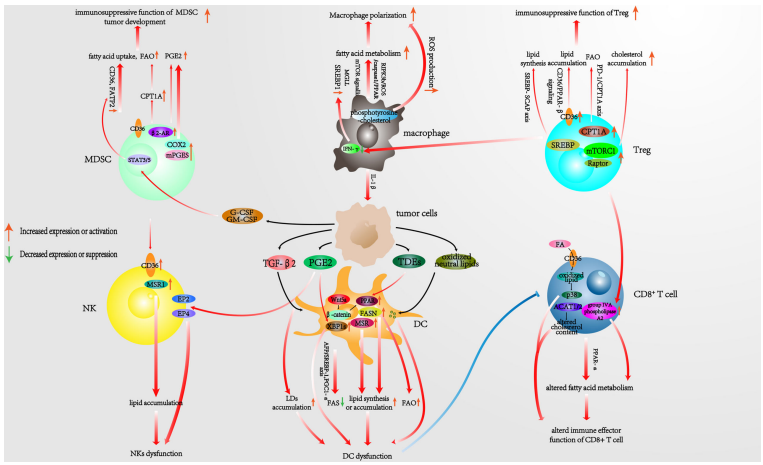

FIGURE 1
Pathways associated with reprogrammed lipid metabolism of infiltrating immunocytes in the TME. TME, tumor microenvironment.

mTORC1 signaling caused an increase in lipid synthesis within these TAMs (25); the underlying mechanisms, however, require further exploration.

In addition, several studies have shown that the cellular accumulation of lipids was crucial for regulating the function of TAMs. TAMs stimulated and isolated from different mouse tumor models exhibited a reduction in monoacylglycerol lipase (MGLL) expression. Meanwhile, macrophages derived from a transgenic mouse model exhibiting MGLL overexpression were shown to accumulate lipids, and such macrophages preferentially polarized into the M1 phenotype in response to cancer-specific stimuli. Conversely, downregulated MGLL contributed to the functional suppression of $CD8^+$ T cells associated with tumor progression. Thereby, the TAM phenotype required a reduction in MGLL expression to stabilize and display immunosuppressive and pro-tumoral functions. Hence, targeting MGLL could be exploited for the treatment of cancer (26). Of note, another study showed that the enrichment of long-chain (LC) omega-3 (ω-3) FAs inhibited the polarization and secretory function of M2 macrophages in a murine prostate tumor model (27, 28). We may therefore hypothesize that the uptake of diverse FA types could give rise to distinct forms of downstream metabolic activity, each exerting different effects on the tumor immune response of macrophages. Moreover, the enzyme-instructed self-assembly of phosphotyrosine-cholesterol was shown to re-educate pro-tumor macrophages into an antitumor phenotype. This phenotype change was achieved by inducing reactive oxygen species (ROS) production and disrupting macrophage-associated filaments, thus inhibiting ovarian cancer progression (29). These findings collectively imply that the underlying mechanism of cholesterol remodeling shapes macrophage effector functions.

2.2 T cells in the tumor microenvironment

T cells are predominantly categorized into $CD4^+$ and $CD8^+$ T-cell subsets; both have crucial functions in the eradication of tumors and pathogens (30). However, the TME has been shown to suppress T-cell function and even remodel their metabolism, resulting in the dysfunction of immune surveillance and the immune evasion of tumor cells (31). $CD8^+$ T cells are the most important T-cell subset in the adaptive immune response against tumors. Compared to normal tissues, tumors contain a lower density of $CD8^+$ T cells and a reduced $CD8^+$ T cell to Treg ratio; these phenomena are associated with poor cancer prognosis (32). $CD4^+$ T cells predominantly differentiate into T helper (Th) 1 and Th2 cell subtypes. Th1 cells improve the killing activity of $CD8^+$ "killer" T cells as well as macrophages, while Th2 cells promote the activation and differentiation of B cells. Thus, the role of $CD4^+$ T cells is to influence other immunocytes and their effector functions to prevent infection and tumor growth (11). Aside from the classic T-cell subtypes, other rare T cells also contribute to human immune system homeostasis, including natural killer T cells (NKTs), Tregs, Th9, Th17, Th22, and T follicular helper (Tfh) cells. We will now in turn discuss the lipid metabolism reprogramming capacity of some of these cells within the TME.

2.2.1 $CD8^+$ T cells in the tumor microenvironment

$CD8^+$ T cells are considered the most important executors of antitumor immunity. Lipids are the essential materials for cell bioactivity, and their depletion in $CD8^+$ T cells inhibits cell proliferation and signal transduction. However, this does not mean that excessive lipid production would lead to better cell function. Unraveling the role of lipids in $CD8^+$ T cells may be beneficial to furthering our understanding of T-cell function.

Raised FA concentrations in the TME have been shown to activate PPAR-α signaling, which had an essential role in facilitating lipid metabolism and preserving the effector functions of $CD8^+$ T cells (33). Nanomedicine, which involves the encapsulation of anti-cancer chemicals and biological tumor necrosis factors (TNFs) in nanoparticles, represents a new form of tumor therapy (34). Kim et al. generated a fenofibrate-encapsulating nanoparticle (F/ANs), the surface of which was modified with an anti-CD3e f(ab′)2 fragment, thus yielding aCD3/F/ANs. PPAR-α and downstream FA metabolism-related genes were overexpressed in aCD3/F/AN-treated T cells. These overexpressed genes resulted in the increased proliferation, killing potency, and infiltration of $CD8^+$ T cells in a glucose-deficient environment mimicking the TME (35). This finding, as a new modality of immune metabolic therapy, highlights the potential of nanotechnology to modulate the reprogramming of lipid metabolism and the value of targeting the PPAR pathway in $CD8^+$ T cells. In addition, Chowdhury et al. proved that potentiated FAO levels could also enhance the antitumor activity of $CD8^+$ T cells in conjunction with anti-programmed cell death protein 1 (PD-1) antibody treatment (36).

However, there is evidence to suggest that lipid accumulation in $CD8^+$ T cells contributes to their immune dysfunction. Cluster of differentiation 36 (CD36), also named FA translocase (FAT), is an integral transmembrane glycoprotein expressed in various tissues, which is involved in the high-affinity uptake of long-chain FAs (LCFAs). Increasing evidence has shown that the abnormal expression of CD36 in immunocytes may be involved in tumor-associated processes, such as tumor angiogenesis and tumor immune evasion (33). CD36 mediates the uptake of FAs by $CD8^+$ tumor-infiltrating T cells and is also implicated in lipid peroxidation and ferroptosis. In the TME, these phenomena are induced by cholesterol and have been shown to decrease cytotoxic cytokine production by $CD8^+$ T cells with their overall antitumor capacity impairment

(37). Xu et al. found the emergence of lipoproteins accumulation in $CD8^+$ tumor-infiltrating lymphocytes (TILs) within the TME. This was also associated with the increased expression of CD36. In accordance with previous findings, the authors proved that CD36 expression was also correlated with progressive T-cell dysfunction. Mechanistically, CD36 promoted the uptake of oxidized low-density lipoprotein (OxLDL) into T cells and concurrently induced lipid peroxidation and activation of the p38 kinase. Consequently, the inhibition of p38 and resolution of lipid peroxidation restored $CD8^+$ TIL functionality. Thus, the OxLDL/CD36/p38 axis promoted intratumoral $CD8^+$ T-cell dysfunction in the context of melanoma/colorectal carcinoma (38) and may also serve as a therapeutic target in other tumors.

Senescent T cells exhibit active glucose metabolism but have an imbalance in their lipid metabolism. Tumor cells and Tregs have been shown to drive the expression of group IVA phospholipase A2 (IVA-PLA2). Such increment was responsible for the altered lipid metabolism and the induction of senescence observed in $CD8^+$ T cells. Inhibition of IVA-PLA2 reprogrammed the lipid metabolism of effector $CD8^+$ T cells, prevented $CD8^+$ T cell senescence *in vitro*, and enhanced antitumor immunity and immunotherapy efficacy (in mouse models of melanoma and breast cancer *in vivo*) (39).

In addition, some studies reported that the fluctuation in cholesterol levels had a key role in regulating the immune function of $CD8^+$ T cells. Ma *et al.* found that when cholesterol accumulated in the cytoplasm of $CD8^+$ T cells, it induced the overexpression of inhibitory checkpoints [PD-1, TIM-3, and lymphocyte activation gene 3 (LAG-3)] in an ER-stress-X-box binding protein 1 (XBP1)-dependent manner, leading to the functional depletion of $CD8^+$ T cells. In contrast, lowering cholesterol levels or ER stress could enhance the antitumor function of $CD8^+$ T cells (40). Tc9 cells (IL-9-producing $CD8^+$ T cells) exhibit stronger antitumor potency compared to conventional $CD8^+$ T cells. These cells were shown low levels of PPAR-α/retinoid X receptor (RXR)α, accompanied by a lower expression of the cholesterol synthesis enzymes (HMGCR and SQLE), and a higher expression of the cholesterol efflux enzymes (ABCA and ABCG1). Moreover, the addition of cholesterol-derived oxysterols inhibited IL-9 expression, induced the apoptosis of Tc9 cells, and resulted in their impaired antitumor activity (41). Nevertheless, Yang et al. pointed out that raising cholesterol levels by blocking cholesterol esterification with ACAT1/2 inhibitors facilitated the migration of T-cell receptor (TCR) microclusters to the immunological synapse center (42). The outcome was an increase in the number and activity of anti-melanoma $CD8^+$ T cells, as demonstrated both *in vitro* and *in vivo*. These findings highlight the conflicting roles of cholesterol in the regulation of immunocyte function, the intricacies of which require further investigation.

2.2.2 Tregs in the tumor microenvironment

Tregs contribute to immune homeostasis and are essential for orchestrating immune tolerance and the prevention of autoimmune diseases. However, Tregs tend to suppress the antitumor immune response as well as the proliferation of other antitumor immunocytes, such as $CD8^+$ T cells and NK cells. Tregs also exert a pro-tumor effect by secreting anti-inflammatory factors like IL-10 and tumor growth factor (TGF)-β, while inhibiting the production of pro-inflammatory cytokines by other immune cells. Thus, Tregs act as negative immune regulators of the antitumor response and promote tumor immune escape and TME maintenance (43).

Xu et al. reported that the Treg-specific ablation of the glutathione peroxidase 4 (GPX4) enzyme repressed melanoma growth and concomitantly promoted antitumor immunity. The mechanism involved in the excessive accumulation of lipid peroxides and ferroptosis in Tregs upon TCR/CD28 co-stimulation (44). FAS mediated by FA synthase (FASN) contributes to the functional maturation of Tregs, with FAO supplying a key energy source for Tregs infiltrating the TME; these features could partly explain why Tregs normally perform their immunosuppressive role in such a glucose-deficient microenvironment (45, 46). CD36 also plays a critical role in Tregs. Wang et al. demonstrated how CD36 depletion decreased the uptake of lipids by Tregs leading to tumor growth deceleration in a melanoma model (33). The authors also observed synergistic effects between the anti-CD36 and anti-PD-1 antitumor therapy. This study indicates that CD36 blockade may represent a powerful enhancer of current immunotherapies by targeting the lipid metabolism of Tregs. Furthermore, another study reported that HCC-associated Tregs expressed PD-1, which promoted the FAO of endogenous lipids by increasing carnitine palmitoyltransferase 1A (CPT1A) protein expression and inducing lipolysis; however, the detailed mechanism has not yet been delineated (47).

Fatty acid-binding proteins (FABPs) are a family of lipid chaperones required for lipid uptake and intracellular lipid trafficking. One of the FABP family members, FABP5, promotes FA absorption from the microenvironment, and FA transportation to specific cellular compartments has been shown to be highly expressed in Tregs. Field et al. showed that in Tregs, the genetic or pharmacologic inhibition of FABP5 function caused mitochondrial changes that were underscored by decreased oxidative phosphorylation (OXPHOS). Consequently, lipid metabolism was impaired, leading to the loss of cristae structure. Interestingly, although FABP5 inhibition in Tregs triggered mitochondrial (mt)DNA release and consequent cGAS-STING-dependent type-I IFN signaling, these changes induced the production of IL-10 by Tregs and promoted their suppressive activity in a murine lymphoma model (48). However, whether long-term mitochondrial

alterations mediated by the depletion of FABP5 could lead to increased Treg death remains unknown.

Lim et al. demonstrated that the activity of SREBPs was upregulated in tumor-infiltrating Tregs (49). Inhibiting lipid synthesis and metabolic signaling by targeting SREBPs in the Tregs effectively activated the antitumor immune response without eliciting autoimmune toxicity in the context of melanoma. In addition, SREBP-cleavage-activating protein (SCAP), a downstream target responsible for regulating SREBP activity in Tregs, was identified. The authors demonstrated that the inhibition of the SREBP–SCAP axis attenuated tumor growth and boosted immunotherapy in combination with PD-1 targeting. Moreover, they further showed that Tregs present in the TME exhibited upregulated PD-1 gene expression dependent on SREBP activity and mevalonate metabolism signaling (which led to protein geranylgeranylation), thus identifying a new target for cancer therapy. Similarly, Pacella et al. confirmed that the activation of SREBP promoted lipid synthesis and in turn supported the local proliferation of $OX40^+$ Tregs in the TME in a mouse colon carcinoma model and samples from patients with liver cancer (46). OX40, also known as TNF receptor superfamily member 4 (TNFRSF4) and CD134, shapes the lipid composition of Tregs and promotes the proliferation of $OX40^+$ Tregs in the TME by inducing FAS and glycolysis.

Regulatory-associated protein of mammalian target of rapamycin (Raptor)/mTORC1 signaling is essential for the suppressive activity of Tregs by promoting cholesterol biosynthesis and lipid metabolism. During the activation of this pathway, mevalonate signaling (which is downstream of the mTOR pathway) is particularly important for the proliferation of Tregs and the upregulation of the suppressive molecules cytotoxic T lymphocyte antigen-4 (CTLA-4) and ICOS to establish Treg functional competency (50). In addition, after selectively deleting ABCG1 in the Tregs of LDL receptor-deficient mice, Cheng et al. observed a 30% increase in Tregs exhibiting intracellular cholesterol accumulation and downregulation of the mTOR pathway, which was responsible for the differentiation of naive $CD4^+$ T cells into Tregs. The increased number of Tregs resulted in reduced antitumor T-cell activation and increased IL-10 production, indicating that ABCG1 regulated T-cell differentiation into Tregs (51).

2.2.3 Other T-cell subtypes in the tumor microenvironment

Th2 cells, a subset of $CD4^+$ T cells, are significantly involved in the clearance of extracellular parasites as well as asthma and other allergic reactions. Th2 cells have been reported to possess a double-edged effect (52, 53) that depends on the specific kind and stage of the tumor. Moreover, it is conventionally assumed that Th2 cells exhibit tumor-promoting function (53). Of note, PPAR-γ controls the expression of genes associated with lipid metabolism, and it is of tremendous importance for the activation and immune function execution of Th2 cells (52), whereas there is little evidence to prove that this molecule could be influenced by Th2 cells within the TME.

Studies implied the vital role of lipid in the functional maturation of Th17 cells (54). Th17 cells not only are correlated with autoimmune diseases but also play paramount roles against pathogens as well as tumor cells (55). In terms of Th17 cells, they have been proved to fluctuate their number in distinct tumor types. However, its precise mechanism, for instance, how to affect cancers, has not been cleared yet, and it is even contradictory to their immune role referring to a recent concept (55, 56). CD5L (CD5 antigen-like protein) is a member of the scavenger receptor cysteine-rich superfamily involved in lipid metabolism. It exerts the function of inhibiting FASN and is indicated as a regulator for the pathogenicity related to Th17 cells. Such alterations by FASN inhibition may promote RORγt (a transcriptional factor) to bind to the anti-inflammatory genes (*IL10*) whereas preventing it from binding to the *IL17a* and *IL23r* loci (pro-inflammatory genes) in Th17 cells. These changes would eventually cause the pathogenicity of Th17 in the autoimmunity context (57). Nonetheless, the study involved in Th17 lipid metabolic alterations within the TME is in shortage; the exact roles of Th17 in specific tumor types and if the rewiring of lipid metabolism would remodel its immune response are still limited.

Th1 assists cytotoxic cells like NK cells, CTLs, and antigen-presenting cells (APCs) through direct touch or indirect signaling activation. Such effort devotes to elevated immune elimination of pathogens and destructive antitumor immune responses of these antitumor cells (58). Sphingolipids, including two central bioactive lipids, ceramide and sphingosine-1-phosphate (S1P), perform opposing roles in sustaining the survival of tumor cells. Accordingly, some studies implied ceramide acted as an antitumor role, whereas S1P behaved in a pro-tumor manner (59–61). Acid sphingomyelinase (ASM) is a lipid hydrolase enzyme converting sphingophospholipids to ceramides in lysosomes, and Bai et al. reported that elevated ASM bioactivity and ceramide production promoted naive $CD4^+$ T cells differentiating into Th1. Moreover, ASM activity also contributed to the expansion of Th17 cells (62).

NKTs, a cluster of CD1d-restricted T cells participating in adaptive and innate immune together, are characterized by recognizing lipid antigens. Lipid metabolism acts as a significant regulator of the cytotoxicity of NKT cells. FAO is of vital importance in maintaining the biofunction of tumor-infiltrating invariant (i)NKTs. Stimulated human (i)NKTs cells utilize fatty acids as the substrates for oxidation more than stimulated conventional T cells, such as $CD4^+$ and $CD8^+$ T cells. In addition, (i)NKTs display a higher level of FAO and high expression of adenosine monophosphate-activated protein kinase (AMPK) pathway genes (63). Given the complex content in various TMEs, (i)NKTs could also be affected to exert their inherent antitumor function by the blockade of lipid metabolism. However, more evidence would be required to

confirm this hypothesis. There is little research focusing on lipid metabolism reprogramming of helper T cells in the TME; perhaps it is noteworthy for us to pay attention to their immune metabolism pattern transition.

2.3 Dendritic cells in the tumor microenvironment

DCs are predominantly classified into three categories according to their expression of cell surface molecules and transcription factors: 1) conventional (c)DCs, which can be further subdivided into two subtypes, cDC1 and cDC2; 2) plasmacytoid (p)DCs; and 3) monocyte-derived (mo)DCs. DCs undertake the role of capturing antigens derived from pathogens or tumor cells. They then present the specific antigens to T cells for the activation of the adaptive immune response. Thus, DCs provide the crucial link between innate and adaptive immunity. In addition, DCs release cytokines to help immune effector cells to exert their antitumor effects.

A high lipid content promotes the accumulation of phospholipids and triacylglycerols but not cholesterol and cholesteryl esters in DCs. Intriguingly, these lipid-rich DCs exhibit higher levels of integrins, co-stimulatory molecules, glycoproteins, pro-inflammatory cytokines, and chemokines than DCs with a low lipid content (64, 65).

FAS is crucial for the maturation of DCs as well as their ability to express costimulatory molecules, undergo toll-like receptor (TLR)-mediated activation, and induce T-cell responses. However, the precise roles of FAS and FAO in regulating DC function await to be defined (66, 67). The activation of DCs depends on TLR signaling through which DCs potentiate their glycolysis to produce high levels of pyruvate. As the fuel of mitochondrial respiration, pyruvate is sequentially transformed into acetyl coenzyme A (acetyl-CoA), which is required for FAS and the normal immune function of DCs (66). Li et al. proposed that the uptake of HCC-derived alpha-fetoprotein (AFP) accounted for the reduced expression of CD1 on moDCs (68); this finding was consistent with the results of Santos and colleagues. Santos et al. found that during the early stages of DC maturation, HCC cells could secrete AFP to inhibit FAS and the mitochondrial metabolism of DCs (69). Mechanistically, AFP was shown to downregulate the expression of SREBP-1 and PPAR-γ co-activator-1α (PGC1-α) in DCs *in vitro*. Both SREBP-1 and PGC1-α functioned as regulatory molecules for FAS and mitochondrial metabolism, which were required by DCs for the execution of the antitumor response. These outcomes imply that the curtailed immune function of DCs could be partially attributed to FAS inhibition, thus providing new insights into DC-mediated cancer immunotherapy approaches.

Although the aforementioned research has highlighted the positive effect of high lipid concentrations and altered FA metabolism on DC function, these parameters have also been assigned contradictory roles in the reprogramming of DCs within the TME. These controversial conclusions remind us of the complex signaling networks implicated in the lipid metabolism of DCs. In addition, other potential factors such as the influence of tumor types, DC phenotypes, lipid species, and the interaction between DCs and the soluble components of the TME should also be considered.

Gao et al. reported how blocking FA uptake or impairing lipid synthesis in DCs within a radiation-induced thymic lymphoma model rescued the immunosuppressive state of the TME by improving the T cell-stimulating capacity of DCs (70). Accordingly, Jiang et al. showed that the degree of FASN expression in tumor-infiltrating DCs in ovarian cancer was associated with the advanced clinical phenotype (71). Consecutive activation of FASN in DCs increased lipid assembly, causing abnormal lipid synthesis and lipid accumulation within the cell. This abnormal state may be responsible for the defective ability of DCs to present antigens and activate the antitumor T cell-mediated immune response within the TME. Macrophage scavenger receptor 1 (MSR1) is expressed in DCs and is deemed to be a positive regulator of the immune response by modulating antigen cross-presentation. However, a study has shown that DCs in the TME (of murine colon carcinoma, melanoma, and lymphoma tumor models) increased their expression of MSR1. This gave rise to superfluous lipid uptake and lipid accumulation in these cells (72). The consequences were a reduction in the expression of costimulatory molecules on the DC surface, and in the DC-mediated cytokine production, which ultimately lowered activated T-cell activation. In addition, Yin et al. reported that inactive DCs in the TME were characterized by abnormal lipid accumulation in the cytoplasm (73). They found that tumor cells (murine breast cancer 4T1, cervical carcinoma TC-1, colon carcinoma MC38-OT I, and MC38 and melanoma B16/F10 cell lines) secreted tumor-derived exosomes (TDEs), which arose the PPAR-α-mediated reaction in DCs; in the meantime, PPAR-α also undertook the role of transporting TDEs into DCs. Since PPAR-α signaling acted as the mediator of lipid metabolism, Yin and colleagues in turn demonstrated that PPAR-α contributed to the excessive biogenesis of LDs and concomitantly enhanced FAO in DCs, culminating in DC dysfunction. Conversely, the genetic depletion or pharmacologic inhibition of PPAR-α effectively reversed the TDE-induced immune dysfunction of DC and enhanced the efficacy of immunotherapy. This work uncovered the role of TDE-mediated immune modulation and lipid metabolism in the reprogramming of DCs. Furthermore, it revealed PPAR-α as a stress-induced target, suggesting a novel mechanism by which tumor cells modulated immune cells. Zhao et al. demonstrated that the Wnt5a/β-catenin/PPAR-γ axis was abnormally activated in the context of melanoma (74). This axis was shown to induce FAO in DCs by upregulating the expression of CPT1A, an FA

transporter. This in turn increased the levels of the protoporphyrin IX prosthetic group of iIDO (a tryptophan catabolic enzyme) and reduced the expression of IL-6 and IL-12, which normally promote the expansion of Tregs. Furthermore, inhibiting the Wnt5a/β-catenin/PPAR-γ axis not only decreased melanoma progression but also improved the efficacy of anti-PD-1 therapy.

Recently, the identification of certain lipid types (including modified species of lipids) has raised increasing concern due to their ability to cause DC dysfunction. In a study by Ramakrishnan et al., the accumulation of oxidized neutral lipids (e.g., triglycerides, cholesterol esters, and FAs) within DCs, triggered by tumor-derived factors (i.e., originating from the supernatant of EL-4 lymphoma, MC38 colon carcinoma, and CT-26 colon carcinoma cell lineages), was shown to retard the cross-presentation of exogenous antigens. Consequently, the expression of peptide (p)MHC class I complexes on DCs was reduced. Contrary to this phenomenon, the accumulation of non-oxidized lipids did not affect the cross-presentation ability of DCs (75).

There is growing evidence that prostaglandin (PG), the metabolite of arachidonic acid, plays a non-negligible role in the modulation of DC function. Gilardini Montani et al. predicted an increase in the mortality of pancreatic cancer patients following valproic acid (VPA) treatment, due to extensive ER stress and dysregulated choline metabolism in DCs (76). Intriguingly, their investigation of the detailed mechanism found elevated concentrations of prostaglandin E2 (PGE2) (released by VPA-treated cancer cells) in the cellular supernatant. DCs cultured in this supernatant consequently exhibited a lower allostimulatory capacity and an increased ability to release IL-10 and IL-8. These findings suggest that the secretion of PGE2 by the tumor transferred the stress of VPA treatment from the tumor cells to DCs. In agreement with this finding, Amberger et al. designed two new PGE1-containing protocols (Pici-PGE1, Kit M) to generate DC/leukemia-derived DC (DCleu) *in vitro* from leukemic peripheral blood mononuclear cells (PBMCs) or directly from leukemic whole blood (WB) (77). The results showed that PGE1-containing Kit M generated significantly higher amounts of mature DCs from not only leukemic but also healthy PBMCs. Furthermore, it was possible to directly produce DCs from leukemic and healthy WB without triggering their extensive proliferation. Also, compared to the PGE2-containing Kit K, Kit M exhibited higher DC numbers and increased anti-leukemic activity, demonstrating that different subtypes of PG may exert distinct effects on the antitumor process. Additionally, E6, one of the most important oncoproteins associated with human papillomavirus (HPV), was shown to regulate PGE2 synthesis and was associated with the overproduction of PGE2 in HPV-16-positive cervical lesions leading to the inhibition of DC migration (78).

LDs, also named lipid bodies (LBs) are an important cellular organelle involved in the regulation of cellular lipid metabolism by balancing lipid storage and degradation to maintain normal cellular activity. Several lines of evidence suggest that LD metabolic disorders participate in the dysfunction of the DC-mediated immune response. The autocrine secretion of TGF-β2 in the TME by mesothelioma has been shown to account for the abnormal LD accumulation in DCs (79). This suppressed the proliferative and migratory capacities of DCs, preventing their localization to the lymph node to induce $CD8^+$ T-cell activation. Tumor-associated DCs (TADCs) with defective antigen cross-presentation ability have been observed in the TME. This defect was partly due to their inability to transport peptide-MHC class I (pMHCI) complexes to the cell surface. Remarkably, DCs in individuals with cancers have been shown to accumulate LBs containing oxidatively truncated (ox-tr) lipids (80). These specific ox-tr-LBs were found covalently bound to the chaperone heat shock protein 70 (Hsp70), thus preventing the translocation of pMHCI to the cell surface. This important research revealed that the species of lipids incorporated into the LBs could determine the role of LBs in the regulation of DC function.

Apart from LDs, lipoprotein metabolism also impacts DC function. Immature moDCs were shown to display notably increased NADPH-oxidase-driven H_2O_2-production and LDL uptake (81). These features contributed to the immunosuppressive function of immature moDCs, whereas blocking LDL uptake restored their maturation capacity and attenuated their immunosuppressive properties. Hence, regulating the uptake of LDL may be a potential strategy for modulating the immune function of DCs. However, further research is required to support this hypothesis.

2.4 Myeloid-derived suppressor cells in the tumor microenvironment

MDSCs are a differentiated type of myeloid cells that can be divided into three major subpopulations in humans: monocytic (M)-MDSCs ($CD14^+CD15^-HLA\text{-}DR^{lo/-}$ cells), polymorphonuclear (PMN)-MDSCs ($CD11b^+CD14^-CD15^+CD66b^+$ low-density cells), and early-MDSCs ($Lin^-CD11b^+CD34^+CD33^+CD117^+HLA\text{-}DR^{lo/-}$ cells) (82). MDSCs have been found in association with various human cancer tissues, where they can act as an independent prognostic factor for the overall survival rate (83). MDSCs usually play an immunosuppressive role in the anti-cancer immune response and support tumor progression and metastasis (84). Therefore, there is an essential need for understanding MDSC function in cancer pathogenesis, with the aim of designing appropriate therapeutic targets or disease markers. Here, we summarize recent research relating to abnormal lipid metabolism in MDSCs.

Cancer-associated MDSCs typically switch their main source of energy from glycolysis to FAO. This metabolic reprogramming is more readily observed in tumor-infiltrating

MDSCs, and features increased CD36-mediated FA uptake and higher expression of key enzymes (e.g., CPT1a, medium-chain acyl-CoA dehydrogenase (ACADM), peroxisome proliferator-activated receptor gamma co-activator 1-β (PGC1-β), and 3-hydroxyacyl-CoA dehydrogenase (HADHA)). As a result, the rate of FAO is upregulated, leading to the increased production of immunosuppressive mediators, such as arginase 1 (ARG1) and the cytokines (granulocyte colony-stimulating factor (G-CSF), granulocyte-macrophage colony-stimulating factor (GM-CSF), IL-1β, IL-6, and IL-10) required for the proliferation of MDSCs (85).

In addition to the production of cytokines by MDSCs themselves, the paracrine production of cancer cell-derived G-CSF and GM-CSF also act on the STAT3/5 pathway of tumor-infiltrating MDSCs within the TME. As the downstream target, CD36 was shown to be sequentially upregulated and enhance the uptake of exogenous FAs, thus contributing to the immunosuppressive function of MDSCs (86). Consistently, FATP2 was reported to be exclusively upregulated in the PMN-MDSCs of mice and humans. Meanwhile, the overexpression of FATP2 was proven to be associated with GM-CSF/STAT5 pathway activation. In addition, the absorption of arachidonic acid and the synthesis of its metabolite, PGE2, were implied as being the key players in the FATP2-associated immunosuppressive activity of MDSCs. Conversely, the deletion of FATP2 abolished the suppressive function of MDSCs and even blocked tumor progression in mouse models (EL4 lymphoma, Lewis lung carcinoma, and CT26 colon carcinoma, as well as in a genetically engineered model of pancreatic cancer), when used in combination with immune checkpoint inhibitors (87).

Of note, two soluble mediators, IFN-γ and TNF-α, which are thought to exert pro-inflammatory and antitumor effects, were shown to contribute to the induction of COX2. COX2, as a key enzyme required for PGE2 synthesis, is responsible for the hyperactivation of MDSCs within the TME of patients with ovarian cancer (88). However, this phenomenon was not deemed to implicate either of these factors alone. These findings highlight the overarching role of cytokines in the switching of lipid metabolism, meaning that an approach that targets specific cytokines and their downstream effector molecules could represent a promising therapeutic strategy.

Prior research has implied the potential link between certain cytokines and PGE2 in MDSCs, while other studies underscored the important immune regulatory function of PGE2 *via* another MDSC-relevant axis. The PGE2-forming enzymes, microsomal PGE2 synthase 1 (mPGES1) and COX2, were shown to be highly expressed within Ly-6C$^+$ MDSCs in the murine bladder tumor model (89). In contrast, inhibiting the COX2, mPGES1/PGE2 pathway lowered the expression of PD-L1 in these cells and resulted in an elevated number of activated CD8$^+$ T cells. The expression of the β2-adrenergic receptor (β2-AR) on MDSCs is positively correlated with breast cancer progression. This phenomenon reveals its role as a pro-tumor factor, which enhances the immunosuppressive activity of MDSCs by reprogramming their metabolism (e.g., by increasing FAO). Interestingly, the increase in CPT1A expression supports the FAO-mediated immunosuppressive effect of MDSCs, consistent with the elevated expression of β2-AR. Moreover, β2-AR signaling is also responsible for increasing the release of the immunosuppressive mediator PGE2 (90). These findings propose an antitumor therapeutic strategy that would rely on lowering the production of PGE2 and its associated upstream and downstream molecules to alleviate the immunosuppressive action of MDSCs.

One study accentuated the difference between the PMN-MDSCs of patients with cancer and healthy individuals by showing that tumor-associated PMN-MDSCs expressed lectin-type oxidized LDL receptor 1 (LOX-1), whereas their normal equivalents did not (91). Accordingly, another finding demonstrated that LOX-1$^+$ PMN-MDSCs had a higher level of dichlorodihydrofluorescein diacetate (DCFDA), ARG1, and inducible nitric oxide synthase (iNOS). These LOX-1$^+$ PMN-MDSCs possessed the capacity to inhibit the proliferation of CD3$^+$ T cells in an ARG1/iNOS-dependent manner. Such suppression of CD3$^+$ T-cell expansion in turn signaled a worse prognosis in patients with glioblastoma multiforme (GBM) (92). These results suggest that LOX-1 could also be a prospective antitumor therapeutic target and that the lipoprotein metabolism of MDSCs may contribute to immunosuppression within the TME.

The above studies have shown that lipid metabolism acted as a negative modulator in the TME, leading to the abnormal activation of MDSC. However, PPAR-γ signaling, which also affects the lipid metabolic activity of MDSCs, was demonstrated to support the regular function of lysosomal acid lipase (LAL) in the dampening transendothelial migration (TEM), suppressing the overactivation of the mTOR pathway and preventing ROS overproduction of MDSCs (93). Since these MDSC-associated properties could promote tumor progression, this study provides a mechanistic basis for targeting MDSCs to reduce the risk of cancer initiation, growth, and metastasis.

2.5 Natural killer cells in the tumor microenvironment

NK cells, working as an indispensable component of the human innate immune, possess direct killing property and participate in anti-tumor and anti-virus infection. NK cells exert their immune function by releasing cytotoxic granules, mediating the antibody-dependent cell-mediated cytotoxicity (ADCC) effect, and priming death receptor signal of targeted cells to sustain immune homeostasis (94). The research about NK cell lipid metabolism alteration has been referred to below.

In the setting of the postoperative period after colorectal cancer resection, granulocytic MDSCs expanding after surgery induced the expression of scavenger receptors (SR) such as MSR1, CD36, and CD68 in NK cells. The changes resulted in intracellular lipid accumulation with diminished NK cell ability to release granzyme B and perforin, eventually contributing to NK cell dysfunction and colorectal cancer relapse (95). Regarding the finding of Bonavita et al., tumor-derived PGE2 selectively acted on EP2 and EP4 expressed on NK cells to reshape immunosuppressive TME and consequently promoted tumor (colorectal carcinoma and melanoma) immune evasion (96).

3 Hypoxia in the tumor microenvironment induces lipid metabolism reprogramming in immunocytes

Under normal physiological conditions, oxygen is taken up by mitochondria to participate in OXPHOS, which provides ATP for typical cellular functions. The extensive depredation of tumor cells and their unlimited growth cause the release of non-cellular components into the TME. These include cytotoxic metabolites. The metabolites ROS (97), lactic acid, and tumor-derived negative regulatory molecules collectively impair the effector function of immunocytes. Although cells possess the flexibility to adapt to an altered milieu, they inevitably sacrifice some bioactivities to guarantee survival. Hypoxia is one of the stressors within the TME that has a significant effect on tumor outcome (98). Hence, broadening our understanding of how hypoxia affects the function of immunocytes is necessary. Here, we have assembled findings related to the switch in lipid metabolism that occurs in immune cells as a result of hypoxia. In addition, we also discuss the molecular targets and pathways that could be utilized to alleviate immune cell dysfunction, which is a result of the hypoxia-driven reprogramming of lipid metabolism (Figure 2).

Hypoxia represents an obstacle for the immune system in the fight against tumors (99). Among the molecules that contribute to the hypoxia-mediated state of immune inhibition, hypoxia-inducible factor (HIF), ROS (elevated production in anoxic conditions), and lactic acid (lactate) (which mostly contributes to an acidic environment) are predominantly responsible for the induction of immune cell dysfunction (100).

The hypoxic TME has been shown to reduce the expansion of $CD8^+$ T cells, in addition to impairing the maturation and activity of DCs and NK cells; in contrast, Tregs and MDSCs remain highly active in the same context (101, 102). HIF is a transcription factor activated by a low-oxygen microenvironment and is composed of two subunits: HIF-α (which occurs in the form of three isoforms: HIF-1α, HIF-2α, and HIF-3α) and HIF-β (103). HIF is reported to promote lipid peroxidation and ER stress and recruit Tregs, M2 macrophages, and MDSCs to construct an immunosuppressive TME (6). However, a recent finding by Velica *et al.* proposed that it was HIF-2α, not HIF-1α, that triggered the increased cytotoxic differentiation and cytolytic function of $CD8^+$ T cells against tumor targets (104). This suggests that distinct subtypes of HIF perform divergent roles in response to immunocyte stressors.

The differentiation of naïve T cells into effector T cells (Teffs) by TCR/CD28 co-stimulation requires PI3K/Akt/mTOR signaling. HIF-1α locates downstream of this pathway, and once HIF-1α is activated, it consequentially triggers aerobic glycolysis and amino acid metabolism in Teffs while suppressing FAO (105). As a result, HIF-1α is often

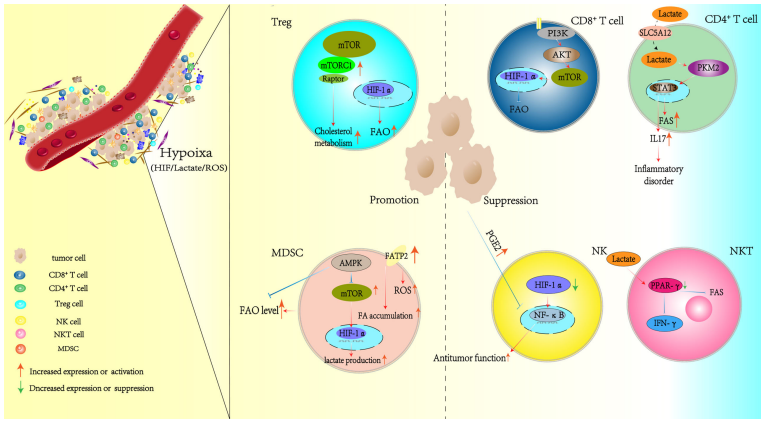

FIGURE 2
Hypoxia alters the lipid metabolism patterns of immunocytes in the TME. TME, tumor microenvironment.

upregulated under such circumstances, and Teffs ultimately exhibit immune dysfunction. These phenomena may suggest that strong FAO suppression makes a potential contribution to Teff dysfunction in the TME.

It appears that the adaptation of Tregs to the TME depends not only on their glycolysis but also on FAO (98). mTORC1 signaling impairment was shown to compromise *de novo* lipid synthesis in $CD3^+$ T cells. Such altered lipid metabolism was associated with the PI3K/mTOR/HIF-α axis, which in turn affected $CD3^+$ T-cell adaptation to hypoxic conditions and their execution of immune regulation *in situ* (106). Earlier, we also reviewed that Raptor/mTORC1 signaling in Tregs could promote cholesterol biosynthesis and support the immunosuppressive function and the activation of Tregs. These observations indicate that mTOR signaling plays a previously underestimated role in T cells (and possibly in other immune cells) by bridging HIF and lipid metabolism. In addition, Miska et al. unveiled that HIF-1α-directed glucose away from mitochondria; thus, Tregs consequently depended on FAs for their energy in the hypoxic tumor tissue. Conversely, inhibiting lipid oxidation enhanced the overall survival of glioma-bearing mice; however, the direct link between HIF-1α and lipid oxidation remained unclear (107). PGE2 is upregulated in the TME (thyroid cancer background), and a high concentration of PGE2 was shown to result in the NF-κB pathway-mediated suppression of NK cells (108). Another study by Ni et al. clarified that the inhibition of HIF-1α enhanced the IL-18-driven activation of the NF-κB pathway. This activated axis in turn elevated the expression of activation markers and effector molecules in tumor-infiltrating NK cells, thus promoting tumor suppression (109). These results reveal the potential link between PGE2, HIF-1α, and NF-κB signaling in NK cells; however, further supporting research is required.

There are dramatic differences in the metabolism of M1 and M2 macrophages. M1 macrophages mainly derive their energy from glycolysis and the existing blockade of the tricarboxylic acid (TCA) cycle, which results in the intracellular accumulation of itaconate and succinate. Succinate overproduction leads to HIF-1α stabilization and, in turn, activates the transcription of glycolytic genes. Such genes are responsible for maintaining the glycolytic metabolism of M1 macrophages. On the contrary, M2 cells are more dependent on OXPHOS for their energy. Moreover, their TCA cycle is intact and provides the substrates with complexes of the electron transport chain (110). The effect of hypoxia on macrophages is also vague. A study has reported the positive effect of hypoxia on macrophages, which sustained their inflammatory responses and migratory capacity (111). In contrast to this report, hypoxia has also been shown to impair macrophage pro-inflammatory activity by eliciting energy metabolism disorder (EMD), which particularly affected glucose metabolism (112, 113). These results have predominantly occurred in the M1 subtype. The possible explanation for these disparate conclusions may be related to the duration of low-oxygen conditions and the preferable differentiation of macrophages from M1 to M2 within the TME (114). The effect of hypoxia on M2 macrophages is well studied and is deemed as a driver of M2-mediated pro-tumor activity (101). Regrettably, although numerous studies have established the mechanism for how hypoxia affects the glucose metabolism of macrophages in the TME, which ultimately results in macrophage dysfunction, the investigations of lipid metabolism alteration remain limited.

Hypoxia was proven to aggravate tumor progression with aberrant PPAR signaling activation. In the setting of glioma, PPAR signaling hyperactivation was shown to immunosuppress by promoting Treg expansion (115). Since PPAR largely regulates cellular lipid metabolism, aiming at an undetected target stressed by hypoxia through this signaling to mediate Treg lipid metabolism and in turn support the immunosuppression function of Tregs may be a prospective research orientation. Liu et al.> proposed the excessive production of IDO1 in DCs within a hypoxic milieu (116). This finding appears to be similar to the result we previously cited (74) and may be the clue to explaining the underlying correlation between hypoxia and the Wnt5a/β-catenin/PPAR-γ signaling pathway, which may mediate the reprogramming of lipid metabolism in DCs within the hypoxic TME.

Lactate is the main metabolite of glycolysis. Hypoxia has been shown to greatly increase lactate levels, causing the acidification of the TME. Such an acidic milieu consequently facilitates tumor progression and suppresses antitumor immunity through T-cell inhibition and PD-L1 upregulation (117). SLC5A12, a lactate transporter, mediates lactate uptake by $CD4^+$ T cells and induces the reshaping of their effector phenotype resulting in increased IL-17 production *via* the nuclear PKM2/STAT3 pathway. Of note, SLC5A12-mediated lactate uptake into $CD4^+$ T cells also promotes FAS. Such abnormal lactate content eventually leads to the onset of chronic inflammatory disorders by $CD4^+$ T cells (118); however, its relationship with the TME demands more research. mTOR signaling is inhibited by AMPK activation and regarded as an effective activator of HIF-1α signaling as well as lactate production. In addition, AMPK was also shown to restrict FAO. Interestingly, the extent of both lactate production and FAO levels is increased in MDSCs within the TME, which is beneficial for their activity. These findings suggest that activators of AMPK signaling could represent promising MDSC-targeting therapeutic candidates (119). Moreover, the acidic milieu of mesothelioma was shown to trigger DC dysfunction and alter the T cell-mediated immune response through a TGF-β2-dependent mechanism (79). In this context, DC anergy was tightly associated with intracellular LD accumulation and the

metabolic rewiring of DCs. Moreover, the aggregation of lactic acid in the TME reduced PPAR-γ expression levels, thus diminishing lipid synthesis and IFN-γ production in invariant (i)NKT cells (120). Conversely, utilizing a PPAR-γ agonist successfully reversed these phenomena and strengthened the antitumor activity of (i)NKT cells in the context of melanoma. Since there are few studies about lactate-induced abnormal lipid metabolism in different immunocyte types within the TME, more effort would be required to progress this field of research.

ROS is easily produced under hypoxic anoxic conditions. A report by Adeshakin et al. proposed the link between ROS and lipid metabolism (121). FATP2 expression in the MDSCs was shown to increase when these cells were present within the TME (thyroid cancer). Meanwhile, the blockade of FATP2 expression in MDSCs by lipofermata lowered their intracellular lipid content, reduced ROS concentration, blocked their immunosuppressive function, and consequently inhibited tumor growth.

4 Current immunotherapies and reagents targeting the lipid metabolism of immunocytes

In recent years, immunotherapy has shown an excellent performance in the treatment of various types of cancer. Generally speaking, current efforts in cancer immunotherapy fall into three main approaches (122): 1) the blockade of immune checkpoints such as anti-PD-1/PD-L1 and anti-CTLA-4 to restore or potentiate the antitumor effect of immune cells (123); 2) adoptive cellular therapy, including the use of TIL therapy (124), engineered T-cell therapy (e.g., chimeric antigen receptor [CAR] T-cell therapy and TCR therapy (125)), CAR-NK cell therapy (126), and CAR-macrophage therapy (127); and 3) therapeutic cancer vaccines (128). Although immunotherapy represents a remarkable breakthrough in the treatment of cancer, it still has limited success in certain types of tumors. Tumor resistance, non-responsiveness, and recurrence following immunotherapy could in part explain why existing immunotherapeutic methods are not as effective against cancers as anticipated. Hence, novel therapeutic targets are urgently needed to complement existing forms of immunotherapy. Since the study of immune cell metabolism has received increasing attention, certain biomarkers have also been established as new checkpoints associated with metabolic activity in specific immunocytes. Targeting these markers either alone or in combination with other forms of immunotherapy could contribute to the dysregulated immune situation reversing. Here, we describe the molecular targets that participate in immunocyte lipid metabolism and introduce the drugs that could be used to modulate these targets in favor of the antitumor immune response (Table 1).

In lung carcinoma and colon adenocarcinoma, etomoxir was shown to target CPT1A to inhibit FAO of MDSCs and reversed its tumor-promoting effects by abrogating the infiltration of MDSCs into the tumor (85). In addition, Su et al. demonstrated

TABLE 1 Current tumor-suppressor reagents that regulate immune cell function by modulating their lipid metabolism.

Reagent	Target molecule	Effect on lipid metabolism in immunocytes	Influence on immunocytes in the TME	Reference
Etomoxir	CPT1A	Inhibition of FAO	Inhibited the infiltration of MDSCs; potential of suppressing pro-tumor capacity of TAMs	(85, 129)
Nivolumab; pembrolizumab; atezolizumab 2	PD-1/PD-L1	Inhibition of FAO; promotion of cholesterol content	Enhanced immune response of immunocytes such as $CD8^+$ T cells	(47, 130)
Ipilimumab	CTLA-4	Interfered with T-cell FAO process	Enhanced antitumor response of T cells	(131)
_	CD36	Inhibition of FA uptake and accumulation	Enhanced intra-tumoral $CD8^+$ T-cell effector function; ablated the function of intra-tumoral Tregs	(33, 37)
C75	FASN	Inhibition of fatty acids synthesis	Reduction of IL-1β, TNF-α, IL-6, and IL-10 levels in macrophages	(132)
AICAR	_	Elevation of fatty acid oxidation of $CD4^+$ T cells	Specifically enhanced the expansion of Treg cells; impairment of Th17 generation	(133)
RGX-104	LXR	Driving *Apoe* and genes involved in cholesterol, fatty acidic transcriptional activation	Activation of LXR/ApoE axis elicited robust anti-tumor responses; enhanced T-cell activation; suppressed survival and immunosuppressive function of MDSCs	(134)
Atorvastatin	mTOR	Restrained cholesterol content	Downregulated the expression of co-inhibitory receptors in T cells with constant secretion of IL-2	(135)
NS-398	COX-2	Inhibition of PGE2 production	Enhanced the antitumor potency of DCs	(136)
Saponin-based adjuvants	_	Induction of intracellular LBs	Elevated cross-presentation and T-cell activation function of $CD11b^+$ DCs	(137)

TME, tumor microenvironment; FAO, fatty acid oxidation; MDSCs, myeloid-derived suppressor cells; TAMs, tumor-associated macrophages; FA, fatty acid; DCs, dendritic cells; LBs, lipid bodies.

that high CTP1A expression modulated TAMs to form a pro-tumor subset (129). PD-1/PD-L1 is ubiquitously expressed on immunocytes. Although the detailed mechanism regarding how PD-1/PD-L1 affects immunocyte immune function has been well studied, new research has uncovered that the drugs targeting PD-1/PD-L1 (e.g., nivolumab, pembrolizumab, and atezolizumab) simultaneously dampen their FAO levels; this effect partially enhanced the response of immune cells (e.g., $CD8^+$ T cells) that were generally inhibited in the TME (47, 130). Of note, in the setting of HCC, the expression levels of PD-1 in HCC patients were reported to be markedly higher than in healthy donors. This phenomenon implies that targeting PD-1 to alleviate the suppression of antitumor immune function in immunocytes (within the hepatic TME) could potentially be achieved by regulating their lipid metabolic patterns (138). Moreover, ipilimumab targets CTLA-4 to positively regulate the antitumor immune response and was also reported to interfere with the FAO process in T cells (131). The CD36 inhibitor and the anti-CD36 antibody are proposed as novel therapeutic molecules used to enhance intratumoral $CD8^+$ T-cell effector function (37) and ablate the immunosuppressive function of intratumoral Tregs (33); related research, however, is still in the preclinical stage. In addition, C75, as a FASN inhibitor, was shown to reduce IL-1β, TNF-α, IL-6, and IL–10 levels in macrophages; further results are anticipated (132).

Gualdoni et al. found that AICAR, an AMP analog, modulated the ratio of Tregs/Th17 cells by regulating FAO in $CD4^+$ T cells (133). Mechanistically, AICAR directly activated AMPK and specifically induced Treg expansion while impairing the generation of Th17 cells. This phenomenon was associated with an increase in FAO in $CD4^+$ T cells. LXR (liver-X nuclear receptor) is a member of the nuclear hormone receptor family. As a transcription factor, LXR has the capacity to drive the transcriptional activation of *APOE* and other genes involved in cholesterol, FA, and glucose metabolism to limit MDSC expansion. Additionally, the activation of the LXR/APOE axis was shown to elicit robust antitumor responses in various tumor models and human tumor cell lineages. RGX-104, an agonist of LXR, was proven to suppress the survival and immunosuppressive function of MDSCs; this research was in the Phase I a/b stage (134).

Atorvastatin, one of the classic cholesterol-lowering drugs, was shown to downregulate the expression of co-inhibitory receptors in T cells accompanied by the prolonged secretion of IL-2, as observed in chronic infections such as HIV, hepatitis C virus (HCV), and cancer. However, atorvastatin treatment actually compromised T-cell proliferation and reduced their capacity to secrete TNF-α; related mechanisms were also involved in the inhibition of Ras-activated MAPK, PI3K-Akt, and subsequent mTOR signaling pathways (135).

The regulation of arachidonic acid metabolism in the TME is also thought to have a positive effect on tumor eradication. Pandey et al. found that the augmented secretion of PGE2 by tumor cells inhibited DC function (136). They utilized the COX-2 inhibitor, NS-398, to reduce PG synthesis and consequently elevated the antitumor potency of DCs by enhancing their immune activity. The mechanism may involve an increased content of the classical DC-lineage-specific transcription factor Zbtb46, as well as a decrease in extracellular signal-regulated kinase (ERK)/the cyclic AMP response-element binding protein (CREB) signaling, which promoted IL-10 synthesis.

Of note, a study showing that the elevated intracellular LB content of $CD11b^+$ DCs, which was induced by saponin-based adjuvants (used for animal and human cancer vaccines), could improve DC-mediated cross-presentation and T-cell activation *in vitro* and *in vivo* (137).

5 Discussion

Since the notion of the TME was proposed, multiple studies have uncovered the role of the TME in tumor initiation, progression, metastasis, and its response to treatment. TME components include tumor-infiltrating immune cells (recruited in response to tumor antigens), chemokines, and other soluble factors, all of which are strongly associated with cancer prognosis. In recent years, immunometabolism has gained increasing attraction for its implication in the regulation of immune cell function (139). Furthermore, evidence of immunometabolism reprogramming has been uncovered in various types of tumors. The studies we have listed in this review collectively reveal the true value of targeting the TME-induced lipid metabolism reprogramming of immunocytes. Hence, in this section, we summarize the lipid metabolism-associated challenges awaiting to be addressed in each type of immunocytes within the TME by future research.

TAMs tend to differentiate into a pro-tumorigenic, immunosuppressive phenotype, which is associated with an M2 signature within the TME. Because of the TME stressor, the altered lipid metabolism of TAMs preferentially favors macrophage polarization into M2 rather than the M1 subset, sequentially contributing to tumor evasion and progression. Nevertheless, some TME-residing macrophages retain their antitumor functions in the TME. Thus, promoting the M1 macrophage immune response while suppressing the activity or expansion of the M2 macrophages could represent a plausible therapeutic strategy.

In humans, $CD8^+$ T cells perform the primary antitumor role, and their function is universally suppressed within the TME. To date, a consensus on how the reprogramming of lipid

metabolism impacts $CD8^+$ T-cell functions has not been reached. As for Tregs, prior research has demonstrated that the lipid metabolism reprogramming of these cells could also be targeted to improve the immunogenicity of tumors. However, the exact mechanism behind how altered lipid metabolism modulates Treg function within the TME of each tumor type remains uncertain. Moreover, the prevalence of altered lipid metabolism in rare T-cell subsets is also unclear. Thereby, more research is needed to clarify the processes involved in the lipid metabolic rewiring of T cells within the TME.

Research on DC dysfunction associated with the immune evasion of tumor cells has raised concerns, especially as the mechanisms implicated remain elusive. DC metabolism controls the development, polarization, and maturation processes within these cells and provides energy to maintain their function. However, the immune activity of DCs is generally inhibited in the TME, while many relevant metabolic pathways are also strongly altered. Thus, it is rational for us to assume the existence of the unknown mutual interaction between the inhibition of immune function and lipid metabolism alteration. Hence, the discovery of novel therapeutic targets associated with lipid metabolic changes in DCs would be of great value. Encouragingly, prior research has already demonstrated the potential benefits of targeting the metabolic switch of tumor-associated DCs. Based on the research progress that we have summarized, we envision that the development of tailored DC-associated therapies for the treatment of patients with specific tumors could one day become a reality.

MDSCs represent one of the major immunosuppressive immunocytes that reside within the TME (140). The quest to eliminate the immunosuppressive function of MDSCs is a promising field of tumor therapy. In-depth research of MDSCs has revealed prospective insights into the metabolic alterations (including changes in lipid metabolism) affecting these cells; these findings could therefore unveil novel ways of eliminating the immunosuppressive function of MDSCs. Studies have shown that the direct inhibition of MDSCs interacted with immune checkpoints on antitumor immunocytes or immediately restricted the secretion of immunosuppressive mediators (such as IL-10, TGF-β, and PGE2), which may be a thinkable method to mitigate such immunosuppressive milieu contributed by MDSCs. However, research is largely limited to a small subset of specific tumors; thus, more attention needs to be devoted to this area of study.

Regrettably, at present, there is insufficient research on the lipid metabolism reprogramming of NK cells within the TME. Adoptive NK cell transfer therapy, one of the most used NK cell-related immunotherapies, still suffers from limitations such as the challenge of producing sufficient NK cell numbers to efficiently recognize and target the tumor or the slow migration of adoptively transferred NK cells toward the tumor site. Thus, investing in the study of the lipid metabolic reprogramming of NK cells in the TME may improve therapeutic NK regimens in cancer.

The TCA cycle is the major method for ATP production in eukaryotes. A low-oxygen milieu orchestrated by the TME would inevitably affect glucose metabolism and, in turn, FAO and FAS. Moreover, the drop in ATP levels would shift metabolism in favor of the consumption of cholesterol and other lipid species. Since lipids maintain multifarious activities that are necessary for cell survival, the alteration of lipid metabolism in immunocytes would inevitably lead to immune dysfunction and tumor evasion in the TME. Of note, the unknown effect of the shift in lipid metabolism in a low-oxygen environment may be easily masked and underestimated, due to our major focus on glucose metabolism. Hence, the investigation of how hypoxia impacts the lipid metabolism of immunocytes within the TME is worth considering for the development of novel antitumor therapies.

Immunotherapy represents a major breakthrough in the improvement of the overall survival (OS)/relapse-free survival (RFS) of patients with cancers in recent years. However, its limitations, arising from tumor heterogeneity, drug resistance, and non-responsiveness, in addition to the risk of autoimmune disease induction, still need to be overcome. Encouragingly, from the research summarized in this review, we would hypothesize that immunotherapy and drugs regulating immune cells' lipid metabolism could represent complementary approaches to rescue the antitumor function of antitumor immunocytes or inhibit the immunosuppressive function of pro-tumor immune cells in the TME. However, there are still some challenges for relevant research at the present stage. Firstly, prior research only focused on one specific tumor type; thus, the universality of such drugs needs more exploration since distinct tumors vary in their intra-tumoral compositions. In addition, few studies examined abnormal lipid metabolism within immunocytes in various TMEs from a comprehensive perspective. Thus, considerable effort will be required to establish solid evidence in this field and apply this therapeutic method to distinct tumor categories. Secondly, current cancer treatment regimens only focus on one type of immunocyte. Hence, it is often not possible to determine whether the function of non-targeted immune cells would be affected when employing immunomodulating drugs. These problems need to be taken into consideration to minimize the unknown side effects of novel drugs and optimize therapeutic strategies for cancer patients.

Collectively, our review unveils a largely unexplored and tangible approach to the treatment of patients with cancer. By concentrating on the studies of lipid metabolism reprogramming in immunocytes within the TME, we unveil part of the mechanisms that contribute to this metabolic alteration. Ultimately, we hope that this review will prove beneficial for

the development of novel effective antitumor therapies in the near future.

Author contributions

MZ and TW wrote the draft manuscript. XZ and DG made critical revisions to the manuscript. All authors contributed to the article and approved the submitted version.

Funding

This study was supported by grants from the National Natural Science Foundation of China (No. 81901571 to DG) and the Henan Provincial Science and Technology Research Project (No. 222102310564 to XZ, No. SBGJ202103056 to DG).

Conflict of interest

The authors declare that the research was conducted in the absence of any commercial or financial relationships that could be construed as a potential conflict of interest.

Publisher's note

References

1. Sung H, Ferlay J, Siegel RL, Laversanne M, Soerjomataram I, Jemal A, et al. Global cancer statistics 2020: Globocan estimates of incidence and mortality worldwide for 36 cancers in 185 countries. *Ca-a Cancer J Clin* (2021) 71(3):209–49. doi: 10.3322/caac.21660

2. Arneth B. Tumor microenvironment. *Medicina-Lithuania* (2020) 56(1):15. doi: 10.3390/medicina56010015

3. Pedersen AK, Mendes Lopes de Melo J, Morup N, Tritsaris K, Pedersen SF. Tumor microenvironment conditions alter akt and Na(+)/H(+) exchanger Nhe1 expression in endothelial cells more than hypoxia alone: Implications for endothelial cell function in cancer. *BMC Cancer* (2017) 17(1):542. doi: 10.1186/s12885-017-3532-x

4. Tormoen GW, Crittenden MR, Gough MJ. Role of the immunosuppressive microenvironment in immunotherapy. *Adv Radiat Oncol* (2018) 3(4):520–6. doi: 10.1016/j.adro.2018.08.018

5. Hu C, Xuan Y, Zhang X, Liu Y, Yang S, Yang K. Immune cell metabolism and metabolic reprogramming. *Mol Biol Rep* (2022)13:1–13. doi: 10.1007/s11033-022-07474-2

6. Xu Y, He L, Fu Q, Hu J. Metabolic reprogramming in the tumor microenvironment with immunocytes and immune checkpoints. *Front Oncol* (2021) 11:759015. doi: 10.3389/fonc.2021.759015

7. Zhang Q, Lou Y, Bai XL, Liang TB. Immunometabolism: A novel perspective of liver cancer microenvironment and its influence on tumor progression. *World J Gastroenterol* (2018) 24(31):3500–12. doi: 10.3748/wjg.v24.i31.3500

8. Andrejeva G, Rathmell JC. Similarities and distinctions of cancer and immune metabolism in inflammation and tumors. *Cell Metab* (2017) 26(1):49–70. doi: 10.1016/j.cmet.2017.06.004

9. Cockcroft S. Mammalian lipids: Structure, synthesis and function. *Essays Biochem* (2021) 65(5):813–45. doi: 10.1042/EBC20200067

10. Cariani E, Missale G. Immune landscape of hepatocellular carcinoma microenvironment: Implications for prognosis and therapeutic applications. *Liver Int* (2019) 39(9):1608–21. doi: 10.1111/liv.14192

11. Ringquist R, Ghoshal D, Jain R, Roy K. Understanding and improving cellular immunotherapies against cancer: From cell-manufacturing to tumor-immune models. *Adv Drug Delivery Rev* (2021) 179:114003. doi: 10.1016/j.addr.2021.114003

12. Aria H, Ghaedrahmati F, Ganjalikhani-Hakemi M. Cutting edge: Metabolic immune reprogramming, reactive oxygen species, and cancer. *J Cell Physiol* (2021) 236(9):6168–89. doi: 10.1002/jcp.30303

13. Yu W, Lei Q, Yang L, Qin G, Liu S, Wang D, et al. Contradictory roles of lipid metabolism in immune response within the tumor microenvironment. *J Hematol Oncol* (2021) 14(1):187. doi: 10.1186/s13045-021-01200-4

14. Wang C, Ma C, Gong L, Guo Y, Fu K, Zhang Y, et al. Macrophage polarization and its role in liver disease. *Front Immunol* (2021) 12:803037. doi: 10.3389/fimmu.2021.803037

15. Shapouri-Moghaddam A, Mohammadian S, Vazini H, Taghadosi M, Esmaeili SA, Mardani F, et al. Macrophage plasticity, polarization, and function in health and disease. *J Cell Physiol* (2018) 233(9):6425–40. doi: 10.1002/jcp.26429

16. Murray PJ, Allen JE, Biswas SK, Fisher EA, Gilroy DW, Goerdt S, et al. Macrophage activation and polarization: Nomenclature and experimental guidelines. *Immunity* (2014) 41(1):14–20. doi: 10.1016/j.immuni.2014.06.008

17. Yunna C, Mengru H, Lei W, Weidong C. Macrophage M1/M2 polarization. *Eur J Pharmacol* (2020) 877:173090. doi: 10.1016/j.ejphar.2020.173090

18. Mantovani A, Biswas SK, Galdiero MR, Sica A, Locati M. Macrophage plasticity and polarization in tissue repair and remodelling. *J Pathol* (2013) 229 (2):176–85. doi: 10.1002/path.4133

19. Pathria P, Louis TL, Varner JA. Targeting tumor-associated macrophages in cancer. *Trends Immunol* (2019) 40(4):310–27. doi: 10.1016/j.it.2019.02.003

20. Yeung OW, Lo CM, Ling CC, Qi X, Geng W, Li CX, et al. Alternatively activated (M2) macrophages promote tumour growth and invasiveness in hepatocellular carcinoma. *J Hepatol* (2015) 62(3):607–16. doi: 10.1016/j.jhep.2014.10.029

21. Marechal L, Laviolette M, Rodrigue-Way A, Sow B, Brochu M, Caron V, et al. The Cd36-ppargamma pathway in metabolic disorders. *Int J Mol Sci* (2018) 19 (5):1529. doi: 10.3390/ijms19051529

22. Wu L, Zhang X, Zheng L, Zhao H, Yan G, Zhang Q, et al. Ripk3 orchestrates fatty acid metabolism in tumor-associated macrophages and hepatocarcinogenesis. *Cancer Immunol Res* (2020) 8(5):710–21. doi: 10.1158/2326-6066.CIR-19-0261

23. Zhang Q, Wang H, Mao C, Sun M, Dominah G, Chen L, et al. Fatty acid oxidation contributes to il-1beta secretion in M2 macrophages and promotes macrophage-mediated tumor cell migration. *Mol Immunol* (2018) 94:27–35. doi: 10.1016/j.molimm.2017.12.011

24. Liu C, Chikina M, Deshpande R, Menk AV, Wang T, Tabib T, et al. Treg cells promote the Srebp1-dependent metabolic fitness of tumor-promoting macrophages *Via* repression of Cd8(+) T cell-derived interferon-gamma. *Immunity* (2019) 51(2):381–97.e6. doi: 10.1016/j.immuni.2019.06.017

25. Hobson-Gutierrez SA, Carmona-Fontaine C. The metabolic axis of macrophage and immune cell polarization. *Dis Model Mech* (2018) 11(8): dmm034462. doi: 10.1242/dmm.034462

26. Xiang W, Shi R, Kang X, Zhang X, Chen P, Zhang L, et al. Monoacylglycerol lipase regulates cannabinoid receptor 2-dependent macrophage activation and cancer progression. *Nat Commun* (2018) 9(1):2574. doi: 10.1038/s41467-018-04999-8

27. Liang P, Henning SM, Guan J, Grogan T, Elashoff D, Cohen P, et al. Effect of dietary omega-3 fatty acids on castrate-resistant prostate cancer and tumor-associated macrophages. *Prostate Cancer Prostatic Dis* (2020) 23(1):127–35. doi: 10.1038/s41391-019-0168-8

28. Shan K, Feng N, Cui J, Wang S, Qu H, Fu G, et al. Resolvin D1 and D2 inhibit tumour growth and inflammation *Via* modulating macrophage polarization. *J Cell Mol Med* (2020) 24(14):8045–56. doi: 10.1111/jcmm.15436

29. Hu Y, Wang H, Li C, Liu J, Xu B, Di W. Enzyme-instructed assembly of a cholesterol conjugate promotes pro-inflammatory macrophages and induces apoptosis of cancer cells. *Biomater Sci* (2020) 8(7):2007–17. doi: 10.1039/d0bm00125b

30. Annunziato F, Romagnani C, Romagnani S. The 3 major types of innate and adaptive cell-mediated effector immunity. *J Allergy Clin Immunol* (2015) 135 (3):626–35. doi: 10.1016/j.jaci.2014.11.001

31. Bader JE, Voss K, Rathmell JC. Targeting metabolism to improve the tumor microenvironment for cancer immunotherapy. *Mol Cell* (2020) 78(6):1019–33. doi: 10.1016/j.molcel.2020.05.034

32. Maimela NR, Liu S, Zhang Y. Fates of Cd8+ T cells in tumor microenvironment. *Comput Struct Biotechnol J* (2019) 17:1–13. doi: 10.1016/j.csbj.2018.11.004

33. Wang H, Franco F, Tsui Y-C, Xie X, Trefny MP, Zappasodi R, et al. Cd36-mediated metabolic adaptation supports regulatory T cell survival and function in tumors. *Nat Immunol* (2020) 21(3):298–308. doi: 10.1038/s41590-019-0589-5

34. Irvine DJ, Dane EL. Enhancing cancer immunotherapy with nanomedicine. *Nat Rev Immunol* (2020) 20(5):321–34. doi: 10.1038/s41577-019-0269-6

35. Kim D, Wu Y, Li Q, Oh YK. Nanoparticle-mediated lipid metabolic reprogramming of T cells in tumor microenvironments for immunometabolic therapy. *Nanomicro Lett* (2021) 13(1):31. doi: 10.1007/s40820-020-00555-6

36. Chowdhury PS, Chamoto K, Kumar A, Honjo T. Ppar-induced fatty acid oxidation in T cells increases the number of tumor-reactive Cd8(+) T cells and facilitates anti-Pd-1 therapy. *Cancer Immunol Res* (2018) 6(11):1375–87. doi: 10.1158/2326-6066.CIR-18-0095

37. Ma X, Xiao L, Liu L, Ye L, Su P, Bi E, et al. Cd36-mediated ferroptosis dampens intratumoral Cd8(+) T cell effector function and impairs their antitumor ability. *Cell Metab* (2021) 33(5):1001–12.e5. doi: 10.1016/j.cmet.2021.02.015

38. Xu S, Chaudhary O, Rodriguez-Morales P, Sun X, Chen D, Zappasodi R, et al. Uptake of oxidized lipids by the scavenger receptor Cd36 promotes lipid peroxidation and dysfunction in Cd8(+) T cells in tumors. *Immunity* (2021) 54 (7):1561–77.e7. doi: 10.1016/j.immuni.2021.05.003

39. Liu X, Hartman CL, Li L, Albert CJ, Si F, Gao A, et al. Reprogramming lipid metabolism prevents effector T cell senescence and enhances tumor immunotherapy. *Sci Transl Med* (2021) 13(587):6314. doi: 10.1126/scitranslmed.aaz6314

40. Ma X, Bi E, Lu Y, Su P, Huang C, Liu L, et al. Cholesterol induces Cd8(+) T cell exhaustion in the tumor microenvironment. *Cell Metab* (2019) 30(1):143–56.e5. doi: 10.1016/j.cmet.2019.04.002

41. Ma X, Bi E, Huang C, Lu Y, Xue G, Guo X, et al. Cholesterol negatively regulates il-9-Producing Cd8(+) T cell differentiation and antitumor activity. *J Exp Med* (2018) 215(6):1555–69. doi: 10.1084/jem.20171576

42. Yang W, Bai Y, Xiong Y, Zhang J, Chen S, Zheng X, et al. Potentiating the antitumour response of Cd8(+) T cells by modulating cholesterol metabolism. *Nature* (2016) 531(7596):651–5. doi: 10.1038/nature17412

43. Whiteside TL. Foxp3+ treg as a therapeutic target for promoting anti-tumor immunity. *Expert Opin Ther Targets* (2018) 22(4):353–63. doi: 10.1080/14728222.2018.1451514

44. Xu C, Sun S, Johnson T, Qi R, Zhang S, Zhang J, et al. The glutathione peroxidase Gpx4 prevents lipid peroxidation and ferroptosis to sustain treg cell activation and suppression of antitumor immunity. *Cell Rep* (2021) 35(11):109235. doi: 10.1016/j.celrep.2021.109235

45. Wawman RE, Bartlett H, Oo YH. Regulatory T cell metabolism in the hepatic microenvironment. *Front Immunol* (2017) 8:1889. doi: 10.3389/fimmu.2017.01889

46. Pacella I, Procaccini C, Focaccetti C, Miacci S, Timperi E, Faicchia D, et al. Fatty acid metabolism complements glycolysis in the selective regulatory T cell expansion during tumor growth. *Proc Natl Acad Sci U.S.A.* (2018) 115(28):E6546–E55. doi: 10.1073/pnas.1720113115

47. Patsoukis N, Bardhan K, Chatterjee P, Sari D, Liu B, Bell LN, et al. Pd-1 alters T-cell metabolic reprogramming by inhibiting glycolysis and promoting lipolysis and fatty acid oxidation. *Nat Commun* (2015) 6:6692. doi: 10.1038/ncomms7692

48. Field CS, Baixauli F, Kyle RL, Puleston DJ, Cameron AM, Sanin DE, et al. Mitochondrial integrity regulated by lipid metabolism is a cell-intrinsic checkpoint for treg suppressive function. *Cell Metab* (2020) 31(2):422–37.e5. doi: 10.1016/j.cmet.2019.11.021

49. Lim SA, Wei J, Nguyen TM, Shi H, Su W, Palacios G, et al. Lipid signalling enforces functional specialization of treg cells in tumours. *Nature* (2021) 591 (7849):306–11. doi: 10.1038/s41586-021-03235-6

50. Zeng H, Yang K, Cloer C, Neale G, Vogel P, Chi H. Mtorc1 couples immune signals and metabolic programming to establish T(Reg)-cell function. *Nature* (2013) 499(7459):485–90. doi: 10.1038/nature12297

51. Cheng HY, Gaddis DE, Wu R, McSkimming C, Haynes LD, Taylor AM, et al. Loss of Abcg1 influences regulatory T cell differentiation and atherosclerosis. *J Clin Invest* (2016) 126(9):3236–46. doi: 10.1172/JCI83136

52. Schreiber S, Hammers CM, Kaasch AJ, Schraven B, Dudeck A, Kahlfuss S. Metabolic interdependency of Th2 cell-mediated type 2 immunity and the tumor microenvironment. *Front Immunol* (2021) 12:632581. doi: 10.3389/fimmu.2021.632581

53. Simson L, Ellyard JI, Parish CR. The role of Th2-mediated anti-tumor immunity in tumor surveillance and clearance. *Cancer Ige.* (2010) 255–75. doi: 10.1007/978-1-60761-451-7_11

54. Shen H, Shi LZ. Metabolic regulation of Th17 cells. *Mol Immunol* (2019) 109:81–7. doi: 10.1016/j.molimm.2019.03.005

55. Wilke CM, Bishop K, Fox D, Zou W. Deciphering the role of Th17 cells in human disease. *Trends Immunol* (2011) 32(12):603–11. doi: 10.1016/j.it.2011.08.003

56. Qianmei Y, Zehong S, Guang W, Hui L, Lian G. Recent advances in the role of Th17/Treg cells in tumor immunity and tumor therapy. *Immunol Res* (2021) 69 (5):398–414. doi: 10.1007/s12026-021-09211-6

57. Wang C, Yosef N, Gaublomme J, Wu C, Lee Y, Clish CB, et al. Cd5l/Aim regulates lipid biosynthesis and restrains Th17 cell pathogenicity. *Cell* (2015) 163 (6):1413–27. doi: 10.1016/j.cell.2015.10.068

58. Dinç Akbulut G, ÖZkazanÇ D, EsendaĞLi G. Th1 cells in cancer-associated inflammation. *Turkish J Biol* (2017) 41:20–30. doi: 10.3906/biy-1602-20

59. Clarke CJ. Neutral sphingomyelinases in cancer: Friend or foe? *Adv Cancer Res* (2018) 140:97–119. doi: 10.1016/bs.acr.2018.04.010

60. Montfort A, Bertrand F, Rochotte J, Gilhodes J, Filleron T, Milhes J, et al. Neutral sphingomyelinase 2 heightens anti-melanoma immune responses and anti-Pd-1 therapy efficacy. *Cancer Immunol Res* (2021) 9(5):568–82. doi: 10.1158/2326-6066.CIR-20-0342

61. Ogretmen B. Sphingolipid metabolism in cancer signalling and therapy. *Nat Rev Cancer* (2018) 18(1):33–50. doi: 10.1038/nrc.2017.96

62. Bai A, Guo Y. Acid sphingomyelinase mediates human Cd4(+) T-cell signaling: Potential roles in T-cell responses and diseases. *Cell Death Dis* (2017) 8(7):e2963. doi: 10.1038/cddis.2017.360

63. Khurana P, Burudpakdee C, Grupp SA, Beier UH, Barrett DM, Bassiri H. Distinct bioenergetic features of human invariant natural killer T cells enable retained functions in nutrient-deprived states. *Front Immunol* (2021) 12:700374. doi: 10.3389/fimmu.2021.700374

64. Dong H, Bullock TN. Metabolic influences that regulate dendritic cell function in tumors. *Front Immunol* (2014) 5:24. doi: 10.3389/fimmu.2014.00024

65. Ibrahim J, Nguyen AH, Rehman A, Ochi A, Jamal M, Graffeo CS, et al. Dendritic cell populations with different concentrations of lipid regulate tolerance and immunity in mouse and human liver. *Gastroenterology* (2012) 143(4):1061–72. doi: 10.1053/j.gastro.2012.06.003

66. Giovanelli P, Sandoval TA, Cubillos-Ruiz JR. Dendritic cell metabolism and function in tumors. *Trends Immunol* (2019) 40(8):699–718. doi: 10.1016/j.it.2019.06.004

67. Nguyen-Phuong T, Chung H, Jang J, Kim JS, Park CG. Acetyl-coa carboxylase-1/2 blockade locks dendritic cells in the semimature state associated with fa deprivation by favoring fao. *J Leukoc Biol* (2022) 111(3):539–51. doi: 10.1002/JLB.1A0920-561RR

68. Li C, Song B, Santos PM, Butterfield LH. Hepatocellular cancer-derived alpha fetoprotein uptake reduces Cd1 molecules on monocyte-derived dendritic cells. *Cell Immunol* (2019) 335:59–67. doi: 10.1016/j.cellimm.2018.10.011

69. Santos PM, Menk AV, Shi J, Tsung A, Delgoffe GM, Butterfield LH. Tumor-derived alpha-fetoprotein suppresses fatty acid metabolism and oxidative phosphorylation in dendritic cells. *Cancer Immunol Res* (2019) 7(6):1001–12. doi: 10.1158/2326-6066.CIR-18-0513

70. Gao F, Liu C, Guo J, Sun W, Xian L, Bai D, et al. Radiation-driven lipid accumulation and dendritic cell dysfunction in cancer. *Sci Rep* (2015) 5:9613. doi: 10.1038/srep09613

71. Jiang L, Fang X, Wang H, Li D, Wang X. Ovarian cancer-intrinsic fatty acid synthase prevents anti-tumor immunity by disrupting tumor-infiltrating dendritic cells. *Front Immunol* (2018) 9:2927. doi: 10.3389/fimmu.2018.02927

72. Herber DL, Cao W, Nefedova Y, Novitskiy SV, Nagaraj S, Tyurin VA, et al. Lipid accumulation and dendritic cell dysfunction in cancer. *Nat Med* (2010) 16 (8):880–6. doi: 10.1038/nm.2172

73. Yin X, Zeng W, Wu B, Wang L, Wang Z, Tian H, et al. Pparalpha inhibition overcomes tumor-derived exosomal lipid-induced dendritic cell dysfunction. *Cell Rep* (2020) 33(3):108278. doi: 10.1016/j.celrep.2020.108278

74. Zhao F, Xiao C, Evans KS, Theivanthiran T, DeVito N, Holtzhausen A, et al. Paracrine Wnt5a-Beta-Catenin signaling triggers a metabolic program that drives dendritic cell tolerization. *Immunity* (2018) 48(1):147–60.e7. doi: 10.1016/j.immuni.2017.12.004

75. Ramakrishnan R, Tyurin VA, Veglia F, Condamine T, Amoscato A, Mohammadyani D, et al. Oxidized lipids block antigen cross-presentation by dendritic cells in cancer. *J Immunol* (2014) 192(6):2920–31. doi: 10.4049/jimmunol.1302801

76. Gilardini Montani MS, Benedetti R, Piconese S, Pulcinelli FM, Timperio AM, Romeo MA, et al. Pge2 released by pancreatic cancer cells undergoing er stress transfers the stress to dcs impairing their immune function. *Mol Cancer Ther* (2021) 20(5):934–45. doi: 10.1158/1535-7163.Mct-20-0699

77. Amberger DC, Doraneh-Gard F, Gunsilius C, Weinmann M, Möbius S, Kugler C, et al. Pge(1)-containing protocols generate mature (Leukemia-derived) dendritic cells directly from leukemic whole blood. *Int J Mol Sci* (2019) 20(18):4590. doi: 10.3390/ijms20184590

78. Huang J, Diao G, Zhang Q, Chen Y, Han J, Guo J. E6–Regulated overproduction of prostaglandin e2 may inhibit migration of dendritic cells in human papillomavirus 16–Positive cervical lesions. *Int J Oncol* (2020) 56(4):921–31. doi: 10.3892/ijo.2020.4983

79. Trempolec N, Degavre C, Doix B, Brusa D, Corbet C, Feron O. Acidosis-induced tgf-Beta2 production promotes lipid droplet formation in dendritic cells and alters their potential to support anti-mesothelioma T cell response. *Cancers (Basel)* (2020) 12(5):1284. doi: 10.3390/cancers12051284

80. Veglia F, Tyurin VA, Mohammadyani D, Blasi M, Duperret EK, Donthireddy L, et al. Lipid bodies containing oxidatively truncated lipids block antigen cross-presentation by dendritic cells in cancer. *Nat Commun* (2017) 8(1):2122. doi: 10.1038/s41467-017-02186-9

81. Menzner AK, Rottmar T, Voelkl S, Bosch JJ, Mougiakakos D, Mackensen A, et al. Hydrogen-peroxide synthesis and ldl-uptake controls immunosuppressive properties in monocyte-derived dendritic cells. *Cancers (Basel)* (2021) 13(3):461. doi: 10.3390/cancers13030461

82. Hofer F, Di Sario G, Musiu C, Sartoris S, De Sanctis F, Ugel S. A complex metabolic network confers immunosuppressive functions to myeloid-derived suppressor cells (Mdscs) within the tumour microenvironment. *Cells* (2021) 10(10):2700. doi: 10.3390/cells10102700

83. Gabitass RF, Annels NE, Stocken DD, Pandha HA, Middleton GW. Elevated myeloid-derived suppressor cells in pancreatic, esophageal and gastric cancer are an independent prognostic factor and are associated with significant elevation of the Th2 cytokine interleukin-13. *Cancer Immunol Immunother* (2011) 60(10):1419–30. doi: 10.1007/s00262-011-1028-0

84. Safarzadeh E, Orangi M, Mohammadi H, Babaie F, Baradaran B. Myeloid-derived suppressor cells: Important contributors to tumor progression and metastasis. *J Cell Physiol* (2018) 233(4):3024–36. doi: 10.1002/jcp.26075

85. Hossain F, Al-Khami AA, Wyczechowska D, Hernandez C, Zheng L, Reiss K, et al. Inhibition of fatty acid oxidation modulates immunosuppressive functions of myeloid-derived suppressor cells and enhances cancer therapies. *Cancer Immunol Res* (2015) 3(11):1236–47. doi: 10.1158/2326-6066.CIR-15-0036

86. Al-Khami AA, Zheng L, Del Valle L, Hossain F, Wyczechowska D, Zabaleta J, et al. Exogenous lipid uptake induces metabolic and functional reprogramming of tumor-associated myeloid-derived suppressor cells. *Oncoimmunology* (2017) 6(10):e1344804. doi: 10.1080/2162402X.2017.1344804

87. Veglia F, Tyurin VA, Blasi M, De Leo A, Kossenkov AV, Donthireddy L, et al. Fatty acid transport protein 2 reprograms neutrophils in cancer. *Nature* (2019) 569(7754):73–8. doi: 10.1038/s41586-019-1118-2

88. Wong JL, Obermajer N, Odunsi K, Edwards RP, Kalinski P. Synergistic Cox2 induction by ifngamma and tnfalpha self-limits type-1 immunity in the human tumor microenvironment. *Cancer Immunol Res* (2016) 4(4):303–11. doi: 10.1158/2326-6066.CIR-15-0157

89. Prima V, Kaliberova LN, Kaliberov S, Curiel DT, Kusmartsev S. Cox2/Mpges1/Pge2 pathway regulates pd-L1 expression in tumor-associated macrophages and myeloid-derived suppressor cells. *Proc Natl Acad Sci U.S.A.* (2017) 114(5):1117–22. doi: 10.1073/pnas.1612920114

90. Mohammadpour H, MacDonald CR, McCarthy PL, Abrams SI, Repasky EA. Beta2-adrenergic receptor signaling regulates metabolic pathways critical to myeloid-derived suppressor cell function within the tme. *Cell Rep* (2021) 37(4):109883. doi: 10.1016/j.celrep.2021.109883

91. Condamine T, Dominguez GA, Youn JI, Kossenkov AV, Mony S, Alicea-Torres K, et al. Lectin-type oxidized ldl receptor-1 distinguishes population of human polymorphonuclear myeloid-derived suppressor cells in cancer patients. *Sci Immunol* (2016) 1(2):aaf8943. doi: 10.1126/sciimmunol.aaf8943

92. Chai E, Zhang L, Li C. Lox-1+ pmn-mdsc enhances immune suppression which promotes glioblastoma multiforme progression. *Cancer Manag Res* (2019) 11:7307–15. doi: 10.2147/CMAR.S210545

93. Bleve A, Durante B, Sica A, Consonni FM. Lipid metabolism and cancer immunotherapy: Immunosuppressive myeloid cells at the crossroad. *Int J Mol Sci* (2020) 21(16):5845. doi: 10.3390/ijms21165845

94. Paul S, Lal G. The molecular mechanism of natural killer cells function and its importance in cancer immunotherapy. *Front Immunol* (2017) 8:1124. doi: 10.3389/fimmu.2017.01124

95. Niavarani SR, Lawson C, Bakos O, Boudaud M, Batenchuk C, Rouleau S, et al. Lipid accumulation impairs natural killer cell cytotoxicity and tumor control in the postoperative period. *BMC Cancer* (2019) 19(1):823. doi: 10.1186/s12885-019-6045-y

96. Bonavita E, Bromley CP, Jonsson G, Pelly VS, Sahoo S, Walwyn-Brown K, et al. Antagonistic inflammatory phenotypes dictate tumor fate and response to immune checkpoint blockade. *Immunity* (2020) 53(6):1215–29.e8. doi: 10.1016/j.immuni.2020.10.020

97. Zorov DB, Juhaszova M, Sollott SJ. Mitochondrial reactive oxygen species (Ros) and ros-induced ros release. *Physiol Rev* (2014) 94(3):909–50. doi: 10.1152/physrev.00026.2013

98. Sormendi S, Wielockx B. Hypoxia pathway proteins as central mediators of metabolism in the tumor cells and their microenvironment. *Front Immunol* (2018) 9:40. doi: 10.3389/fimmu.2018.00040

99. Riera-Domingo C, Audige A, Granja S, Cheng WC, Ho PC, Baltazar F, et al. Immunity, hypoxia, and metabolism-the menage a trois of cancer: Implications for immunotherapy. *Physiol Rev* (2020) 100(1):1–102. doi: 10.1152/physrev.00018.2019

100. De Santis M, Locati M, Selmi C. The elegance of a macrophage. *Cell Mol Immunol* (2018) 15(3):196–8. doi: 10.1038/cmi.2017.64

101. Mortezaee K, Majidpoor J. The impact of hypoxia on immune state in cancer. *Life Sci* (2021) 286:120057. doi: 10.1016/j.lfs.2021.120057

102. Ge Y, Yoon SH, Jang H, Jeong JH, Lee YM. Decursin promotes hif-1alpha proteasomal degradation and immune responses in hypoxic tumour microenvironment. *Phytomedicine* (2020) 78:153318. doi: 10.1016/j.phymed.2020.153318

103. Moniz S, Biddlestone J, Rocha S. Grow(2): The hif system, energy homeostasis and the cell cycle. *Histol Histopathol* (2014) 29(5):589–600. doi: 10.14670/HH-29.10.589

104. Velica P, Cunha PP, Vojnovic N, Foskolou IP, Bargiela D, Gojkovic M, et al. Modified hypoxia-inducible factor expression in Cd8(+) T cells increases antitumor efficacy. *Cancer Immunol Res* (2021) 9(4):401–14. doi: 10.1158/2326-6066.CIR-20-0561

105. Waickman AT, Powell JD. Mtor, metabolism, and the regulation of T-cell differentiation and function. *Immunol Rev* (2012) 249(1):43–58. doi: 10.1111/j.1600-065X.2012.01152.x

106. Nakamura H, Makino Y, Okamoto K, Poellinger L, Ohnuma K, Morimoto C, et al. Tcr engagement increases hypoxia-inducible factor-1 alpha protein synthesis *Via* rapamycin-sensitive pathway under hypoxic conditions in human peripheral T cells. *J Immunol* (2005) 174(12):7592–9. doi: 10.4049/jimmunol.174.12.7592

107. Miska J, Lee-Chang C, Rashidi A, Muroski ME, Chang AL, Lopez-Rosas A, et al. Hif-1alpha is a metabolic switch between glycolytic-driven migration and oxidative phosphorylation-driven immunosuppression of tregs in glioblastoma. *Cell Rep* (2019) 27(1):226–37 e4. doi: 10.1016/j.celrep.2019.03.029

108. Park A, Lee Y, Kim MS, Kang YJ, Park YJ, Jung H, et al. Prostaglandin E2 secreted by thyroid cancer cells contributes to immune escape through the suppression of natural killer (Nk) cell cytotoxicity and nk cell differentiation. *Front Immunol* (2018) 9:1859. doi: 10.3389/fimmu.2018.01859

109. Ni J, Wang X, Stojanovic A, Zhang Q, Wincher M, Bühler L, et al. Single-cell rna sequencing of tumor-infiltrating nk cells reveals that inhibition of transcription factor hif-1α unleashes nk cell activity. *Immunity* (2020) 52(6):1075–87.e8. doi: 10.1016/j.immuni.2020.05.001

110. Viola A, Munari F, Sanchez-Rodriguez R, Scolaro T, Castegna A. The metabolic signature of macrophage responses. *Front Immunol* (2019) 10:1462. doi: 10.3389/fimmu.2019.01462

111. Semba H, Takeda N, Isagawa T, Sugiura Y, Honda K, Wake M, et al. Hif-1alpha-Pdk1 axis-induced active glycolysis plays an essential role in macrophage migratory capacity. *Nat Commun* (2016) 7:11635. doi: 10.1038/ncomms11635

112. Alexander RK, Liou YH, Knudsen NH, Starost KA, Xu C, Hyde AL, et al. Bmal1 integrates mitochondrial metabolism and macrophage activation. *Elife* (2020) 9:e54090. doi: 10.7554/eLife.54090

113. Zhihua Y, Yulin T, Yibo W, Wei D, Yin C, Jiahao X, et al. Hypoxia decreases macrophage glycolysis and M1 percentage by targeting microrna-30c and mtor in human gastric cancer. *Cancer Sci* (2019) 110(8):2368–77. doi: 10.1111/cas.14110

114. He Z, Zhang S. Tumor-associated macrophages and their functional transformation in the hypoxic tumor microenvironment. *Front Immunol* (2021) 12:741305. doi: 10.3389/fimmu.2021.741305

115. Chang WH, Lai AG. The pan-cancer mutational landscape of the ppar pathway reveals universal patterns of dysregulated metabolism and interactions with tumor immunity and hypoxia. *Ann N Y Acad Sci* (2019) 1448(1):65–82. doi: 10.1111/nyas.14170

116. Liu M, Wang X, Wang L, Ma X, Gong Z, Zhang S, et al. Targeting the Ido1 pathway in cancer: From bench to bedside. *J Hematol Oncol* (2018) 11(1):100. doi: 10.1186/s13045-018-0644-y

117. Feng J, Yang H, Zhang Y, Wei H, Zhu Z, Zhu B, et al. Tumor cell-derived lactate induces taz-dependent upregulation of pd-L1 through Gpr81 in human lung cancer cells. *Oncogene* (2017) 36(42):5829–39. doi: 10.1038/onc.2017.188

118. Pucino V, Certo M, Bulusu V, Cucchi D, Goldmann K, Pontarini E, et al. Lactate buildup at the site of chronic inflammation promotes disease by inducing Cd4(+) T cell metabolic rewiring. *Cell Metab* (2019) 30(6):1055–74 e8. doi: 10.1016/j.cmet.2019.10.004

119. Salminen A, Kauppinen A, Kaarniranta K. Ampk activation inhibits the functions of myeloid-derived suppressor cells (Mdsc): Impact on cancer and aging. *J Mol Med (Berl)* (2019) 97(8):1049–64. doi: 10.1007/s00109-019-01795-9

120. Fu S, He K, Tian C, Sun H, Zhu C, Bai S, et al. Impaired lipid biosynthesis hinders anti-tumor efficacy of intratumoral inkt cells. *Nat Commun* (2020) 11 (1):438. doi: 10.1038/s41467-020-14332-x

121. Adeshakin AO, Liu W, Adeshakin FO, Afolabi LO, Zhang M, Zhang G, et al. Regulation of ros in myeloid-derived suppressor cells through targeting fatty acid transport protein 2 enhanced anti-Pd-L1 tumor immunotherapy. *Cell Immunol* (2021) 362:104286. doi: 10.1016/j.cellimm.2021.104286

122. Yousefi H, Yuan J, Keshavarz-Fathi M, Murphy JF, Rezaei N. Immunotherapy of cancers comes of age. *Expert Rev Clin Immunol* (2017) 13 (10):1001–15. doi: 10.1080/1744666X.2017.1366315

123. He X, Xu C. Immune checkpoint signaling and cancer immunotherapy. *Cell Res* (2020) 30(8):660–9. doi: 10.1038/s41422-020-0343-4

124. Paijens ST, Vledder A, de Bruyn M, Nijman HW. Tumor-infiltrating lymphocytes in the immunotherapy era. *Cell Mol Immunol* (2021) 18(4):842–59. doi: 10.1038/s41423-020-00565-9

125. Zhao L, Cao YJ. Engineered T cell therapy for cancer in the clinic. *Front Immunol* (2019) 10:2250. doi: 10.3389/fimmu.2019.02250

126. Wang L, Dou M, Ma Q, Yao R, Liu J. Chimeric antigen receptor (Car)-modified nk cells against cancer: Opportunities and challenges. *Int Immunopharmacol* (2019) 74:105695. doi: 10.1016/j.intimp.2019.105695

127. Sloas C, Gill S, Klichinsky M. Engineered car-macrophages as adoptive immunotherapies for solid tumors. *Front Immunol* (2021) 12:783305. doi: 10.3389/fimmu.2021.783305

128. Sabado RL, Balan S, Bhardwaj N. Dendritic cell-based immunotherapy. *Cell Res* (2017) 27(1):74–95. doi: 10.1038/cr.2016.157

129. Su P, Wang Q, Bi E, Ma X, Liu L, Yang M, et al. Enhanced lipid accumulation and metabolism are required for the differentiation and activation of tumor-associated macrophages. *Cancer Res* (2020) 80(7):1438–50. doi: 10.1158/0008-5472.CAN-19-2994

130. Odorizzi PM, Pauken KE, Paley MA, Sharpe A, Wherry EJ. Genetic absence of pd-1 promotes accumulation of terminally differentiated exhausted Cd8+ T cells. *J Exp Med* (2015) 212(7):1125–37. doi: 10.1084/jem.20142237

131. Hu B, Lin JZ, Yang XB, Sang XT. Aberrant lipid metabolism in hepatocellular carcinoma cells as well as immune microenvironment: A review. *Cell Prolif* (2020) 53(3):e12772. doi: 10.1111/cpr.12772

132. Rabold K, Aschenbrenner A, Thiele C, Boahen CK, Schiltmans A, Smit JWA, et al. Enhanced lipid biosynthesis in human tumor-induced macrophages contributes to their protumoral characteristics. *J Immunother Cancer* (2020) 8(2): e000638. doi: 10.1136/jitc-2020-000638

133. Gualdoni GA, Mayer KA, Goschl L, Boucheron N, Ellmeier W, Zlabinger GJ. The amp analog aicar modulates the Treg/Th17 axis through enhancement of fatty acid oxidation. *FASEB J* (2016) 30(11):3800–9. doi: 10.1096/fj.201600522R

134. Tavazoie MF, Pollack I, Tanqueco R, Ostendorf BN, Reis BS, Gonsalves FC, et al. Lxr/Apoe activation restricts innate immune suppression in cancer. *Cell* (2018) 172(4):825–40.e18. doi: 10.1016/j.cell.2017.12.026

135. Okoye I, Namdar A, Xu L, Crux N, Elahi S. Atorvastatin downregulates Co-inhibitory receptor expression by targeting ras-activated mtor signalling. *Oncotarget* (2017) 8(58):98215–32. doi: 10.18632/oncotarget.21003

136. Pandey VK, Amin PJ, Shankar BS. Cox-2 inhibitor prevents tumor induced down regulation of classical dc lineage specific transcription factor Zbtb46 resulting in immunocompetent dc and decreased tumor burden. *Immunol Lett* (2017) 184:23–33. doi: 10.1016/j.imlet.2017.01.019

137. den Brok MH, Bull C, Wassink M, de Graaf AM, Wagenaars JA, Minderman M, et al. Saponin-based adjuvants induce cross-presentation in dendritic cells by intracellular lipid body formation. *Nat Commun* (2016) 7:13324. doi: 10.1038/ncomms13324

138. Kalathil S, Lugade AA, Miller A, Iyer R, Thanavala Y. Higher frequencies of Garp(+)Ctla-4(+)Foxp3(+) T regulatory cells and myeloid-derived suppressor cells in hepatocellular carcinoma patients are associated with impaired T-cell functionality. *Cancer Res* (2013) 73(8):2435–44. doi: 10.1158/0008-5472.CAN-12-3381

139. Fan C, Zhang S, Gong Z, Li X, Xiang B, Deng H, et al. Emerging role of metabolic reprogramming in tumor immune evasion and immunotherapy. *Sci China Life Sci* (2021) 64(4):534–47. doi: 10.1007/s11427-019-1735-4

140. Engblom C, Pfirschke C, Pittet MJ. The role of myeloid cells in cancer therapies. *Nat Rev Cancer* (2016) 16(7):447–62. doi: 10.1038/nrc.2016.54

Glossary

TME	tumor microenvironment
OXPHOS	oxidative phosphorylation
FAO	fatty acid oxidation
FAS	fatty acid synthesis
LD	lipid droplet
DC	dendritic cell
NK	natural killer cell
MDSC	myeloid-derived suppressor cell
N	neutrophils
TAM	tumor-associated macrophage
PPAR	peroxisome proliferator-activated receptor
RIPK3	receptor-interacting protein kinase 3
HCC	hepatocellular carcinoma
MDM	M2 monocyte-derived macrophage
MGLL	monoacylglycerol lipase
FAs	fatty acids
SREBP	sterol regulatory element-binding protein
IFN-γ	interferon-γ
CTL	cytotoxic T lymphocyte
NKT	natural killer T cell
T_{reg}	regulatory T cell
Th	helper T cell
Tfh	follicular helper T cell
OxLDL	oxidized low-density lipoprotein
TGF-β	transforming growth factor-β
FASN	fatty acid synthase
CPT1A	carnitine palmitoyltransferase-1A
FABP	fatty acid-binding proteins
AMPK	adenosine monophosphate-activated protein kinase
AFP	alpha-fetoprotein
LB	lipid body
NOS	nitric oxide synthase
HIF	hypoxia-inducible factor
Teff	effector T cells

frontiers | Frontiers in Immunology

TYPE Review
PUBLISHED 14 October 2022
DOI 10.3389/fimmu.2022.1030831

OPEN ACCESS

EDITED BY
Xuyu Gu,
Southeast University, China

REVIEWED BY
Jie Tang,
The University of Queensland, Australia
Yiqing Zhao,
Case Western Reserve University, United States

*CORRESPONDENCE
Xiao Liang
xiaoliang9101@163.com

SPECIALTY SECTION
This article was submitted to Cancer Immunity and Immunotherapy, a section of the journal Frontiers in Immunology

RECEIVED 29 August 2022
ACCEPTED 29 September 2022
PUBLISHED 14 October 2022

CITATION
Lin Y, Zhou X, Ni Y, Zhao X and Liang X (2022) Metabolic reprogramming of the tumor immune microenvironment in ovarian cancer: A novel orientation for immunotherapy.
Front. Immunol. 13:1030831.
doi: 10.3389/fimmu.2022.1030831

Metabolic reprogramming of the tumor immune microenvironment in ovarian cancer: A novel orientation for immunotherapy

Yi Lin, Xiaoting Zhou, Yanghong Ni, Xia Zhao and Xiao Liang*

Department of Gynecology and Obstetrics, Key Laboratory of Obstetrics & Gynecologic and Pediatric Diseases and Birth Defects of Ministry of Education, Development and Related Diseases of Women and Children Key Laboratory of Sichuan Province, West China Second Hospital, Sichuan University, Chengdu, China

Ovarian cancer is the most lethal gynecologic tumor, with the highest mortality rate. Numerous studies have been conducted on the treatment of ovarian cancer in the hopes of improving therapeutic outcomes. Immune cells have been revealed to play a dual function in the development of ovarian cancer, acting as both tumor promoters and tumor suppressors. Increasingly, the tumor immune microenvironment (TIME) has been proposed and confirmed to play a unique role in tumor development and treatment by altering immunosuppressive and cytotoxic responses in the vicinity of tumor cells through metabolic reprogramming. Furthermore, studies of immunometabolism have provided new insights into the understanding of the TIME. Targeting or activating metabolic processes of the TIME has the potential to be an antitumor therapy modality. In this review, we summarize the composition of the TIME of ovarian cancer and its metabolic reprogramming, its relationship with drug resistance in ovarian cancer, and recent research advances in immunotherapy.

KEYWORDS

ovarian cancer, tumor immune microenvironment, metabolic reprogramming, metabolism, immunotherapy

1 Introduction

Ovarian cancer (OC) is the most lethal gynecological neoplasm due to its high mortality (1–3). Due to inadequate early detection methods and few early symptoms, ovarian cancer is the most challenging disease to identify in the female reproductive system (4). The majority of patients are frequently identified at an advanced stage, while

therapeutic interventions are relatively limited. Only approximately 16% of patients are diagnosed at an early stage (FIGO I stage) and have a greater possibility of long-term survival (5, 6). The treatment of OC varies depending on its stage and classification (7). OC has an epithelial origin in more than 90% of cases, and high-grade serous ovarian cancer (HGSOC) makes up 70% of these cases (1, 8). According to the National Comprehensive Cancer Network (NCCN) Guidelines, debulking surgery combined with platinum-based chemotherapy is currently the first line of treatment for OC (7). The mortality of OC has decreased globally over the past decade as a result of lifestyle modifications and technological advancements in treatment (9). However, research has shown that early screening does not appear to reduce mortality from OC (10). More frustratingly, regardless of the type of treatment used, approximately 80% of cases of advanced ovarian cancer eventually recur and result in the progression of the disease and death (11). Given these findings, it is imperative to develop novel and reliable therapies and prevent recurrence.

Immune cells are a cluster of different cells that have differentiated from bone marrow hematopoietic stem cells (12). In tumors, immune cells have a dual role, either killing or promoting them (13). Immune cells can even become accomplices of tumor cells in the event of immune escape (14). In this regard, Stephen Paget put forth the well-known "seed and soil" hypothesis, according to which the environment in which a tumor develops determines how that tumor expresses its phenotype (15). The tumor immune microenvironment (TIME) refers to the immune infiltrative microenvironment, which consists of a large number of immune cells clustered within and around the tumor (16). With the advent of high-throughput and single-cell sequencing, research on the TIME has been fueled.

Immunotherapy is the next generation of treatment that is rapidly developing after traditional treatments such as surgery, radiotherapy, and chemotherapy (17). It functions by activating the immune defenses of the human body to eliminate tumor cells (17). A seemingly endless stream of cancer immunotherapies derived from tumor immunity have been developed, including immune checkpoint inhibitors (ICIs), adoptive cellular immunotherapy, tumor vaccines and others (17–19). Among these, ICIs have made significant progress and demonstrated excellent antitumor activity in gynecological cancer (20). However, not all patients with OC are candidates for immunotherapy, and only a small percentage of them will benefit (21, 22). Due to its cool tumor nature, OC has few infiltrating lymphocytes and responds poorly to immunotherapy (22, 23). Indubitably, OC is an immunogenic disease, and its immunogenicity is solely dependent on approximately 13% of $CD8^+$ tumor-infiltrating T cells with a high affinity for antigens (24). Most likely, the underlying cause of drug resistance and treatment failure is metabolic reprogramming (25). Metabolic reprogramming, a hallmark of cancer, is the reprogramming of specific metabolic pathways inside and outside the cell to meet the demands of rapid proliferation by affecting gene expression, cellular state, and the tumor microenvironment (26). It may be crucial to investigate metabolic reprogramming of the TIME to increase therapeutic effectiveness and improve drug resistance in OC. This review focuses on the TIME in OC with an emphasis on its metabolic reprogramming and concludes with immunotherapy related to TIME metabolic reprogramming, with the goal of providing a new vision for immunotherapy in OC.

2 Overview of TIME metabolism in ovarian cancer

Tumors have a complicated metabolic pattern that is a highly adaptable response to hypoxia and nutritional deficiency (25). They have the ability to select the optimal metabolic phenotype based on the microenvironment. The metabolic overview of the ovarian cancer TIME is a network of substance exchange incorporating biochemical reactions. The metabolism of both tumor cells and immune cells is briefly discussed next.

2.1 Metabolism of ovarian cancer cells

Ovarian cancer cells have a heterogeneous metabolism, which means they are able to modify their metabolic patterns in response to their microenvironment (Figure 1A). The metabolic characteristics of ovarian cancer cells can be described as prominent glucose metabolism and lipid metabolism (Figure 1B).

The selection of aerobic glycolysis and oxidative phosphorylation as energy sources is a marked manifestation of the heterogeneity of ovarian cancer (27). Through aerobic glycolysis, often known as the Warburg effect, ovarian cancer cells primarily consume glucose to obtain energy (28). Ovarian cancer tumor cells use a substantial quantity of glucose during this process, which is finally generated and expelled as lactic acid, resulting in a localized hypoxic, hypoglycemic, and acidic microenvironment (29). The local low-glucose environment contributes to the expansion of chemical resistance to paclitaxel in ovarian cancer cells, creating a vicious cycle (30). Mitochondrial oxidative phosphorylation (OXPHOS) and the pentose phosphate pathway (PPP) were upregulated in ovarian cancer cells with metastatic capacity (31, 32). Glutamate is used by ovarian cancer cells in mitochondrial OXPHOS to produce adenosine triphosphate (ATP) and other biomolecules necessary for aggressive expansion and migration (33). Platinum-based chemotherapy increases mitochondrial OXPHOS activity of ovarian cancer cells but contributes to cancer stem cell enrichment (34).

Another characteristic of ovarian cancer cells is abnormal active lipid metabolism, which is intimately associated with tumor progression and metastasis (35). The preferential metastasis of ovarian cancer to lipid-rich tissues such as the omentum suggests that adipocyte-derived fatty acids are a significant source of energy for the rapid spreading and metastasis of ovarian cancer cells (36, 37).

2.2 Metabolism of immune cells in ovarian cancer

TIME has tissue heterogeneity, which means that the type and function of immune cells entering the microenvironment in various cancer types differs substantially. There is a certain gap between the resting and activated states of immune cells in ovarian cancer, as well as between different stages of tumor development. Tumor-infiltrating immune cells are an essential component of the TIME and can be classified as pro-tumor cells (tumor-associated macrophages and myeloid-derived suppressor cells) and antitumor cells (such as effector T cells and natural killer cells). The proportion and distribution of immune cells are crucial for the development and spread of tumors. Table 1 provides a summary of immune cell metabolic propensity in the ovarian cancer TIME.

2.2.1 Natural killer (NK) cells

Natural killer (NK) cells can be cytotoxic as well as immunomodulatory (38, 39). The primary mechanism by which NK cells attack ovarian cancer cells is antibody-dependent cellular cytotoxicity (52). The activation of NK cells depends on aerobic glycolysis (53, 54).

2.2.2 Tumor-associated macrophages (TAMs)

Tumor-associated macrophages (TAMs) are significantly infiltrated in ovarian cancer, and the extent of their polarization is tightly tied to the local microenvironment (55). Under different conditions, TAMs can polarize into two types: M1-TAMs (proinflammatory/antitumor) and M2-TAMs (anti-inflammatory/protumor) (56). The expression of both M1 and M2 markers was elevated in ovarian cancer according to genome-wide expression profiling of TAMs (57). From this, it may be inferred that the monocyte phenotype of ovarian cancer is mixed polarization. The aggressiveness of ovarian cancer is directly related to the degree of infiltration of M2-TAMs. In ovarian cancer, a high M2/M1 ratio indicates a poor prognosis (58). Typically, M1-TAMs rely on aerobic glycolysis, whereas M2-TAMs are more dependent on OXPHOS (40, 41).

2.2.3 T cells

T cells can be classified into a number of subtypes based on their varied roles, and these subtypes also differ in their corresponding metabolic patterns. When naive T cells differentiate into effector T cells (Teffs) in tumors, they switch from relying mostly on OXPHOS for energy to relying primarily on glycolysis (42). Memory T cells (Tmems) show high OXPHOS levels (42, 43). In particular, regulatory T lymphocytes (Tregs) have an immunosuppressive function in tumors, where their recruitment contributes to the immune escape of ovarian cancer (59). Tregs have higher levels of glucose uptake and glycolysis because their genes associated with glucose metabolism are substantially expressed (46). A high glycolytic level of $CD4^+$ Tregs was likewise found in coculture with SKOV3 ovarian cancer cells (46). In addition, Tregs can

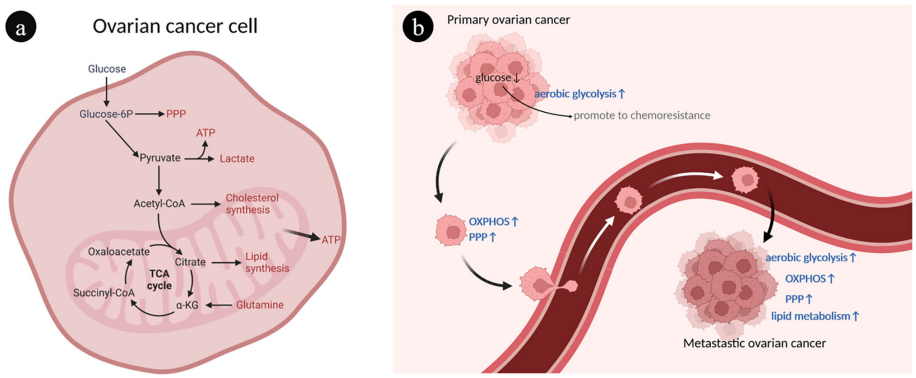

FIGURE 1
Overview of ovarian cancer cell metabolism. **(A)** Interaction of different metabolic pathways within ovarian cancer cells. There are connections between different metabolisms through metabolites. **(B)** The heterogeneity of ovarian cancer metabolism is characterized by abnormal glucose and lipid metabolism. During the development of ovarian cancer, different metabolic phenotypes are gradually acquired, such as enhanced OXPHOS, PPP and FAO. ATP, Adenosine triphosphate; FAO, Fatty acid oxidation; OXPHOS, Oxidative phosphorylation; PPP, Pentose phosphate pathway; TCA, Tricarboxylic acid.

also rely on OXPHOS produced by fatty acid oxidation (FAO) to provide energy (60).

2.2.4 Dendritic cells (DCs)

Dendritic cells are antigen-presenting cells that act as a bridge between innate and cellular immunity. Resting immature DCs primarily utilize mitochondrial β-oxidation of lipids and OXPHOS for energy (44). Glycolytic reprogramming takes place when DCs are activated (44). Early glycolytic reprogramming is supported by glycogen metabolism in DCs (45). The TIME inhibits the function of DCs in malignancies. In the ID8 ovarian cancer mouse model, tumor cells led to overexpression of suppressor of cytokine signaling 3 (SOCS3) in DCs and lowered the activity of the corresponding pyruvate kinase (a crucial enzyme for glycolysis), which inhibited the function of DCs (61).

2.2.5 Myeloid-derived suppressor cells (MDSCs)

A group of immature heterogeneous cells from the bone marrow known as myeloid-derived suppressor cells (MDSCs) have immunosuppressive properties (62). It has been proven that enhanced lipid uptake and FAO by MDSCs activate immunosuppressive mechanisms (48). OXPHOS (fueled by glutamine) and tricarboxylic acid (TCA) cycling were elevated in MDSCs, which were demonstrated to have a high-energy metabolic profile in the ID8 ovarian cancer mouse model (49). Additionally, arginine metabolism is of great importance in MDSCs. MDSCs can regulate T cell function by removing essential metabolites such as arginine from the microenvironment (50). MDSCs were found to be dependent on arginase-1 (ARG1) to exert their T cell immunosuppressive phenotype (51).

The metabolism of immune cells in ovarian cancer is heterogeneous. Immune-activated cells are more dependent on anaerobic glycolysis, whereas immunosuppressive cells tend to use multiple metabolic pathways, including OXPHOS, to meet their energy needs. Modulation and intervention of immune cell metabolic patterns can aid in breaking the immunosuppressive TIME of ovarian cancer.

2.3 Overall metabolism of ovarian cancer patients

Compared to healthy individuals, patients with OC have a generally altered metabolism. The analysis of serum metabolomic data from epithelial ovarian cancer (EOC) revealed considerable heterogeneity in the metabolism of distinct subtypes of ovarian cancer (63). This demonstrates the metabolic heterogeneity of various subtypes in ovarian cancer. For instance, Hishinuma, E., et al. found an increase in tryptophan and its metabolite kynurenine by a wide-target metabolomic analysis of plasma from patients with epithelial ovarian cancer, and a larger ratio in its proportion was associated with a worse prognosis (57). The metabolism of ovarian clear cell carcinoma (OCCC), on the other hand, shows increased expression of glycolysis and oxidative stress genes, as well as improved mitochondrial OXPHOS and glycolysis (64). Additionally, the oncogene ARID1A has loss-of-function mutations in more than 50% of OCCC patients, which leads to decreased glutaminase (GLS) inhibition (65). This consequently contributes to a particular metabolic need for glutamine in OCCC.

Furthermore, metabolism differs between stages of ovarian cancer. Altered metabolism occurs even in the early stages of ovarian cancer. High-accuracy metabolomics detection of early-stage ovarian cancer indicated increased manufacture of fatty acids and cholesterol, as well as increased expression of enzymes that block FAO (66).

TABLE 1 Main metabolic tendencies of immune cells in ovarian cancer.

Cell type	Main metabolic pattern	Function	Refs
Immune activation			
NK cell	Aerobic glycolysis	Cytotoxicity and immunomodulation	(38, 39)
M1-TAM	Glycolysis, PPP	Inflammatory	(40, 41)
Teff	Aerobic glycolysis	Cytotoxicity	(42)
Tmem	OXPHOS	Cytotoxicity and proliferation	(42, 43)
DC	Aerobic glycolysis	Antigen presentation	(44, 45)
Immune suppression			
Treg	OXPHOS	Immune suppression and tolerance	(46)
M2-TAM	OXPHOS	Invasion Metastasis	(40, 41, 47)
MDSC	OXPHOS, FAO, Argnine metabolism	Suppression of the immune response	(48–51)

OXPHOS, Oxidative phosphorylation; PPP, pentose phosphate pathway; TAM, Tumor-associated macrophage; Teff, effector T cell; Tmem, memory T cell; Treg, Regulatory T cell; MDSC, Myeloid-derived suppressor cell; NK, Natural killer.

3 Metabolic reprogramming of the TIME in ovarian cancer based on various factors

How the metabolic reprogramming of the TIME in ovarian cancer occurs is one of the hot topics of research, and multiple factors are now known to influence it. Tumor-derived cytokines, chemokines, and even the metabolic microenvironment (pH, oxygen levels, and nutrition) can have an impact on the metabolism and function of immune cells (29). Metabolic reprogramming is used to carry out the procedure. Here, we will summarize the metabolic reprogramming of the TIME in ovarian cancer in terms of different common metabolic pathways. Finally, the effect of metabolic signaling pathways on TIME reprogramming is added.

3.1 Glucose metabolism

Lactate is a necessary byproduct of glycolysis, and tumor cells in the TIME are extremely dependent on glycolytic capacity, excreting large amounts of lactate, resulting in a localized low glucose, low oxygen, and acidic environment. Kumagai, S., et al. found that in a highly glycolytic tumor microenvironment, Tregs actively take up lactate through monocarboxylate cotransporter 1 (MCT1) and enhance the expression of programmed death receptor 1 (PD-1) by promoting NFAT1 entry into the nucleus (67). However, PD-1 expression was reduced in Teffs (67). As a result, PD-1 treatment was doomed to fail. Furthermore, increased lactate in ovarian cancer promotes the production of VEGF, a potent inducer of angiogenesis in tumors (68). The ensuing cellular invasion is a critical element in the proliferation and metastasis of ovarian cancer. In conjunction with GM-CSF and M-CSF, tumor-derived lactic acidosis in ovarian cancer was discovered to drive macrophage differentiation into a preinflammatory tumor phenotype ($VEGF^{high}$ $CXCL8^{+}$ $IL1\beta^{+}$) (69). Furthermore, sphingosine kinase-1 in A2780 ovarian cancer cells is involved in the induction of aerobic glycolysis (70). This was demonstrated by an increase in lactate levels and expression of the MCT1, as well as a decrease in TCA cycle intermediate accumulation and the production of carbon dioxide (70). A recent study by I. Elia et al. found that tumor-derived lactate could redirect glucose metabolism in $CD8^{+}$ T cells. Specifically, it induced a shift in pyruvate carboxylase activity to pyruvate dehydrogenase (a key enzyme of gluconeogenesis) catalytic reaction, leading to a reduction in the back-supplementation pathway of the TCA cycle, thereby suppressing tumor immunity (71).

Several enzymes involved in glucose metabolism have been implicated in the development of the malignant phenotype of ovarian cancer. Pyruvate kinase is the glycolysis rate-limiting enzyme that catalyzes the conversion of phosphoenolpyruvate and ADP to pyruvate and ATP (72). M-type pyruvate kinase is supportive of anabolic metabolism in cancers, with PKM1 and PKM2 isoforms. Normally proliferating cells are dominated by the high-activity tetrameric form of PKM2, while the low-activity dimeric form is primarily seen in cancer cells (72). TBC1D8 binds to PKM2 *via* its Rab-GAP TBC domain in invasive ovarian cancer cells, preventing PKM2 tetramerization (73). This leads to a decrease in pyruvate kinase activity, promotes aerobic glycolysis and nuclear translocation of PKM2, and induces activation of glucose metabolism and cell cycle-related genes (73). In contrast, SOCS3, which has been shown to be increased in DCs by tumor-derived substances, interacts with PKM2, resulting in decreased ATP generation under hypoxic conditions and a profound effect on the function of DCs (61). Follicle-stimulating hormone (FSH) was found to upregulate the expression of PKM2 and glycolysis in SKOV3 and OVCAR3 ovarian cancer cells in an *in vitro* assay (74).

Glyceraldehyde-3-phosphate dehydrogenase (GAPDH), a glycolytic enzyme, controls IFN-γ production in Teffs by binding to AU-rich elements within the 3' UTR of IFN-γ mRNA (75). As a result, the ability of activated Teffs to produce IFN-γ is severely hampered when they are prohibited from participating in glycolysis even under suitable conditions (75).

In mitochondria, pyruvate is decarboxylated by pyruvate dehydrogenase kinase 1 (PDK1) to generate acetyl coenzyme A (76). It is heavily expressed in ovarian cancer and serves as a crucial hub between glycolysis and the TCA cycle (77). Inhibition of PDK1 could reverse the Warburg effect by switching cytoplasmic glucose metabolism to mitochondrial OXPHOS (78, 79). In ovarian cancer cells, abnormal elevation of PDK1 can upregulate programmed death ligand-1 (PD-L1) expression and induce increased apoptosis of $CD8^{+}$ T cells, ultimately impairing T cell immune function (80). Pyruvate dehydrogenase kinase 2 (PDK2) is favorably connected with the prognosis of OCCC, and increased PDK2 expression decreases apoptosis, resulting in cisplatin resistance in OCCC (81). By increasing the production of reactive oxygen species although mitochondrial metabolism, PDK2 inhibition can synergistically boost sensitivity to cisplatin (81). Another classical metabolic reprogramming occurs in the TCA cycle of macrophages. Macrophages are transferred from the TCA cycle and transform cis-aconitate to itaconic acid by the activity of aconitic acid decarboxylase 1 in the TIME of ovarian cancer (82). Itaconic acid, a metabolite with anti-inflammatory activity, can exert an inhibitory effect on glycolysis (83). A brief schematic of the reprogramming of glycolytic metabolism in ovarian cancer TIME is shown in Figure 2.

3.2 Lipid metabolism

Reprogramming of ovarian cancer cells toward lipid metabolism is the initiating step for metastasis to the peritoneal cavity (84). Ovarian cancer cells can take up exogenous fatty acids (FAs) to promote dissemination in the peritoneal cavity. CD36 (FA receptor) is upregulated in metastatic human ovarian tumors (85). It was shown that ovarian cancer cells that were cocultured with primary human omental adipocytes underwent lipid metabolic reprogramming in the plasma membrane and expressed high levels of CD36 (85). Lipidomic analysis demonstrated that the high levels of polyunsaturated fatty acids, particularly linoleic acid, in ovarian cancer contributed to the tumor-promoting activity of TAMs as an efficient PPARβ/δ agonist (86).

Lysophosphatidic acid (LPA) is an important intermediate in glycerophospholipid metabolism. Through the transcriptional activation of VEGF, stimulation of Fas translocation, and other mechanisms, LPA in ovarian cancer ascites can promote tumor invasion, metastasis, and immune evasion (87, 88). TAMs were found to be a significant source of LPA in ovarian cancer by metabolomics (89). In T lymphoma cells, LPA was found to mediate apoptosis and glucose metabolism, supporting tumor cell survival (90). The corresponding metabolic regulation has yet to be demonstrated in ovarian cancer.

Prostaglandin E-2 (PGE2) is a hormone-like lipid metabolite generated by arachidonic acid *via* cyclooxygenase catalysis (91). Ovarian cancer can enhance proliferation and invasion through the PGE2/nuclear factor-kappa B signaling pathway (92). At the same time, tumor-derived PGE2 controls the production of CXCL12 and CXCR4, thereby inducing the migration of MDSCs to ascites (93, 94). In contrast, MDSC-derived PGE2 not only increases the stem cell-like properties of EOC but also increases PD-L1 expression in tumor cells (95).

3.3 Amino acid metabolism

The metabolism of amino acids has also been dramatically altered in ovarian cancer TIME to accommodate rapid growth. Figure 3 illustrates how amino acid metabolites connect various cells. This entire process entails reprogramming glutamine, arginine, tryptophan, aspartate, and one-carbon metabolism. The details are discussed as follows.

3.3.1 Glutamine

Glutamine is a significant nutrient source for the development of tumor cells (96). Its metabolism is significantly associated with the aggressiveness of OC, where glutamine synthetase (GS) is silenced in ovarian cancer cells in favor of

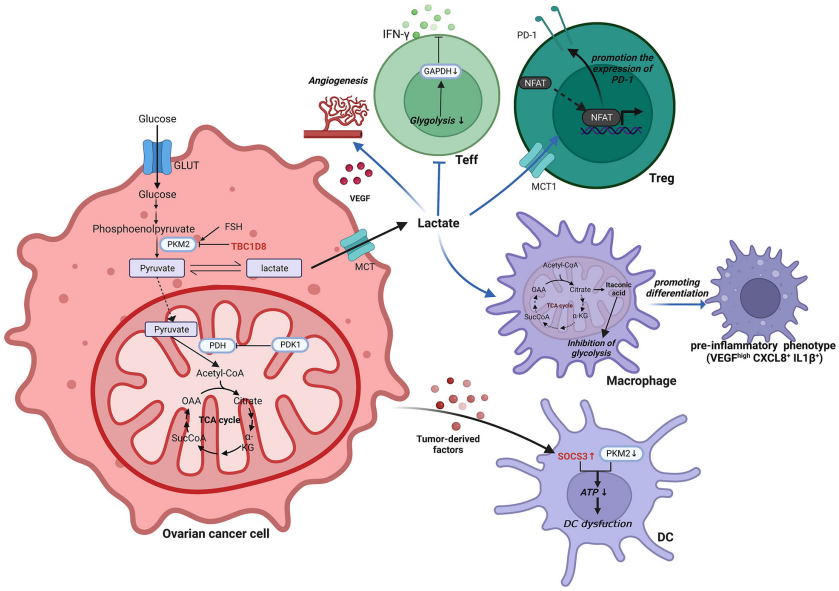

FIGURE 2
Reprogramming of glycolytic metabolism in the TIME of ovarian cancer. In the TIME of ovarian cancer, the reprogramming of glycolytic metabolism occurs in cells such as ovarian cancer cells, T cells, macrophages and DCs, resulting in a suppressive immune microenvironment that facilitates tumorigenesis and progression. ATP, Adenosine triphosphate; CXCL, C-X-C motif chemokine ligand; DC, Dendritic cell; FSH, Follicle-stimulating hormone; GAPDH, Glyceraldehyde-3-phosphate dehydrogenase; GLUT, Glucose transporter; IL, Interleukin; INF-γ, interferon-γ; MCT, Monocarboxylate cotransporter; NFAT, Nuclear factor of activated T cells; OAA, Oxalacetate; PDH, pyruvate dehydrogenase; PDK1, Pyruvate dehydrogenase kinase 1; PD-1, Programmed death receptor 1; PKM2, Pyruvate kinase M2; SOCS3, Cytokine signaling 3; TBC1D8, TBC1 domain family member 8; TCA, Tricarboxylic acid; Teff, effector T cell; Treg, Regulatory T cell; VEGF, Vascular endothelial growth factor.

extracellular glutamine addiction (96, 97). In highly invasive ovarian cancer, macrophages were found to be driven toward the M2-like subtype by glutamine metabolism (98). N-acetylaspartate (NAA) is secreted by ovarian cancer cells as an antagonist to suppress NMDA receptors on macrophages, causing macrophages to assume an M2-like phenotype with increased GS expression (98). Malignant ascites in ovarian cancer patients have reduced glucose uptake, decreased mitochondrial activity and downregulated glutamine carrier abundance in T cells (99, 100). This leads to poor T cell mitochondrial function and evasion of immunity under low glucose conditions.

3.3.2 Arginine

Arginase converts L-arginine to L-ornithine and urea, which is known as the urea cycle. In the early stages of ovarian cancer, arginine metabolism is essential for the activation of T cells and control of immunological responses. In animal experiments, it was discovered that ovarian cancer cells express and release extracellular vesicles (EVs) containing ARG-1, which are taken up by DCs and prevent the proliferation of T cells (101). In contrast, ARG-1 released from activated neutrophils or dead cells induced apoptosis of cancer cells *via* the endoplasmic reticulum stress pathway (102). High amounts of arginine-1 boosted arginine metabolism in Tim-4^{+} TAMs (refilled from circulating monocytes), which in turn improved mitochondrial phagocytic activity in TAMs and ultimately inhibited T cell function (103). So do MDSCs. Strong arginine-1 expression and the production of ROS by MDSCs in human and mouse peritoneal ovarian cancers contribute to the immunosuppression of T cells (51). Arginine deficiency not only causes T cell malfunction but also decreases NK cell survival and cytotoxicity. *In vitro* experiments demonstrated that low L-Arg concentrations reduced the expression of activating receptors, NKp46 and NKp30, as well as the development of the NK zeta chain and the generation of IFN-gamma in NK-92 cell lines (104).

The production of nitric oxide (NO) by nitric oxide synthase is another catabolic mode of arginine. By raising NADPH and glutathione levels, NO lowers ROS levels and promotes glutamine and TCA cycling in ovarian cancer cells (105). Th17 cell growth is aided by physiological NO concentrations produced by MDSCs from ovarian cancer patients (106).

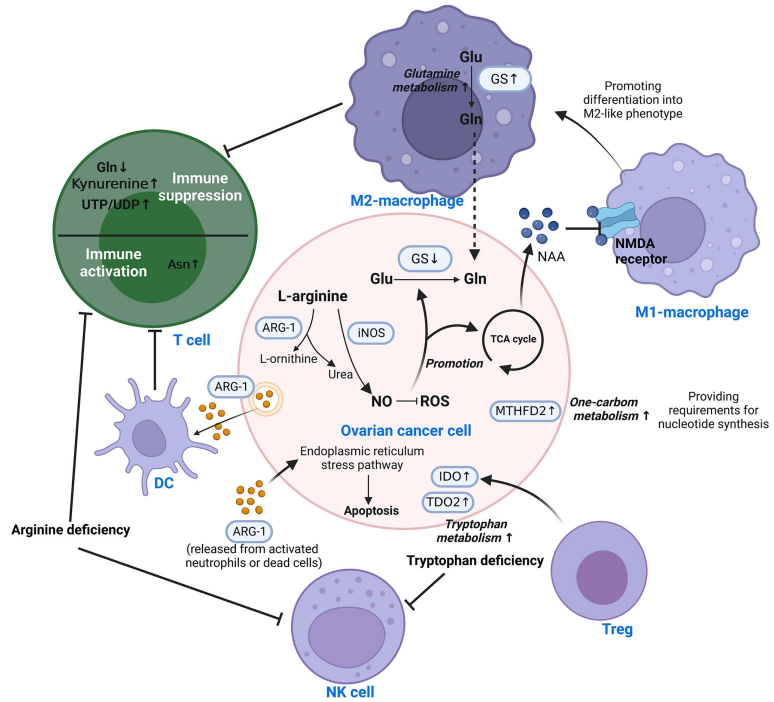

FIGURE 3
Reprogramming of amino acid metabolism in the TIME of ovarian cancer. Amino acid metabolism of ovarian cancer cells and immune cells in TIME is complementarily enhanced by metabolic reprogramming, which is responsible for mediating tumor progression and immune escape. Different cells are interconnected by amino acid metabolites. This involves the reprogramming of glutamine, arginine, tryptophan, aspartate, and one-carbon metabolism. Asn, Asparagine; ARG-1, Arginase-1; DC, Dendritic cell; Glu, Glutamate; Gln, Glutamine; GS, Glutamine synthetase; IDO, Indoleamine 2,3-dioxygenase; iNOS/NOS2, Nitric oxide synthase-2; ROS, Reactive oxygen species; TCA, Tricarboxylic acid; TDO2, tryptophan 2,3-dioxygenase; Teff, effector T cell; Treg, Regulatory T cell; MTHFD2, Methylenetetrahydrofolate dehydrogenase 2; NAA, N-acetylaspartate; NAMD receptor, N-methyl-D-aspartate receptor; NK, Natural killer; NO, nitric oxide; UDP, Uridine Diphosphate; UTP, Uridine Triphosphate.

Nitric oxide synthase 1 (NOS1) modulates S-nitrosylation at Cys351 of PFKM, which contributes to the reprogramming of glucose metabolism in ovarian cancer cells (107). Nitric oxide synthase-2 (NOS2/iNOS) expressed by endogenous T cells and NO generated by T cells are required for *de novo* Th17 differentiation from naive precursors and for induction of the Th17 phenotype in memory cells (106).

3.3.3 Tryptophan

Tryptophan is an essential amino acid that can be catabolized or used to make tissue proteins. Patients with ovarian cancer showed accelerated tryptophan breakdown (108). There is evidence that in ovarian cancer, the enzyme indoleamine 2,3-dioxygenase (IDO) catalyzes the breakdown of tryptophan through the kynurenine pathway, resulting in immunosuppressive compounds that accelerate the growth of tumor cells and reduce antitumor immunity (109, 110). Specifically, it reduces tryptophan availability in immune cells, resulting in immunological escape by inhibiting the recruitment of NK cells and the infiltration of T cells (110, 111). Tregs can enhance IDO expression in ovarian cancer cells and synergize with hypoxia to extend the aggressiveness of OC (112). Meanwhile, tryptophan 2,3-dioxygenase (TDO2), the rate-limiting enzyme of the kynurenine pathway, was found to be upregulated in ovarian cancer tissues, which promotes tumor cell proliferation, migration and invasion (113).

3.3.4 Aspartic acid and asparagine

Asparagine (Asn) is a metabolic byproduct that is released into the extracellular compartment by tumor cells in large amounts. A metabolomics-based study of EOC serum metabolites found that Asn may be an important factor influencing the pathogenesis of ovarian cancer (114). However, specific mechanisms have yet to be explored. The presence of Asn in the microenvironment dramatically enhances the activation, proliferation and tumor killing ability of $CD8^+$ T cells both *in vivo* and *in vitro* (115).

3.3.5 One-carbon metabolism

Large quantities of pyrimidines, thymidines, S-adenosylmethionine, and glutathione are necessary for rapid tumor proliferation for the synthesis of nucleotides. One-carbon (1C) metabolism backs up these substances required by tumors (116, 117). By affecting T cell functions, the folate-coupled metabolic enzyme methylenetetrahydrofolate dehydrogenase 2 (MTHFD2) serves as a crucial metabolic checkpoint in the 1C metabolic pathway (118). As a nicotinamide adenine dinucleotide (NAD^+)-dependent enzyme with a considerable level of expression in ovarian cancer tissues, MTHFD2 positively correlates with both malignancy and prognosis (119). The synthesis of uridine-related metabolites, including UTP/UDP, is enhanced in the TIME by MTHFD2-mediated high levels of folate metabolism (120). It consequently stimulates PD-L1 transcription for the purpose of immune evasion (120). Furthermore, in IC metabolism, the methionine cycle is a major methyl donor, which is required for protein and nucleic acid methylation. Research has revealed the important role of methionine metabolism in T cell proliferation and differentiation (121). Cysteine is another significant metabolite in IC metabolism. It was discovered that ovarian cancer enhances tolerance to hypoxia through cysteine-mediated reprogramming of sulfur and carbon metabolism (122).

3.4 Metabolic signaling pathways in TIME reprogramming

The signaling pathways are linked to the shift of the metabolic landscape in ovarian cancer. Cancer cells exhibit persistent proliferative signals, and metabolic reprogramming facilitates this behavior.

The PI3K/Akt signaling pathway stimulates gluconeogenesis and lipid metabolism and activates tumor metabolism (123, 124). Salt-inducible kinase 2 (SIK2) overexpression in ovarian cancer cells activates the PI3K/AKT/HIF-1α pathway, upregulates HIF-1α expression, directly upregulates the transcription of major glycolytic genes and promotes glycolysis (123). SIK2 can promote mitochondrial fission and inhibit mitochondrial oxidative phosphorylation through phosphorylation of Drp1 at the Ser616 site (123). Moreover, SIK2 activates the PI3K/Akt signaling pathway and upregulates sterol regulatory element binding protein 1c (SREBP1c) and sterol regulatory element binding protein 2 (SREBP2), thus promoting the transcription of lipase FASN and cholesterol synthase HMGCR (124). This process improved the synthesis of cholesterol and FAs in ovarian cancer cells (124). In addition, ovarian cancer cells are capable of producing several forms of laminins (125). The Akt and MEK signaling pathways are activated in DCs cultivated with laminins *in vitro*, and a shift in the metabolic state of DCs induces the development of their reprogramming from bone marrow precursors to a suppressive phenotype (125).

The metabolic reprogramming of tumors is strongly correlated with the PI3K/Akt/mTOR pathway, which regulates cell growth and metabolism. The protein kinase mTOR is a serine/threonine enzyme that is a component of the mTORC1 and mTORC2 signaling complexes. In ovarian cancer, mTORC1 regulates glucose metabolism during $CD8^+$ Treg differentiation by modulating HIF1α expression (126). Research has revealed that inhibiting GLScan synergize with the therapeutic effect of mTOR inhibitors on ovarian cancer (127).

Additionally, an aberrant MAPK signaling pathway is inextricably tied to metabolic reprogramming in ovarian cancer. It was found that TGF-β1 secreted by ovarian cancer cells could induce CD8+ Tregs through the p38 MAPK signaling pathway (128). In ovarian cancer, the widespread degradation of

HIF-1 is encouraged by the silencing of TRPM7, which possesses ion channel and kinase activity. This promotes AMPK activation and changes glycolysis into oxidative phosphorylation (129).

As previously discussed, the Wingless (Wnt)/β-catenin pathway is hypothesized to be a driver of altered glycolysis, glutaminolysis, and lipogenesis (130). In ovarian cancer, hexokinase 2 increases CyclinD1/c-myc through the Wnt/β-catenin pathway, which in turn enhances oncogenesis and proliferation (131). In addition, macrophages that support ovarian cancer metastasis are linked to β-catenin expression (132). Inhibition of the Wnt/β-catenin pathway decelerates ovarian cancer progression and regulates the TIME by increasing cytotoxic T cell infiltration and decreasing MDSC infiltration (133).

4 Immunotherapeutic strategies targeting TIME metabolic reprogramming in ovarian cancer

Not only does metabolic adaptation of tumors take place throughout the course of OC, but it also happens during the course of therapy, which results in drug resistance (134–137). Metabolic reprogramming of the TIME in ovarian cancer leads to chemoresistance. M2-TAMs have a higher glucose uptake and utilization capacity, which stimulate the O-GlcNAcylation of lysosomal Cathepsin B (138). And it has been demonstrated that M2-TAMs could promote cancer metastasis and chemoresistance by increasing the activity of the hexosamine biosynthesis pathway (138). High levels of G6PD and glutathione-producing oxidoreductase are favorably associated with cisplatin resistance in OC (135). Moreover, paclitaxel resistance in ovarian cancer is associated with choline metabolism reprogramming. The expression of glycerophosphocholine phosphodiesterase 1 and glycerophosphodiester phosphodiesterase 1 in EOC was discovered to be elevated using proton magnetic resonance spectroscopy, and total choline was found to be elevated (136). Owing to the cunning metabolic adaptations of OC, monotherapy is frequently ineffective. For instance, when exposed to IDO1 inhibitors, ovarian cancer cells develop a metabolic adaptation that switches tryptophan catabolism to the 5-hydroxytryptamine pathway (137). NAD^+ is increased as a result, which reduces T cell function and proliferation (137). The extracellular vesicles secreted by ovarian cancer can confer carboplatin resistance to tumor cells through hypoxia-induced metabolic dysregulation (mainly glycolysis and FAO) (139). Based on the metabolic adaptations described above in ovarian cancer, it is essential to take action to inhibit metabolic reprogramming during the treatment.

Immunotherapy allows the restoration of the T cell antitumor immune response through targeted metabolic reprogramming. Previously, we outlined the pertinent medications that target the metabolism of ovarian cancer as well as their clinical trials (29). Since there is an overlap of agents for the immunosuppressive microenvironment in ovarian cancer, we focused on immunotherapeutic strategies related to metabolic reprogramming targeting the TIME. Table 2 summarizes the immunotherapy therapies and medicines listed herein for TIME in ovarian cancer.

4.1 Supplementation or deprivation of metabolism

Certain antitumor effects can be achieved by directly supplementing metabolites. For example, L-asparaginase is a potential therapeutic enzyme. When cocultured with OVCAR-8 ovarian cancer cells, asparagine is rapidly depleted both inside and outside the cells, converting it to aspartic acid and assisting in tumor death (140). However, supplementation with amino acids *in vitro* shows no discernible benefit against malignancies. However, a potential involvement in disease recurrence and metastasis cannot be excluded. *In vivo* experiments on ovarian cancer-bearing mice showed that intraperitoneal injection of glutamine could enhance immune function and synergistically enhance paclitaxel's antitumor effects (141).

On the other hand, metabolic deprivation is a form of starvation therapy for the treatment of ovarian cancer. The use of the specific glycolysis inhibitor 2-deoxyglucose triggers caspase-dependent apoptosis, reduces lactate production, and blocks the expression of resistance-associated proteins under low glucose conditions (30). AMPK activators can imitate the cytotoxicity induced by glucose starvation (142). Through arginine deprivation, human recombinant arginase I [HuArgI (Co)-PEG5000] can trigger autophagy and influence the motility and adhesion of ovarian cancer cells (143). Yu, J., et al. also discovered that simultaneous dual deprivation of lactate and glucose improved the antitumor effect (152). Furthermore, dietary changes might be beneficial in cancer prevention and treatment. A low-fat, high-fiber diet can help in the prevention and treatment of ovarian cancer (153, 154).

However, this adjustment of metabolic endpoint levels is extremely restricted, and most investigations have revealed no meaningful contribution to anticancer therapy in OC. It only works in a few ovarian cancer subtypes. For example, galactose intake may play a role in the development of borderline ovarian cancer in women who carry the galactose-1-phosphate uridyl transferase N314D polymorphism (155). Due to its accessibility and convenience, even though its therapeutic effect is modest, it is worthwhile to continue researching.

Adoptive cell transfer therapy (ACT) is a popular field of immunotherapy research. ACT is the collection of the patient's own immune cells, followed by identification and *in vitro* cultivation to increase their quantity or improve their capacity for targeted killing (156). It can be helpful to improve the immune escape of ovarian cancer, especially for patients with

TABLE 2 Immunotherapy targeting the metabolism of immune cells in ovarian cancer.

Immunotherapy approaches	Agents	Targets	Functions	Stage/ Phase	Refs
Supplementation or deprivation of metabolism					
Metabolites supplementation	L-asparaginase	Depletion of asparagine	Cytotoxicity	Preclinical study	(140)
Metabolites supplementation	Glutamine	Supplement of glutamine	Synergistic enhancement of the antitumor effect of paclitaxel	Preclinical study	(141)
Metabolic deprivation through inhibition of glycolysis	2-deoxyglucose	hexokinase	Cytotoxicity, reducing lactate production, and blocking the expression of drug resistance-associated proteins.	Preclinical study	(30, 142)
Arginine deprivation	HuArgI (Co)-PEG5000	Human recombinant arginase I	Cytotoxicity and influencing viability and adhesion	Preclinical study	(143)
Allogeneic NK cell plus DCs and cytokines	6B11-OCIK	Autologous T cells plus dendritic cells and cytokines	Enhancement the function of immune system, rebuilding anti-tumor specific immunity and increasing the immune response of T cells	Phase I	(144)
Immune checkpoint inhibitors					
IDO and kynurenine pathways	CH223191	AHR antagonist	Reduction of AHR-induced PD-1 expression in T cells	Preclinical study	(145)
Combined therapy	GDC-0919 combined atezolizumab	IDO inhibitor and PD-L1 inhibitor	No significant therapeutic effect	Phase I	(146)
Combined therapy	An isotype of anti-PD-L1 antibody combined 968	PD-L1 inhibitors combined GLS inhibitor	Enhancement of T cell response and synergistic anti-tumor effects	Preclinical study	(147)
Others					
Autologous DC vaccination	DCVAC	An autologous DC-based vaccine	Improving progression-free survival in EOC	Phase II	(148, 149)
Autologous DC vaccination	Th17-induced FRα-loaded autologous DC vaccine	DCs programmed to induce a Th17 response to the OC antigen FRα	Inducingantigen-specific immunity and prolonging remission	Phase I	(150)
Oncolytic virotherapy	SV. IL12 in combination with anti-OX40	Inducing OX40 expression on $CD4^+$ T cells	Significantly altering the transcriptome profile and metabolic program of T cells and activating T cell activity	Preclinical study	(151)

AHR, Aryl hydrocarbon receptor; DC, Dendritic cell; EOC, Epithelial ovarian cancer; FR, folate receptor; GLS, glutaminase; IDO, Indoleamine 2,3-dioxygenase; IL, Interleukin; OC, ovarian cancer; PD-L1, Programmed death ligand-1; Th17, IL-17-producing T helper; NK, Natural killer.

recurrent ovarian cancer. An adoptive cell therapy of autologous T cells induced by a humanized anti-adiotypic antibody 6B11 minibody plus DCs and cytokines demonstrated preliminary safety and potential clinical efficacy in a phase I clinical trial of platinum-resistant recurrent or refractory ovarian cancer (144). A phase II study of allogeneic NK cell therapy for recurrent ovarian cancer showed suboptimal efficacy, and Treg cells were revealed to represent a treatment barrier (157). Allogeneic NK cell infusion in the most recent phase 1 clinical trial is still recruiting participants (158). In ovarian cancer TIME, the self-generated nanosystem known as KT-NE (KIRA6 loaded α-Tocopherol nanoemulsion) dramatically reduced lipid buildup in DCs and restored their immunological activity (159). In tumor-bearing mice, adoptive transfer of KT-NE-treated ID8-DCs increased host progression-free survival (159). Furthermore, PD-1 immunotherapy and KT-NE had synergistic effects (159). Additional clinical studies are needed to explore the therapeutic effects of ACT in ovarian cancer.

4.2 Immune checkpoint inhibitors

Checkpoint receptors on the surface of T cells, such as PD-1 and cytotoxic T lymphocyte-associated antigen 4 (CTLA-4), can suppress energy and metabolic changes in T cells and mediate immunosuppression when activated by the corresponding ligands (160). Immune checkpoint blockade (ICB) therapy enhances the tumor infiltration and effector functions of T cells by reprogramming metabolism. Classical PD-1, PD-L1, and CTLA-4 inhibitors have made great progress in the treatment of ovarian cancer. Immune checkpoints show a positive modulatory effect on metabolism (160, 161). PD-1 and CTLA-4 inhibitors can modulate the amount and activity of ARG-1, which prevents MDSCs from suppressing the immune system in ovarian cancer (161).

The IDO and kynurenine pathways are emerging metabolic checkpoints that promote T cell proliferation by preventing the synthesis of kynurenine (162). The aryl hydrocarbon receptor

(AHR) antagonist CH223191 significantly decreased AHR-induced PD-1 expression in T cells (145).

However, the efficacy of ICB in the treatment of ovarian cancer is not obvious (163). In patients with advanced malignancies, combinations of PD-L1 inhibitors and IDO inhibitors have demonstrated acceptable safety and resistance (146). But there is no proof to back up the benefits of the combination. The metabolic reprogramming of the TIME is probably an important cause for the weak efficacy of ICB. The combination of drugs targeting metabolic reprogramming and ICIs is expected to improve the efficacy of ICB. Based on the glutamine dependence of ovarian cancer, the GLS inhibitor 968 increased the infiltration of $CD3^+$ T cells and enhanced the apoptosis-inducing ability of cancer cells by $CD8^+$ T cells. Combination with PD-L1 blockade enhanced the immune response to ovarian cancer (147).

The in-depth exploration of metabolic reprogramming has allowed for the continuous refinement of immunotherapy in ovarian cancer. For example, ICB induces not only IDO1 but also interleukin-4-induced-1 (IL4I1). The failure of clinical studies of ICB combined with IDO1 inhibition may be due to the presence of IL4I1 (164). The discovery of new metabolic immune checkpoints opens up a new path for cancer therapy.

4.3 Others

By targeting intracellular metabolic reprogramming, the metabolic state of T cells was induced to change, resulting in a more effective ovarian cancer treatment. Specific metabolism-related cell surface receptors can be identified as targets for selective delivery therapies based on the metabolic reprogramming properties of ovarian cancer. Folate receptor (FR) β in one-carbon metabolism can also be used as a regulatory target. It is expressed on activated macrophages in patients with EOC, and its blockade can inhibit nucleotide production, leading to significant immunotherapeutic effects (165, 166).

As more is known about tumor immunity, cancer vaccines have received increasing attention. Various cancer vaccines targeting immune cells have demonstrated a promising therapeutic landscape in ovarian cancer. In a phase II clinical trial, an autologous DC-based vaccination (DCVAC) significantly increased progression-free survival, and peripheral blood analysis revealed that DCVAC increases anti-cancer immunity in ovarian cancer patients with cool tumor nature (148, 149). A single-arm open-label phase I clinical trial indicates the safety of a Th17-induced FR-loaded autologous DC vaccination in inducing antigen-specific immunity and prolonging remission in ovarian cancer patients (150). Oncolytic virotherapy is an emerging immunotherapy. Oncolytic viruses invade tumor cells through cell surface molecules, infect and kill tumor cells, activate the immune response, and thus exert their tumor-killing effect (167). Lysozyme virus has high selectivity to tumor cells and high immune response intensity, thus maximizing the effect of immunotherapy. Gene set enrichment analysis showed that SV. IL12 in combination with anti-OX40 increased intracellular glycolysis and OXPHOS in T cells at the genetic level (151). Hulin-Curtis, S. L., et al. designed a phage peptide that binds to FRα on SKOV3 cell lines based on the selective high expression of FRα on ovarian cancer cells (168). It binds specifically to FRα, however, due to defective intracellular transport, it cannot yet be effectively targeted through FRα (168).

The above researches show promising therapeutic effects of tumor vaccines and oncolytic virotherapy for the treatment of ovarian cancer. However, because the relevant technology and exploration are not yet very mature, most of the current development is still only at the preclinical stage. More immunotherapy targeting TIME need to be developed in the future.

5 Perspectives and prospects

New insights suggest that tumors are not only a genetic disease but also highly associated with a suppressive immune microenvironment (16). Cellular metabolism is the key link between the extracellular environment and intracellular processes. Therefore, it is essential to explore the immunity and metabolism of ovarian cancer. By exploring the immunosuppressive microenvironment of ovarian cancer, we decipher what significant role environmental factors, especially immune cells, play in tumorigenesis, development, treatment and prognosis. Single-cell sequencing and integrated bioinformatics analysis have led to a greater understanding of ovarian cancer. J. Sun et al. described the immunogenomic landscape of HGSOC and identified immunological subtypes appropriate for immunotherapy (169). The application of immunogenomics, immunogenomics and molecular typing in ovarian cancer will contribute to subsequent targeted therapies. By deeply researching different immune subtypes, the application of precision therapy in ovarian cancer can be further expanded.

Ovarian cancer patients inevitably develop resistance to drugs, leading to treatment failure, which is the leading cause of death. Metabolic reprogramming of tumors occurs not only in tumorigenesis, progression, and metastasis, but different therapeutic measures also reshape tumor metabolism. It has been proven that surgery could increase the immune suppression of first-line ovarian cancer treatment (21). Metabolic reprogramming is extremely complex. In addition to the discussion in this review, epigenetics also plays an indelible role in the process of metabolic

reprogramming (170). For example, ubiquitination and deubiquitination could alter cancer metabolism as one of the types of posttranslational modifications (171). Ovarian cancer restricts methyltransferase EZH2 expression in T cells by limiting aerobic glycolysis, thereby impairing T-cell-mediated antitumor immunity (172). Epigenetic regulation, in turn, can also affect cellular metabolism by modifying kinase activity. To illustrate, the DNA demethylating agent 5-aza-2-deoxycytidine reduces chemoresistance in cisplatin-resistant A2780cis cells and restores GS expression (173). Therefore, integrating the mechanism of interaction between metabolic reprogramming and epigenetics is also an important direction for future metabolic research in ovarian cancer, which could provide a theoretical foundation for treatment.

However, the metabolic phenotype of cancer is not invariant. Treatment resistance and metastases also cause metabolic reprogramming. It is feasible to increase the sensitivity of immunotherapy and chemotherapy as a new complement to the treatment of malignancies by targeting this feature. It is extremely promising to create medications to postpone the progression of tumors and to improve the sensitivity of cancer treatment based on the relevant theories. Therefore, it is crucial to continue researching metabolic reprogramming to enhance tumor immunotherapy.

Author contributions

Conceptualization, YL and XL. Writing, review, and editing, YL and XtZ. Visualization, YL and YN. Supervision, XL and XZ. Funding acquisition, XZ and XL. All authors have read and agreed to the published version of the manuscript.

Funding

This research was funded by the National Natural Science Foundation of China, grant number No. 81902662, the Natural Science Foundation of Sichuan Province, grant number No.2022NSFSC1531, the National Natural Science Foundation of China, grant number No. 81821002, Sichuan Science and Technology Program, grant number 2021YJ0011, and Foundation of Development and Related Diseases of Women and Children Key Laboratory of Sichuan Province, grant number No. 2022003. The APC was funded by West China Second Hospital.

Acknowledgments

Figures in this review were created with BioRender.com.

Conflict of interest

The authors declare that the research was conducted in the absence of any commercial or financial relationships that could be construed as a potential conflict of interest.

Publisher's note

All claims expressed in this article are solely those of the authors and do not necessarily represent those of their affiliated organizations, or those of the publisher, the editors and the reviewers. Any product that may be evaluated in this article, or claim that may be made by its manufacturer, is not guaranteed or endorsed by the publisher.

References

1. Torre LA, Trabert B, DeSantis CE, Miller KD, Samimi G, Runowicz CD, et al. Ovarian cancer statistics, 2018. *CA Cancer J Clin* (2018) 68(4):284–96. doi: 10.3322/caac.21456

2. Coburn SB, Bray F, Sherman ME, Trabert B. International patterns and trends in ovarian cancer incidence, overall and by histologic subtype. *Int J Cancer* (2017) 140(11):2451–60. doi: 10.1002/ijc.30676

3. Siegel RL, Miller KD, Fuchs HE, Jemal A. Cancer statistics, 2021. *CA Cancer J Clin* (2021) 71(1):7–33. doi: 10.3322/caac.21654

4. Stewart C, Ralyea C, Lockwood S. Ovarian cancer: An integrated review. *Semin Oncol Nurs* (2019) 35(2):151–6. doi: 10.1016/j.soncn.2019.02.001

5. Bogani G, Ditto A, Pinelli C, Lopez S, Chiappa V, Raspagliesi F. Ten-year follow-up study of long-term outcomes after conservative surgery for early-stage ovarian cancer. *Int J Gynaecol Obstet* (2020) 150(2):169–76. doi: 10.1002/ijgo.13199

6. Mazzoni A, Bronte V, Visintin A, Spitzer JH, Apolloni E, Serafini P, et al. Myeloid suppressor lines inhibit T cell responses by an NO-dependent mechanism. *J Immunol* (2002) 168(2):689–95. doi: 10.4049/jimmunol.168.2.689

7. Armstrong DK, Alvarez RD, Bakkum-Gamez JN, Barroilhet L, Behbakht K, Berchuck A, et al. Ovarian cancer, version 2.2020, NCCN clinical practice guidelines in oncology. *J Natl Compr Canc Netw* (2021) 19(2):191–226. doi: 10.6004/jnccn.2021.0007

8. Shih IM, Wang Y, Wang TL. The origin of ovarian cancer species and precancerous landscape. *Am J Pathol* (2021) 191(1):26–39. doi: 10.1016/j.ajpath.2020.09.006

9. Dalmartello M, La Vecchia C, Bertuccio P, Boffetta P, Levi F, Negri E, et al. European Cancer mortality predictions for the year 2022 with focus on ovarian cancer. *Ann Oncol* (2022) 33(3):330–9. doi: 10.1016/j.annonc.2021.12.007

10. Menon U, Gentry-Maharaj A, Burnell M, Singh N, Ryan A, Karpinskyj C, et al. Ovarian cancer population screening and mortality after long-term follow-up in the UK collaborative trial of ovarian cancer screening (UKCTOCS): A randomised controlled trial. *Obstet Gynecol Survey* (2021) 76(9):537–8. doi: 10.1097/01.ogx.0000792624.55995.3e

11. Luvero D, Milani A, Ledermann JA. Treatment options in recurrent ovarian cancer: latest evidence and clinical potential. *Ther Adv Med Oncol* (2014) 6(5):229–39. doi: 10.1177/1758834014544121

12. Granata V, Crisafulli L, Nastasi C, Ficara F, Sobacchi C. Bone marrow niches and tumour cells: Lights and shadows of a mutual relationship. *Front Immunol* (2022) 13:884024. doi: 10.3389/fimmu.2022.884024

13. Lakshmi Narendra B, Eshvendar Reddy K, Shantikumar S, Ramakrishna S. Immune system: a double-edged sword in cancer. *Inflamm Res* (2013) 62(9):823–34. doi: 10.1007/s00011-013-0645-9

14. Bhatia A, Kumar Y. Cellular and molecular mechanisms in cancer immune escape: a comprehensive review. *Expert Rev Clin Immunol* (2014) 10(1):41–62. doi: 10.1586/1744666X.2014.865519

15. Paget S. The distribution of secondary growths in cancer of the breast. 1889. *Cancer Metastasis Rev* (1989) 8(2):98–101. doi: 10.1016/s0140-6736(00)49915-0

16. Binnewies M, Roberts EW, Kersten K, Chan V, Fearon DF, Merad M, et al. Understanding the tumor immune microenvironment (TIME) for effective therapy. *Nat Med* (2018) 24(5):541–50. doi: 10.1038/s41591-018-0014-x

17. Odunsi K. Immunotherapy in ovarian cancer. *Ann Oncol* (2017) 28 (suppl_8):viii1–7. doi: 10.1093/annonc/mdx444

18. Tan S, Li D, Zhu X. Cancer immunotherapy: Pros, cons and beyond. *BioMed Pharmacother* (2020) 124:109821. doi: 10.1016/j.biopha.2020.109821

19. Sobhani N, Scaggiante B, Morris R, Chai D, Catalano M, Tardiel-Cyril DR, et al. Therapeutic cancer vaccines: From biological mechanisms and engineering to ongoing clinical trials. *Cancer Treat Rev* (2022) 109:102429. doi: 10.1016/j.ctrv.2022.102429

20. Pirs B, Skof E, Smrkolj V, Smrkolj S. Overview of immune checkpoint inhibitors in gynecological cancer treatment. *Cancers (Basel)* (2022) 14(3):631. doi: 10.3390/cancers14030631

21. De Bruyn C, Ceusters J, Landolfo C, Baert T, Thirion G, Claes S, et al. Neo-adjuvant chemotherapy reduces, and surgery increases immunosuppression in first-line treatment for ovarian cancer. *Cancers (Basel)* (2021) 13(23):5899. doi: 10.3390/cancers13235899

22. Le Saux O, Ray-Coquard I, Labidi-Galy SI. Challenges for immunotherapy for the treatment of platinum resistant ovarian cancer. *Semin Cancer Biol* (2021) 77:127–43. doi: 10.1016/j.semcancer.2020.08.017

23. Morand S, Devanaboyina M, Staats H, Stanbery L, Nemunaitis J. Ovarian cancer immunotherapy and personalized medicine. *Int J Mol Sci* (2021) 22 (12):6532. doi: 10.3390/ijms22126532

24. Anadon CM, Yu X, Hanggi K, Biswas S, Chaurio RA, Martin A, et al. Ovarian cancer immunogenicity is governed by a narrow subset of progenitor tissue-resident memory T cells. *Cancer Cell* (2022) 40(5):545–557e13. doi: 10.1016/j.ccell.2022.03.008

25. Yoshida GJ. Metabolic reprogramming: The emerging concept and associated therapeutic strategies. *J Exp Clin Cancer Res* (2015) 34:111. doi: 10.1186/s13046-015-0221-y

26. Hanahan D. Hallmarks of cancer: New dimensions. *Cancer Discovery* (2022) 12(1):31–46. doi: 10.1158/2159-8290.CD-21-1059

27. Dar S, Chhina J, Mert I, Chitale D, Buekers T, Kaur H, et al. Bioenergetic adaptations in chemoresistant ovarian cancer cells. *Sci Rep* (2017) 7(1):8760. doi: 10.1038/s41598-017-09206-0

28. Liberti MV, Locasale JW. The warburg effect: How does it benefit cancer cells? *Trends Biochem Sci* (2016) 41(3):211–8. doi: 10.1016/j.tibs.2015.12.001

29. Lin Y, Liang X, Zhang X, Ni Y, Zhou X, Zhao X. Metabolic cross-talk between ovarian cancer and the tumor microenvironment-providing potential targets for cancer therapy. *Front Biosci (Landmark Ed)* (2022) 27(4):139. doi: 10.31083/j.fbl2704139

30. Park GB, Jeong JY, Choi S, Yoon YS, Kim D. Glucose deprivation enhances resistance to paclitaxel *via* ELAVL2/4-mediated modification of glycolysis in ovarian cancer cells. *Anticancer Drugs* (2022) 33(1):e370–80. doi: 10.1097/CAD.0000000000001215

31. Ding Y, Labitzky V, Legler K, Qi M, Schumacher U, Schmalfeldt B, et al. Molecular characteristics and tumorigenicity of ascites-derived tumor cells: Mitochondrial oxidative phosphorylation as a novel therapy target in ovarian cancer. *Mol Oncol* (2021) 15(12):3578–95. doi: 10.1002/1878-0261.13028

32. Bose S, Huang Q, Ma Y, Wang L, Rivera GO, Ouyang Y, et al. G6PD inhibition sensitizes ovarian cancer cells to oxidative stress in the metastatic omental microenvironment. *Cell Rep* (2022) 39(13):111012. doi: 10.1016/j.celrep.2022.111012

33. Prasad P, Roy SS. Glutamine regulates ovarian cancer cell migration and invasion through ETS1. *Heliyon* (2021) 7(5):e07064. doi: 10.1016/j.heliyon.2021.e07064

34. Sriramkumar S, Sood R, Huntington TD, Ghobashi AH, Vuong TT, Metcalfe TX, et al. Platinum-induced mitochondrial OXPHOS contributes to cancer stem cell enrichment in ovarian cancer. *J Transl Med* (2022) 20(1):246. doi: 10.1186/s12967-022-03447-y

35. Ji Z, Shen Y, Feng X, Kong Y, Shao Y, Meng J, et al. Deregulation of lipid metabolism: The critical factors in ovarian cancer. *Front Oncol* (2020) 10:593017. doi: 10.3389/fonc.2020.593017

36. Dogra S, Neelakantan D, Patel MM, Griesel B, Olson A, Woo S. Adipokine Apelin/APJ pathway promotes peritoneal dissemination of ovarian cancer cells by regulating lipid metabolism. *Mol Cancer Res* (2021) 19(9):1534–45. doi: 10.1158/1541-7786.MCR-20-0991

37. Nieman KM, Kenny HA, Penicka CV, Ladanyi A, Buell-Gutbrod R, Zillhardt MR, et al. Adipocytes promote ovarian cancer metastasis and provide energy for rapid tumor growth. *Nat Med* (2011) 17(11):1498–503. doi: 10.1038/nm.2492

38. Nersesian S, Glazebrook H, Toulany J, Grantham SR, Boudreau JE. Naturally killing the silent killer: NK cell-based immunotherapy for ovarian cancer. *Front Immunol* (2019) 10:1782. doi: 10.3389/fimmu.2019.01782

39. Pugh-Toole M, Nicolela AP, Nersesian S, Leung BM, Boudreau JE. Natural killer cells: The missing link in effective treatment for high-grade serous ovarian carcinoma. *Curr Treat Options Oncol* (2022) 23(2):210–26. doi: 10.1007/s11864-021-00929-x

40. Mortezaee K, Majidpoor J. Dysregulated metabolism: A friend-to-foe skewer of macrophages. *Int Rev Immunol* (2022) 135:1–17. doi: 10.1080/08830185.2022.2095374

41. Liu Y, Xu R, Gu H, Zhang E, Qu J, Cao W, et al. Metabolic reprogramming in macrophage responses. *biomark Res* (2021) 9(1):1. doi: 10.1186/s40364-020-00251-y

42. Franco F, Jaccard A, Romero P, Yu YR, Ho PC. Metabolic and epigenetic regulation of T-cell exhaustion. *Nat Metab* (2020) 2(10):1001–12. doi: 10.1038/s42255-020-00280-9

43. Martin MD, Badovinac VP. Defining memory CD8 T cell. *Front Immunol* (2018) 9:2692. doi: 10.3389/fimmu.2018.02692

44. Dong H, Bullock TN. Metabolic influences that regulate dendritic cell function in tumors. *Front Immunol* (2014) 5:24. doi: 10.3389/fimmu.2014.00024

45. Thwe PM, Pelgrom LR, Cooper R, Beauchamp S, Reisz JA, D'Alessandro A, et al. Cell-intrinsic glycogen metabolism supports early glycolytic reprogramming required for dendritic cell immune responses. *Cell Metab* (2017) 26(3):558–567e5. doi: 10.1016/j.cmet.2017.08.012

46. Xu R, Wu M, Liu S, Shang W, Li R, Xu J, et al. Glucose metabolism characteristics and TLR8-mediated metabolic control of CD4(+) treg cells in ovarian cancer cells microenvironment. *Cell Death Dis* (2021) 12(1):22. doi: 10.1038/s41419-020-03272-5

47. Yin M, Li X, Tan S, Zhou HJ, Ji W, Bellone S, et al. Tumor-associated macrophages drive spheroid formation during early transcoelomic metastasis of ovarian cancer. *J Clin Invest* (2016) 126(11):4157–73. doi: 10.1172/JCI87252

48. Al-Khami AA, Zheng L, Del Valle L, Hossain F, Wyczechowska D, Zabaleta J, et al. Exogenous lipid uptake induces metabolic and functional reprogramming of tumor-associated myeloid-derived suppressor cells. *Oncoimmunology* (2017) 6(10): e1344804. doi: 10.1080/2162402X.2017.1344804

49. Udumula MP, Sakr S, Dar S, Alvero AB, Ali-Fehmi R, Abdulfatah E, et al. Ovarian cancer modulates the immunosuppressive function of CD11b(+)Gr1(+) myeloid cells *via* glutamine metabolism. *Mol Metab* (2021) 53:101272. doi: 10.1016/j.molmet.2021.101272

50. Leonard W, Dufait I, Schwarze JK, Law K, Engels B, Jiang H, et al. Myeloid-derived suppressor cells reveal radioprotective properties through arginase-induced l-arginine depletion. *Radiother Oncol* (2016) 119(2):291–9. doi: 10.1016/j.radonc.2016.01.014

51. Bak SP, Alonso A, Turk MJ, Berwin B. Murine ovarian cancer vascular leukocytes require arginase-1 activity for T cell suppression. *Mol Immunol* (2008) 46(2):258–68. doi: 10.1016/j.molimm.2008.08.266

52. Zhu H, Blum RH, Bjordahl R, Gaidarova S, Rogers P, Lee TT, et al. Pluripotent stem cell-derived NK cells with high-affinity noncleavable CD16a mediate improved antitumor activity. *Blood* (2020) 135(6):399–410. doi: 10.1182/blood.2019000621

53. Sheppard S, Santosa EK, Lau CM, Violante S, Giovanelli P, Kim H, et al. Lactate dehydrogenase a-dependent aerobic glycolysis promotes natural killer cell anti-viral and anti-tumor function. *Cell Rep* (2021) 35(9):109210. doi: 10.1016/j.celrep.2021.109210

54. Deng M, Wu D, Zhang Y, Jin Z, Miao J. MiR-29c downregulates tumor-expressed B7-H3 to mediate the antitumor NK-cell functions in ovarian cancer. *Gynecol Oncol* (2021) 162(1):190–9. doi: 10.1016/j.ygyno.2021.04.013

55. Biswas SK, Sica A, Lewis CE. Plasticity of macrophage function during tumor progression: regulation by distinct molecular mechanisms. *J Immunol* (2008) 180(4):2011–7. doi: 10.4049/jimmunol.180.4.2011

56. Wang H, Yung MMH, Ngan HYS, Chan KKL, Chan DW. The impact of the tumor microenvironment on macrophage polarization in cancer metastatic progression. *Int J Mol Sci* (2021) 22(12). doi: 10.3390/ijms22126560

57. Hishinuma E, Shimada M, Matsukawa N, Saigusa D, Li B, Kudo K, et al. Wide-targeted metabolome analysis identifies potential biomarkers for prognosis prediction of epithelial ovarian cancer. *Toxins (Basel)* (2021) 13(7):461. doi: 10.3390/toxins13070461

58. Zhang M, He Y, Sun X, Li Q, Wang W, Zhao A, et al. A high M1/M2 ratio of tumor-associated macrophages is associated with extended survival in ovarian cancer patients. *J Ovarian Res* (2014) 7:19. doi: 10.1186/1757-2215-7-19

59. Winkler I, Wilczynska B, Bojarska-Junak A, Gogacz M, Adamiak A, Postawski K, et al. Regulatory T lymphocytes and transforming growth factor beta in epithelial ovarian tumors-prognostic significance. *J Ovarian Res* (2015) 8:39. doi: 10.1186/s13048-015-0164-0

60. Pompura SL, Wagner A, Kitz A, LaPerche J, Yosef N, Dominguez-Villar M, et al. Oleic acid restores suppressive defects in tissue-resident FOXP3 tregs from patients with multiple sclerosis. *J Clin Invest* (2021) 131(2):138519. doi: 10.1172/JCI138519

61. Zhang Z, Liu Q, Che Y, Yuan X, Dai L, Zeng B, et al. Antigen presentation by dendritic cells in tumors is disrupted by altered metabolism that involves pyruvate kinase M2 and its interaction with SOCS3. *Cancer Res* (2010) 70(1):89–98. doi: 10.1158/0008-5472.CAN-09-2970

62. Mabuchi S, Sasano T, Komura N. Targeting myeloid-derived suppressor cells in ovarian cancer. *Cells* (2021) 10(2):329. doi: 10.3390/cells10020329

63. Olkowicz M, Rosales-Solano H, Kulasingam V, Pawliszyn J. SPME-LC/MS-based serum metabolomic phenotyping for distinguishing ovarian cancer histologic subtypes: A pilot study. *Sci Rep* (2021) 11(1):22428. doi: 10.1038/s41598-021-00802-9

64. Dier U, Shin DH, Hemachandra LP, Uusitalo LM, Hempel N. Bioenergetic analysis of ovarian cancer cell lines: Profiling of histological subtypes and identification of a mitochondria-defective cell line. *PloS One* (2014) 9(5):e98479. doi: 10.1371/journal.pone.0098479

65. Wu S, Fukumoto T, Lin J, Nacarelli T, Wang Y, Ong D, et al. Targeting glutamine dependence through GLS1 inhibition suppresses ARID1A-inactivated clear cell ovarian carcinoma. *Nat Cancer* (2021) 2(2):189–200. doi: 10.1038/s43018-020-00160-x

66. Gaul DA, Mezencev R, Long TQ, Jones CM, Benigno BB, Gray A, et al. Highly-accurate metabolomic detection of early-stage ovarian cancer. *Sci Rep* (2015) 5:16351. doi: 10.1038/srep16351

67. Kumagai S, Koyama S, Itahashi K, Tanegashima T, Lin YT, Togashi Y, et al. Lactic acid promotes PD-1 expression in regulatory T cells in highly glycolytic tumor microenvironments. *Cancer Cell* (2022) 40(2):201–218e9. doi: 10.1016/j.ccell.2022.01.001

68. Bhattacharya R, Ray Chaudhuri S, Roy SS. FGF9-induced ovarian cancer cell invasion involves VEGF-A/VEGFR2 augmentation by virtue of ETS1 upregulation and metabolic reprogramming. *J Cell Biochem* (2018) 119(10):8174–89. doi: 10.1002/jcb.26820

69. Paolini L, Adam C, Beauvillain C, Preisser L, Blanchard S, Pignon P, et al. Lactic acidosis together with GM-CSF and m-CSF induces human macrophages toward an inflammatory protumor phenotype. *Cancer Immunol Res* (2020) 8(3):383–95. doi: 10.1158/2326-6066.CIR-18-0749

70. Bernacchioni C, Ghini V, Cencetti F, Japtok L, Donati C, Bruni P, et al. NMR metabolomics highlights sphingosine kinase-1 as a new molecular switch in the orchestration of aberrant metabolic phenotype in cancer cells. *Mol Oncol* (2017) 11(5):517–33. doi: 10.1002/1878-0261.12048

71. Elia I, Rowe JH, Johnson S, Joshi S, Notarangelo G, Kurmi K, et al. Tumor cells dictate anti-tumor immune responses by altering pyruvate utilization and succinate signaling in CD8(+) T cells. *Cell Metab* (2022) 34(8):1137–1150e6. doi: 10.1016/j.cmet.2022.06.008

72. Israelsen WJ, Vander Heiden MG. Pyruvate kinase: Function, regulation and role in cancer. *Semin Cell Dev Biol* (2015) 43:43–51. doi: 10.1016/j.semcdb.2015.08.004

73. Chen M, Sheng XJ, Qin YY, Zhu S, Wu QX, Jia L, et al. TBC1D8 amplification drives tumorigenesis through metabolism reprogramming in ovarian cancer. *Theranostics* (2019) 9(3):676–90. doi: 10.7150/thno.30224

74. Li S, Ji X, Wang R, Miao Y. Follicle-stimulating hormone promoted pyruvate kinase isozyme type M2-induced glycolysis and proliferation of ovarian cancer cells. *Arch Gynecol Obstet* (2019) 299(5):1443–51. doi: 10.1007/s00404-019-05100-4

75. Chang CH, Curtis JD, Maggi LBJr., Faubert B, Villarino AV, O'Sullivan D, et al. Posttranscriptional control of T cell effector function by aerobic glycolysis. *Cell* (2013) 153(6):1239–51. doi: 10.1016/j.cell.2013.05.016

76. Anwar S, Shamsi A, Mohammad T, Islam A, Hassan MI. Targeting pyruvate dehydrogenase kinase signaling in the development of effective cancer therapy. *Biochim Biophys Acta Rev Cancer* (2021) 1876(1):188568. doi: 10.1016/j.bbcan.2021.188568

77. Yao S, Shang W, Huang L, Xu R, Wu M, Wang F. The oncogenic and prognostic role of PDK1 in the progression and metastasis of ovarian cancer. *J Cancer* (2021) 12(3):630–43. doi: 10.7150/jca.47278

78. Zhang W, Su J, Xu H, Yu S, Liu Y, Zhang Y, et al. Dicumarol inhibits PDK1 and targets multiple malignant behaviors of ovarian cancer cells. *PloS One* (2017) 12(6):e0179672. doi: 10.1371/journal.pone.0179672

79. Zhou L, Liu L, Chai W, Zhao T, Jin X, Guo X, et al. Dichloroacetic acid upregulates apoptosis of ovarian cancer cells by regulating mitochondrial function. *Onco Targets Ther* (2019) 12:1729–39. doi: 10.2147/OTT.S194329

80. Wang JJ, Siu MK, Jiang YX, Leung TH, Chan DW, Cheng RR, et al. Aberrant upregulation of PDK1 in ovarian cancer cells impairs CD8(+) T cell function and survival through elevation of PD-L1. *Oncoimmunology* (2019) 8(11):e1659092. doi: 10.1080/2162402X.2019.1659092

81. Kitamura S, Yamaguchi K, Murakami R, Furutake Y, Higasa K, Abiko K, et al. PDK2 leads to cisplatin resistance through suppression of mitochondrial function in ovarian clear cell carcinoma. *Cancer Sci* (2021) 112(11):4627–40. doi: 10.1111/cas.15125

82. Weiss JM, Davies LC, Karwan M, Ileva L, Ozaki MK, Cheng RY, et al. Itaconic acid mediates crosstalk between macrophage metabolism and peritoneal tumors. *J Clin Invest* (2018) 128(9):3794–805. doi: 10.1172/JCI99169

83. Chen LL, Morcelle C, Cheng ZL, Chen X, Xu Y, Gao Y, et al. Itaconate inhibits TET DNA dioxygenases to dampen inflammatory responses. *Nat Cell Biol* (2022) 24(3):353–63. doi: 10.1038/s41556-022-00853-8

84. Sato M, Kawana K, Adachi K, Fujimoto A, Yoshida M, Nakamura H, et al. Detachment from the primary site and suspension in ascites as the initial step in metabolic reprogramming and metastasis to the omentum in ovarian cancer. *Oncol Lett* (2018) 15(1):1357–61. doi: 10.3892/ol.2017.7388

85. Ladanyi A, Mukherjee A, Kenny HA, Johnson A, Mitra AK, Sundaresan S, et al. Adipocyte-induced CD36 expression drives ovarian cancer progression and metastasis. *Oncogene* (2018) 37(17):2285–301. doi: 10.1038/s41388-017-0093-z

86. Schumann T, Adhikary T, Wortmann A, Finkernagel F, Lieber S, Schnitzer E, et al. Deregulation of PPARbeta/delta target genes in tumor-associated macrophages by fatty acid ligands in the ovarian cancer microenvironment. *Oncotarget* (2015) 6(15):13416–33. doi: 10.18632/oncotarget.3826

87. So J, Wang FQ, Navari J, Schreher J, Fishman DA. LPA-induced epithelial ovarian cancer (EOC) *in vitro* invasion and migration are mediated by VEGF receptor-2 (VEGF-R2). *Gynecol Oncol* (2005) 97(3):870–8. doi: 10.1016/j.ygyno.2005.03.004

88. Meng Y, Kang S, So J, Reierstad S, Fishman DA. Translocation of fas by LPA prevents ovarian cancer cells from anti-fas-induced apoptosis. *Gynecol Oncol* (2005) 96(2):462–9. doi: 10.1016/j.ygyno.2004.10.024

89. Reinartz S, Lieber S, Pesek J, Brandt DT, Asafova A, Finkernagel F, et al. Cell type-selective pathways and clinical associations of lysophosphatidic acid biosynthesis and signaling in the ovarian cancer microenvironment. *Mol Oncol* (2019) 13(2):185–201. doi: 10.1002/1878-0261.12396

90. Gupta VK, Jaiswara PK, Sonker P, Rawat SG, Tiwari RK, Kumar A. Lysophosphatidic acid promotes survival of T lymphoma cells by altering apoptosis and glucose metabolism. *Apoptosis* (2020) 25(1-2):135–50. doi: 10.1007/s10495-019-01585-1

91. Wang J, Yuen BH, Leung PC. Stimulation of progesterone and prostaglandin E2 production by lipoxygenase metabolites of arachidonic acid. *FEBS Lett* (1989) 244(1):154–8. doi: 10.1016/0014-5793(89)81182-2

92. Zhang X, Yan K, Deng L, Liang J, Liang H, Feng D, et al. Cyclooxygenase 2 promotes proliferation and invasion in ovarian cancer cells *via* the PGE2/NF-kappaB pathway. *Cell Transplant* (2019) 28(1_suppl):1S–13S. doi: 10.1177/0963689719890597

93. Obermajer N, Muthuswamy R, Odunsi K, Edwards RP, Kalinski P. PGE(2)-induced CXCL12 production and CXCR4 expression controls the accumulation of human MDSCs in ovarian cancer environment. *Cancer Res* (2011) 71(24):7463–70. doi: 10.1158/0008-5472.CAN-11-2449

94. Obermajer N, Muthuswamy R, Lesnock J, Edwards RP, Kalinski P. Positive feedback between PGE2 and COX2 redirects the differentiation of human dendritic cells toward stable myeloid-derived suppressor cells. *Blood* (2011) 118(20):5498–505. doi: 10.1182/blood-2011-07-365825

95. Chen X, Ying X, Wang X, Wu X, Zhu Q, Wang X. Exosomes derived from hypoxic epithelial ovarian cancer deliver microRNA-940 to induce macrophage M2 polarization. *Oncol Rep* (2017) 38(1):522–8. doi: 10.3892/or.2017.5697

96. Wise DR, Thompson CB. Glutamine addiction: A new therapeutic target in cancer. *Trends Biochem Sci* (2010) 35(8):427–33. doi: 10.1016/j.tibs.2010.05.003

97. Yang L, Moss T, Mangala LS, Marini J, Zhao H, Wahlig S, et al. Metabolic shifts toward glutamine regulate tumor growth, invasion and bioenergetics in ovarian cancer. *Mol Syst Biol* (2014) 10:728. doi: 10.1002/msb.20134892

98. Menga A, Favia M, Spera I, Vegliante MC, Gissi R, De Grassi A, et al. N-acetylaspartate release by glutaminolytic ovarian cancer cells sustains protumoral macrophages. *EMBO Rep* (2021) 22(9):e51981. doi: 10.15252/embr.202051981

99. Song M, Sandoval TA, Chae CS, Chopra S, Tan C, Rutkowski MR, et al. IRE1alpha-XBP1 controls T cell function in ovarian cancer by regulating mitochondrial activity. *Nature* (2018) 562(7727):423–8. doi: 10.1038/s41586-018-0597-x

100. MacPherson S, Keyes S, Kilgour MK, Smazynski J, Chan V, Sudderth J, et al. Clinically relevant T cell expansion media activate distinct metabolic programs uncoupled from cellular function. *Mol Ther Methods Clin Dev* (2022) 24:380–93. doi: 10.1016/j.omtm.2022.02.004

101. Czystowska-Kuzmicz M, Sosnowska A, Nowis D, Ramji K, Szajnik M, Chlebowska-Tuz J, et al. Small extracellular vesicles containing arginase-1 suppress T-cell responses and promote tumor growth in ovarian carcinoma. *Nat Commun* (2019) 10(1):3000. doi: 10.1038/s41467-019-10979-3

102. Garcia-Navas R, Gajate C, Mollinedo F. Neutrophils drive endoplasmic reticulum stress-mediated apoptosis in cancer cells through arginase-1 release. *Sci Rep* (2021) 11(1):12574. doi: 10.1038/s41598-021-91947-0

103. Xia H, Li S, Li X, Wang W, Bian Y, Wei S, et al. Autophagic adaptation to oxidative stress alters peritoneal residential macrophage survival and ovarian cancer metastasis. *JCI Insight* (2020) 5(18):141115. doi: 10.1172/jci.insight.141115

104. Lamas B, Vergnaud-Gauduchon J, Goncalves-Mendes N, Perche O, Rossary A, Vasson MP, et al. Altered functions of natural killer cells in response to l-arginine availability. *Cell Immunol* (2012) 280(2):182–90. doi: 10.1016/j.cellimm.2012.11.018

105. Caneba CA, Yang L, Baddour J, Curtis R, Win J, Hartig S, et al. Nitric oxide is a positive regulator of the warburg effect in ovarian cancer cells. *Cell Death Dis* (2014) 5:e1302. doi: 10.1038/cddis.2014.264

106. Obermajer N, Wong JL, Edwards RP, Chen K, Scott M, Khader S, et al. Induction and stability of human Th17 cells require endogenous NOS2 and cGMP-dependent NO signaling. *J Exp Med* (2013) 210(7):1433–445. doi: 10.1084/jem.20121277

107. Gao W, Huang M, Chen X, Chen J, Zou Z, Li L, et al. The role of s-nitrosylation of PFKM in regulation of glycolysis in ovarian cancer cells. *Cell Death Dis* (2021) 12(4):408. doi: 10.1038/s41419-021-03681-0

108. Sperner-Unterweger B, Neurauter G, Klieber M, Kurz K, Meraner V, Zeimet A, et al. Enhanced tryptophan degradation in patients with ovarian carcinoma correlates with several serum soluble immune activation markers. *Immunobiology* (2011) 216(3):296–301. doi: 10.1016/j.imbio.2010.07.010

109. Inaba T, Ino K, Kajiyama H, Yamamoto E, Shibata K, Nawa A, et al. Role of the immunosuppressive enzyme indoleamine 2,3-dioxygenase in the progression of ovarian carcinoma. *Gynecol Oncol* (2009) 115(2):185–92. doi: 10.1016/j.ygyno.2009.07.015

110. Nonaka H, Saga Y, Fujiwara H, Akimoto H, Yamada A, Kagawa S, et al. Indoleamine 2,3-dioxygenase promotes peritoneal dissemination of ovarian cancer through inhibition of natural killercell function and angiogenesis promotion. *Int J Oncol* (2011) 38(1):113–20. doi: 10.3892/ijo_00000830

111. Tanizaki Y, Kobayashi A, Toujima S, Shiro M, Mizoguchi M, Mabuchi Y, et al. Indoleamine 2,3-dioxygenase promotes peritoneal metastasis of ovarian cancer by inducing an immunosuppressive environment. *Cancer Sci* (2014) 105 (8):966–73. doi: 10.1111/cas.12445

112. Liu J, Zhang H, Jia L, Sun H. Effects of treg cells and IDO on human epithelial ovarian cancer cells under hypoxic conditions. *Mol Med Rep* (2015) 11 (3):1708–14. doi: 10.3892/mmr.2014.2893

113. Zhao Y, Tao F, Jiang J, Chen L, Du J, Cheng X, et al. Tryptophan 2, 3dioxygenase promotes proliferation, migration and invasion of ovarian cancer cells. *Mol Med Rep* (2021) 23(6):445. doi: 10.3892/mmr.2021.12084

114. Wang X, Zhao X, Zhao J, Yang T, Zhang F, Liu L. Serum metabolite signatures of epithelial ovarian cancer based on targeted metabolomics. *Clin Chim Acta* (2021) 518:59–69. doi: 10.1016/j.cca.2021.03.012

115. Wu J, Li G, Li L, Li D, Dong Z, Jiang P. Asparagine enhances LCK signalling to potentiate CD8(+) T-cell activation and anti-tumour responses. *Nat Cell Biol* (2021) 23(1):75–86. doi: 10.1038/s41556-020-00615-4

116. Morellato AE, Umansky C, Pontel LB. The toxic side of one-carbon metabolism and epigenetics. *Redox Biol* (2021) 40:101850. doi: 10.1016/j.redox.2020.101850

117. Ducker GS, Rabinowitz JD. One-carbon metabolism in health and disease. *Cell Metab* (2017) 25(1):27–42. doi: 10.1016/j.cmet.2016.08.009

118. Sugiura A, Andrejeva G, Voss K, Heintzman DR, Xu X, Madden MZ, et al. MTHFD2 is a metabolic checkpoint controlling effector and regulatory T cell fate and function. *Immunity* (2022) 55(1):65–81e9. doi: 10.1016/j.immuni.2021.10.011

119. Cui X, Su H, Yang J, Wu X, Huo K, Jing X, et al. Up-regulation of MTHFD2 is associated with clinicopathological characteristics and poor survival in ovarian cancer, possibly by regulating MOB1A signaling. *J Ovarian Res* (2022) 15 (1):23. doi: 10.1186/s13048-022-00954-w

120. Shang M, Yang H, Yang R, Chen T, Fu Y, Li Y, et al. The folate cycle enzyme MTHFD2 induces cancer immune evasion through PD-L1 up-regulation. *Nat Commun* (2021) 12(1):1940. doi: 10.1038/s41467-021-22173-5

121. Sinclair LV, Howden AJ, Brenes A, Spinelli L, Hukelmann JL, Macintyre AN, et al. Antigen receptor control of methionine metabolism in T cells. *Elife* (2019) 8:44210. doi: 10.7554/eLife.44210

122. Nunes SC, Ramos C, Santos I, Mendes C, Silva F, Vicente JB, et al. Cysteine boosts fitness under hypoxia-mimicked conditions in ovarian cancer by metabolic reprogramming. *Front Cell Dev Biol* (2021) 9:722412. doi: 10.3389/fcell.2021.722412

123. Gao T, Zhang X, Zhao J, Zhou F, Wang Y, Zhao Z, et al. SIK2 promotes reprogramming of glucose metabolism through PI3K/AKT/HIF-1alpha pathway and Drp1-mediated mitochondrial fission in ovarian cancer. *Cancer Lett* (2020) 469:89–101. doi: 10.1016/j.canlet.2019.10.029

124. Zhao J, Zhang X, Gao T, Wang S, Hou Y, Yuan P, et al. SIK2 enhances synthesis of fatty acid and cholesterol in ovarian cancer cells and tumor growth through PI3K/Akt signaling pathway. *Cell Death Dis* (2020) 11(1):25. doi: 10.1038/s41419-019-2221-x

125. Phillippi B, Singh M, Loftus T, Smith H, Muccioli M, Wright J, et al. Effect of laminin environments and tumor factors on the biology of myeloid dendritic cells. *Immunobiology* (2020) 225(1):151854. doi: 10.1016/j.imbio.2019.10.003

126. Zhang S, Wu M, Wang F. Immune regulation by CD8(+) treg cells: novel possibilities for anticancer immunotherapy. *Cell Mol Immunol* (2018) 15(9):805–7. doi: 10.1038/cmi.2018.170

127. Guo L, Zhou B, Liu Z, Xu Y, Lu H, Xia M, et al. Blockage of glutaminolysis enhances the sensitivity of ovarian cancer cells to PI3K/mTOR inhibition involvement of STAT3 signaling. *Tumour Biol* (2016) 37(8):11007–15. doi: 10.1007/s13277-016-4984-3

128. Wu M, Chen X, Lou J, Zhang S, Zhang X, Huang L, et al. TGF-beta1 contributes to CD8+ treg induction through p38 MAPK signaling in ovarian cancer microenvironment. *Oncotarget* (2016) 7(28):44534–44. doi: 10.18632/oncotarget.10003

129. Chen Y, Liu L, Xia L, Wu N, Wang Y, Li H, et al. TRPM7 silencing modulates glucose metabolic reprogramming to inhibit the growth of ovarian cancer by enhancing AMPK activation to promote HIF-1alpha degradation. *J Exp Clin Cancer Res* (2022) 41(1):44. doi: 10.1186/s13046-022-02252-1

130. Vallee A, Lecarpentier Y, Vallee JN. The key role of the WNT/beta-catenin pathway in metabolic reprogramming in cancers under normoxic conditions. *Cancers (Basel)* (2021) 13(21):5557. doi: 10.3390/cancers13215557

131. Liu X, Zuo X, Sun X, Tian X, Teng Y. Hexokinase 2 promotes cell proliferation and tumor formation through the wnt/beta-catenin pathway-mediated cyclin D1/c-myc upregulation in epithelial ovarian cancer. *J Cancer* (2022) 13(8):2559–69. doi: 10.7150/jca.71894

132. To SKY, Tang MKS, Tong Y, Zhang J, Chan KKL, Ip PPC, et al. A selective beta-Catenin-Metadherin/CEACAM1-CCL3 axis mediates metastatic heterogeneity upon tumor-macrophage interaction. *Adv Sci (Weinh)* (2022) 9 (16):e2103230. doi: 10.1002/advs.202103230

133. Wall JA, Meza-Perez S, Scalise CB, Katre A, Londono AI, Turbitt WJ, et al. Manipulating the wnt/beta-catenin signaling pathway to promote anti-tumor immune infiltration into the TME to sensitize ovarian cancer to ICB therapy. *Gynecol Oncol* (2021) 160(1):285–94. doi: 10.1016/j.ygyno.2020.10.031

134. Alonezi S, Tusiimire J, Wallace J, Dufton MJ, Parkinson JA, Young LC, et al. Metabolomic profiling of the synergistic effects of melittin in combination with cisplatin on ovarian cancer cells. *Metabolites* (2017) 7(2):14. doi: 10.3390/metabo7020014

135. Yamawaki K, Mori Y, Sakai H, Kanda Y, Shiokawa D, Ueda H, et al. Integrative analyses of gene expression and chemosensitivity of patient-derived ovarian cancer spheroids link G6PD-driven redox metabolism to cisplatin chemoresistance. *Cancer Lett* (2021) 521:29–38. doi: 10.1016/j.canlet.2021.08.018

136. Lu J, Li Y, Li YA, Wang L, Zeng AR, Ma XL, et al. *In vivo* detection of dysregulated choline metabolism in paclitaxel-resistant ovarian cancers with proton magnetic resonance spectroscopy. *J Transl Med* (2022) 20(1):92. doi: 10.1186/s12967-022-03292-z

137. Odunsi K, Qian F, Lugade AA, Yu H, Geller MA, Fling SP, et al. Metabolic adaptation of ovarian tumors in patients treated with an IDO1 inhibitor constrains antitumor immune responses. *Sci Transl Med* (2022) 14(636):eabg8402. doi: 10.1126/scitranslmed.abg8402

138. Shi Q, Shen Q, Liu Y, Shi Y, Huang W, Wang X, et al. Increased glucose metabolism in TAMs fuels O-GlcNAcylation of lysosomal cathepsin b to promote cancer metastasis and chemoresistance. *Cancer Cell* (2022), S1535-6108(22)00376-2. doi: 10.1016/j.ccell.2022.08.012

139. Alharbi M, Lai A, Sharma S, Kalita-de Croft P, Godbole N, Campos A, et al. Extracellular vesicle transmission of chemoresistance to ovarian cancer cells is associated with hypoxia-induced expression of glycolytic pathway proteins, and prediction of epithelial ovarian cancer disease recurrence. *Cancers (Basel)* (2021) 13 (14):3388. doi: 10.3390/cancers13143388

140. Purwaha P, Lorenzi PL, Silva LP, Hawke DH, Weinstein JN. Targeted metabolomic analysis of amino acid response to l-asparaginase in adherent cells. *Metabolomics* (2014) 10(5):909–19. doi: 10.1007/s11306-014-0634-1

141. Wang L, Li Y, Wang J. Effect of glutamine on the immune function of paclitaxel intervention in ovarian cancer mice. *Cell Mol Biol (Noisy-le-grand)* (2020) 66(2):193–7. doi: 10.14715/cmb/2020.66.2.30

142. Priebe A, Tan L, Wahl H, Kueck A, He G, Kwok R, et al. Glucose deprivation activates AMPK and induces cell death through modulation of akt

in ovarian cancer cells. *Gynecol Oncol* (2011) 122(2):389–95. doi: 10.1016/j.ygyno.2011.04.024

143. El-Mais N, Fakhoury I, Abdellatef S, Abi-Habib R, El-Sibai M. Human recombinant arginase I [HuArgI (Co)-PEG5000]-induced arginine depletion inhibits ovarian cancer cell adhesion and migration through autophagy-mediated inhibition of RhoA. *J Ovarian Res* (2021) 14(1):13. doi: 10.1186/s13048-021-00767-3

144. Cheng H, Ma R, Wang S, Wang Y, Li Y, Tang Z, et al. Preliminary safety and potential effect of 6B11-OCIK adoptive cell therapy against platinum-resistant recurrent or refractory ovarian cancer. *Front Immunol* (2021) 12:707468. doi: 10.3389/fimmu.2021.707468

145. Amobi-McCloud A, Muthuswamy R, Battaglia S, Yu H, Liu T, Wang J, et al. IDO1 expression in ovarian cancer induces PD-1 in T cells *via* aryl hydrocarbon receptor activation. *Front Immunol* (2021) 12:678999. doi: 10.3389/fimmu.2021.678999

146. Jung KH, LoRusso P, Burris H, Gordon M, Bang YJ, Hellmann MD, et al. Phase I study of the indoleamine 2,3-dioxygenase 1 (IDO1) inhibitor navoximod (GDC-0919) administered with PD-L1 inhibitor (Atezolizumab) in advanced solid tumors. *Clin Cancer Res* (2019) 25(11):3220–8. doi: 10.1158/1078-0432.CCR-18-2740

147. Wang JJ, Siu MK, Jiang YX, Leung TH, Chan DW, Wang HG, et al. A combination of glutaminase inhibitor 968 and PD-L1 blockade boosts the immune response against ovarian cancer. *Biomolecules* (2021) 11(12):1749. doi: 10.3390/biom11121749

148. Fucikova J, Hensler M, Kasikova L, Lanickova T, Pasulka J, Rakova J, et al. An autologous dendritic cell vaccine promotes anticancer immunity in patients with ovarian cancer with low mutational burden and cold tumors. *Clin Cancer Res* (2022) 28(14):3053–65. doi: 10.1158/1078-0432.CCR-21-4413

149. Rob L, Cibula D, Knapp P, Mallmann P, Klat J, Minar L, et al. Safety and efficacy of dendritic cell-based immunotherapy DCVAC/OvCa added to first-line chemotherapy (carboplatin plus paclitaxel) for epithelial ovarian cancer: A phase 2, open-label, multicenter, randomized trial. *J Immunother Cancer* (2022) 10(1):e003190. doi: 10.1136/jitc-2021-003190

150. Block MS, Dietz AB, Gustafson MP, Kalli KR, Erskine CL, Youssef B, et al. Th17-inducing autologous dendritic cell vaccination promotes antigen-specific cellular and humoral immunity in ovarian cancer patients. *Nat Commun* (2020) 11(1):5173. doi: 10.1038/s41467-020-18962-z

151. Scherwitzl I, Opp S, Hurtado AM, Pampeno C, Loomis C, Kannan K, et al. Sindbis virus with anti-OX40 overcomes the immunosuppressive tumor microenvironment of low-immunogenic tumors. *Mol Ther Oncolytics* (2020) 17:431–47. doi: 10.1016/j.omto.2020.04.012

152. Yu J, Wei Z, Li Q, Wan F, Chao Z, Zhang X, et al. Advanced cancer starvation therapy by simultaneous deprivation of lactate and glucose using a MOF nanoplatform. *Adv Sci (Weinh)* (2021) 8(19):e2101467. doi: 10.1002/advs.202101467

153. Prentice RL, Thomson CA, Caan B, Hubbell FA, Anderson GL, Beresford SA, et al. Low-fat dietary pattern and cancer incidence in the women's health initiative dietary modification randomized controlled trial. *J Natl Cancer Inst* (2007) 99(20):1534–43. doi: 10.1093/jnci/djm159

154. Zhang M, Lee AH, Binns CW. Reproductive and dietary risk factors for epithelial ovarian cancer in China. *Gynecol Oncol* (2004) 92(1):320–6. doi: 10.1016/j.ygyno.2003.10.025

155. Cozen W, Peters R, Reichardt JK, Ng W, Felix JC, Wan P, et al. Galactose-1-phosphate uridyl transferase (GALT) genotype and phenotype, galactose consumption, and the risk of borderline and invasive ovarian cancer (United states). *Cancer Causes Control* (2002) 13(2):113–20. doi: 10.1023/a:1014384027523

156. Fan J, Shang D, Han B, Song J, Chen H, Yang JM. Adoptive cell transfer: Is it a promising immunotherapy for colorectal cancer? *Theranostics* (2018) 8(20):5784–800. doi: 10.7150/thno.29035

157. Geller MA, Cooley S, Judson PL, Ghebre R, Carson LF, Argenta PA, et al. A phase II study of allogeneic natural killer cell therapy to treat patients with recurrent ovarian and breast cancer. *Cytotherapy* (2011) 13(1):98–107. doi: 10.3109/14653249.2010.515582

158. Hoogstad-van Evert J, Bekkers R, Ottevanger N, Schaap N, Hobo W, Jansen JH, et al. Intraperitoneal infusion of ex vivo-cultured allogeneic NK cells in recurrent ovarian carcinoma patients (a phase I study). *Med (Baltimore)* (2019) 98(5):e14290. doi: 10.1097/MD.0000000000014290

159. Lu YC, Shi YY, Luo ZY, Guo XM, Jiang MS, Li X, et al. Reactivation of dysfunctional dendritic cells by a stress-relieving nanosystem resets anti-tumor immune landscape. *Nano Today* (2022) 43:101416. doi: 10.1016/j.nantod.2022.101416

160. Benesova K, Kraus FV, Carvalho RA, Lorenz H, Horth CH, Gunther J, et al. Distinct immune-effector and metabolic profile of CD8(+) T cells in patients with autoimmune polyarthritis induced by therapy with immune checkpoint inhibitors. *Ann Rheumatic Dis* (2022) 43:101416. doi: 10.1136/ard-2022-222451

161. Liu Y, Yu Y, Yang S, Zeng B, Zhang Z, Jiao G, et al. Regulation of arginase I activity and expression by both PD-1 and CTLA-4 on the myeloid-derived suppressor cells. *Cancer Immunol Immunother* (2009) 58(5):687–97. doi: 10.1007/s00262-008-0591-5

162. Awuah SG, Zheng YR, Bruno PM, Hemann MT, Lippard SJ. A Pt(IV) pro-drug preferentially targets indoleamine-2,3-dioxygenase, providing enhanced ovarian cancer immuno-chemotherapy. *J Am Chem Soc* (2015) 137(47):14854–7. doi: 10.1021/jacs.5b10182

163. Kuznicki ML, Bennett C, Yao M, Joehlin-Price A, Rose PG, Mahdi H. Predictors of response to immune checkpoint inhibition in a real world gynecologic cancer population. *Gynecol Oncol Rep* (2020) 34:100671. doi: 10.1016/j.gore.2020.100671

164. Sadik A, Somarribas Patterson LF, Ozturk S, Mohapatra SR, Panitz V, Secker PF, et al. IL4I1 is a metabolic immune checkpoint that activates the AHR and promotes tumor progression. *Cell* (2020) 182(5):1252–1270e34. doi: 10.1016/j.cell.2020.07.038

165. Wallace-Povirk A, Rubinsak L, Malysa A, Dzinic SH, Ravindra M, Schneider M, et al. Targeted therapy of pyrrolo[2,3-d]pyrimidine antifolates in a syngeneic mouse model of high grade serous ovarian cancer and the impact on the tumor microenvironment. *Sci Rep* (2022) 12(1):11346. doi: 10.1038/s41598-022-14788-5

166. Hou Z, Gattoc L, O'Connor C, Yang S, Wallace-Povirk A, George C, et al. Dual targeting of epithelial ovarian cancer *Via* folate receptor alpha and the proton-coupled folate transporter with 6-substituted Pyrrolo[2,3-d]pyrimidine antifolates. *Mol Cancer Ther* (2017) 16(5):819–30. doi: 10.1158/1535-7163.MCT-16-0444

167. Li L, Liu S, Han D, Tang B, Ma J. Delivery and biosafety of oncolytic virotherapy. *Front Oncol* (2020) 10:475. doi: 10.3389/fonc.2020.00475

168. Hulin-Curtis SL, Davies JA, Nestic D, Bates EA, Baker AT, Cunliffe TG, et al. Identification of folate receptor alpha (FRalpha) binding oligopeptides and their evaluation for targeted virotherapy applications. *Cancer Gene Ther* (2020) 27(10-11):785–98. doi: 10.1038/s41417-019-0156-0

169. Sun J, Yan C, Xu D, Zhang Z, Li K, Li X, et al. Immuno-genomic characterisation of high-grade serous ovarian cancer reveals immune evasion mechanisms and identifies an immunological subtype with a favourable prognosis and improved therapeutic efficacy. *Br J Cancer* (2022) 126(11):1570–80. doi: 10.1038/s41416-021-01692-4

170. Sun L, Zhang H, Gao P. Metabolic reprogramming and epigenetic modifications on the path to cancer. *Protein Cell* (2022) 13(12):877–919. doi: 10.1007/s13238-021-00846-7

171. Sun T, Liu Z, Yang Q. The role of ubiquitination and deubiquitination in cancer metabolism. *Mol Cancer* (2020) 19(1):146. doi: 10.1186/s12943-020-01262-x

172. Zhao E, Maj T, Kryczek I, Li W, Wu K, Zhao L, et al. Cancer mediates effector T cell dysfunction by targeting microRNAs and EZH2 *via* glycolysis restriction. *Nat Immunol* (2016) 17(1):95–103. doi: 10.1038/ni.3313

173. Guo J, Satoh K, Tabata S, Mori M, Tomita M, Soga T. Reprogramming of glutamine metabolism *via* glutamine synthetase silencing induces cisplatin resistance in A2780 ovarian cancer cells. *BMC Cancer* (2021) 21(1):174. doi: 10.1186/s12885-021-07879-5

Glossary

ACT	Adoptive cell transfer therapy
ADP	Adenosine diphosphate
AHR	Aryl hydrocarbon receptor
ARG1	Arginase-1
Asn	Asparagine
ATP	Adenosine triphosphate
AMPK	Adenosine monophosphate activated protein kinase
CTLA-4	Cytotoxic T lymphocyte-associated antigen 4
Cys	cysteine
CXCL	C-X-C motif chemokine ligand
DC	Dendritic cell
EOC	Epithelial ovarian cancer
EVs	Extracellular vesicles
FAs	Fatty acids
FAO	Fatty acid oxidation
FASN	Fatty acid synthase
FIGO	Federation of Gynecology and Obstetrics
FR	folate receptor
FSH	Follicle-stimulating hormone
GAPDH	Glyceraldehyde-3-phosphate dehydrogenase
GDE1	Glycerophosphodiester phosphodiesterase 1
GLS	glutaminase
GM-CSF	granulocyte-macrophage colony-stimulating factor
GPCPD1	Glycerophosphocholine phosphodiesterase 1
GS	glutamine synthetase
HIF-1α	Hypoxia-inducible factor-1
HGSOC	high-grade serous ovarian cancer
HMGCR	3-hydroxy-3-methylglutaryl-coenzyme A reductase
ICB	Immune checkpoint blockade
ICI	Immune checkpoint inhibitor
IDO	Indoleamine 2, 3-dioxygenase
IFN	Interferon
IL	Interleukin
IL4I1	Interleukin-4-induced-1
LPA	Lysophosphatidic acid
OC	ovarian cancer
OCCC	Ovarian clear cell carcinoma
OXPHOS	Oxidative phosphorylation
PDK1	Pyruvate dehydrogenase kinase 1
PDK2	Pyruvate dehydrogenase kinase 2
PD-1	Programmed death receptor 1
PD-L1	Programmed death ligand-1
PGE2	Prostaglandin E-2
PFKM	Phosphofructokinase-M
PI3K/Akt	Phosphatidylinositol 3-kinase/protein kinase B
PKM1	Pyruvate kinase M1
PKM2	Pyruvate kinase M2
PPAR	peroxisome proliferators-activated receptor
PPP	pentose phosphate pathway
Ser	Serine
SIK2	Salt-inducible kinase 2
SOCS3	cytokine signaling 3
SREBP	Sterol regulatory element binding protein
ROS	Reactive oxygen species
TAM	Tumor-associated macrophage
TCA	tricarboxylic acid
TDO2	tryptophan 2, 3-dioxygenase
Teff	effector T cell
TGF	transforming growth factor
Th17	IL-17-producing T helper
TIME	tumor immune microenvironment
Tmem	memory T cell
Treg	Regulatory T cell
TRPM7	Transient receptor potential melastatin 7L
MAPK	Mitogen-activated protein kinase
M-CSF	Macrophage colony-stimulating factor
MCT1	Monocarboxylate cotransporter 1
MDSCs	Myeloid-derived suppressor cells
MEK	methyl ethyl ketone
mRNA	Messenger ribose nucleic acid
MTHFD2	Methylenetetrahydrofolate dehydrogenase 2
mTOR	Mammalian target of rapamycin
NAA	N-acetylaspartate
NAD^+	Nicotinamide adenine dinucleotide
NADPH	Nicotinamide adenine dinucleotide phosphate
NAMD receptor	N-methyl-D-aspartate receptor
NCCN	National Comprehensive Cancer Network
NK	Natural killer
NMDA receptor	N-methyl-D-aspartic acid receptor
NO	Nitric oxide
NOS1	Nitric oxide synthase 1
NOS2/iNOS	Nitric oxide synthase-2
UDP	Uridine Diphosphate
UTP	Uridine Triphosphate
VEGF	Vascular Endothelial Growth Factor
Wnt	Wingless
1C	One-carbon

frontiers | Frontiers in Immunology

TYPE Original Research
PUBLISHED 01 February 2023
DOI 10.3389/fimmu.2022.1047661

OPEN ACCESS

EDITED BY
Soumya R. Mohapatra,
School of Medicine (KIMS), India

REVIEWED BY
Anjie Zhen,
University of California, Los Angeles, United States
Vanaja Konduri,
Baylor College of Medicine, United States
Govindarajan Thangavelu,
University of Minnesota Twin Cities, United States

*CORRESPONDENCE
Shashi Gujar
shashi.gujar@dal.ca

SPECIALTY SECTION
This article was submitted to Cancer Immunity and Immunotherapy, a section of the journal Frontiers in Immunology

RECEIVED 18 September 2022
ACCEPTED 20 December 2022
PUBLISHED 01 February 2023

CITATION
Holay N, Kennedy BE, Murphy JP, Konda P, Giacomantonio M, Brauer-Chapin T, Paulo JA, Kumar V, Kim Y, Elaghil M, Sisson G, Clements D, Richardson C, Gygi SP and Gujar S (2023) After virus exposure, early bystander naïve CD8 T cell activation relies on NAD$^+$ salvage metabolism.
Front. Immunol. 13:1047661.
doi: 10.3389/fimmu.2022.1047661

After virus exposure, early bystander naïve CD8 T cell activation relies on NAD$^+$ salvage metabolism

Namit Holay[1], Barry E. Kennedy[1,2], J. Patrick Murphy[1,3], Prathyusha Konda[4,5], Michael Giacomantonio[1], Tatjana Brauer-Chapin[1,7], Joao A. Paulo[7], Vishnupriyan Kumar[1], Youra Kim[1], Mariam Elaghil[1,2], Gary Sisson[3], Derek Clements[1,8], Christopher Richardson[4,9,10], Steven P. Gygi[7] and Shashi Gujar[1,4,11,12,13]*

[1]Department of Pathology, Dalhousie University, Halifax, NS, Canada, [2]IMV Inc, Halifax, NS, Canada, [3]Department of Biology, University of Prince Edward Island, Charlottetown, PEI, Canada, [4]Department of Microbiology and Immunology, Dalhousie University, Halifax, NS, Canada, [5]Dana Farber Cancer Institute, Harvard Medical School, Boston, MA, United States, [6]Flow Cytometry Core Facility, Dalhousie University, Halifax, NS, Canada, [7]Department of Cell Biology, Harvard Medical School, Harvard University, Boston, MA, United States, [8]Department of Microbiology and Immunology, Stanford University, Stanford, CA, United States, [9]Canadian Centre for Vaccinology, IWK Health Centre, Goldbloom Pavilion, Halifax, NS, Canada, [10]Department of Pediatrics, Dalhousie University, Halifax, NS, Canada, [11]Department of Biology, Dalhousie University, Halifax, NS, Canada, [12]Beatrice Hunter Cancer Research Institute, Halifax, NS, Canada, [13]Cancer Immunotherapy: Innovation & Global Partnerships, Faculty of Medicine, Dalhousie University, Halifax, NS, Canada

CD8 T cells play a central role in antiviral immunity. Type I interferons are among the earliest responders after virus exposure and can cause extensive reprogramming and antigen-independent bystander activation of CD8 T cells. Although bystander activation of pre-existing memory CD8 T cells is known to play an important role in host defense and immunopathology, its impact on naïve CD8 T cells remains underappreciated. Here we report that exposure to reovirus, both *in vitro* or *in vivo*, promotes bystander activation of naïve CD8 T cells within 24 hours and that this distinct subtype of CD8 T cell displays an innate, antiviral, type I interferon sensitized signature. The induction of bystander naïve CD8 T cells is STAT1 dependent and regulated through nicotinamide phosphoribosyl transferase (NAMPT)-mediated enzymatic actions within NAD$^+$ salvage metabolic biosynthesis. These findings identify a novel aspect of CD8 T cell activation following virus infection with implications for human health and physiology.

KEYWORDS

antiviral immunity, CD8 T cells, bystander activation, naïve CD8 T cells, type I interferons, immunometabolism, NAD$^+$ salvage metabolism, metabolic reprogramming

Introduction

CD8 T cells are an important arm of cellular immunity to viruses and are responsible for identifying and eliminating virus-infected cells during the adaptive phase of the immune response. Following virus exposure, T cells can be activated by T cell receptor (TCR)-dependent and -independent mechanisms. Upon TCR engagement, T cells rapidly lose their naive phenotype, become CD44hi, and are known as differentiated T cells (1). In TCR- independent activation, known as bystander activation, cytokines play an important role in the activation of effector functions in pre-existing memory T cells. Specifically, the cytokines IL-15 and IL-18 can drive antigen independent IFN-γ secretion or cytolytic activity *via* NKG2D in non-specific, pre-existing memory T cells (2, 3). Naïve CD8 T cells can also undergo bystander activation because of their presence in an inflammatory milieu. Some studies have demonstrated that bystander activation during chronic virus exposure can drive naïve CD8 T cells with memory-like phenotype (4) or cause them to differentiate into memory-like T cells upon late priming (5). Interestingly, infections and inflammation driven by the cohousing of laboratory mice with pet store mice can activate naïve CD8 T cells in a bystander manner and impact their homeostasis and function (6). Type I interferons are rapidly produced early in infection in response to viral exposure. Some viruses, such as SARS-CoV2, drive severe disease by dysregulating and delaying host type I interferon production (7, 8). Exposure of naïve CD8 T cells to type I interferons drives rapid acquisition of effector function upon antigenic stimulation (9, 10). The complex interplay between naïve CD8 T cells and type I interferons during bystander activation *early on* following virus exposure remains poorly understood.

Recent advances in immunometabolism firmly suggest that T cell function is closely linked with metabolism (11, 12). Virus exposure as well as type I interferons have been reported to cause metabolic restructuring in immune cells (13, 14). While most studies in the area of T cell immunometabolism have focussed on effector and memory T cell subsets (15, 16), very little is known about the metabolic reprogramming that occurs within naïve CD8 T cells, especially immediately following virus exposure. While the majority of studies on T cell metabolism thus far have captured the roles of the key metabolic pathways glycolysis and oxidative phosphorylation, further investigation of other metabolic pathways and metabolites including NAD^+ is needed. NAD^+ is a substrate and redox cofactor for several important metabolic pathways and is required for the function of T cells (17). Intracellular NAD^+ is an essential cofactor for glycolysis and glycolytic flux is well known to mediate effector vs memory function in T cells (18). Also, the activity of NAD^+-dependent deacetylase SIRT1 has been shown to promote the formation of memory T cells (19). Further, extracellular NAD^+ promotes immune response through receptor-mediated downregulation of regulatory T cell populations (20). Similarly, tumor cyclic ADP ribose hydrolase CD38-mediated breakdown of extracellular NAD^+ promotes T cell exhaustion in tumor microenvironments (21).Therapeutic modulation of NAD^+ levels has been implemented to control T cell function in conditions like graft versus host disease (GVHD) (22) and experimental allergic encephalomyelitis (EAE) (23, 24). However, the implications for NAD^+ metabolism in the context of antiviral CD8 T cell immunity remain relatively unknown.

In the present study, using a combination of flow cytometry, quantitative proteomics, metabolomics, and pharmacological inhibition approaches within *in vivo* and *in vitro* settings, we report an NAD^+ salvage-dependent, type I interferon-driven induction of bystander naïve CD8 T cells (CD8 bT_N) within 24 hours of viral exposure. Given the importance of bystander activation and the early determinants of antiviral adaptive immunity, this study highlights underappreciated consequences of type I interferon-mediated metabolic reprogramming of naïve CD8 T cells immediately after exposure to viruses.

Results

Reovirus exposure drives early induction of CD8 bT_N cells *in vivo*

To understand the earliest phenotypic changes in CD8 T cells upon virus exposure, we exposed C57BL/6 mice to reovirus, a naturally occurring prototypic dsRNA virus that causes acute infection and drives immune response (25, 26), *via* intraperitoneal (i.p.) injection and studied CD8 T cell subsets *via* flow cytometry in the spleen. We first gated on live cells followed by sequential gating on single cells, lymphocytes and CD3+CD8+ T cells to identify 4 subsets of CD8 T cells- naïve, central memory, effector memory, and CD44lowCD62Llow- using CD44 and CD62L as shown in the representative dot plots (Figure 1A). The Ly6 family of proteins including Ly6C and Ly6A/E (Sca-1) are important early indicators of bystander activation (6, 27). We observed that Ly6C was upregulated in CD44lowCD62L+ naïve CD8 T cells within 24 hours of virus exposure (Figures 1B, C). Sca-1 was observed to be *uniquely* upregulated on virus exposed naïve CD8 T cells and not in T cells from non-treated spleens and was hence, used as a marker to identify bystander naïve CD8 T cells (CD8 bT_N) henceforth. Expression of these markers was also observed on the parent CD8 T cell population (Figures S1A, B) and it was noted that upregulation in Sca-1 after exposure to virus was not unique to T_N cells (Figure S1C). Since, CD8 T cells still maintained a naive (CD44lowCD62L+) phenotype, it was unlikely that the increase in Sca-1 and Ly6C expression is due to TCR triggering, however, to confirm this we measured the expression of CD69, CD25, KLRG1, and CD49d (Figures 1D, S1C), markers known to be upregulated upon activation *via* TCR (6). Naïve CD8 T cells failed to upregulate any of these markers within 24 hours after

10.3389/fimmu.2022.1047661

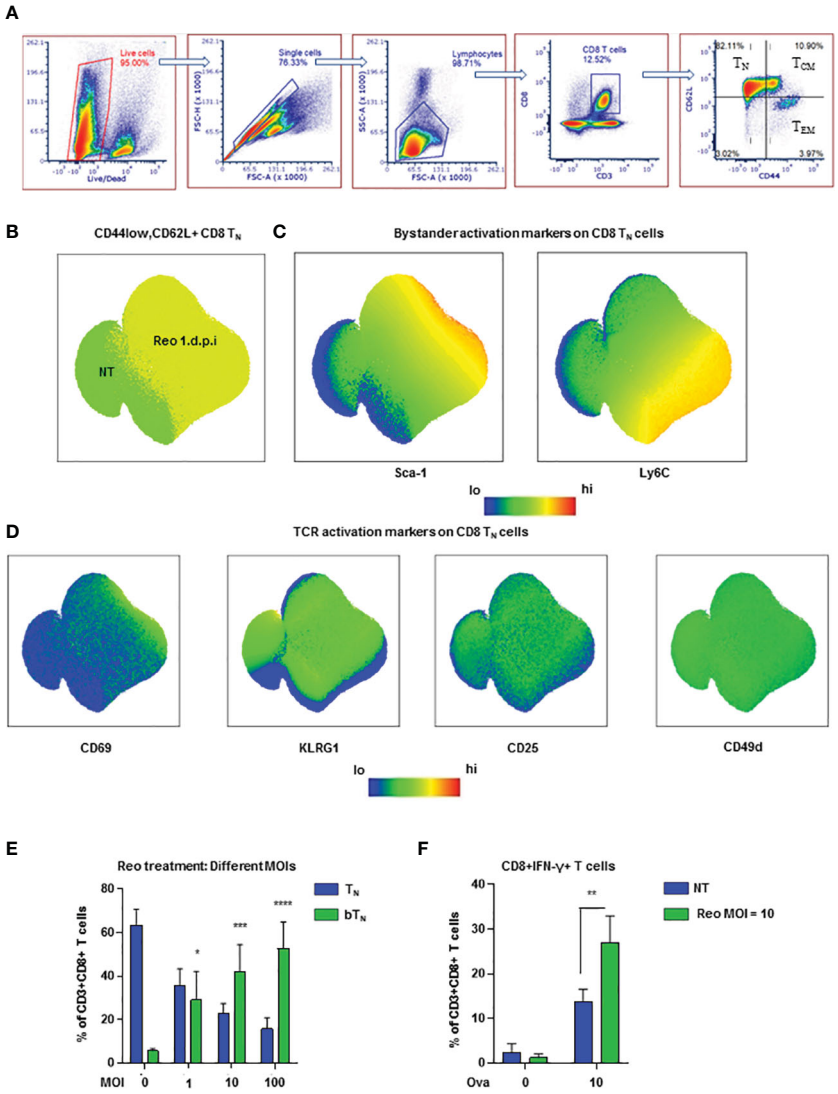

FIGURE 1
Reovirus induces early bystander activated naïve CD8 T cells *in vivo* **(A)** Representative dot plots demonstrating the gating strategy for the identification of CD8 T cell subsets- T_N, T_{CM}, T_{EM} and CD44lowCD62Llow (n=3 mice per non-treated group). **(B)** UMAP showing CD8 T_N cells in non-treated (NT) and reovirus treated (Reo 1 d.p.i.) C57BL/6 splenocytes. **(C)** UMAP depicting bystander activation markers in CD8 T_N cells. **(D)** UMAP representing TCR activation markers in CD8 T_N cells. (n=9 mice; NT-3 mice, Reo 1 d.p.i.-6 mice in all UMAP plots). **(E)** Bar graphs for the induction of CD8 bT_N cells upon treatment of splenocytes from C57BL/6 mice with varying MOIs of reovirus (n=3 independent experiments). **(F)** Bar graphs for % of CD8+IFN-γ+ T cells in OT-1 splenocytes (n=3 independent experiments). Two-way ANOVA with 95% confidence interval was used for statistical analysis in bar graphs. Significance has been indicated only for CD8 bT_N cell populations induced within 24 hours in comparison with untreated control population levels. Not significant (ns) = $p > 0.05$; *$p < 0.05$; **$p < 0.01$; ***$p < 0.001$; **** $p < 0.0001$.

virus exposure confirming that they were indeed activated in a bystander manner (Figure 1D).

Next, we evaluated the presence of CD8 bT_N cells over time in different tissues after exposure to reovirus. In the spleen, we found that a significant percentage of CD8 bT_N cells were maintained at day 7 after virus exposure- by which timepoint an effector CD8 T cell response was developed (Figure S2A). In the mesenteric lymph nodes, CD8 bT_N cells were not only maintained but formed the majority population even on day 7 (Figure S2B) while in the peritoneal flush extracted from the site of exposure, CD8 bT_N cells were also observed albeit at lower percentages (Figure S2C). This data demonstrated that CD8 bT_N cells were differentially maintained at different sites following virus exposure suggesting that their role and persistence may be context dependent after virus exposure. Since reovirus is a dsRNA virus, we also investigated whether the induction of CD8 bT_N cells was dependent on TLR3, a dsRNA sensor in the cytoplasm (28). We discovered that CD8 bT_N cell induction was independent of TLR3 (Figure S2D). The induction of CD8 bT_N cells was also found to be independent of mouse background as a

robust CD8 bT_N induction was also seen in BALB/c mice after reovirus exposure (Figure S2E).

To study CD8 bT_N cells *ex vivo*, we exposed mouse splenocytes to varying MoIs of reovirus and observed that they were induced in a dose dependent manner (Figure 1E). Upon exposure of OT-1 splenocytes to reovirus for 18h followed by priming with ova peptide for 6h, we observed an increase in the percentage of IFN-γ+ CD8 T cells (Figure 1F) suggesting that bystander activation of naïve CD8 T cells led to enhanced functional capabilities. Together, these data show that the exposure to virus prompts the induction of functionally distinct CD8 bT_N cells.

CD8 bT_N cells have an innate anti-viral proteomic signature

In light of phenotypic and functional changes noted above, we next asked whether CD8 bT_N cells held a distinct proteomic landscape. For this, a proteomic snapshot of these cells in comparison with other T cell subsets was generated using tandem mass tag (TMT)- labelled multiplexed mass spectrometry. FACS-isolated pure populations of CD8 T_N cells, CD8 bT_N cells (Day 1), CD8 bT_N cells (Day 7) and T_{EM} cells (Day 7) from the spleen were digested, labelled with TMT, and processed for mass spectrometry-based proteome profiling as depicted in the workflow schematic (Figure 2A). A heatmap representing 4718 proteins that were identified by the proteomic analysis shows these proteins grouped into various clusters by K-means clustering across the tested T cell subtypes (Figure S3A). The top 2 hits in each of the clusters have been listed in Table S1. When comparing CD8 bT_N cells on Day 1 and Day 7, we discovered that CD8 bT_N cells on Day 7 had increased granzyme K expression (Figure 2B) although no changes were seen in levels of granzyme A or B (Figure S3B). Further, when compared with the other dominant population on Day 7 i.e., T_{EM} cells- CD8 bT_N cells had increased expression of memory markers TCF7 and FOXO1 (Figure 2C). Using flow cytometry, we also noted that CD8 bT_N cells on day 7 were mostly positive for CD127 expression as compared to T_{EM} cells that include distinct CD127 + and CD127- populations (Figure 2D) that are known to comprise memory precursors and short-lived effectors, respectively (29–31). Taken together, this data suggests that CD8 bT_N cells bear distinct proteome changes accompanying alerted functional capabilities.

To get an insight into the molecular signature of these early induced CD8 bT_N cells and understand how they differed from T_N cells within 24 hours of virus exposure, we next focussed our analysis on the proteomic data from these two groups of cells, identifying proteins that were significantly changed (at least 2-fold) between them (Figure 2E). From among the K-means clusters described earlier, cluster 3 represents proteins that are upregulated in CD8 bT_N cells when compared to T_N cells. Gene Ontology (GO) term analysis for proteins in this cluster revealed differential expression of proteins related to defense responses to virus, innate immune response, type I interferon, and purine biosynthesis (Figure 2F). As mentioned previously, the induction of CD8 bT_N cells after reovirus exposure was observed to be independent of TLR3 signalling (Figure S1B), however, among the proteins related to defense response to virus and innate immune response, RIG-I related proteins were upregulated in CD8 bT_N cells (Figure S3C). Along with TLR3, RIG-I is also involved in dsRNA recognition and regulation of immune responses (32). One of the major pathways associated with viral defense, however, identified in CD8 bT_N cells *via* proteomics was the type I interferon pathway (Figure 2E). Levels of interferon-driven proteins including the IFIT family, ZBP1, BST2, ADR, IFI35 and EIF2AK2 were upregulated in CD8 bT_N cells (Figure 2G). These data demonstrated a clear signature of type I interferon sensitization, a characteristic event driven during virus recognition, in CD8 bT_N cells.

Antiviral type I interferons induce CD8 bT_N cells in a STAT1-dependent manner

In order to further investigate the role of type I interferons in the induction of CD8 bT_N cells, we first confirmed that an increased level of type I interferon was observed in the spleen of mice exposed to reovirus (Figure S3D). Hence, we next asked if type I interferons might be able to directly drive the induction of CD8 bT_N cells without reovirus. To test this, we treated *ex vivo* isolated C57BL/6 splenocytes with exogeneous IFN-α1 and IFN-β1. Both treatments induced a robust, dose-dependent induction of CD8 bT_N cells (Figures 3A, B respectively). We further tested whether type I interferon signalling had a role to play in the induction of CD8 bT_N cells. Using quantitative PCR, we noted that the levels of *Ifnar1* and *Ifnar2* remained unchanged in splenocytes on day 1 after treatment of mice with reovirus (Figure S3E). We proceeded to block the IFNAR1 receptor with a blocking antibody during treatment of splenocytes with reovirus *ex vivo*. This led to the abolishment of CD8 bT_N cell induction (Figure 3C). Within the type I interferon signalling pathway, the ISGF3 (STAT1-STAT2-IRF9) complex forms an important regulator of type I interferon signalling in cells (33). Although signalling proteins in other type I interferon signalling pathways remained unchanged (Figure 2G, lower half of heatmap), IRF9 of the ISGF3 complex was significantly upregulated in CD8 bT_N cells (Figure 3D). In the proteomics data, all STAT proteins, except STAT2, were identified and STAT1 levels were found to be increased, albeit not to statistically significant levels (Figure S3F). Nonetheless, given the importance of STATs in the response to type I interferons and the upregulation of IRF9 of the ISGF3 complex in the proteomics data, we decided to test the induction of CD8 bT_N cells in STAT1 KO mice. Reovirus

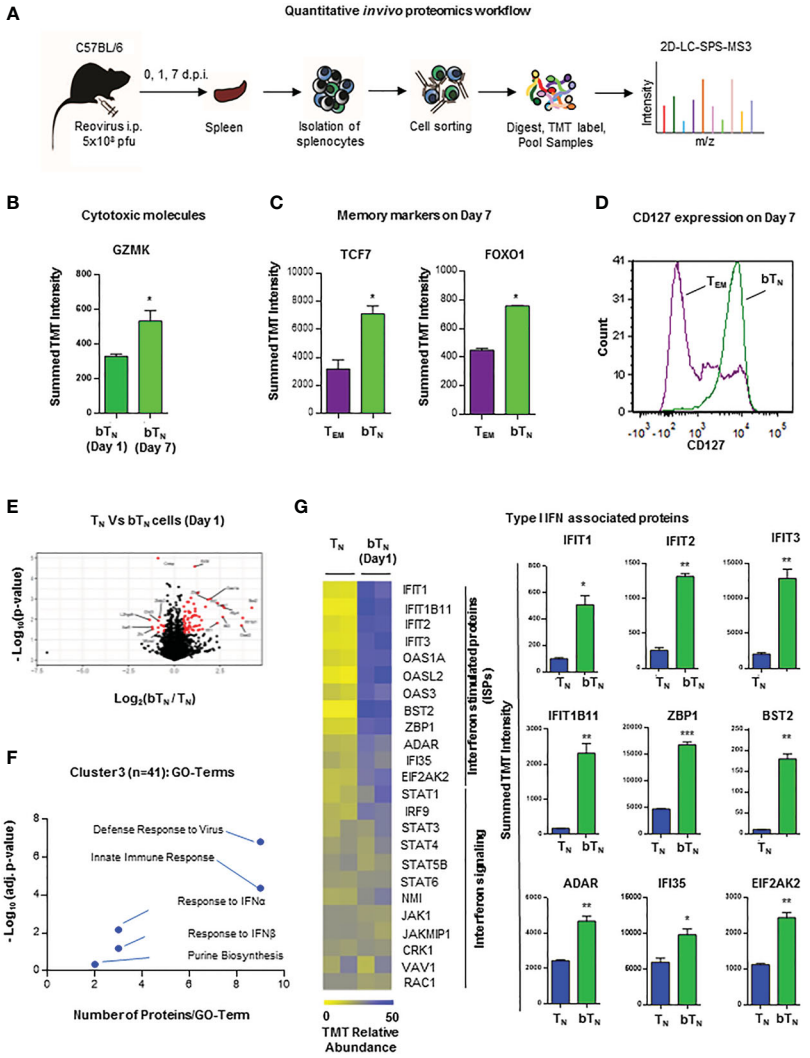

FIGURE 2
Quantitative *in vivo* proteomic analysis of CD8 bT_N cells. **(A)** Schematic for the workflow of quantitative *in vivo* proteomics with T cells isolated from spleens of C57BL/6 mice (n=5 mice pooled for isolation of each cell type in an independent experiment). **(B)** Bar graph for protein expression from quantitative proteomics of granzyme K expression in CD8 bT_N cells (1 d.p.i. and 7 d.p.i.). **(C)** Bar graphs for protein expression from quantitative proteomics of memory markers TCF7 and FOXO1 expression in T_{EM} cells (7 d.p.i.) and CD8 bT_N cells (7 d.p.i.). **(D)** Histogram overlay for memory marker CD127 in T_{EM} cells (7 d.p.i.) and CD8 bT_N cells (7 d.p.i.). Representative histogram shown from spleen of one mouse (n=3 mice) **(E)** Volcano plot compares all identified proteins across CD8 T_N and CD8 bT_N cells (1 d.p.i.). **(F)** Cluster 3 of GO TERM analysis of proteomics depicting differentially regulated pathways in CD8 bT_N cells compared to T_N cells. **(G)** Heatmap for the relative levels of interferon-stimulated proteins and interferon signalling proteins identified in T_N and CD8 bT_N cells (1 d.p.i.). Corresponding bar graphs show the levels of several type I interferon-associated proteins in T_N and CD8 bT_N cells. Two-tailed Student's *t*-test with 95% confidence interval was used for statistical analysis. Not significant (ns) = $p > 0.05$; *$p < 0.05$; **$p < 0.01$; ***$p < 0.001$.

failed to induce CD8 bT_N cells in splenocytes isolated from STAT1 KO mice (Figure 3E). Similar results were also observed with type I interferons wherein no induction of CD8 bT_N cells was observed with IFN-α1 and IFN-β1 (Figure 3F). In addition, it should be noted that our model of STAT1 KO mice also had a SLAM knock-in. SLAM or CD150 is a receptor for measles virus and this model was previously designed for the study of measles infection (34). To confirm that the lack of induction of CD8 bT_N cells in the STAT1 KO mice was not a result of SLAM knock-in, we tested splenocytes from SLAM knock-in only control mice and found robustly induced CD8 bT_N cells following treatment with reovirus and IFN-β1 (Figure S3G). Altogether, these data conclusively demonstrate a role for type I interferon signalling in the induction of CD8 bT_N cells and provide evidence that this induction occurs in a STAT1-dependent manner.

10.3389/fimmu.2022.1047661

Induction of CD8 bT_N cells with different viruses depends on their interferon activating capacity

To assess whether different viruses were equally capable of inducting bystander activation of naïve CD8 T cells, we investigated the induction of CD8 bT_N cells upon *ex vivo* exposure to a number of different viruses. We observed that two different strains of herpes simplex virus- HSV- ICP0 (35) and 1716 (36)- robustly induced CD8 bT_N cells at a low MoI of 0.1 (Figure 4A). Next, the Indiana strain of VSV (37) induced CD8 bT_N cells at a higher MoI (Figure 4B). Further, we employed measles virus and discovered that the Edmonston vaccine strain of measles (38)- induced CD8 bT_N cells at an MoI of 0.1 (Figure 4C) however, the IC323 strain of measles virus (39) failed to induce a significant CD8 bT_N cell response (Figure 4D). Within the array of viruses employed, IC323 strain of measles is known for its inferior capacity to stimulate type I interferons (40, 41) Taken together, this data suggested that CD8 bT_N cell induction occurred variably in different viruses and was a function of their interferon inducing capabilities.

NAMPT-mediated NAD^+ biosynthesis through salvage pathway metabolism regulates CD8 bT_N cell induction

Type I interferons have been shown to drive a rewiring of metabolism in a variety of cell types including hepatic cells (42) and innate immune cells (14). In our proteomics analysis, we discovered that proteins related to NAD^+-dependent ADP-ribosyl transferase activity like PARP9 and PARP14 (Figure S4A), as well as many proteins from the OAS family with ATP binding activity were also upregulated (Figure S4B) in CD8 bT_N cells when compared to T_N cells. Consequently, we hypothesized that CD8 bT_N cells might be metabolically reprogrammed as compared to CD8 T_N cells after reovirus exposure. To test this hypothesis, we employed a semi-targeted approach to study the metabolism of CD8 T_N and CD8 bT_N cells. CD8 T_N cells and CD8 bT_N cells (Day 1) were isolated from the spleens of reovirus-injected C57BL/6 mice by flow cytometry and then processed for metabolome analysis (Figure 5A). A heatmap comparing the metabolomic signatures of CD8 T_N and CD8 bT_N cells clearly showed distinct metabolic rewiring of CD8 bT_N cells as compared to CD8 T_N cells (Figure 5B). A list of the top upregulated and downregulated metabolites (fold change greater than or equal to 2, $p<0.05$) in CD8 bT_N cells as compared to T_N cells is shown in Figure 5C. An enrichment analysis revealed a role for central energy metabolism (glycolysis and oxidative phosphorylation) in CD8 bT_N cells (Figure 5D). As glycolysis and oxidative phosphorylation have been extensively studied in T cells (12, 43, 44) and both require NAD^+, we focussed on NAD^+ metabolism that has shown emergent applications within immune cell biology (21, 22, 45) and was discovered in our analysis (Figure 5E). In mammalian cells, the NAD^+ salvage pathway is a major source for NAD^+ synthesis (46) and consists of metabolites nicotinamide (NAM), nicotinamide ribotide or nicotinamide mononucleotide (NMN), and NAD^+ (Figure 5F). Using metabolite standards, we conducted a targeted analysis of metabolites involved in the NAD^+ salvage pathway and found higher relative levels of NAM, NMN, and lower levels of NAD^+ (normalized to cell number) in CD8 bT_N cells compared to CD8 T_N cells (Figure 6A). Furthermore, our proteomics analysis revealed that Nicotinamide phosphoribosyltransferase (NAMPT), which is the rate limiting enzyme of the NAD^+ salvage pathway, is increased in CD8 bT_N cells (Figure 6B). Using qPCR, we found that transcript levels of *Nampt* were also increased in CD8 bT_N cells as compared to T_N cells (Figure 6B). Interestingly, the transcript levels of other enzymes associated with various NAD^+ pathways (Figure S4C) including *Nmnats* (Figure S4D) that are part of the salvage pathway as well as other synthesis pathways, enzymes of the *de novo* pathway (Figure S4E), and the nicotinamide riboside/nicotinic acid riboside pathway (Figure S4F) remained unchanged, indicating a possibly preferential reliance of CD8 bT_N cells on NAD^+ synthesis *via* NAMPT.

To further consolidate our understanding of the role of the NAD^+ salvage pathway and NAMPT, we tested the effect of FK866, an inhibitor of NAMPT (47, 48), on the induction of CD8 bT_N cells upon reovirus exposure. As shown in Figure 6C, splenocytes from C57BL/6 mice exposed to reovirus and treated with FK866 showed less induction of CD8 bT_N cells compared to those with only reovirus exposure. The robust induction of CD8 bT_N cells was rescued when nicotinamide mononucleotide (NMN), a metabolite downstream of the NAMPT enzymatic action, was supplemented in the media (Figure 6C). These results showed that FK866 can impair the virus-driven induction of CD8 bT_N cells and further consolidated the role of NAMPT within this phenomenon. One possibility was that the reduced induction of CD8 bT_N cells could have occurred *via* an indirect effect of FK866 treatment by reducing the production of proinflammatory mediators in splenocytes (23, 49). To elucidate whether FK866 could impair the induction of CD8 bT_N cells in the presence of abundant type I interferons, we treated C57BL/6 splenocytes with exogeneous IFN-α1 or IFN-β1 along with FK866 and found impaired induction of CD8 bT_N cells compared to splenocytes treated with only interferons (Figures 6D, E respectively). Once again, the impaired induction of CD8 bT_N cells upon FK866 treatment was rescued by the supplementation of NMN in the media with both IFN-α1 (Figure 6D) and IFN-β1 (Figure 6E) treatments. In conclusion, these findings suggested that NAD^+ production *via* NAMPT-mediated salvage pathway is required for the induction of CD8 bT_N cells after reovirus or type I interferon exposure.

10.3389/fimmu.2022.1047661

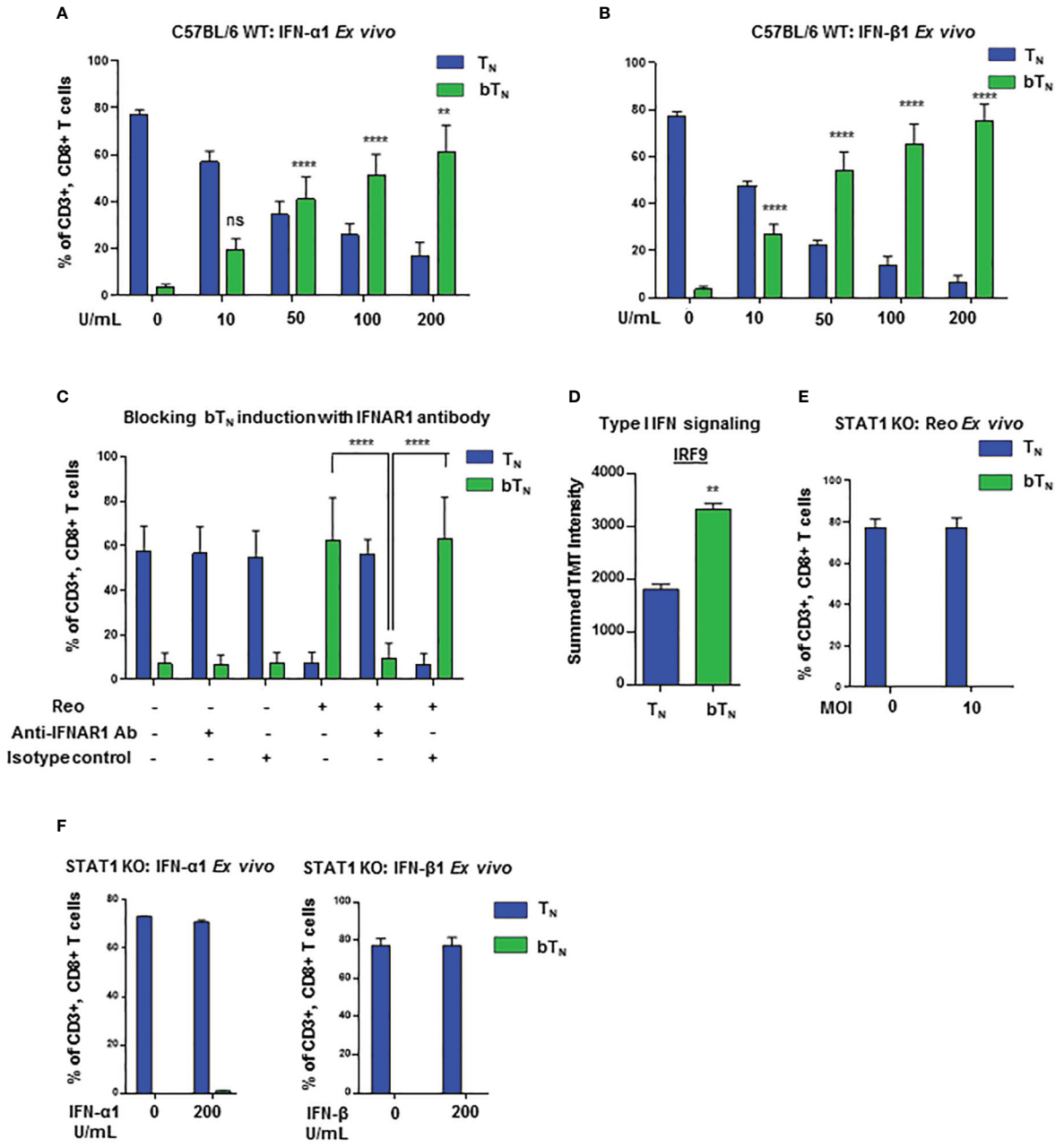

FIGURE 3
Induction of CD8 bT_N cells occurs in a STAT1-dependent manner. Bar graphs showing induction of CD8 bT_N cells upon *ex vivo* treatment of splenocytes from C57BL/6 mice with **(A)** varying concentrations of IFN-α1 from 10 U/mL- 200 U/mL (n=3 independent experiments), **(B)** varying concentrations of IFN-β1 from 10 U/mL- 200 U/mL (n=3 independent experiments) and **(C)** reovirus (MOI = 10) + IFNAR1 antibody (10μg/mL, n=3 independent experiments; Significance shown as indicated in figure) or isotype control. **(D)** IRF9 protein intensity (Two-tailed Student's t-test). **(E, F)** Bar graphs for induction of CD8 bT_N cells upon *ex vivo* treatment of splenocytes from STAT1 KO mice with reovirus MoI = 10 (n=3 independent experiments) **(E)** and, IFN-α1 and IFNβ1 (200 units (U)/ml each) (n=2 independent experiements) **(F)**. Two-way ANOVA with Tukey's multiple comparisons test and 95% confidence interval was used for statistical analysis unless otherwise indicated. Significance has been indicated for CD8 bT_N cells in treatment conditions versus non-treated conditions unless otherwise indicated. Not significant (ns) = $p > 0.05$; **$p < 0.01$; **** $p < 0.0001$.

Discussion

As is being recognized in the context of the SARS-CoV2 pandemic, the understanding of early immunological events that occur after virus exposure is extremely important. It has become quite clear from various studies on COVID-19 that one the most important factors determining the clinical outcome of the disease is the early induction of type I interferons (7, 8). Early

10.3389/fimmu.2022.1047661

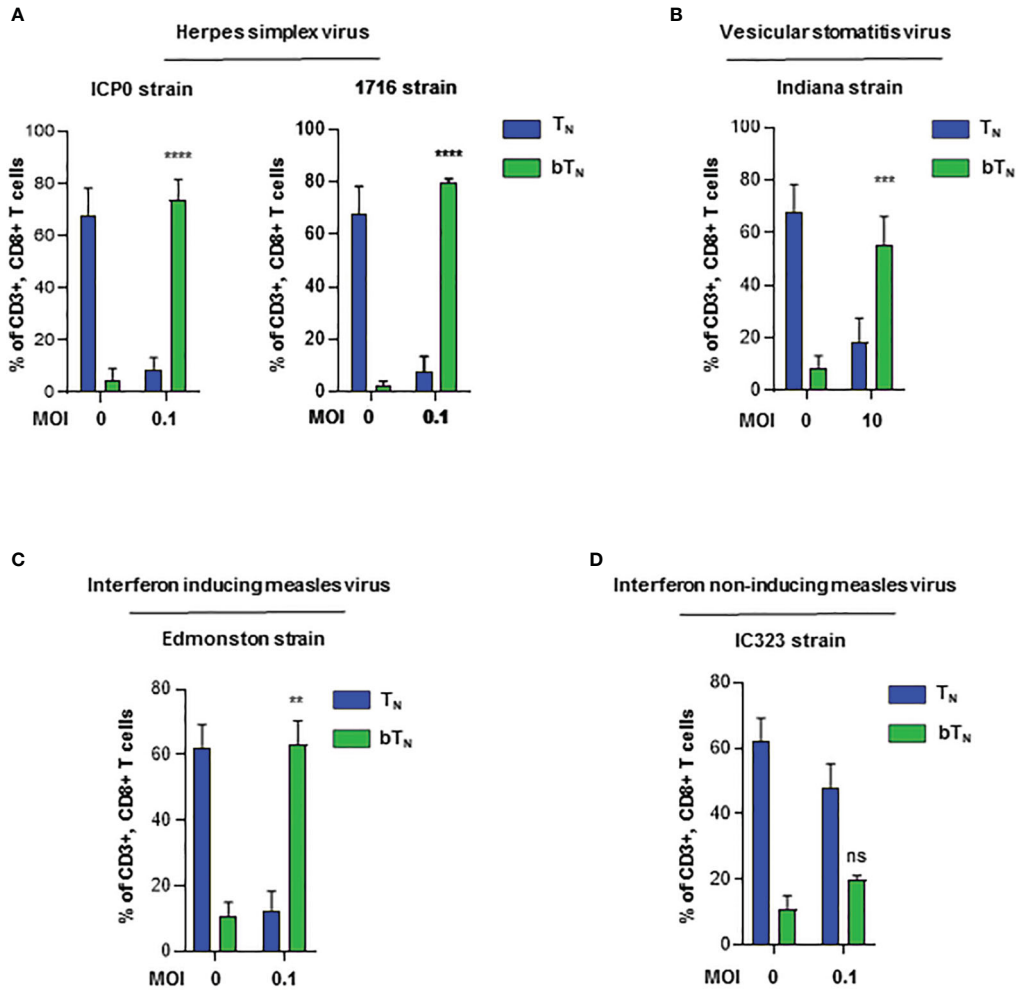

FIGURE 4
Induction of CD8 bT_N cells *ex vivo* upon exposure to different viruses. Bar graphs showing the induction of CD8 bT_N cells upon *ex vivo* exposure of C57BL/6 splenocytes to **(A)** two different strains of herpes simplex virus (ICP0 and 1716, n=3 independent experiments each) at MoI = 0.1, **(B)** vesicular stomatitis virus (Indiana strain, n=3 independent experiments) at MoI = 10, **(C)** interferon activating strain of measles (Edmonston, n=2 independent experiments) at MoI = 0.1 and **(D)** wild type strain of measles (IC323, n=2 independent experiments) at MoI = 0.1. Two-way ANOVA with Sidak's multiple comparisons test and 95% confidence interval was used for statistical analysis in bar graphs. Significance has been indicated only for CD8 bT_N cell populations induced within 24 hours in comparison with untreated control population levels. Not significant (ns) = $p > 0.05$; **$p < 0.01$; ***$p < 0.001$; **** $p < 0.0001$.

type I interferon responses are associated with mild COVID whereas delayed type I interferon responses leads to poor viral control, delayed and persistent activation of adaptive immunity, and severe COVID (50). In addition, early bystander activation of T cells has also been shown to be an important characteristic of mild disease compared to delayed bystander activation which has been associated with severe disease (51). Bystander activation is one of the earliest ways in which naïve CD8 T cells are activated occurring even before the cells have had an opportunity to be primed with antigen. Most studies focus on the biology of CD8 T cells after antigenic priming or on the bystander activation of pre-existing memory T cells. In this study, we have delineated the molecular mechanisms that govern the induction of early naïve bystander activated CD8 T cells. We demonstrated that CD8 bT_N cells are induced and have an anti-viral, type I interferon signature within 24 hours of reovirus exposure, a timepoint that is not typically studied for CD8 T cells. Further, STAT-1 has been demonstrated to play an important role in the maintenance of quiescence in naïve CD8 T cells (52). We demonstrated that the induction of CD8 bT_N cells was dependent on STAT-1, an important finding that can provide clues as to the mechanism of differential maintenance of these cells at different sites as observed in our study. We further demonstrated that the induction of CD8 bT_N cells was also dependent on the interferon inducing capacity of viruses.

Like our study, another study has investigated bystander activation in naïve CD8 T cells after virus exposure, albeit at later timepoints, and employed Ly6C, another member of the Ly6

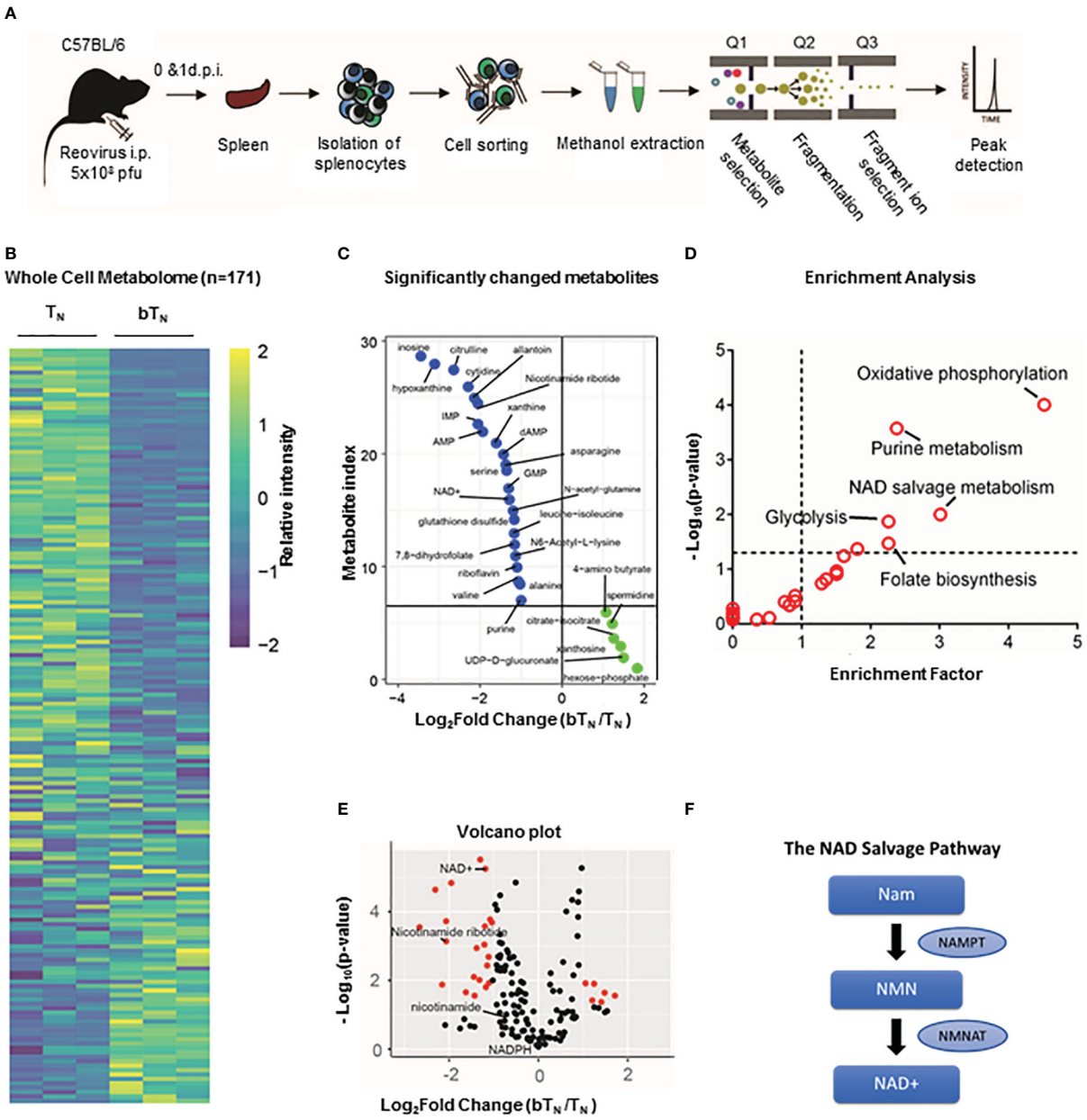

FIGURE 5
Semi-targeted metabolome analysis of CD8 bT_N cells. **(A)** Schematic for the workflow of metabolome analysis of T cells. **(B)** Whole cell metabolome heatmap. **(C)** List of significant top upregulated and downregulated metabolites in CD8 bT_N cells. **(D)** Significant metabolite Enrichment analysis of significantly changed metabolites. **(E)** Volcano plot depiciting metabolites that are significantly changed in CD8 bT_N cells versus CD8 T_N cells. NAD^+ salvage metabolites are highlighted in red. **(F)** NAD^+ salvage pathway. NAM- Nicotinamide, NMN- Nicotinamide mononucleotide and NAD^+- Nicotinamide adenosine dinucleotide.

family of proteins like Sca-1, to identify these cells (6). The study demonstrated that bystander activated Ly6C+ T_N cells had enhanced homing to lymph nodes, improved homeostatic properties and enhanced function. Taken together with this study, ourfindings further highlight the importance of studying early interferon production upon exposure to viruses and provide insight into another avenue through which CD8 T cells can be modulated early on by viruses.

Recent literature on COVID-19 pathobiology has generated an increased appreciation for the role of immunometabolic reprogramming that occurs during virus exposure (53). Viruses can alter the metabolism of cells directly during their replication or *via* the effects of type I interferons (54). For example, type I interferons induce important changes in the metabolism of plasmacytoid dendritic cells by acting on them in an autocrine manner and

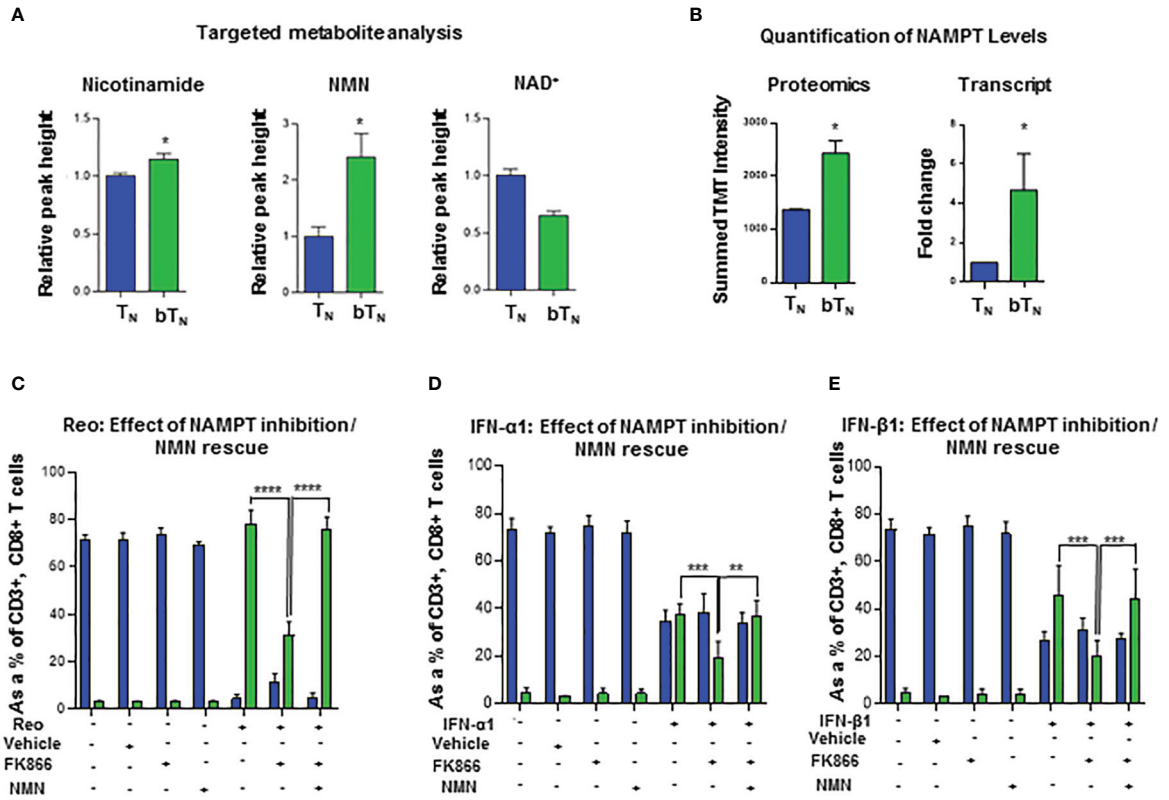

FIGURE 6
NAD^+ salvage metabolism regulates induction of CD8 bT_N cells. **(A)** Bar graphs depicting the relative peak heights of NAD^+ salvage metabolites - NAM, NMN and NAD^+ - using targeted metabolomics (n=4 mice per group). **(B)** Bar graphs for NAMPT levels- proteomics (n=5 mice pooled per condition) and quantitative PCR analysis (n = 3 independent experiments). **(C–E)** Bar graphs show the induction of CD8 bT_N cells upon *ex vivo* treatment of splenocytes from C57BL/6 mice with reovirus (MoI = 10) **(C)** IFN-α1 (20 U/mL) **(D)**, and IFN-β1 (20 U/mL) **(E)** in the presence of FK866 (5nM) and NMN (200μM) (n=3 independent experiments for each treatment, ethanol vehicle control for FK866). Two-tailed student t-test used for statistical analysis for **(A, B)** Two-way ANOVA with Tukey's multiple comaprisons and 95% confidence interval was used for statistical analysis of **(C–E)** Not significant (ns) = $p > 0.05$; *$p < 0.05$; **$p < 0.01$; ***$p < 0.001$; **** $p < 0.0001$.

these changes allow for enhanced immune function (14). Type I interferons can also modulate T cells, especially CD8 T_N cells, which are important during virus exposure. Although some studies have investigated the metabolism of T_N cells (55), the impact of metabolism in the context of bystander activated CD8 T_N cells remains unexplored. In our study we discovered that CD8 bT_N cells, despite being phenotypically similar to prototypic T_N cells, demonstrate a completely different metabolic signature. In this regard, our findings on the role of the NAD^+ salvage pathway in CD8 bT_N cell induction adds a crucial piece to the metabolic puzzle being investigated. Targeting NAD^+ salvage metabolism by inhibiting its rate limiting enzyme NAMPT has been previously shown to reduce effector T cell function in the tumor microenvironment (18, 21). In GVHD the functionality of alloreactive T cells was inhibited by targeting NAMPT (22) and similarly, the depletion of NAD^+ in T cells *via* FK866 treatment reduced demyelination in EAE (23, 24). Studies of metabolism, specifically the NAD^+ metabolic circuitry in T_N cells following activation in native settings by viral exposure, remain few. We have demonstrated a clear role for NAD^+ salvage metabolism in the reprogramming of bystander activated CD8 T_N cells during the acute phase of the immune response, further underscoring the importance of NAD^+ salvage metabolism in early T cell biology.

Finally, the virus of choice in this study- reovirus- is an oncolytic virus being developed as a cancer immunotherapy agent for the treatment of various tumor types in clinics (56). Induction of type I interferons and bystander naïve CD8 T cells upon exposure to oncolytic viruses can have important consequences for cancer immunotherapy. The role of type I interferons in tumor immunology is widely appreciated (57, 58) and naïve-like T cells with functional capacities have been detected in tumors (59). Further, cancer metabolism can have a direct detrimental impact on T_N cells (60). Understanding the impact of oncolytic viruses like reovirus on T_N cells *via* bystander activation and consequent metabolic reprogramming represents an important emerging area of research. We believe

that the research in this study provides new avenues for immunometabolism research in T cells, specifically CD8 T_N cells, and potential therapeutic targets for the reprogramming of T cell immunity. Ultimately, an improved understanding of bystander activated T_N cells and immunometabolism following virus exposure will inform fundamental concepts leading to better development of vaccines and treatments against viral infections and for the effective design and development of oncolytic virotherapies.

Material and methods

Viruses, cell lines, and reagents

Reovirus (serotype 3, Dearing strain) was cultured, amplified, and isolated using a previously established protocol (61, 62). L929 cells were cultured in minimum essential media (MEM) with (5% vol/vol Glutamax, 5% fetal bovine serum (FBS), 1X sodium pyruvate, 1X nonessential amino acids, and 1X Anti-Anti [Invitrogen, Carlsbad, CA]). Measles viruses (Edmonston and IC323 strains) were obtained from Dr. Christopher Richardson at the Canadian Centre for Vaccinology, Halifax, Nova Scotia. Herpes simplex viruses (ICP0 and 1716) and vesicular stomatitis virus (Indiana strain) was obtained from Dr. Tommy Alain at the University of Ottawa.

Animal studies

All animal work and *in vivo* experiments were conducted with prior approval from the Ethics Committee at Dalhousie University, Halifax, Nova Scotia. Wild type C57BL/6 and BALB/c mice were purchased from Charles River Laboratory (Montreal, Quebec, Canada). OT-1 transgenic and TLR3 KO mice were obtained from The Jackson Laboratory, United States. SLAM knock-in (KI) mice and SLAM KI, STAT1 KO mice for harvesting splenocytes and *ex vivo* virus treatment were obtained from Dr. Christopher Richardson. Intraperitoneal injections of reovirus (5 x 10^8 plaque-forming units/ml) were carried out and mice were sacrificed 1, 3 or 7 days post injection to harvest splenocytes for analysis of T cell populations. All animals used for experiments were between the ages of 6-10 weeks.

Flow cytometry analysis and immune cell sorting

Sample processing for flow cytometry was carried out by harvesting splenocytes in 5mL PBS-EDTA. The cells were filtered using a 40-micron filter and treated with RBC-lysing ammonium chloride (ACK) buffer. The cells were then incubated with CD16/32 Fc blocking antibody in FACS buffer (PBS + 1% EDTA + 1% FBS) for 25 minutes at 4°C, washed and stained with fluorophore labelled primary antibodies in BD Brilliant Stain buffer or FACS buffer for 25 minutes at 4°C. Stained cells were then washed and fixed with 4% paraformaldehyde for 15 minutes. For intracellular staining, fixation/permeabilization of the cells was carried out using the FoxP3/Transcription Factor Staining Buffer Set after staining with extracellular antibodies. Intracellular labelling with IFN-γ antibody in permeabilization buffer was done for 25 minutes at 4°C. The cells were finally washed and resuspended in FACS buffer. Sample data acquisition was done using the BD FACS Symphony A5 or the LSR Fortessa SORP flow cytometers. Data analysis was carried out using BD FACS Diva (BD Bioscience), FCS Express 7 (DeNovo Software, Los Angeles, CA) and FlowJo version 10 (BD biosciences, Ashland, OR). Dimensionality reduction performed on total CD8 T cells and CD8 T cell subsets using the UMAP (version 2.4) FlowJo plugin. Bar graphs were generated using GraphPad (GraphPad Software Inc., San Diego, CA). Anti-mouse BV785 CD45, BV650 CD62L, BV510 CD3, PerCP-Cy5.5 CD8, and APC-H7 CD4 antibodies were purchased from BD Biosciences. FITC CD44, PerCP CD44, BV711 CD44, BV650 CD62L, PE CD62L, PerCP CD8, PE-Cy7 CD3, PE CD3, APC IFN-γ, PE Sca-1, and AF647 Sca-1 were purchased from Biolegend. For cell sorting, splenocytes were harvested and stained *via* the same protocol described for flow cytometry. The paraformaldehyde fixation step was eliminated, and cells were sorted live using FACSAria III, BD Biosciences with a 95-98% purity. The gating strategy for sorting involved gating on lymphocytes (FSC-A vs SSC-A) followed by gating out the doublets. Singlets were then gated for CD3+CD8+ T cells. Following this, CD44 and CD62L expression was observed on CD8+ T cells and CD44lowCD62L+ were further sub-gated as Sca-1+ or Sca-1- to identify and collect bT_N and T_N cells respectively. In some cases (for proteomic analysis), T_{EM} cells (CD44hiCD62L+) were also identified and collected.

Ex vivo treatment of splenocytes

C57BL/6 mice and others, depending on the experiment, were sacrificed and splenocytes were harvested and prepared using initial steps described for flow cytometry processing. After treatment with ACK buffer for RBC lysis, 3 x 10^6 cells were plated in 12-well plates for 24 hours and treated with varying MoIs of reovirus, different strains of measles or herpes simplex viruses or vesicular stomatitis virus. For OT-1 mice experiments, splenocytes were isolated as described above and plated in 96-well plates at a concentration of 1-2 x 10^6 cells/well. These cells were then stimulated with ovalbumin peptide (SIINFEKL) at the 18-hour timepoint for 6 hours. Other *ex vivo* treatments included treatment of splenocytes with varying concentrations

of IFN-α1 and IFN-β1. Combination treatments were also carried out such as treatment of splenocytes with reovirus/IFN-β1 and anti-IFNAR1 antibody or isotype control or treatment of splenocytes with reovirus/IFN-α1/IFN-β1 in the presence of FK866 and NMN. For intracellular staining, brefeldin A (2μg/mL) was added to the cells at the 18-hour timepoint for 6 hours. After 24 hours, cells were collected, washed and processed for analysis *via* flow cytometry. Anti-IFNAR1 antibody (catalog no. 127324), isotype control (catalog no. 400198), IFN-α1 (catalog no. 752802) and IFN-β1 (catalog no. 581302) were purchased from Biolegend. FK866 (product no. F8557) and NMN (product no. N3501) and brefeldin A (catalog no. B7651) were purchased from Sigma. Ovalbumin peptide (257-264) was purchased from Genscript (catalog no. RP10611).

Quantitative *in vivo* proteomics

Animals were injected with reovirus as described above, and T cell subsets were collected either from the naive spleen or spleens on 1 and 7 days post infection (d.p.i.) *via* the cell sorting process described above. Each sample was prepared by pooling spleens of 5 animals for isolation. Isolated cells were washed with PBS, pelleted, and lysed in 6 M guanidine-HCl, 50 mM HEPES, pH 8.5, containing Roche complete mini protease inhibitor mixture (1 tablet per 10 mL) (Roche, Madison, WI). Lysis was performed *via* sonication and cleared by centrifugation. Cysteine residues were reduced using 5 mM dithiothreitol and then alkylated with 14 mM iodoacetamide. Aliquots containing 50 μg of protein were diluted to 1.5 M guanidine-HCl, 50 mM HEPES (pH 8.5) and digested with trypsin (Promega, Madison, WI). Digested peptides were desalted using 60 mg solid-phase C18-extraction cartridges (Waters, Milford, MA), lyophilized, and labelled using TMT 10-plex reagents as described previously (63). Samples were then mixed equally, desalted using solid-phase C18 extraction cartridges (Waters, Milford, MA), and lyophilized. TMT10-labelled samples were fractionated using high-pH reversed phase chromatography performed with an Onyx monolithic 100 × 4.6 mm C18 column (Phenomenex, Torrance, CA). The flow rate was 800 μL/min, and a gradient of 5–40% acetonitrile (10 mM ammonium formate, pH 8) was applied over 60 min using an Agilent 1100 pump (Agilent) from which 12 fractions were collected. Fractions were desalted using homemade Stage Tips, lyophilized, and analyzed with an Orbitrap Fusion mass spectrometer (64) using the SPS-MS3 method (McAlister et al., 2014). Protein identification was performed using a database search against a mouse proteome database (downloaded from UniProtKB in September 2014) concatenated to a mammalian orthoreovirus 3 (Dearing strain) database (downloaded from UniProtKB in September 2014). All false discovery rate (FDR) filtering and protein quantitation was performed as previously described (63). A protein was required to have a minimum total signal-to-noise ratio of 100 in all TMT reporter channels, and the maximum number of missing channels was equal to 8. Data for heat maps and individual protein profiles are represented by relative TMT intensity, which is based on the summed signal-to-noise. The data set was subsequently analyzed *via* K-means clustering with Euclidean distance using MultiExperiment Viewer (MeV) followed by DAVID Bioinformatics Resources (https://david.ncifcrf.gov/) to conduct GO-term analysis for biological processes, molecular functions and cellular compartments on specific clusters. Our total data set was utilized as the background for the data analysis searches. Volcano plot was generated using R statistical analysis package and bar graphs were generated using GraphPad

Ex vivo T cell metabolomics

For metabolomic analysis, each sample was prepared by pooling spleens of 3-5 mice. Live T cell populations were sorted, washed with PBS-EDTA, and resuspended in 100 μl 80% ice cold methanol. 20 μl of methanol extracted cells were combined with 180 μl of HPLC buffer A [95% (vol/vol) water, 5% (vol/vol) acetonitrile, 20 mM ammonium hydroxide, 20 mM ammonium acetate (pH = 9.0)]. The sample was split in triplicates and run using a triple quadrupole mass spectrometer 5500 QTRAP and metabolite levels were analyzed. Based on known Q1 (precursor ion) and Q3 (fragment ion) transitions, the metabolite name, the dwell time and the appropriate collision energies (CEs) for both positive and negative ion modes were identified. Using this protocol, a selected reaction monitoring transition list of 289 (approximately 10–14 scans per metabolite peak) metabolites can be accurately identified. MultiQuant v2.0 software was used to integrate the peak areas from the Q3 TIC values across the chromatographic elution. Each metabolite from every sample was manually confirmed; typically, a single dominant peak will be present for most detectable compounds. Peak heights normalized to the sum of peak heights per sample were used to determine relative metabolite concentrations between samples. For computational analysis, the metabolomics database was analyzed using R, to identify metabolites with significant fold changes and p values. Metabolite rank was obtained by comparing significantly changing metabolites in the order of decreasing fold change (CD8 bT_N/CD8 T_N). NAM, NMN, and NAD^+ were further analyzed using a targeted analysis on a QExactive Orbitrap Mass Spectrometer. Here, a targeted selective ion monitoring (tSIM) method was employed with a resolution of 140,000. Metabolic features identified by tSIM were confirmed using Maven software and peak heights were exported to excel. Peak heights were again normalized using cell number and relative peak heights calculated. Graphs were generated GraphPad Prism.

Enrichment analysis

All detectable metabolites were organized into specific and general metabolic pathways based on Kyoto Encyclopedia of Genes and Genomes (KEGG) metabolic pathways. To determine pathways that were enriched in CD8 bT_N cells, an overrepresentation analysis was completed. Briefly, metabolites that were increased or decreased by 2-fold and t test probability less than or equal to 0.05 were selected, and compared with the original list of metabolites, and then we calculated percent of metabolites changed. We used this percentage to calculate the expected number of metabolites that would change if the metabolites were randomly distributed throughout the various metabolic pathways. We then calculated fold enrichment by dividing metabolites changed by 2-fold by the number of metabolites expected to have changed if random. Probability was calculated by the hypergeometric test.

Quantitative real-time PCR

T cells were sorted from splenocytes using flow cytometry and used for RNA extraction and qPCR. 3-5 animals were pooled for isolation of every sample, and this was repeated 2-3 times. RNA extractions were conducted using standard TRIzol methodology following manufacturer's instructions (Qiagen). Extracted RNA was quantified, diluted to a total of 2 µg, and synthesized into cDNA using Superscript II (Invitrogen, Burlington, ON). SsoAdvanced Universal SYBR Green Supermix (Biorad catalog no. 1708882) was used for qPCR and run on the BioRad CFX96 mice for amplification and quantification. Gene-specific primers for murine *Ifna2*, *Ifnr1*, *Ifnr2*, *Nampt, Kynu, Kyat1, Qprt, Nmrk1, Nmnat1, Nmnat2, Nmnat3, Gapdh* and *Hprt* were purchased from Invitrogen (Table S2). The data from the qPCR were collected and analyzed using Livak and Schmittgen's $2^{-\Delta\Delta CT}$ method (65). The fold change was calculated by first normalizing the quantification cycle (Cq) of the indicated gene against *Gapdh* or *Hprt* followed by a comparison against the respective controls and bar graphs were generated using GraphPad.

Statistical analysis

Depending on the indicated experiment, two-way ANOVA with Sidak/Tukey's post-test or a two-tailed Student's *t*-test with 95% confidence interval were used for statistical analysis, and *p* values of <0.05 were considered significant. Asterisks were used to signify *p* values as follows: not significant (ns) = $p > 0.05$; *$p < 0.05$; **$p < 0.01$; ***$p < 0.001$; **** $p < 0.0001$.

Data availability statement

The original contributions presented in the study are publicly available. This data can be found here: PRIDE database - https://www.ebi.ac.uk/pride/. accession: PXD039614.

Ethics statement

The animal study was reviewed and approved by University Committee on Laboratory Animals (UCLA), Dalhousie University.

Author contributions

Conceptualization, NH and SG. Methodology, NH, BK, JM, GS, JP. Software, NH, BK, JM, JP, PK, MG, TB-C. Validation, NH, BK, ME. Formal Analysis, NH, BK, JM, PK, MG TB-C. Investigation, NH, BK, JM, ME, VK, YK, GS, JP. Writing-Original Draft, NH. Writing- Review & Editing, YK, BK, GS. Visualization, NH, BK, PK, MG, TB-C. Supervision, StG, CR, SG. Project Administration, NH, SG. All authors contributed to the article and approved the submitted version.

Funding

This work was supported by grants from the Canadian Institutes of Health Research (CIHR), Canadian Cancer Society (CCS), and Dalhousie Medical Research Foundation (DMRF) to SG. NH was funded by the Infection, Immunity, Inflammation & Vaccinology (I3V; Faculty of Medicine) Graduate Studentship and the Vitamin Scholarship (Dalhousie University). BK, VK, and JM were supported through the Cancer Research Training Program (CRTP) of Beatrice Hunter Cancer Research Institute (BHCRI). PK was funded by the Killam Predoctoral Scholarship. YK was supported by the CIHR and DMRF. DC was supported previously by CIHR, CRTP and the Nova Scotia Health Research Foundation (NSHRF). Work by JP was funded in part by NIH/NIGMS grant R01 GM132129.

Acknowledgments

We acknowledge Drs. Devanand Pinto and Ken Chisholm (National Research Council), Alejandro Cohen at the Dalhousie Proteomics Core Facility, Derek Rowter & Renee Raudonis at Dalhousie Flow cytometry suites, and the staff of Dalhousie Animal Care Facility. We would also like to thank Dr. Ian Haidl for helpful discussions and critical review of the manuscript. The authors declare no competing interests.

Conflict of interest

Authors BK and ME were employed by company IMV Inc,.

The remaining authors declare that the research was conducted in the absence of any commercial or financial relationships that could be construed as a potential conflict of interest.

Publisher's note

All claims expressed in this article are solely those of the authors and do not necessarily represent those of their affiliated organizations, or those of the publisher, the editors and the reviewers. Any product that may be evaluated in this article, or claim that may be made by its manufacturer, is not guaranteed or endorsed by the publisher.

Supplementary material

The Supplementary Material for this article can be found online at: https://www.frontiersin.org/articles/10.3389/fimmu.2022.1047661/full#supplementary-material

References

1. Hwang J-R, Byeon Y, Kim D, Park S-G. Recent insights of T cell receptor-mediated signaling pathways for T cell activation and development. *Exp Mol Med* (2020) 52:750–61. doi: 10.1038/s12276-020-0435-8

2. Kim T-S, Shin E-C. The activation of bystander CD8+ T cells and their roles in viral infection. *Exp Mol Med* (2019) 51:1–9. doi: 10.1038/s12276-019-0316-1l

3. Lee H, Jeong S, Shin E-C. Significance of bystander T cell activation in microbial infection. *Nat Immunol* (2022) 23:13–22. doi: 10.1038/s41590-021-00985-3

4. Alanio C, Nicoli F, Sultanik P, Flecken T, Perot B, Duffy D, et al. Bystander hyperactivation of preimmune CD8+ T cells in chronic HCV patients. *eLife* (2015) 4:e07916. doi: 10.7554/eLife.07916

5. Snell LM, MacLeod BL, Law JC, Osokine I, Elsaesser HJ, Hezaveh K, et al. CD8+ T cell priming in established chronic viral infection preferentially directs differentiation of memory-like cells for sustained immunity. *Immunity* (2018) 49:678–694.e5. doi: 10.1016/j.immuni.2018.08.002

6. Jergović M, Coplen CP, Uhrlaub JL, Besselsen DG, Cheng S, Smithey MJ, et al. Infection-induced type I interferons critically modulate the homeostasis and function of CD8+ naïve T cells. *Nat Commun* (2021) 12:5303. doi: 10.1038/s41467-021-25645-w

7. Acharya D, Liu G, Gack MU. Dysregulation of type I interferon responses in COVID-19. *Nat Rev Immunol* (2020) 20:397–8. doi: 10.1038/s41577-020-0346-x

8. Lee JS, Shin E-C. The type I interferon response in COVID-19: Implications for treatment. *Nat Rev Immunol* (2020) 20:585–6. doi: 10.1038/s41577-020-00429-3

9. Marshall HD, Prince AL, Berg LJ, Welsh RM. IFN-αβ and self-MHC divert CD8 T cells into a distinct differentiation pathway characterized by rapid acquisition of effector functions. *J Immunol* (2010) 185:1419. doi: 10.4049/jimmunol.1001140

10. Urban SL, Berg LJ, Welsh RM. Type 1 interferon licenses naïve CD8 T cells to mediate anti-viral cytotoxicity. *Virology* (2016) 493:52–9. doi: 10.1016/j.virol.2016.03.005

11. Biase SD, Ma X, Wang X, Yu J, Wang Y-C, Smith DJ, et al. Creatine uptake regulates CD8 T cell antitumor immunity. *J Exp Med* (2019) 216(12):2869–82. doi: 10.1084/jem.20182044

12. Menk AV, Scharping NE, Moreci RS, Zeng X, Guy C, Salvatore S, et al. Early TCR signaling induces rapid aerobic glycolysis enabling distinct acute T cell effector functions. *Cell Rep* (2018) 22:1509–21. doi: 10.1016/j.celrep.2018.01.040

13. Ayres JS. Immunometabolism of infections. *Nat Rev Immunol* (2020) 20:79–80. doi: 10.1038/s41577-019-0266-9

14. Wu D, Sanin DE, Everts B, Chen Q, Qiu J, Buck MD, et al. Type 1 interferons induce changes in core metabolism that are critical for immune function. *Immunity* (2016) 44:1325–36. doi: 10.1016/j.immuni.2016.06.006

15. Buck MD, Sowell RT, Kaech SM, Pearce EL. Metabolic instruction of immunity. *Cell* (2017) 169:570–86. doi: 10.1016/j.cell.2017.04.004

16. Klein Geltink RI, Kyle RL, Pearce EL. Unraveling the complex interplay between T cell metabolism and function. *Annu Rev Immunol* (2018) 36:461–88. doi: 10.1146/annurev-immunol-042617-053019

17. Yoshino J, Baur JA, Imai S-I. NAD+ intermediates: The biology and therapeutic potential of NMN and NR. *Cell Metab* (2018) 27:513–28. doi: 10.1016/j.cmet.2017.11.002

18. Beier UH, Quinn WJ, Jiao J, TeSlaa T, Stadanlick J, Hancock WW, et al. Nicotinamide adenine dinucleotide (NAD) oxidation preserves T cell function under lactic acidosis characteristic of the tumor microenvironment (TME). *J Immunol* (2018) 200:177.4–4. doi: 10.4049/jimmunol.200.Supp.177.4

19. Jeng MY, Hull PA, Fei M, Kwon H-S, Tsou C-L, Kasler H, et al. Metabolic reprogramming of human CD8+ memory T cells through loss of SIRT1. *J Exp Med* (2018) 215:51–62. doi: 10.1084/jem.20161066

20. Hubert S, Rissiek B, Klages K, Huehn J, Sparwasser T, Haag F, et al. Extracellular NAD+ shapes the Foxp3+ regulatory T cell compartment through the ART2–P2X7 pathway. *J Exp Med* (2010) 207:2561–8. doi: 10.1084/jem.20091154

21. Chatterjee S, Daenthanasanmak A, Chakraborty P, Wyatt MW, Dhar P, Selvam SP, et al. CD38-NAD+Axis regulates immunotherapeutic anti-tumor T cell response. *Cell Metab* (2018) 27:85–100.e8. doi: 10.1016/j.cmet.2017.10.006

22. Gerner RR, Macheiner S, Reider S, Siegmund K, Grabherr F, Mayr L, et al. Targeting NAD immunometabolism limits severe graft-versus-host disease and has potent antileukemic activity. *Leukemia* (2020) 34:1885–97. doi: 10.1038/s41375-020-0709-0

23. Bruzzone S, Fruscione F, Morando S, Ferrando T, Poggi A, Garuti A, et al. Catastrophic NAD+ depletion in activated T lymphocytes through nampt inhibition reduces demyelination and disability in EAE. *PloS One* (2009) 4: e7897. doi: 10.1371/journal.pone.0007897

24. Tullius SG, Biefer HRC, Li S, Trachtenberg AJ, Edtinger K, Quante M, et al. NAD + protects against EAE by regulating CD4 + T-cell differentiation. *Nat Commun* (2014) 5:1–17. doi: 10.1038/ncomms6101

25. Abad AT, Danthi P. Early events in reovirus infection influence induction of innate immune response. *J Virol* (2022) 96:e0091722. doi: 10.1128/jvi.00917-22

26. Bouziat R, Hinterleitner R, Brown JJ, Stencel-Baerenwald JE, Ikizler M, Mayassi T, et al. Reovirus infection triggers inflammatory responses to dietary antigens and development of celiac disease. *Science* (2017) 356:44–50. doi: 10.1126/science.aah5298

27. DeLong JH, Hall AO, Konradt C, Coppock GM, Park J, Harms Pritchard G, et al. Cytokine- and TCR-mediated regulation of T cell expression of Ly6C and sca-1. *J Immunol Baltim. Md* (2018) 200:1761–70. doi: 10.4049/jimmunol.1701154

28. Botos I, Liu L, Wang Y, Segal DM, Davies DR. The toll-like receptor 3: dsRNA signaling complex. *Biochim Biophys Acta* (2009) 1789:667–74. doi: 10.1016/j.bbagrm.2009.06.005

29. Chng MHY, Lim MQ, Rouers A, Becht E, Lee B, MacAry PA, et al. Large-Scale HLA tetramer tracking of T cells during dengue infection reveals broad acute activation and differentiation into two memory cell fates. *Immunity* (2019) 51 (6):1119–35.e5. doi: 10.1016/j.immuni.2019.10.007

30. Rivadeneira DB, DePeaux K, Wang Y, Kulkarni A, Tabib T, Menk AV, et al. Oncolytic viruses engineered to enforce leptin expression reprogram tumor-infiltrating T cell metabolism and promote tumor clearance. *Immunity* (2019) 51:548–560.e4. doi: 10.1016/j.immuni.2019.07.003

31. Youngblood B, Hale JS, Kissick HT, Ahn E, Xu X, Wieland A, et al. Effector CD8 T cells dedifferentiate into long-lived memory cells. *Nature* (2017) 552:404–9. doi: 10.1038/nature25144

32. Saito T, Hirai R, Loo Y-M, Owen D, Johnson CL, Sinha SC, et al. Regulation of innate antiviral defenses through a shared repressor domain in RIG-I and LGP2. *Proc Natl Acad Sci U. S. A.* (2007) 104:582–7. doi: 10.1073/pnas.0606699104

33. Fu XY, Kessler DS, Veals SA, Levy DE, Darnell JE. ISGF3 the transcriptional activator induced by interferon alpha consists of multiple interacting polypeptide chains. *Proc Natl Acad Sci U. S. A.* (1990) 87:8555–9. doi: 10.1073/pnas.87.21.8555

34. Hsu EC, Iorio C, Sarangi F, Khine AA, Richardson CD. CDw150(SLAM) is a receptor for a lymphotropic strain of measles virus and may account for the immunosuppressive properties of this virus. *Virology* (2001) 279:9–21. doi: 10.1006/viro.2000.0711

35. Everett RD. ICP0 a regulator of herpes simplex virus during lytic and latent infection. *BioEssays* (2000) 22:761–70. doi: 10.1002/1521-1878(200008)22:8<761::AID-BIES10>3.0.CO;2-A

36. Valyi-Nagy T, Fareed MU, O'Keefe JS, Gesser RM, MacLean AR, Brown SM, et al. The herpes simplex virus type 1 strain 17+ gamma 34.5 deletion mutant 1716 is avirulent in SCID mice. *J Gen Virol* (1994) 75(Pt 8):2059–63. doi: 10.1099/0022-1317-75-8-2059

37. Freer G, Burkhart C, Ciernik I, Bachmann MF, Hengartner H, Zinkernagel RM. Vesicular stomatitis virus Indiana glycoprotein as a T-cell-dependent and -independent antigen. *J Virol* (1994) 68:3650–5. doi: 10.1128/JVI.68.6.3650-3655.1994

38. Bankamp B, Takeda M, Zhang Y, Xu W, Rota PA. Genetic characterization of measles vaccine strains. *J Infect Dis* (2011) 204 Suppl 1:S533–548. doi: 10.1093/infdis/jir097

39. Takeuchi K, Takeda M, Miyajima N, Kobune F, Tanabayashi K, Tashiro M. Recombinant wild-type and edmonston strain measles viruses bearing heterologous h proteins: Role of h protein in cell fusion and host cell specificity. *J Virol* (2002) 76:4891–900. doi: 10.1128/JVI.76.10.4891-4900.2002

40. Nguyen NV, Kato S, Nagata K, Takeuchi K. Differential induction of type I interferons in macaques by wild-type measles virus alone or with the hemagglutinin protein of the edmonston vaccine strain. *Microbiol Immunol* (2016) 60:501–5. doi: 10.1111/1348-0421.12392

41. Shingai M, Ebihara T, Begum NA, Kato A, Honma T, Matsumoto K, et al. Differential type I IFN-inducing abilities of wild-type versus vaccine strains of measles virus. *J Immunol* (2007) 179:6123–33. doi: 10.4049/jimmunol.179.9.6123

42. Ghazarian M, Revelo XS, Nøhr MK, Luck H, Zeng K, Lei H, et al. Type I interferon responses drive intrahepatic T cells to promote metabolic syndrome. *Sci Immunol* (2017) 2(10):eaai7616. doi: 10.1126/sciimmunol.aai7616

43. Chang C-H, Curtis JD, Maggi LB, Faubert B, Villarino AV, O'Sullivan D, et al. Posttranscriptional control of T cell effector function by aerobic glycolysis. *Cell* (2013) 153:1239–51. doi: 10.1016/j.cell.2013.05.016

44. van der Windt GJW, Everts B, Chang C-H, Curtis JD, Freitas TC, Amiel E, et al. Mitochondrial respiratory capacity is a critical regulator of CD8+ T cell memory development. *Immunity* (2012) 36:68–78. doi: 10.1016/j.immuni.2011.12.007

45. Cameron AM, Castoldi A, Sanin DE, Flachsmann LJ, Field CS, Puleston DJ, et al. Inflammatory macrophage dependence on NAD + salvage is a consequence of reactive oxygen species–mediated DNA damage. *Nat Immunol* (2019) 20:420–32. doi: 10.1038/s41590-019-0336-y

46. Revollo JR, Grimm AA, Imai S. The NAD biosynthesis pathway mediated by nicotinamide phosphoribosyltransferase regulates Sir2 activity in mammalian cells. *J Biol Chem* (2004) 279:50754–63. doi: 10.1074/jbc.M408388200

47. Lee J, Kim H, Lee JE, Shin S-J, Oh S, Kwon G, et al. Selective cytotoxicity of the NAMPT inhibitor FK866 toward gastric cancer cells with markers of the epithelial-mesenchymal transition due to loss of NAPRT. *Gastroenterology* (2018) 155:799–814.e13. doi: 10.1053/j.gastro.2018.05.024

48. Schuster S, Penke M, Gorski T, Gebhardt R, Weiss TS, Kiess W, et al. FK866-induced NAMPT inhibition activates AMPK and downregulates mTOR signaling in hepatocarcinoma cells. *Biochem Biophys Res Commun* (2015) 458:334–40. doi: 10.1016/j.bbrc.2015.01.111

49. Al-Shabany AJ, Moody AJ, Foey AD, Billington RA. Intracellular NAD+ levels are associated with LPS-induced TNF-α release in pro-inflammatory macrophages. *Biosci Rep* (2016) 36(1):e00301. doi: 10.1042/BSR20150247

50. Moss P. The T cell immune response against SARS-CoV-2. *Nat Immunol* (2022) 23:186–93. doi: 10.1038/s41590-021-01122-w

51. Bergamaschi L, Mescia F, Turner L, Hanson AL, Kotagiri P, Dunmore BJ, et al. Longitudinal analysis reveals that delayed bystander CD8+ T cell activation and early immune pathology distinguish severe COVID-19 from mild disease. *Immunity* (2021) 54:1257–1275.e8. doi: 10.1016/j.immuni.2021.05.010

52. Kye Y-C, Lee G-W, Lee S-W, Ju Y-J, Kim H-O, Yun C-H, et al. STAT1 maintains naïve CD8+ T cell quiescence by suppressing the type I IFN-STAT4-mTORC1 signaling axis. *Sci Adv* (2021) 7:eabg8764. doi: 10.1126/sciadv.abg8764

53. O'Carroll SM, O'Neill LAJ. Targeting immunometabolism to treat COVID-19. *Immunother. Adv* (2021) 1:ltab013. doi: 10.1093/immadv/ltab013

54. Moreno-Altamirano MMB, Kolstoe SE, Sánchez-García FJ. Virus control of cell metabolism for replication and evasion of host immune responses. *Front Cell Infect Microbiol* (2019) 9:95. doi: 10.3389/fcimb.2019.00095

55. Mendoza A, Fang V, Chen C, Serasinghe M, Verma A, Muller J, et al. Lymphatic endothelial S1P promotes mitochondrial function and survival in naive T cells. *Nature* (2017) 546:158–61. doi: 10.1038/nature22352

56. Müller L, Berkeley R, Barr T, Ilett E, Errington-Mais F. Past present and future of oncolytic reovirus. *Cancers* (2020) 12:3219. doi: 10.3390/cancers12113219

57. Cao X, Liang Y, Hu Z, Li H, Yang J, Hsu EJ, et al. Next generation of tumor-activating type I IFN enhances anti-tumor immune responses to overcome therapy resistance. *Nat Commun* (2021) 12:5866. doi: 10.1038/s41467-021-26112-2

58. Zitvogel L, Galluzzi L, Kepp O, Smyth MJ, Kroemer G. Type I interferons in anticancer immunity. *Nat Rev Immunol* (2015) 15:405–14. doi: 10.1038/nri3845

59. Sheng SY, Gu Y, Lu CG, Tang YY, Zou JY, Zhang YQ, et al. The characteristics of naive-like T cells in tumor-infiltrating lymphocytes from human lung cancer. *J Immunother.* (2017) 40:1–10. doi: 10.1097/CJI.0000000000000147

60. Xia H, Wang W, Crespo J, Kryczek I, Li W, Wei S, et al. Suppression of FIP200 and autophagy by tumor-derived lactate promotes naïve T cell apoptosis and affects tumor immunity. *Sci Immunol* (2017) 2:eaan4631. doi: 10.1126/sciimmunol.aan4631

61. Coffey MC, Strong JE, Forsyth PA, Lee PWK. Reovirus therapy of tumors with activated ras pathway. *Science* (1998) 282(5392):1332–4. doi: 10.1126/science.282.5392.1332

62. Kennedy BE, Giacomantonio M, Murphy JP, Cutler S, Sadek M, Konda P, et al. NAD+ depletion enhances reovirus-induced oncolysis in multiple myeloma. *Mol Ther - Oncolytics.* (2022) 24:695–706. doi: 10.1016/j.omto.2022.02.017

63. Murphy JP, Stepanova E, Everley RA, Paulo JA, Gygi SP. Comprehensive temporal protein dynamics during the diauxic shift in saccharomyces cerevisiae. *Mol Cell Proteomics MCP.* (2015) 14:2454–65. doi: 10.1074/mcp.M114.045849

64. McAlister GC, Nusinow DP, Jedrychowski MP, Wühr M, Huttlin EL, Erickson BK, et al. MultiNotch MS3 enables accurate sensitive and multiplexed detection of differential expression across cancer cell line proteomes. *Anal Chem* (2014) 86(14):7150–8. doi: 10.1021/ac502040v

65. Livak KJ, Schmittgen TD. Analysis of relative gene expression data using real-time quantitative PCR and the 2(-delta delta C(T)) method. *Methods San. Diego. Calif.* (2001) 25:402–8. doi: 10.1006/meth.2001.1262

frontiers | Frontiers in Immunology

TYPE Original Research
PUBLISHED 09 February 2023
DOI 10.3389/fimmu.2023.1033497

OPEN ACCESS

EDITED BY
Soumya R. Mohapatra,
KIIT University, India

REVIEWED BY
Yinming Liang,
Xinxiang Medical University, China
Antonio Giovanni Solimando,
University of Bari Aldo Moro, Italy

*CORRESPONDENCE
Geng Chen
chengeng66666@163.com
Yinghong Shi
shi.yinghong@zs-hospital.sh.cn
Duojiao Wu
wu.duojiao@zs-hospital.sh.cn

†These authors have contributed equally to this work

SPECIALTY SECTION
This article was submitted to Cancer Immunity and Immunotherapy, a section of the journal Frontiers in Immunology

RECEIVED 31 August 2022
ACCEPTED 04 January 2023
PUBLISHED 09 February 2023

CITATION
Yang Y, Sun L, Chen Z, Liu W, Xu Q, Liu F, Ma M, Chen Y, Lu Y, Fang H, Chen G, Shi Y and Wu D (2023) The immune-metabolic crosstalk between CD3$^+$C1q$^+$TAM and CD8$^+$T cells associated with relapse-free survival in HCC.
Front. Immunol. 14:1033497.
doi: 10.3389/fimmu.2023.1033497

The immune-metabolic crosstalk between CD3$^+$C1q$^+$TAM and CD8$^+$T cells associated with relapse-free survival in HCC

Yanying Yang[1,2†], Lu Sun[3†], Zhouyi Chen[3†], Weiren Liu[4,5,6†], Qiyue Xu[7†], Fangming Liu[3], Mingyue Ma[8], Yuwen Chen[1], Yan Lu[8], Hao Fang[9], Geng Chen[7*], Yinghong Shi[4,5,6*] and Duojiao Wu[1,3*]

[1]Jinshan Hospital Center for Tumor Diagnosis & Therapy, Jinshan Hospital, Fudan University, Shanghai, China, [2]Shanghai Key Laboratory of Bioactive Small Molecules, Department of Physiology and Pathophysiology, School of Basic Medical Sciences, Fudan University, Shanghai, China, [3]Shanghai Key Laboratory of Lung Inflammation and Injury, Institute of Clinical Science, Zhongshan Hospital, Fudan University, Shanghai, China, [4]Department of Liver Surgery and Transplantation, Liver Cancer Institute, Zhongshan Hospital, Fudan University, Shanghai, China, [5]Key Laboratory of Carcinogenesis and Cancer Invasion of Ministry of Education, Chinese Academy of Medical Sciences, Shanghai, China, [6]Research Unit of Bench and Clinic Research for Liver cancer Recurrence and Metastasis, Chinese Academy of Medical Sciences, Shanghai, China, [7]Center for Bioinformatics and Computational Biology, Shanghai Key Laboratory of Regulatory Biology, Institute of Biomedical Sciences, School of Life Sciences, East China Normal University, Shanghai, China, [8]Department of Endocrinology and Metabolism, Zhongshan Hospital, Key Laboratory of Metabolism and Molecular Medicine, the Ministry of Education, Fudan University, Shanghai, China, [9]Department of Anesthesiology, Zhongshan Hospital, Fudan University, Shanghai, China

Introduction: Although multiple targeted treatments have appeared, hepatocellular carcinoma (HCC) is still one of the most common causes of cancer-related deaths. The immunosuppressive tumor microenvironment (TME) is a critical factor in the oncogenesis and progression of HCC. The emerging scRNA-seq makes it possible to explore the TME at a high resolution. This study was designed to reveal the immune-metabolic crosstalk between immune cells in HCC and provide novel strategies to regulate immunosuppressive TME.

Method: In this study, we performed scRNA-seq on paired tumor and peri-tumor tissues of HCC. The composition and differentiation trajectory of the immune populations in TME were portrayed. Cellphone DB was utilized to calculate interactions between the identified clusters. Besides, flow cytometry, RT-PCR and seahorse experiments were implemented to explore potential metabolic and epigenetic mechanisms of the inter-cellular interaction.

Result: A total of 19 immune cell clusters were identified and 7 were found closely related to HCC prognosis. Besides, differentiation trajectories of T cells were also presented. Moreover, a new population, CD3+C1q+ tumor-associated macrophages (TAM) were identified and found significantly interacted with CD8+ CCL4+T cells. Compared to the peri-tumor tissue, their interaction was attenuated in tumor. Additionally, the dynamic presence of this newly found cluster was also verified in the peripheral blood of patients with sepsis. Furthermore, we found that CD3+C1q+TAM affected T cell immunity through C1q signaling-induced metabolic and epigenetic reprogramming, thereby potentially affecting tumor prognosis.

Conclusion: Our study revealed the interaction between CD3+C1q+TAM and CD8 + CCL4+T cells and may provide implications for tackling the immunosuppressive TME in HCC.

KEYWORDS

immunometabolism, C1q, tumor-associated macrophage, T cell, HCC

1 Introduction

With a high mortality rate, liver cancer is the second leading cause of cancer-related deaths under the age of 80 worldwide (1, 2). Hepatocellular carcinoma (HCC) accounts for 70% to 85% of primary liver cancers (3). HCC is an inflammation-driven disease. Surgery, radiofrequency ablation (RFA), transcatheter arterial chemoembolization, and targeted therapies are the most common treatments (4). The tumor microenvironment (TME) of HCC is strongly immunosuppressive; thus, it is extremely important to illustrate the immune characteristics of TME and develop new immunotherapies for HCC.

Immune cell infiltration is a well-known significant regulator of HCC progression (5). The density of tumor-infiltrating $CD8^+$T cells was proved to be an effective prognostic indicator in HCC or many solid tumors (6, 7). It can be affected by multiple regulatory procedures in HCC TME, including the secretion of transforming growth factor β (TGF-β) and interleukin 10 (IL-10), the recruitment of regulatory T cells (Tregs) and myeloid-derived suppressor cells (MDSCs), high levels of programmed cell death 1 (PD-1), programmed death ligand-1 (PD-L1) and so on (4, 5, 8, 9). All the factors cause a rather low response rate of HCC to immunotherapy (10). Therefore it is critical to illustrate the complex network of cell-to-cell interactions within the TME. However, the traditional immunological technology has certain limitations. For example, the chasm between *in vitro* and *in vivo* systems, low throuhput, and limited information on immunohistochemistry, et al.

ScRNA-seq is an emerging and powerful tool for investigating the cellular components even rare populations and their interactions in TME (11, 12). It also helps to illustrate connections between TME and clinical outcomes in cancers (13–15). Recently several studies have portrayed the landscape of HCC at single-cell level (16–20). For example, heterogeneity of exhausted T cells (Tex) has been reported (16, 17). The study aims to deepen our understanding of cell-cell interactions and molecular pathways in TME based on scRNA-seq data of paired HCC tissues, and discover new cell subsets which cannot be achieved by traditional methods (21, 22).

We revealed TILs differentiation trajectories and identified certain populations associated with HCC prognosis. The scRNA-seq found that macrophage populations were much more complex than the M1/M2 dichotomy. Although macrophages and T cells are generally considered to belong to different cell lineages, recently a novel macrophage sub-population expressing CD3 molecule was reported in infectious, inflammatory diseases (23). However, the specific role of $CD3^+$ tumor-associated macrophages (TAM) is poorly understood. In the study, we found that a new population of $CD3^+C1q^+$TAM regulated the anti-tumor immunity of the tumor-infiltrated $CD8^+CCL4^+$T cells through the C1q signaling pathway and subsequent metabolic and epigenetic remodeling, thereby potentially affecting tumor prognosis. Our study supported that the versatile molecular C1q expressed in TAM has functions beyond the complement cascade. The data reveals the interaction between C1q and the metabolism of $CD8^+$T cells and provides implications for regulating immunosuppressive TME.

2 Methods

2.1 Human specimens

Paired carcinomatous and para-carcinomatous tissues were from patients with HCC. No chemotherapy or radiation therapy was performed on patients before tumor resection. Peri-tumor tissue was 3cm away from the edge of the conjugated tumor tissue. Samples were then obtained for the subsequent $CD3^+$cell sorting, single-cell RNA sequencing analysis, or *in vitro* testing implement.

Peripheral blood was collected from sepsis patients on the 1^{st}, 3^{rd}, 7^{th} and14^{th} day for flow cytometry. We obtained approval from the ethics committee of Zhongshan Hospital, Fudan University, and written informed consent from all HCC patients.

2.2 Sample preparation

We immersed specimens of fresh tumor and adjacent normal tissue in RPMI-1640 (Gibco) containing 10% FBS, shredded, ground the blocks and then passed the suspension through 40 μm cell strainers. Next, the single cell suspension was centrifuged (1500 rpm, for 10 min) and the supernatant was removed. The bottom cell pellets were resuspended in erythrocyte lysis buffer (Solarbio), kept on ice for 5 min and then washed twice with 1 × PBS.

2.3 Cell isolation and scRNA-Seq

Single-cell suspension was stained with fluorescent-labeled anti-CD3 (0.5%, Biolegend, Cat No.300308, Clone HIT3a) anti-CD45RO (0.5%, Biolegend, Cat No.304210, Clone UCHL1) for 30 min at 4°C. Subsequently, cells were rinsed and resuspended for FACS sorting. $CD3^+CD45RO^+$ T cells were isolated through FACS sorting (BD FACS Aria II).

For scRNA-Seq, the sorted cells were counted with a hemocytometer and diluted to 700–1200 cells/μl with targeted cell viability (>70%). Single cells were separated on a Chromium controller (10×Genomics) as the manufacturer's instructions. 20 cDNA libraries were prepared using Single-Cell 3′ Reagent Kits V2 (10xGenomics, Pleasanton, California) after single cell purification on a Chromium controller (10×Genomics) following the manufacturer's instructions. Library sequencing was conducted *via* Illumina sequencer following stringent quality control by fragment analysis (AATI) and the output data was processed through the Cell Ranger pipeline (version 2.1.1, 10×Genomics) default. Cells expressing less than 200 genes or with an improperly high fraction (> 5%) of mitochondrial genes were removed. The raw data was normalized on a log scale, facilitating the following clustering and principal component analysis. CytoTRACE (https://cytotrace.stanford.edu) helped to predict cell differentiation fate based on single-cell RNA-sequencing data Cell development trajectory was performed through ScVelo, an extensible RNA velocity analysis toolkit.

2.4 $CD8^+$ T cells culture

Spleens of wild-type mice were extracted, ground, and filtered to single-cell suspension. $CD8^+$ T cells were purified through negatively magnetic sorting (Biolegend, Cat. 480008), activated with anti-CD3 (eBioscience, Cat.16-0031-85) and anti-CD28 (eBioscience, Cat.16-0281-85) for 3 days, and then cultured with 100 U/ml IL-2 (Peprotech, Cat.200-02-50) or 10 μg/ml IL-15 (R&D, Cat.247-ILB-005) for another 3 days while adding 10 ug/mL or 25ug/mL C1q (Sigma, Cat.C1740-1MG).

2.5 FACS analysis

For flowing staining, viable cells identified through Fixable Viability Stain 510(BD). And cells were stained with CD3 (BioLegend, clone: HIT3a), CD8 (BioLegend, clone: SK1), CD45 (BioLegend, clone: HI30), CD68 (BioLegend, clone: Y1/82A), CD11B (BioLegend, clone: ICRF44), CD80 (BioLegend, clone: 2D10), CD206 (BioLegend, clone: 15-2), CD163 (BioLegend, clone: RM3/1), C1QA (abcam, clone: EPR2980Y), C1QC (abcam, clone: EPR2984Y), PD-1 (BioLegend, clone: RMP1-30), PD-L1 (BioLegend, clone: 10F.9G2), BCL2 (BioLegend, clone: 100), Ki67 ((BioLegend, clone: 11F6), GZMA (Biolegend, clone: CB9),GZMB (Biolegend, clone: QA16A02), IFNγ (Biolegend, clone: XMG1.2), TNFα (Biolegend, clone: MP6-XT22), LDHA (biocompare), Acetyl-Histone H3 (Lys27) Antibody (Cell Signaling), Acetyl-Histone H3 (Lys9) (C5B11) Antibody (Cell Signaling). Intracellular markers were stained before cell re-stimulation by PMA/ionomycin (Biolegend, Cat. 423303). Flow cytometry was performed on BD FACS Aria III flow cytometer and the data was analyzed by FlowJo6 software.

2.6 Metabolic gene-expression analysis by RT-PCR

Relative expression levels of selected genes were quantified by qRT-PCR. cDNA was synthesized *via* PrimeScript RT Master Mix (TAKARA, Cat. RR036A). TB Green Premix Ex Taq II (TAKARA, Cat. RR820A) was used for qRT-PCR analysis on the Roche LightCycler 480 System with primer sets in Supplementary Table 1. Expression data of all candidate genes were normalized to the housekeeping gene *36b4*.

2.7 Metabolic assay

XF-96 extracellular flux analyzer (Seahorse Bioscience) was used for the mitochondrial fitness test, Oxygen consumption rate (OCR) was measured at basal (1.5 × 10^5 cells/well), and after treatment with oligomycin (1 μM), protonophore carbonyl cyanide p-trifluoromethoxyphenylhydrazone (FCCP,1.5 μM), etomoxide (200 μM) in some cases, and rotenone (100 nM) plus antimycin A (1 μM) sequentially. The lactate assay kit (Life Technologies) was used to measure the lactate content in cells and cell cultures.

2.8 Statistical analysis

Post-acquisition analysis was carried out on FlowJo Software (v10.5.30) and representative plots were exhibited. Statistical analysis and corresponding quantitative plots were conducted using GraphPad Prism 8 software. Significance levels were assessed by Student t-test or ANOVA test, where appropriate.

2.9 Data availability

Relevant data in this study are available within the article and supplementary files. Additional information is available upon reasonable request from the corresponding author

3 Results

3.1 Cell populations identification in HCC samples

To identify the cellular diversity in HCC patients, we implemented ScRNA-Seq using the 10x Genomics single-cell 3′ V2 chemistry. We generated a single-cell suspension of 6 samples from the paired tumor (T) and peri-tumor tissue (P) and enriched $CD3^+$T cells by magnetic bead sorting. Barcoded sequencing reads went to the corresponding cells and transcriptome, then individual mRNA molecules were counted through unique molecular identifiers (UMIs). After quality control, we acquired single-cell transcriptomes of 24267 cells. Multiple single-cell analysis was carried out *via* R package *Seurat* (version 3.0; https://satijalab.org/seurat/) and high-quality transcriptome and visualization cells were presented over uniform manifold approximation and projection (UMAP) (Figure 1A). A total of 19 immune cell clusters were identified, including $CD8^+$T cells (5 clusters) and $CD4^+$T cells (4 clusters), NKT cells (2 clusters), gamma delta T cells, $CD3^+$monocytes and some clusters undergoing proliferating or differentiating process, et al. (Figure 1A; Table 1). In addition to the typical ones, including

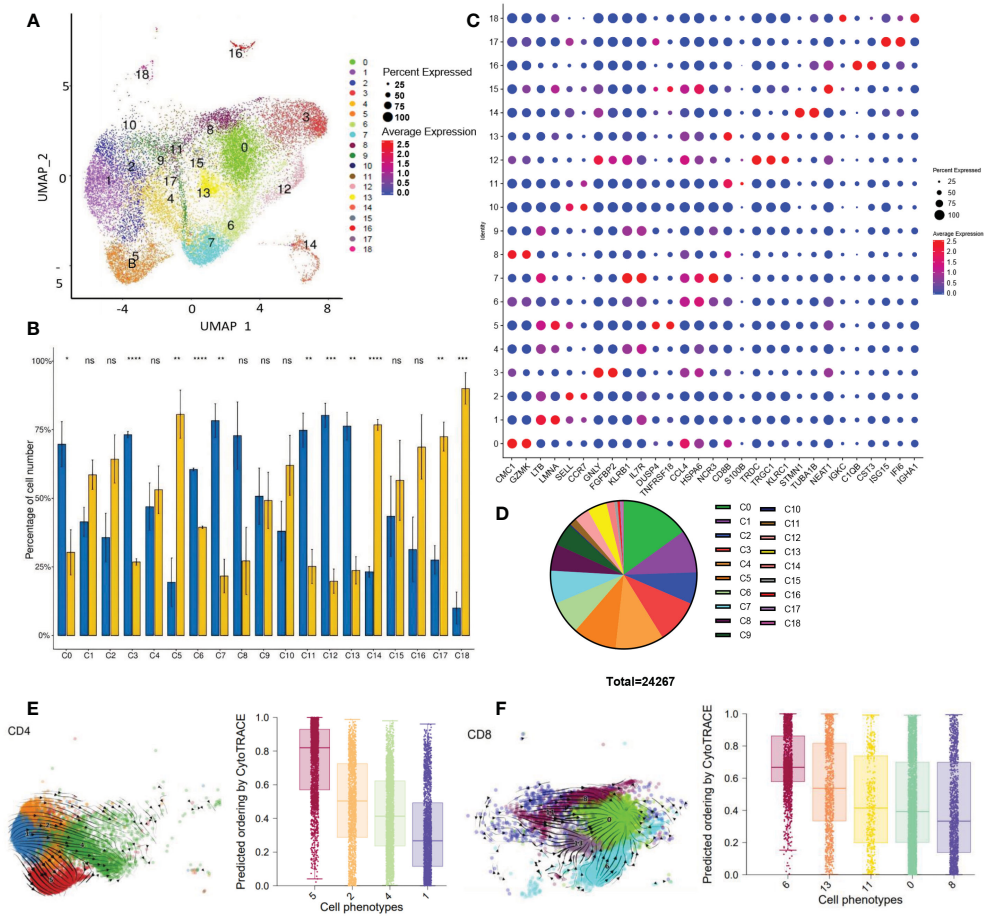

FIGURE 1
Single CD3$^+$ cell transcriptome analysis **(A)** UMAP visualization of T cells clusters based on 24267 single-cell transcriptomes of 6 samples (paired tumor and peri-tumor tissue of HCC), showing the formation of 19 cell clusters. **(B)** Histogram visualization shows the tissue distribution of 19 clusters. The percentage of cell number of each cluster was compared between tumor and peri-tumor. The means of the 2 groups were tested for significant differences based on the *t-test*. ns, no significance; *P<0.05 **P<0.01; ***P<0.001; ****P<0.0001. **(C)** Dot plot showed the expression of representative genes for each cluster. **(D)** Pie charts showed the proportion of different clusters. **(E)** Developmental trajectories of CD4$^+$T clusters in UAMP space by scvelo (right) and CytoTRACE (left). Values per phenotype using boxplots in CD4$^+$ clusters. Scores from 0 to 1 represent progressively lower differentiation potential. **(F)** Developmental trajectories of CD8$^+$T clusters in UAMP space by scvelo (right) and CytoTRACE(left). Summarize the median and distribution of CytoTRACE values per phenotype using boxplots in CD8$^+$T clusters. Scores from 0 to 1 represent progressively lower differentiation potential.

naïve T cells (TN), central memory T cells (TCM), effector memory T cells (TEM), recently activated effector memory or effector T cells (TEMRA/TEFF, designated TEMRA hereafter), gamma delta T cells, tumor-Treg cells, and exhausted T (Tex) cells, we also identified two virus-responsive cell clusters, with the CD3-IFI6 and CD3-IGHA1 clusters expressing some markers of type I interferon-stimulated genes.

We found that 11 clusters were differentially distributed in P and T. Statistical analysis was performed on the number of cells in each cluster (Figure 1B). Except for the C8, other CD8$^+$ T cell clusters (C0, C6, C11, C13) had a remarkable reduction in tumor tissue than adjacent tissue. Among the CD4$^+$ T cell clusters, C5(Treg) was significantly accumulated in the tumors, centering in establishing and maintaining an immunosuppressive environment. We then listed representative genes for each cluster in Figure 1C. Each cluster exhibited a distinct distribution and characteristics. From C0 to C9, the top 10 clusters of most CD3$^+$cells infiltrated in HCC samples are mainly composed of CD4 and CD8 T cells (Figure 1D). Other cell types, C3(NK) C7(NKT), and C12 (Gamma delta T) are notably reduced in tumors; on the contrary, the proportion of C14: CD3-STMN1 (proliferating cells), C17: CD3-IFI6 (type I interferon signaling pathway activated T cells) increased significantly in the tumor.

3.2 Time differentiation trajectory map of different cluster cells

Next, we explored a hypothetical differentiation trajectory with multiple intermediate states and gene expression gradients by using scVelo and CytoTRACE. The scVelo and CytoTRACE analysis respectively reflect the direction and potential of cell differentiation.

Firstly, we obtained the developmental trajectory of CD4$^+$ and CD8$^+$ T cells on UAMP space *via* scVelo. As listed in Table 1, we identified 4 clusters of CD4$^+$T cells. It was found that C1 showed progress trends toward 3 other clusters (Figure 1E). Using CytoTRACE to predict the differentiation potential of 4 clusters, in order from high to low is C1> C4> C2> C5(from purple to red,

TABLE 1 The presentative genes of each cluster.

Cluster NO.	Name	Definition	Representative genes
0	CD8-CMC1	Central memory CD8 T	CMC1, GZMK, CCL4, CCL3, CCL4L2
1	CD4-GPR183	Central memory CD4 T	LTB, LMNA, GPR183, VIM, IL7R
2	CD4-LEF1	Effector memory CD4 T	SELL, CCR7, LEF1, LDHB, GPR183
3	CD3-GNLY	NK	GNLY, FGFBP2, GZMB, GZMH, NKG7
4	CD4-CD69	TEMRA	KLRB1, IL7R, FOS, NFKBIA, CD69, CD40LG
5	CD4-FOXP3	Treg	FOXP3, TIGIT, IL2RA
6	CD8-CCL4	Effector CD8 T	CD8A, CCL4, HSPA6, FOSB, DUSP1, ID2
7	CD3-KLRB1	NKT	KLRB1, NCR3, CEBPD, CD69, DUSP1
8	CD8-GZMK	Central memory CD8 T	GZMK, CMC1, CCL5, CD8B, CD8A, NKG7
9	CD3-NCR3	NKT	NCR3, LTB, IL7R, KLRB1
10	CD3-SATB1	Differentiating T	MAL, LEF1, SATB1, CCR7, SELL
11	CD8-S100B	Effector memory CD8 T	LEF1, S100B, CD8A, CD8B
12	CD3-TRGC1	Gamma delta T	TRDC, TRGC1, GNLY, KLRD1, KLRC1
13	CD8-KLRC1	Effector CD8T	KLRC1, CD8B, KLRC2, CCL5, XCL1, KLRD1
14	CD3-STMN1	Proliferating cells	STMN1, PCNA, MKI67
15	CD3-CTLA4	Exhausted T cells	NEAT1, FOSB, CTLA4, TIGIT, HAVCR2
16	CD3-CD68	TAM	C1QB, C1QA, C1QC, APOEFTL, SELENOP, FCER1G, HLA-DRA, CD68
17	CD3-IFI6	Virus responsive T	IFI6, ISG15, MX1, IFI44L, IFIT3
18	CD3-IGHA1	Undetermined	IGKC, LTB, IGHA1, IFI6

Figure 1E; Supplementary Figure 1A), which is consistent with the results of scVelo. The results showed that C1 (GPR183^{hi}IL7R^{hi}CD4^{+}T cells) was speculated to be a group of cells with "stem cell-like" multiple differentiation potential. The memory CD4 T C2 with up-regulated expression of SELL, CCR7, and LEF1, may differentiate into effector CD4 (C4) or regulatory T cells (C5). C4 has TEMRAs. C4 and C5 developed into two individual branches without further differentiation potentials. The top 10 genes related to stemness (red) or differentiation (blue) were listed in Supplementary Figure 1B by calculating the correlation with CytoTRACE. It is not surprising that multiple genes coding ribosome proteins were related to CD4^{+}T cell differentiation (Supplementary Figure 1B, blue part). Ribosome biogenesis is critical for T-cell activation because of its rate-limiting role in cell growth and proliferation (24). More interestingly, several immune checkpoint genes (TIGIT, CTLA4) were linked to stemness character (Supplementary Figure 1B, red part), reflecting a paradox that dysfunctional TILs *in situ* may be capable of stem cell-like behavior (25).

By analyzing the differentiation trajectory of CD8^{+}T cells using the same strategy, scVelo depicted that the differentiation direction started from C11 to other clusters (Figure 1F). CytoTRACE predicted that the differentiation potential of the clusters varied from high to low by C8> C0> C11> C13> C6 (Figure 1F, purple to red). Track analysis showed the same trends (Supplementary Figure 1C). Different from the results of CD4^{+}T cells, multiple genes coding ribosome proteins were linked to cell differentiation and stemness of CD8^{+}T cells (Supplementary Figure 1D, blue part, and red part respectively), pinpointing the importance of metabolism in CD8^{+}T cells. Besides, other genes including long non-coding RNA were found associated with CD8^{+}T cell differentiation (Supplementary Figure 1D, blue part), suggesting diverse factors are required for the process.

3.3 Survival analysis of each cluster for liver cancer patients

Based on the TCGA data of 368 liver cancer patients, the survival analysis results obtained 7229 genes related to liver cancer prognosis. In each cluster, we counted the number of survival-related genes. It was found that C14 had the most survival-related genes, followed by C16, and C18, while there were no survival-related genes in C9, C10, and C11. To further understand the role of different cell subsets in prognosis, we performed a K-means cluster analysis on TCGA data based on the survival-related characteristic genes of liver cancer for each cluster. We divided liver cancer patients into two groups and calculated the survival curve to judge the role of this cluster in predicting the prognosis of patients (Figure 2).

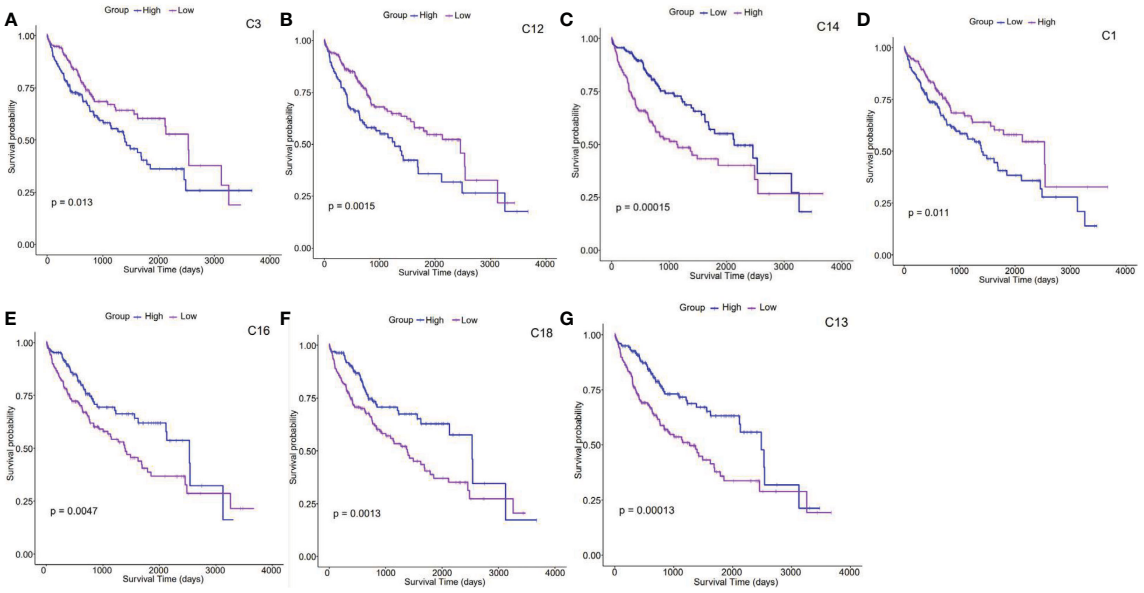

FIGURE 2
Survival analysis of clusters **(A–G)**. Kaplan–Meier survival analysis curves compare the high and low expression of characteristic genes in each cluster based on the TCGA HCC cohort. .

According to survival analysis results, survival curves of 7 clusters (C1, C3, C12, C13, C14, C16, and C18) could be significantly separated. Patients highly expressing C3, C12, and C14-featured genes presented a lower survival probability than those with moderate levels, indicating that the prognosis of patients with liver cancer enriched with this type of cells *in vivo* is relatively poor (the upper panel, Figures 2A–C). On the contrary, those with high expression ofC1, C13, C16, and C18-featured genes showed improved survival probability, suggesting that these clusters may point to better prognosis in liver cancer patients (the lower panel, Figures 2D–G). Interestingly, cell cycle genes STMN1 and TUBA1B were found increasingly expressed on C14. As switch molecules of the cell cycle from G1 to S phase, they were known for their crucial rules in eukaryotic cell proliferation (26). As shown in Figure 1B, the proportion of C14 increased by 3 times in HCC tumors. Although the destiny of these proliferating cells remains unknown, survival analysis suggests that it is detrimental to the prognosis of cancer patients (Figure 2C).

3.4 The interaction between clusters

It is essential to comprehend the interactions between clusters. Inter-cellular interactions by various molecules, such as receptors, ligands, structural proteins, secreted proteins, hormones, cytokines, neurotransmitters, etc, mediate cell communication and cell activities. Cellphone DB provides comprehensive recourses of curated receptors, ligands, and interactions(https://pypi.org/project/CellPhoneDB/).

In the study, we utilized scRNA-Seq data and Cellphone DB (version 3.1.0) to calculate the interaction scores between clusters, visualized the receptor-ligands interaction quantity, and analyzed the regulatory relationship. The output results are counted and presented in Figures 3A, B. Figures 3A, B respectively showed the interaction of clusters within peri-tumor and tumor tissue. We found that in HCC, the network with the most notable changes involved clusters C5, C16, and C4. In para-cancerous tissue, C6 and C16 had stronger interactions (Figure 3A). However, C16 not only lost self-regulation but also had a weaker connection with C6 in the tumor. In contrast, tumor-infiltrated C6 and C14 gained enhanced interactions (Figure 3B). Overall, the changed connections between clusters of TME suggested the potential immune suppressive mechanisms which need further investigation.

A meaningful receptor-ligand interaction leads to a physiological response. We identified 141 pairs of ligand-receptor interactions enriched in tumor samples. And the top five were KLRB1_CLEC2D, CD74_MIF, MIF_TNFRSF14, CD8 receptor_LCK, and CD2_CD58. There were 156 pairs in the samples of adjacent tissues, and the top five with the highest frequency were CD74_MIF, CD55_ADGRE5, MIF_TNFRSF14, SELL_SELPLG, CCL4L2_VSIR. The role of these ligand-receptor interactions in shaping TME still needs further investigation.

Next, we defined C16 as $CD3^+C1q^+$TAM. The presentative marker genes for C16 included the genes encoding the C1q protein family (C1QB, C1QA, C1QC, and CD68) (Figure 1C). The C6 was $CD8^+CCL4^+$T cells identified as effector T cells. Therefore, we speculate that C16 possibly regulates C6 function through the complement signaling pathway. The cluster C16 ($CD3^+C1q^+$TAM) found in our study has not been reported before. To further evaluate the existence of C16, we stain $CD3^+$ $CD45^+$ $CD68^+$ $CD11B^+$ cells for single-cell suspension of paired tumor and peri-tumor tissue (Figure 3C). Using flow cytometry, we detected the presence of $CD3^+C1q^+$TAM in HCC and found the proportion of this population was significantly lower in tumors (Figure 3C). The observation is consistent with the shift revealed by scRNA-Seq analysis (Figures 3A, B). Furthermore, we labeled M1-LIKE

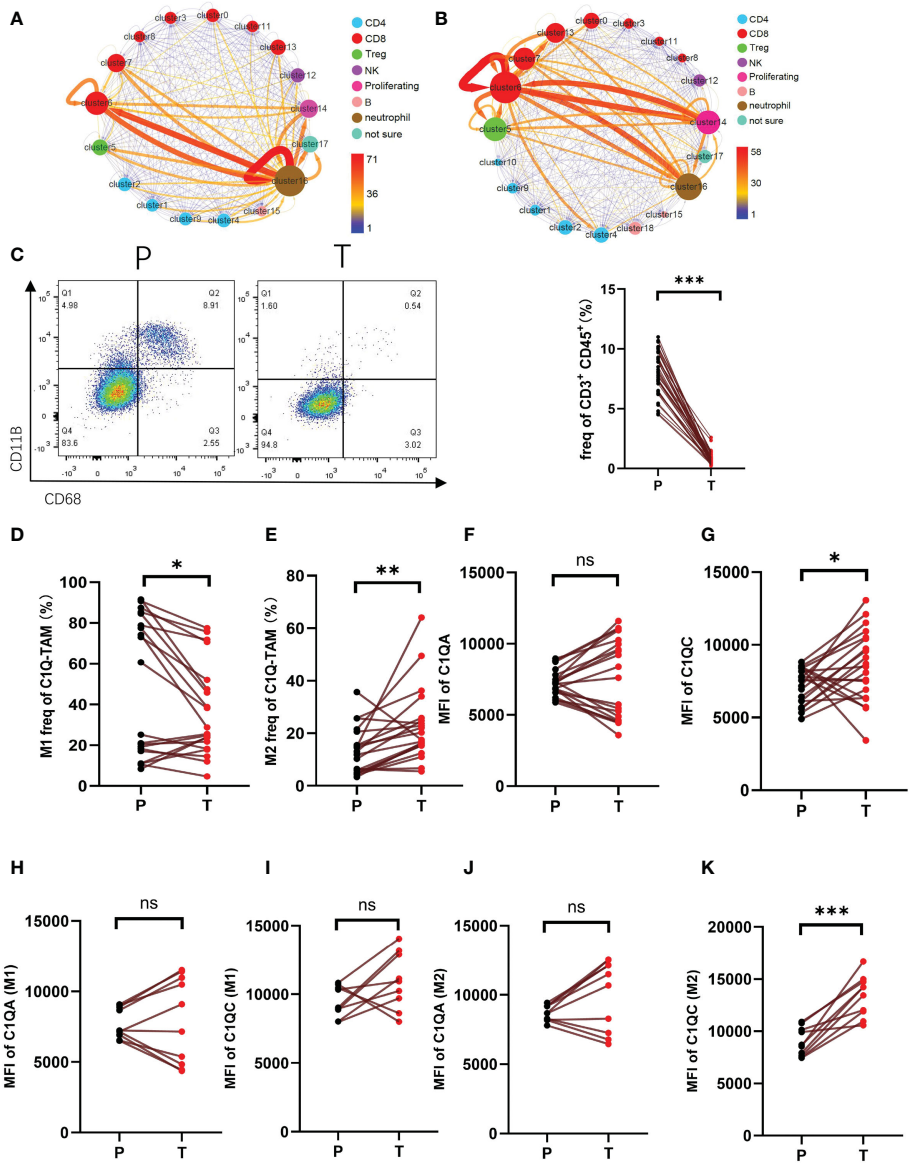

FIGURE 3
The interaction of $CD3^+C1q^+$TAM and $CD8^+CCL4^+$T cells a-b. Interaction between clusters of HCC para-cancer **(A)** and tumor tissues **(B)**. The arrow represents the interaction from this cluster to that cluster. The thickness of the line indicates the value of the interaction pair. The size of the point refers to the interaction of the cluster as an end. The color of the point refers to the interaction of the cluster as a start. **(C)** Flow cytometric gating of C1q-T ($CD11B^+$ and $CD68^+$) staining on $CD45^+CD3^+$ cells of HCC. Right panel shows the proportion of $CD11B^+$ $CD68^+$ in total $CD45^+CD3^+$ cells. **(D, E)**. The proportion of M1 ($CD86^+CD80^+$) **(D)**, M2 ($CD163^+CD206^+$) **(E)** in total C1Q-TAM ($CD11B^+$ and $CD68^+$) were compared at P and T. **(F–K)**. The expression level of C1QA and C1QC of C1Q-TAM cells **(F, G)**, M1 **(H, I)** and M2 **(J, K)** were detected by cell flow cytometry. ns, no significance; *P<0.05; **P<0.01; ***P<0.001.

($CD86^+CD80^+$) and M2-LIKE($CD206^+CD163^+$) to explore its entity (Supplementary Figure 2). The staining suggested that the population $CD3^+C1q^+$TAM was a mixture of M1 or M2-LIKE cells. There are more M1-LIKE cells in tumor-adjacent tissues (Figure 3D). In contrast, a remarkably increased number of M2-LIKE cells was observed in tumor tissues (Figure 3E). Since the C1q signaling pathway was significantly expressed in C16 (Figure 1C). C1QC expression was elevated in tumors, especially in M2 cells, and C1QA did not change significantly (Figure 3F–K).

To further verify the existence of this population, we collected peripheral blood from patients with sepsis to measure the proportion of $CD3^+C1q^+$macrophage in infection by flow cytometry. We found that the $CD3^+C1q^+$macrophage ratio increased in the early stage of sepsis (day 1) and decreased after day 3 (Figures 4A, B). Furthermore, we labeled M1-LIKE ($CD80^+$) and M2-LIKE ($CD163^+$) and the data indicated that M2-LIKE cells were significantly higher than M1-LIKE cells in the peripheral blood of sepsis patients (Figures 4C–F). At the same time, we also detected the C1q signaling pathway and found that the expression of C1QC was elevated in the peripheral blood of patients with sepsis, while C1QA had no significant change (Figures 4G–J). These results are consistent with the HCC results, so we believe that $CD3^+C1q^+$TAM

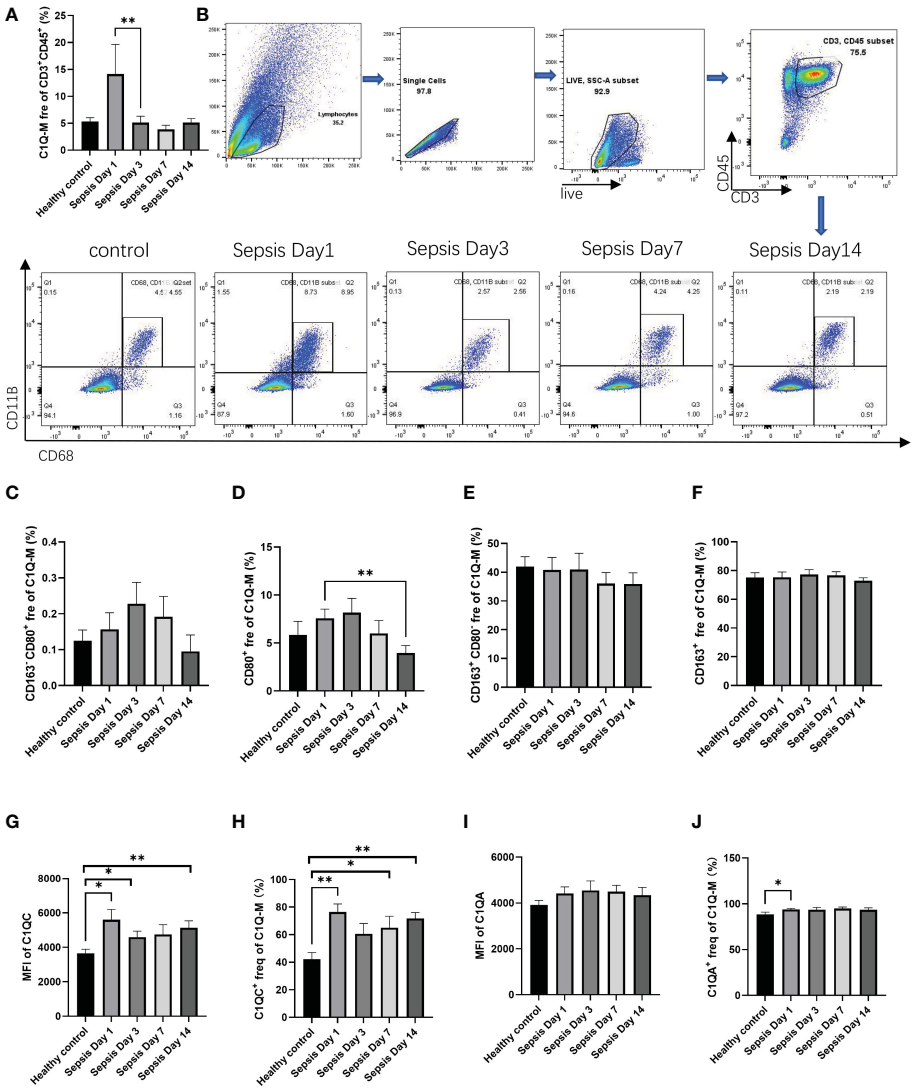

FIGURE 4
The existence of $CD3^+C1q^+$macrophage in peripheral blood of sepsis patients **(A)** The histogram shows the proportion of $CD11B^+CD68^+$ in the total $CD45^+CD3^+$ cells in the peripheral blood of healthy controls and sepsis patients. **(B)** Flow cytometry gating of C1Q-M ($CD11B^+$ and $CD68^+$) staining on $CD45^+CD3^+$ cells in healthy controls and sepsis. c-f. The histogram shows the proportion of $CD163^-CD80^+$ **(C)**, $CD80^+$ **(D)**, $CD163^+CD80^-$ **(E)**, $CD163^+$ **(F)** cells in total C1Q-M ($CD11B^+$ and $CD68^+$) by flow staining. **(G–J)** The expression levels **(G, I)** and ratios **(H, J)** of C1QA and C1QC in C1Q-TAM cells **(F–G)**, M1 **(H–I)** and M2 **(J–K)** were detected by flow cytometry. ns, no significance; *P<0.05; **P<0.01.

plays a pro-inflammatory and anti-tumor role in the initial stage of infection and tumors.

3.5 Effects of C1q on T cell metabolism

Since energy metabolism is essential for T cell differentiation and function, we next explored how C1q modulates T cell metabolism. We tested the expression panel of metabolic genes and found most were upregulated in C1q-treated Teff cells, including HK1, TPI1, GPD2, GPM2, ENO3, PDK1, and LDHA (Supplementary Figure 3). In Tmem cells, only the expression of ALDOA and LDHA were increased after C1q treatment (Supplementary Figure 3). For both Teff and Tmem, the MFI of Carnitine palmitoyl transferase 1A(CPT1α) and Lactate dehydrogenase A(LDHA) increased significantly after C1q treatment (Figures 5A, B). CPT1α and LDHA respectively center in the process of fatty acid oxidation and glycolysis. Besides, the expression of transcription factor HIF1α, an important oxygen sensor and metabolic modulator, also increased after C1q treatment (Figure 5C). The data suggested that C1q treatment can increase T cell metabolism, which was confirmed by the seahorse experiment (Figures 5D, E). Consistent with metabolic changes aforesaid, the lactate content was found increased in Teff and Tmem internally and culture medium of Teff after C1q treatment (Figures 5F, G). Increased glycolysis and higher lactate production further confirmed the effects of C1q treatment on T cell metabolism. Taken together, the results suggested that Teff was considerably responsive to C1q on metabolic regulation.

Some metabolites have been proved to involve in epigenetic regulation as substrates, donors, cofactors, or antagonists of chromatin- and DNA-modifying enzymes, indicating cross-talk between cell metabolism and differentiation (27). Previous studies

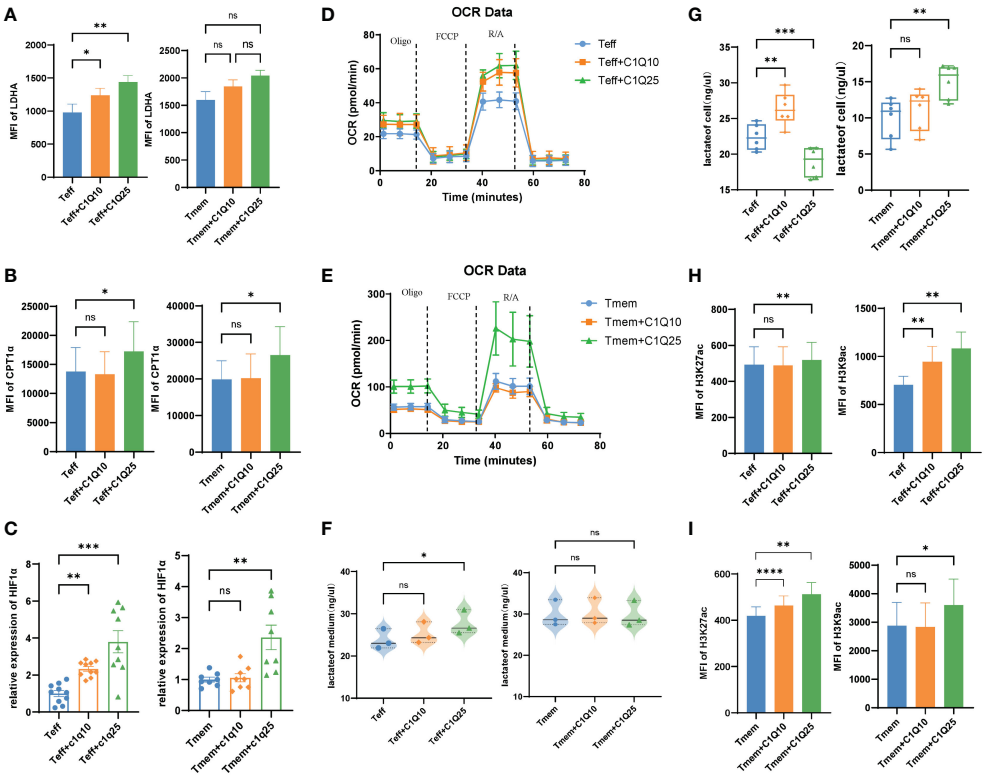

FIGURE 5
Effects of C1Q on T cell differentiation and function **(A)** The expression of LDHA in Teff and Tmem cells with and without C1q. **(B)** The expression of CPT1α in Teff and Tmem cells with and without C1q. **(C)** The mRNA expression of HIF1a in Teff and Tmem cells with and without C1q. **(D, E)**. Oxygen consumption rate (OCR) spectra of Teff and Tmem cells with and without C1q using Seahorse XF96 analyzer. **(F)** The lactate levels in Teff and Tmem cells with and without C1q. **(G)** The lactate levels in Teff and Tmem cells culture medium. **(H)** The expression of H3K27ac in Teff and Tmem cells with and without C1q. **(I)** The expression of H3K9ac in Teff and Tmem cells with and without C1q. ns, no significance; *P<0.05; **P<0.01; ***P<0.001; ****P<0.0001.

have found that LDHA could regulate cell differentiation through the epigenetic axis (28). We next focused on whether the alternation of epigenetic profiling occurred in $CD8^+$ T cells after C1q treatment. Since lactate is generated in the cytoplasm which gives rise to acetyl-CoA and increases the level of histone acetylation, H3K27 and H3K9 acetylation levels were also elevated in both Teff and Tmem after C1q treatment (Figures 5H, I), which is consistent with our observation of increased lactate concentration in treated cells (Figures 5F, G).

3.6 C1q regulates T cell differentiation and function

Then we turned to the impact of C1q from C16 on T cell activation and proliferation. Naïve $CD8^+$T cells were isolated from wild type mice, then stimulated by anti-CD3 and anti-CD28 antibodies, along with C1q to simulate the effect of $CD3^+C1q^+$TAM on T cells function. We found that C1q treatment promoted Teff and Tmem differentiation (Figures 6A, B) through T cell responses analysis by flow cytometry. Then we assessed the effects of C1q on the production of IFN-γ, tumor necrosis factor–α (TNF-α), Perforin (PRF), Granzyme A (GZMA) and Granzyme B (GZMB) in Teff and Tmem cells. For both Teff and Tmem, after C1q treatment, cells had increased expression of Ki67 and Bcl2, possibly highlighting a link between C1q and T cell proliferation and survival capacity although the effector function was only significantly enhanced in Teff (Figures 6C, D). The treatment did not affect PD1 or PDL1 expression of T cells, thereby excluding that C1q might induce T cell exhaustion (Supplementary Figure 4).

4 Discussion

Understanding the tumor immune microenvironment of HCC is critical for developing individualized immunotherapy. The study performed cell clustering and annotated them based on scRNA-seq from paired HCC tumor or peri-tumor tissues. Combing the TCGA data, we established the correlation between each cluster and the prognosis of liver cancer patients (Figure 2). Some clusters (C1, C13, C16, and C18) predicted better survival; in contrast, C3, C12, and C14 were linked to poor prognosis.

In view of the prognostic value of C16, it is conceivable that these cells play a crucial role in anti-tumor immunity. C16 is a new population simultaneously expressing CD3, C1Q, CD68, APOEFTL, SELENOP, FCER1G, and HLA-DRA (Table 1). CD68 is a classic marker for macrophages. Complement component C1q is a marker of a particular subpopulation of tissue-resident macrophages and tumor-associated macrophages (TAM). It is hard to define this

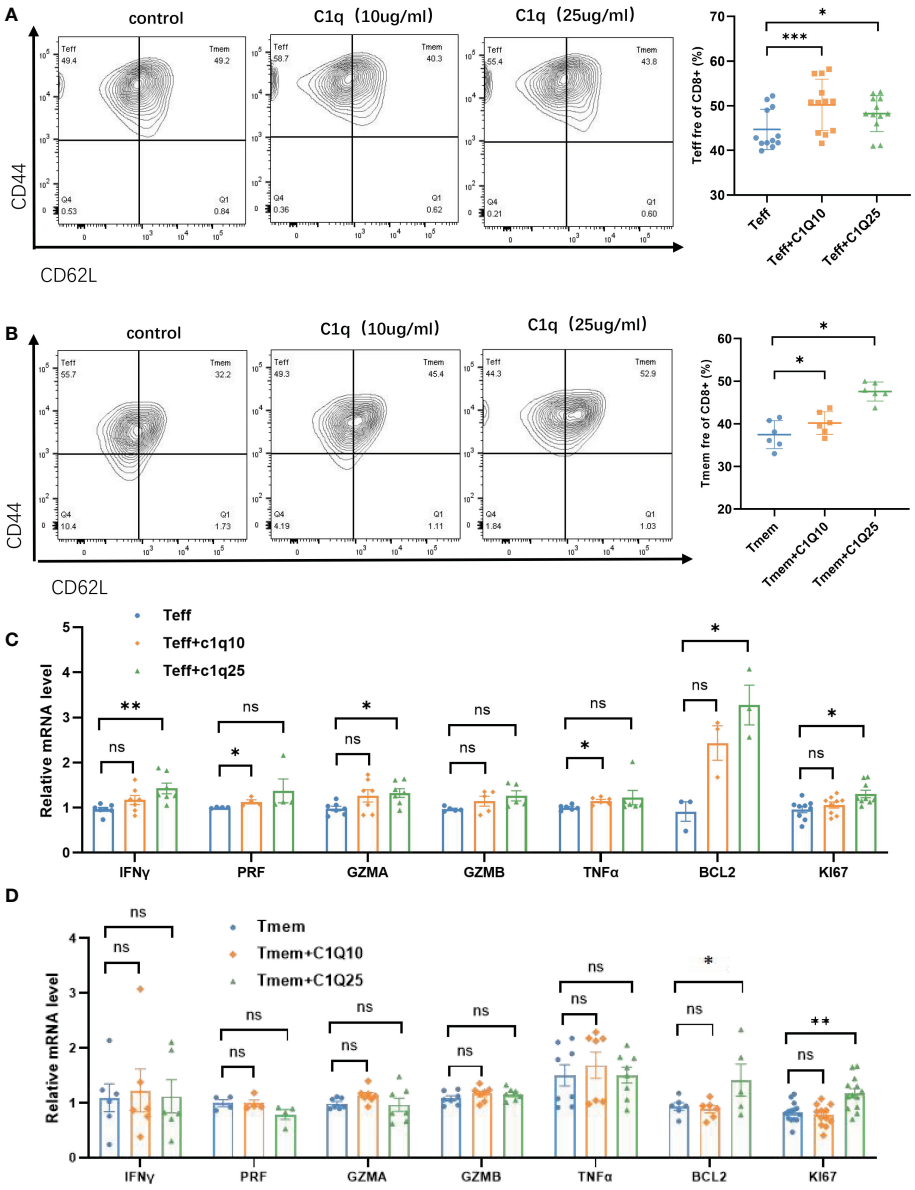

FIGURE 6
Effects of C1q on T cell differentiation and function **(A)** Flow cytometric gating of CD44 and CD62L in $CD8^+$Teff (left) cells and quantification (right) on Teff cells with and without C1q. **(B)** Flow cytometric gating of CD44 and CD62L in $CD8^+$Tmem (left) cells and quantification (right) on Tmem cells with and without C1q. **(C)** The expression of IFNγ, GZMA, PRF, GZMB, TNFα, BCL2, and KI67 in Teff cells with and without C1q. **(D)** The expression of IFNγ, GZMA, PRF, GZMB, TNFα, BCL2 and KI67 in Tmem cells with and without C1q. ns, no significance; *P<0.05; **P<0.01; ***P<0.001. IFNγ, Interferon Gamma, GZMA, Granzyme A, GZMB, Granzyme B, PRF, Perforin, TNFα, Tumor Necrosis Factor Alpha, BCL2, BCL2 Apoptosis Regulator, KI67, Marker Of Proliferation Ki-67.

population as M1(pro-inflammation) or M2(anti-inflammation) based on their DEGs generated from scRNA-seq data. Then we verified its entity by staining well-known markers for M1 (CD80, CD86) and M2(CD206, CD163) signaling, and the results suggested it is a unique population of cells that possess both M1 and M2 features.

With high plasticity, the differentiation process of macrophages often produces heterogeneous results. Recently, a novel subset of macrophages called $CD3^+$ macrophages was found accumulating in both infectious and non-infectious condition (23).They have been reported to originate from monocytic myeloid-derived suppressor cells (M-MDSCs) (29). Meanwhile, $CD3^+$monocyte-derived macrophages can be further differentiated into $TCR\alpha\beta^+$ and $TCR\alpha\beta^-$ sub-population. Adriana et al. found that Tumor necrosis factor (TNF) knockout caused lower frequency of $CD3^+$ $TCR\alpha\beta^+$ macrophage and higher mortality in Bacillus Calmette-Guérin (BCG) -infected mice (23). Consistently, the ϵ and ζ chains of CD3 were recently reported to express on RAW, a classical murine macrophage cell line, and present increased transcriptional levels after BCG infection (30). In this study, we identified $CD3^+C1q^+$macrophages, a new subset in both HCC tumors (Figure 1) and peripheral blood of sepsis patients (Figure 4). In sepsis samples, the population of $CD3^+C1q^+$macrophages had a sharp rise at Day1 after infection and subsequent decline when the infection subsided (Figure 4A). So, we believe that the tumor-infiltrated $CD3^+C1q^+$TAM mainly plays

a pro-inflammatory and anti-tumor role in the initial stage of infection and tumors although the population is experiencing differential and heterogeneous characteristics. It also could explain why the increased $CD3^+C1q^+$TAM links to a better survival prognosis for liver cancer patients (Figure 2E).

We quantified the interaction information between clusters for visual analysis. The results showed that the cluster-cluster interactions differed in HCC tumors and para-cancerous tissue. To further understand the transcriptional heterogeneity of clusters, we discovered transcription factors related to the oncogenesis and development of HCC. For C6 and C16, the gene regulation network of specific high expression transcription factors was constructed. Some key transcription factors were found, such as KDM5B, UQCRB, and CREM in C6, at the same time DAB2 in C16(data not shown).

It has been reported that $C1q^+$TAMs could modulate tumor-infiltrating $CD8^+$T cells *via* multiple immunomodulatory ligands (31). However, in our study the new identified $CD3^+C1q^+$TAM hasn't been reported before. Therefore, the explanation for the relationship between newly identified C16($CD3^+C1q^+$TAM) and C6 ($CD8^+CCL4^+$T) cells also remains unknown. Based on multiple roles of C1q independent of complement activation (32), we explored how $CD3^+C1q^+$TAM affected the $CD8^+CCL4^+$T cells.

In vitro experiment suggested that this population can promote specific T cell functions by some mechanisms independent of complement activation. In the study (Figure 5), C1q treatment affected multiple metabolic genes expression and which was confirmed by a seahorse experiment. Besides, an abundant metabolite produced during glycolysis, lactate, was increased along with enhanced histone acetylation in both Teff and Tmem after C1q treatment (Figures 5H, I). In other studies, complement C1q binding protein (C1qbp) has been reported to promote differentiation of Teff *via* metabolic-epigenetic reprogramming (33). Besides, research showed that C1q could restrain responses to self-antigens in $CD8^+$T cells by modulating mitochondrial metabolism (34). Altogether these data link C1q to $CD8^+$T cell metabolism and activation and point the protective role of this newly identified population. Dynamic changes of histone acetylation lead to differential expression of effectors, facilitating rapid and robust responses in $CD8^+$Tmem (35). The nature of incoming environmental factors and the diversion of inherent metabolic programs during T cell activation heavily impact the differentiation and function of effector T cell subpopulations. Thus, our findings depict how C1q influences the metabolism of $CD8^+$T cells and highlights the importance of interaction between complement and immunometabolism in anti-tumor immunity.

With the development of gene detection technology, genomic network-based stratification (NBS)-guided treatments have made great progress clinically. Tumor mutations were proved to help identify subtypes in ovarian, uterine, endometrial and lung cancer and head and neck squamous cell carcinoma (HNSCC) (36–39). A metabolic network-driven approach facilitated to divide HCC into 3 subsets with distinct metabolic features and different prognosis (39). Besides, transcription regulators were also reported to label immunoreactive or silent subtypes in cancer (40). Genomic directed stratification made it possible to implement personalized medicine. Our data showed that C16 was significantly associated with patient outcomes. Together, our results identify $C1q^+CD3^+$TAM cells relate with cancer patients prognosis and highlight these cells, as well as C1q itself, as potential targets to address TME-associated immune dysfunction. One of the limitations of our study is the lackness of *in vivo* animal model to evaluate whether T cell function can regain after restoration of the attenuate crosstalk(C16-C6) within HCC TME. Besides, more researches await to be done to explore how to strengthen this connection pointedly in clinical practice.

Data availability statement

Data transparency. The datasets used or analyzed during the current study are available from the corresponding author on reasonable request. The data presented in the study are deposited in the China National Center for Bioinformation / Beijing Institute of Genomics, accession number HRA003563 (https://ngdc.cncb.ac.cn/gsa-human).

Ethics statement

The studies involving human participants were reviewed and approved by Zhongshan Hospital ethics committee. The patients/participants provided their written informed consent to participate in this study. The animal study was reviewed and approved by Zhongshan Hospital ethics committee.

Author contributions

YY designed and conducted the research, collected and interpreted the data, and wrote the paper. LS, ZC, FL, MM, YC, YL performed and assisted with the experiments, helped to analyze the data and edit the manuscript. QX and GC performed scRNA-seq data analysis. WL, HF and YS provided the patient samples and assisted in the analysis of experimental results. LS, FL, WL, QX, MM, YC, YL, GC and YS provided advice and edited the paper. DW oversaw the research and revised the paper. The authors declared that they had no conflicts of interest. All authors contributed to the article and approved the submitted version.

Funding

This study was supported by the National Natural Science Foundation of China (No.81771672), "Cross key project of mathematics and medical health" of the National Natural Science Foundation of China (No.12026608), Open fund project of Shenzhen BGI Institute of Life Science(No.BGIRSZ20200004) and Special Fund for Clinical Research of Zhongshan Hospital, Fudan University (No.2020ZSLC07), Key Subject Construction Program of Shanghai Health Administrative Authority (ZK2019B30), and Shanghai Engineering Research Center of Tumor Multi-Target Gene Diagnosis (20DZ2254300). The funding agencies had no role in the

study's design and conduct, collecting, analyzing, and interpreting the data or preparation.

Conflict of interest

The authors declare that the research was conducted in the absence of any commercial or financial relationships that could be construed as a potential conflict of interest.

Publisher's note

Supplementary material

The Supplementary Material for this article can be found online at: https://www.frontiersin.org/articles/10.3389/fimmu.2023.1033497/full#supplementary-material

SUPPLEMENTARY FIGURE 1
Differentiation and stemness potential analysis of CD4 and CD8 cell subsets.

SUPPLEMENTARY FIGURE 2
Flow cytometry gating of M1 ($CD80^+$ $CD86^+$), M2 ($CD163^+$ $CD206^+$) staining on C1q-TAM ($CD11B^+$ $CD68^+$) cells in HCC.

SUPPLEMENTARY FIGURE 3
Effects of C1q on T cell metabolic genes expression.

SUPPLEMENTARY FIGURE 4
Effects of C1q on T cell exhaustion induction.

SUPPLEMENTARY TABLE 1
Primer sequences of genes related to glycolysis and effector functions are provided.

References

1. Llovet JM, Kelley RK, Villanueva A, Singal AG, Pikarsky E, Roayaie S, et al. Hepatocellular carcinoma. *Nat Rev Dis Primers* (2021) 7(1):6. doi: 10.1038/s41572-020-00240-3

2. Sung H, Ferlay J, Siegel RL, Laversanne M, Soerjomataram I, Jemal A, et al. Global cancer statistics 2020: GLOBOCAN estimates of incidence and mortality worldwide for 36 cancers in 185 countries. *CA Cancer J Clin* (2021) 71(3):209–49. doi: 10.3322/caac.21660

3. McGlynn KA, Petrick JL, El-Serag HB. Epidemiology of hepatocellular carcinoma. *Hepatology* (2021) 73 Suppl 1:4–13. doi: 10.1002/hep.31288

4. Leone P, Solimando AG, Fasano R, Argentiero A, Malerba E, Buonavoglia A, et al. The evolving role of immune checkpoint inhibitors in hepatocellular carcinoma treatment. *Vaccines* (2021) 9(5):532–50. doi: 10.3390/vaccines9050532

5. Hinshaw DC, Shevde LA. The tumor microenvironment innately modulates cancer progression. *Cancer Res* (2019) 79(18):4557–66. doi: 10.1158/0008-5472.CAN-18-3962

6. Fridman WH, Zitvogel L, Sautès-Fridman C, Kroemer G. The immune contexture in cancer prognosis and treatment. *Nat Rev Clin Oncol* (2017) 14(12):717–34. doi: 10.1038/nrclinonc.2017.101

7. Fridman WH, Pagès F, Sautès-Fridman C, Galon J. The immune contexture in human tumours: impact on clinical outcome. *Nat Rev Cancer* (2012) 12(4):298–306. doi: 10.1038/nrc3245

8. Kumar V, Patel S, Tcyganov E, Gabrilovich DI. The nature of myeloid-derived suppressor cells in the tumor microenvironment. *Trends Immunol* (2016) 37(3):208–20. doi: 10.1016/j.it.2016.01.004

9. Eggert T, Greten TF. Tumor regulation of the tissue environment in the liver. *Pharmacol Ther* (2017) 173:47–57. doi: 10.1016/j.pharmthera.2017.02.005

10. Xing R, Gao J, Cui Q, Wang Q. Strategies to improve the antitumor effect of immunotherapy for hepatocellular carcinoma. *Front Immunol* (2021) 12:783236. doi: 10.3389/fimmu.2021.783236

11. Wagner J, Rapsomaniki MA, Chevrier S, Anzeneder T, Langwieder C, Dykgers A, et al. A single-cell atlas of the tumor and immune ecosystem of human breast cancer. *Cellα* (2019) 177(5):1330–45.e18. doi: 10.1016/j.cell.2019.03.005

12. Qian J, Olbrecht S, Boeckx B, Vos H, Laoui D, Etlioglu E, et al. A pan-cancer blueprint of the heterogeneous tumor microenvironment revealed by single-cell profiling. *Cell Res* (2020) 30(9):745–62. doi: 10.1038/s41422-020-0355-0

13. Tirosh I, Izar B, Prakadan SM, Wadsworth MH2nd, Treacy D, Trombetta JJ, et al. Dissecting the multicellular ecosystem of metastatic melanoma by single-cell RNA-seq. *Sci (New York NY)* (2016) 352(6282):189–96. doi: 10.1126/science.aad0501

14. Guo X, Zhang Y, Zheng L, Zheng C, Song J, Zhang Q, et al. Global characterization of T cells in non-small-cell lung cancer by single-cell sequencing. *Nat Med* (2018) 24(7):978–85. doi: 10.1038/s41591-018-0045-3

15. Savas P, Virassamy B, Ye C, Salim A, Mintoff CP, Caramia F, et al. Single-cell profiling of breast cancer T cells reveals a tissue-resident memory subset associated with improved prognosis. *Nat Med* (2018) 24(7):986–93. doi: 10.1038/s41591-018-0078-7

16. Zhang Q, He Y, Luo N, Patel SJ, Han Y, Gao R, et al. Landscape and dynamics of single immune cells in hepatocellular carcinoma. *Cellα* (2019) 179(4):829–45 e20. doi: 10.1016/j.cell.2019.10.003

17. Zheng C, Zheng L, Yoo JK, Guo H, Zhang Y, Guo X, et al. Landscape of infiltrating T cells in liver cancer revealed by single-cell sequencing. *Cellα* (2017) 169(7):1342–56 e16. doi: 10.1016/j.cell.2017.05.035

18. Lim CJ, Lee YH, Pan L, Lai L, Chua C, Wasser M, et al. Multidimensional analyses reveal distinct immune microenvironment in hepatitis b virus-related hepatocellular carcinoma. *Gutα* (2019) 68(5):916–27. doi: 10.1136/gutjnl-2018-316510

19. Younossi Z, Tacke F, Arrese M, Chander Sharma B, Mostafa I, Bugianesi E, et al. Global perspectives on nonalcoholic fatty liver disease and nonalcoholic steatohepatitis. *Hepatologyα* (2019) 69(6):2672–82. doi: 10.1002/hep.30251

20. Sun Y, Wu L, Zhong Y, Zhou K, Hou Y, Wang Z, et al. Single-cell landscape of the ecosystem in early-relapse hepatocellular carcinoma. *Cellα* (2021) 184(2):404–21 e16. doi: 10.1016/j.cell.2020.11.041

21. Zhang L, Li Z, Skrzypczynska KM, Fang Q, Zhang W, O'Brien SA, et al. Single-cell analyses inform mechanisms of myeloid-targeted therapies in colon cancer. *Cellα* (2020) 181(2):442–59.e29. doi: 10.1016/j.cell.2020.03.048

22. Ren X, Zhang L, Zhang Y, Li Z, Siemers N, Zhang Z. Insights gained from single-cell analysis of immune cells in the tumor microenvironment. *Annu Rev Immunol* (2021) 39:583–609. doi: 10.1146/annurev-immunol-110519-071134

23. Rodriguez-Cruz A, Vesin D, Ramon-Luing L, Zuñiga J, Quesniaux VFJ, Ryffel B, et al. CD3(+) macrophages deliver proinflammatory cytokines by a CD3- and transmembrane TNF-dependent pathway and are increased at the BCG-infection site. *Front Immunol* (2019) 10:2550. doi: 10.3389/fimmu.2019.02550

24. Tan TCJ, Knight J, Sbarrato T, Dudek K, Willis AE, Zamoyska R. Suboptimal T-cell receptor signaling compromises protein translation, ribosome biogenesis, and proliferation of mouse CD8 T cells. *Proc Natl Acad Sci United States America* (2017) 114(30):E6117–E26. doi: 10.1073/pnas.1700939114

25. Vodnala SK, Eil R, Kishton RJ, Sukumar M, Yamamoto TN, Ha NH, et al. T Cell stemness and dysfunction in tumors are triggered by a common mechanism. *Science* (2019) 363(6434):eaau0135. doi: 10.1126/science.aau0135

26. Lu C, Zhang J, He S, Wan C, Shan A, Wang Y, et al. Increased alpha-tubulin1b expression indicates poor prognosis and resistance to chemotherapy in hepatocellular carcinoma. *Dig Dis Sci* (2013) 58(9):2713–20. doi: 10.1007/s10620-013-2692-z

27. Fanucchi S, Dominguez-Andres J, Joosten LAB, Netea MG, Mhlanga MM. The intersection of epigenetics and metabolism in trained immunity. *Immunityα* (2021) 54(1):32–43. doi: 10.1016/j.immuni.2020.10.011

28. Peng M, Yin N, Chhangawala S, Xu K, Leslie CS, Li MO. Aerobic glycolysis promotes T helper 1 cell differentiation through an epigenetic mechanism. *Sci (New York NY)* (2016) 354(6311):481–4. doi: 10.1126/science.aaf6284

29. Zhang N, Gao X, Zhang W, Xiong J, Cao X, Fu ZF, et al. JEV infection induces m-MDSC differentiation into CD3+ macrophages in the brain. *Front Immunol* (2022). doi: 10.3389/fimmu.2022.838990

30. Ocaña-Guzmán R, Ramón-Luing LA, Rodríguez-Alvarado M, Voss TD, Fuchs T, Chavez-Galan L. Murine RAW macrophages are a suitable model to study the CD3 signaling in myeloid cells. *Cellsα* (2022) 11(10):1635–50. doi: 10.3390/cells11101635

31. Dong L, Chen C, Zhang Y, Guo P, Wang Z, Li J, et al. The loss of RNA N(6)-adenosine methyltransferase Mettl14 in tumor-associated macrophages promotes CD8(+)

T cell dysfunction and tumor growth. *Cancer Cell* (2021) 39(7):945–57 e10. doi: 10.1016/j.ccell.2021.04.016

32. Thielens NM, Tedesco F, Bohlson SS, Gaboriaud C, Tenner AJ. C1q: A fresh look upon an old molecule. *Mol Immunol* (2017) 89:73–83. doi: 10.1016/j.molimm.2017.05.025

33. Zhai X, Liu K, Fang H, Zhang Q, Gao X, Liu F, et al. Mitochondrial C1qbp promotes differentiation of effector CD8(+) T cells via metabolic-epigenetic reprogramming. *Sci Adv* (2021) 7(49):eabk0490. doi: 10.1126/sciadv.abk0490

34. Ling GS, Crawford G, Buang N, Bartok I, Tian K, Thielens NM, et al. C1q restrains autoimmunity and viral infection by regulating CD8(+) T cell metabolism. *Sci (New York NY)* (2018) 360(6388):558–63. doi: 10.1126/science.aao4555

35. Araki Y, Fann M, Wersto R, Weng NP. Histone acetylation facilitates rapid and robust memory CD8 T cell response through differential expression of effector molecules (eomesodermin and its targets: perforin and granzyme b). *J Immunol (Baltimore Md 1950)* (2008) 180(12):8102–8. doi: 10.4049/jimmunol.180.12.8102

36. Hofree M, Shen JP, Carter H, Gross A, Ideker T. Network-based stratification of tumor mutations. *Nat Methods* (2013) 10(11):1108–15. doi: 10.1038/nmeth.2651

37. Sanati N, Iancu OD, Wu G, Jacobs JE, McWeeney SK. Network-based predictors of progression in head and neck squamous cell carcinoma. *Front Genet* (2018) 9:183. doi: 10.3389/fgene.2018.00183

38. Urick ME, Bell DW. Clinical actionability of molecular targets in endometrial cancer. *Nat Rev Cancer* (2019) 19(9):510–21. doi: 10.1038/s41568-019-0177-x

39. Bidkhori G, Benfeitas R, Klevstig M, Zhang C, Nielsen J, Uhlen M, et al. Metabolic network-based stratification of hepatocellular carcinoma reveals three distinct tumor subtypes. *Proc Natl Acad Sci United States America* (2018) 115(50):E11874–e83. doi: 10.1073/pnas.1807305115

40. Mall R, Saad M, Roelands J, Rinchai D, Kunji K, Almeer H, et al. Network-based identification of key master regulators associated with an immune-silent cancer phenotype. *Briefings Bioinf* (2021) 22(6):bbab168. doi: 10.1093/bib/bbab168

frontiers | Frontiers in Immunology

TYPE Original Research
PUBLISHED 23 February 2023
DOI 10.3389/fimmu.2023.1125594

OPEN ACCESS

EDITED BY
Soumya R. Mohapatra,
KIIT University, India

REVIEWED BY
Hong Zhou,
Institute of Health Service and Transfusion Medicine, China
Joerg Buescher,
Max Planck Institute of Immunobiology and Epigenetics, Germany

*CORRESPONDENCE
Eva-Maria Wolfschmitt
eva-maria.wolfschmitt@uni-ulm.de
Peter Radermacher
peter.radermacher@uni-ulm.de

SPECIALTY SECTION
This article was submitted to Cancer Immunity and Immunotherapy, a section of the journal Frontiers in Immunology

RECEIVED 16 December 2022
ACCEPTED 13 February 2023
PUBLISHED 23 February 2023

CITATION
Wolfschmitt E-M, Hogg M, Vogt JA, Zink F, Wachter U, Hezel F, Zhang X, Hoffmann A, Gröger M, Hartmann C, Gässler H, Datzmann T, Merz T, Hellmann A, Kranz C, Calzia E, Radermacher P and Messerer DAC (2023) The effect of sodium thiosulfate on immune cell metabolism during porcine hemorrhage and resuscitation.
Front. Immunol. 14:1125594.
doi: 10.3389/fimmu.2023.1125594

The effect of sodium thiosulfate on immune cell metabolism during porcine hemorrhage and resuscitation

Eva-Maria Wolfschmitt[1]*, Melanie Hogg[1], Josef Albert Vogt[1], Fabian Zink[1], Ulrich Wachter[1], Felix Hezel[1], Xiaomin Zhang[1], Andrea Hoffmann[1], Michael Gröger[1], Clair Hartmann[2], Holger Gässler[3], Thomas Datzmann[1,2], Tamara Merz[1], Andreas Hellmann[4], Christine Kranz[4], Enrico Calzia[1], Peter Radermacher[1]* and David Alexander Christian Messerer[1,2,5]

[1]Institute of Anesthesiological Pathophysiology and Process Engineering, University Hospital Ulm, Ulm, Germany, [2]Clinic for Anesthesia and Intensive Care, University Hospital Ulm, Ulm, Germany, [3]Department of Anaesthesiology, Intensive Care Medicine, Emergency Medicine and Pain Therapy, Federal Armed Forces Hospital Ulm, Ulm, Germany, [4]Institute of Analytical and Bioanalytical Chemistry, Ulm University, Ulm, Germany, [5]Department of Transfusion Medicine and Hemostaseology, Friedrich-Alexander University Erlangen-Nuremberg, University Hospital Erlangen, Erlangen, Germany

Introduction: Sodium thiosulfate ($Na_2S_2O_3$), an H_2S releasing agent, was shown to be organ-protective in experimental hemorrhage. Systemic inflammation activates immune cells, which in turn show cell type-specific metabolic plasticity with modifications of mitochondrial respiratory activity. Since H_2S can dose-dependently stimulate or inhibit mitochondrial respiration, we investigated the effect of $Na_2S_2O_3$ on immune cell metabolism in a blinded, randomized, controlled, long-term, porcine model of hemorrhage and resuscitation. For this purpose, we developed a Bayesian sampling-based model for ^{13}C isotope metabolic flux analysis (MFA) utilizing 1,2-$^{13}C_2$-labeled glucose, $^{13}C_6$-labeled glucose, and $^{13}C_5$-labeled glutamine tracers.

Methods: After 3 h of hemorrhage, anesthetized and surgically instrumented swine underwent resuscitation up to a maximum of 68 h. At 2 h of shock, animals randomly received vehicle or $Na_2S_2O_3$ (25 mg/kg/h for 2 h, thereafter 100 mg/kg/h until 24 h after shock). At three time points (prior to shock, 24 h post shock and 64 h post shock) peripheral blood mononuclear cells (PBMCs) and granulocytes were isolated from whole blood, and cells were investigated regarding mitochondrial oxygen consumption (high resolution respirometry), reactive oxygen species production (electron spin resonance) and fluxes within the metabolic network (stable isotope-based MFA).

Results: PBMCs showed significantly higher mitochondrial O_2 uptake and lower $O_2^{\bullet-}$ production in comparison to granulocytes. We found that in response to $Na_2S_2O_3$ administration, PBMCs but not granulocytes had an increased mitochondrial oxygen consumption combined with a transient reduction of the citrate synthase flux and an increase of acetyl-CoA channeled into other compartments, e.g., for lipid biogenesis.

Conclusion: In a porcine model of hemorrhage and resuscitation, $Na_2S_2O_3$ administration led to increased mitochondrial oxygen consumption combined with stimulation of lipid biogenesis in PBMCs. In contrast, granulocytes remained unaffected. Granulocytes, on the other hand, remained unaffected. $O_2^{\bullet-}$ concentration in whole blood remained constant during shock and resuscitation, indicating a sufficient anti-oxidative capacity. Overall, our MFA model seems to be is a promising approach for investigating immunometabolism; especially when combined with complementary methods.

KEYWORDS

hemorrhagic shock, innate immunity, mitochondrial respiration, reactive oxygen species, immunometabolism, metabolic flux analysis, metabolic modeling, hydrogen sulfide

1 Introduction

Treatment with hydrogen sulfide (H_2S) resulted in controversial data in clinically relevant, long-term large animal models of hemorrhage and subsequent resuscitation, inasmuch as unchanged, attenuated and aggravated organ dysfunction were reported (1–5). These divergent findings were at least in part due the fact that depending on the dosing and timing, model and mode of administration, H_2S exerted either anti- (6–10) or pro-inflammatory (11, 12) effects. Moreover, during hemorrhage and subsequent resuscitation, H_2S caused variable effects on whole body energy expenditure (1, 3, 13–15), at least in part as a result of its concentration-dependent effects on mitochondrial respiration (16, 17). However, any H_2S-related effect on energy metabolism may assume particular importance for the inflammatory response, since recent publications have reported on the involvement of H_2S in dysregulation of the immune response by alterations in the immunometabolism, specifically suppression of glycolysis (18); while other sources reported on increased glycolysis and stimulation of lipid biosynthesis from glutamine by carboxylation of α-ketoglutarate (αKG) (19, 20).

Sodium thiosulfate ($Na_2S_2O_3$) is a H_2S-releasing agent (21, 22) that is recognized as an antidote in cyanide poisoning (23) as well as for its mitigation of cisplatin-induced side effects (24). Administration of $Na_2S_2O_3$ exerted organ-protective effects in murine neuronal ischemia reperfusion injury (25, 26), LPS-induced lung injury, and polymicrobial sepsis (27). Beneficial effects of $Na_2S_2O_3$ treatment were attributed to its anti-inflammatory, anti-oxidative and/or hypometabolic characteristics (26–28). In this context, the potential effects of $Na_2S_2O_3$ on metabolism and mitochondrial respiration are poorly understood.

Furthermore, the cellular metabolic network has a crucial impact on inflammation and immune function: Systemic inflammation activates immune cells, which in turn show cell type-specific metabolic plasticity with modifications of mitochondrial respiratory activity. These metabolic changes were demonstrated to not only impact, but determine immune cell function (29–32). Many innate immune cells, like granulocytes, heavily rely on glycolysis and consume little oxygen. This is further enhanced upon activation, when these cells engage in glycolysis despite sufficient availability of oxygen, a phenomenon termed Warburg effect initially observed in cancer cells (32, 33). In addition to increasing the glycolytic rate, granulocytes also increase their activity through the pentose phosphate pathway (PPP), regenerating nicotinamide adenine dinucleotide phosphate (NADPH) in the process, an important cofactor for the NADPH oxidase. This enzymatic complex is a major source of the anti-microbial reactive oxygen species (ROS) superoxide ($O_2^{\bullet-}$) and, therefore, hydrogen peroxide (H_2O_2), which play a crucial role in innate immune defense (33, 34). In contrast, resting lymphocytes show lower rates of glycolysis and primarily rely on oxidizing glucose-derived pyruvate in the tricarboxylic acid (TCA) cycle, while generating $O_2^{\bullet-}$ radicals as a byproduct of oxidative phosphorylation (OXPHOS) (32, 35). After activation, higher ATP demand is met by an increase in the rate of glycolysis, while fatty acid oxidation is repressed to guarantee the supply of substrates for membrane synthesis (33, 36). These mechanisms of metabolic adaptation to inflammatory stress provide a complex and highly plastic network that is distinct for each cell type (37).

Tracing individual molecules through metabolic pathways is an ongoing challenge. We have developed a model for ^{13}C-based

metabolic flux analysis (MFA) that utilizes glucose and glutamine tracers to be able to investigate the effect a factor might have on immunometabolism. Incubating cells with stable, non-radioactive isotope-labeled nutrients yields ^{13}C labeling patterns on important metabolites which can be detected by gas chromatography/mass spectrometry (GC/MS) (38–40).

Concerning MFA, one of the most frequent strategies is to analyze labeling patterns of metabolites and deduce relative pathway utilization (39, 41). When going further and transforming these labeling patterns into fluxes, it is paramount to assess precision and accuracy. Bayesian analysis is one of the most straight forward and reliable ways to analyze error propagation and receive accurately assessed error bounds of calculated fluxes (42). We therefore propose our sampling-based model as a suitable method for estimating fluxes within the metabolic network. A preliminary version of this model has already been applied to study the effects of glucocorticoids on macrophage metabolism (43) and, in a more rudimentary form, to investigate the effect of acute subdural hematoma-induced brain injury on peripheral blood mononuclear cell (PBMC) metabolism (44).

To the best of our knowledge, data is scarce for metabolic flux during hemorrhagic shock in general and especially for interventions potentially affecting metabolism and mitochondria, such as the administration of $Na_2S_2O_3$ and/or H_2S. Therefore, we applied our novel MFA method to isolated circulating immune cells and tested whether $Na_2S_2O_3$ has an impact on the metabolism of innate immunity during experimental hemorrhage and subsequent resuscitation.

2 Materials and methods

2.1 Animal procedures

The reported data utilized material obtained during a recently published study investigating the effect of $Na_2S_2O_3$ in a long-term porcine model of hemorrhage (5). Experiments were conducted according to the National Institutes of Health Guidelines on the Use of Laboratory Animals and the European Union 'Directive 2010/63 EU on the protection of animals used for scientific purposes' after approval by the University of Ulm Animal Care Committee and the Federal Authorities for Animal Research (Regierungspräsidium Tübingen, Germany, Reg.-Nr. 1341, date of approval 02.05.2017). A total of 17 adult Bretoncelles-Meishan-Willebrand (BMW) pigs of both sexes (7 castrated males, 10 females) with a median weight of 62 kg (interquartile range (IQR) 56;67) and a median age of 15 months (IQR 13;16) were included in this study. The STS group included 4/5 male-castrated/female pigs and the vehicle control group consisted of 3/5 male-castrated/female animals. The BMW strain is characterized by a decreased activity of the von Willebrand factor resulting in a coagulatory state similar to that of human blood (45, 46).

2.2 Anesthesia and surgery

Anesthesia and surgical instrumentation are described in detail in Messerer et al.; analyzing the impact of $Na_2S_2O_3$ on organ damage within the same cohort (5). Briefly, animals were randomly assigned to a control (n = 8) or $Na_2S_2O_3$-treatment group (n = 9), and the staff performing the experiment was blinded to the group assignment. Hemorrhagic shock was induced by passive removal of the blood with a titration of mean arterial blood pressure (MAP) to 40 ± 5 mmHg. After 3 h of hemorrhage, swine underwent resuscitation up to a maximum of 68 h, while noradrenaline was continuously administered intravenously to restore the MAP to pre-shock levels. At 2 h of shock, animals received either vehicle (NaCl 0.9%) or $Na_2S_2O_3$ (25 mg/kg/h for 2 h, thereafter 100 mg/kg/h until 24 h after shock, Dr. Franz Köhler Chemie GmbH, Bensheim, Germany) according to their group assignment. The choice of dose and time of administration is explained in detail in Messerer et al. (47). Briefly, it was performed in accordance with previous studies as well as established concentrations for treatment of cyanide poisoning (23, 47, 48).

2.3 Cell isolation from whole blood

Blood was drawn after the induction of anesthesia and a subsequent stabilization period (T1) as well as 24 h (T2) and 64 h (T3) after shock induction (Figure 1). 14 lithium-heparin (LiHep) monovettes with a volume of 9 mL each (Sarstedt, Nümbrecht, Germany) were used to collect approximately 120 mL of arterial whole blood each time point. After 1:1 dilution with PBS (without $CaCl_2$, $MgCl_2$), the drawn blood was layered onto a two density gradient solutions (9 mL 1.119 and 8 mL 1.088 g/mL solution, Pancoll, PAN Biotech, Aidenbach, Germany). Centrifugation at 764 g without break at room temperature (RT) for 20 min resulted in a PBMC top layer and a bottom layer containing red blood cells (RBCs) and granulocytes. The cells were resuspended in water for short-time osmotic lysis to remove residual RBCs before stopping the reaction with 10 × PBS to avoid lysis of leukocytes. Osmotic lysis was applied to PBMCs only once, while three procedures were required for granulocytes due to the high fraction of RBCs in the bottom layer. After removal of all RBC contamination, cells were washed once with 1 × PBS and subsequently counted in a Neubauer counting chamber. On average, isolated cells could be used for experiments 2 – 3 h after blood withdrawal was firstly initiated.

2.4 High resolution respirometry

Mitochondrial respiration was measured by high-resolution respirometry using the Oroboros® Oxygraph-2K (Oroboros Instruments, Innsbruck, Austria). This device allows for simultaneous recording of the O_2 concentration in two parallel

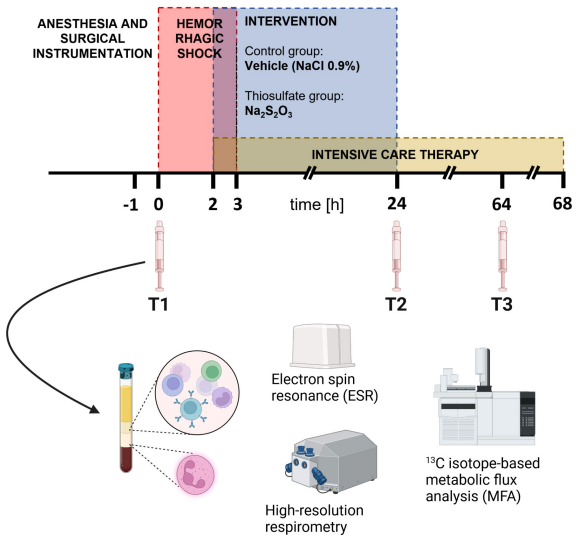

FIGURE 1
Experimental setup. In the red period, pigs were subjected to hemorrhagic shock. After 3 h of shock, animals underwent resuscitation up to a maximum of 68 h. In accordance with their group assignment, they received either $Na_2S_2O_3$ (n = 9, 25 mg/kg/h for 2 h, thereafter 100 mg/kg/h until 24 h after shock) or vehicle (n = 8, NaCl 0.9%) during the blue-marked period. The Figure is adapted from (5).

chambers calibrated for 2 mL of mitochondrial respiration medium MiR05 (49). This medium contains 110 mM D-sucrose (Sigma Aldrich, St. Louis, MO, USA), 60 mM K-lactobionate (Sigma Aldrich, St. Louis, MO, USA), 0.5 mM ethylene glycol tetra acetic acid (Sigma Aldrich, St. Louis, MO, USA), 1 g/L bovine serum albumin free from essential fatty acids (Sigma Aldrich, St. Louis, MO, USA), 3 mM $MgCl_2$ (Scharlau, Hamburg, Germany), 20 mM taurine (Sigma Aldrich, St. Louis, MO, USA), 10 mM KH_2PO_4 (Merck, Darmstadt, Germany), 20 mM HEPES (Sigma Aldrich, St. Louis, MO, USA), adjusted to pH 7.1 with KOH and equilibrated with 21% O_2 at 37°C. Directly after cell isolation, 10×10^6 PBMCs/granulocytes suspended in MiR05 were filled into a chamber and stirred at 750 rpm. Sealing the chambers of the device according to the manufacturers protocol started the continuous recording of mitochondrial respiration. Quantification of the oxygen flux (JO_2) was based on the rate of change in the O_2 concentration in the chambers and normalized for the cell number. Once the chambers were sealed, specific analysis of mitochondrial respiratory function was achieved by sequential injections of substrates and inhibitors into the respiration medium. Firstly, routine respiration was recorded once a stable JO_2-value was achieved after closing the chambers. Subsequently, 2.5 µM oligomycin was injected to block the ATP-synthase. This yielded the LEAK-state, which represents the respiratory activity required to maintain a stable membrane potential in absence of ATP-turnover. The titration of carbonyl cyanide p-(trifluoromethoxy)-phenylhydrazone (FCCP) in 1 µM steps allowed to achieve the maximum respiratory activity in the uncoupled state (ETS-state). The ETS state corresponds to state 3 as defined in Chance and Williams et al. (50) and is neither limited by substrate availability, cell energy demand, nucleotide availability or ATP synthase activity. Finally, 0.5 µM rotenone + 5 µM antimycin were added to block complex I and III respectively, yielding the residual (non-mitochondrial) oxygen consumption.

2.5 Quantification of reactive oxygen species

$O_2^{\bullet -}$ concentration in whole blood was determined immediately after blood removal. 25 µL of whole blood were mixed with an aliquot of 25 µL freshly thawed CMH (1-Hydroxy-3-methoxycarbonyl-2,2,5,5-tetramethylpyrrolidine) spin probe solution. The CMH solution contained 400 µM CMH spin probe, 25 µM deferoxamine, and 5 µM diethyldithiocarbamate to chelate transition metal ions in Krebs-HEPES-Buffer (KHB) (Noxygen, Elzach, Germany). After mixing whole blood with CMH spin probe solution, it was transferred to a 50 µL glass capillary, sealed, and measured with an EMXnano electron spin resonance (ESR) spectrometer (Bruker, Billerica, MA, USA) after 5 min incubation at 37°C (Bio-III, Noxygen, Elzach, Germany). The device settings are detailed in the Supplements. Radical concentration was quantified by comparison with a series of CP° (3-Carboxy-2,2,5,5-tetramethyl-1-pyrrolidinyloxy) radical standards solved in KHB. As a blank sample, KHB added to the respective amount of CMH spin probe solution was measured and subtracted from the sample value.

For determination of radical production by immune cells, 25 µL of a cell suspension containing 2.5×10^6 cells/mL RPMI 1640 medium (Glucose 1.8 mg/mL, Glutamine 0.6 mg/mL, $NaHCO_3$ 100 µg/mL) were mixed with 25 µL of CMH spin probe solution. In contrast to whole blood, cell samples were measured over a 30 min interval to calculate the radical production rate. A sample of RPMI 1640 medium mixed 1:1 with CMH spin probe solution was used as a blank value for measuring cell suspensions and subtracted from sample values. Data were evaluated with the Xenon_nano software (version 1.3; Bruker BioSpin GmbH, Rheinstetten, Germany) and Microsoft Excel. Results regarding ROS determination by ESR were included in a dissertation by one of our co-authors (51). Additionally, the extracellular H_2O_2 concentration was determined in a suspension of 1×10^6 PBMCs/granulocytes in 100 µL PBS after 30 min at RT. A three-electrode setup that has been previously thoroughly described was used for this purpose (52). The determination of the H_2O_2 concentration was not performed for each animal due to limited availability of the measurement device.

2.6 Stable isotope incubation and detection of metabolites

For investigating nutrient utilization of cells, we incubated three times 5×10^6 freshly isolated cells in parallel in 1 mL RPMI containing one of the following tracers: 1,2-$^{13}C_2$-labeled glucose, $^{13}C_6$-labeled glucose, and $^{13}C_5$-labeled glutamine (Cambridge Isotope Laboratories, Andover, MA, USA). Concentrations are specified in the Table S3 in the Supplements. The pH of the medium was adjusted to 7.4 before experimentation through

addition of 1M HCl or NaOH. After incubation at 37°C for 2 h, cells were spun down and 850 µL of the supernatant was transferred to a crimp neck glass vial. The vial was frozen upside down at −20°C for later GC/MS analysis of $^{13}CO_2$ production and lactate released into the medium. The cell pellet was washed once with PBS and subsequently stored at −80°C after removal of all liquid. For MFA analysis, we required both the supernatant ($^{13}CO_2$ production; mass isotopomer distributions (MIDs) of secreted lactate) and the cell pellet (MIDs of the selected metabolites lactate, glutamate, and aspartate). Samples were stored for 1 – 2 months until analysis.

The cumulative cellular $^{13}CO_2$ production was estimated by enrichment analysis from the spiked amount of CO_2 released from $NaHCO_3$ in the supernatant (Table S1). The frozen supernatant was thawed, and 25 µL 1 M HCl were injected through the septum into the liquid to drive out CO_2 into the gaseous phase. For each vial, 10 replicates of 5 µL headspace gas each were injected into the GC/MS system (Agilent 6890 GC/5975B MSD, Agilent Technologies, Waldbronn, Germany) while analyzing the m/z of 44 and 45; corresponding to unlabeled and labeled CO_2, respectively. The average ratio of $^{13}CO_2/^{12}CO_2$ amounted to 0.56% with an average standard error of 2% of the nominal value.

After $^{13}CO_2$ detection from the supernatant, we analyzed lactate secretion into the medium. Determination was performed by taking two aliquots of 100 µL supernatant and adding 500 µL acetonitrile. Samples were centrifuged at RT (13000 rpm for 5 min) and afterwards decanted into vials suited for derivatization. After drying in a Savant2010 SPD 2010 SpeedVac concentrator (Thermo Scientific, Waltham, MA, USA) (45°C, 14 mTorr) for about 50 min, derivatization was initiated with 100 µL acetonitrile and 25 µL N-(tert-butyldimethylsilyl)-N-methyltrifluoroacetamide (MTBSTFA). Samples were incubated at 80°C for 1 h with the lid closed and afterwards transferred into GC/MS vials. One of the initial 100 µL samples was incubated with 1 µg of internal standard (IS, corresponding to 20 µL of 50 µg/mL $^{13}C_3$ sodiumlactate solution) for 10 min beforehand to serve for quantification. A variety of essential calibration samples were prepared in replicates: 0.1 µg/0.2 µg/0.5 µg/0.75 µg/1 µg of lactate with an additional 1 µg of IS each, 1 µg of IS only, blank RPMI, and RPMI with 1 µg of IS. Details of calibration and quantification are specified in the Supplements.

For metabolite extraction from the cell pellet, 100 µL cold H_2O was added to the frozen pellets. The mixture was vortexed and sonicated for 10 min. Subsequently, 500 µl acetonitrile was added and the samples were centrifuged for 5 min at 13000 rpm. All samples were decanted into vials and dried for derivatization. Steps of derivatization follow those of lactate determined from medium. Standard mixes with 0.1 µg/0.2 µg/0.5 µg/0.75 µg/1 µg of analytes were prepared as control: the first with the respective amounts of lactate; the second with aspartate, glutamine, and glutamate.

For GC/MS detection, we used selected ion monitoring for optimal signal to noise ratios. Details of device settings and m/z of measured TBDMS derivatives are specified in the Supplements. Peak area integration was performed with our in-house program and MIDs were converted into carbon mass distributions (CMD) with a correction matrix approach (53, 54). MIDs were corrected for all isotopic interferences except for the natural ^{13}C abundance, which is included in our CMDs.

2.7 Metabolic flux analysis

For MFA, we established a combined model for glycolysis, the PPP and TCA cycle, which has been previously described and utilized in Stifel et al. (43). It predicts ^{13}C mass distributions on metabolites based on flow rates of the metabolic system by utilizing the EMU concept (40, 55–57) and was implemented in RStan [R interface to Stan, a tool for Bayesian analysis (58)]. Comparing predictions for ^{13}C mass distributions with the corresponding GC/MS measurements (section 2.6) using sampling-based Bayesian statistics allowed for identifying suitable fluxes within the network. It further estimated how the precision in measurements affects the precision of estimated fluxes, including standard deviations and confidence intervals. Conveniently, unidentifiable fluxes can be recognized by wide confidence ranges.

Our PPP estimation is built on the same method as the one used by Lee, Katz, and Rognstad (59, 60) that is based on the assumption that PPP utilization can be represented as a shift in the label ('carbon scrambling') of the top carbon atoms of PPP metabolites. For this approach, usually only the m+1/m+2 ratio on lactate would be used as a proxy for triose labeling using a 1,2-$^{13}C_2$-labeled glucose input, but we expanded the method so that the complete CMD of the full metabolite as well as the CMD of the lactate fragment across carbon 2 and 3 were taken into account. The model firstly estimated relative fluxes from GC/MS measurements and subsequently utilized $^{13}CO_2$ production and the secretion of lactate into the medium to transform these relative fluxes into absolute values. The parallel tracer setup of 1,2-$^{13}C_2$-labeled glucose, $^{13}C_6$-labeled glucose, and $^{13}C_5$-labeled glutamine enabled improved flux determination, as the estimated fluxes must apply to sets of measurements obtained from each tracer. The details of the metabolic model are available in the Supplements.

2.8 Statistical analysis

17 BMW pigs were included in this study. Animals were randomly assigned to a control vehicle (n = 8) or $Na_2S_2O_3$-treatment group (n = 9). Data are presented as median with IQR and the number of animals that could be included in the corresponding analyses are indicated in the respective figure legends. Missing values at later time points indicate animals with premature experiment termination in accordance with a list of predetermined criteria (5). Statistical and graphical presentation was performed with GraphPad Prism 9, version 9.4.1 (GraphPad Software Inc., La Jolla, CA, USA). Experimental data was considered to be non-parametric due to small sample sizes. We

conducted the comparison between groups with Mann-Whitney U tests, while the effect of time within one group was analyzed with the Kruskal-Wallis rank sum test and a *post hoc* Dunn's multiple comparisons test. Figure 1 uses templates provided by www.biorender.com.

3 Results

In general, the administration of $Na_2S_2O_3$ neither altered survival nor dramatically impacted cardiocirculatory parameters, biomarkers of organ damage, or inflammatory markers; as previously published in detail in Messerer et al. (5).

3.1 $Na_2S_2O_3$ administration significantly increased mitochondrial oxygen consumption in PBMCs but not in granulocytes

To determine mitochondrial oxygen consumption, we evaluated routine respiration and ETS capacity; the former describing baseline respiration and the latter representing the maximum capacity of the mitochondria independent of factors like substrate availability, oxygen availability, ATP synthase activity and cell energy demand (50). Since the respective treatment was initiated at 2 h of shock, variances in groups caused by differential treatment should become apparent at the T2 (24 h after shock) or T3 (64 h after shock) time points, while baseline T1 was expected to be comparable (Figure 1). Both routine and ETS mitochondrial oxygen consumption increased over the course of the experiment for PBMCs and granulocytes (Figure 2). Generally, PBMCs demonstrated higher respiration than granulocytes. Interestingly, $Na_2S_2O_3$-treated PBMCs showed a significantly higher oxygen consumption compared to the vehicle-treated cells at T2, which was not present in granulocytes. By T3, this intergroup difference disappeared.

3.2 Whole blood radicals and immune cell ROS production did not significantly differ between groups

The capability to generate ROS was uncompromised, as determined by ESR spectroscopy, the gold standard for radical measurements. As depicted in Figure 3, differences in production of $O_2^{\bullet-}$ of both cell types as well as $O_2^{\bullet-}$ levels in whole blood were non-significant between both groups at all times of measurement. When it comes to Regarding cell type specific effects, granulocytes demonstrated higher superoxide production levels than PBMCs. PBMCs slightly increased $O_2^{\bullet-}$ production over the course of the experiment, while granulocytes displayed significantly higher production levels at T2, which returned to baseline at the end of the experiment (Figure 3B). To further confirm the findings obtained by ESR, we determined H_2O_2 produced by PBMCs or granulocytes electrochemically and found it mirroring the ESR-measured pattern despite utilizing completely different means of detection and measuring different oxidative agents (Figure 3C). However, only few samples could be analyzed for their H_2O_2 concentration, making it difficult to obtain reliable statistical informative values.

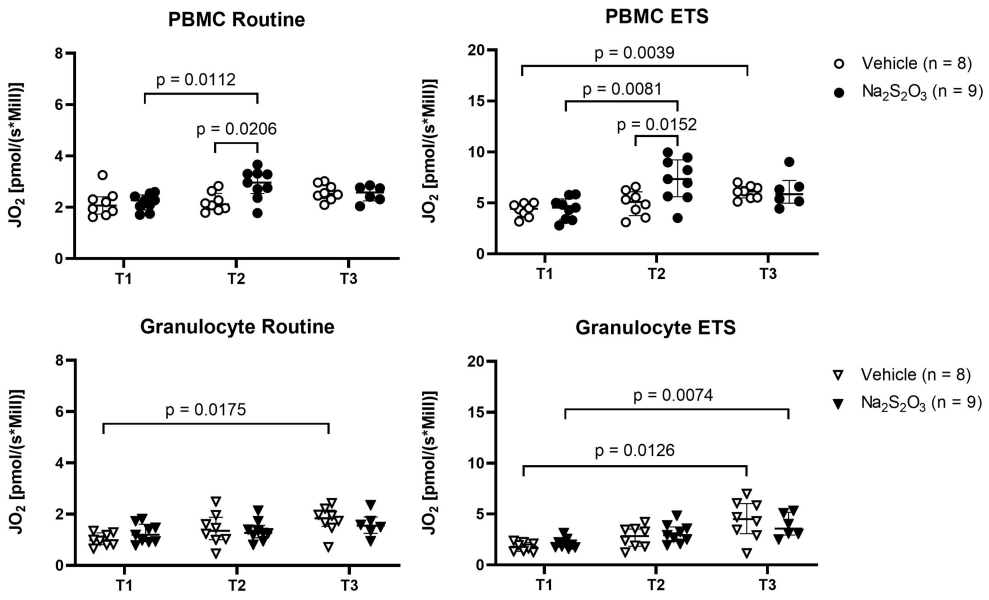

FIGURE 2
Mitochondrial oxygen consumption of PBMCs and granulocytes. JO_2 was measured as baseline (routine) respiration and ETS with high resolution respirometry at indicated time points at the time points T1 (before shock), T2 (24 h post shock) and T3 (64 h post shock). Individual data of vehicle-treated animals are indicated as bright symbols; $Na_2S_2O_3$-treated animals as dark ones. PBMCs are displayed as circles and granulocytes as triangles. Significant p values are presented in the graphs; Mann-Whitney U test for intergroup differences, Kruskal-Wallis rank sum test for time-related effects. Data are presented as median with IQR.

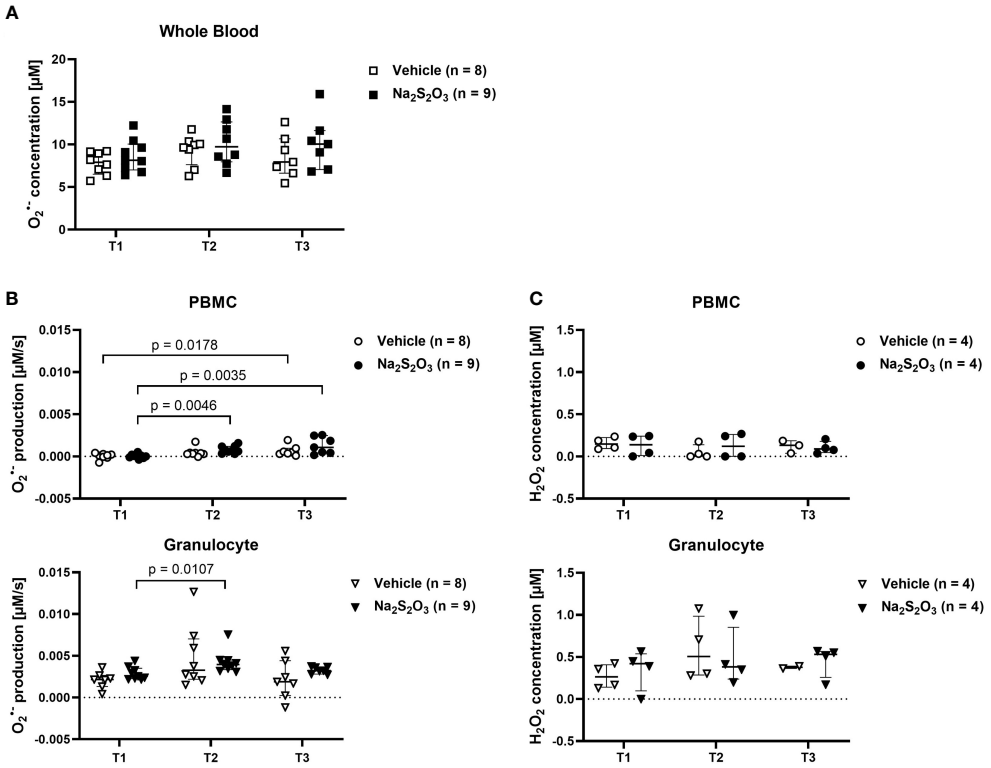

FIGURE 3
Radical production in PBMCs and granulocytes. ROS measured by ESR or electrochemical detection at the indicated time points at the time points T1 (before shock), T2 (24 h post shock) and T3 (64 h post shock). Vehicle-treated animals are indicated as bright symbols; $Na_2S_2O_3$-treated animals as dark ones. PBMCs are displayed as circles and granulocytes as triangles. **(A)** $O_2^{\bullet-}$ radical concentration in whole blood quantified by ESR. **(B)** $O_2^{\bullet-}$ radical production in PBMCs and granulocytes quantified by ESR. **(C)** H_2O_2 concentration in PBMCs and granulocytes quantified by electrochemical detection after incubation at RT for 30 min. Significant p values are presented in the graphs; Mann-Whitney U test for intergroup differences, Kruskal-Wallis rank sum test for time-related effects. Data are presented as median with IQR.

3.3 $Na_2S_2O_3$ administration led to a cell type-specific transient reduction of the flow mediated by the citrate synthase flux with an interlinked increase in mitochondrial oxygen consumption

We analyzed immune cell metabolism with a model formulated in RStan (visualized in Figure 4A). Our ^{13}C-based MFA method managed to successfully reproduce textbook knowledge regarding cell type specific preferences in metabolism such as granulocytes displaying higher glycolytic rates while PBMCs rather utilized the TCA cycle (Figure 4B) (32, 61, 62). Moreover, PBMCs displayed much higher glutamate metabolism (F8) in comparison to granulocytes: about 40 – 50% (Median 0.44; IQR 0.39; 0.48) of the main TCA cycle flux F3 originated from glutamine *via* glutamate in PBMCs, while it only added up to 13% for granulocytes (IQR 0.11; 0.19).

Although the glutamate input also slightly increased with shock progression for granulocytes, it only reached 22% at its highest at T3. PPP utilization was similar for both cell subsets, however, granulocytes showed completely divergent PPP utilization at the last measurement time point. So far, we could not find correlations with other parameters that could explain the two extremes.

Generally, cell metabolism reacted similarly in response to the intensive care treatment, inasmuch almost all fluxes gradually increased from T1 to T3 (Figure 4B). These changes were significant for PMBCs, while granulocytes only demonstrated a slight trend. The only notable exception were TCA cycle fluxes, which remained mostly constant, and PBMCs from $Na_2S_2O_3$-treated animals, where citrate synthesis significantly decreased at T2 (Figure 5A).

When it comes to the effect of $Na_2S_2O_3$ on immunometabolism, it seems like neither glycolytic nor PPP or TCA cycle fluxes of granulocytes were impacted by its administration (Figure 4B). While PBMCs also failed to show intergroup differences regarding glycolytic and PPP metabolism, there was a notable and significant difference in F4, the flux from oxaloacetate (OAA) over citrate to α-ketoglutarate, pertaining to the change over the course of the experiment (Figure 5A): $Na_2S_2O_3$-treated PBMCs significantly decreased their F4 flux from T1 to T2, while this was not the case for vehicle-treated PBMCs. Intriguingly, this difference in F4 between measurement time points highly correlated with the intergroup differences observed in routine respiration ($R^2 = 0.8425$, $p < 0.0001$). This negative linear regression was neither present in the control group nor in granulocytes. PBMCs from $Na_2S_2O_3$-treated animals further displayed a significantly increased loss in acetyl-CoA, representing the amount of acetyl-CoA exiting the described subsystems of Figure 4A, compared to vehicle-treated ones at T2 (Figure 5B). As an indicator of potential reductive

10.3389/fimmu.2023.1125594

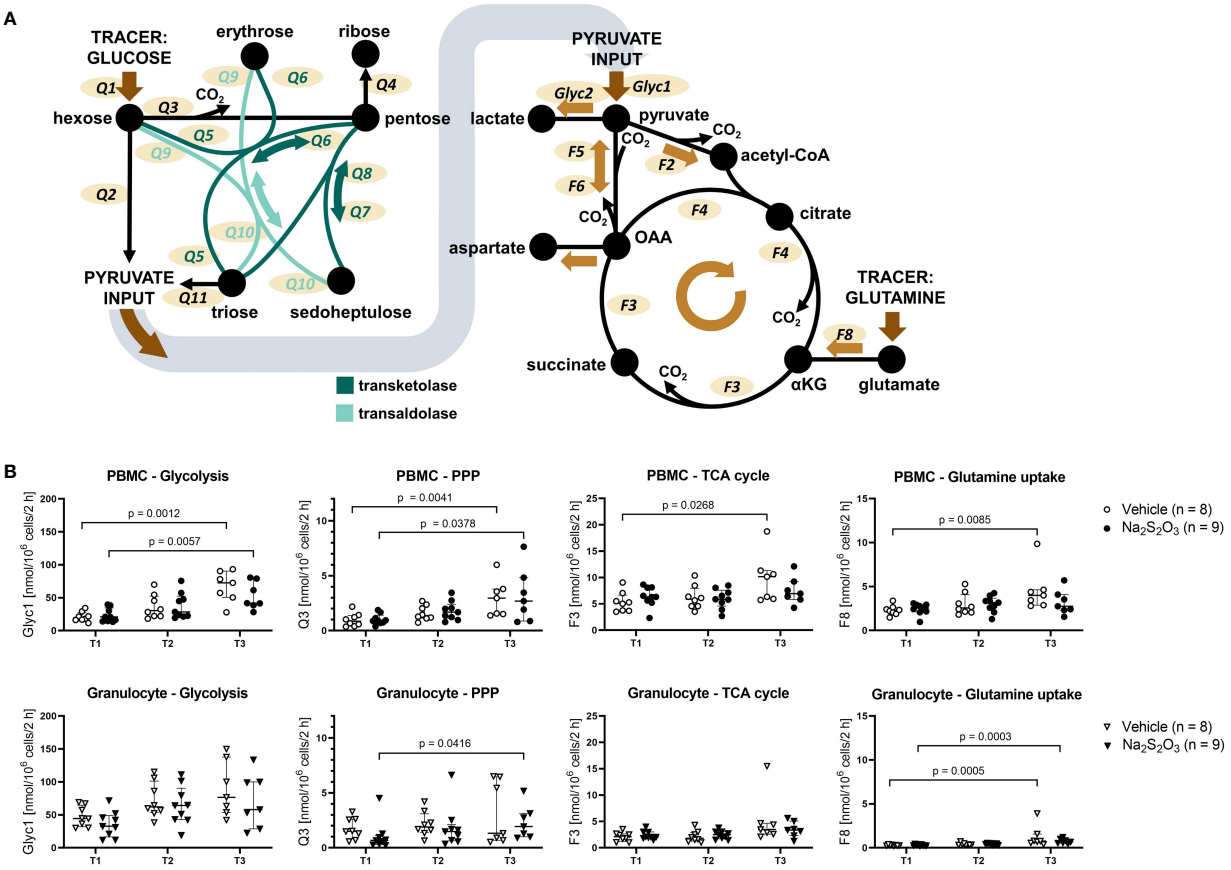

FIGURE 4
Metabolic fluxes of porcine immune cells calculated from ^{13}C labeling patterns on metabolites. **(A)** Visualization of the model used for Bayesian sampling. Left: PPP model. Right: TCA cycle model. Glyc: glycolytic flux. Q: flux within the PPP. F: flux within the TCA cycle. **(B)** Glycolytic, PPP and TCA cycle fluxes of PBMCs and granulocytes. Animals were treated either with vehicle (n = 8, bright symbols) or $Na_2S_2O_3$ (n = 9, dark symbols). αKG: α-ketoglutarate, OAA: oxaloacetate. Significant p values are indicated in the graphs; Mann-Whitney U test for intergroup differences, Kruskal-Wallis rank sum test for time-related effects. Data are presented as median with IQR.

carboxylation, we compared the m+3 ^{13}C label on the complete aspartate fragment between vehicle and $Na_2S_2O_3$-treated animals at T2. There was no difference between groups (Vehicle: 1.94%, $Na_2S_2O_3$: 1.78%; p = 0.2925), implying that the higher amount of acetyl-CoA loss was not coupled to reductive carboxylation. The change in acetyl-CoA loss, like the change in mitochondrial oxygen consumption, correlated with the change in F4 (Figure 5B).

4 Discussion

We investigated the effect of $Na_2S_2O_3$ on the metabolism of circulating immune cells in a porcine model of hemorrhage and resuscitation over a period of max 68 h. The main findings included that $Na_2S_2O_3$ administration for a 24 h period i) did not impact granulocyte metabolism or ROS production, while ii) it increased the mitochondrial oxygen consumption of PBMCs at the end of the administration period. Furthermore, iii) in PBMCs there was a transient reduction of the citrate synthase flux, which significantly correlated with the increase in mitochondrial oxygen consumption and acetyl-CoA exiting the TCA cycle network, potentially to be utilized in lipid biogenesis.

$Na_2S_2O_3$ administration had displayed organ-protective and anti-inflammatory effects in previous studies. Through inhibition of caspase 3, $Na_2S_2O_3$ administration initiated anti-apoptotic effects by attenuation of cerebral ischemia (25, 63) and reduction of myocardial ischemia reperfusion injury in rats (26). The latter study also demonstrated mitochondrial preservation through $Na_2S_2O_3$ by opening ATP-sensitive potassium channels (KATP) channels as well as preserving activity of various mitochondrial enzymes, proteins and functions involved in ROS homeostasis (26). The most prominent were NADH dehydrogenase, the major contributor to electron transport chain complex I activity and one of the main producer of the $O_2^{\bullet -}$ radical, the malate aspartate shuttle which provides NADH for complex I, as well as peroxisome proliferator-activated receptor γ coactivator 1α (PGC-1α), which is an important anti-oxidant factor in ROS detoxification (26, 64).

As $Na_2S_2O_3$ is an approved drug and is considered for potential intervention during shock, we investigated its impact on the immune response. When applying our novel MFA model, we reproduced known cell-specific preferences of metabolic pathways: The overall lower mitochondrial oxygen consumption (routine and ETS respiration) of granulocytes in comparison to PBMCs maps with their characteristic preference of glycolytic

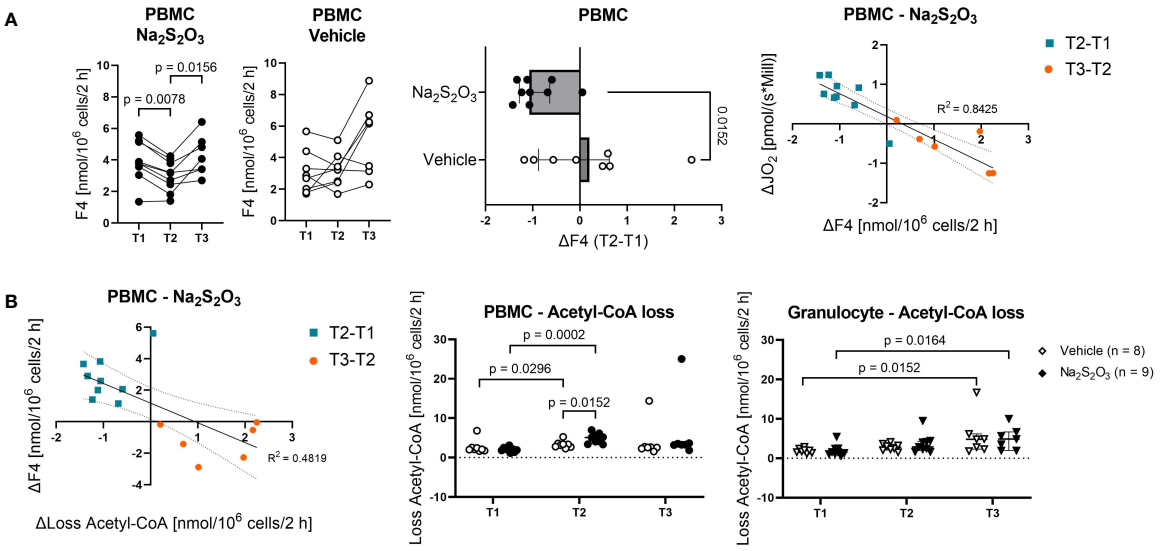

FIGURE 5
The effect of $Na_2S_2O_3$ on porcine PBMCs. Metabolic fluxes calculated from ^{13}C labeling patterns on metabolites. PBMCs are displayed as circles and granulocytes as triangles. Animals were treated either with vehicle (n = 8, bright symbols) or $Na_2S_2O_3$ (n = 9, dark symbols). **(A)** F4 trends in PBMCs in vehicle vs $Na_2S_2O_3$-treated animals and correlations between the difference in F4 and the difference in routine respiration over time. **(B)** Acetyl-CoA loss of PBMCs and granulocytes. Correlation between the difference in F4 and the difference in Acetyl-CoA loss over time. Significant P values are indicated in the graphs; Mann-Whitney U test for intergroup differences, Kruskal-Wallis rank sum test for time-related effects. Data are presented as median with IQR. Correlations are presented with 95% confidence intervals.

pathways which only require baseline TCA cycle activity and minimal glutamine uptake (32, 37). These findings were confirmed with MFA, where we found that the flux patterns follow this exact pattern. Interestingly, there was no significant difference in PPP utilization between granulocytes and PBMCs. However, it should be noted that due to us not detecting metabolites directly involved in the PPP, the margin of error for these fluxes is much higher as estimations are only based on ^{13}C isotope patterns on lactate.

In terms of metabolic changes in response to shock and resuscitation, mitochondrial oxygen consumption significantly increased in both PBMCs and granulocytes, potentially due to immune activation and higher energy expenditure (32). Interestingly, whole blood ROS concentration reacted neither to $Na_2S_2O_3$ administration, shock initiation, retransfusion, nor noradrenalin administration, which stands in contrast to literature observing an increase in oxidative activity; mainly due to ischemia reperfusion injury (65, 66). This might indicate that the anti-oxidative capacity of whole blood is too high to reflect small scale fluctuations in radical concentration and that the increase in radical concentration is mainly localized at the site of ischemic tissue.

In our experiments, $Na_2S_2O_3$ administration impacted neither whole blood radical concentration nor immune cell superoxide production. Intriguingly, there was also no effect on glycolysis, thus posing a contrast to current findings of other groups (18, 19). These divergent findings might be due to us utilizing a porcine ex-vivo model, as Rahman et al. (18) worked with cystathionine-γ-lyase $(CSE)^{-/-}$ mice and Carballal et al. (19) *in vitro*. However, we did observe an effect pertaining to PBMC metabolism at the end of the administration period: Cells obtained from $Na_2S_2O_3$-treated animals had increased oxygen consumption as well a transient reduction of the citrate synthase flux. This raises the question about the impact of $Na_2S_2O_3$ on mitochondria. H_2S, which can be released by $Na_2S_2O_3$ especially under hypoxic conditions, characteristically demonstrates concentration-dependent effects (17). Originally, H_2S was mainly known for its cytotoxic properties by inhibition of cytochrome c oxidase (complex IV) (67), resulting in suppressed mitochondrial electron transport. However, after being recognized as the third gasotransmitter, a variety of beneficial effects have been reported (16, 17). At low concentrations, H_2S stimulates mitochondria by acting as an electron donor with an effect comparable to that of NADH or $FADH_2$ (17, 68, 69). Consequently, H_2S can contribute to energetic homeostasis under conditions of impaired oxygen supply and attenuate damage due to hypoxia. Our results of increased oxygen consumption seem to support this notion. However, it is important to keep in mind that an increased oxygen consumption does not equal increased mitochondrial activity but could simply indicate a change in ATP/O_2 ratio, e.g., less 'effective' ATP generation. Furthermore, it has been reported that H_2S is mainly metabolized in a process of mitochondrial detoxification (70).

The $Na_2S_2O_3$-induced transient reduction in the citrate synthase flux observed over the course of the experiment in the citrate synthase flux observed in PBMCs correlated with the increase correlated with the increase in both the oxygen consumption and the acetyl-CoA exiting the TCA cycle network. These findings support the notion that $Na_2S_2O_3$ administration might contribute to lipogenesis in some circulating immune cell subsets. H_2S-stimulated lipid synthesis from glutamine is a well-

documented effect in cell culture and algae, which is characterized by acetyl-CoA generation through citrate (19, 71). To investigate whether the acetyl-CoA lost for lipid biogenesis or similar mechanisms has a glucose or a glutamine origin, we compared the $^{13}C_5$-glutamine tracer-induced m+3 label on aspartate, which Zhang et al. (72) and Alkan et al. (73) reported to be indicative of reductive glutamine catabolism. While our experiment produced a significantly higher label in PBMCs than in granulocytes, there was no difference between cells originating from vehicle and $Na_2S_2O_3$-treated animals, which speaks against the putative increase in lipogenesis being an effect induced by reductive carboxylation and rather suggests a glucose origin.

Since we utilized $Na_2S_2O_3$ as an intervention, the question arises whether $Na_2S_2O_3$ itself or $Na_2S_2O_3$-released H_2S is the acting agent in the alteration of immunometabolism. As we focused on the effect on circulating immune cells and the blood pO_2 was always maintained within normoxemic levels, it is likely that only minor amounts of H_2S were released. Overall, however, the dose and route of administration of $Na_2S_2O_3$ used in this study seemed to be appropriate for maintaining immune cell integrity, as the increase in mitochondrial oxygen consumption mirrored stimulating effects observed in other groups (16, 17, 19), and no further deleterious effect could be detected.

4.1 Limitations of the study

As we used density gradient centrifugation to isolate immune cells, it became increasingly difficult to obtain pure PBMC populations at later time points. Low density granulocytes are a population of granulocytes found in the PBMC layer of density gradients and tend to increase in number upon inflammation and, consequently, shock and resuscitation (74, 75). As they are metabolically not particularly well defined, this fraction within the PBMC population could potentially distort results at the later time points of blood withdrawal. Moreover, as PBMCs are not a metabolically uniform population, changes in one subpopulation might be masked by others. With our MFA routine, only conclusions about the whole population but not of their subsets can be drawn. Another factor to consider is potential immune cell activation during cell purification.

4.2 Conclusion

In summary, our novel MFA model is a suitable tool for detecting small scale metabolic alterations in immune cells. Further studies with more homogenic populations could elucidate which PBMC subset precisely is responsible for the treatment-induced metabolic effect.

Data availability statement

The raw data supporting the conclusions of this article will be made available by the authors, without undue reservation.

Ethics statement

The animal study was reviewed and approved by Federal Authorities for Animal Research, Regierungspräsidium Tübingen, Germany, Reg.-Nr. 1341, date of approval 02.05.2017.

Author contributions

Study design/planning: PR, DM, EC, CK, CH, JV, UW, TM. Data acquisition: E-MW, FZ, FH, XZ, MH, DM, AHo, MG, UW, JV, HG, AHe, CK, EC, PR, TD. Data analysis: E-MW, FZ, XZ, MH, JV, DM. Writing paper: E-MW, PR, DM. Revising paper: all authors.

Funding

The presented study was supported by the Deutsche Forschungsgemeinschaft (DFG, German Research Foundation, project 251293561 – collaborative research center CRC 1149), the research training group GRK2203 PULMOSENS (Ulm University) and the German Ministry of Defense (Forschungsvorhaben E/U2AD/ID013/IF564).

Acknowledgments

We are deeply grateful to Rosemarie Meyer, Bettina Stahl, Carolin Renner, Jessica Hofmiller, Edina Ahmetovic, and Sandra Kress for their excellent technical assistance.

Conflict of interest

The authors declare that the research was conducted in the absence of any commercial or financial relationships that could be construed as a potential conflict of interest.

The reviewer JB declared a past collaboration with the authors E-MW, MG and MH to the handling editor.

Publisher's note

Supplementary material

The Supplementary Material for this article can be found online at: https://www.frontiersin.org/articles/10.3389/fimmu.2023.1125594/full#supplementary-material

References

1. Bracht H, Scheuerle A, Gröger M, Hauser B, Matallo J, McCook O, et al. Effects of intravenous sulfide during resuscitated porcine hemorrhagic shock*. *Crit Care Med* (2012) 40:2157–67. doi: 10.1097/CCM.0b013e31824e6b30

2. Datzmann T, Hoffmann A, McCook O, Merz T, Wachter U, Preuss J, et al. Effects of sodium thiosulfate (Na2S2O3) during resuscitation from hemorrhagic shock in swine with preexisting atherosclerosis. *Pharmacol Res* (2020) 151:104536. doi: 10.1016/j.phrs.2019.104536

3. Drabek T, Kochanek PM, Stezoski J, Wu X, Bayir H, Morhard RC, et al. Intravenous hydrogen sulfide does not induce hypothermia or improve survival from hemorrhagic shock in pigs. *Shock* (2011) 35:67–73. doi: 10.1097/SHK.0b013e3181e86f49

4. Satterly SA, Salgar S, Hoffer Z, Hempel J, DeHart MJ, Wingerd M, et al. Hydrogen sulfide improves resuscitation *via* non-hibernatory mechanisms in a porcine shock model. *J Surg Res* (2015) 199:197–210. doi: 10.1016/j.jss.2015.04.001

5. Messerer DA, Gaessler H, Hoffmann A, Gröger M, Benz K, Huhn A, et al. The H2S donor sodium thiosulfate (Na2S2O3) does not improve inflammation and organ damage after hemorrhagic shock in cardiovascular healthy swine. *Front Immunol* (2022) 13:901005. doi: 10.3389/fimmu.2022.901005

6. Chai W, Wang Y, Lin J-Y, Sun X-D, Yao L-N, Yang Y-H, et al. Exogenous hydrogen sulfide protects against traumatic hemorrhagic shock *via* attenuation of oxidative stress. *J Surg Res* (2012) 176:210–9. doi: 10.1016/j.jss.2011.07.016

7. Gao C, Xu D-Q, Gao C-J, Ding Q, Yao L-N, Li Z-C, et al. An exogenous hydrogen sulphide donor, NaHS, inhibits the nuclear factor κB inhibitor kinase/nuclear factor κb inhibitor/nuclear factor-κB signaling pathway and exerts cardioprotective effects in a rat hemorrhagic shock model. *Biol Pharm Bull* (2012) 35:1029–34. doi: 10.1248/bpb.b110679

8. Ganster F, Burban M, de La Bourdonnaye M, Fizanne L, Douay O, Loufrani L, et al. Effects of hydrogen sulfide on hemodynamics, inflammatory response and oxidative stress during resuscitated hemorrhagic shock in rats. *Crit Care* (2010) 14:R165. doi: 10.1186/cc9257

9. Issa K, Kimmoun A, Collin S, Ganster F, Fremont-Orlowski S, Asfar P, et al. Compared effects of inhibition and exogenous administration of hydrogen sulphide in ischaemia-reperfusion injury. *Crit Care* (2013) 17:R129. doi: 10.1186/cc12808

10. Wepler M, Merz T, Wachter U, Vogt J, Calzia E, Scheuerle A, et al. The mitochondria-targeted H2S-donor AP39 in a murine model of combined hemorrhagic shock and blunt chest trauma. *Shock* (2019) 52:230–9. doi: 10.1097/SHK.0000000000001210

11. Mok Y-YP, Atan MS, Yoke Ping C, Zhong Jing W, Bhatia M, Moochhala S, et al. Role of hydrogen sulphide in haemorrhagic shock in the rat: protective effect of inhibitors of hydrogen sulphide biosynthesis. *Br J Pharmacol* (2004) 143:881–9. doi: 10.1038/sj.bjp.0706014

12. Mok Y-YP, Moore PK. Hydrogen sulphide is pro-inflammatory in haemorrhagic shock. *Inflammation Res* (2008) 57:512–8. doi: 10.1007/s00011-008-7231-6

13. Dyson A, Dal-Pizzol F, Sabbatini G, Lach AB, Galfo F, Dos Santos Cardoso J, et al. Ammonium tetrathiomolybdate following ischemia/reperfusion injury: Chemistry, pharmacology, and impact of a new class of sulfide donor in preclinical injury models. *PloS Med* (2017) 14:e1002310. doi: 10.1371/journal.pmed.1002310

14. Morrison ML, Blackwood JE, Lockett SL, Iwata A, Winn RK, Roth MB. Surviving blood loss using hydrogen sulfide. *J Trauma* (2008) 65:183–8. doi: 10.1097/TA.0b013e3181507579

15. van de Louw A, Haouzi P. Oxygen deficit and H2S in hemorrhagic shock in rats. *Crit Care* (2012) 16:R178. doi: 10.1186/cc11661

16. Módis K, Bos EM, Calzia E, van Goor H, Coletta C, Papapetropoulos A, et al. Regulation of mitochondrial bioenergetic function by hydrogen sulfide. part II. pathophysiological and therapeutic aspects. *Br J Pharmacol* (2014) 171:2123–46. doi: 10.1111/bph.12368

17. Szabo C, Ransy C, Módis K, Andriamihaja M, Murghes B, Coletta C, et al. Regulation of mitochondrial bioenergetic function by hydrogen sulfide. part i. biochemical and physiological mechanisms. *Br J Pharmacol* (2014) 171:2099–122. doi: 10.1111/bph.12369

18. Rahman MA, Cumming BM, Addicott KW, Pacl HT, Russell SL, Nargan K, et al. Hydrogen sulfide dysregulates the immune response by suppressing central carbon metabolism to promote tuberculosis. *Proc Natl Acad Sci U.S.A.* (2020) 117:6663–74. doi: 10.1073/pnas.1919211117

19. Carballal S, Vitvitsky V, Kumar R, Hanna DA, Libiad M, Gupta A, et al. Hydrogen sulfide stimulates lipid biogenesis from glutamine that is dependent on the mitochondrial NAD(P)H pool. *J Biol Chem* (2021) 297:100950. doi: 10.1016/j.jbc.2021.100950

20. Carter RN, Morton NM. Cysteine and hydrogen sulphide in the regulation of metabolism: insights from genetics and pharmacology. *J Pathol* (2016) 238:321–32. doi: 10.1002/path.4659

21. Szabo C, Papapetropoulos A. International union of basic and clinical pharmacology. CII: Pharmacological modulation of H2S levels: H2S donors and H2S biosynthesis inhibitors. *Pharmacol Rev* (2017) 69:497–564. doi: 10.1124/pr.117.014050

22. Olson KR, Deleon ER, Gao Y, Hurley K, Sadauskas V, Batz C, et al. Thiosulfate: a readily accessible source of hydrogen sulfide in oxygen sensing. *Am J Physiol Regul Integr Comp Physiol* (2013) 305:R592–603. doi: 10.1152/ajpregu.00421.2012

23. Bebarta VS, Brittain M, Chan A, Garrett N, Yoon D, Burney T, et al. Sodium nitrite and sodium thiosulfate are effective against acute cyanide poisoning when administered by intramuscular injection. *Ann Emerg Med* (2017) 69:718–725.e4. doi: 10.1016/j.annemergmed.2016.09.034

24. Brock PR, Maibach R, Childs M, Rajput K, Roebuck D, Sullivan MJ, et al. Sodium thiosulfate for protection from cisplatin-induced hearing loss. *N Engl J Med* (2018) 378:2376–85. doi: 10.1056/NEJMoa1801109

25. Marutani E, Yamada M, Ida T, Tokuda K, Ikeda K, Kai S, et al. Thiosulfate mediates cytoprotective effects of hydrogen sulfide against neuronal ischemia. *J Am Heart Assoc* (2015) 4. doi: 10.1161/JAHA.115.002125

26. Ravindran S, Jahir Hussain S, Boovarahan SR, Kurian GA. Sodium thiosulfate post-conditioning protects rat hearts against ischemia reperfusion injury *via* reduction of apoptosis and oxidative stress. *Chem Biol Interact* (2017) 274:24–34. doi: 10.1016/j.cbi.2017.07.002

27. Sakaguchi M, Marutani E, Shin H, Chen W, Hanaoka K, Xian M, et al. Sodium thiosulfate attenuates acute lung injury in mice. *Anesthesiology* (2014) 121:1248–57. doi: 10.1097/ALN.0000000000000456

28. Ravindran S, Kurian GA. Effect of sodium thiosulfate postconditioning on ischemia-reperfusion injury induced mitochondrial dysfunction in rat heart. *J Cardiovasc Transl Res* (2018) 11:246–58. doi: 10.1007/s12265-018-9808-y

29. Buck MD, O'Sullivan D, Klein Geltink RI, Curtis JD, Chang C-H, Sanin DE, et al. Mitochondrial dynamics controls T cell fate through metabolic programming. *Cell* (2016) 166:63–76. doi: 10.1016/j.cell.2016.05.035

30. O'Neill LA, Pearce EJ. Immunometabolism governs dendritic cell and macrophage function. *J Exp Med* (2016) 213:15–23. doi: 10.1084/jem.20151570

31. Palmer CS, Ostrowski M, Balderson B, Christian N, Crowe SM. Glucose metabolism regulates T cell activation, differentiation, and functions. *Front Immunol* (2015) 6:1. doi: 10.3389/fimmu.2015.00001

32. Pearce EL, Pearce EJ. Metabolic pathways in immune cell activation and quiescence. *Immunity* (2013) 38:633–43. doi: 10.1016/j.immuni.2013.04.005

33. Pearce EL, Poffenberger MC, Chang C-H, Jones RG. Fueling immunity: insights into metabolism and lymphocyte function. *Science* (2013) 342:1242454. doi: 10.1126/science.1242454

34. Kleikers PW, Wingler K, Hermans JJ, Diebold I, Altenhöfer S, Radermacher KA, et al. NADPH oxidases as a source of oxidative stress and molecular target in ischemia/reperfusion injury. *J Mol Med* (2012) 90:1391–406. doi: 10.1007/s00109-012-0963-3

35. Geltink RI, Kyle RL, Pearce EL. Unraveling the complex interplay between T cell metabolism and function. *Annu Rev Immunol* (2018) 36:461–88. doi: 10.1146/annurev-immunol-042617-053019

36. Fox CJ, Hammerman PS, Thompson CB. Fuel feeds function: energy metabolism and the T-cell response. *Nat Rev Immunol* (2005) 5:844–52. doi: 10.1038/nri1710

37. Kramer PA, Ravi S, Chacko B, Johnson MS, Darley-Usmar VM. A review of the mitochondrial and glycolytic metabolism in human platelets and leukocytes: implications for their use as bioenergetic biomarkers. *Redox Biol* (2014) 2:206–10. doi: 10.1016/j.redox.2013.12.026

38. Antoniewicz MR, Kelleher JK, Stephanopoulos G. Accurate assessment of amino acid mass isotopomer distributions for metabolic flux analysis. *Anal Chem* (2007) 79:7554–9. doi: 10.1021/ac0708893

39. Buescher JM, Antoniewicz MR, Boros LG, Burgess SC, Brunengraber H, Clish CB, et al. A roadmap for interpreting (13)C metabolite labeling patterns from cells. *Curr Opin Biotechnol* (2015) 34:189–201. doi: 10.1016/j.copbio.2015.02.003

40. Antoniewicz MR, Kelleher JK, Stephanopoulos G. Elementary metabolite units (EMU): a novel framework for modeling isotopic distributions. *Metab Eng* (2007) 9:68–86. doi: 10.1016/j.ymben.2006.09.001

41. Lee MH, Malloy CR, Corbin IR, Li J, Jin ES. Assessing the pentose phosphate pathway using 2, 3-13 C2 glucose. *NMR BioMed* (2019) 32:e4096. doi: 10.1002/nbm.4096

42. Ringland V, Lewis MA, Dunleavy D. Beyond the p-value: Bayesian statistics and causation. *J Evid Based Soc Work (2019)* (2021) 18:284–307. doi: 10.1080/26408066.2020.1832011

43. Stifel U, Wolfschmitt E-M, Vogt J, Wachter U, Vettorazzi S, Tews D, et al. Glucocorticoids coordinate macrophage metabolism through the regulation of the tricarboxylic acid cycle. *Mol Metab* (2021) 57:101424. doi: 10.1016/j.molmet.2021.101424

44. Zink F, Vogt J, Wachter U, Hartert J, Horchler M, Zhang X, et al. Effects of acute subdural hematoma-induced brain injury on energy metabolism in peripheral blood mononuclear cells. *Shock* (2021) 55:407–17. doi: 10.1097/SHK.0000000000001642

45. Knöller E, Stenzel T, Broeskamp F, Hornung R, Scheuerle A, McCook O, et al. Effects of hyperoxia and mild therapeutic hypothermia during resuscitation from porcine hemorrhagic shock. *Crit Care Med* (2016) 44:e264–77. doi: 10.1097/CCM.0000000000001412

46. Nichols TC, Bellinger DA, Merricks EP, Raymer RA, Kloos MT, Defriess N, et al. Porcine and canine von willebrand factor and von willebrand disease: hemostasis, thrombosis, and atherosclerosis studies. *Thrombosis* (2010) 2010:461238. doi: 10.1155/2010/461238

47. Bebarta VS, Tanen DA, Lairet J, Dixon PS, Valtier S, Bush A. Hydroxocobalamin and sodium thiosulfate versus sodium nitrite and sodium thiosulfate in the treatment of acute cyanide toxicity in a swine (Sus scrofa) model. *Ann Emerg Med* (2010) 55:345–51. doi: 10.1016/j.annemergmed.2009.09.020

48. Bebarta VS, Pitotti RL, Dixon P, Lairet JR, Bush A, Tanen DA. Hydroxocobalamin versus sodium thiosulfate for the treatment of acute cyanide toxicity in a swine (Sus scrofa) model. *Ann Emerg Med* (2012) 59:532–9. doi: 10.1016/j.annemergmed.2012.01.022

49. Doerrier C, Garcia-Souza LF, Krumschnabel G, Wohlfarter Y, Mészáros AT, Gnaiger E. High-resolution FluoRespirometry and OXPHOS protocols for human cells, permeabilized fibers from small biopsies of muscle, and isolated mitochondria. *Methods Mol Biol* (2018) 1782:31–70. doi: 10.1007/978-1-4939-7831-1_3

50. Chance B, Williams GR. Respiratory enzymes in oxidative phosphorylation. *J Biol Chem* (1955) 217:409–27. doi: 10.1016/S0021-9258(19)57191-5

51. Zink F. Quantification of oxygen radicals and surrogate parameters of oxidative stress. *PhD Thesis. Ulm Germany* (2021).

52. Hellmann A, Daboss S, Zink F, Hartmann C, Radermacher P, Kranz C. Electrocatalytically modified microelectrodes for the detection of hydrogen peroxide at blood cells from swine with induced trauma. *Electrochimica Acta* (2020) 353:136458. doi: 10.1016/j.electacta.2020.136458

53. van Winden WA, Wittmann C, Heinzle E, Heijnen JJ. Correcting mass isotopomer distributions for naturally occurring isotopes. *Biotechnol Bioeng* (2002) 80:477–9. doi: 10.1002/bit.10393

54. Vogt JA, Yarmush DM, Yu YM, Zupke C, Fischman AJ, Tompkins RG, et al. TCA cycle flux estimates from NMR- and GC-MS-determined 13Cglutamate isotopomers in liver. *Am J Physiol* (1997) 272:C2049–62. doi: 10.1152/ajpcell.1997.272.6.C2049

55. Wiechert W. 13C metabolic flux analysis. *Metab Eng* (2001) 3:195–206. doi: 10.1006/mben.2001.0187

56. Alger JR, Sherry AD, Malloy CR. tcaSIM: A simulation program for optimal design of 13C tracer experiments for analysis of metabolic flux by NMR and mass spectroscopy. *Curr Metabolomics* (2018) 6:176–87. doi: 10.2174/2213235X07666181219115856

57. Weitzel M, Nöh K, Dalman T, Niedenführ S, Stute B, Wiechert W. 13CFLUX2–high-performance software suite for (13)C-metabolic flux analysis. *Bioinformatics* (2013) 29:143–5. doi: 10.1093/bioinformatics/bts646

58. Stan Development Team. *RStan: the r interface to Stan* (2020). Available at: http://mc-stan.org/.

59. Lee WN, Boros LG, Puigjaner J, Bassilian S, Lim S, Cascante M. Mass isotopomer study of the nonoxidative pathways of the pentose cycle with 1,2-13C2glucose. *Am J Physiol* (1998) 274:E843–51. doi: 10.1152/ajpendo.1998.274.5.E843

60. Katz J, Rognstad R. The labeling of pentose phosphate from glucose-14C and estimation of the rates of transaldolase, transketolase, the contribution of the pentose cycle, and ribose phosphate synthesis. *Biochemistry* (1967) 6:2227–47. doi: 10.1021/bi00859a046

61. Hu C, Xuan Y, Zhang X, Liu Y, Yang S, Yang K. Immune cell metabolism and metabolic reprogramming. *Mol Biol Rep* (2022) 49:9783–95. doi: 10.1007/s11033-022-07474-2

62. O'Neill LA, Kishton RJ, Rathmell J. A guide to immunometabolism for immunologists. *Nat Rev Immunol* (2016) 16:553–65. doi: 10.1038/nri.2016.70

63. Zhang MY, Dugbartey GJ, Juriasingani S, Sener A. Hydrogen sulfide metabolite, sodium thiosulfate: Clinical applications and underlying molecular mechanisms. *Int J Mol Sci* (2021) 22. doi: 10.3390/ijms22126452

64. Lu M, Zhou L, Stanley WC, Cabrera ME, Saidel GM, Yu X. Role of the malate-aspartate shuttle on the metabolic response to myocardial ischemia. *J Theor Biol* (2008) 254:466–75. doi: 10.1016/j.jtbi.2008.05.033

65. Fan J, Li Y, Levy RM, Fan JJ, Hackam DJ, Vodovotz Y, et al. Hemorrhagic shock induces NAD(P)H oxidase activation in neutrophils: role of HMGB1-TLR4 signaling. *J Immunol* (2007) 178:6573–80. doi: 10.4049/jimmunol.178.10.6573

66. Premaratne S, Amaratunga DT, Mensah FE, McNamara JJ. Significance of oxygen free radicals in the pathophysiology of hemorrhagic shock - a protocol. *Int J Surg Protoc* (2018) 9:15–9. doi: 10.1016/j.isjp.2018.04.002

67. Paul BD, Snyder SH, Kashfi K. Effects of hydrogen sulfide on mitochondrial function and cellular bioenergetics. *Redox Biol* (2021) 38:101772. doi: 10.1016/j.redox.2020.101772

68. Goubern M, Andriamihaja M, Nübel T, Blachier F, Bouillaud F. Sulfide, the first inorganic substrate for human cells. *FASEB J* (2007) 21:1699–706. doi: 10.1096/fj.06-7407com

69. Matallo J, Vogt J, McCook O, Wachter U, Tillmans F, Groeger M, et al. Sulfide-inhibition of mitochondrial respiration at very low oxygen concentrations. *Nitric Oxide* (2014) 41:79–84. doi: 10.1016/j.niox.2014.06.004

70. Bouillaud F. Sulfide oxidation evidences the immediate cellular response to a decrease in the mitochondrial ATP/O2 ratio. *Biomolecules* (2022) 12. doi: 10.3390/biom12030361

71. Cheng J, Wang Z, Lu H, Yang W, Fan Z. Hydrogen sulfide improves lipid accumulation in nannochloropsis oceanica through metabolic regulation of carbon allocation and energy supply. *ACS Sustain Chem Eng* (2020) 8:2481–9. doi: 10.1021/acssuschemeng.9b06748

72. Zhang J, Ahn WS, Gameiro PA, Keibler MA, Zhang Z, Stephanopoulos G. 13C isotope-assisted methods for quantifying glutamine metabolism in cancer cells. *Methods Enzymol* (2014) 542:369–89. doi: 10.1016/B978-0-12-416618-9.00019-4

73. Alkan HF, Walter KE, Luengo A, Madreiter-Sokolowski CT, Stryeck S, Lau AN, et al. Cytosolic aspartate availability determines cell survival when glutamine is limiting. *Cell Metab* (2018) 28:706–720.e6. doi: 10.1016/j.cmet.2018.07.021

74. Herteman N, Vargas A, Lavoie J-P. Characterization of circulating low-density neutrophils intrinsic properties in healthy and asthmatic horses. *Sci Rep* (2017) 7:7743. doi: 10.1038/s41598-017-08089-5

75. Wright HL, Makki FA, Moots RJ, Edwards SW. Low-density granulocytes: functionally distinct, immature neutrophils in rheumatoid arthritis with altered properties and defective TNF signalling. *J Leukoc Biol* (2017) 101:599–611. doi: 10.1189/jlb.5A0116-022R

frontiers | Frontiers in Immunology

TYPE Original Research
PUBLISHED 16 March 2023
DOI 10.3389/fimmu.2023.1076587

OPEN ACCESS

EDITED BY
Soumya R. Mohapatra,
KIIT University, India

REVIEWED BY
Wenbo Zou,
Chinese PLA General Hospital, China
Deepika Rai,
Cedars Sinai Medical Center, United States
Divya Vimal,
Columbia University Irving Medical Center, United States

*CORRESPONDENCE
Rufu Chen
chenrufu@mail.sysu.edu.cn
Yu Zhou
zhouyu@gdph.org.cn

†These authors have contributed equally to this work and share first authorship

SPECIALTY SECTION
This article was submitted to Cancer Immunity and Immunotherapy, a section of the journal Frontiers in Immunology

RECEIVED 21 October 2022
ACCEPTED 08 February 2023
PUBLISHED 16 March 2023

CITATION
Yang J, Zeng L, Chen R, Zheng S, Zhou Y and Chen R (2023) Characterization of heterogeneous metabolism in hepatocellular carcinoma identifies new therapeutic target and treatment strategy. *Front. Immunol.* 14:1076587. doi: 10.3389/fimmu.2023.1076587

Characterization of heterogeneous metabolism in hepatocellular carcinoma identifies new therapeutic target and treatment strategy

Jiabin Yang[1,2†], Liangtang Zeng[1,2†], Ruiwan Chen[3†], Shangyou Zheng[2], Yu Zhou[2*] and Rufu Chen[1,2*]

[1]School of Medicine, South China University of Technology, Guangzhou, Guangdong, China, [2]Department of Pancreatic Surgery, Guangdong Provincial People's Hospital (Guangdong Academy of Medical Sciences), Southern Medical University, Guangzhou, China, [3]Department of Radiation Oncology, The First Affiliated Hospital, Sun Yat-sen University, Guangzhou, Guangdong, China

Background: Metabolic reprogramming is a well-known hallmark of cancer. Systematical identification of clinically relevant metabolic subtypes of Hepatocellular carcinoma (HCC) is critical to understand tumor heterogeneity and develop efficient treatment strategies.

Methods: We performed an integrative analysis of genomic, transcriptomic, and clinical data from an HCC patient cohort in The Cancer Genome Atlas (TCGA).

Results: Four metabolic subtypes were defined: mHCC1, mHHC2, mHCC3, and mHCC4. These subtypes had distinct differences in mutations profiles, activities of metabolic pathways, prognostic metabolism genes, and immune features. The mHCC1 was associated with poorest outcome and was characterized by extensive metabolic alterations, abundant immune infiltration, and increased expression of immunosuppressive checkpoints. The mHHC2 displayed lowest metabolic alteration level and was associated with most significant improvement in overall survival in response to high CD8+ T cell infiltration. The mHHC3 was a "cold-tumor" with low immune infiltration and few metabolic alterations. The mHCC4 presented a medium degree of metabolic alteration and high CTNNB1 mutation rate. Based on our HCC classification and in vitro study, we identified palmitoyl-protein thioesterase 1 (PPT1) was a specific prognostic gene and therapeutic target for mHCC1.

Conclusion: Our study highlighted mechanistic differences among metabolic subtypes and identified potential therapeutic targets for subtype-specific treatment strategies targeting unique metabolic vulnerabilities. The immune heterogeneities across metabolic subtypes may help further clarify the

association between metabolism and immune environment and guide the development of novel strategies through targeting both unique metabolic vulnerabilities and immunosuppressive triggers.

KEYWORDS

hepatocellular carcinoma, metabolism, differential gene expression, personalized treatment, metabolic subtype, PPT1

Introduction

Hepatocellular carcinoma (HCC) is the leading cause of cancer-related death in many parts of the world (1). In the past decade, considerable improvements have been made in prevention, surveillance, early detection, diagnosis, and treatment, but HCC remains one of the few cancers with a continued increase in both incidence and mortality (1, 2). The positive results of treatment with sorafenib, a small-molecule multi-kinase inhibitor, in the first-line systemic treatment of advanced HCC, triggered the evaluation of molecular targeted therapy in this disease (3). However, despite several new multi-kinase inhibitors showed survival benefits (4–6), there are still limited therapy options in patients with HCC, with HCC prognosis remaining poor (7, 8). Therefore, an improved understanding of HCC biology that will contribute to expansion of therapeutic arsenal for HCC is clearly and urgently needed.

Cellular metabolism reprogramming is a well-established hallmark of cancer that presents opportunities for cancer diagnosis and therapy (9). Tumors adjust their metabolism to provide sufficient energy and biosynthetic metabolites, which is necessary for malignant cellular proliferation (10, 11). Due to their pivotal cellular functions, recent efforts have sought to devise novel cancer treatments through targeting metabolism vulnerabilities. In addition to metabolism targeted therapy, tumor immunotherapy is raising with both approaches being promising tools to treat tumors (12); in particular, strategies targeting immune checkpoints have shown substantial efficacy in a variety of tumors (13, 14). In HCC, promising responses to immune checkpoint inhibitors PD-1/PD-L1 have been recently reported (15), but similarly to other solid tumors, the response rate was low. Therefore, strategies to improve the efficacy of immune checkpoint inhibitors and to direct individualized medication are urgently required (16, 17).

Since liver is a key organ for whole body energy homeostasis, pathological changes of liver, especially during carcinogenesis, often involve the reprogramming of normal metabolic processes (18). In this scenario, the HCC represents an optimal candidate as a malignancy for developing therapeutics targeting altered metabolism (19). However, HCC is a highly heterogeneous tumor (20). It has not been well established, whether this heterogeneity is caused by distinct metabolic pathways that can be used to stratify HCC into subgroups with clinical significance and biological characteristics (21). Classification of total metabolic characteristics could undoubtedly provide useful information on the metabolic pathways at the systems level of HCC (22). Besides, increasing evidences suggest that alterations in tumor metabolism can also contribute to the inhibition of antitumor response (23, 24). Immunosuppression in the tumor microenvironment is suggested to be based on the mutual metabolic requirements of immune cells and tumor cells (25, 26). Therefore, the investigation of metabolic heterogeneity as well as the association between the tumor metabolism and the tumor immune microenvironment could provide a better understanding of the complex molecular pathogenesis of HCC and lead to discoveries of new possible treatment targets and strategies.

Methods

Data resources and reprocessing

The normalized level 3 RNA-sequencing (RNA-seq) data and corresponding clinical information of HCC patients were collected from The Cancer Genome Atlas (TCGA) database portal. RNA-seq data (FPKM values) were transformed into transcripts per kilobase million (TPM) values, which are closer in format to those resulting from microarrays and more comparable between samples. Mutational data for all samples with RNA-seq data available was also downloaded. Furthermore, other HCC datasets were obtained from the GEO public database.

Consensus clustering for metabolic subtype

Genes belonging to the KEGG subset of canonical pathways were searched in the Molecular Signature Database (MSigDB, https://www.gsea-msigdb.org/gsea/msigdb) (27), and genes involved in the metabolism pathways were collected. Genes displaying a median TPM < 1 across patients were considered extremely low expression and were removed from the consensus clustering analysis. Consensus clustering was performed on metabolic genes using ConsensusClusterPlus R package (parameters: 160 reps=50, pItem=0.8, pFeature=1). The optimum cluster number was determined by testing 2 to 10 clusters, and based on CDF and Δ(K). The collected pathways and their respective genes were subjected clustering analysis are listed in Supplementary Table S1.

Identification of maker genes of HCC subtypes

Hierarchical clustering is used to classify samples into different categories based on the sample's gene expression matrix, and label different sample categories (28). Taking the expression value of the gene as an input feature and the classification of the sample as an output value, a random forest algorithm was used to construct a prediction model. We used the out-of-bag error rate as an index to evaluate the importance of the features and rank them, and take the first 100 and the first 50 features as the features for subsequent analysis. Scikit-learn was used as a tool for related calculations (29).

Differentially expressed mRNA analysis

Level-3 RNA-sequencing (RNA-seq) data containing 374 HCC samples and 50 normal controls was downloaded from The Cancer Genome Atlas (TCGA). The differentially expressed genes (DEGs) were identified using the Edge R package for R software. |Fold change| > 2 and adjusted P-values < 0.05 were set as the thresholds.

Gene set enrichment analysis

The Gene set enrichment analysis (GSEA) was performed to identify enrichment degree of gene set among tumors of a certain metabolic subtype and compared with other samles (27). Significance was considered for values of corrected P as recommended by the software (https://www.gsea-msigdb.org/gsea/downloads.jsp). Gene sets were downloaded from the MSigDB. The GSEA results were merged by using GSVA R package.

Estimation of metabolic pathways' activity

Gene Set Variation Analysis (GSVA) is a pathway/gene set-based analysis approach that provides an overall pathway or gene-set activity score for each sample (30). We estimated the activities of metabolic pathways through GSVA. GSVA z-scores for KEGG metabolic gene-sets from the MSigDB and other gene-sets were calculated using the GSVA R package. We considered that the activity a given metabolic pathway was different between two groups if the median of GSVA values across one group differed significantly (Mann-Whitney q-value<0.1) and more than 0.2 from that measured across another group. Besides, we estimated T cell exhaustion scores for each HCC sample by using GSVA and a gene set including signature genes of exhausted CD8+ T cells (31).

Estimation of the abundance of immune cell populations

GSVA and the single sample Gene Set Enrichment Analysis (ssGSEA) are two most widely used methods that carry out sample level enrichment analysis. Both are unsupervised gene set enrichment methods that compute an enrichment score integrating the collective expression of a given gene set relative to the other genes in the sample. A previous study revealed a significant consistency of the two methods in evaluating immune populations across 28 cancer types (32). Besides, they also compared different signatures identifying immune cell populations reported in previous articles and constructed a new set of gene signatures with better discrimination than that shown in previous sets. According to their experience, we chose GSVA method because its advantage in reducing the noise of the data; the immune signatures were also retrieved from the same publication (32).

Analysis of PPT1 expression in different cell types in HCC at the single-cell level.

Tumor Immune Single Cell Hub (TISCH, http://tisch.comp-genomics.org), a single cell RNA sequencing (scRNA-seq) application platform that can systematically and comprehensively study the heterogeneity of tumor microenvironment (TME) (33), was used to explore the relationship between PPT1 and the TME on cell level.

Cell culture

The human HCC cell lines Huh-7 (JCRB0403) and JHH-7 (JCRB1031) were obtained from the Health Science Research Resources Bank (Osaka, Japan). Cells were grown in Dulbecco's Modified Essential Media (DMEM, Hyclone) supplemented with 10% fetal bovine serum (FBS) and penicillin/streptomycin (Gibco, Grand Island, NY, USA) in a humidified incubator at 37°C in a 5% CO_2 atmosphere.

Vector construction and lentivirus transfection

Human pyruvate kinase M2 (PKM2) cDNA was cloned into the pCDH-CMV-MCS-EF1-Neo vector and palmitoyl-protein thioesterase 1 (PPT1) was cloned into the pCDH-CMV-MCS-EF1-Puro vector by IGE (Guangzhou, China). After confirming the PKM2 and PPT1 sequence by sequencing, the plasmid was co-transfected into HEK293T cells (ATCC, RRID: CVCL_0063) with the lentivirus packaging plasmids psPAX2 and pMD2G to produce lentivirus particles. To knock down the PKM2 and PPT1 expression, the shRNA sequence of PKM2 was cloned into the pLKO.1-Neo lentiviral vector and the shRNA sequence of PPT1 was cloned into the pLKO.1-Puro lentiviral vector by IGE (Guangzhou, China). The oligonucleotide sequences of shRNAs are listed in Supplementary Table S5. Similarly, the lentiviral vector was transfected into HEK293T cells together with packaging vectors pMD2.G and psPAX2 to produce lentivirus particles. The media containing retroviruses were collected 72h after transfection, centrifuged to remove cell debris, and then filtered. The lentivirus

particles were then used to transduce Huh-7 and JHH-7 cells. Control cells were transfected with a control empty vector.

Western blotting

Total protein was extracted by using RIPA lysis buffer containing a cocktail of protease and phosphatase inhibitors. Using the BCA Protein Assay Kit (CWBio, China, Cat#CW0014S), the concentration of the protein was determined. Following the previous process, 20 μg total proteins extracted from Huh-7 cells were separated electrophoretically in 10% SDS polyacrylamide gels. Separated proteins are transferred to polyvinylidene fluoride (PVDF) membranes. The membrane was then blocked with 5% BSA at room temperature for 1h before being incubated with the primary antibodies overnight at 4°C. Next day, the membranes were incubated for 1h at room temperature with secondary antibodies. Eventually, the immunoblotting was tested using the ECL Chemiluminescence Kit (Thermo Fisher Scientific, USA, Cat#32109). The antibodies are shown in Supplementary Table S4.

Cell viability assay

MTT assay was used to evaluate cell viability. Cells were seeded in 96-well plates (2×10^3/well) (in triplicate for each condition) and were cultured for different hours (34). The 20 μl MTT (Sigma, Saint Louis, USA) stock solution (5 mg/ml) was added to each well and incubated for 2h, the absorbance was measured at a wavelength of 570 nm.

Glycolysis stress tests (ECAR)

ECAR was estimated by using Seahorse assays with a Seahorse XFp Analyzer, 2.0×10^4 Huh-7 cells per well were plated onto 8-well plates and glycolysis stress test was performed following the manufacturer's specifications (35, 36). The assay DMEM media was free of glucose and pyruvate. The concentration of drugs used for test were as following: glucose (10.0 μM), oligomycin A (1.0 μM), and 2-deoxy-D-glucose (2-DG, 100 μM).

Lactate production assay

5 x 10^5 HCC cells were incubated in phenol red-free medium at 37°C, 5% CO_2 for 1h. The supernatant medium was collected. The lactate secreted by the cells was measured using the Lactate Colorimetric/Fluorometric Assay Kit according to the manufacturer's protocol (BioVision, Inc.) (37).

Statistical tests

All quantitative data were conducted at least three independent experiments and expressed as the mean ± SD. For comparisons between two groups, statistical significance for normal distribution data was estimated by unpaired Student t-test, otherwise Mann-Whitney U test was applied. For comparisons of more than two groups, One-way ANOVA multiple comparison was used. Correlation coefficients were computed by Spearman and distance correlation analyses. The influence of a single factor on the survival was evaluated through the Cox proportional hazard model, Kaplan-Meier survival curves, or Log-rank test. All statistical analyses were conducted using R (https://www.r-project.org/) or SPSS software (version 17.0). Two-sided P values of less than 0.05 were considered statistically significant.

Results

Classification of metabolic subtypes in HCC

We obtained four robust subtypes of HCC in TCGA dataset (Supplementary Table S2). A heatmap based on one hundred genes obtained with machine learning was shown in Figure 1A. The robust classification revealed that HCC tumors displayed highly heterogeneous expression of genes that were directly involved in metabolism. The mHCC1 was defined as the largest group (144/371; 38.8%), followed by mHCC2 (138/371; 37.2%), mHCC4 (51/371; 13.7%), and mHCC3 (38/371; 10.2%). These subtypes are henceforth termed mHCC1 (cluster 1), mHCC2 (cluster 2), mHCC3 (cluster 3), and mHCC4 (cluster 4). We noted distinct patterns of gene mutations across the four different metabolic subtypes (Figures 1B, C). For example, mutations in TP53 were enriched in mHCC1, and 76% of MHCC4 tumors showed mutations in CTNNB1. In addition, co-occurrence analysis using the five most frequent mutations in HCC indicated different relationships among the five common mutations across four subtypes. A mutual exclusion between TP53 mutations and CTNNB1 mutations in mHCC1 tumors was observed, while co-occurrence between TTN mutations and mutations in CTNNB1 or ALB were found in mHCC2. These results indicated that there are multiple metabolic phenotypes in HCC driven by different oncogenic mutations. The mHCC1 was associated with the shortest survival while the prognosis of other three subtypes were similar (Figures 1D, E).

Landscape of functional annotations across four subtypes

To identify the underlying biological functional characteristics of each subtype, signature genes in each group were collected. KEGG analysis of the signature genes was conducted and the results were visualized in Figure 2. Among those signature genes dysregulated in each subtype/cluster, we identified that the mHCC1 had much larger proportion of genes enriched in metabolism-related pathways than that in other clusters; especially including "carbohydrate metabolism", "lipid metabolism", and "amino acid metabolism", which were major

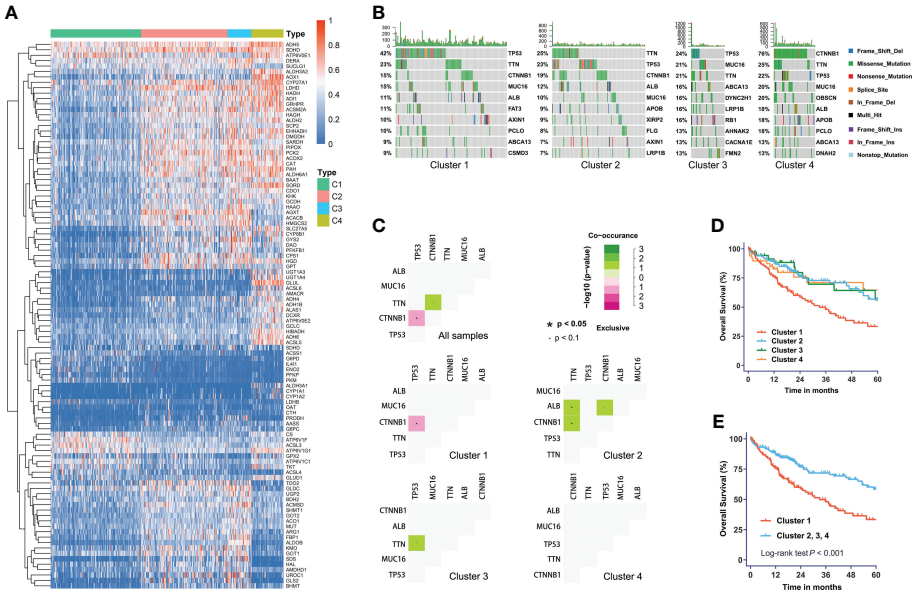

FIGURE 1
The metabolic subtypes in HCC. **(A)** Unsupervised clustering of HCC samples for 371 HCC patients in the TCGA cohort. **(B)** Correlation between the distribution of highly variant mutated genes and metabolic subtypes. **(C)** Co-occurrence analysis of mutations in whole cohort and each subtype. **(D)** Kaplan-Meier curves with univariate analyses of overall survival in patients stratified by metabolic subgroup. **(E)** Kaplan-Meier curves with univariate analyses of overall survival in patients of cluster 1 versus those of other three clusters. Log-rank test P values are shown.

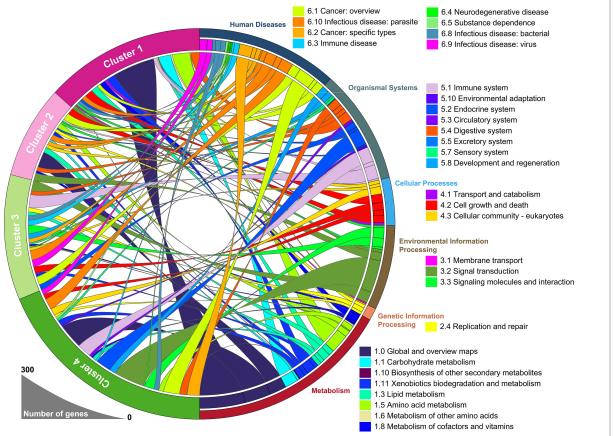

FIGURE 2
A circular plot showing the differentially expressed genes and their associated biological processes. The differentially expressed genes in each group were calculated separately, using 50 normal liver samples as control group.

reprogrammed metabolic pathways in malignant cells. In addition, we noted that most genes that were enriched in "signal transduction", "signaling molecules and interaction", and "cellular community" came from mHCC4, followed by mHCC2 and mHCC3, but barely from mHCC1. Besides, immune-related pathways were more likely to be enriched by genes from mHCC3 and mHCC4, such as "Immune system", "Infectious disease: bacterial", "Infectious disease: viral", "Infectious disease: parasite", and "Immune disease".

Association of different subtypes with metabolic pathway profiles

We next supposed that subtypes produced through gene clustering had specific features in different metabolic pathways and employed a sample-level gene set enrichment method (GSVA) to compute the GSVA enrichment scores of the selected metabolic pathways. The differences in GSVA scores for each pathway between normal liver and four subtypes were calculated. As shown in Figure 3A, compared with other subtypes, mHCC1 displayed significantly dysregulated fold change in GSVA scores with reference to those in normal livers. It was well known that HCC cells are metabolically distinct from normal hepatocytes and express different metabolic enzymes (38, 39). Our next gene set enrichment analysis (GSEA) using a gene set involving metabolic genes of normal liver revealed a significant absence of normal metabolic genes in samples of mHCC1 and mHCC4, but no significant differences in mHCC2 and mHCC3 (Figure 3B). These results were consistent with the KEGG analysis visualized in Figure 2 and suggested different types of metabolism impairments among subtypes. Similarly, as shown in Figures 3C, D, there was a remarkable difference between GSVA scores for most metabolic pathways of the mHCC1 and other three clusters as well as normal liver samples; in contrast, GSVA scores of the most pathways in both mHCC2 and mHCC3 showed limited differences compared with normal liver samples, which is consistent with the GSEA results.

We next compared GSVA scores of major metabolism reactions that are critical to carcinogenesis, including carbohydrate metabolism (Figure 3E), amino acid metabolism (Figure 3F), and lipid metabolism (Figure 3G). Overall, compared with normal liver

10.3389/fimmu.2023.1076587

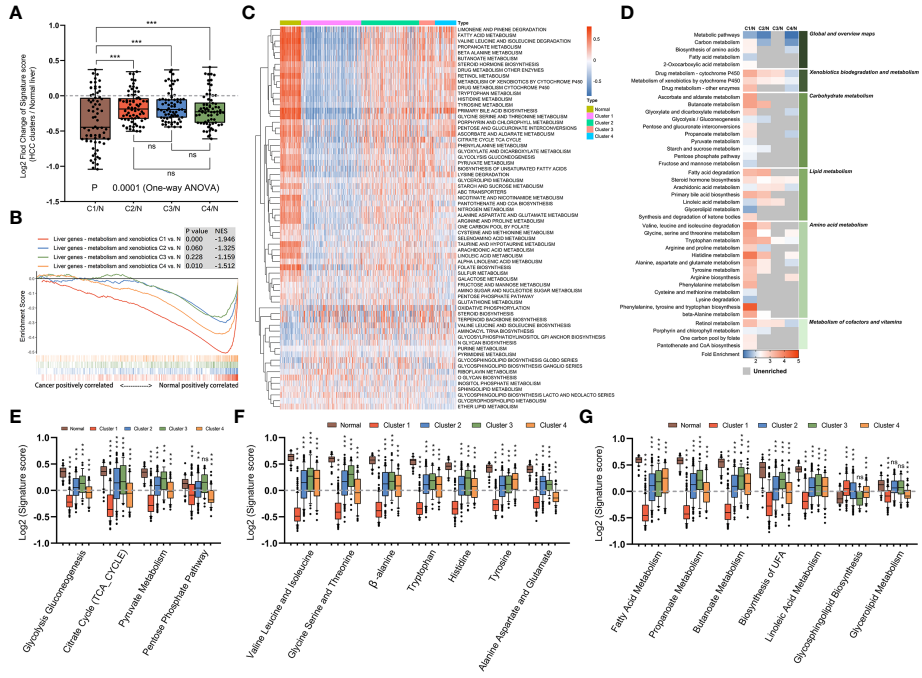

FIGURE 3
Metabolic landscape across metabolic subgroups. **(A)** In samples of normal livers and each subtype, the GSVA values of 69 KEGG metabolic pathways were measured respectively. With the normal liver as the control group, fold changes of GSVA values in each subtype were obtained and shown in a box plot. Each dot represents the fold change in GSVA value of one metabolic pathway between a subtype and the control group. **(B)** Gene set enrichment analysis of a gene sets including metabolic genes in healthy liver, with all transcripts ranked by the log2 (Fold Change) between clusters and normal liver. **(C)** Heatmap depicting GSVA values of metabolic pathways across each subgroup. **(D)** Heatmap showing the results of KEGG clustering results based on differentially expressed genes in each subgroup. **(E–G)** The GSVA values of pathways involved in glucose metabolism **(E)**, amino acid metabolism **(F)**, and fatty acid metabolism **(G)** for samples in each subgroup were shown in box plots. (ns: not significant, **: P < 0.01, ***: P < 0.001).

samples, tumors in mHCC1 were most significantly differentially enriched for almost all the selected pathways. The GSVA enrichment pattern in different pathways of carbohydrate metabolism was identical, mHCC1 had most significant differences in GSVA scores than in normal liver, followed by mHCC4, while mHCC2 and mHCC3 had similar scores compared with each other. In the respect of amino acid metabolism and lipid metabolism, mHCC2, mHCC3, and mHCC4 had similar enrichment in many pathways but mHCC1 still showed a significantly differential enrichment for all pathways. Specifically, mHCC4 displayed much more significant enrichment in "Pentose phosphate pathway" than other clusters and showed a similar enrichment in both "Alanine aspartate and glutamate pathway" and "Glycolipid metabolism pathway" compared with mHCC1. In addition to the characteristic metabolic pathways specifically present above, there are some amino acid metabolic pathways that are significantly reduced in mHCC1.

Analysis of differences in specific metabolic pathways across four subtypes

To complete the landscape of the metabolic pathways across the four subtypes, we further evaluated whether each subtype had unique metabolic pathways enriched. If a pathway was especially different (Mann-Whitney q-value<0.05 and difference between medians of GSVA was more than 0.2) in only one cluster, it was regarded as a characteristic metabolic pathway in corresponding subtype. As shown in Figures 4A–C, there were six characteristic pathways in total identified in mHCC1, mHCC3, and mHCC4. "Lysine Degradation" and "On-Carbon-Pool by Folate" were identified as characteristic metabolic pathways of mHCC1, "Oxidative Phosphorylation" and "O-Glycan Biosynthesis" in mHCC3, and two sub-pathways of "Glycosphingolipid Biosynthesis" in mHCC4, while none in mHCC2. In addition to the characteristic metabolic pathways specifically present above, there are some amino acid metabolic pathways that are significantly reduced in mHCC1.

Identification of survival signatures and its heterogeneity across metabolic subtypes

The above observations led us to question how these differences among metabolic subtypes relate to clinical outcome of the patients. Therefore, the prognostic value of metabolic genes in each subtype was investigated using log-rank test and univariate Cox regression model. The results of survival analysis are summarized in Supplementary Table S3. Remarkably, only a small portion of metabolic genes with prognostic significance were shared by multi-subtypes, and none was shared by all four subtypes (Figures 5A, B), suggesting distinct role of genes across subtypes even for the same metabolic pathway. Furthermore, survival analysis based on genes

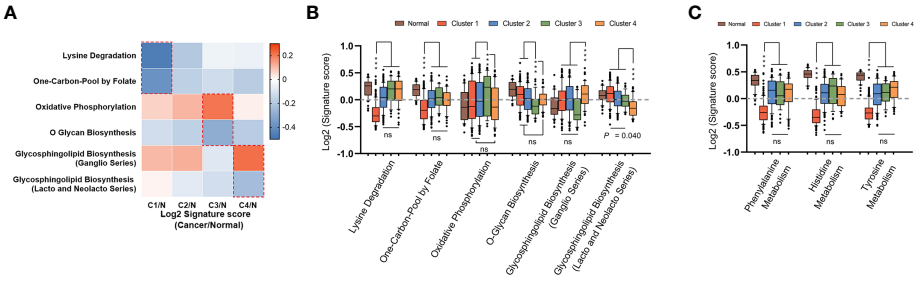

FIGURE 4
Identification of unique metabolic characteristics in each subtype. **(A)** Heatmap displaying the GSVA score of which pathway has exclusivity significant difference between a subtype and normal control group. Pathways that showed significant difference in only one group were marked with dotted box, and were shown in box plots of **(B, C)**, respectively. (ns: not significant, ***: P < 0.001).

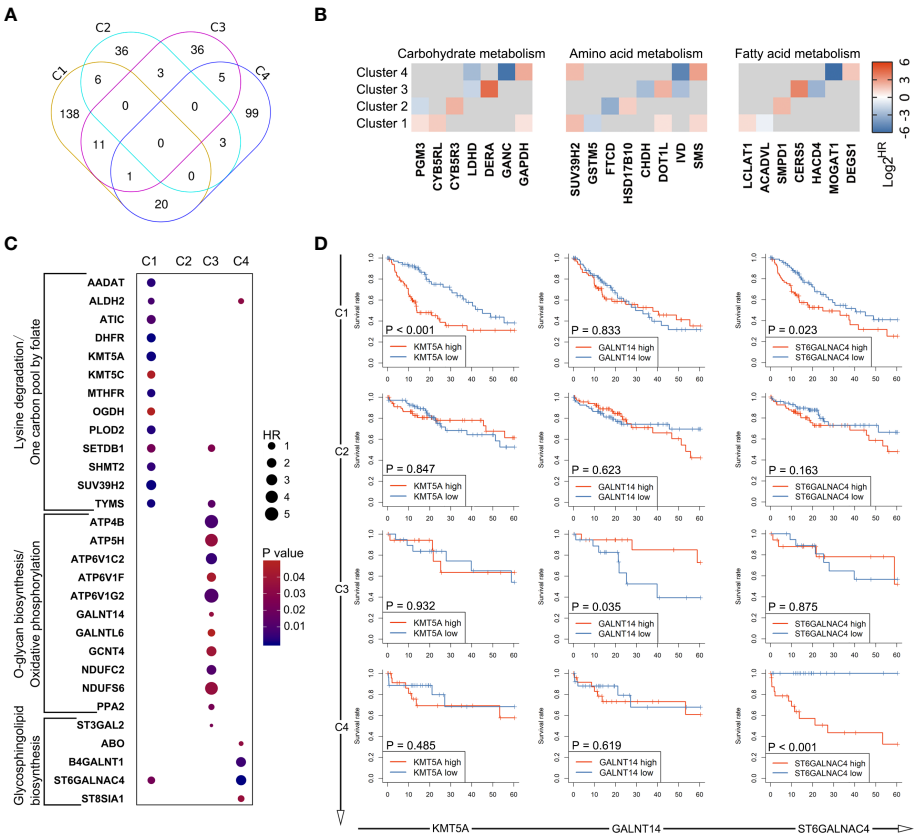

FIGURE 5
Heterogeneity in prognostic significance of metabolic genes stratified by the metabolic subtypes. **(A)** A venn diagram showing common and specific prognostic genes across four subtypes. **(B)** The hazard ratio values (HRs) of prognostic genes involved in glucose metabolism, amino acid metabolism, and fatty acid metabolism are depicted in heatmap. Only HRs of genes with significant prognostic significance are shown. **(C)** Dot plot depicting the prognostic genes involved in unique metabolic pathways described in Figure 4B. **(D)** Several genes were selected from **(C)**, including KMT5A, GALNT14, and ST6GALNAC4. Survival curves showing the predictive role of these genes for over survival in each subtype.

involved in the six characteristic metabolic pathways also revealed specific prognostic value of metabolic genes in their corresponding clusters (Figures 5C, D). These data suggested subtype-specific roles for these unique tumor metabolic pathways as mechanisms contributing to tumor progression and identified some genes of unique metabolic pathways as potential targetable metabolic vulnerabilities in subtype-specific manner.

Relevance of metabolic clusters in immune features

The immune response is associated with dramatic modifications in tissue metabolism, and emerging evidences suggested the tremendous impact of tumor metabolic reprogramming on the immune response (40). Therefore, we assessed the relationship

between the metabolic subtypes and previously defined scores which indicating the abundance of various immune cell populations. The immune landscape revealed significant intra-cluster heterogeneity (Figure 6A). Consistent with an immune-cold phenotype, tumors in mHCC3 had the lowest rate of leukocytes infiltration. Contrary to the immune-cold mHCC3, tumors in mHCC1 had the highest cell infiltration fraction and it was mainly characterized by higher infiltration of lymphocytes. Interestingly, although tumors in mHCC1 displayed the highest infiltration of cytotoxic cells including CD8+ T cells, Tgd, and NK cells, mHCC1 was the subtype with both poorest prognosis and highest T cell exhaustion score (Figure 6B), suggesting that the tumor microenvironment of mHCC1 was immune-hot but highly immune-exhausted type. Most suppressive ligands and receptors for immune checkpoint showed the highest expression levels in mHCC1 (Figure 6C), which is consistent with an immune-suppressive phenotype. Emerging experimental data indicated that the presence of a pre-existing intra-tumoral T cell infiltration, checkpoint molecules (PD-1, PD-L1 expression) could favor a clinical response (41), therefore, we hypothesized that this subtype could benefit much from immune therapy only if the immunosuppressive situation was relieved.

Different from the extreme low/high immune infiltration shown above for mHCC3 and mHCC1, mHCC2 demonstrated a more balanced and favorable immune profile. One major difference from mHCC1 is that the immune composition in mHCC2 was enriched with B cells, macrophages, mast cells, and neutrophils, suggesting an immune microenvironment tended to towards innate immunity and inflammation. The remaining mHCC4 were more diverse with intermediate levels of immune features. The mHCC4 had high infiltration levels of NKdim, Th, Tcm, and Tgd, but showed a low level of other lymphocytic cells, and extremely low levels of B cells, macrophages, mast cells, and neutrophils, which was opposite to mHCC2. Additionally, mHCC4 had the highest level of eosinophils. Together with the specificity of eosinophils infiltration as an index for good prognosis in mHCC4, the above findings supported the major anti-tumor role of eosinophils in the metabolic subtype mHCC4.

The prognostic role of immune cells shown by survival analysis between inter-and intra-cluster was in a high degree of heterogeneity (Figure 6D). For example, among the important cytotoxic T cells, such as CD8+ T cells, and Tgd cells, we found that increased rate of CD8+ T cell infiltration was associated with good prognosis in mHCC1, mHCC2, and mHCC3, but it was not linked with prognosis in mHCC4; in contrast, Tgd infiltration was associated with significantly poor prognosis in mHCC4, but showed no correlation with prognosis in other three clusters. Meanwhile, some immune cells had the opposite prognostic role in different clusters, such as that infiltration of Treg cells was a poor factor in the prognosis of mHCC4 but a good factor of prognosis in mHCC3. The prognostic heterogeneity of immune infiltration revealed different roles of immune cells in different HCC subtypes. Since the metabolic subtypes were produced based on metabolism genes that did not involve signature genes of immune cells, these results suggest a high heterogeneity in component and function of immune microenvironment across these four metabolic subtypes, and support a combination treatment strategy targeting metabolism and immune microenvironment, or the attempt to dig out new target of dual function that combined metabolism-regulation as well as immune-modulation.

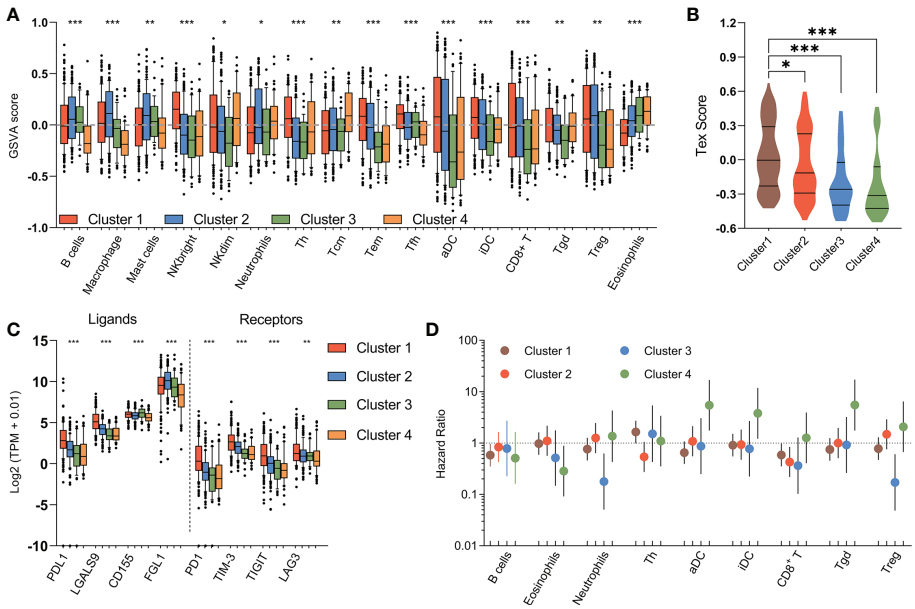

FIGURE 6
Immune characteristics of metabolic subtypes. **(A)** Box plots depicting the abundance of immune cell populations in each subgroup. **(B)** Violin plots showing the distribution of T cell exhaustion scores (Tex Score) in samples of each group. **(C)** Box plots depicting the expression of immune checkpoints across metabolic subtypes. **(D)** The prognostic significance of the abundance of each immune cell population in each subtype are summarized in a forest plot. (*P < 0.05, **P < 0.01, ***P < 0.001).

10.3389/fimmu.2023.1076587

Identification of palmitoyl-protein thioesterase 1, a metabolic gene, as a therapy target for T cell exhaustion with metabolic subgroup specific

Considering that mHCC1 had the poorest prognosis, we tried to identify new therapeutic targets for this subtype. The prognostic metabolic genes were identified, and their correlation with T cell exhaustion, the important feature of mHCC1, was investigated (Figure 7A). Of genes most closely related with T cell exhaustion, we identified palmitoyl-protein thioesterase 1 (PPT1), which was specifically upregulated in mHCC1 and was a specific prognosis factor for mHCC1 (Figures 7B, C). The positive correlation between PPT1 and Tex score (Figure 7D, R = 0.3495, P<0.0001) suggested that PPT1 might contribute to T cell exhaustion. To determine the relationship between PPT1 and glucose metabolism, we analyzed the data of Transcriptomics and metabolomics in the study of Chaisaingmongkol et al. (42). Data LIHC_GSE76297 was used to confirm the high expression of PPT1 in HCC tumor tissues. Through the analysis of glucose metabolism-related metabolites, the content of glucose, maltose and maltotriose decreased in the high expression group of PPT1, suggested that the level of glycolysis

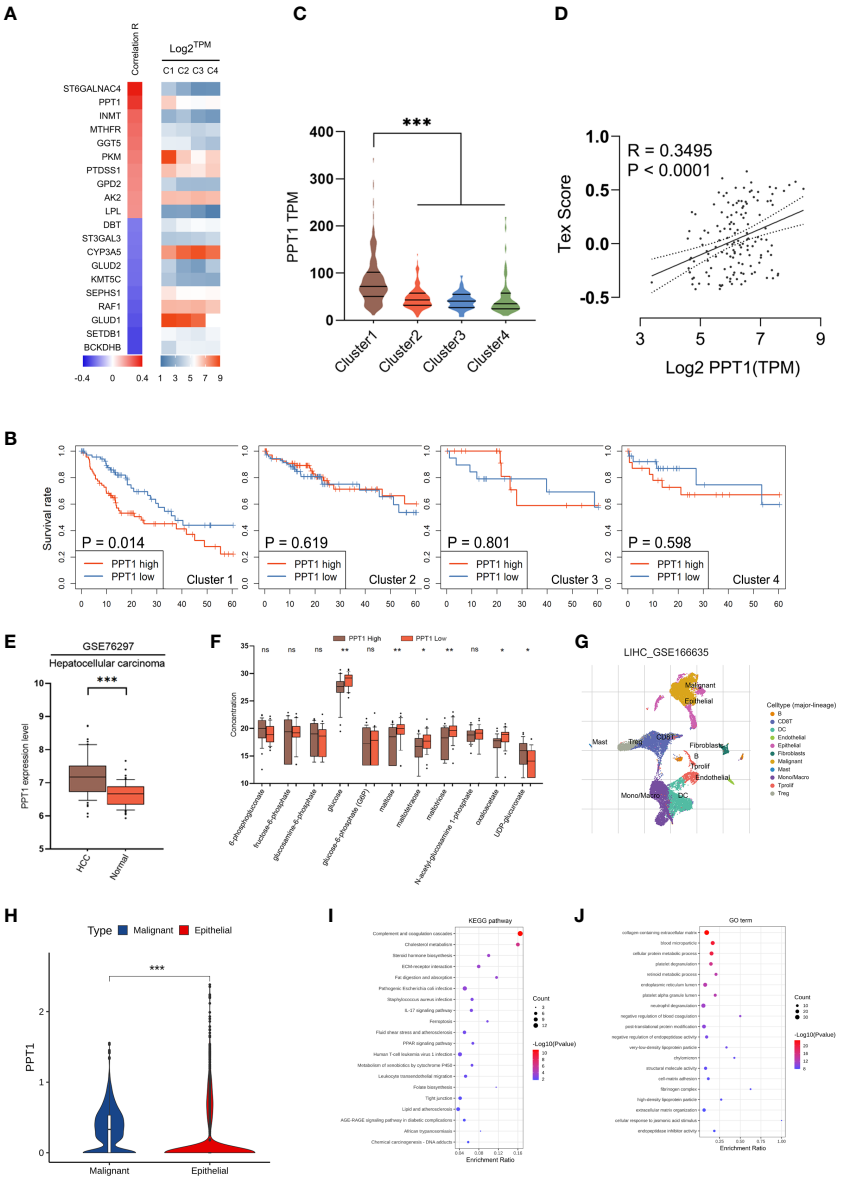

FIGURE 7
Identification of PPT1 as a therapy target. **(A)** Heatmap showing the correlation between prognostic metabolic genes and Tex score. The top 10 most positively/negatively correlated genes are shown. **(B)** Survival curves showing the distinctive prognostic value of PPT1 in different metabolic subtypes. **(C)** Violin plots showing the expression of PPT1 in samples of different subtypes. **(D)** Scatter plot depicting the correlation between PPT1 gene expression and Tex score. **(E)** PPT1 expression in HCC and non-tumorous tissues was analyzed using data in the LIHC_GSE76297. **(F)** Box plots depicting the glycolytic related metabolites between low and high PPT1 expression subgroup. **(G)** Single-cell RNA sequencing revealed the cell types and distribution of HCC. **(H)** Violin plots showing the PPT1 expression between malignant and epithelial cells. **(I, J)** The KEGG pathways **(I)** and GO biological processes **(J)** enrichment analysis of PPT1 in malignant cells. (ns: not significant, *: P < 0.05, **: P < 0.01, ***: P < 0.001).

was exuberant in tissues with high expression of PPT1 (Figures 7E, F). Then, we analyzed the data LIHC_GSE166635 in GEO database using TISCH platform, and the results showed that the expression of PPT1 in malignant cell was strikingly higher than that in epithelial cells (Figures 7G, H). To verify the biological function and mechanism of PPT1, functional annotation analysis was performed on PPT1 in malignant cell. The KEGG pathways and GO biological processes enrichment suggested that PPT1 was closely related to tumor metabolism, immunity, tumor microenvironment and extracellular matrix (Figures 7I, J), which was consistent with the above results that PPT1 is related to tumor metabolism and immunosuppression (43, 44).

In a very recent study, Rebecca et al. identified PPT1 is the molecular target of a novel chloroquine derivative, the DC661; they found that knockout of PPT1 in several cancer cell lines using CRISPR-Cas9 editing resulted in significant impairment of tumor growth similar to that observed with DC661 treatment, which supported the tumor driver role of PPT1 in cancer (45, 46). Therefore, a further question was raised whether PPT1 as a therapeutic target had subtype-specific property and immunomodulating function. *In vitro* study was carried out to verify the above questions. We enhanced the glycolysis activity through overexpression of PKM2 in Huh-7 and JHH-7 cells, cell lines with the intermediate glycolysis level. Downregulation of PPT1 significantly neutralized the proliferative advantage of PKM2 overexpression cells (Figures 8A–C). In addition, PKM2 overexpression markedly increased ECAR (Figure 8D), and we found downregulation of PPT1 in PKM2-overexpressed cells induced a larger drop in ECAR than it did in normal cells, and the same was observed for the lactate production ability (Figure 8E), which partly explained the positive correlation between PPT1 expression and Tex score. We next divided TCGA samples into two groups based on the expression of PKM2, HK2, or FBP1, respectively. Interestingly, the prognostic value of PPT1 expression was only significant in TCGA samples with higher expression of PKM2 (Figure 8F) or HK2 (Figure 8G), two enzymes promote glycolysis, or in TCGA samples with lower expression of FBP1 (Figure 8H), an enzyme inhibits glycolysis.

PPT1 promotes the proliferation, migration, and invasion of HCC *in vitro* and vivo.

Recently, it has been reported that PPT1 is essential for the function of lysosomes, which, as the center of cellular energy sensing and metabolic regulation, play a driving role in the malignant progression of tumor cells (45). In HCC, the increase of glycolysis level and the further enhancement of lysosome and autophagy activity lead to poor prognosis of patients (47). PKM2 is a key rate-limiting enzyme in glycolysis and an important factor in HCC metabolism (48). Therefore, we decided to find out whether PPT1 depends on PKM2 to promote tumor progression through autophagy. Chloroquine, a lysosomal autophagy inhibitor, was used to inhibit autophagy. In Colony formation assay (Figures 9A–D and Supplementary Figures S1A–D), Transwell assay (Figures 9E–H and Supplementary Figures S1E–H) and EdU assay (Figures 9I–L and Supplementary Figures S1I–L), compared with the stably knockdown PKM2 cells, PPT1 could significantly promote the proliferation, migration and invasion of HCC tumor cells in stable overexpression of PKM2 between Huh-7 and JHH-7 cells, interestingly, the proliferation, migration and invasion of tumor cells decreased strikingly after the treatment of chloroquine. Furthermore, Western blotting analysis showed that under the condition of high expression of PKM2, PPT1 could significantly affect the expression of autophagosome protein marker LC3B, while the accumulation of LC3B -II expression increased after chloroquine was added, suggesting that the lysosomal function might be impaired (Figures 9M, N). Collectively, PPT1 may be dependent on PKM2 to promote the progress of HCC through the autophagy.

To further verify the role of PPT1, we constructed Mouse subcutaneous xenograft models. Compared with the control group, the injection of Huh-7 cells stably overexpressing PPT1 and PKM2 significantly promoted tumor growth, while after treatment with chloroquine, tumor growth was inhibited to some extent (Figures 10A–D). In addition, IHC staining showed that Ki-67 levels were notably increased in the tissues of mice treated with stable overexpression of PPT1 and PKM2, suggesting that tumor proliferation was obvious (Figures 10E, F). Taken together, PPT1 relies on PKM2 to promote the malignant progression of HCC by mediating autophagy.

Discussion

HCC is highly heterogeneous and thus difficult for treatment cancer (49). In this regard, continuous progress in the understanding of molecular tumor subtypes is needed to accelerate the development of personalized treatment for HCC patients. Our study established four HCC subtypes with distinct profiles based on the expression of metabolic genes. We found distinct differences in metabolic pathways, immune profiles, and in clinical survival between four major HCC subtypes. Moreover, the markedly immune heterogeneity among the metabolic subtypes provides more biological and clinical significance to our classifier and suggests subtype-specific therapeutic strategies targeting metabolic dependencies and immune regulators alone each or in combination.

Clear evidences supported that metabolic alterations are common for all tumor types (50). As a key organ for whole body energy homeostasis, the liver carries out many metabolic functions (51). Consequently, it is not surprising that metabolic reprogramming is critical during HCC carcinogenesis. Our study demonstrated that HCC was characterized by the absence of normal metabolic genes in noncancerous liver, which was more evident in individual subtypes. This result suggested that alterations in the expression of genes involved in metabolism of normal liver contributed to HCC metabolic heterogeneity. An enzyme or a metabolic pathway enriched in HCC and not in the corresponding normal liver tissue could be used to selectively target tumor cells. Therefore, the degree of normal metabolic genes loss seems an indicator for the success of therapies targeting metabolism.

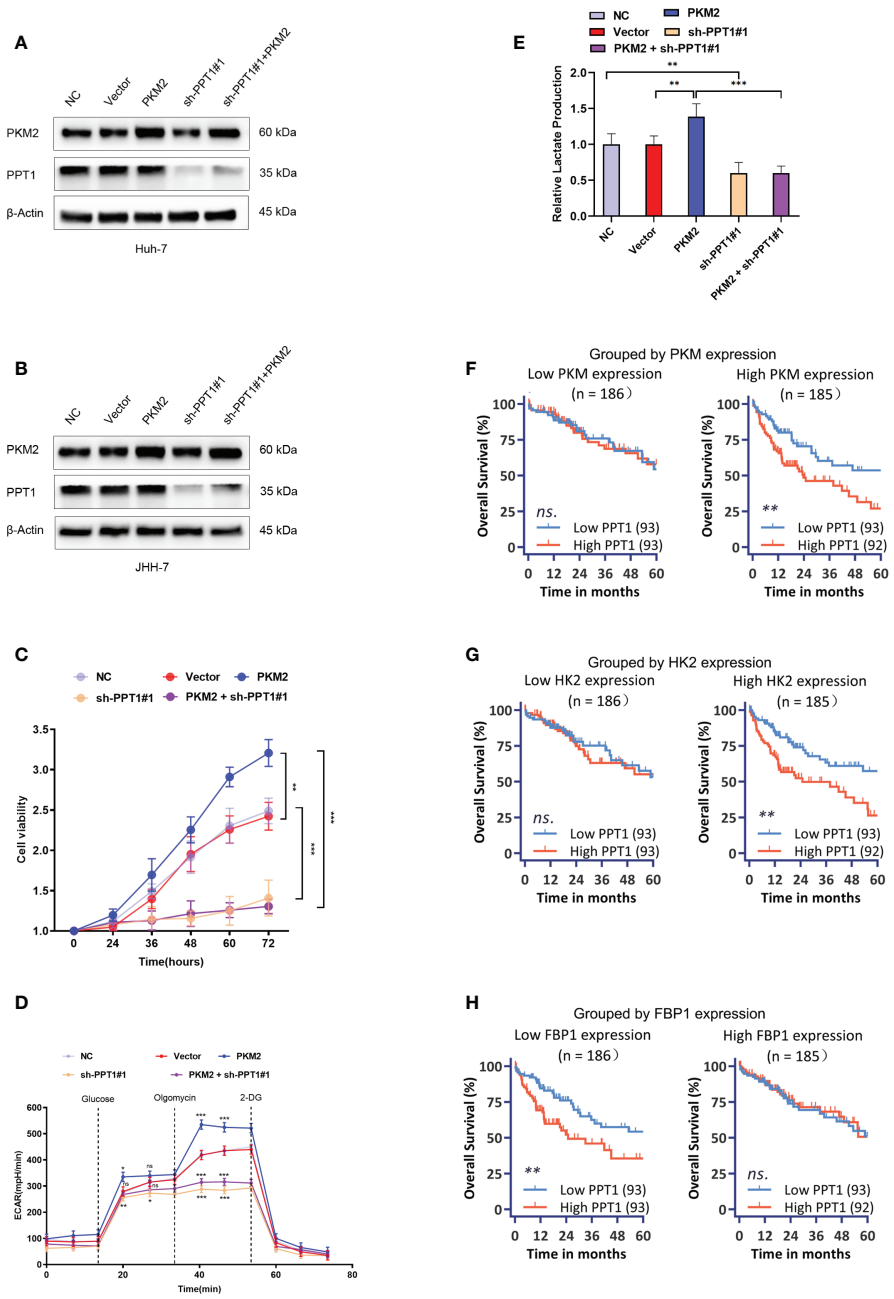

FIGURE 8
Effect of PPT1 knockdown on human HCC cells. **(A, B)** Stable knockdown of PPT1, and overexpression of PKM2 in Huh-7 **(A)** and JHH-7 **(B)** cells by lentiviral vector transfection. The knockdown effect on protein levels were shown for normal control cells (NC), cells transfected with empty vector (Vector), PPT1 knockdown cells (sh-PPT1#1), PKM2 overexpression cells (PKM2), and combination of PKM2 overexpression and PPT1 knockdown (PKM2 + sh-PPT1#1). β-Actin was used as a loading control. **(C)** *In vitro* cell proliferation curves showing the effect of PKM2 overexpression, PPT1 knockdown, or in combination of PKM2 overexpression and PPT1 knockdown on huh-7 cells. **(D)** Seahorse metabolic analysis (ECAR) of normal control cells (NC), cells transfected with empty vector (Vector), PPT1 knockdown cells (sh-PPT1#1), PKM2 overexpression cells (PKM2), and combination of PKM2 overexpression and PPT1 knockdown (PKM2+ sh-PPT1#1). **(E)** Relative lactate production from hun-7 cells upon treatment as annotated. **(F–H)** Survival curves showing the predictive role of PPT1 for prognosis stratified by PKM2 expression **(F)**, HK2 expression **(G)**, or FBP1 expression **(H)**. The error bars are expressed as the mean ± SD of three independent experiments. (ns: not significant, *: P < 0.05, **: P < 0.01, ***: P < 0.001).

Among all four subtypes, the first subtype (mHCC1) demonstrated the worst prognosis, significant downregulation of metabolic genes enriched in normal liver, and broad alternations in most metabolic pathways. HCC involves multiple metabolic abnormalities. In addition to unique metabolic features, alternations in glucose metabolism, lipid metabolism, and amino acid metabolism attracted much wider attention over the past few years (52–54). Most cancer cells reprogram cellular glucose metabolism to constitute a selective advantage for proliferation (55). Among them, HCC probably displays the most comprehensive reprogramming of glucose metabolism, which was essential for the maintaining of tumor growth and progression (56). Altered amino

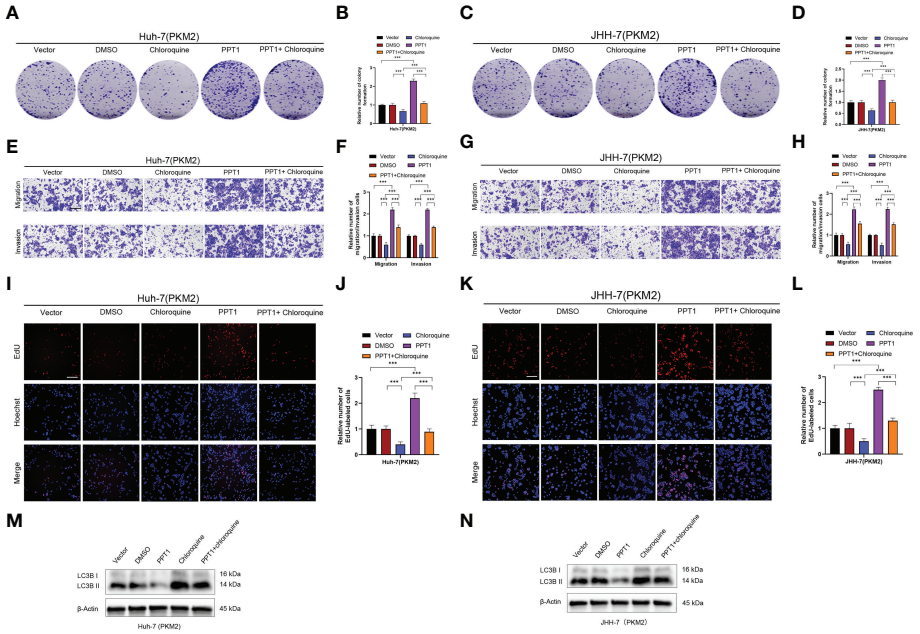

FIGURE 9
PPT1 promotes the proliferation, migration and invasion of HCC *via* lysosomes *in vitro*. **(A–D)** The colony formation was counted in stable overexpression of PKM2 between Huh-7 **(A, B)** and JHH-7 **(C, D)** cells. **(E–H)** Representative images and histogram analysis of Transwell migration and Matrigel invasion assays in stable overexpression of PKM2 between Huh-7 **(E, F)** and JHH-7 **(G, H)** cells. Scale bars: 100 μm. **(I-L)** Representative images and histogram analysis of EdU assays in stable overexpression of PKM2 between Huh-7 **(I, J)** and JHH-7 **(K, L)** cells. Scale bars: 100 μm. **(M, N)** Western blotting analysis of PPT1 and LC3B in stable overexpression of PKM2 between Huh-7 **(M)** and JHH-7 **(N)** cells. β-Actin was used as a loading control. The error bars are expressed as the mean ± SD of three independent experiments. (***: $P < 0.001$).

acid metabolism and lipid metabolism also characterize HCC compared with other liver diseases. GSVA analysis indicated that tumors of the first subtype had significant alternations in all pathways associated with glucose metabolism, and most pathways involved in lipid and amino metabolism in comparison with other tumors and normal liver tissues. This finding suggests that tumors in this subtype rely heavily on reprogramed metabolism, which is therefore an appropriate candidate for metabolism-target therapy.

One of the clinical-translational relevance of this subtype classification is that it suggested that different metabolic subtypes have different therapeutic and prognostic targets, since the prognostic significance of a particular metabolic gene could be different between each subtype. For example, PPT1, a gene that was detected as a special prognostic factor only for mHCC1, regulates the lysosomal acidity necessary for cellular catabolism. The catabolic function and nutrient sensing activity of the lysosome make it as a metabolic signaling center (57). Lysosome is a key central delivery port for substrates destined for breakdown and serve to recycle the constituent building blocks (58). The central position of the lysosome system in cancer have made it a promising target in anti-tumor therapy, especially for those alterations that are highly dependent on metabolism to fulfill their anabolic demands (46). A previous study has identified that KO PPT1 cells showed impaired lysosomal deacidification, decreased proliferation, and increased apoptosis both *in vitro* and *in vivo* (45). Consistent with the above assumption, we found PPT1 have special prognostic value in the first subtype, and knockdown of PPT1 significantly neutralized the PKM2 overexpression-induced growth advantage in HCC cells. Despite PPT1 being a promising target for HCC tumors with relatively abundant metabolism alternations, these findings supported that the therapy strategy in a metabolic subtype-specific manner might be more efficient than those trying to cover all patients. The subtype classification of this study provided clues for future research.

In healthy tissues, neighboring cells cooperate to build a harmonious metabolic environment, which is usually disrupted in cancer tissues (59). As a result of altered tumor metabolism, cells in tumor microenvironment suffer from lacking essential nutrients while atypical metabolites accumulate, along with impaired antitumor immunity (40, 60, 61). One example is the competition for glucose between T lymphocytes and tumor cells; T cells consume extracellular glucose to fulfill their activation, and suppression of glucose take up, such as knockout glucose transporters, inhibited proliferation of activated CD4+ T cells and generation of effector T cells (62). In turn, elevated lactate production in glycolytic cancer cells suppressed survival of effector T and NK cells and promoted immune escape (63). In this study, perhaps surprisingly, we found distinct immune infiltration profiles, as well as expression of immune checkpoints and T cell exhaustion levels in different metabolic subtypes. Additionally, the prognostic significance of infiltration level for the same immune cell was distinct in different subgroups. These findings revealed an intimate link between metabolic subtypes and immune heterogeneity; suggested personalized immunotherapy strategy according to the metabolic subtypes. For example, the mHCC1, despite its significantly altered metabolic pathways, was characterized by high immune infiltration, high T cell-exhausted signature, and high expression of suppressive

10.3389/fimmu.2023.1076587

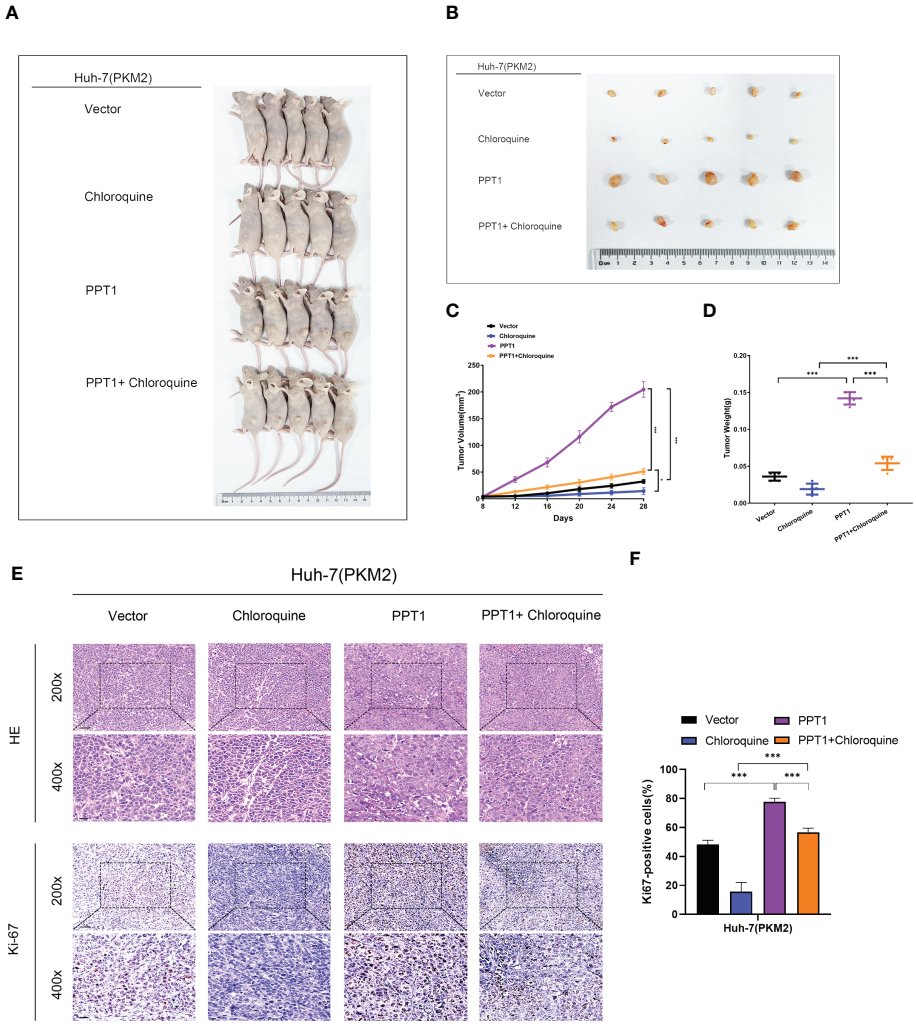

FIGURE 10
PPT1 promotes HCC tumorigenicity and progression *in vivo*. **(A, B)** Representative images of subcutaneous xenograft tumors in stable overexpression of PKM2 Huh-7 cells treated with Vector, Chloroquine, PPT1 lentivirus and PPT1 lentivirus + Chloroquine (n=5). **(C, D)** The tumor volume **(C)** and weight **(D)** were evaluated in each group. **(E, F)** Representative images **(E)** and histogram analysis **(F)** of IHC for Ki-67. Scale bars: 200× =50 μm; 400× =20 μm. The error bars are expressed as the mean ± SD of three independent experiments. (*: P < 0.05, ***: P < 0.001).

immune checkpoints; all indicating the applicability of treatment strategy through combination of metabolism-targeted and immune-targeted therapies in this subtype. In contrast, mHCC2 was the only subtype which did not show significantly altered expression of normal metabolic genes in the GSEA analysis, suggesting that metabolism-targeted therapy is not a priority for patients with this subtype.

Tumors in mHCC4 had distinct mutations compared with other three groups. More than 76% of patients with this subtype harbored mutations in CTNNB1. A very recent report discovered that Wnt/CTNNB1 mutations could characterize the immune excluded class (cold tumors) and might represent the biomarkers predicting resistance to immune checkpoint inhibitors (64, 65). Consistent with this report, subtype 4 showed a low enrichment level for signatures of most immune cells. Only in subtype 4, CD8+ T cell infiltration had almost no correlation with the prognosis. Besides, many immunosuppressive checkpoints, including PD1, PD-L1, TIM-3, LAG3, and others, showed the lowest expression levels in this subtype. All these suggested innate resistance to checkpoint inhibitors. But fortunately, tumors of this subtype demonstrate highly altered metabolism which is second only to subtype 1. Therefore, effort to uncover new metabolism-related targets in this subtype might be helpful. Additionally, unlike the other three subtypes, increased infiltration of aDC, iDC, or Tgd were all associated with poor prognosis. The unique roles of these immune cells and their correlation with metabolism merits further study.

Another interesting finding in the present study was that some molecules might be good target to "kill two birds with one stone". For example, PPT1 showed much more correlation with cell viability, glucose metabolism activity, lactate production, and T cell exhaustion in HCCs with enhanced metabolic alterations, which should be especially applicable for the mHCC1 tumors with obvious alterations in metabolism and enhanced proliferation. This also provided clues for the treatment strategy for other subtypes. The tumors in subtype 3 also seemed like "cold' tumors"; they had aberrant decreased enrichment of immune signatures and showed a low level of metabolism alteration. However, the mHCC3 had its own

unique characteristic: CTNNB1 mutations was rare in this subtype; it was the only subtype that benefited from enrichment in aDC; moreover, CD8+ T cell enrichment showed the lowest HR value, suggesting a high anti-tumor activity of effector T cells in tumors of this subtype. Therefore, the barrier for immunotherapy in this subtype seemed more from impaired in immune chemotaxis, immune presentation, and expansion, but which has rare relation with CTNNB1 mutations and PD1/PD-L1. We noted that mHCC3 was characterized by significant altered O-Glycan biosynthesis metabolisms. Although the impact of tumor glycans on anti-tumor immunity has not yet been fully elucidated, the abundant and aberrant cancer glycosylation profile is currently accepted as a distinct hallmark of cancer, and tumor-associated O-glycans bind a variety of receptors on immune cells to facilitate the subsequently induction of immunosuppression (66). Determining whether O-Glycan metabolism could play a dual role as both metabolism and immunotherapy targets requires further investigation.

In summary, our study introduced a novel metabolic class in HCC cases, which comprise not only metabolic heterogeneity but also immune heterogeneity. The metabolic heterogeneity demonstrated that some reprogrammed metabolic pathways affected tumor progression in different rates depending on the subtype, which supports the development of subtype-specific treatment strategies targeting unique metabolic vulnerabilities. The immune heterogeneity across metabolic subtypes suggested that it might be effective to select different immune therapeutic strategies according to different metabolic subtypes. The correlation between immune characters and metabolic features also helped us to find an individualized therapeutic target, the PPT1. Further investigations of the effect of metabolism pathways on both tumor progression and immunologic microenvironment is worthy of study.

Data availability statement

Publicly available datasets were analyzed in this study. This data can be found here: TCGA database (https://portal.gdc.cancer.gov/), GEO database (https://www.ncbi.nlm.nih.gov/geo/),Molecular Signature Database (MSigDB, https://www.gsea-msigdb.org/gsea/msigdb).The datasets presented in this study can be found in online repositories. The names of the repository/repositories and accession number(s) can be found in the article/Supplementary Figures and Method.

Ethics statement

The animal study was reviewed and approved by the Guangdong Provincial People's Hospital and the Animal Experimental Research Ethics Committee of South China University of Technology. [Approval number: KY-N-2022-130-01].

Author contributions

RFC and YZ conceived and designed the study. JY, LZ, and RWC collected and analyzed the data. JY and LZ performed *in vitro* and vivo studies. SZ and RWC review the literature. JY, LZ and RFC wrote the manuscript. All authors contributed to the article and approved the submitted version.

Funding

This work was financially supported the National Natural Science Foundation of China (grant number: 82072639), and the Special Fund of "Dengfeng Plan" of Guangdong Provincial People's Hospital, China (KJ012019509, DFJH2020027), the Outstanding Youth Scholars Project of Guangdong Provincial People's Hospital (No. KJ012019096).

Conflict of interest

The authors declare that the research was conducted in the absence of any commercial or financial relationships that could be construed as a potential conflict of interest.

Publisher's note

Supplementary material

The Supplementary Material for this article can be found online at: https://www.frontiersin.org/articles/10.3389/fimmu.2023.1076587/full#supplementary-material

References

1. Siegel RL, Miller KD, Fuchs HE, Jemal A. Cancer statistics, 2022. *CA Cancer J Clin* (2022) 72(1):7–33. doi: 10.3322/caac.21708

2. Maluccio M, Covey A. Recent progress in understanding, diagnosing, and treating hepatocellular carcinoma. *CA Cancer J Clin* (2012) 62(6):394–9. doi: 10.3322/caac.21161

3. Llovet JM, Ricci S, Mazzaferro V, Hilgard P, Gane E, Blanc J-F, et al. Sorafenib in advanced hepatocellular carcinoma. *N Engl J Med* (2008) 359(4):378–90. doi: 10.1056/NEJMoa0708857

4. Bruix J, Qin S, Merle P, Granito A, Huang Y-H, Bodoky G, et al. Regorafenib for patients with hepatocellular carcinoma who progressed on sorafenib treatment

(Resorce): A randomised, double-blind, placebo-controlled, phase 3 trial. *Lancet* (2017) 389(10064):56–66. doi: 10.1016/S0140-6736(16)32453-9

5. Bruix J, Tak W-Y, Gasbarrini A, Santoro A, Colombo M, Lim H-Y, et al. Regorafenib as second-line therapy for intermediate or advanced hepatocellular carcinoma: Multicentre, open-label, phase ii safety study. *Eur J Cancer (Oxford Engl 1990)* (2013) 49(16):3412–9. doi: 10.1016/j.ejca.2013.05.028

6. Finn RS, Merle P, Granito A, Huang Y-H, Bodoky G, Pracht M, et al. Outcomes of sequential treatment with sorafenib followed by regorafenib for hcc: Additional analyses from the phase iii resorce trial. *J Hepatol* (2018) 69(2):353–8. doi: 10.1016/j.jhep.2018.04.010

7. Parikh ND, Pillai A. Recent advances in hepatocellular carcinoma treatment. *Clin Gastroenterol Hepatol* (2021) 19(10):2020–4. doi: 10.1016/j.cgh.2021.05.045

8. Geh D, Leslie J, Rumney R, Reeves HL, Bird TG, Mann DA. Neutrophils as potential therapeutic targets in hepatocellular carcinoma. *Nat Rev Gastroenterol Hepatol* (2022) 19(4):257–73. doi: 10.1038/s41575-021-00568-5

9. Pavlova NN, Zhu J, Thompson CB. The hallmarks of cancer metabolism: Still emerging. *Cell Metab* (2022) 34(3):355–77. doi: 10.1016/j.cmet.2022.01.007

10. Martínez-Reyes I, Chandel NS. Cancer metabolism: Looking forward. *Nat Rev Cancer* (2021) 21(10):669–80. doi: 10.1038/s41568-021-00378-6

11. Icard P, Shulman S, Farhat D, Steyaert J-M, Alifano M, Lincet H. How the warburg effect supports aggressiveness and drug resistance of cancer cells? *Drug Resist Update* (2018) 38:1–11. doi: 10.1016/j.drup.2018.03.001

12. Pinter M, Scheiner B, Peck-Radosavljevic M. Immunotherapy for advanced hepatocellular carcinoma: A focus on special subgroups. *Gut* (2021) 70(1):204–14. doi: 10.1136/gutjnl-2020-321702

13. Tan PS, Aguiar P, Haaland B, Lopes G. Comparative effectiveness of immune-checkpoint inhibitors for previously treated advanced non-small cell lung cancer - a systematic review and network meta-analysis of 3024 participants. *Lung Cancer* (2018) 115:84–8. doi: 10.1016/j.lungcan.2017.11.017

14. Robert C, Ribas A, Schachter J, Arance A, Grob J-J, Mortier L, et al. Pembrolizumab versus ipilimumab in advanced melanoma (Keynote-006): *Post-hoc* 5-year results from an open-label, multicentre, randomised, controlled, phase 3 study. *Lancet Oncol* (2019) 20(9):1239–51. doi: 10.1016/S1470-2045(19)30388-2

15. Peeraphatdit TB, Wang J, Odenwald MA, Hu S, Hart J, Charlton MR. Hepatotoxicity from immune checkpoint inhibitors: A systematic review and management recommendation. *Hepatol (Baltimore Md)* (2020) 72(1):315–29. doi: 10.1002/hep.31227

16. Llovet JM, De Baere T, Kulik L, Haber PK, Greten TF, Meyer T, et al. Locoregional therapies in the era of molecular and immune treatments for hepatocellular carcinoma. *Nat Rev Gastroenterol Hepatol* (2021) 18(5):293–313. doi: 10.1038/s41575-020-00395-0

17. Pinter M, Jain RK, Duda DG. The current landscape of immune checkpoint blockade in hepatocellular carcinoma: A review. *JAMA Oncol* (2021) 7(1):113–23. doi: 10.1001/jamaoncol.2020.3381

18. Trefts E, Gannon M, Wasserman DH. The liver. *Curr Biol* (2017) 27(21):R1147–R51. doi: 10.1016/j.cub.2017.09.019

19. De Matteis S, Ragusa A, Marisi G, De Domenico S, Casadei Gardini A, Bonafè M, et al. Aberrant metabolism in hepatocellular carcinoma provides diagnostic and therapeutic opportunities. *Oxid Med Cell Longev* (2018) 2018:7512159. doi: 10.1155/2018/7512159

20. Craig AJ, von Felden J, Garcia-Lezana T, Sarcognato S, Villanueva A. Tumour evolution in hepatocellular carcinoma. *Nat Rev Gastroenterol Hepatol* (2020) 17(3):139–52. doi: 10.1038/s41575-019-0229-4

21. Liao H, Du J, Wang H, Lan T, Peng J, Wu Z, et al. Integrated proteogenomic analysis revealed the metabolic heterogeneity in noncancerous liver tissues of patients with hepatocellular carcinoma. *J Hematol Oncol* (2021) 14(1):205. doi: 10.1186/s13045-021-01195-y

22. Ng CKY, Dazert E, Boldanova T, Coto-Llerena M, Nuciforo S, Ercan C, et al. Integrative proteogenomic characterization of hepatocellular carcinoma across etiologies and stages. *Nat Commun* (2022) 13(1):2436. doi: 10.1038/s41467-022-29960-8

23. Ramapriyan R, Caetano MS, Barsoumian HB, Mafra ACP, Zambalde EP, Menon H, et al. Altered cancer metabolism in mechanisms of immunotherapy resistance. *Pharmacol Ther* (2019) 195:162–71. doi: 10.1016/j.pharmthera.2018.11.004

24. Afonso J, Santos LL, Longatto-Filho A, Baltazar F. Competitive glucose metabolism as a target to boost bladder cancer immunotherapy. *Nat Rev Urol* (2020) 17(2):77–106. doi: 10.1038/s41585-019-0263-6

25. Ho DW-H, Tsui Y-M, Chan L-K, Sze KM-F, Zhang X, Cheu JW-S, et al. Single-cell rna sequencing shows the immunosuppressive landscape and tumor heterogeneity of hbv-associated hepatocellular carcinoma. *Nat Commun* (2021) 12(1):3684. doi: 10.1038/s41467-021-24010-1

26. Nguyen PHD, Ma S, Phua CZJ, Kaya NA, Lai HLH, Lim CJ, et al. Intratumoural immune heterogeneity as a hallmark of tumour evolution and progression in hepatocellular carcinoma. *Nat Commun* (2021) 12(1):227. doi: 10.1038/s41467-020-20171-7

27. Subramanian A, Tamayo P, Mootha VK, Mukherjee S, Ebert BL, Gillette MA, et al. Gene set enrichment analysis: A knowledge-based approach for interpreting genome-wide expression profiles. *Proc Natl Acad Sci U.S.A.* (2005) 102(43):15545–50. doi: 10.1073/pnas.0506580102

28. Galili T. Dendextend: An r package for visualizing, adjusting and comparing trees of hierarchical clustering. *Bioinformatics* (2015) 31(22):3718–20. doi: 10.1093/bioinformatics/btv428

29. Pedregosa F, Varoquaux G, Gramfort A, Michel V, Thirion B, Grisel O, et al. Scikit-learn: Machine learning in Python. *J Mach Learn Res* (2011) 12(null):2825–30. doi: 10.5555/1953048.2078195

30. Hanzelmann S, Castelo R, Guinney J. Gsva: Gene set variation analysis for microarray and rna-seq data. *BMC Bioinf* (2013) 14:7. doi: 10.1186/1471-2105-14-7

31. Zheng C, Zheng L, Yoo J-K, Guo H, Zhang Y, Guo X, et al. Landscape of infiltrating T cells in liver cancer revealed by single-cell sequencing. *Cell* (2017) 169(7):1342–56 e16. doi: 10.1016/j.cell.2017.05.035

32. Tamborero D, Rubio-Perez C, Muiños F, Sabarinathan R, Piulats JM, Muntasell A, et al. A pan-cancer landscape of interactions between solid tumors and infiltrating immune cell populations. *Clin Cancer Res* (2018) 24(15):3717–28. doi: 10.1158/1078-0432.CCR-17-3509

33. Sun D, Wang J, Han Y, Dong X, Ge J, Zheng R, et al. Tisch: A comprehensive web resource enabling interactive single-cell transcriptome visualization of tumor microenvironment. *Nucleic Acids Res* (2021) 49(D1):D1420–D30. doi: 10.1093/nar/gkaa1020

34. Feng S, Gao L, Zhang D, Tian X, Kong L, Shi H, et al. Mir-93 regulates vascular smooth muscle cell proliferation, and neointimal formation through targeting Mfn2. *Int J Biol Sci* (2019) 15(12):2615–26. doi: 10.7150/ijbs.36995

35. Pan T, Sun S, Chen Y, Tian R, Chen E, Tan R, et al. Immune effects of Pi3k/Akt/Hif-1alpha-Regulated glycolysis in polymorphonuclear neutrophils during sepsis. *Crit Care* (2022) 26(1):29. doi: 10.1186/s13054-022-03893-6

36. Wang L, Pavlou S, Du X, Bhuckory M, Xu H, Chen M. Glucose transporter 1 critically controls microglial activation through facilitating glycolysis. *Mol Neurodegener* (2019) 14(1):2. doi: 10.1186/s13024-019-0305-9

37. Zhou Y, Lin F, Wan T, Chen A, Wang H, Jiang B, et al. Zeb1 enhances warburg effect to facilitate tumorigenesis and metastasis of hcc by transcriptionally activating pfkm. *Theranostics* (2021) 11(12):5926–38. doi: 10.7150/thno.56490

38. Hu B, Lin J-Z, Yang X-B, Sang X-T. Aberrant lipid metabolism in hepatocellular carcinoma cells as well as immune microenvironment: A review. *Cell Prolif* (2020) 53(3):e12772. doi: 10.1111/cpr.12772

39. Rui L. Energy metabolism in the liver. *Compr Physiol* (2014) 4(1):177–97. doi: 10.1002/cphy.c130024

40. Patel CH, Leone RD, Horton MR, Powell JD. Targeting metabolism to regulate immune responses in autoimmunity and cancer. *Nat Rev Drug Discovery* (2019) 18(9):669–88. doi: 10.1038/s41573-019-0032-5

41. Sia D, Jiao Y, Martinez-Quetglas I, Kuchuk O, Villacorta-Martin C, Castro de Moura M, et al. Identification of an immune-specific class of hepatocellular carcinoma, based on molecular features. *Gastroenterology* (2017) 153(3):812–26. doi: 10.1053/j.gastro.2017.06.007

42. Chaisaingmongkol J, Budhu A, Dang H, Rabibhadana S, Pupacdi B, Kwon SM, et al. Common molecular subtypes among Asian hepatocellular carcinoma and cholangiocarcinoma. *Cancer Cell* (2017) 32(1):57–70 e3. doi: 10.1016/j.ccell.2017.05.009

43. Kanehisa M, Goto S. Kegg: Kyoto encyclopedia of genes and genomes. *Nucleic Acids Res* (2000) 28(1):27–30. doi: 10.1093/nar/28.1.27

44. Carbon S, Ireland A, Mungall CJ, Shu S, Marshall B, Lewis S, et al. Amigo: Online access to ontology and annotation data. *Bioinformatics* (2009) 25(2):288–9. doi: 10.1093/bioinformatics/btn615

45. Rebecca VW, Nicastri MC, Fennelly C, Chude CI, Barber-Rotenberg JS, Ronghe A, et al. Ppt1 promotes tumor growth and is the molecular target of chloroquine derivatives in cancer. *Cancer Discovery* (2019) 9(2):220–9. doi: 10.1158/2159-8290.CD-18-0706

46. Rebecca VW, Nicastri MC, McLaughlin N, Fennelly C, McAfee Q, Ronghe A, et al. A unified approach to targeting the lysosome's degradative and growth signaling roles. *Cancer Discovery* (2017) 7(11):1266–83. doi: 10.1158/2159-8290.CD-17-0741

47. Jiao L, Zhang HL, Li DD, Yang KL, Tang J, Li X, et al. Regulation of glycolytic metabolism by autophagy in liver cancer involves selective autophagic degradation of Hk2 (Hexokinase 2). *Autophagy* (2018) 14(4):671–84. doi: 10.1080/15548627.2017.1381804

48. Rao J, Wang H, Ni M, Wang Z, Wang Z, Wei S, et al. Fstl1 promotes liver fibrosis by reprogramming macrophage function through modulating the intracellular function of Pkm2. *Gut* (2022) 71(12):2539–50. doi: 10.1136/gutjnl-2021-325150

49. Dagogo-Jack I, Shaw AT. Tumour heterogeneity and resistance to cancer therapies. *Nat Rev Clin Oncol* (2018) 15(2):81–94. doi: 10.1038/nrclinonc.2017.166

50. DeBerardinis RJ, Lum JJ, Hatzivassiliou G, Thompson CB. The biology of cancer: Metabolic reprogramming fuels cell growth and proliferation. *Cell Metab* (2008) 7(1):11–20. doi: 10.1016/j.cmet.2007.10.002

51. Piccinin E, Villani G, Moschetta A. Metabolic aspects in nafld, Nash and hepatocellular carcinoma: The role of Pgc1 coactivators. *Nat Rev Gastroenterol Hepatol* (2019) 16(3):160–74. doi: 10.1038/s41575-018-0089-3

52. Todisco S, Convertini P, Iacobazzi V, Infantino V. Tca cycle rewiring as emerging metabolic signature of hepatocellular carcinoma. *Cancers (Basel)* (2019) 12(1):68. doi: 10.3390/cancers12010068

53. Nakagawa H, Hayata Y, Kawamura S, Yamada T, Fujiwara N, Koike K. Lipid metabolic reprogramming in hepatocellular carcinoma. *Cancers (Basel)* (2018) 10(11):447. doi: 10.3390/cancers10110447

54. Björnson E, Mukhopadhyay B, Asplund A, Pristovsek N, Cinar R, Romeo S, et al. Stratification of hepatocellular carcinoma patients based on acetate utilization. *Cell Rep* (2015) 13(9):2014–26. doi: 10.1016/j.celrep.2015.10.045

55. Liberti MV, Locasale JW. The warburg effect: How does it benefit cancer cells? *Trends Biochem Sci* (2016) 41(3):211–8. doi: 10.1016/j.tibs.2015.12.001

56. Shang R-Z, Qu S-B, Wang D-S. Reprogramming of glucose metabolism in hepatocellular carcinoma: Progress and prospects. *World J Gastroenterol* (2016) 22 (45):9933–43. doi: 10.3748/wjg.v22.i45.9933

57. Lawrence RE, Zoncu R. The lysosome as a cellular centre for signalling, metabolism and quality control. *Nat Cell Biol* (2019) 21(2):133–42. doi: 10.1038/s41556-018-0244-7

58. Lamming DW, Bar-Peled L. Lysosome: The metabolic signaling hub. *Traffic* (2019) 20(1):27–38. doi: 10.1111/tra.12617

59. Madi A, Cui G. Regulation of immune cell metabolism by cancer cell oncogenic mutations. *Int J Cancer* (2020) 147(2):307–16. doi: 10.1002/ijc.32888

60. Ngwa VM, Edwards DN, Philip M, Chen J. Microenvironmental metabolism regulates antitumor immunity. *Cancer Res* (2019) 79(16):4003–8. doi: 10.1158/0008-5472.CAN-19-0617

61. Riera-Domingo C, Audigé A, Granja S, Cheng W-C, Ho P-C, Baltazar F, et al. Immunity, hypoxia, and metabolism-the ménage à trois of cancer: Implications for immunotherapy. *Physiol Rev* (2020) 100(1):1–102. doi: 10.1152/physrev.00018.2019

62. Macintyre AN, Gerriets VA, Nichols AG, Michalek RD, Rudolph MC, Deoliveira D, et al. The glucose transporter Glut1 is selectively essential for Cd4 T cell activation and effector function. *Cell Metab* (2014) 20(1):61–72. doi: 10.1016/j.cmet.2014.05.004

63. Brand A, Singer K, Koehl GE, Kolitzus M, Schoenhammer G, Thiel A, et al. Ldha-associated lactic acid production blunts tumor immunosurveillance by T and nk cells. *Cell Metab* (2016) 24(5):657–71. doi: 10.1016/j.cmet.2016.08.011

64. Pinyol R, Sia D, Llovet JM. Immune exclusion-Wnt/Ctnnb1 class predicts resistance to immunotherapies in hcc. *Clin Cancer Res* (2019) 25(7):2021–3. doi: 10.1158/1078-0432.CCR-18-3778

65. Gao Q, Zhu H, Dong L, Shi W, Chen R, Song Z, et al. Integrated proteogenomic characterization of hbv-related hepatocellular carcinoma. *Cell* (2019) 179(2):561–77.e22. doi: 10.1016/j.cell.2019.08.052

66. Cornelissen LAM, Van Vliet SJ. A bitter sweet symphony: Immune responses to altered O-glycan epitopes in cancer. *Biomolecules* (2016) 6(2):26. doi: 10.3390/biom6020026

frontiers | Frontiers in Immunology

TYPE Original Research
PUBLISHED 23 March 2023
DOI 10.3389/fimmu.2023.1116760

OPEN ACCESS

EDITED BY
Soumya R. Mohapatra,
KIIT University, India

REVIEWED BY
Clovis Palmer,
Tulane University, United States
Khushboo Borah Slater,
University of Surrey, United Kingdom

*CORRESPONDENCE
Emma Leacy
leacyej@tcd.ie
Mark A. Little
mlittle@tcd.ie

†These authors have contributed equally to this work

SPECIALTY SECTION
This article was submitted to Cancer Immunity and Immunotherapy, a section of the journal Frontiers in Immunology

RECEIVED 05 December 2022
ACCEPTED 03 March 2023
PUBLISHED 23 March 2023

CITATION
Leacy E, Batten I, Sanelli L, McElheron M, Brady G, Little MA and Khouri H (2023) Optimal LC-MS metabolomic profiling reveals emergent changes to monocyte metabolism in response to lipopolysaccharide.
Front. Immunol. 14:1116760.
doi: 10.3389/fimmu.2023.1116760

Optimal LC-MS metabolomic profiling reveals emergent changes to monocyte metabolism in response to lipopolysaccharide

Emma Leacy[1*], Isabella Batten[1], Laetitia Sanelli[2], Matthew McElheron[1], Gareth Brady[1†], Mark A. Little[1,3*†] and Hania Khouri[4†]

[1]Trinity Translational Medicine Institute, Faculty of Health Sciences, Trinity College Dublin, Dublin, Ireland, [2]Faculty of Health Medicine and Life Sciences, Maastricht University, Maastricht, Netherlands, [3]Trinity Health Kidney Centre, Tallaght University Hospital, Dublin, Ireland, [4]Agilent Technologies, Stockpoty, England, United Kingdom

Introduction: Immunometabolism examines the links between immune cell function and metabolism. Dysregulation of immune cell metabolism is now an established feature of innate immune cell activation. Advances in liquid chromatography mass spectrometry (LC-MS) technologies have allowed discovery of unique insights into cellular metabolomics. Here we have studied and compared different sample preparation techniques and data normalisation methods described in the literature when applied to metabolomic profiling of human monocytes.

Methods: Primary monocytes stimulated with lipopolysaccharide (LPS) for four hours was used as a study model. Monocytes (n=24) were freshly isolated from whole blood and stimulated for four hours with lipopolysaccharide (LPS). A methanol-based extraction protocol was developed and metabolomic profiling carried out using a Hydrophilic Interaction Liquid Chromatography (HILIC) LC-MS method. Data analysis pipelines used both targeted and untargeted approaches, and over 40 different data normalisation techniques to account for technical and biological variation were examined. Cytokine levels in supernatants were measured by ELISA.

Results: This method provided broad coverage of the monocyte metabolome. The most efficient and consistent normalisation method was measurement of residual protein in the metabolite fraction, which was further validated and optimised using a commercial kit. Alterations to the monocyte metabolome in response to LPS can be detected as early as four hours post stimulation. Broad and profound changes in monocyte metabolism were seen, in line with increased cytokine production. Elevated levels of amino acids and Krebs cycle metabolites were noted and decreases in aspartate and β-alanine are also reported for the first time. In the untargeted analysis, 154 metabolite entities were significantly altered compared to unstimulated cells. Pathway analysis

revealed the most prominent changes occurred to (phospho-) inositol metabolism, glycolysis, and the pentose phosphate pathway.

Discussion: These data report the emergent changes to monocyte metabolism in response to LPS, in line with reports from later time points. A number of these metabolites are reported to alter inflammatory gene expression, which may facilitate the increases in cytokine production. Further validation is needed to confirm the link between metabolic activation and upregulation of inflammatory responses.

KEYWORDS

monocyte, metabolomics, LPS, LC-MS, data normalization

Introduction

Immunometabolism

Immunometabolism examines the links between immune cell function and metabolism. The field has burgeoned from early discoveries linking succinate accumulation to interleukin-1β (IL-1β) production in macrophages (1, 2), and we now know that metabolic pathways and immunologic functions are a complex concatenation of processes with distinct, context-dependent outputs. There are two primary pathways used by cells to generate energy in the form of adenosine triphosphate (ATP): the glycolytic pathway (glycolysis) and oxidative phosphorylation (OXPHOS) (3). Glycolytic intermediates can be diverted to feed multiple metabolic pathways including the pentose phosphate pathway (PPP), tricarboxylic acid (TCA) cycle, and lipid synthesis pathways (3). Although glycolysis is less energy efficient than OXPHOS in terms of ATP production, it is often adopted by immune cells as a rapid means of generating energy during acute activation, in a process called the "Warburg effect" (4).

Monocytes and their role in inflammation

Monocytes are myeloid cells accounting for approximately 10% of circulating leukocytes, whose primary role is immune defence. These cells are derived from myeloid bone marrow precursors and can transmigrate into tissues to differentiate into macrophages or dendritic cells. However, these cells are more than just a precursor, and are becoming more recognised for their heterogeneous responses to inflammation and roles in tissue repair and trained immunity (5). Prior to differentiation, monocytes are typically pro-inflammatory cells. They can rapidly propagate inflammation directly by phagocytosis and antigen presentation, as well as through release of cytokines, reactive oxygen species (ROS) and other inflammatory signalling molecules (6, 7). During inflammation (sterile or infectious), circulating monocytes extravasate to inflamed tissues *via* the leukocyte recruitment cascade, and can rapidly become the dominant infiltrating mononuclear phagocyte in damaged tissues and draining lymph nodes.

Monocyte metabolism

To perform these diverse functions, monocytes need dynamic energy processing systems. Monocytes exist in a "metabolically poised" state (8, 9), where they can react rapidly and specifically to different stimuli. These cells are also metabolically flexible and can utilise diverse fuel sources to fuel inflammation (10). Even in conditions of low oxygen – such as arthritic joints – these cells have been shown to adapt their metabolism to continue to preserve inflammatory cytokine production (11, 12). Glucose does appear to be a requirement for monocyte activation (13), differentiation (14), and cytokine production (15, 16). However, the way glucose is utilised during its breakdown may be of greater importance for cellular function. Glycolysis could be creating substrates for DNA (via the PPP) and cell membrane (via lipid metabolism) synthesis to facilitate cell growth and differentiation (17). Alternatively, glucose breakdown could be directed towards the TCA cycle, where fumarate and alpha-ketoglutarate can alter DNA methylation and gene expression (18).

Monocytes have been most closely studied in the context of LPS activation. LPS-stimulated TLR4 initiates a signalling cascade *via* MyD88 or TRIF leading to NF-κB/MAPK/IRF5 or IRF3 activation, respectively (19). Depleting NAD+ in monocytes inhibits TLR4 signalling, ultimately abrogating IL-1β production and highlighting a dependence on metabolic machinery (20). Lachmandas et al. investigated the differential metabolomic effects of various microbial stimulants in human monocytes and found diverse metabolic and inflammatory phenotypes (15). LPS did increase glycolysis rates at the expense of OXPHOS, however Pam3CysK4 and other bacterial lysates favoured increased oxygen consumption (15). *Candida* albicans (*C.* albicans) stimulation for instance led to sustained increases in both glycolysis and OXPHOS (16). A study replicating the effects of sepsis in monocyte-like THP1 cells detailed the switch from anabolic energy consumption during early immune activation (0-8h), to a catabolic energy-conserving process during

immune deactivation (24-48h), before re-establishing energy homeostasis during resolution (48-96h) (21).

Aims

Investigations into primary monocyte metabolism have thus far focused on metabolomic profiling after 24 hours of stimulation or more (11, 12, 15, 16, 22). In addition, none of these investigations have provided sufficient detail of how to replicate their sample processing of LC-MS methods. In this work, we set out to optimise and standardise LC-MS protocols for primary human monocytes and to define the early metabolomic changes that occur with LPS stimulation.

Methods

Blood collection and PBMC preparation

Fresh blood samples were taken from patients attending the outpatient's haemochromatosis clinic in St. James' Hospital. Whole blood donations were collected in CPDA-1 anti-coagulant bags (Fannin Scientific, MSE6500L) from consenting donors with no known infections and who disclosed their age and sex. PBMCs were isolated by density gradient centrifugation. Briefly, blood was added to 2% dextran (in PBS) mixed thoroughly at a 1:3 ratio and incubated for 30 mins at room temperature. This step was necessary to decrease the total blood volume while still ensuring sufficient monocyte numbers for optimisation studies, and can be omitted from future studies with a lower starting blood volume. The supernatant layer was removed and layered onto Lymphoprep™ and centrifuged at 400g for 25 mins with minimal acceleration and no breaking. The PBMC layer was aspirated and cells washed twice before resuspension in MACS buffer (PBS + 2mM EDTA + 0.5% BSA).

Monocyte isolation and stimulation

Monocytes were isolated from PBMCs by CD14+ magnetic bead isolation. 100µL of anti-CD14 microbeads (Miltenyi Biotec,130-050-201) were added to 2.9mL PBMCs in MACS buffer and cells were incubated for 15 minutes at 4°C. CD14+ cells were eluted using an LS column and counted. The concentration was adjusted to $1x10^6$/mL in complete RPMI (RPMI + 10% FCS + 100U/mL streptomycin + 1mg/mL penicillin). Monocytes were seeded at $1x10^6$ cells/mL in a 24-well plate and left to rest at 37°C with 5% CO_2 for at least 30 mins before stimulation. Cells were stimulated with 5µg/mL of monoclonal anti-MPO (Meridian BioSciences, H87207M) or anti-PR3 (Merck, MABT340) for 4 hours at 37°C with 5% CO_2. In some experiments, monocytes were pre-treated with CBR-5884 (Sigma, SML1656) for 30 minutes before LPS stimulation. At the end of the stimulation, plates were centrifuged at 400g for 7 mins and supernatants removed for cytokine or cytotoxicity assay (Lactate dehydrogenase assay, LDH). $5x10^6$ monocytes were processed for metabolomic analysis.

Measurement of cytokines and cytotoxicity assay

DuoSet ELISA kits (R&D Systems) were used to measure cytokine production in supernatants from ANCA-stimulated monocytes. Supernatants were diluted 1:5, 1:25, and 1:50 for tumour necrosis factor (TNF)-α (DY210), IL-1β (DY201), and IL-6 (DY206) assays, respectively. Quantification of LDH in post-stimulation cell supernatants was performed using the CytoTox 96® Non-Radioactive Cytotoxicity Assay (Promega, G1780) to assess cell death/viability. Both protocols were performed as per manufacturer's instructions.

Sample preparation for LC-MS

An optimised sample preparation protocol was used to extract metabolites from isolated monocytes post-stimulation (see Figure 1A). Following cell stimulation, $5x10^6$ treated monocytes were washed with ice-cold 0.9% NaCl and centrifuged in 1.5mL Eppendorf tubes at 400g for 7 mins. Supernatants were removed completely, and samples were quenched on dry ice. 100µL of ice cold 80% ACS reagent-grade methanol, (MeOH, Acros Organics, 10607221) was added, and cells were vortexed for 30 secs, then sonicated in an ice bath for 1 min, and vortexed for another 30secs. Samples were centrifuged at 16,000g for 10 mins at 4°C and the metabolite fraction (supernatant) removed for LC-MS analysis. The extraction procedure was repeated twice for a final metabolite fraction volume of 200µL. 5µL of metabolite fraction for each sample was added to an Eppendorf tube immediately after extraction to generate pooled quality control (PQC) samples. Extraction blanks were prepared using empty Eppendorf tubes as a negative control. Samples were stored at -80°C until analysis. A 50µM synthetic standard mix containing amino acids (Sigma, A9906), TCA cycle intermediates (Sigma, ML0010), and other metabolites of interest was formulated in 80% MeOH (see Table S1). To limit variations in metabolite abundances, all samples were processed on the same day with the same batch of reagents.

Modified BCA assay for measurement of residual protein in metabolite fraction

Protein levels in metabolite fraction (and cell pellets) were measured using the Pierce™ BCA Protein Assay (Thermo Scientific, 23227). A top standard of 200µg/mL (300nM) bovine serum albumin (BSA) in was prepared in 80% MeOH (Acros Organics, 10607221) and serially diluted 1:2 down to 1.56µg/mL plus a negative blank sample. BCA Working Reagent was prepared by diluting Reagent B 1:50 with BCA Reagent A. 100µL of BCA Working Reagent was added to each well and the plate was mixed briefly on a plate shaker. The plate was sealed tightly with parafilm

and left to incubate at 37°C for 18 hours. After cooling to room temperature, the absorbance was measured at 562nm with an Epoch™ Microplate Spectrophotometer (BioTek Instruments, Inc.).

LC-MS metabolomic analysis

LC-MS metabolomics was performed as described by Hsiao et al. (23) with minor modifications. Samples were analysed on an Agilent 6546 Q-TOF (G6546A) paired with an Agilent 1290 Infinity LC. A 150mm×2.1mm InfinityLab Poroshell 120 HILIC-Z column (Agilent Technologies, 683775-924) was used and column temperature was maintained at 25°C. Mobile phase A consisted of 10mM ammonium acetate, pH 9.0 in water plus 5µM InfinityLab Deactivator Additive (Agilent Technologies, 5191-4506); and mobile phase B was 10mM ammonium acetate, pH 9.0 in 90% acetonitrile. The instrument was operated in negative electrospray ionisation (ESI-) mode. Flow rate was 0.25ml/min and an injection volume of 2µL was used. Gradient was as follows: 90% B; 70% B 11.5min; 60% B 12min; 100% 15min. The column was held at 90% B for 5mins between sample injections. MS data were acquired using a Dual Agilent Jet Stream ESI source operating at fragmentor and capillary voltages of 3500V and 125V, respectively. The nebulizer pressure was set at 40psi and the nitrogen drying gas flow rate was set at 10L/min. The drying gas temperature was maintained at 200°C. The Sheath gas temperature and flow were 300°C and 12L/min, respectively. The MS acquisition rate was 2 spectra/sec and m/z data range from 40-1000 were stored in profile mode. Dynamic mass axis calibration was achieved by continuous infusion of a reference mass solution using an Agilent 1260 isocratic pump (Agilent Technologies, G7110B) connected to the ESI source. All samples were run in a single LC-MS batch to limit variation from instrument effects.

LC-MS data analysis

Analysis was performed using Agilent MassHunter ProFinder (version 10.0) in a similar manner to Cruickshank-Quinn et al. (24) Briefly, the "Batch Targeted Feature Extraction" and "Batch Recursive Feature Extraction" methods were used for the targeted and untargeted analyses, respectively. Formula targets were limited to Negative H- ion species and charge states limited to a range of 1-2. Mass and retention time (RT) tolerances were limited to ±10ppm +2mDa, and ±0.00%+0.5min, respectively. Features with an absolute height below 1,000 and saturation >20% were excluded. Detected metabolite features had to satisfy conditions in at least 33% of files in at least 1 sample group. Compounds detected in extraction blank samples and with %CV >20% in PooledQC samples were excluded from analysis. Metabolite abundances were calculated using areas integrated at the apex of selected chromatographic peaks. Values were exported as. CSV or. CEF files for further analysis and visualisation. Significantly altered entities were distinguished by paired t-test with a Benjamini-Hochberg FDR correction. Only metabolites with a fold change ≥1.5 and a p value <0.05 were considered significant.

Metabolite annotation

Significantly altered metabolites were imported into Mass Profiler Professional (MPP, Version 15.0) ID Browser (version 10.0). Tentative metabolite IDs (25) were assigned using the Agilent MassHunter METLIN Metabolomics Database (curated in Agilent PCDL Manager, version B.08.00). Compounds were annotated in the first instance by Library/Database search, and by formula generation when there were no Library/Database hits. LC/MS tolerances for precursor ion m/z were ± 10ppm + 2mDa. Identification parameter (Database search, Molecular Formula Generation score) score weights were all evenly set to 40. Search results were limited to the 10 best hits per compound and scores above 70 were considered reliable. Features were annotated with tentative metabolite IDs assigned based on 1) score, 2) the presence of a commercialised standard, and 3) brief literature review to determine likelihood of metabolite's impact on human monocyte function. Endogenous metabolites (as listed in HMDB) were preferred. Where no metabolite IDs or formulae were available, metabolite features were annotated by their mass and RT values (e.g., 601.2048@4.95).

Class prediction analysis

Partial Least Squares Discrimination Analysis (PLS-DA) and Random Forrest (RF) class predication analyses were carried out in Agilent Mass Profiler Professional (MPP). Both models were built using all 24 samples. The PLS-DA model used 2 components and was autoscaled. The RF model was built on 500 trees using 14 predictors and used a GINI variable importance calculation. Variable importance in projection (VIP) scores above 1 were considered significant.

Flow cytometry

Dextran sediment (as a surrogate for whole blood) and isolated monocytes were analysed for purity, viability, and surface ANCA expression. 100µL of dextran sediment or $1x10^6$ purified monocytes were used for flow cytometry experiments. Red blood cells in dextran samples were lysed with 1mL of diluted BD lysis buffer before washing and staining. Cells were stained with CD14- PE-Vio770 (TÜK4), MPO-PE (2C7), and fixable viability dye eFluor450 for 30 mins in the dark. Cells were washed and immediately acquired on a FACSCanto II flow cytometer using BD FACSDiva™ software, and results analysed using Kaluza software (Version 2.1, Beckman Coulter, Inc.).

Statistics

Statistical tests were carried out in GraphPad Prism software (Version 9.3.1). LPS-stimulated cells were compared to unstimulated using paired t-tests. Where multiple readouts were analysed, a Benjamini, Kreiger, and Yekutieli false discovery rate (FDR) correction (Q=1%) was performed. Pearson correlation was used to assess relationships between metabolites and flow/cytokine

readouts. Results are only statistically significant ($p < 0.05$) where specified.

Results

Optimised sample preparation of primary human monocytes for LC-MS analysis requires data normalisation to residual protein content

Given the dearth of standardised protocols for metabolomic analysis of primary cells, in particular primary blood monocytes, we first sought to develop an optimised sample preparation method. In a pilot study of 6 biological replicates, a combination of methanol-based extraction and ice bath sonication was the most effective extraction protocol in terms of numbers of detectable features and reproducibility (Figure 1A). This method provided excellent coverage of the monocyte metabolome. We found sample quenching and log transformation to be essential steps for sample preparation and data analysis, respectively (Figure 1B). Another essential [and challenging (26)] element of metabolomic analysis is data normalisation. After reviewing over forty biological and algorithmic data analysis strategies, the most efficient and consistent technique was an external scalar normalisation to residual protein content in the metabolite fraction. This was measured using a commercial BCA assay, with minor modifications. We first confirmed that methanol (MeOH) did not interfere with the assay system by comparing its performance to PBS-BSA solutions. MeOH correlated very well with PBS in both plate- and tube-based assays (Figure 1C, $R^2 = 0.9823$, $p<0.0001$). Further, sample volumes as low as 10µL maintained consistency in protein measurements with this plate-based assay (Figure 1D). Normalising metabolite concentrations to BCA-corrected data improved the appearance of Principal Component Analysis (PCA) plots for the targeted analysis (Figure 1E). Residual protein content was also strongly correlated with cell number, more so than cell pellet and cellular DNA content (Figure 1F). Overall, the BCA protein assay was compatible with 80% MeOH and suitable for measurement of residual protein content measurements in metabolomic extractions. All subsequent results reported have been $\log_2$ transformed and BCA-normalised.

Targeted metabolomic analysis reveals alterations in amino acids with ANCA stimulation

Twenty-nine of the 53 synthetic standard metabolites were detected in experimental samples, and forty in PQCs. In the targeted analysis changes between treatment groups were relatively small at this early time point, however, 17 metabolites

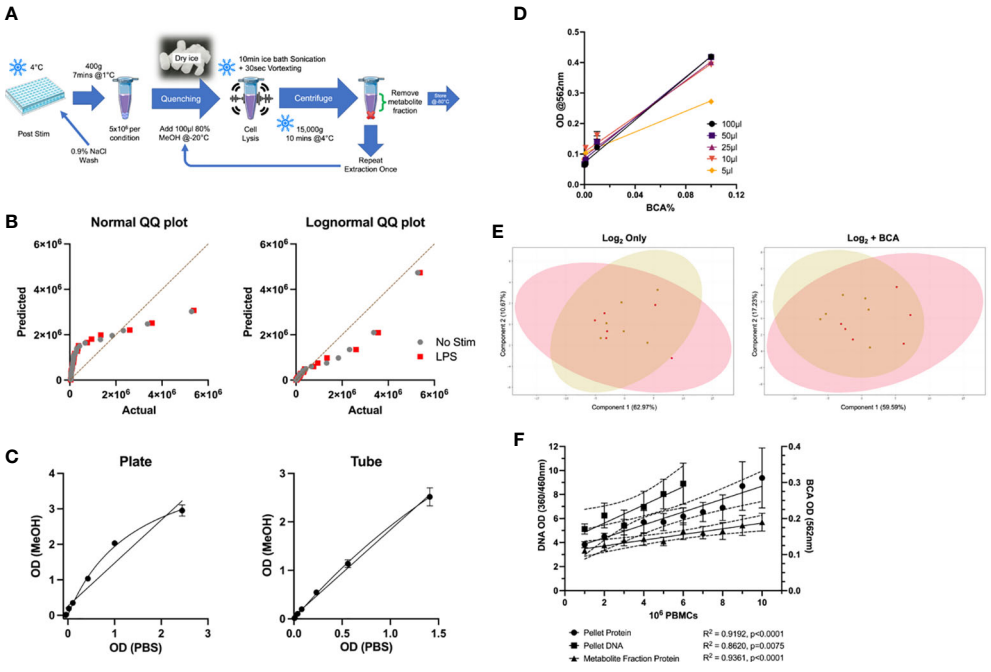

FIGURE 1
Optimisation of LC-MS Protocols for Metabolomic Profiling of Primary Monocytes. **(A)** Overview of optimised sample preparation protocol. **(B)** QQ plots of targeted metabolomics data (n=24) for normality testing by Anderson-Darling test, D'agostino & Pearson test, Shapiro-Wilk test, and Kolmogorov-Smirnov test. **(C)** Comparison of plate and tube protocols for BCA assay in various protein levels in PBS and MeOH. **(D)** Comparison of metabolite fraction (80% MeOH) volume used for protein determination by BCA assay. **(E)** PCA plots comparing log2 transformed to BCA-normalised targeted metabolomics data in unstimulated (gold) and LPS-stimulated (red) monocytes. **(F)** Comparison of biomass normalisation methods in PBMCs for metabolomic data normalisation. Protein levels of different cell numbers in the metabolite and pellet fractions were quantified by BCA assay, and DNA levels in the cell pellet were also measured. LC-MS, Liquid chromatography mass spectrometry; BCA, bicinchoninic acid; MeOH, methanol; PCA, Principal Component Analysis.

out of the 29 did reach statistical significance. Thirteen were upregulated in LPS-treated cells, and four downregulated (Figure 2A). The heatmap of AUC values (Figure 2B) demonstrates changes in a wide range of metabolites upon LPS stimulation. These mostly comprised amino acids, as well as TCA cycle metabolites (fumaric acid, L-malic acid) and nucleotides (inosine 5'-monophosphate [IMP]). Among these, the branch-chained amino acids (BCAAs) leucine, isoleucine (Figure 2C) and valine were among the most significantly increased by LPS stimulation (Figure 2D). In contrast, aspartic acid and two alanine isomers were depleted upon LPS activation (Figure 2E). These results demonstrate that, metabolic changes can be detected as early as four hours post LPS stimulation.

Inositol and glucose metabolism are altered in monocytes stimulated with LPS

For a more global overview of the metabolic changes, we performed untargeted analysis of LPS-stimulated monocytes. A summary of the untargeted workflow is shown in Figure 3A. A total of 1,376 features were detected after manual chromatography review and removal of peaks present in extraction blank samples. These were assigned tentative metabolite IDs. Out of 1,376 features detected, 154 were significantly altered in the LPS-treated monocytes (Figure 3B): 87 with decreased abundance, and 67 with increased levels compared to unstimulated cells. Of note, itaconic acid, an important modulator of inflammatory responses in macrophages (27), was found to be highly upregulated in LPS-activated cells at this early time point.

To better understand the specific influence and fundamental relations of these features, class prediction analyses were carried out using PLS-DA and RF analysis. Both models had an overall accuracy of 97.92%: 95.83% for unstimulated cells, 100% for the LPS-treated group. VIP scores and heatmaps for PLS-DA and RF are shown in Figures 3C, D, respectively. The PLS-DA model returned 434 features with a score above one, and 47 above two. The RF model had 17 features >1, with six of these common to both analyses. Four of these features were assigned as: L-lactic acid, uracil 5-carboxylate, D-myo-Inositol-1,3-diphosphate, and PI(38:4). A heatmap of the 58 influential metabolites is displayed in Figure 3E. We see changes in a number of lipid-like molecules, particularly several glycerophosphoinositols (PI) and glycerophosphoserine (PS) species, as well as a number of amino acids.

Pathway analysis for all 1,367 assigned features detected in the untargeted analysis was carried out using MetaboAnalyst (Version 5.0, https://www.metaboanalyst.ca/). Figure 3F shows annotated bubble plots for the most significantly altered metabolites in LPS-stimulated monocytes. Phosphatidylinositol signalling and inositol phosphate metabolism were the most significantly enriched pathways in LPS-treated cells, however, both of these pathways had a very low pathway coverage and thus a low pathway impact score. Other pathways previously reported to be altered by LPS were also seen at this early time point, including the Pentose phosphate pathway (PPP), glycolysis/gluconeogenesis, and nicotinate and nicotinamide metabolism. This suggests increased utilisation of glucose by early branches of the glycolysis pathway. Quantitative enrichment analysis confirmed the impact of LPS on the inositol phosphate metabolism and phosphatidylinositol signalling pathways (Figure 3G). BCAA degradation and biosynthesis were

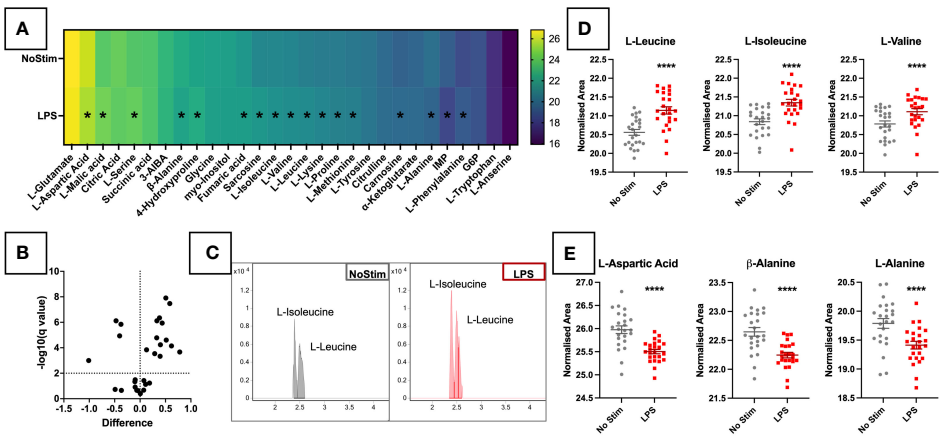

FIGURE 2
Targeted Metabolomic Analysis of LPS Stimulated Primary Monocytes. **(A)** CD14+ monocytes were stimulated for four hours with 200ng/ml LPS. Monocytes were analysed by LC-MS and targeted metabolomic analysis of 53 metabolites was completed in ESI-. **(A)** Heatmap of targeted metabolites in LPS-stimulated monocytes. LPS-stimulated monocytes were analysed by LC-MS and targeted metabolomic analysis of 53 metabolites was completed. 29 of the 53 metabolites were detected in experiment samples. Intergroup values are reported as BCA and Log2 normalised AUCs. Significant metabolites of varying degrees are marked with *. **(B)** Volcano plot analysis of targeted metabolites in LPS-stimulated monocytes. Metabolite features were analysed by Mann-Whitney paired test with a Benjamini-Hochberg FDR correction, and features with fold change ≥1.5 and p value <0.05 were considered significant. Fold change and p-value thresholds are shown in dotted lines on the X and Y axes, respectively. EICs for leucine and isoleucine are displayed in **(C)**, and sample plots of BCAAs **(D)** and metabolites reduced in the LPS-stimulated cells **(E)** are shown in individual dot plots. TIC, Total Ion Chromatograms; ESI, Electrospray Ionisation; BCAAs, Branched-Chain Amino Acids; EIC, Extracted Ion Chromatogram.*** $p < 0.001$.

also impacted, confirming the findings of the targeted analysis (Figure 2D). These results must be considered cautiously, as metabolite annotations were only available for a small subset of the metabolites, and at a lower confidence level (28) than those in the targeted analysis. Additional analyses are needed to improve coverage of these metabolite pathways and confirm their importance LPS-activated inflammation.

Targeted metabolomics and links to surface MPO and cytokine production

We next wanted to determine if these alterations in monocyte metabolism in response to LPS occur in line with cellular activation. Cytokine production is a key function of monocytes, and significant increases in IL-1β, IL-6, and TNF-α were observed after four hours of LPS stimulation (Figure 4A). Increased cytokine production correlated with levels of a number of metabolites. Of note, inosine 5'-monophosphate (IMP) significantly correlated with all three cytokines (Figure 4B). Further correlations were found for a number of amino acids, including the BCAAs, L-lysine, L-methionine, and L-phenylalanine. Despite this, these correlations had rather low R^2 values, likely owing to the short timescale of these experiments. Surface expression of myeloperoxidase (MPO) was measured in a subset of samples prior to stimulation. The percentage of MPO-positive monocytes and median fluorescence intensity (MFI) of MPO appeared to correlate with subsequent IL-1β production upon LPS stimulation (Figure 4C), suggesting that surface MPO levels may act as a surrogate marker for cellular activation. Serine has previously been shown to be essential for IL-1β production in LPS-stimulated murine macrophages (29). Given the increase in glycolysis upon LPS activation, it is feasible that flux through the serine pathway could be increased to support IL-1β production in human monocytes. Inhibiting serine production with CBR-5884 for 30 mins prior to stimulation completely abrogated IL-1β production (Figure 4D). These data suggest that CBR-5884 can inhibit IL-1β production by limiting serine synthesis. These data present clues to the emergent changes to monocyte metabolism in response to LPS.

Discussion

To date, most investigations of monocyte metabolomics have been carried out at later time points, such as >24h stimulations, a steady state in terms of metabolism. Here we defined the inchoate monocyte response to LPS-stimulation after four hours and provide detailed protocols for effective reproducibility of these works. Our method limits hands-on sample time with a quick single phase methanolic extraction and a single complementary and comprehensive LC-MS method.

First, we describe optimised sample preparation protocols for monocyte metabolomic investigations. A methanol-based

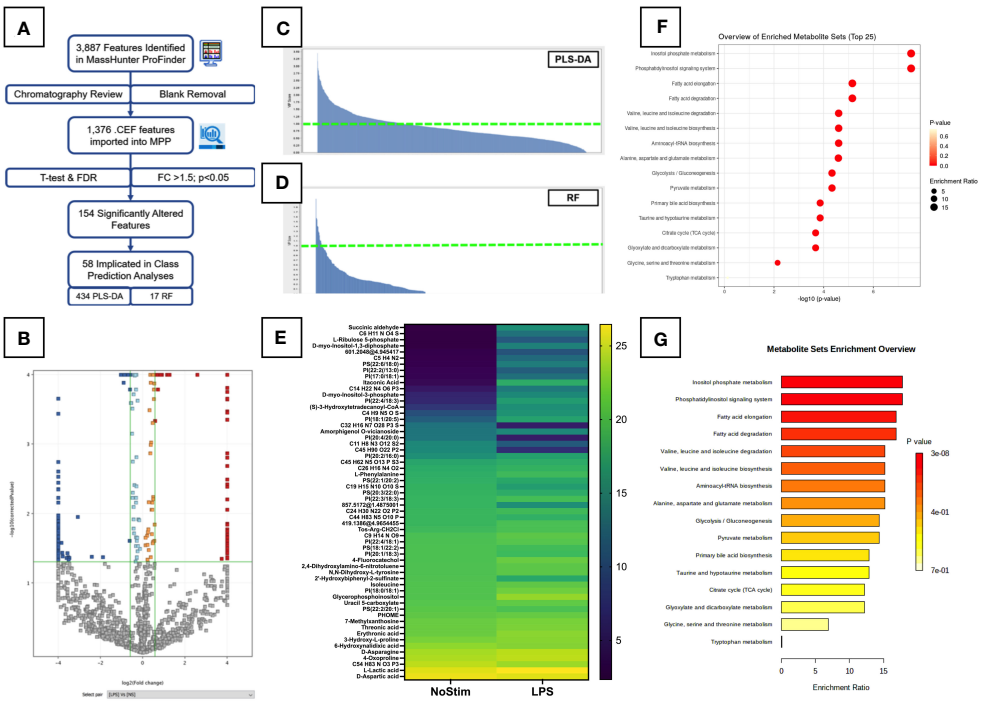

FIGURE 3
Untargeted Metabolomic Analysis of LPS Stimulated Primary Monocytes. **(A)** Summary workflow for untargeted metabolomic analysis with numbers of features/entities specified at each stage. **(B)** Volcano plot of LPS-treated monocytes are shown with significantly upregulated features highlighted in red and downregulated features in dark blue. Light blue and orange features did not meet the fold change threshold limits, and grey features were insignificant. Fold change and p-value thresholds are shown in green lines on the X and Y axes respectively. Class prediction analyses of significantly altered untargeted metabolites carried out by PLS-DA **(C)** and Random Forrest analysis **(D)**. Entities with a VIP score >1 are plotted on the heatmap in **(E)**. Pathway analysis of significantly altered metabolites identified in untargeted analysis was performed on the online MetaboAnalyst platform (Version 5.0, https://www.metaboanalyst.ca/). Results are displayed as dot plots **(F)** and bar chart **(G)**.

extraction and gentle cell lysis method was found to be optimal (Figure 1A). This method has been effective in adherent cells (30, 31), and is commonly used in cellular metabolomics investigations (32). Harvesting cells by plate scraping or trypsin-EDTA can influence the intracellular metabolome (33). Suspension cells such as monocytes can be easily extracted by adding cold extraction solvent directly to stimulation plate(s) before being transferred to the tube. This allows thorough extraction of any metabolites from remaining cells, limiting contamination from cell supernatants (exometabolome).

Experimental design and technical variation can affect the outcomes of metabolomics studies. As such, a number of data normalisation methods have been developed to correct for these errors (26, 34). We found that residual protein in the metabolite fraction measured by BCA protein assay was the optimum normalisation method. This method has been successfully used in previous work (35) and, in contrast to prior reports (26), protein levels did correlate with metabolite abundances in this analysis. Extending the (BCA assay) sample incubation time to 18 hours improved detection of small protein volumes, and the plate-based assay facilitates minimal sample loss, preserving low volume samples for LC-MS analysis (Figure 1D). We also found that acetonitrile was compatible with the commercial BCA assay (data not shown). The compatibility of other metabolite extraction solvents should be explored further.

Previously published LC-MS methods for monocyte metabolomic profiling were carried out by commercial metabolic profiling companies (15, 22) which combine RP and HILIC liquid chromatography to measure four metabolite subfractions. While we initially sought to replicate these techniques, the HILIC ESI- method consistently returned the greatest numbers of viable metabolite features. HILIC methods can detect a larger number of molecular features than RPLC and at higher abundances (36). Certain lipid classes in myeloid cells have been reliably detected by HILIC single phase extraction (31), and a recent publication noted the detection of over 1,900 lipid species across 26 subclasses from a single 12-minute HILIC LC-MS method (37). These are largely polar, small lipids, and the relevance of these compounds to monocyte inflammatory responses should be investigated in future profiling experiments.

Using these optimised protocols, we found novel metabolomic changes in primary monocytes after four hours of LPS stimulation. There have already been a number of investigations of monocyte metabolism at 24 hours (15, 16, 18, 21, 22), a timepoint which represents steady state monocyte metabolism. Zhu et al. (21) investigated a sepsis model in monocyte-like THP1 cells through activation, deactivation, and resolution of LPS-induced inflammation.

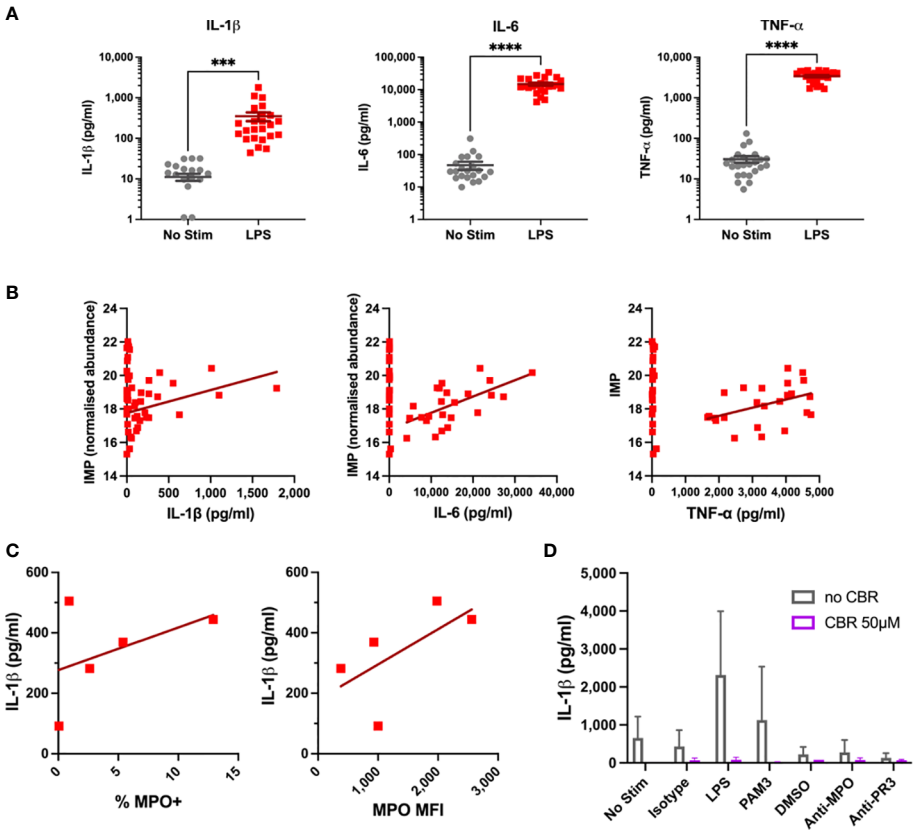

FIGURE 4
Cytokine and Flow Results for LPS-Stimulated Monocytes. **(A)** IL-1β, IL-6, TNF-α levels were measured in supernatants of monocytes by ELISA after four hour LPS stimulation. **(B)** Cytokine levels are correlated with IMP concentration in primary monocytes. **(C)** Correlation of baseline MPO surface expression with IL-1β production in stimulated primary monocytes. **(D)** Effects of serine synthesis pathway inhibition on IL-1β production in LPS-Stimulated Monocytes. *** $p < 0.001$, **** $p < 0.0001$.

At eight hours cells were already sufficiently activated, with significant changes across a range of metabolic pathways. Given the broad range of metabolic and inflammatory responses to LPS, longer timepoints pose a threat of artefacts from autocrine effects. TNF-α signalling can alter a broad range of metabolic pathways and affect insulin sensitivity in obesity (38). Conversely, succinate can induce IL-1β expression to promote inflammation (1). To preserve the LPS-specific effects of metabolism and the additional reasons above, we opted to investigate the early changes in monocyte metabolism after four hours of stimulation.

A number of amino acids were enriched in these cells, including the BCAA isomers leucine and isoleucine. Leucine in particular, is key for inflammatory cytokine production in these cells. Leucine influx *via* SLC7A5 contributes to metabolic reprogramming and IL-1β production in primary monocytes (39). This receptor is also upregulated on monocytes of RA patients where it correlated with disease severity markers (39). Decreased intracellular L-aspartate upon LPS activation has been reported at 6 hours (12), and is exacerbated by glucose deprivation. However, Arts et al. (18) found that aspartic acid was depleted in medium from trained monocytes. This may indicate increased breakdown of aspartate to produce more bioactive amino acids such as those described above. The precise reasons for depletion of aspartate and alanine metabolites should be further explored at different time points.

Serine is another amino acid important for inflammatory cytokine production. In murine macrophages serine production was found to be essential for IL-1β (and TNF-α) production upon LPS activation, and inhibiting serine synthesis abrogated inflammatory cytokine release (29). CBR-5884 inhibits 3-phosphoglycerate dehydrogenase (PHGDH) – the first step of the *de novo* serine synthesis pathway which directly branches off from glycolysis (40). The increased glycolysis reported in LPS-stimulated monocytes could therefore be fuelling serine production, and subsequent IL-1β release. In macrophages the one-carbon pool facilitates epigenetic changes during proinflammatory macrophage (M1) differentiation, fed in part by serine synthesis (41, 42). However, serine was not increased in LPS-stimulated monocytes in this work, and has not been reported in more long-term stimulations. We did find that the inhibitory effects of CBR-5884 on IL-1β production were lost when cells were stimulated for 18 hours (data not shown). Whether serine synthesis has a prolonged role in cytokine production in monocytes should be a focus of future research.

The untargeted analysis revealed further novel metabolic pathways perturbed by LPS in monocytes. Inositol phosphate metabolism and phosphatidylinositol signalling were the top two metabolic pathways implicated by LPS activation (Figures 3F, G). Myo-inositol was increased at four hours (Figure 2A), and was also found to be increased after 24 hours of LPS stimulation (15, 22). Other pathway metabolites were also increased (Figures 3E), indicating that these pathways are important for early monocyte activation. Additional validation experiments are required to confirm the influence of these metabolic pathways on monocyte function upon LPS activation.

Fatty acid metabolism was also significantly altered at this early time point. Other fatty acids have been implicated at later time points (12, 15, 22), and Fatty Acid Oxidation (FAO) has been shown to be essential for CCL20 production by RA monocytes (11). In low glucose/oxygen conditions (or where competition for glucose/oxygen is high) monocytes increase FAO *via* oxidative phosphorylation to meet their energy demands (12). This broad increase may indicate a metabolic emergency, whereby multiple energy generating pathways become activated prior to a specific metabolic (and associated inflammatory) response. Recently lipid metabolism was shown to be important in COVID-19 (43), and these pathways should be investigated further.

Pro-resolving M2 macrophages preferentially utilise FAO (as well as OXPHOS and glutaminolysis) as a means of energy generation (44, 45), though these cells are unlikely to be undergoing pro-resolving differentiation at this early time point. Itaconic acid is a well-known anti-inflammatory metabolite increased in activated macrophages (27). Increased itaconic acid has also been reported in LPS-stimulated monocytes (15, 22), and was found to be increased at our early time point (Figure 3E). Understanding the role of this metabolite prior to macrophage differentiation should be a focus of future work.

We report a novel increase in surface MPO expression which appears to link to inflammatory activation of primary monocytes (Figure 4C). Little is known about surface MPO expression and its relationship to metabolism. Our group has previously shown differences in MPO expression between monocyte subsets, and subsequent differences in pro-inflammatory cytokine release (46). Despite this, we found only a mild relationship between inflammatory cytokine production and metabolism. Additional activation markers should be explored to confirm the link between metabolic activation and upregulation of inflammatory responses.

Data availability statement

The data presented in the study are deposited in the MetaboLights repository (https://www.ebi.ac.uk/metabolights/index), accession number MTBLS6730.

Ethics statement

The studies involving human participants were reviewed and approved by The St. James' Hospital (SJH)/Tallaght University Hospital (TUH) Joint Research Ethics Committee (REC). Written informed consent for participation was not required for this study in accordance with the national legislation and the institutional requirements.

Author contributions

EL designed and performed experiments, analysed data, and wrote the manuscript. IB performed experiments and assisted in data analysis. LS performed experiments. MMcE assisted in data analysis. GB, MAL, and HK supervised the project and reviewed the manuscript. HK performed experiments and assisted in data analysis. All authors contributed to the article and approved the submitted version.

Funding

This work was funded by Irish Research Council Enterprise Partnership Scheme (Postgraduate) Award EPSPG/2017/321 in collaboration with Agilent Technologies. Agilent Technologies was not involved in the study design, collection, analysis, interpretation of data, the writing of this article, nor the decision to submit it for publication.

Conflict of interest

Author HK was employed by Agilent Technologies.

The remaining authors declare that the research was conducted in the absence of any commercial or financial relationships that could be construed as a potential conflict of interest.

Publisher's note

Supplementary material

The Supplementary Material for this article can be found online at: https://www.frontiersin.org/articles/10.3389/fimmu.2023.1116760/full#supplementary-material

References

1. Tannahill GM, Curtis AM, Adamik J, Palsson-McDermott EM, McGettrick AF, Goel G, et al. Succinate is an inflammatory signal that induces IL-1β through HIF-1α. *Nature.* (2013) 496(7444):238–42. doi: 10.1038/nature11986

2. Ryan DG, O'Neill LAJ. Krebs Cycle reborn in macrophage immunometabolism. *Annu Rev Immunol* (2020) 38(1):289–313. doi: 10.1146/annurev-immunol-081619-104850

3. Wood EJ. Instant notes: Biochemistry. *Biochem Mol Biol Education* (2006) 34 (1):59–60. doi: 10.1002/bmb.2006.49403401059

4. Warburg O. On the origin of cancer cells. *Science.* (1956) 123(3191):309–14. doi: 10.1126/science.123.3191.309

5. Guilliams M, Mildner A, Yona S. Developmental and functional heterogeneity of monocytes. *Immunity.* (2018) 49(4):595–613. doi: 10.1016/j.immuni.2018.10.005

6. Serbina NV, Jia T, Hohl TM, Pamer EG. Monocyte-mediated defense against microbial pathogens. *Annu Rev Immunol* (2008) 26(1):421–52. doi: 10.1146/annurev.immunol.26.021607.090326

7. Deshmane SL, Kremlev S, Amini S, Sawaya BE. Monocyte chemoattractant protein-1 (MCP-1): An overview. *J Interferon Cytokine Res* (2009) 29(6):313–26. doi: 10.1089/jir.2008.0027

8. Mitchell AJ, Roediger B, Weninger W. Monocyte homeostasis and the plasticity of inflammatory monocytes. *Cell Immunol* (2014) 291(1):22–31. doi: 10.1016/j.cellimm.2014.05.010

9. Stienstra R, Netea-Maier RT, Riksen NP, Joosten LAB, Netea MG. Specific and complex reprogramming of cellular metabolism in myeloid cells during innate immune responses. *Cell Metab* (2017) 26(1):142–56. doi: 10.1016/j.cmet.2017.06.001

10. Jones N, Blagih J, Zani F, Rees A, Hill DG, Jenkins BJ, et al. Fructose reprogrammes glutamine-dependent oxidative metabolism to support LPS-induced inflammation. *Nat Commun* (2021) 12(1):1209. doi: 10.1038/s41467-021-21461-4

11. Rodgers LC, Cole J, Rattigan KM, Barrett MP, Kurian N, McInnes IB, et al. The rheumatoid synovial environment alters fatty acid metabolism in human monocytes and enhances CCL20 secretion. *Rheumatology.* (2020) 59(4):869–78. doi: 10.1093/rheumatology/kez378

12. Raulien N, Friedrich K, Strobel S, Rubner S, Baumann S, von Bergen M, et al. Fatty acid oxidation compensates for lipopolysaccharide-induced warburg effect in glucose-deprived monocytes. *Front Immunol* (2017) 8. doi: 10.3389/fimmu.2017.00609

13. Lee MKS, Al-Sharea A, Shihata WA, Bertuzzo Veiga C, Cooney OD, Fleetwood AJ, et al. Glycolysis is required for LPS-induced activation and adhesion of human CD14+CD16– monocytes. *Front Immunol* (2019) 10. doi: 10.3389/fimmu.2019.02054

14. Suzuki H, Hisamatsu T, Chiba S, Mori K, Kitazume MT, Shimamura K, et al. Glycolytic pathway affects differentiation of human monocytes to regulatory macrophages. *Immunol Letters* (2016) 176:18–27. doi: 10.1016/j.imlet.2016.05.009

15. Lachmandas E, Boutens L, Ratter JM, Hijmans A, Hooiveld GJ, Joosten LAB, et al. Microbial stimulation of different toll-like receptor signalling pathways induces diverse metabolic programmes in human monocytes. *Nat Microbiol* (2016) 2(3):16246. doi: 10.1038/nmicrobiol.2016.246

16. Domínguez-Andrés J, Arts RJW, ter Horst R, Gresnigt MS, Smeekens SP, Ratter JM, et al. Rewiring monocyte glucose metabolism *via* c-type lectin signaling protects against disseminated candidiasis. *PloS Pathogens* (2017) 13(9):e1006632. doi: 10.1371/journal.ppat.1006632

17. Palmer CS, Cherry CL, Sada-Ovalle I, Singh A, Crowe SM. Glucose metabolism in T cells and monocytes: New perspectives in HIV pathogenesis. *eBioMedicine.* (2016) 6:31–41. doi: 10.1016/j.ebiom.2016.02.012

18. Arts RJW, Novakovic B, ter Horst R, Carvalho A, Bekkering S, Lachmandas E, et al. Glutaminolysis and fumarate accumulation integrate immunometabolic and epigenetic programs in trained immunity. *Cell Metab* (2016) 24(6):807–19. doi: 10.1016/j.cmet.2016.10.008

19. Dorrington MG, Fraser IDC. NF-κB signaling in macrophages: Dynamics, crosstalk, and signal integration. *Front Immunol* (2019) 10. doi: 10.3389/fimmu.2019.00705

20. Yang K, Lauritzen KH, Olsen MB, Dahl TB, Ranheim T, Ahmed MS, et al. Low cellular NAD+ compromises lipopolysaccharide-induced inflammatory responses *via* inhibiting TLR4 signal transduction in human monocytes. *J Immunol* (2019) 203 (6):1598–608. doi: 10.4049/jimmunol.1801382

21. Zhu X, Meyers A, Long D, Ingram B, Liu T, Yoza BK, et al. Frontline science: Monocytes sequentially rewire metabolism and bioenergetics during an acute inflammatory response. *J Leukocyte Biol* (2019) 105(2):215–28. doi: 10.1002/JLB.3HI0918-373R

22. Kerstholt M, Vrijmoeth H, Lachmandas E, Oosting M, Lupse M, Flonta M, et al. Role of glutathione metabolism in host defense against borrelia burgdorferi infection. *Proc Natl Acad Sci* (2018) 115(10):E2320–E8. doi: 10.1073/pnas.1720833115

23. Hsiao JJ, Potter OG, Chu T-W, Yin H. Improved LC/MS methods for the analysis of metal-sensitive analytes using medronic acid as a mobile phase additive. *Analytical Chem* (2018) 90(15):9457–64. doi: 10.1021/acs.analchem.8b02100

24. Cruickshank-Quinn C, Powell R, Jacobson S, Kechris K, Bowler RP, Petrache I, et al. Metabolomic similarities between bronchoalveolar lavage fluid and plasma in humans and mice. *Sci Rep* (2017) 7(1):5108. doi: 10.1038/s41598-017-05374-1

25. Schrimpe-Rutledge AC, Codreanu SG, Sherrod SD, McLean JA. Untargeted metabolomics strategies–challenges and emerging directions. *J Am Soc Mass Spectrometry* (2016) 27(12):1897–905. doi: 10.1007/s13361-016-1469-y

26. Misra BB. Data normalization strategies in metabolomics: Current challenges, approaches, and tools. *Eur J Mass Spectrometry* (2020) 26(3):165–74. doi: 10.1177/1469066720918446

27. O'Neill LAJ, Artyomov MN. Itaconate: The poster child of metabolic reprogramming in macrophage function. *Nat Rev Immunol* (2019) 19(5):273–81. doi: 10.1038/s41577-019-0128-5

28. Broadhurst D, Goodacre R, Reinke SN, Kuligowski J, Wilson ID, Lewis MR, et al. Guidelines and considerations for the use of system suitability and quality control samples in mass spectrometry assays applied in untargeted clinical metabolomic studies. *Metabolomics.* (2018) 14(6):72. doi: 10.1007/s11306-018-1367-3

29. Rodriguez AE, Ducker GS, Billingham LK, Martinez CA, Mainolfi N, Suri V, et al. Serine metabolism supports macrophage IL-1β production. *Cell Metab* (2019) 29 (4):1003–11.e4. doi: 10.1016/j.cmet.2019.01.014

30. Dettmer K, Nürnberger N, Kaspar H, Gruber MA, Almstetter MF, Oefner PJ. Metabolite extraction from adherently growing mammalian cells for metabolomics studies: Optimization of harvesting and extraction protocols. *Analytical bioanalytical Chem* (2011) 399(3):1127–39. doi: 10.1007/s00216-010-4425-x

31. Fei F, Bowdish DME, McCarry BE. Comprehensive and simultaneous coverage of lipid and polar metabolites for endogenous cellular metabolomics using HILIC-

TOF-MS. *Analytical Bioanalytical Chem* (2014) 406(15):3723–33. doi: 10.1007/s00216-014-7797-5

32. Hayton S, Maker GL, Mullaney I, Trengove RD. Experimental design and reporting standards for metabolomics studies of mammalian cell lines. *Cell Mol Life Sci* (2017) 74(24):4421–41. doi: 10.1007/s00018-017-2582-1

33. Luo X, Gu X, Li L. Development of a simple and efficient method of harvesting and lysing adherent mammalian cells for chemical isotope labeling LC-MS-based cellular metabolomics. *Analytica Chimica Acta* (2018) 1037:97–106. doi: 10.1016/j.aca.2017.11.054

34. Wu Y, Li L. Sample normalization methods in quantitative metabolomics. *J Chromatogr A* (2016) 1430:80–95. doi: 10.1016/j.chroma.2015.12.007

35. Serafini A, Tan L, Horswell S, Howell S, Greenwood DJ, Hunt DM, et al. Mycobacterium tuberculosis requires glyoxylate shunt and reverse methylcitrate cycle for lactate and pyruvate metabolism. *Mol Microbiol* (2019) 112(4):1284–307. doi: 10.1111/mmi.14362

36. Bi H, Krausz KW, Manna SK, Li F, Johnson CH, Gonzalez FJ. Optimization of harvesting, extraction, and analytical protocols for UPLC-ESI-MS-based metabolomic analysis of adherent mammalian cancer cells. *Analytical Bioanalytical Chem* (2013) 405 (15):5279–89. doi: 10.1007/s00216-013-6927-9

37. Medina J, Borreggine R, Teav T, Gao L, Ji S, Carrard J, et al. Omic-scale high-throughput quantitative LC–MS/MS approach for circulatory lipid phenotyping in clinical research. *Analytical Chem* (2023) 95(6):3168–79. doi: 10.1021/acs.analchem.2c02598

38. Sethi JK, Hotamisligil GS. Metabolic messengers: Tumour necrosis factor. *Nat Metab* (2021) 3(10):1302–12. doi: 10.1038/s42255-021-00470-z

39. Yoon BR, Oh Y-J, Kang SW, Lee EB, Lee W-W. Role of SLC7A5 in metabolic reprogramming of human Monocyte/Macrophage immune responses. *Front Immunol* (2018) 9. doi: 10.3389/fimmu.2018.00053

40. Mullarky E, Lucki NC, Beheshti Zavareh R, Anglin JL, Gomes AP, Nicolay BN, et al. Identification of a small molecule inhibitor of 3-phosphoglycerate dehydrogenase to target serine biosynthesis in cancers. *Proc Natl Acad Sci* (2016) 113(7):1778–83. doi: 10.1073/pnas.1521548113

41. Miyajima M. Amino acids: key sources for immunometabolites and immunotransmitters. *Int Immunol* (2020) 32(7):435–46. doi: 10.1093/intimm/dxaa019

42. Yu W, Wang Z, Zhang K, Chi Z, Xu T, Jiang D, et al. One-carbon metabolism supports s-adenosylmethionine and histone methylation to drive inflammatory macrophages. *Mol Cell* (2019) 75(6):1147–60.e5. doi: 10.1016/j.molcel.2019.06.039

43. Park MD. Fatty monocytes in COVID-19. *Nat Rev Immunol* (2020) 20(11):649–. doi: 10.1038/s41577-020-00462-2

44. Liu Y, Xu R, Gu H, Zhang E, Qu J, Cao W, et al. Metabolic reprogramming in macrophage responses. *biomark Res* (2021) 9(1):1. doi: 10.1186/s40364-020-00251-y

45. Nomura M, Liu J, Rovira II, Gonzalez-Hurtado E, Lee J, Wolfgang MJ, et al. Fatty acid oxidation in macrophage polarization. *Nat Immunol* (2016) 17(3):216–7. doi: 10.1038/ni.3366

46. O'Brien EC, Abdulahad WH, Rutgers A, Huitema MG, O'Reilly VP, Coughlan AM, et al. Intermediate monocytes in ANCA vasculitis: Increased surface expression of ANCA autoantigens and IL-1β secretion in response to anti-MPO antibodies. *Sci Rep* (2015) 5(1):11888. doi: 10.1038/srep11888

frontiers | Frontiers in Immunology

TYPE Review
PUBLISHED 19 May 2023
DOI 10.3389/fimmu.2023.1125874

OPEN ACCESS

EDITED BY
Soumya R. Mohapatra,
KIIT University, India

REVIEWED BY
Vadim V. Sumbayev,
University of Kent, United Kingdom
Zhe Yang,
Xi'an Jiaotong University, China

*CORRESPONDENCE
John H. Stewart IV
jste17@lsuhsc.edu
Vijay Kumar
vkuma2@lsuhsc.edu
vij_tox@yahoo.com

RECEIVED 16 December 2022
ACCEPTED 02 May 2023
PUBLISHED 19 May 2023

CITATION
Kumar V and Stewart JH IV (2023) Immunometabolic reprogramming, another cancer hallmark.
Front. Immunol. 14:1125874.
doi: 10.3389/fimmu.2023.1125874

Immunometabolic reprogramming, another cancer hallmark

Vijay Kumar [1*] and John H. Stewart IV[1,2*]

[1]Department of Interdisciplinary Oncology, Stanley S. Scott Cancer Center, School of Medicine, Louisiana State University Health Science Center (LSUHSC), New Orleans, LA, United States,
[2]Louisiana State University- Louisiana Children's Medical Center, Stanley S. Scott, School of Medicine, Louisiana State University Health Science Center (LSUHSC), New Orleans, LA, United States

Molecular carcinogenesis is a multistep process that involves acquired abnormalities in key biological processes. The complexity of cancer pathogenesis is best illustrated in the six hallmarks of the cancer: (1) the development of self-sufficient growth signals, (2) the emergence of clones that are resistant to apoptosis, (3) resistance to the antigrowth signals, (4) neo-angiogenesis, (5) the invasion of normal tissue or spread to the distant organs, and (6) limitless replicative potential. It also appears that non-resolving inflammation leads to the dysregulation of immune cell metabolism and subsequent cancer progression. The present article delineates immunometabolic reprogramming as a critical hallmark of cancer by linking chronic inflammation and immunosuppression to cancer growth and metastasis. We propose that targeting tumor immunometabolic reprogramming will lead to the design of novel immunotherapeutic approaches to cancer.

KEYWORDS

cancer, immunity, inflammation, immunometabolism, immunometabolic reprogramming, TME, TIME

1 Introduction

Cancer is the second leading cause of death worldwide as 10 million deaths resulted from cancer in 2020 and 70% of cancer deaths occurred in developing or low-middle-income countries (LMICs). Furthermore, it is projected that the incidence of cancer will increase to 28.4 million cases in 2040 (1). Sub-Saharan countries will witness a 92% cancer increase between 2020 and 2040. Several factors contribute to the rising incidence of cancer in these countries, including environmental pollution, the adoption of western diets, increased alcohol uptake, lack of exercise, and increased tobacco use.

Advances in medicine have now established that cancer cells differ from normal cells in many ways. For example, cancer cells exhibit uncontrolled cell division and proliferation, never mature, ignore signals required for the orderly progression of the cell cycle, cell death (apoptosis), specialization, and shedding. In addition, cancer cells express neoantigens and evade the host's immune recognition (2, 3). Hence, cancer cells develop intratumoral heterogeneity, including

altered cellular architecture/morphology, physiology (including their metabolism), subtypes, and evade cell death and their immune recognition (4–7). Additionally, nuclear compartmentalization (chromatin re-organization) in the tumor microenvironment (TME) regulates the gene expression that controls many processes, including immune cell development and programing, discussed in detail elsewhere (8–10). Furthermore, extrachromosomal DNAs (ecDNAs) are emerging as crucial mediators of cancer pathogenesis, gene regulation and epxression, and emerging treatment resistance (11–14). For example, ecDNAs promote increased oncogene expression and subsequent poor prognosis in many cancers (15–18).

Further development in the field led to the recognition of the six hallmarks of cancers almost 20 years ago (19, 20). Metabolic reprogramming among cancer cells and immune escape were also included later as additional hallmarks (21). Many reviews have further emphasized cancer and immune cell metabolism as a foundation mechanism for tumor immunology (22–27). For example, DePeaux and Delgoffe have discussed in detail the importance of decreasing TME metabolic barriers to increase the efficacy of tumor immunotherapy, including oncolytic viral therapy (OVT) (22). Whereas, Leone and Powell have discussed the metabolism of immune cells, specifically T cells, in the TME and exploiting differential metabolic plasticity for increasing the efficacy of immune checkpoint inhibitors (ICIs) (23). Hence, immunometabolism in the TME is critical in tumor immunopathogenesis, metastasis, and efficacy of existing immunotherapies. Hanahan recently upgraded the list of cancer hallmarks to include canonical and prospective characteristics (28). Different metabolic determinants of tumor initiation have been identified and discussed in detail (29). Therefore, we propose to add tumor-supportive immunometabolic reprogramming to the list of cancer hallmarks. The work herein discusses immunometabolic reprogramming of tumor-infiltrating immune cells as a critical hallmark of cancer progression.

2 Immune surveillance failure in cancer

Immune surveillance protects the host from endogenous and exogenous threats, including cancer development, infections, and premature aging (Figure 1) (30–34). However, aging and certain medications (antibiotics and antivirals) dysregulate immune surveillance to induce a tumor supportive environment (35–38). The immune system-mediated patrolling and monitoring to prevent cancer is called cancer or tumor immunosurveillance (39, 40). Tumor immune surveillance (immunosurveillance) requires tumor cell-derived molecules, including heat-shock proteins (HSPs) and double-stranded DNA (ds-DNA), which are recognized by pattern recognition receptors (PRRs) (41, 42). For example, CD91 (a receptor for HSP gp96)is crucial in cancer immune surveillance and cancer arising in the absence of CD91 are highly immunogenic (42, 43). However, the tumor microenvironment (TME) supports immunosurveillance escape and therefore supports cancer growth, differentiation, and metastasis (Figure 1) (44, 45). For example, TME T cells induce galectin-9 secretion from tumor cells derived from various malignant tumors. The released galectin-9 suppresses the antitumor cytotoxic activity of $CD8^+$ T and natural killer (NK) cells (46). Galectin-9 in cancer cells combines with V-domain Ig-containing suppressor of T cell activation (VISTA, an immune checkpoint protein) to support the protumorigenic immunosuppressive TME (46, 47). The transforming growth factor-β (TGF-β) via TGF-β receptors (TGF-βRs) and suppressor of mothers against decapentaplegic-3 (smad-3) protein induce the VISTA expression on cancer and T cells in the TME to promote immunosuppression. TGF-β and VISTA mediate immunosuppression by polarizing naïve T cells to regulatory T cells (T_{regs}) and pro-inflammatory M1 macrophages to M2 macrophages by increasing the SNAIL or snail family transcriptional repressor 1 (SNAI1) expression and increasing the myeloid-derived suppressor cells (MDSCs) activity (48–52). Thus, cancer cells and immune cells in the TME coordinate to create a tumor suppressive tumor immune microenvironment (TIME) for the growth, division, and metastasis of cancer cells. Cancer cell metabolism also plays a significant role in escaping from tumor immune surveillance via different mechanisms, including altering immunometabolic reprogramming.

3 Metabolic reprogramming among cancer cells in TME

Cancer cells differ from normal cells in maintaining homeostasis regarding their energy demand. Cancer cells undergo metabolic reprogramming to maintain their fastidious growth and proliferation status. For example, they reprogram themselves for rapid adenosine triphosphate (ATP) synthesis to meet increased energy demand, macromolecule synthesis, and tight maintenance of their redox status (53). The cancer cell metabolic reprogramming is crucial for their survival in the stressful TME with its spatially and temporally heterogenous concentrations of glucose, glutamine, and oxygen favoring hypoxia (54). For example, TGF-β in the TME increases aerobic glycolysis via glucose transporters and glycolysis enzymes to meet their high energy demand (55). Additionally, TGF-β also increases TME lactate level, which directly correlates with cancer cell metastasis. Furthermore, the acidic TME supports tumor cell survival, proliferation, and resistance to apoptosis (56–58).

The Warburg effect is an excellent example of cancer cell metabolic reprogramming, shifting from oxidative phosphorylation (OXPHOS) to aerobic glycolysis (Figure 2) (59–61). However, the observed Warburg effect in the TME does not depend on oxygen availability and the carcinogenic origin of cancer (54, 62). Hypoxia induces the hypoxia-inducible factor-1α (HIF-1α) that regulates the transcription of at least 60 genes regulating tumor cell survival, growth, proliferation, tumor angiogenesis, invasion/metastasis, glucose metabolism, immune cell function (63–66). High pyruvate dehydrogenase kinase (PDK) activity in tumor cells increases glycolysis. It also suppresses reactive oxygen species (ROS) production and accumulation, enhancing their stem cell and tumorigenic potential (Figure 2) (67). The aerobic glycolysis in TME can even occur in the non-dividing cells, indicating that the Warburg effect controls the tumor biomass and enhances their stem cell-like phenotype and oncogenic potential (67). Thus, the increased glucose uptake in tumor cells decreases its

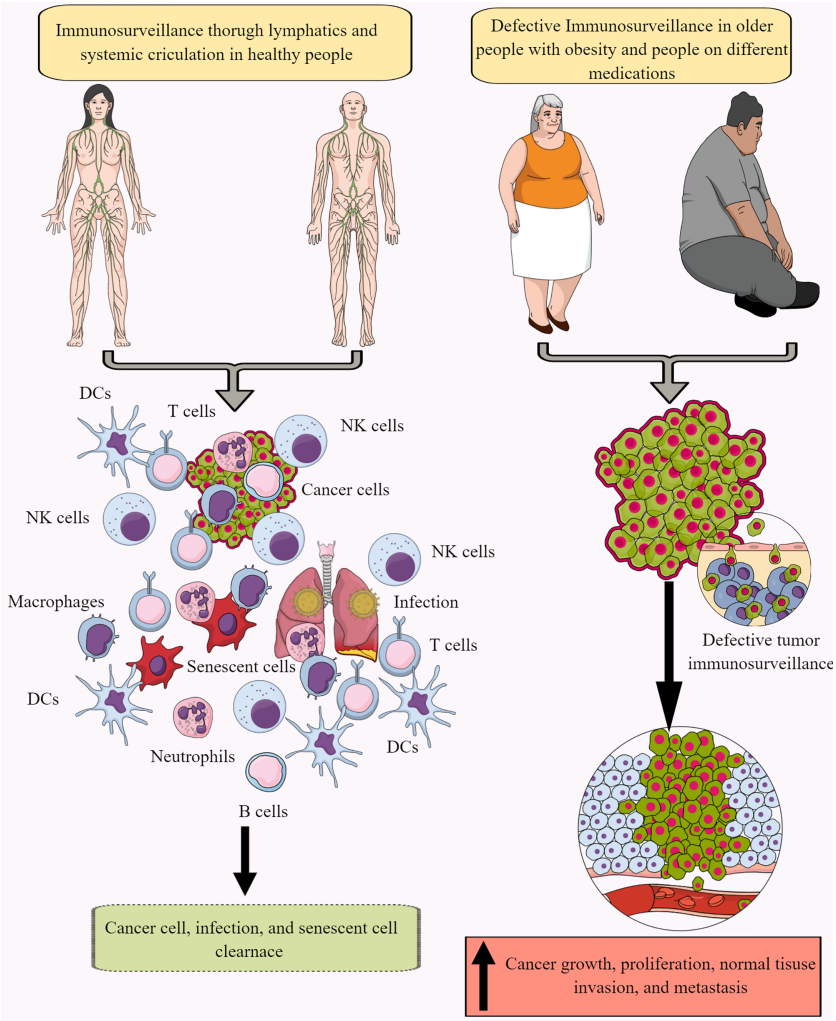

FIGURE 1
Immunosurveillance and cancer. The continuous immune surveillance of target organs by immune cells (innate and adaptive immunity) through lymphatics and systemic circulation keeps a check on altered or cancer cells in healthy individuals. This helps to maintain homeostasis by removing altered or cancer cells. However, several factors, including aging, obesity, repeated or chronic infections, and different medications, dysregulate or suppress regular immune surveillance leading to a tumor or cancer development. See text for details.

concentration in the tumor interstitial fluid (TIF) and increases extracellular lactate levels with increased lactate dehydrogenase (LDH) activity Figure 2 (68). Tumors expressing nucleus accumbens-associated protein-1 (NAC1) also upregulate LDH-A activity that further supports lactate accumulation in TME (69). The increased lactate level in the TME inhibits antitumor immune responses by T cells, macrophages, and DCs, through different mechanisms, including immunometabolic reprogramming (70–75).

A recent study has provided some of the first experimental evidence of the Warburg effect in patients with cancer (76). For example, clear cell renal carcinoma (ccRC) exhibits increased aerobic glycolysis compared to the adjacent normal kidney, and ccRC has suppressed glucose oxidation compared to tumors of other anatomical sites, including the brain and lungs (76, 77). Hence, ccRC is the first human tumor to demonstrate a convincing shift toward glycolysis, as indicated by the intraoperative ^{13}C infusions. It is important to note that the altered metabolic environment in the TME induces a metabolic competition between tumor and immune cells that helps in cancer progression (78, 79). Like glucose metabolism, the increased glutaminolysis in cancer cells also creates a glutamine-deficient tumor immune microenvironment (TIME) for immune cells (Figure 2). Tumor cells exhibit the highest glutamine uptake in TME compared to infiltrated immune cells (80). Notably, the increased glutamine uptake suppresses the glucose uptake across tumor-resident cell types, emphasizing that glutamine metabolism suppresses glucose uptake without glucose being a limiting factor in the TME (80). Cancer cells over express the methionine transporter SLC43A2. Therefore, they outcompete $CD8^+$ T cells for methionine uptake and utilization (81). The decreased methionine availability to $CD8^+$ T cells decreases the methyl donor *S*-adenosylmethionine (SAM), inhibiting dimethylation at lysine 79 of histone H3 (H3K79me2). The loss of H3K79me2 in $CD8^+$ T cells decreases signal transducer and activator of transcription 5 (STAT5) expression and alters their cytotoxic action against tumor cells. Furthermore, the methionine utilization by tumor cells in the TME of hepatic cell carcinoma increases T cell exhaustion (82). Thus, strategies to deprive methionine uptake by cancers cells or providing

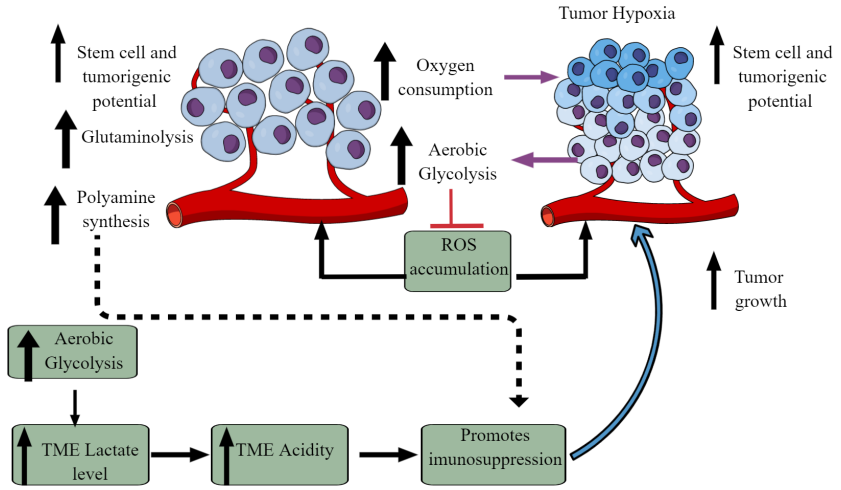

FIGURE 2
Altered cellular metabolism among cancer cells. Due to the altered physiological and metabolic demands, cancer cells undergo metabolic reprogramming. For example, due to their high energy demand as a response to their fastidious growth and proliferation, cancer cells depend on aerobic glycolysis, causing lactate accumulation and an increased acidic environment. Furthermore, increased aerobic glycolysis elevates oxygen consumption inducing hypoxia. The increased hypoxia and acidity (lactate accumulation) cause immunosuppression to escape from the host immune response. Immunosuppression promotes tumor growth. Additionally, other metabolic mechanisms (polyamine synthesis, glutamine metabolism) also increase in tumor cells, limiting nutrient availability to residential and infiltrated immune cells, causing their immunosuppression. Details are mentioned in the text.

methionine to TME T cells has a potential cell-specific immunometabolic targeting in different solid cancers.

Additionally, increased polyamine biosynthesis and transport occur in tumor cells as indicated by the induction of ornithine decarboxylase (ODC), a hallmark for tumorigenesis (Figure 2) (83–86). Polyamines suppress the immune response to promote tumor growth and directly influence it through numerous tumor-supportive mechanisms (Figure 2) (87–90). Along with tumor cells, myeloid cells (tumor-associated macrophages (TAMs), dendritic cells (DCs), and MDSCs compete with T cells to utilize polyamines to exert their immunosuppressive action (91). Hence, cancer and immuno suppressive myeloid cells compete with T cells in the TIME for polyamine uptake and utilization. In addition, polyamine metabolism is a central determinant of $CD4^+$T cells to differentiate into different functional Th subtypes (Th1, Th2, Th17, and T_{regs}). Therefore, polyamine deficiency in $CD4^+$T cells results in the failure to adopt a correct subset specification by affecting the tricarboxylic acid (TCA) cycle and histone deacetylation (92). Also, the decreased availability of polyamines to T cells supports their differentiation to immunosuppressive T_{regs} and its targeting reverses the TME immunosuppression (93–96). Thus, cancer cell metabolism alters the TIME via affecting immunometabolic reprogramming.

4 Immunometabolism in TIME

Immunometabolism combines classical metabolism and immunology to understand the immune cell phenotype and function by combining immunology and metabolism experimental approaches and paradigms (97). Immunometabolism has two subdisciplines: (1) cellular immunometabolism and (2) tissue immunometabolism. Cellular immunometabolism governs the fate of immune cells. At the same time, tissue immunometabolism includes the governing of tissue and systemic metabolism by immune cells to support the adaptations of the host to the surrounding environment (97, 98). Six major metabolic pathways, including glycolysis, the Krebs's cycle, fatty acid synthesis (FAS), fatty acid oxidation (FAO), amino-acid (AA) metabolism, and the pentose-phosphate pathway (PPP) regulate immune cell function (99). The details of immunometabolism during inflammation or inflammatory immune cell function have been discussed elsewhere (100–102).

Despite having the maximum capacity to uptake intratumoral glucose, myeloid cells in the TIME shift their immunometabolic reprogramming to tumor-promoting anti-inflammatory, immunosuppressive phenotype such as M2 macrophages, N2 neutrophils, MDSCs, and tolerogenic DCs (80). Hence, nutrient partitioning in the TIME is programmed in a cell-intrinsic manner through mammalian target of rapamycin complex 1 (mTORC1) signaling and the expression of genes related to glucose and glutamine metabolism. For example, glucose deprivation to immune cells prevents their pro-inflammatory tumor suppressive action in the TIME, indicating that tumor cells are still the biggest glucose consumer. Therefore, we will primarily focus on immunometabolic reprogramming among different immune cells that support tumor growth via immunosuppression.

4.1 Immunometabolic reprogramming among tumor-resident or infiltrated macrophages to support tumor growth, proliferation, and metastasis

Most immune cells are present within the invasive margins and central zone of tumors (103). However, macrophages often

comprise the dominant immune cell population in TIME as they include the first pro-inflammatory innate immune cell responders in the chronic inflammatory environment, which later polarize to tumor-supportive immunosuppressive M2 or TAMs (104–106). M1 to M2 macrophages polarization occurs in response to low glucose, glutamine, and FAs availability in a nutrient competitive TME. M2 polarization is further supported by increased TGF-β, IL-4, IL-5, IL-6, and IL-10 availability in the TME (Figure 3). TAMs support tumor growth, survival, proliferation, and metastasis by supporting tumor angiogenesis, chemoresistance, and immunosuppression (107–110). Hence, understanding their immunometabolic reprogramming in TME or TIME is warranted.

For example, M1 macrophages depend on aerobic glycolysis to infiltrate the hypoxic TME and exert their pro-inflammatory and anti-tumor actions (98, 111). The IL-4-dependent M1 to M2 macrophage polarization supports OXPHOS through interferon regulatory factor 4 (IRF4) and mTORC2 activation (112). However, IL-4-mediated M2 macrophage polarization does not require immunometabolic reprogramming to FAO (113). Also, the IL-4-mediated M1 macrophage polarization to M2 phenotype

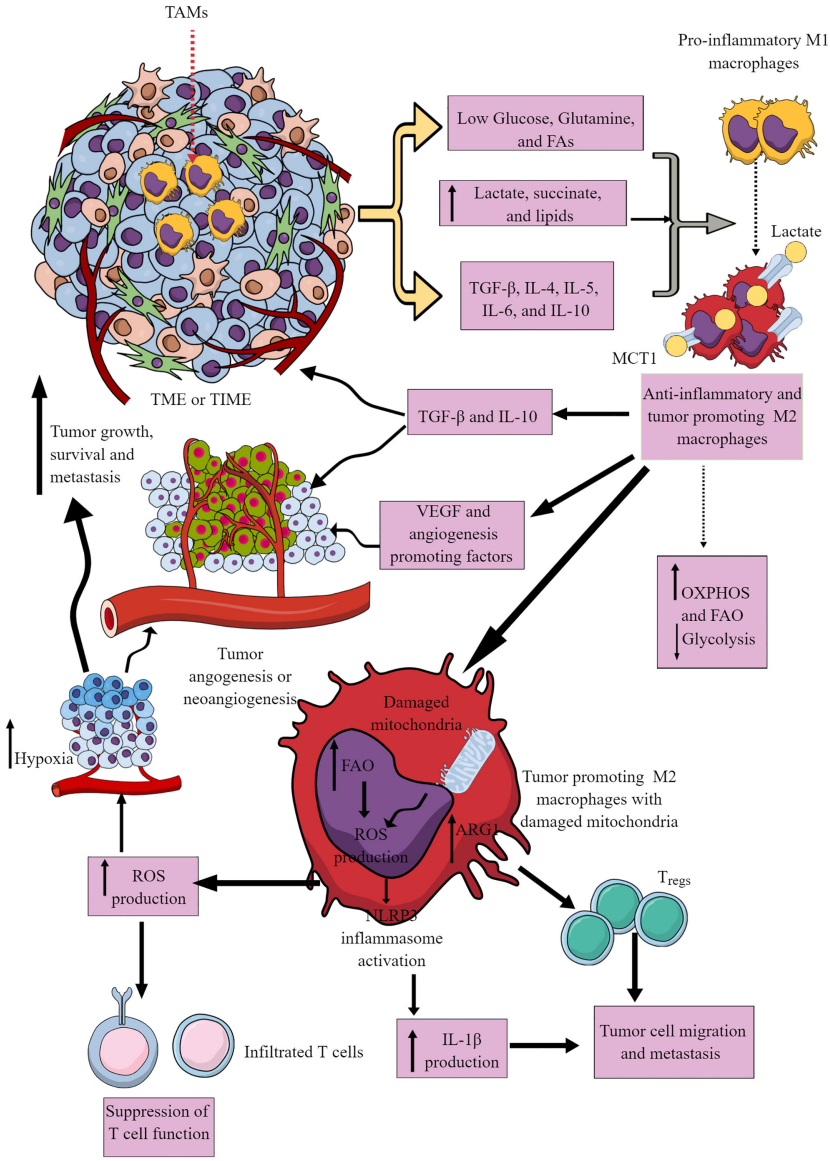

FIGURE 3
Tumor-associated macrophages (TAMs) in immunosuppressive TME or TIME and their immunometabolic reprogramming. Several factors, including low nutrient availability, increased lactate, succinate, and lipid levels, and different Th2 cytokines (TGF-β, IL-4, IL-5, IL-6, and IL-10) polarize antitumor and pro-inflammatory M1 TAMs to tumor-promoting and immunosuppressive M2 TAMs. These M2 TAMs release immunosuppressive cytokines (IL-10 and TGF-β) to support an immunosuppressive TIME by supporting T_{regs}. M1 TAMs undergo immunometabolic reprogramming to polarize to M2 TAMs. For example, M2 TAMs show increased OXPHOS and FAO to survive in the nutrient-deprived TIME or TME. The increased ROS production due to the damaged mitochondria in M2 TAMs suppresses the antitumor T cell immune response. Intracellular ROS in M2 TAMs activates NLRP3 inflammasome to produce IL-1β supporting tumor cell migration and metastasis. The increased ROS production supports TME or TIME hypoxia, supporting tumor angiogenesis, growth, survival, and metastasis. For details, see the text.

only occurs only when NO˙ generation is blocked due to the dysregulated mitochondrial function (114, 115). TME/TIME and IL-4 synergistically increase protein kinase RNA-like ER kinase (PERK)-signaling cascade in macrophages to promote immunosuppressive M2 transition, activation, and proliferation (116). PERK activation induces phosphoserine aminotransferase 1 (PSAT1) and serine biosynthesis via activation transcription factor-4 (ATF-4). The increased serine biosynthesis supports an enhanced mitochondrial function and α-ketoglutarate (α-KG) synthesis required for Jumonji domain-containing protein-3 (JMJD3)-dependent epigenetic modification (116). On the other hand, PERK activity loss impedes mitochondrial respiration and FAO crucial for M2 macrophages. Hence, the immunometabolic reprogramming among macrophages depends on stimulus, tissue environment, and mitochondria health. TME and associated TIME are complex due to severely altered tumor cell phenotype, function, and different oncometabolites.

The hypoxic and glucose-deprived TME induces regulated in development and DNA damage response 1 (REDD1) on TAMs that suppresses mTORC1 signaling and associated glycolysis (Figure 3) (117, 118). The increased levels of other oncometabolites, including lactate and succinate in TME, further support the M1 to M2 macrophages or TAMs polarization (Figure 3) through different mechanisms, including yes-1 associated protein (YAP) and NF-κB inhibition via G protein-coupled receptor 81 (GPR-81)-mediated signaling (119, 120). Macrophages in TIME or TME uptake lactate via increased expression of monocarboxylate transporter 1 (MCT1) that increases OXPHOS and FAO to generate M2 macrophages or TAMs (Figure 3) (121, 122). There are three types of M2 macrophages (M2a, M2b, and M2c), which secrete common immunosuppressive cytokines (TGF-β and IL-10) and chemokines to support tumor growth (Figure 3) (123). Also, TAMs promote angiogenesis via secreting VEGF and other angiogenesis-promoting factors to support tumor growth, proliferation, and metastasis (Figure 3) (117–119).

Cancer cells secrete M-CSF that promotes fatty acid synthase (FASN) activity in myeloid cells, including TAMs (124). FASN in TAMs via peroxisome proliferator-activated receptor (PPAR)β/δ activation promotes increased IL-10 synthesis and release. IL-10 promotes immunosuppression, angiogenesis, tumor growth, and metastasis (Figure 3). Also, tumor-cell-produced lipids simultaneously orchestrate M1 to M2 macrophage polarization and survival in TME or TIME via inducing ER stress response by reshuffling lipid composition and saturation on the ER membrane (Figure 3) (125). Furthermore, ER stress induces inositol-requiring enzyme 1 (IRE1, an endoplasmic reticulum stress sensor)-mediated spliced X-box-binding protein 1 (XBP1) production and STAT3 activation. The IRE1 production and STAT3 activation support M2 macrophage polarization and immunosuppressive TIME development (125–127). Hence, conditions favoring M2 macrophage transition exert a strong push towards OXPHOS in TAMs, which damages their mitochondria, producing increased ROS (Figure 3) (128). The increased ROS production further supports hypoxia and angiogenesis in TME, adding to tumor growth and metastasis. ROS further suppresses the antitumor action of infiltrated T cells (Figure 3). FAO-dependent ROS generation activates NLRP3 inflammasome to release IL-1β from TIME M2 macrophages, supporting tumor cell migration and metastasis (Figure 3) (129). Also, exosomes released from tumor cells in TME support the M1 to M2 macrophage transition via activating NLRP6/NF-κB pathway to support immunosuppressive TIME and cancer cell metastasis (130). Arginase 1 (Arg1) expression in TAMs lowers the L-arginine availability to T cells in TME or TIME. It recruits immunosuppressive T_{regs} to support tumor growth and development (Figure 3) (131). The simultaneous Arg1 and inducible nitric oxide synthesis (iNOS) expression in TAMs (M1/M2 phenotype) at low arginine concentration may favor ROS and RNS production that may inhibit antitumor T cell function in TIME (132–134).

Also, TAMs show a decreased receptor-interacting protein kinase 3 (RIPK3, a central factor in necroptosis) that inhibits caspase 1 (CASP1)-mediated cleavage of PPAR-γ to support FAO (135). The M2 macrophage polarization also involves increased glutamine catabolism (glutaminolysis) and UDP-GlcNAc-associated modules (136). The increased glutaminolysis replenishes the TCA cycle in immunosuppressive TAMs (137). Thus, the glutamine deprivation or N-glycosylation inhibition decreases M2 polarization and CCL22 production and promotes their polarization to M1-like macrophages (136, 138). The indoleamine 2,3-dioxygenase (IDO) expression in M2 macrophages also increases, which depletes local tryptophan via generating immunosuppressive kynurenine metabolites (139, 140). Hence, immunometabolic reprogramming among TAMs (highest in number among TIME immune cells) gives them an immunosuppressive phenotype. These immunosuppressive macrophages suppress other immune cells, including T cells through direct interaction or secreting immunosuppressive metabolites, switching their immunometabolism to immunosuppressive or exhausted phenotype (141–145).

4.2 Neutrophils and Myeloid-derived suppressor cells immunometabolism in TIME

Tumor cells and immune cells release several factors, including TNF-α, IL-8, IL-1α, CXCL1, CXCL2, and CXCL5 to stimulate neutrophil chemotaxis to the TME (146, 147). Although only mature neutrophils leave bone marrow (BM) for the circulation and target organs, TIME also harbors immature neutrophils (Figure 4) (146, 148). At initial stages, neutrophils exert antitumor action but become tumor and metastasis supportive later. They can be classified as antitumor N1 neutrophils that are supported by IFN-β and hepatocyte growth factor (HGF) and protumor N2 neutrophils that are supported by TGF-β and G-CSF (147). The complex immunological functions of neutrophils and their targeting in cancer are discussed elsewhere (147, 149–151).

In cancer-bearing mice, neutrophils leaving the BM show more spontaneous migration than in typical tumor-free mice (152). For example, these neutrophils lack immunosuppressive action, having increased OXPHOS and glycolysis rate than neutrophils of typical tumor-free individuals (Figure 4). The aggravated autocrine ATP

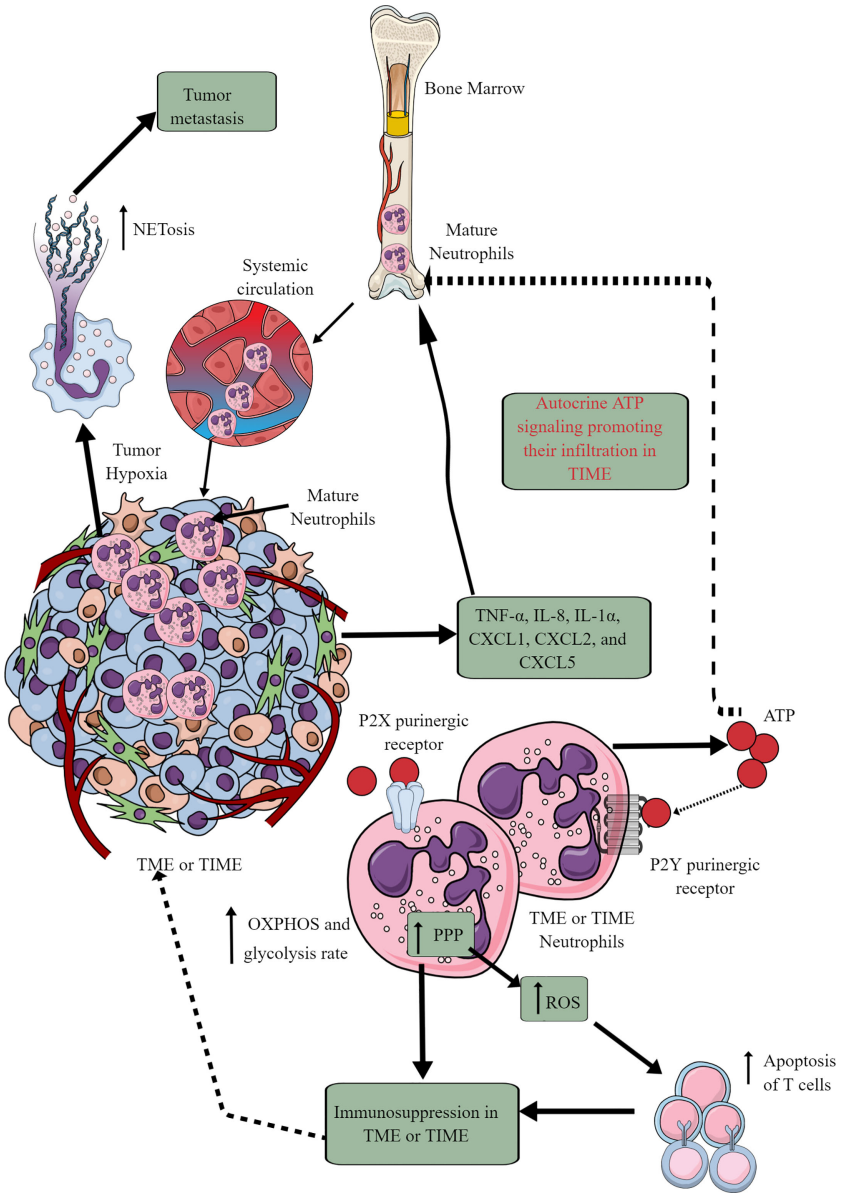

FIGURE 4
Neutrophils in TME or TIME and their immunometabolic reprogramming. The systemic neutrophil number increases in tumor patients. This increase is due to the increased neutrophil generation in the bone marrow (BM), causing increased infiltration in the TME or TIME. Although only mature neutrophils leave the BM, TIME contains both immature and mature neutrophils. Therefore, different chemokines and cytokines released from TME or TIME cells send the signals to BM for neutrophil chemotaxis. Additionally, ATP released from tumor-associated neutrophils (TANs) acts in an autocrine manner via P2Y purinergic receptors to further support their chemotaxis in TME or TIME. TANs show an increased rate of OXPHOS and glycolysis along with an elevated PPP. The ROS released from TANs induced apoptotic cell death among infiltrated antitumor T cells, causing immunosuppression. Hypoxia in TME or TIME causes NETosis that further supports tumor metastasis. See the text for details.

signaling supports the increased neutrophil infiltration to TIME via purinergic receptors (Figure 4) (152). The hypoxic environment in the TME or TIME increases HIF-1α and HIF-2α levels (65). HIF-1α increases neutrophil survival via supporting glycolysis (OXPHOS is not crucial for neutrophils) at initial stages, creating a chronic pro-inflammatory environment to support tumor progression (153). At the same time, HIF-2α increases the lifespan of pro-inflammatory neutrophils called tumor-associated neutrophils (TANs) (154). Also, the PPP in neutrophils supports increased ROS generation that induces apoptotic cell death among infiltrated T cells to support further a tumor suppressive TIME (Figure 4) (155, 156). PPP is also involved in the neutrophil extracellular trap (NETs) formation or NETosis by fueling NADPH oxidase with NADPH to produce superoxide that supports cancer metastasis (157). However, immunosuppressive mediators, including TGF-β released at later stages of the tumor, polarize antitumor N1 TANs to pro-tumor N2 TANs (158–160). Also, the glutamine and proline uptake in immature low-density neutrophils (iLDNs) supports their pro-metastasis action inducing NETosis under hypoxic and glucose-deprived conditions (Figure 4)

(161, 162). NETs promote cancer growth, progression, and metastasis and provide a protective shield to them through different mechanisms discussed somewhere else (163).

MDSCs are well-known immunosuppressive innate immune cells found only in pathological conditions, including cancer (164–166). They are of two types (1) monocytic-MDSCs or M-MDSCs, and (2) polymorphonuclear-MDSCs or PMN-MDSCs (167). Hence, MDSCs are the pathological phenotypes of neutrophils and monocytes accumulating in pathological lesions, including TME or TIME (164, 165). PMN-MDSCs of patients with cancer also show an increased spontaneous migration characteristic and are present at very early cancer stages (152, 168). Different chemokines, including IL-8 (CXCL8) and CXCR4 chemoattract (in response to miR-494) MDSCs to TME or TIME (Figure 5) (169–171). They secrete different immunosuppressive cytokines, including IL-10 and TGF-β, responsible for their immunosuppressive function to support tumor growth, proliferation, neoangiogenesis, and metastasis (170, 172). MDSCs also secrete vascular endothelial growth factor (VEGF)-A, fibroblast growth factor (FGF), and Bv8 (prokineticin or PK), and different MMPs to promote tumor growth and metastases (Figure 5) (173, 174).

MDSCs depend on AMPK and FAO for their immunosuppressive function (175, 176). Glutamate or L-glutamine (L-Gln) taken by MDSCs in TME or TIME is oxidized in an AMPK-dependent manner to support their immunosuppressive function by regulating the TCA cycle (Figure 5) (177). Even tumor-infiltrated/associated MDSCs (T-MDSCs) synthesize their L-Gln and with increased transglutaminase (TGM) expression that supports their immunosuppressive function and tumor metastases (178, 179). T-MDSCs show an increased FAO, OXPHOS, and glycolysis due to an increased lipid/FAs content in TME or TIME (Figure 5) (176). However, the increased FAs in TME or TIME promote FAO in MDSCs via CD36-mediated FA uptake, and FAO inhibition suppresses their immunosuppressive function in TME (176, 180, 181).

The fatty acid transport protein 2 (FATP2) on PMN-MDSCs through arachidonic acid (AA) uptake and prostaglandin E2 (PGE2) synthesis also support the immunosuppressive function of MDSCs (Figure 5) (182, 183). Furthermore, the PGE2-mediated negative feedback loop FATP2 and receptor-interacting protein kinase 3 (RIPK3, A negative regulator of FATP2) promotes PMN-MDSCs' immunosuppressive function (184, 185). GM-CSF controls the FATP2 overexpression on PMN-MDSCs in TIME via STAT5 activation. TME or TIME hypoxia increases the immunosuppressive function of T-MDSCs by increasing the HIF-1α level (Figure 5) (186, 187). Furthermore, HIF-1α, along with promoting their immunometabolic reprogramming to immunosuppressive phenotype, also increases the PD-L1 expression that suppresses the cytotoxic and immune-promoting functions of $CD8^+$ and $CD4^+$T cells in TIME (188). A high lactate level in TME increases the survival and proliferation of immunosuppressive MDSCs through G protein-coupled receptor 81 (GPR81)/mTOR/HIF-1α/STAT3 pathway (189–191). Also, the increased TME lactate level increases the number and proliferation of MDSCs, which inhibit NK cell cytotoxicity (NKCC) (Figure 5) (190). Hence, hypoxic TME or TIME supports MDSCs' immunometabolic reprogramming to FAO to favor their tumor and metastasis-supportive function.

4.3 DCs and their immunometabolic reprogramming in TME/TIME

DCs are potent antigen-presenting cells (APCs), which play a crucial role in generating and regulating immune response via recognizing different pathogens and inflammogens and presenting antigens to adaptive immune cells (T and B cells) (192). They also serve a part of first responding innate immune cells against cancer via antigen presentation despite constituting a rare immune cell population ($CD103^+$DCs) within TME or TIME capable of activating $CD8^+$T cells (Figure 6) (193, 194). Conventional DCs (cDCs) at early malignancy recognize dying tumor cells and migrate to draining lymph nodes (DLNs) to present tumor antigens to $CD4^+$ and $CD8^+$ T cells (195, 196). For example, type 1 cDCs (cDC1s) prime cytotoxic $CD8^+$T cells, and type 2 cDCs (cDC2s) activate antitumor helper $CD4^+$T cells (197–199). The antitumor action of cDC1s in TIME depends on NK cells as they release cDC1 chemo-attractants CCL5 and XCL1 to bring them in (Figure 6) (200, 201). However, the prostaglandin E2 (PGE2) release by tumor cells in TME or TIME suppresses NKCC and the production of cDC1 chemo-attractive chemokines (Figure 6). Thus, cDC1s lose their antitumor function due to the evasion of the NK cell-cDC1 axis and other immune cells with tumor growth. Furthermore, cDC2s ($CD11b^+$DCs) in tumor DLNs also express PDL-1 and suppress T cell-mediated antitumor immunity (Figure 6) (202, 203). Additionally, monocyte-derived DCs (mo-DCs) with pro-inflammatory properties comprise another type of DCs populating tumors (198). Also, the plasmacytoid DCs (pDCs) in tumor DLNs release IDO that directly activates mature T_{regs} to create an immunosuppressive TIME (Figure 6) (204). The details of immunologic and immunoregulatory functions of DCs in TME or TIME are mentioned elsewhere (205–208). We will focus their immunometabolic reprogramming in TME or TIME.

Under a steady state, DCs depend on OXPHOS for their energy demand to maintain immune homeostasis (209). For example, bone marrow-derived DCs (BMDCs) depend on FAO for OXPHOS to meet the energy demand, but the involvement of FAO for OXPHOS in cDCs and pDCs is not yet clear (192, 209). FAO and OXPHOS do not provide the maximum threshold for DCs to secrete cytokines and activate T cells to create a pro-inflammatory environment. The pro-inflammatory PRRs, like toll-like receptor-4 (TLR-4) stimulation, reprograms DC immunometabolic state from OXPHOS to glycolysis within minutes, like other myeloid immune cells (209–211). The shift from OXPHOS to glycolysis induces their antigen presentation potential through increased major histocompatibility complex (MHC)-I and -II expression, co-stimulatory molecules (CD80 and CD86), and cytokine synthesis and release. Although increased glucose uptake by DCs during the early stages of activation is accompanied by lactate production, this does not reflect a commitment to Warburg metabolism as a mechanism for ATP production because, during this time, ATP is provided by OXPHOS (211). Instead, glycolysis fulfills the citrate needs of DCs is filled by glycolysis (211). The export of citrate from the mitochondria into the cytoplasm through the citrate transporter SLC25A is significant for fueling FAS required for activated DCs to increase the size of critical

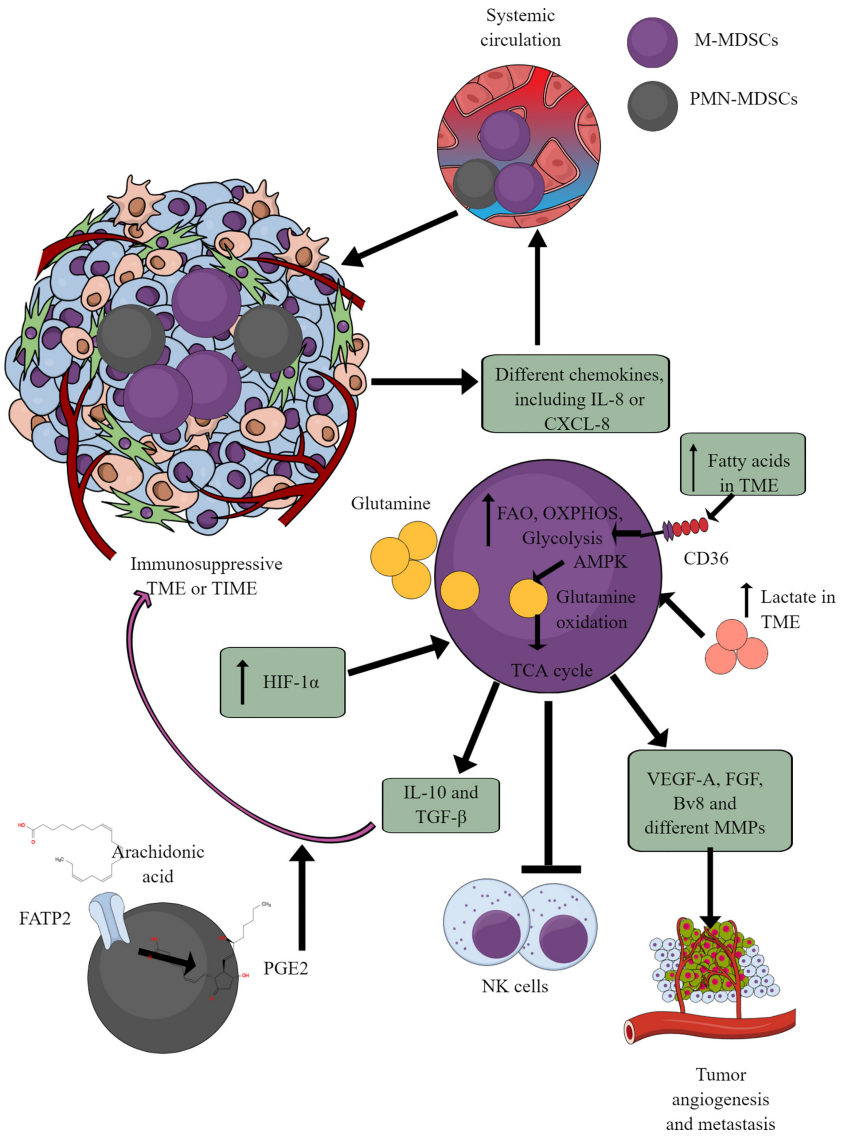

FIGURE 5
MDSCs in TME or TIME and their immunometabolism. MDSCs infiltration in TME or TIME supports the immunosuppressive microenvironment. IL-8 and many other TME or TIME-released chemokines support their infiltration. To exert their immunosuppressive function, MDSCs show an increased FAO, OXPHOS, and glycolysis. AMPK increase induces glutamine oxidation to support the TCA cycle. The increased lactate level in TME or TIME favors the immunosuppressive function of MDSCs. For example, MDSCs release immunosuppressive cytokines (TGF-β and IL-10), suppress cytotoxic NK cell activity and promote tumor angiogenesis, growth, proliferation, and metastasis. Additionally, arachidonic acid (AA) metabolism to PGE2 in PMN-MDSCs further supports immunosuppressive TIME.

organelles (Golgi bodies and endoplasmic reticulum or ER) involved in protein synthesis and secretion. Intriguingly, the enlargement of these compartments co-occurs with increased gene expression downstream of TLRs but is regulated post-transcriptionally by increased glycolytic flux. This is controlled by the Akt-dependent phosphorylation and subsequent activation of hexokinase II (essential to catalyze the first step of glycolysis) (211).

The Akt activation involves TANK-binding kinase 1 (TBK1)/I-kappa-B kinase epsilon (IKKε), activation downstream of RIG-I–like receptor (RLR), indicating that the rapid glycolysis is a typical response to any innate immune recognition by DCs. This Akt activation occurs regardless of PI3K or mTOR (two canonical Akt upstream activators) inhibition (210, 211). Different PRRs, including TLR2, TLR6, TLR9, Dectin-1, and -2 activation, induce immunometabolic reprogramming to glycolysis in DCs that governs their inflammatory status and motility (212, 213). Notably, early glycolysis induction in DCs occurs independently of their pro-inflammatory phenotype. This allows DCs to rapidly respond metabolically to these danger signals originating in the TME (211).

DCs fail to mature in the absence of OXPHOS to glycolysis transition. Also, DCs showing weak inflammatory response lack long-term glycolytic reprogramming requiring increased glycolytic gene expression (212). Thus, a prolonged and increased glycolysis enzymatic gene expression is crucial for maintaining pro-inflammatory DCs and their migration. Also, DCs utilize pre-existing glycogen stores to support shifting from OXPHOS to

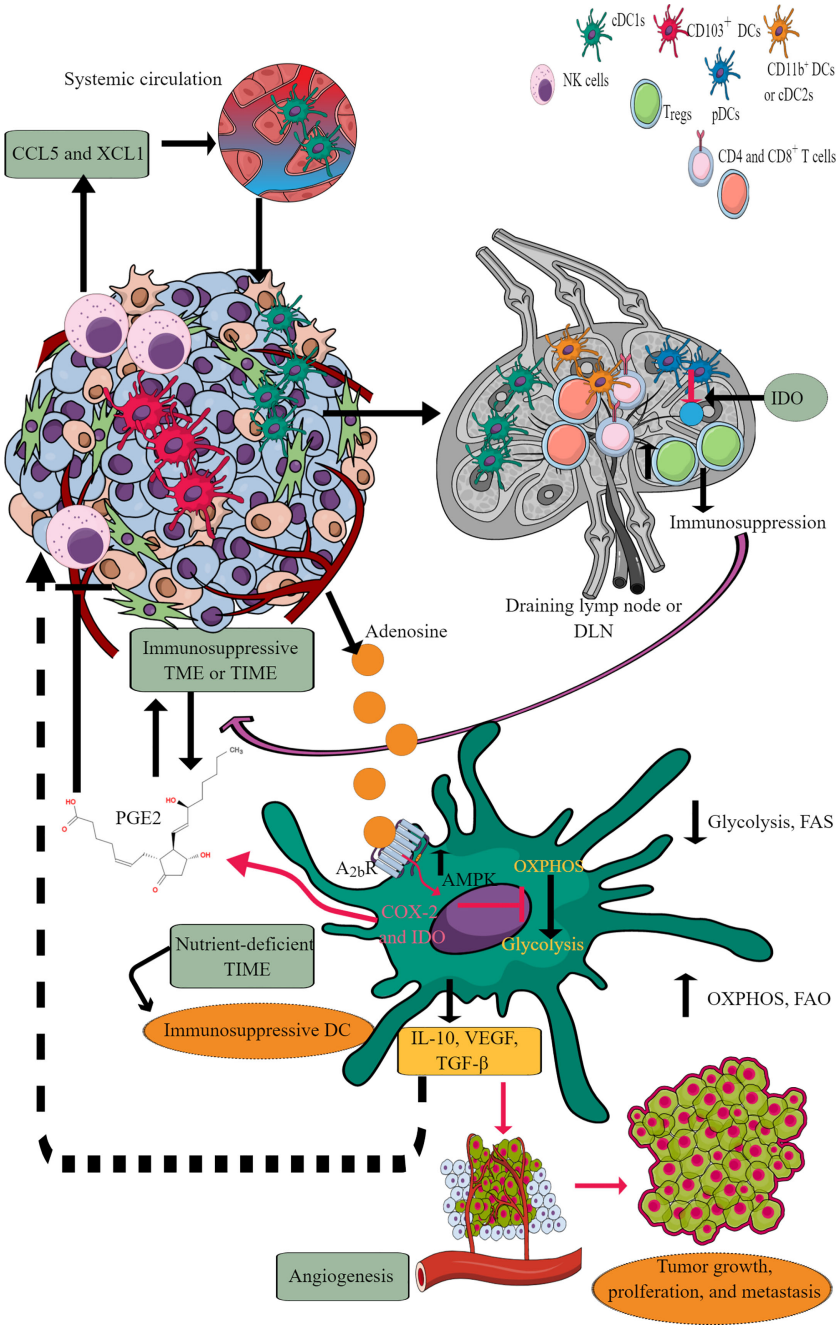

FIGURE 6
DCs in TIME and their immunometabolic reprogramming. TME or TIME-released chemokines induce DC chemotaxis. cDCs migrate to tumor DLNs for antigen presentation for adaptive immune cells (T and B cells) to induce antitumor immunity. However, IDO release from pDCs induces immunosuppression. Furthermore, adenosine in TME or TIME via A2bR blocks immunometabolic shift to glycolysis from OXPHOS and increases AMPK levels. Thus, tumor-associated DCs (TADCs) show an increased OXPHOS and FAO giving them an immunosuppressive phenotype to survive in the nutrient-deficient TME or TIME. These immunosuppressive TADCs release different factors and molecules to support immunosuppressive TIME, angiogenesis, and tumor growth and metastasis. Details are mentioned in the text.

glycolysis during their inflammatory stimuli to drive their TLR-dependent activation (214). The glycogenolysis inhibition attenuates TLR-mediated DC maturation and impairs their ability to act as APCs. Therefore, it is likely that even weak inflammatory signals can induce early glycolytic reprogramming through glycogenolysis without a significant and prolonged gene transcription crucial for glycolysis reprogramming. However, this is not true for other myeloid cells, including macrophages, which depend on external glucose supply through glucose transporter 1 (Glut1) upon inflammatory stimuli. Thus, only strong pro-inflammatory signals can induce prolonged inflammatory phenotype and DC motility in LNs.

IL-10 and AMP-activated protein kinase (AMPK, the central regulator of catabolic pathways and OXPHOS) inhibit glycolysis

(215). The FAS inhibition enhances DCs' capacity to activate allogeneic and Ag-restricted $CD4^+$ and $CD8^+$ T cells and induce CTL responses (216). Further, FAS blockade increases DC expression of Notch ligands and enhances their ability to activate NK cell immune phenotype and IFN-γ production. ER stress enhances DC's immunogenic function upon FAS inhibition, accounting for its higher immunogenicity (216). Conversely, the ER stress lowering by 4-phenylbutyrate (4-PBA) suppresses their increased immunogenic action due to FAS inhibition. TLR7/8 stimulation with promoter-associated RNA (pRNA) increases FAO and OXPHOS in human mo-DCs due to branched-chain alpha-keto acid dehydrogenase complex E1-alpha subunit (BCKDE1α) phosphorylation in a phosphatase and tensin homolog (PTEN)-induced putative kinase 1(PINK1)-dependent manner. Interestingly, inducing PINK1 activity in tolerogenic DCs stimulates FAO and renders them immunostimulatory (217).

Tumor-associated DCs (TADCs), like tumor-associated T cells, also face the harsh nutrient-deficient environment that activates AMPK, inhibiting the immunometabolic reprogramming from OXPHOS to glycolysis. For example, AMPK supports OXPHOS by upregulating proliferator-activated receptor γ co-activator (PGC-1α) that binds to PPAR-γ to promote mitochondrial biogenesis, oxidative metabolism and antagonize anabolic metabolism (218, 219). Thus, TADCs lose their APC properties and migration capacity to DLNs to prime and induce a robust adaptive immune response against tumor antigens. The recognition of exogenous adenosine monophosphate (AMP) by adenosine A_{2b} receptor expressed on DCs, including TADCs, upregulates their pro-tumorigenic functions, including angiogenesis via releasing VEGF, TGF-β, and creating an immunosuppressive environment through releasing IL-10 and expressing cyclooxygenase-2 (COX-2) and IDO (220–223). IDO (IDO1 and IDO2) activity metabolizes tryptophan (an essential amino acid) into kynurenine (224). Thus, the tryptophan depletion activates a stress response kinase called general control non-derepressing 2 (GCN2) in T cells that inhibits their proliferation and biases naïve $CD4^+$T cells to develop into $FoxP3^+T_{regs}$ (225–227). Also, the kynurenine and other metabolites bind to the aryl hydrocarbon receptor (AhR) on T cells, promoting their differentiation to T_{regs} along with supporting the immunosuppressive macrophage and DC phenotype (226, 228–230).

Catabolism of pre-existing glycogen in DCs is crucial to initiate glycolysis independent of external glucose supply in response to the TLR activation (214). However, in TME or TIME, the continuous TLR signaling, including the TLR9 activation in response to the host cell-derived DNA creates an immunosuppressive TIME due to the increased IDO expression (231–233). Furthermore, TLR9 ligand CpG ODN 2006 is a poor adjuvant to induce $CD8^+$T cells responsible for clearing tumor cells (234). This may be due to the poor DCs activation or their suppression through IDO generation. Further studies are required in this direction. The increased AMPK expression in TADCs also transforms them into tolerogenic DCs due to increased FAO and OXPHOS (210, 235). Furthermore, the aberrant lipid accumulation in TADCs due to the transport of extracellular lipids via macrophages scavenger receptor 1 (MSR1) diminishes their antigen-presenting capacity that suppresses their adaptive immune activation property to fight against tumors (236, 237). Also, the tumor-released Wnt5 molecule triggers PPAR-γ activation through β-catenin, which activates FAO by upregulating carnitine palmitoyltransferase-1A (CPT1A, a fatty acid transporter) in TADCs and induces a tolerogenic phenotype and secrete IDO to create an immunosuppressive TIME by upregulating T_{regs} (238, 239). Furthermore, the Wnt5 also blocks the immunometabolic shift to glycolysis in TADCs and induces an increased FAO. In addition, β-catenin induces vitamin-A metabolism in TADCs and FAO to produce retinoic acid (RA), further promoting T_{regs} generation to create an immunosuppressive TIME (240) Thus, TME or TIME DCs also become potent immunosuppressive immune cells and lose their antigen presentation characteristics to further support adaptive immunity against tumors due to their immunometabolic reprogramming supporting their survival but not potent immune function.

4.4 Immunometabolic reprogramming among innate lymphoid cells, including NK cells in TIME

ILCs are a relatively new class of immune cells, which phenotypically appear as adaptive lymphoid cells. However, they are lineage negative and do not express antigen-specific receptors encoded by rearranged genes, including T cell or B cell receptors (TCRs or BCRs). ILCs also do not show V(*D*)J recombination required for somatic hypermutation (SHM)/recombination, like T and B cells (241). However, they respond to various immunogenic stimuli, including pathogens, to mounting a pro-inflammatory immune response. Additionally, they are highly localized to mucosal surfaces (gastrointestinal, reproductive, and respiratory tracts). The details about different types of ILCs, including ILC1s or group 1 ILCs (NK cells and helper ILC1s), ILC2s (group 2 ILCs, produce Th2 cytokines), and ILC3s (group 3 ILCs, include $ROR\gamma t^+$ ILCs and lymphoid tissue inducer or LTi cells) inflammation and their interaction with adaptive immune cells have been discussed elsewhere (242–246).

ILCs increase in the circulation of patients with cancer compared to healthy controls, indicating that they also infiltrate TME or TIME of different cancers (Figure 7) (247–251). Patients with a high number of circulating ILCs, including NK cells with great cytotoxic action, are less prone to develop cancer and metastasis (252–254). The ILC (NK cells, ILC1s, ILC2s, and ILC3s) infiltration into the TME at the early (premalignant) stage induces anti-tumor TIME to kill tumor cells through different mechanisms, including direct cytotoxic action and recruitment of different immune cells, including cytotoxic T cells, and eosinophils (255–259). The details of ILCs, including NK cells in early TME, have been discussed elsewhere (260, 261).

At later stages, NK cells infiltrating TME become less cytotoxic ILC1s (inefficient in controlling the growth and metastasis of tumor cells) in the presence of TGF-β secreted by tumor cells and other immunosuppressive immune cells (262–264). TGF-β also downregulates eomesodermin (EOMES) or T-box brain protein 2 (Tbr2) expression (Figure 7) (262). EOMES and T-box protein in T

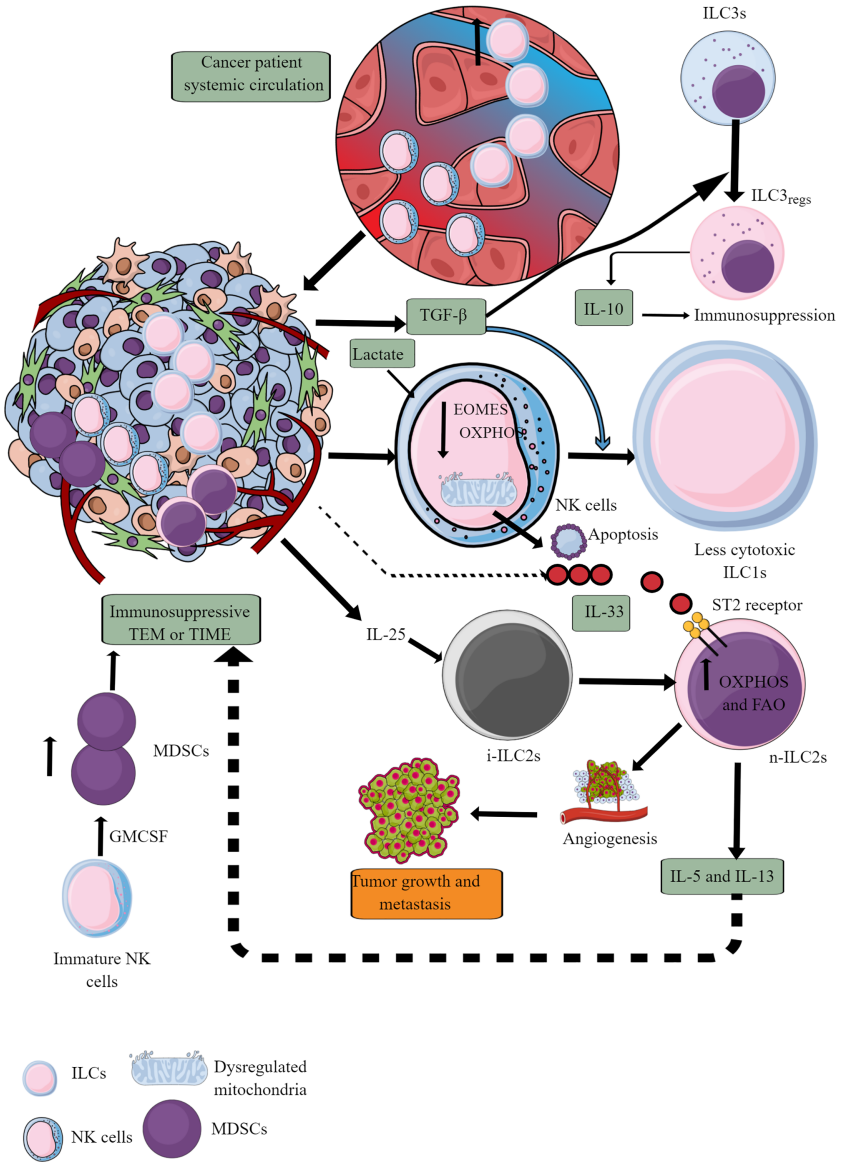

FIGURE 7
ILCs and NK cells in TIME and their immunometabolism. Different ILCs, including cytotoxic NK cells, are present in TME or TIME. The increased TGF-β levels in TIME transform high cytotoxic NK cells to less cytotoxic ILC1s and ILC3s to ILC3regs, which release IL-10 to support immunosuppressive TIME. Also, the high lactate levels in TIME or TME decrease NK cell OXPHOS, induce mitochondrial damage, and their apoptosis. Hence, the NK cell cytotoxicity (NKCC) is blocked in the immunosuppressive TIME that supports tumor growth. Furthermore, i-ILC2s polarize to n-ILC2s in the presence of TIME IL-25, further supporting angiogenesis, tumor growth, and metastasis by releasing immunosuppressive cytokines (IL-5 and IL-13). IL-5 and IL-13 are released from n-ILC2s in response to IL-33, increasing their OXPHOS and FAO. GM-CSF release from immature NK cells increases MDSCs proliferation, supporting immunosuppression. See text for details.

cells (T-bet) are crucial for NK cell development, maturation, and cytotoxic function (265–267). Also, EOMES is crucial for invariant NK (iNK)T cell development and differentiation in the thymus and their differentiation to memory-like KLRG1^{+}iNKT cells in the periphery (268). iNKT cells facilitate the potent anticancer cytotoxic action of CD8^{+}T cells by presenting different lipid and glycolipid antigens to expressed MHC class I-like molecule CD1d, in addition to direct killing (269, 270). iNKT cells also release IFN-γ that further supports tumor cell killing by NK cells (270). Hence, it will be novel to study the impact of TGF-β on iNKT cell development and function in TME or TIME, which depends on EOMES expression. Furthermore, TGF-β in TME also reprograms otherwise antitumor ILC3s to tumor-promoting regulatory ILC3s (ILC_{regs}) and secrete IL-10 (271).

IL-25, an IL-17 cytokine subfamily member in TME or TIME, transforms inflammatory ILC2s (iILC2s) to natural ILC2s (nILC2s) or ILC3-like cells to create an innate tumor-permissive microenvironment through activating ILC2s via inducing IL-17 expression (272, 273). iILC2s have a low RORγt expression, but nILC2s do not (274). Also, these tumor infiltrating ILC2s are highly IL-25R^{+} (273). These nILC2s secrete large amounts of IL-5 and IL-13 (Th2 cytokines), creating an anti-inflammatory or immunosuppressive TIME (272). However, IL-

25 exerts a tumor regulatory role through different mechanisms, including eosinophil and B cell infiltration, apoptosis, and Th2 cytokines secretion in TME to create an immunosuppressive TIME (275). The therapeutic blockade of IL-25R in colorectal cancer (CRC) lowers the tumor burden and activates an anti-tumor immune response in mice (273). These ILC2s join IL-25R$^+$ MDSCs to create an immunosuppressive TIME in different cancers (276–278). Another study has shown that blocking IL-25 (released from gastrointestinal tuft cells) suppresses gastric cancer in mice, and the ILC2 axis, which is responsible for immunosuppressive IL-13 release (279). IL-33 (a member of IL-1 cytokine family) also promotes tumor survival and progression through different mechanisms, including T_{regs} functional stabilization (280, 281). Also, IL-33 exerts tumor supportive action via regulating PPAR-γ-mediated IL-4, IL-13, and IL-15 (Th2 cytokines) release from ILC2s (Figure 7) (282). Thus, antitumor functions of ILCs, including NK cells, ILC2s, and ILC3s, reprogram to tumor-promoting immune activity governed by their immunometabolic reprogramming.

ILCs, including NK cells recruited to the nutrient-competitive TME with tumor cells, adjust their immunometabolic requirement affecting their antitumor immune function. For example, NK cells depend on glycolysis and OXPHOS for their energy requirement under immune homeostasis due to their limited energy or biosynthetic demand (283, 284). Under inflammatory conditions due to increased energy demand to perform a cytotoxic function and cytokine release, immunometabolic reprogramming shifts more towards aerobic glycolysis than OXPHOS, although an increase in OXPHOS also occurs like effector CD8$^+$T cells that depends on mTORC1 activation (285–287). However, TME does not support their increased glucose demand to exert their antitumor action. For example, increased TGF-β in TME induces NK cell suppression through decreasing mitochondrial metabolism, including OXPHOS, which is crucial to maintain its high metabolic demand to maintain its antitumor activity (288). This process occurs independently of mTORC1 inhibition. However, TGF-β blocks IL-15-dependent NK cell proliferation and maturation via inhibiting mTOR signaling (289). Thus, it will be interesting to delineate factors responsible for a differential effect of TGF-β on mTOR signaling and dependent metabolic reprogramming, as mTORC1 signaling is crucial for NK cell maturation and proliferation in patients with metastatic cancers (290).

It is important to note that blocking TGF-β restores the anti-tumor function (including metastasis prevention) of NK cells via restoring their immunometabolic reprogramming crucial for cytotoxicity and IFN-γ release (288, 289). Additionally, lactate accumulation in TME also blocks NK cells' OXPHOS via inducing mitochondrial dysfunction due to increased ROS release, making them energy deficient and causing their apoptosis (Figure 7) (291). Thus, it will be interesting to delineate that to escape from apoptosis of TIME NK cells in the presence of TGF-β to polarize to less cytotoxic ILC1s having less energy demand to survive. Also, GM-CSF in TME converts immature NK cells to MDSCs, helping in cancer progression and metastasis (292).

The immunometabolic reprogramming of ILC2s is complex compared to other immune cells. For example, they use OXPHOS and branched-chain amino acids (valine, leucine, and isoleucine) to fuel their polarized mitochondria at their steady state during homeostasis (293). However, their developmental maturation depends on the HIF-1α-glycolysis axis (294). Hence, OXPHOS, branched amino acids, and glycolysis are crucial to maintaining ILC2s' immune homeostatic function by regulating development and maturation. The release of IL-4, IL-6, and IL-13 (Th2 cytokines) from ILC2s is maintained by increased glutaminolysis, glycolysis, mTOR activation, and FAO (295, 296). However, they continue to OXPHOS through amino acid uptake to maintain their cellular fitness and proliferation (296). The increased FAO takes place in ILC2s of nutrient (glucose and glutamine)-deficient TME or TIME, which reprograms their antitumor function to tumor-promoting via releasing Th2 cytokines causing immunosuppression and angiogenesis (Figure 7) (297).

Furthermore, the increased IL-33 level in TME or TIME promotes ILC2's pro-tumor function via binding to its cognate receptor ST2, promoting temporary storage of externally acquired FA in lipid droplets to make cell membranes (298). These accumulating lipid droplets transform into phospholipids to promote ILC2s proliferation. An enzyme called diacylglycerol o-acyltransferase 1 (DGAT1) regulates this process. PPAR-γ, a key transcription factor, governs this immunometabolic reprogramming crucial for lipid uptake, metabolism, and ILC2 function (297, 298). For example, genetic deletion or pharmacological inhibition of PPAR-γ and DGAT1 in ILC2s blocks the IL-33-mediated cancer growth and metastasis (282). The IL-33-mediated optimal immunometabolic reprogramming in ILC2s also requires ROS, and its inhibition can prevent its tumor-promoting role by suppressing IL-5 and IL-13 release (299). Thus, TME supports immunometabolic reprogramming among ILC2s to create an immunosuppressive TIME that supports tumor growth and metastasis.

4.5 Immunometabolic reprogramming among T cells in the TIME

T cells are crucial adaptive immune cells, which have the potential to regulate the immune system through helper T (Th) cell phenotype and direct killing of tumor cells through their cytotoxic action (CD8$^+$T cells) (102). The pro-inflammatory T cells (Th1, Th2, and Th17 phenotypes collectively called T effector (T_{eff}) phenotype) depend more on increased glycolysis than OXPHOSS (300, 301). The aerobic glycolysis controls T_{eff} function, including the IFN-γ release through binding the glycolysis enzyme glyceraldehyde 3-phosphate dehydrogenase (GAPDH) to AU-rich elements within the 3' untranslated region (3' UTR) of IFN-γ mRNA (302). Also, the lactate dehydrogenase A (LDHA) induction in T cells supports aerobic glycolysis but supports IFN-γ release or Th1 differentiation independent of 3'UTR through epigenetic mechanisms (303). In addition, in acidic TME (due to lactate accumulation), LDH converts lactate to pyruvate and lowers nicotinamide adenine dinucleotide (NAD^+) levels. The decreased NAD^+:NADH further blocks glycolysis in T cells (Figure 8) (304). The increased lactate level in TME inhibits NAD^+-dependent GAPDH and 3-phosphoglycerate dehydrogenase (PGDH) activity crucial for NADH reduction and serine production, important for T cell proliferation (Figure 8) (304). Serine supplementation rescues T cell proliferation in high lactate TME.

LDHA maintains a high acetyl-coenzyme A (acetyl-CoA) level that promotes histone acetylation and IFN-γ transcription. LDHA deletion in T cells suppresses their IFN-γ-mediated pro-inflammatory action and induces their differentiation to FoxP3$^+$ T_{regs}. FoxP3 expression in T_{regs} reprograms their immunometabolism to OXPHOS via suppressing Myc activity and glycolysis and increasing NAD^+ oxidation (Figure 8) (305). Due to this, T_{regs} resist highly acidic (lactate) TME and grow and proliferate (306). T_{regs} also take more lactate than T_{effs} to utilize it as a fuel for the TCA cycle or gluconeogenesis, which decreases their glucose need in the highly nutrient-competitive TME (305, 307). T_{regs} highly express lactate transporter, monocarboxylate transporter 1 (MCT-1), for lactate uptake in TME (307). Furthermore, TME lactate induces programmed cell death protein 1 (PD-1 or CD279) expression in T_{regs}, and PD-1 inhibition strengthens T_{regs} in TIME, causing treatment failure with PD-1-based checkpoint inhibitors (308, 309). However, a co-treatment with anti-PD-1 and a LDH inhibitor serves as a better anticancer treatment as this approach inhibits lactylation of Lys72 in MOESIN (a member of the ERM (ezrin, radixin, and moesin) proteins). The MOESIN lactylation inhibition improves MOESIN interaction with TGF-β receptor I and downstream SMAD (suppressor of mothers against decapentaplegic) family member 3 (SMAD3) signaling activating FoxP3 in T_{regs} (310).

T_{reg} differentiation in TME or TIME depends on the Basic leucine zipper transcription factor, ATF-like or BATF transcription factor (311). T_{regs} are highly dependent on FAO or β lipid oxidation

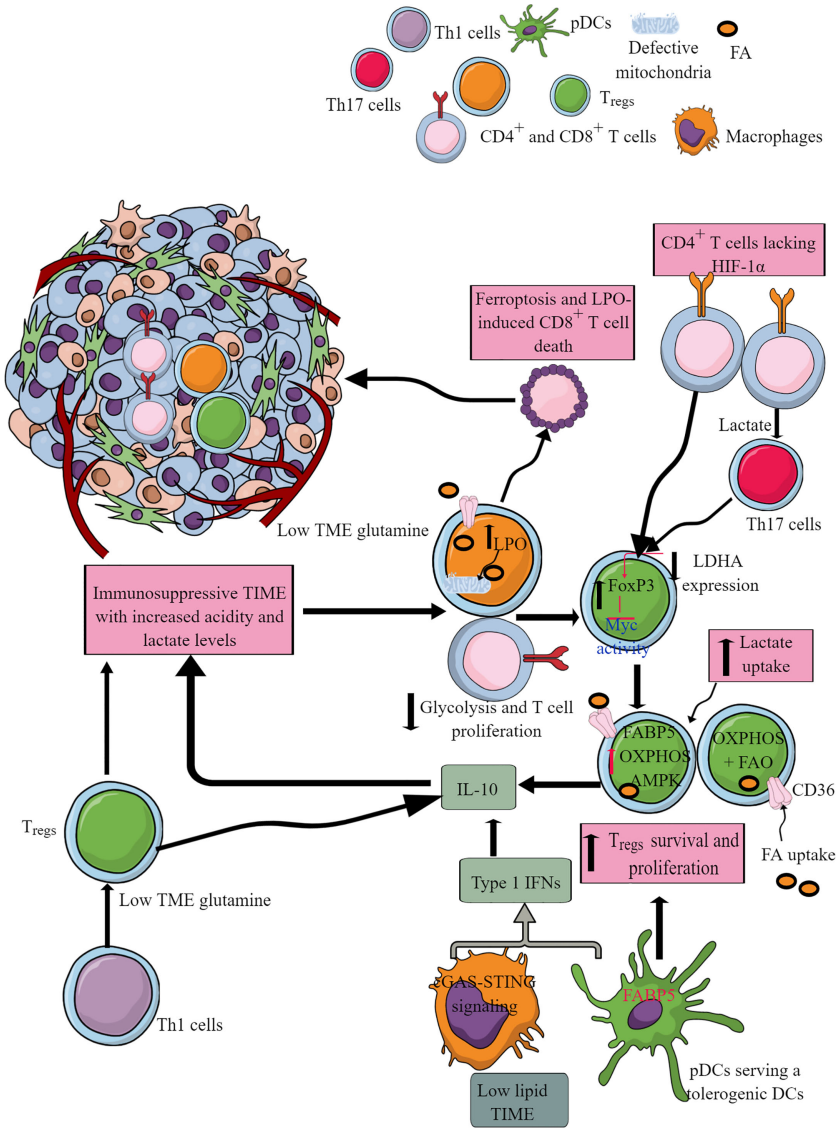

FIGURE 8
T cell subtypes and their immunometabolic reprogramming in the immunosuppressive TME or TIME. Different Th1 and cytotoxic T cells infiltrate initially to care for growing or premalignant tumors. However, the nutrient-deprived TME or TIME and the presence of immunosuppressive myeloid cells alter their function, including immunometabolic reprogramming. For example, CD8$^+$ cytotoxic T cells undergo cell death, including ferroptosis. Additionally, Th1 and Th17 cells in the high lactate and nutrient-deprived (glucose and glutamine) TIME polarize to immunosuppressive T_{regs}. All these events support T cell immunometabolic reprogramming to their tumor-supportive phenotype and function, including CD8+T cell death. Details are mentioned in the text.

and OXPHOS for their immunoregulatory function due to the lower Glut1 and higher AMPK expression (300, 301). The fatty acid binding protein 5 (FABP5, a cellular chaperone long-chain FAs) in T_{regs} regulates OXPHOS and immunosuppressive function by inducing the IL-10 release in response to the type 1 IFN (released in response to cGAS-STING signaling) in low lipid availability TME for immune cells (Figure 8) (312). Hence, FABP5 is a gatekeeper for mitochondrial integrity modulating T_{regs}. Furthermore, FABP5 expression in pDCs in TME or TIME supports their tolerogenic role via supporting the generation of T_{regs} (Figure 8) (313).

T_{regs} generation do not need mTOR kinase (314). Also, the CD36 expression increases in T_{regs}, supporting their survival and proliferation in TME or TIME via increased FA uptake (Figure 8) (315). Furthermore, CD36 fine-tunes mitochondrial fitness via PPAR-β signaling to increase T_{regs} survival in a lactate-rich acidic TME by increasing OXPHOS (Figure 8) (315, 316). On the other hand, CD36 expressed on $CD8^+$ cytotoxic T cells increases oxidized lipids/low-density lipoproteins (oxLDLs) uptake that increases lipid peroxidation (LPO) (Figure 8) (317). LPO activates p38 mitogen-activated protein kinase (p38MAPK) that induces $CD8^+$T cell dysfunction through defective mitochondrial biogenesis in mTOR-independent signaling pathway governing their autophagy and glycolysis (Figure 8) (317, 318). CD36-mediated lipid uptake by $CD8^+$T cells in TME also causes their ferroptosis and LPO to cause their death and immunosuppression (Figure 8) (319). Thus, CD36-mediated FA uptake determines T cell-dependent immunosuppressive TIME. Also, death/damage-associated molecular proteins (DAMPs) in TME promoting chronic inflammation can activate T_{regs} TLRs that, with FoxP3, balance mTORC1 signaling and glucose metabolism to control their proliferation and immunosuppressive function (320, 321). Hence, TME and TIME support T_{regs} for tumor growth and metastasis and induce resistance to chemotherapies and checkpoint inhibitors through immunometabolic reprogramming.

Th17 cells selectively express HIF-1α governed by mTOR signaling, a central regulator of cellular metabolism (301). HIF-1α is crucial for glycolysis induction and maintenance. The lack of HIF-1α in T cells at their differentiation stage reprograms them to develop into T_{regs} (Figure 8) (301). The tumor-associated Th17 cells with low glycolysis capacity reprogram to $FoxP3^+T_{regs}$ (Figure 8) (322). Thus, the local tissue environment, including metabolic status, is crucial determines T cell differentiation to their different phenotypes and function.

Low extracellular lactate promotes immune cell infiltration and proliferation at the premalignant stage, including T cells at the site to create a pro-inflammatory TIME to clear tumor cells. For example, $CD8^+$T cells under physiologic normoxia utilize glycolysis to exert antitumor action, including IFN-γ release and cytotoxicity (323). The prolyl-hydroxylase (PHD) proteins are intrinsic oxygen-sensing molecules that promote T_{regs} growth and proliferation during hypoxia that develops at later stages of cancer (323). The T cell-specific internal deletion or pharmacological inhibition of PHD increases the antitumor action of tumor-infiltrating T cells. The increased energy demand among tumor cells reprograms their metabolism to increased glycolysis and creates a hypoxic TME. The increased glycolysis among tumor cells in TME increases extracellular lactate accumulation, which impairs the nuclear factor of activated T-cells (NFAT) activation and IFN-γ production by T and NK cells (324–326). This impairs the anticancer/tumor action of tumor infiltrating $CD4^+$ and $CD8^+$ T cells in the pro-inflammatory environment. For example, tumor infiltrating T cells in the glucose-deprived TME could not reprogram their immunometabolism to glycolysis, forcing them to rely on OXPHOS without exhibiting the T_{eff} phenotype that causes their mitochondrial depolarization and exhaustion (327–329). IL-12 treatment rescues T cell exhaustion by increasing their mitochondrial potential and reducing their dependence of glycolysis (330). Hence, IL-12 treatment prevents forced OXPHOS while maintaining the balanced glycolysis and OXPHOS to maintain their full effector function.

The increased PD-1-PD-L1 signaling (TAMs, cancer cells, and tolerogenic DCs express PD-1 and PD-L1), altered epigenetic reprogramming, and nutrient-deprived stressful TME through coordinating with the TCR signaling prove lethal to tumor-infiltrating $CD8^+$T cells by altering their immunometabolic reprogramming (131, 327, 331, 332). Thus, low access to appropriate nutrients (glucose, glutamine, and lipids) imposes a significant barrier to T_{effs} via metabolic stress (333–336). For example, T cells under hypoxic conditions with limited glucose conditions exhibit mTORC1 signaling pathway inhibition, decreased antigen-induced expression of genes (including cell adhesion molecules, cell cycle progression), and $CD8^+$T cell proliferation and effector function (335, 337).

The insufficient glucose level in TME or TIME induces apoptosis among T_{effs}*via*activating pro-apoptosis genes/proteins, including phorbol-12-myristate-12 acetate-induced protein 1 (MAIP1/Noxa, a Bcl2 family protein) and Bcl-2-associated X protein (Bax), destabilizing myeloid cell leukemia 1 (Mcl1), an antiapoptotic Bcl-2 family protein (338). However, memory T_{effs} are not programmed to upregulate FAS, OXPHOS, and reductive glutaminolysis in limited glucose conditions, including TIME, which allows them to maintain their function in the nutrient-limited/depleted microenvironment (339). Thus, naïve T cells survive the nutrient-depleted TME or TIME but lose their effector function, but only memory T_{effs} survive and function in the environment. In addition, increasing FAO activity in $CD8^+$T cells in TME or TIME can enhance their cytotoxic action as they show an increased PPAR-α signaling and FA catabolism, which preserves their cytotoxic action (340, 341). However, it should be noted that tumor progression also increases co-inhibitor expression on $CD8^+$T cells, and PD-1 blockers delay tumor progression by affecting tumor-infiltrating lymphocyte (TIL) metabolism and function.

The cell motility is controlled by subtype-specific transporters called MCT1 (Slc5a12 and Slc16a1), specifically expressed on $CD4^+$ and $CD8^+$ T cells. The lactate accumulation suppresses the cytotoxic action of $CD8^+$T cells and promotes the $CD4^+$T cells switching to Th17 cells (Figure 8) (324). Also, IL-2 (a cytokine critical for antitumor T cell function) signaling-mediated STAT5 activation becomes limited in a highly acidic TME (342). This further suppresses antitumor $CD8^+$T cell function. The tumor-associated Th17 cells reprogram to $FoxP3^+T_{regs}$ in TME. The genetic targeting of LDHA in tumors decreases the pyruvate to lactate conversion

restoring T and NK cell infiltration and their antitumor cytotoxic function (325). Pyruvate dehydrogenase kinase 1 (PDHK1) via inhibiting PDH determines the cytosolic lactate levels in T cells that varies with T cell subtype (343). For example, Th17 cells show a robust PDHK1 expression, whereas T_{regs} have it at an intermediate level and Th1 cells have very little PDHK1. Hence, TME promotes Th1 cells reprogramming to Th17 cells, then to T_{regs} under intratumoral high lactate level that also suppresses IL-2 signaling (342). The increase in the glutaminolysis in tumor cells also deprives infiltrated T cells of glutamine, further compromising their growth and proliferation (Figure 8) (344). The glutamine-deficient TME reduces cytosolic α-KG in Th1 cells supporting their differentiation to T_{regs} (345). The glutaminase (a key enzyme involved in glutaminolysis) genetic deletion or glutamine uptake blockade in tumor cells increases TME glutamine and upregulates T cell infiltration (128, 346). The glutaminolysis is linked to polyamine biosynthesis via a Myc-dependent metabolic pathway in T cells (347). Hence, immunometabolic reprogramming among tumor-infiltrated T cells is governed by TME, including the hypoxia and lactate level.

HIF-1α during hypoxia induces the PDL-1 (CD274) expression in tumor cells, DCs, TAMs, and MDSCs to support immunosuppressive TIME (188). For example, PD-1^+ $CD8^+$T cells in TIME are most immunodysfunctional due to the mitochondria loss (348). The mitochondria loss affects their oxidative (TCA cycle, FAO, and OXPHOS) and membrane potential (ROS and ATP production) due to PPAR-γ coactivator 1α (PGC1α) loss, which programs mitochondrial biosynthesis by Akt signaling (348). B-lymphocyte-induced maturation protein 1 (BLIMP1) activation causes PGC1α loss. The PGC1α loss increases ROS production that, through phosphatase inhibition and the consequent activity of NFAT, promotes T cell exhaustion through mitochondrial dysfunction and loss (349–351). The mitochondrial mass loss in $CD8^+$T cells of TIME correlates well with PD-1 expression. Thus, the PD-1/PDL-1 interaction in TIME suppresses T cell immune response governed by their metabolic stage or alters T cell immunometabolism responsible for immunosuppression (142). The increased lipolysis of endogenous lipids and FAO among PD-1^+CD8^+T cells continuously exposed to PDL-1-expressing cells survive longer to support the immunosuppressive TIME. These immunosuppressive $CD8^+$T cells highly express CPT1A and the adipose triglyceride lipase (ATGL), the lipolysis marker glycerol, and the release of FAs (142). On the other hand, the T_{regs} PD-1 engagement with PDL-1 promotes FAO and mitochondrial OXPHOS to fuel their energy requirement in the presence of TGF-β (142, 352).

TGF-β suppresses PI3K-mediated mTOR signaling and inhibits glucose transporter and *hexokinase 2* (*Hk2*) expression that favors OXPHOS in induced-T_{regs} (iT_{regs}). PD-1 reduces the TGF-β threshold for its immunosuppressive action, including the T_{reg} development and function in the TIME (353). Reduced TGF-β signaling via TGF-β type 1 receptor (TβR1) is crucial for T cell activation and associated immune response (354). Hence, the increased TGF-β in TME and TIME suppresses antitumor T cell immune response through metabolic reprogramming. The details of PD-1 signaling mediated T cell immunometabolic reprogramming responsible for T cell immunosuppression are discussed elsewhere (141). Blocking PD-1/PDL-1 signaling restores glucose in TME, which permits T cell glycolysis and IFN-γ production as an antitumor immune response (78). However, blocking PD-L1 directly in tumors inhibits their glycolysis via suppressing mTOR signaling and glycolysis enzymes (78). Tumor and immune cell-secreted and expressed molecules create a T cell-mediated immunosuppressive TIME in the TME to support tumor growth, proliferation, and metastasis *via* immunometabolic reprogramming.

4.6 B cells in TIME and their immunometabolic reprogramming

Murine cancer models have indicated the role of B cells in tumor pathogenesis and immunity, including their regulatory role in innate immune cell infiltration in the premalignant tissue to promote chronic inflammation, which promotes epithelial carcinogenesis (Figure 9) (355, 356). For example, antibodies released from activated B cells in premalignant tissues fuel chronic inflammation through Fcγ receptor (FcγR)-dependent innate immune cell infiltration into the preneoplastic and neoplastic TME (Figure 9). Hence, B cells have been shown to promote cancer through promoting early malignancy via supporting chronic inflammation. However, in established tumors, B cells act as antitumor immune cells by promoting IFN-γ secreting Th1 immune cells, which are crucial for generating an adequate antitumor immunity in response to checkpoint inhibitors (357, 358). Even, intratumoral immunotherapy success depends on B and T cell collaboration (359, 360). In humans, intratumoral B cells are good prognosis markers for different cancers (361). However, the clonal diversity among infiltrated B cells affects survival of patients with cancer depending on type (362–364). For example, in TME or TIME, intratumoral B cell number highly depends on tertiary lymphoid structures (TLSs), as tumors without TLS have low B cell numbers (365, 366). Furthermore, B cell maturation, selection, and expansion occur in the mature TLS of tumor tissue that determines their antitumor (367, 368).

The mature TLS B cells increase antitumor T-cell activity in TIME and the responsiveness of tumors to immunotherapies (Figure 9) (368). On the other hand, B cells in immature TLSs do not have potent antitumor action. Instead, they become tumor-supportive (Figure 9). The B cell numbers, including the presence of switched memory B cells in tumor TLSs, guide the success of potential tumor immunotherapy and the associated patient survival (365). The details of B cells in TME and TIME are discussed elsewhere (361, 369–371). However, TLS maturation depends on the availability of extracellular ATP molecules (including the microbe-derived ones), which use ILC3-driven (IL-22, TNF-α, IL-8 and IL-2) and colony-stimulating factor 2 (CSF2)-dependent axis to induce the monocyte to macrophage transition in TIME (372, 373). These NCR^+ILC3s are in higher numbers in the early stages (stage 1 or 2) than in later tumor stages, and their presence directly correlates with the density of TLSs in TIME (373). For example, gut microbiota may influence the efficacy of tumor immunotherapy via many immunomodulatory mechanisms,

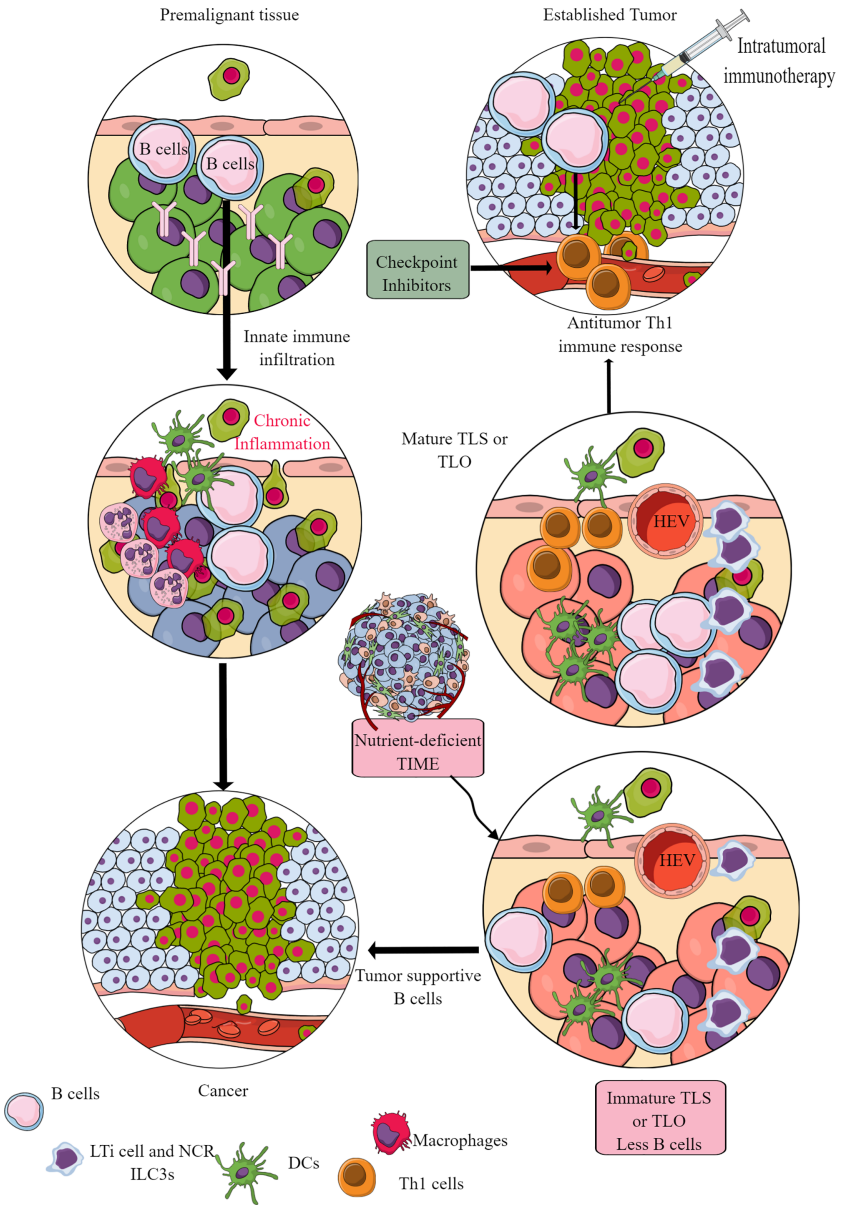

FIGURE 9
B cells in TIME. B cells in the premalignant tissue are the first immune cells to send signals to innate immune cells. This causes chronic inflammation. Unresolved chronic inflammation is linked to several cancers, including lung, breast, and colorectal cancers. However, in established tumors, B cells serve as antitumor immune cells and support intratumoral immunotherapies and Th1 immune response. However, only mature B cells perform antitumor functions, and their maturation occurs in the TLS or TLOs. The nutrient-deprived TME or TIME does not support TLS maturation, and immature B cells and B_{regs} increase immunosuppressive TIME. See text for details.

including the secretion of metabolites supporting the development and maturation of TLSs in TIME (374). Hence, a nutrient-competitive TME does not support the maturation of TLSs in TIME to escape from B cells and other immune cell-based antitumor immunity (Figure 9).

B cells are divided into B1 B cells, conventional B2 cells, and marginal zone B (MZB) cells. MZB cells have an innate-like function and are present mainly in the spleen along with LNs and blood to take care of blood-borne pathogens and circulating antigens or foreign particles (375, 376). Out of B1 (form in fetal life and then depend on self-renewal in adult life) and B2 B cells (constantly keep developing in BM), B1 B cells are more dependent on OXPHOS and glycolysis and are more active at the resting stage than B2 B cells (377–379). In addition, B1 B cells acquire external lipids as lipid droplets. Furthermore, B1 B cells have a unique immunometabolic programming that depends on their location and specific functional properties as autophagy-deficient B1-a B cells down-regulate critical metabolic genes and accumulate dysfunctional mitochondria (379). Hence, the autophagy gene Atg7 is crucial to maintain their immunometabolic status to support their high proliferative and secretary functions.

Non-proliferative naïve B cells depend on OXPHOS due to the glycogen synthase kinase 3 (GSK3) activity required to maintain their metabolic quiescence and prevent proliferation (380).

However, tumors have insufficient naive non-proliferating B cells (371). The germinal center (GC) B cells have different immunometabolic requirements depending on their location in the light zone (LZ) and dark zone (DZ). For example, in mature GCs (the microanatomical sites of antibody diversification (B cell clonal expansion) and affinity maturation), the DZ has large and mitotically active proliferating B cells (centroblasts) undergoing somatic hypermutation (SHM). These DZ B cells depend on glycolysis for the energy demand and differentiate into LZ B cells (381). Whereas the LZ of the GC contains a large portion of infiltrating and non-proliferative quiescent naïve B cells, which are also called centrocytes and compete for antigen presentation to follicular helper T (T_{fh}) cells mainly depend on OXPHOS (382, 383). However, LZ B cells expressing BCR and CD40 are rewired to highly express c-Myc, stimulating mitochondrial biosynthesis and genes required for glycolysis, promoting their re-entry to the DZ of the GC (384–386). These c-Myc-expressing centrocytes also express HIF-1α to support anaerobic glycolysis (387).

Memory B cells depend on OXPHOS for their metabolic demand. In contrast, plasma cells (PCs) or antibody-secreting B cells depend on OXPHOS and other carbon-utilizing metabolic pathways, including the TCA cycle, and nucleotide biosynthesis (PPS or PPP) that supports ribosome synthesis or ribogenesis, but not glycolysis (388–390). This glucose deprivation of PCs does not affect their humoral functions, but OXPHOS and glutaminolysis inhibition impairs their growth and differentiation. Hence, B cell activation requires considerable mitochondrial remodeling due to extensive OXPHOS. In addition, long-lived plasma cells (LLPCs) also depend on amino acid metabolism (glutaminolysis) and autophagosome formation (391, 392). Notably, PC metabolic reprogramming may also be affected by other factors, including the type of antibody production, location, and other metabolites (vitamins). For example, vitamin B1 supports the TCA cycle in Peyer's patches in IgM-producing PCs without affecting IgA production (393). The tumor-infiltrating IgM memory B cells and switched memory B cells (IgG- and IgA-producing PCs) are present in different cancers, including breast cancer (BC), renal cell carcinoma (RCC), and head and neck squamous cell carcinoma (HNSCC) (394–396). The GC B cells, plasmablasts, and plasma cells are present in non-small cell lung cancers (NSCLCs), RCCs, HNSCC, and ovarian and prostate cancers (367, 395–397).

In TME or TIME infiltrated B cells under the influence of IL-6, IL-1β, IL-12p35, and low oxygen (tumor-promoting molecules), which polarize to regulatory B cells (B_{regs}), producing TGF-β, granzyme B (GZMB), IL-10, and IL-35, which promote tumor growth and metastasis (398–402). The metabolic reprogramming among B_{regs} in TIME is unclear, but IL-10 secretion depends on glucose influx-dependent OXPHOS, PPP, amino acid metabolism, and oxygen level in the TME. Also, a balance between B_{regs} and PCs derives potential antitumor immunity during pancreatic cancer (403). However, IL-35 in TME breaks this balance and stimulates the STAT3-paried box 5 protein (PAX5, a transcription factor crucial for B cell differentiation) complex, upregulating B cell lymphoma 6 (BCL6, a transcriptional regulator) in naive B cells. BCL6 inhibition in tumor-educated B cells reverses dysregulated B cell differentiation and stimulates the intra-tumoral accumulation of PCs and T_{effs}. This renders pancreatic tumors sensitive to anti-PD-1 blockade (403). Hence, B cell metabolic reprogramming in the TME or TIME alters their antitumor action and promotes their polarization to tumor-supportive B_{regs}.

5 Targeting immunometabolic reprogramming in cancer

The dendrimer-mediated nanomedicine-based therapeutic targeting of TAM-specific mitochondria in glioblastoma has stimulated their anticancer function (404, 405). Also, targeting TAMs of pancreatic ductal adenocarcinoma (PDA) to block the pyrimidine metabolites' release, including deoxycytidine, sensitizes tumors to the anticancer drug gemcitabine (a pyrimidine anti-nucleoside) (406). The pyrimidine synthesis in M2 macrophages occurs in response to the increased FAO and TCA cycle (406). Also, serine metabolism is crucial for M1 to M2 macrophage polarization to support immunosuppressive TIME. Serine depletion, either by inhibiting phosphoglycerate dehydrogenase (PHGDH, crucial in the serine biosynthesis pathway) or by exogenous serine and glycine restriction, robustly enhances the polarization of M1 macrophages with antitumor potential along with suppressing M2 macrophages (407). Serine metabolism inhibition in macrophages increases the insulin-like growth factor-1 (IGF1) expression via decreasing the S-adenosyl methionine (SAM)-dependent histone H3 lysine 27 trimethylation. IGF1 then stimulates p38-dependent Janus kinase or JAK–STAT1 axis, promoting M(IFN-γ) or M1 polarization and suppressing M(IL-4)) or M2 macrophages (407). Hence, targeting macrophage metabolism in different cancers can increase the efficacy of available chemotherapies.

Also, targeting glutamine metabolism in TME blocks the immunosuppressive effects of MDSCs, induces their activation-induced cell death (AICD), and the MDSC transition to antitumor M1 macrophages (138). Glutamine metabolism inhibition, specifically to tumor and myeloid cells with a prodrug called 6-diazo-5-oxo-L-norleucine (DON), decreases CSF3 level in TME that blocks MDSCs recruitment and induces immunogenic cell death, promoting the recruitment of M1 macrophages. Targeting glutamine metabolism also inhibits the tryptophan metabolism generating immunosuppressive kynurenine metabolites (138). However, glutamine deprivation in $CD8^+$T cells of hepatocellular carcinoma (HCC) induces their apoptosis due to mitochondrial dysfunction (408). Hence, cell-specific glutamine metabolism targeting specifically in the TME/TIME may serve as a potential immunometabolism regulatory approach. However, lactate treatment increases the stemness of $CD8^+$T cells to augment their antitumor action by inhibiting histone deacetylase (HDAC) activity that acetylates H3K27 of the transcription factor 7 (Tcf7) super-enhancer locus causing its increased gene expression (409). Furthermore, the adoptive transfer of $CD8^+$T cells treated *in vitro* with lactate show an increased antitumor action. Hence, adoptive transfer of oncometabolites' treated T cells may serve as immune cell-based therapeutics for cancer due to their epigenetic modification and resistance development to harsh TME. However, further studies are needed in this direction.

The CD28-mediated co-stimulation among tumor (ccRCC) infiltrated $CD8^+$T cells has restored their defective glycolysis and mitochondrial oxidative metabolism by upregulating Glut3 (410, 411). However, an early study indicated that glycolysis does not support long-term memory $CD8^+$T cell formation and their antitumor action (412). Hence, it becomes crucial to explore these effects related to glycolysis in naïve $CD8^+$T cells or tumor-infiltrated $CD8^+$T cells to better design immunometabolic reprogramming approaches specific to different cancers. CD47 regulates $CD8^+$ T cell activation, proliferation, and fitness in a context-dependent manner, including cancer (413). So, it will be novel to understand the impact of CD47 engagement on glycolysis in $CD8^+$T cells in TIME or homeostasis. For example, CD47 blockage on $CD8^+$T cells mediates immunogenic tumor destruction (414, 415). Furthermore, the decreased CD47 expression on cancer cells increases macrophage infiltration in tumors with an enhanced potential to phagocytose cancer cells (416). CD47 expression increases in TME in response to IL-18 released from macrophages during chemotherapy (doxorubicin). IL-18 upregulates L-amino acid transporter 2 (LAT2) expression in tumor cells, enhancing leucine and glutamine uptake. Glutamine and leucine are two potent mTORC1 signaling stimulators. Thus, increased cellular leucine levels and glutaminolysis activate mTORC1 signaling, which by c-Myc activation, induces CD47 transcription and expression (416). Hence, CD47 blocking in $CD8^+$T cells and tumor cells may increase tumor clearance and patient survival through metabolic alteration of tumor and immune cells.

Additionally, glutarate administration reduces the tumor burden by increasing $CD8^+$T cells in the TME and systemic circulation and their antitumor function by immunometabolic reprogramming (417). The glutarate reprograms $CD8^+$T cell immunometabolism responsible for their cytotoxic function, involving a post-translational modification of the pyruvate dehydrogenase E2 (PDHE2) subunit of the PDH complex (PDHc). The PDHc glutarylation induces a rapid pyruvate conversion to lactate and increased glycolysis in $CD8^+$T cells to reprogram their antitumor function (417). Furthermore, the magnesium (Mg^{2+}) treatment increases the co-stimulatory function of leukocyte function-associated antigen-1 (LFA-1) on $CD8^+$T cells to exert their cytotoxic action against tumor cells via different mechanisms, including immunometabolic reprogramming (418, 419). CAR-T cells also exert an improved and more extended antitumor function upon Mg^{2+} supplementation. Notably, TME has less available Mg^{2+} for immune cells, including $CD8^+$T cells, due to its high usage by tumor cells. Hence, intratumoral Mg^{2+} supplementation improves antitumor TIME to fight against tumors and improves CAR-T cell-based immunotherapy.

L-arginine availability to T cells increases their survival by immunometabolic reprogramming (transition of glycolysis to OXPHOS). It promotes their differentiation to central memory-like T cells with anti-tumor activity without inducing mTOR signaling (420). L-arginine increases T cell survival in TME through targeting transcriptional regulators bromodomain adjacent to the zinc finger domain 1B (BAZ1B) or Williams syndrome transcription factor (WSTF), PC4 and SFRS1 interacting protein 1 (PSIP1), and translin (TSN) (420). The mitochondrial arginase 2 (Arg2) depletion in $CD8^+$T cells increases their survival and antitumor action (421). The $CD8^+$T cell-specific Arg2 inhibition synergizes the antitumor action of PD-1 blocking checkpoint inhibitors. Thus, l-arginine depletion in the TME or TIME by tumor cells and myeloid suppressor cells due to the activation enzymes (Arg1 and iNOS2) compromises an efficient antitumor action of T cells, including $CD8^+$T cells to clear tumor cells (422). The use of genetically modified bacteria (*Escherichia coli* Nissle 1917 strain) or ECN that utilizes ammonia to synthesize L-arginine in tumors has increased antitumor T cell infiltration in TME or TIME to clear the tumor (423, 424). This genetically modified bacteria used as bacterial anticancer therapy (BAT) works synergistically with PD-1 blockers to clear tumors. Hence, emerging immunometabolic reprogramming targeting different cancers has a better future as a specific-immune cell-based tumor targeting and synergizing the available checkpoint inhibitors.

6 Future perspective and conclusion

The immune system is key to checking the induction, development, growth, and metastasis of cancer. Immunometabolic reprogramming among immune cells governs their stimulatory and inhibitory immune functions depending on the stimuli and tissue environment. Thus, it has become crucial to understanding immunometabolic reprogramming and its governing factors in TIME. The development of a robust immunosuppressive TIME has become a landscape for tumor growth, proliferation, and metastasis. For example, increased lactate levels in TME or TIME induce immunosuppressive immunometabolic reprogramming and block the antitumor function of immune cell-based immunotherapies (adoptive T cell therapies) and checkpoint inhibitors (425, 426). LDHA inhibitor (GSK2837808A) has improved the antitumor activity of $CD8^+$T cells via altering their immunometabolic reprogramming responsible for their exhaustion and apoptosis (426). Furthermore, TME or TIME lactate levels can be lowered using MCT1 and MCT4 lactate transporter inhibitors (AZD3965) to improve the existing immune cell-based therapies (427–429).

The increased lactate accumulation in TME or TIME occurs due to overwhelming glycolysis in tumor cells (426). Thus, tumor cell-specific glycolysis can also be a therapeutic approach that directly targets tumor cells, and will also increase the efficacy of immune cell-based immunotherapies and checkpoint inhibitors via decreasing the TME lactate levels (430–433). Fumarate accumulation in TME also inhibits B cell function via covalent inhibition of a tyrosine kinase LYNN of the B cell receptor (BCR) signaling pathway (434). The fumarate deposition blocks BCR signaling-mediated antitumor action, including antibody production and cytokine release. Additionally, fumarate has other tumor-supportive effects by altering different immune cells, but its impact on their immunometabolic reprogramming remains to study (435). Hence, targeting tumor cell-specific glycolysis and lactate and fumarate accumulation in TME indirectly enhances the antitumor action of immune cells by immunometabolic reprogramming. Many metabolic inhibitors with potential to clinical translation are at different clinical trial stages (II and III), which can be used to reprogram TME immunometabolism (23, 25).

Calcium carbonate ($CaCO_3$) nanoparticles coated with 4-phenylimidazole (4PI) inhibit IDO1 to increase the radiotherapy efficacy (436). These nanoparticles are called acidity-IDO1-modulation nanoparticles (AIM NPs), which instantly neutralize protons (H^+) and release 4PI to inhibit the immunosuppressive IDO1 activity in the TME. Thus, AIM NPs reinforce the radiotherapy via modulating the immunosuppressive metabolic reprograming in the TME. Another nanoparticle-based approach during low dose radiotherapy has increased ICIs (PD-1/PD-L1 blockers) efficacy via reprograming immunosuppressive TME immunometabolism in triple negative breast cancer (TNBC) patients (437). This approach involves scavenging the reduced nicotinamide adenine dinucleotide phosphate (NADPH) inside tumor cells by developing the nanomolecule (BMS202@HZP) targeting hypoxia and PD-1/PD-L1 interaction during low dose radiotherapy against TNBC (437). Along with conventional nanomedicine, thermal-immuno nanomedicine is emerging as potential antitumor therapy (438–440). Hence understanding and developing nanomedicine-based approaches specifically targeting TME immunometabolism have a bright future for tumor immunotherapy. For instance, understanding metabolic reprograming, including immunometabolism can rewire radio-oncology for better therapeutic ratio or outcome (441). We need further studies in this direction.

Aging is one of several predisposing factors for cancer as it alters immune cell functions via inducing altered immunometabolism (442, 443). For example, the B cells of older people show a significant reduction in their OXPHOS compared to glycolysis (444). Also, T cells isolated from older adults exhibit decreased glycolysis and OXPHOS but increased mitochondrial ROS generation, indicating an impaired mitochondrial function (442). Aging-associated immunometabolic reprogramming among older adults induces a stage of chronic inflammation that may serve as cancer predisposing factor. Thus, the immunometabolic profile of aged people may indicate their future risk for cancer. Spermidine, a polyamine considered an antiaging molecule enhances the antitumor action of $CD8^+$T or nanobody-based CAR-T cells (Nb CAR-T) cells via immunometabolic reprogramming that increases IFN-γ and IL-2 production (445).

OVT is an emerging area to convert cold tumors to hot tumors or TME through reprogramming immunosuppressive TIME to pro-inflammatory antitumor immunity when used alone or with available checkpoint inhibitors (446–449). However, how OVT modulates the immunometabolic reprogramming among specific immune cells of TIME is an exciting research area to delineate. Also, immunometabolism has emerged as a novel way to target specific immune cell populations in diverse diseases, including sepsis, autoimmunity, and other infectious diseases. The information discussed in the present article specifies that the immunometabolic reprogramming among infiltrated immune cells alters in TME or TIME and needs great attention as it diverts immune cells' normal antitumor function to support tumor growth and metastasis. Hence, immunometabolic reprogramming is another cancer hallmark with significant therapeutic potential based on cancer stages and immune cell population. Thus, studying cancer-associated immunometabolic reprogramming will help to design better immune cell-based therapies, BATs, and OVTs in the future.

Author contributions

VK has developed the idea, wrote the article and conceptualized and developed the figures. JS has done the proofreading and final edits.

Conflict of interest

The authors declare that the research was conducted in the absence of any commercial or financial relationships that could be construed as a potential conflict of interest.

Publisher's note

References

1. Sung H, Ferlay J, Siegel RL, Laversanne M, Soerjomataram I, Jemal A, et al. Global cancer statistics 2020: GLOBOCAN estimates of incidence and mortality worldwide for 36 cancers in 185 countries. *CA: A Cancer J Clin* (2021) 71:209–49. doi: 10.3322/caac.21660

2. Aquino A, Formica V, Prete SP, Correale PP, Massara MC, Turriziani M, et al. Drug-induced increase of carcinoembryonic antigen expression in cancer cells. *Pharmacol Res* (2004) 49:383–96. doi: 10.1016/j.phrs.2003.12.007

3. Ebrahimi N, Akbari M, Ghanaatian M, Roozbahani Moghaddam P, Adelian S, Borjian Boroujeni M, et al. Development of neoantigens: from identification in cancer cells to application in cancer vaccines. *Expert Rev Vaccines* (2022) 21:941–55. doi: 10.1080/14760584.2021.1951246

4. Pardal R, Clarke MF, Morrison SJ. Applying the principles of stem-cell biology to cancer. *Nat Rev Cancer* (2003) 3:895–902. doi: 10.1038/nrc1232

5. Sell S, Pierce GB. Maturation arrest of stem cell differentiation is a common pathway for the cellular origin of teratocarcinomas and epithelial cancers. *Lab Invest* (1994) 70:6–22.

6. Fearon ER, Burke PJ, Schiffer CA, Zehnbauer BA, Vogelstein B. Differentiation of leukemia cells to polymorphonuclear leukocytes in patients with acute nonlymphocytic leukemia. *N Engl J Med* (1986) 315:15–24. doi: 10.1056/NEJM198607033150103

7. Li Z, Seehawer M, Polyak K. Untangling the web of intratumour heterogeneity. *Nat Cell Biol* (2022) 24:1192–201. doi: 10.1038/s41556-022-00969-x

8. Meldi L, Brickner JH. Compartmentalization of the nucleus. *Trends Cell Biol* (2011) 21:701–8. doi: 10.1016/j.tcb.2011.08.001

9. Spilianakis CG, Flavell RA. Long-range intrachromosomal interactions in the T helper type 2 cytokine locus. *Nat Immunol* (2004) 5:1017–27. doi: 10.1038/ni1115

10. Spilianakis CG, Lalioti MD, Town T, Lee GR, Flavell RA. Interchromosomal associations between alternatively expressed loci. *Nature* (2005) 435:637–45. doi: 10.1038/nature03574

11. Yi E, Chamorro González R, Henssen AG, Verhaak RGW. Extrachromosomal DNA amplifications in cancer. *Nat Rev Genet* (2022) 23:760–71. doi: 10.1038/s41576-022-00521-5

12. Hung KL, Mischel PS, Chang HY. Gene regulation on extrachromosomal DNA. *Nat Struct Mol Biol* (2022) 29:736–44. doi: 10.1038/s41594-022-00806-7

13. Hung KL, Yost KE, Xie L, Shi Q, Helmsauer K, Luebeck J, et al. ecDNA hubs drive cooperative intermolecular oncogene expression. *Nature* (2021) 600:731–6. doi: 10.1038/s41586-021-04116-8

14. van Leen E, Brückner L, Henssen AG. The genomic and spatial mobility of extrachromosomal DNA and its implications for cancer therapy. *Nat Genet* (2022) 54:107–14. doi: 10.1038/s41588-021-01000-z

15. Wu S, Turner KM, Nguyen N, Raviram R, Erb M, Santini J, et al. Circular ecDNA promotes accessible chromatin and high oncogene expression. *Nature* (2019) 575:699–703. doi: 10.1038/s41586-019-1763-5

16. Kim H, Nguyen NP, Turner K, Wu S, Gujar AD, Luebeck J, et al. Extrachromosomal DNA is associated with oncogene amplification and poor outcome across multiple cancers. *Nat Genet* (2020) 52:891–7. doi: 10.1038/s41588-020-0678-2

17. Wu S, Bafna V, Chang HY, Mischel PS. Extrachromosomal DNA: an emerging hallmark in human cancer. *Annu Rev Pathol* (2022) 17:367–86. doi: 10.1146/annurev-pathmechdis-051821-114223

18. Bafna V, Mischel PS. Extrachromosomal DNA in cancer. *Annu Rev Genomics Hum Genet* (2022) 23:29–52. doi: 10.1146/annurev-genom-120821-100535

19. Hanahan D, Weinberg RA. The hallmarks of cancer. *Cell* (2000) 100:57–70. doi: 10.1016/S0092-8674(00)81683-9

20. Hanahan D, Robert A. Hallmarks of cancer: the next generation. *Cell* (2011) 144:646–74. doi: 10.1016/j.cell.2011.02.013

21. Floor SL, Dumont JE, Maenhaut C, Raspe E. Hallmarks of cancer: of all cancer cells, all the time? *Trends Mol Med* (2012) 18:509–15. doi: 10.1016/j.molmed.2012.06.005

22. DePeaux K, Delgoffe GM. Metabolic barriers to cancer immunotherapy. *Nat Rev Immunol* (2021) 21:785–97. doi: 10.1038/s41577-021-00541-y

23. Leone RD, Powell JD. Metabolism of immune cells in cancer. *Nat Rev Cancer* (2020) 20:516–31. doi: 10.1038/s41568-020-0273-y

24. O'Sullivan D, Sanin DE, Pearce EJ, Pearce EL. Metabolic interventions in the immune response to cancer. *Nat Rev Immunol* (2019) 19:324–35. doi: 10.1038/s41577-019-0140-9

25. Li X, Wenes M, Romero P, Huang SC-C, Fendt S-M, Ho P-C. Navigating metabolic pathways to enhance antitumour immunity and immunotherapy. *Nat Rev Clin Oncol* (2019) 16:425–41. doi: 10.1038/s41571-019-0203-7

26. Martínez-Reyes I, Chandel NS. Cancer metabolism: looking forward. *Nat Rev Cancer* (2021) 21:669–80. doi: 10.1038/s41568-021-00378-6

27. Elia I, Haigis MC. Metabolites and the tumour microenvironment: from cellular mechanisms to systemic metabolism. *Nat Metab* (2021) 3:21–32. doi: 10.1038/s42255-020-00317-z

28. Hanahan D. Hallmarks of cancer: new dimensions. *Cancer Discov* (2022) 12:31–46. doi: 10.1158/2159-8290.CD-21-1059

29. Brunner JS, Finley LWS. Metabolic determinants of tumour initiation. *Nat Rev Endocrinol* (2023) 19:134–50. doi: 10.1038/s41574-022-00773-5

30. Perez-Lanzon M, Zitvogel L, Kroemer G. Failure of immunosurveillance accelerates aging. *Oncoimmunology* (2019) 8:e1575117. doi: 10.1080/2162402X.2019.1575117

31. Vesely MD, Kershaw MH, Schreiber RD, Smyth MJ. Natural innate and adaptive immunity to cancer. *Annu Rev Immunol* (2011) 29:235–71. doi: 10.1146/annurev-immunol-031210-101324

32. Ribatti D. The concept of immune surveillance against tumors. *first theories. Oncotarget* (2017) 8:7175–80. doi: 10.18632/oncotarget.12739

33. Swann JB, Smyth MJ. Immune surveillance of tumors. *J Clin Invest* (2007) 117:1137–46. doi: 10.1172/JCI31405

34. Gajewski TF, Schreiber H, Fu Y-X. Innate and adaptive immune cells in the tumor microenvironment. *Nat Immunol* (2013) 14:1014–22. doi: 10.1038/ni.2703

35. Martins Lopes MS, Machado LM, Ismael Amaral Silva PA, Tome Uchiyama AA, Yen CT, Ricardo ED, et al. Antibiotics, cancer risk and oncologic treatment efficacy: a practical review of the literature. *Ecancermedicalscience* (2020) 14:1106. doi: 10.3332/ecancer.2020.1106

36. Simin J, Fornes R, Liu Q, Olsen RS, Callens S, Engstrand L, et al. Antibiotic use and risk of colorectal cancer: a systematic review and dose-response meta-analysis. *Br J Cancer* (2020) 123:1825–32. doi: 10.1038/s41416-020-01082-2

37. Li CH, Haider S, Boutros PC. Age influences on the molecular presentation of tumours. *Nat Commun* (2022) 13:208. doi: 10.1038/s41467-021-27889-y

38. Henry CJ, Marusyk A, DeGregori J. Aging-associated changes in hematopoiesis and leukemogenesis: what's the connection? *Aging (Albany NY)* (2011) 3:643–56. doi: 10.18632/aging.100351

39. Burnet FM. The concept of immunological surveillance. *Prog Exp Tumor Res* (1970) 13:1–27. doi: 10.1159/000386035

40. Burnet FM. Immunological surveillance in neoplasia. *Transplant Rev* (1971) 7:3–25. doi: 10.1111/j.1600-065X.1971.tb00461.x

41. Nayak DA, Binder RJ. Agents of cancer immunosurveillance: HSPs and dsDNA. *Trends Immunol* (2022) 43:404–13. doi: 10.1016/j.it.2022.03.004

42. Sedlacek AL, Younker TP, Zhou YJ, Borghesi L, Shcheglova T, Mandoiu II, et al. CD91 on dendritic cells governs immunosurveillance of nascent, emerging tumors. *JCI Insight* (2019) 4(7):e127239. doi: 10.1172/jci.insight.127239

43. Binder RJ, Han DK, Srivastava PK. CD91: a receptor for heat shock protein gp96. *Nat Immunol* (2000) 1:151–5. doi: 10.1038/77835

44. Hiam-Galvez KJ, Allen BM, Spitzer MH. Systemic immunity in cancer. *Nat Rev Cancer* (2021) 21:345–59. doi: 10.1038/s41568-021-00347-z

45. Xu L, Zou C, Zhang S, Chu TSM, Zhang Y, Chen W, et al. Reshaping the systemic tumor immune environment (STIE) and tumor immune microenvironment (TIME) to enhance immunotherapy efficacy in solid tumors. *J Hematol Oncol* (2022) 15:87. doi: 10.1186/s13045-022-01307-2

46. Schlichtner S, Yasinska IM, Lall GS, Berger SM, Ruggiero S, Cholewa D, et al. T Lymphocytes induce human cancer cells derived from solid malignant tumors to secrete galectin-9 which facilitates immunosuppression in cooperation with other immune checkpoint proteins. *J Immunother Cancer* (2023) 11:e005714. doi: 10.1136/jitc-2022-005714

47. Yuan L, Tatineni J, Mahoney KM, Freeman GJ. VISTA: a mediator of quiescence and a promising target in cancer immunotherapy. *Trends Immunol* (2021) 42:209–27. doi: 10.1016/j.it.2020.12.008

48. Schlichtner S, Yasinska IM, Ruggiero S, Berger SM, Aliu N, Prunk M, et al. Expression of the immune checkpoint protein VISTA is differentially regulated by the TGF-β1 - Smad3 signaling pathway in rapidly proliferating human cells and T lymphocytes. *Front Med (Lausanne)* (2022) 9:790995. doi: 10.3389/fmed.2022.790995

49. Wang YA, Li XL, Mo YZ, Fan CM, Tang L, Xiong F, et al. Effects of tumor metabolic microenvironment on regulatory T cells. *Mol Cancer* (2018) 17:168. doi: 10.1186/s12943-018-0913-y

50. Shi X, Yang J, Deng S, Xu H, Wu D, Zeng Q, et al. TGF-β signaling in the tumor metabolic microenvironment and targeted therapies. *J Hematol Oncol* (2022) 15:135. doi: 10.1186/s13045-022-01349-6

51. Rabadi D, Sajani AA, Noelle RJ, Lines JL. The role of VISTA in the tumor microenvironment. *J Cancer Metastasis Treat* (2022) 8:24. doi: 10.20517/2394-4722.2022.06

52. Zhang F, Wang H, Wang X, Jiang G, Liu H, Zhang G, et al. TGF-β induces M2-like macrophage polarization via SNAIL-mediated suppression of a pro-inflammatory phenotype. *Oncotarget* (2016) 7:52294–306. doi: 10.18632/oncotarget.10561

53. Cairns RA, Harris IS, Mak TW. Regulation of cancer cell metabolism. *Nat Rev Cancer* (2011) 11:85–95. doi: 10.1038/nrc2981

54. Soga T. Cancer metabolism: key players in metabolic reprogramming. *Cancer Sci* (2013) 104:275–81. doi: 10.1111/cas.12085

55. Hua W, ten Dijke P, Kostidis S, Giera M, Hornsveld M. TGFβ-induced metabolic reprogramming during epithelial-to-mesenchymal transition in cancer. *Cell Mol Life Sci* (2020) 77:2103–23. doi: 10.1007/s00018-019-03398-6

56. Vander Heiden MG, Cantley LC, Thompson CB. Understanding the warburg effect: the metabolic requirements of cell proliferation. *Science* (2009) 324:1029–33. doi: 10.1126/science.1160809

57. Gatenby RA, Gawlinski ET, Gmitro AF, Kaylor B, Gillies RJ. Acid-mediated tumor invasion: a multidisciplinary study. *Cancer Res* (2006) 66:5216–23. doi: 10.1158/0008-5472.CAN-05-4193

58. Hirschhaeuser F, Sattler UGA, Mueller-Klieser W. Lactate: a metabolic key player in cancer. *Cancer Res* (2011) 71:6921–5. doi: 10.1158/0008-5472.CAN-11-1457

59. Warburg O. On the origin of cancer cells. *Science* (1956) 123:309–14. doi: 10.1126/science.123.3191.309

60. Semenza GL, Artemov D, Bedi A, Bhujwalla Z, Chiles K, Feldser D, et al. 'The metabolism of tumours': 70 years later. *Novartis Found Symp* (2001) 240:251–60. doi: 10.1002/0470868716.ch17

61. Liberti MV, Locasale JW. The warburg effect: how does it benefit cancer cells? *Trends Biochem Sci* (2016) 41:211–8. doi: 10.1016/j.tibs.2015.12.001

62. Bustamante E, Morris HP, Pedersen PL. Energy metabolism of tumor cells. requirement for a form of hexokinase with a propensity for mitochondrial binding. *J Biol Chem* (1981) 256:8699–704. doi: 10.1016/S0021-9258(19)68900-3

63. Quintero M, Mackenzie N, Brennan PA. Hypoxia-inducible factor 1 (HIF-1) in cancer. *Eur J Surg Oncol* (2004) 30:465–8. doi: 10.1016/j.ejso.2004.03.008

64. Semenza GL. Targeting HIF-1 for cancer therapy. *Nat Rev Cancer* (2003) 3:721–32. doi: 10.1038/nrc1187

65. Wu Q, You L, Nepovimova E, Heger Z, Wu W, Kuca K, et al. Hypoxia-inducible factors: master regulators of hypoxic tumor immune escape. *J Hematol Oncol* (2022) 15:77. doi: 10.1186/s13045-022-01292-6

66. Icard P, Shulman S, Farhat D, Steyaert J-M, Alifano M, Lincet H. How the warburg effect supports aggressiveness and drug resistance of cancer cells? *Drug Resistance Updates* (2018) 38:1–11. doi: 10.1016/j.drup.2018.03.001

67. Sebastian C, Ferrer C, Serra M, Choi J-E, Ducano N, Mira A, et al. A non-dividing cell population with high pyruvate dehydrogenase kinase activity regulates

metabolic heterogeneity and tumorigenesis in the intestine. *Nat Commun* (2022) 13:1503. doi: 10.1038/s41467-022-29085-y

68. Sullivan MR, Danai LV, Lewis CA, Chan SH, Gui DY, Kunchok T, et al. Quantification of microenvironmental metabolites in murine cancers reveals determinants of tumor nutrient availability. *eLife* (2019) 8:e44235. doi: 10.7554/eLife.44235

69. Ren Y, Kumar A, Das JK, Peng HY, Wang L, Balllard D, et al. Tumorous expression of NAC1 restrains antitumor immunity through the LDHA-mediated immune evasion. *J Immunother Cancer* (2022) 10(9):e004856. doi: 10.1136/jitc-2022-004856

70. Fischer K, Hoffmann P, Voelkl S, Meidenbauer N, Ammer J, Edinger M, et al. Inhibitory effect of tumor cell–derived lactic acid on human T cells. *Blood* (2007) 109:3812–9. doi: 10.1182/blood-2006-07-035972

71. Mu X, Shi W, Xu Y, Xu C, Zhao T, Geng B, et al. Tumor-derived lactate induces M2 macrophage polarization via the activation of the ERK/STAT3 signaling pathway in breast cancer. *Cell Cycle* (2018) 17:428–38. doi: 10.1080/15384101.2018.1444305

72. Noe JT, Rendon BE, Geller AE, Conroy LR, Morrissey SM, Young LEA, et al. Lactate supports a metabolic-epigenetic link in macrophage polarization. *Sci Adv* (2021) 7:eabi8602. doi: 10.1126/sciadv.abi8602

73. Raychaudhuri D, Bhattacharya R, Sinha BP, Liu CSC, Ghosh AR, Rahaman O, et al. Lactate induces pro-tumor reprogramming in intratumoral plasmacytoid dendritic cells. *Front Immunol* (2019) 10. doi: 10.3389/fimmu.2019.01878

74. Marin E, Bouchet-Delbos L, Renoult O, Louvet C, Nerriere-Daguin V, Managh AJ, et al. Human tolerogenic dendritic cells regulate immune responses through lactate synthesis. *Cell Metab* (2019) 30:1075–1090.e8. doi: 10.1016/j.cmet.2019.11.011

75. Ratter JM, Rooijackers HMM, Hooiveld GJ, Hijmans AGM, de Galan BE, Tack CJ, et al. *In vitro* and *in vivo* effects of lactate on metabolism and cytokine production of human primary PBMCs and monocytes. *Front Immunol* (2018) 9:2564. doi: 10.3389/fimmu.2018.02564

76. Courtney KD, Bezwada D, Mashimo T, Pichumani K, Vemireddy V, Funk AM, et al. Isotope tracing of human clear cell renal cell carcinomas demonstrates suppressed glucose oxidation *In vivo*. *Cell Metab* (2018) 28:793–800.e2. doi: 10.1016/j.cmet.2018.07.020

77. Sanderson SM, Locasale JW. Revisiting the warburg effect: some tumors hold their breath. *Cell Metab* (2018) 28:669–70. doi: 10.1016/j.cmet.2018.10.011

78. Chang CH, Qiu J, O'Sullivan D, Buck MD, Noguchi T, Curtis JD, et al. Metabolic competition in the tumor microenvironment is a driver of cancer progression. *Cell* (2015) 162:1229–41. doi: 10.1016/j.cell.2015.08.016

79. Buck MD, Sowell RT, Kaech SM, Pearce EL. Metabolic instruction of immunity. *Cell* (2017) 169:570–86. doi: 10.1016/j.cell.2017.04.004

80. Reinfeld BI, Madden MZ, Wolf MM, Chytil A, Bader JE, Patterson AR, et al. Cell-programmed nutrient partitioning in the tumour microenvironment. *Nature* (2021) 593:282–8. doi: 10.1038/s41586-021-03442-1

81. Bian Y, Li W, Kremer DM, Sajjakulnukit P, Li S, Crespo J, et al. Cancer SLC43A2 alters T cell methionine metabolism and histone methylation. *Nature* (2020) 585:277–82. doi: 10.1038/s41586-020-2682-1

82. Hung MH, Lee JS, Ma C, Diggs LP, Heinrich S, Chang CW, et al. Tumor methionine metabolism drives T-cell exhaustion in hepatocellular carcinoma. *Nat Commun* (2021) 12:1455. doi: 10.1038/s41467-021-21804-1

83. Weiss TS, Bernhardt G, Buschauer A, Thasler WE, Dolgner D, Zirngibl H, et al. Polyamine levels of human colorectal adenocarcinomas are correlated with tumor stage and grade. *Int J Colorectal Dis* (2002) 17:381–7. doi: 10.1007/s00384-002-0394-7

84. Akinyele O, Wallace HM. Understanding the polyamine and mTOR pathway interaction in breast cancer cell growth. *Med Sci (Basel)* (2022) 10(3):51. doi: 10.3390/medsci10030051

85. O'Brien TG, Megosh LC, Gilliard G, Soler AP. Ornithine decarboxylase overexpression is a sufficient condition for tumor promotion in mouse skin. *Cancer Res* (1997) 57:2630–7.

86. Linsalata M, Caruso MG, Leo S, Guerra V, D'Attoma B, Di Leo A. Prognostic value of tissue polyamine levels in human colorectal carcinoma. *Anticancer Res* (2002) 22:2465–9.

87. Lan L, Trempus C, Gilmour SK. Inhibition of ornithine decarboxylase (ODC) decreases tumor vascularization and reverses spontaneous tumors in ODC/Ras transgenic mice. *Cancer Res* (2000) 60:5696–703.

88. McNamara KM, Gobert AP, Wilson KT. The role of polyamines in gastric cancer. *Oncogene* (2021) 40:4399–412. doi: 10.1038/s41388-021-01862-x

89. Holbert CE, Cullen MT, Casero RAJr., Stewart TM. Polyamines in cancer: integrating organismal metabolism and antitumour immunity. *Nat Rev Cancer* (2022) 22:467–80. doi: 10.1038/s41568-022-00473-2

90. Soda K. The mechanisms by which polyamines accelerate tumor spread. *J Exp Clin Cancer Res* (2011) 30:95. doi: 10.1186/1756-9966-30-95

91. Latour YL, Gobert AP, Wilson KT. The role of polyamines in the regulation of macrophage polarization and function. *Amino Acids* (2020) 52:151–60. doi: 10.1007/s00726-019-02719-0

92. Puleston DJ, Baixauli F, Sanin DE, Edwards-Hicks J, Villa M, Kabat AM, et al. Polyamine metabolism is a central determinant of helper T cell lineage fidelity. *Cell* (2021) 184:4186–4202.e20. doi: 10.1016/j.cell.2021.06.007

93. Wagner A, Wang C, Fessler J, DeTomaso D, Avila-Pacheco J, Kaminski J, et al. Metabolic modeling of single Th17 cells reveals regulators of autoimmunity. *Cell* (2021) 184:4168–4185.e21. doi: 10.1016/j.cell.2021.05.045

94. Shi H, Chi H. Polyamine: a metabolic compass for T helper cell fate direction. *Cell* (2021) 184:4109–12. doi: 10.1016/j.cell.2021.07.012

95. Harbison RA, Pandey R, Considine M, Leone RD, Murray-Stewart T, Erbe R, et al. Interrogation of T cell-enriched tumors reveals prognostic and immunotherapeutic implications of polyamine metabolism. *Cancer Res Commun* (2022) 2:639–52. doi: 10.1158/2767-9764.CRC-22-0061

96. Hayes CS, Shicora AC, Keough MP, Snook AE, Burns MR, Gilmour SK. Polyamine-blocking therapy reverses immunosuppression in the tumor microenvironment. *Cancer Immunol Res* (2014) 2:274–85. doi: 10.1158/2326-6066.CIR-13-0120-T

97. Man K, Kutyavin VI, Chawla A. Tissue immunometabolism: development, physiology, and pathobiology. *Cell Metab* (2017) 25:11–26. doi: 10.1016/j.cmet.2016.08.016

98. Kumar V. Targeting macrophage immunometabolism: dawn in the darkness of sepsis. *Int Immunopharmacol* (2018) 58:173–85. doi: 10.1016/j.intimp.2018.03.005

99. O'Neill LAJ, Kishton RJ, Rathmell J. A guide to immunometabolism for immunologists. *Nat Rev Immunol* (2016) 16:553–65. doi: 10.1038/nri.2016.70

100. Kumar V. Inflammation research sails through the sea of immunology to reach immunometabolism. *Int Immunopharmacol* (2019) 73:128–45. doi: 10.1016/j.intimp.2019.05.002

101. Kumar V. Immunometabolism: another road to sepsis and its therapeutic targeting. *Inflammation* (2019) 42:765–88. doi: 10.1007/s10753-018-0939-8

102. Kumar V. T Cells and their immunometabolism: a novel way to understanding sepsis immunopathogenesis and future therapeutics. *Eur J Cell Biol* (2018) 97:379–92. doi: 10.1016/j.ejcb.2018.05.001

103. Becht E, Giraldo NA, Germain C, de Reyniès A, Laurent-Puig P, Zucman-Rossi J, et al. Immune contexture, immunoscore, and malignant cell molecular subgroups for prognostic and theranostic classifications of cancers. *Adv Immunol* (2016) 130:95–190. doi: 10.1016/bs.ai.2015.12.002

104. Cassetta L, Fragkogianni S, Sims AH, Swierczak A, Forrester LM, Zhang H, et al. Human tumor-associated macrophage and monocyte transcriptional landscapes reveal cancer-specific reprogramming, biomarkers, and therapeutic targets. *Cancer Cell* (2019) 35:588–602.e10. doi: 10.1016/j.ccell.2019.02.009

105. Mantovani A, Marchesi F, Jaillon S, Garlanda C, Allavena P. Tumor-associated myeloid cells: diversity and therapeutic targeting. *Cell Mol Immunol* (2021) 18:566–78. doi: 10.1038/s41423-020-00613-4

106. Christofides A, Strauss L, Yeo A, Cao C, Charest A, Boussiotis VA. The complex role of tumor-infiltrating macrophages. *Nat Immunol* (2022) 23:1148–56. doi: 10.1038/s41590-022-01267-2

107. Dallavalasa S, Beeraka NM, Basavaraju CG, Tulimilli SV, Sadhu SP, Rajesh K, et al. The role of tumor associated macrophages (TAMs) in cancer progression, chemoresistance, angiogenesis and metastasis - current status. *Curr Med Chem* (2021) 28:8203–36. doi: 10.2174/0929867328666210720143721

108. Szulc-Kielbik I, Kielbik M. Tumor-associated macrophages: reasons to be cheerful, reasons to be fearful. *Exp* (2022) Suppl 113:107–40. doi: 10.1007/978-3-030-91311-3_4

109. Fu LQ, Du WL, Cai MH, Yao JY, Zhao YY, Mou XZ. The roles of tumor-associated macrophages in tumor angiogenesis and metastasis. *Cell Immunol* (2020) 353:104119. doi: 10.1016/j.cellimm.2020.104119

110. Bindea G, Mlecnik B, Tosolini M, Kirilovsky A, Waldner M, Anna C, et al. Spatiotemporal dynamics of intratumoral immune cells reveal the immune landscape in human cancer. *Immunity* (2013) 39:782–95. doi: 10.1016/j.immuni.2013.10.003

111. Zheng X, Mansouri S, Krager A, Grimminger F, Seeger W, Pullamsetti SS, et al. Metabolism in tumour-associated macrophages: a quid pro quo with the tumour microenvironment. *Eur Respir Rev* (2020) 29(157):200134. doi: 10.1183/16000617.0134-2020

112. Huang SC-C, Smith AM, Everts B, Colonna M, Pearce EL, Schilling JD, et al. Metabolic reprogramming mediated by the mTORC2-IRF4 signaling axis is essential for macrophage alternative activation. *Immunity* (2016) 45:817–30. doi: 10.1016/j.immuni.2016.09.016

113. Namgaladze D, Brüne B. Fatty acid oxidation is dispensable for human macrophage IL-4-induced polarization. *Biochim Biophys Acta (BBA) - Mol Cell Biol Lipids* (2014) 1841:1329–35. doi: 10.1016/j.bbalip.2014.06.007

114. O'Neill LAJ. A metabolic roadblock in inflammatory macrophages. *Cell Rep* (2016) 17:625–6. doi: 10.1016/j.celrep.2016.09.085

115. Van den Bossche J, Baardman J, Otto NA, van der Velden S, Neele AE, Van Den Berg SM, et al. Mitochondrial dysfunction prevents repolarization of inflammatory macrophages. *Cell Rep* (2016) 17:684–96. doi: 10.1016/j.celrep.2016.09.008

116. Raines LN, Zhao H, Wang Y, Chen H-Y, Gallart-Ayala H, Hsueh P-C, et al. PERK is a critical metabolic hub for immunosuppressive function in macrophages. *Nat Immunol* (2022) 23:431–45. doi: 10.1038/s41590-022-01145-x

117. Wenes M, Shang M, Di Matteo M, Goveia J, Martín-Pérez R, Serneels J, et al. Macrophage metabolism controls tumor blood vessel morphogenesis and metastasis. *Cell Metab* (2016) 24:701–15. doi: 10.1016/j.cmet.2016.09.008

118. Mantovani A, Locati M. Macrophage metabolism shapes angiogenesis in tumors. *Cell Metab* (2016) 24:653–4. doi: 10.1016/j.cmet.2016.10.016

119. Kes MMG, Van den Bossche J, Griffioen AW, Huijbers EJM. Oncometabolites lactate and succinate drive pro-angiogenic macrophage response in tumors. *Biochim Biophys Acta Rev Cancer* (2020) 1874:188427. doi: 10.1016/j.bbcan.2020.188427

120. Yang K, Xu J, Fan M, Tu F, Wang X, Ha T, et al. Lactate suppresses macrophage pro-inflammatory response to LPS stimulation by inhibition of YAP and NF-κB activation via GPR81-mediated signaling. *Front Immunol* (2020) 11:587913. doi: 10.3389/fimmu.2020.587913

121. Sun X, Wang M, Wang M, Yao L, Li X, Dong H, et al. Role of proton-coupled monocarboxylate transporters in cancer: from metabolic crosstalk to therapeutic potential. *Front Cell Dev Biol* (2020) 8:651. doi: 10.3389/fcell.2020.00651

122. Li B, Yang Q, Li Z, Xu Z, Sun S, Wu Q, et al. Expression of monocarboxylate transporter 1 in immunosuppressive macrophages is associated with the poor prognosis in breast cancer. *Front Oncol* (2020) 10. doi: 10.3389/fonc.2020.574787

123. Kumar V. Macrophages: the potent immunoregulatory innate immune cells. In: Hussain BK, editor. *Macrophage activation*. Rijeka Ch: IntechOpen (2019).

124. Park J, Lee SE, Hur J, Hong EB, Choi J-I, Yang J-M, et al. M-CSF from cancer cells induces fatty acid synthase and PPARβ/δ activation in tumor myeloid cells, leading to tumor progression. *Cell Rep* (2015) 10:1614–25. doi: 10.1016/j.celrep.2015.02.024

125. Di Conza G, Tsai C-H, Gallart-Ayala H, Yu Y-R, Franco F, Zaffalon L, et al. Tumor-induced reshuffling of lipid composition on the endoplasmic reticulum membrane sustains macrophage survival and pro-tumorigenic activity. *Nat Immunol* (2021) 22:1403–15. doi: 10.1038/s41590-021-01047-4

126. Chen Y, Brandizzi F. IRE1: ER stress sensor and cell fate executor. *Trends Cell Biol* (2013) 23:547–55. doi: 10.1016/j.tcb.2013.06.005

127. Sriburi R, Jackowski S, Mori K, Brewer JW. XBP1 : a link between the unfolded protein response, lipid biosynthesis, and biogenesis of the endoplasmic reticulum. *J Cell Biol* (2004) 167:35–41. doi: 10.1083/jcb.200406136

128. Kao KC, Vilbois S, Tsai CH, Ho PC. Metabolic communication in the tumour-immune microenvironment. *Nat Cell Biol* (2022) 24(11):1574–83. doi: 10.1038/s41556-022-01002-x

129. Zhang Q, Wang H, Mao C, Sun M, Dominah G, Chen L, et al. Fatty acid oxidation contributes to IL-1β secretion in M2 macrophages and promotes macrophage-mediated tumor cell migration. *Mol Immunol* (2018) 94:27–35. doi: 10.1016/j.molimm.2017.12.011

130. Rao X, Zhou X, Wang G, Jie X, Xing B, Xu Y, et al. NLRP6 is required for cancer-derived exosome-modified macrophage M2 polarization and promotes metastasis in small cell lung cancer. *Cell Death Dis* (2022) 13:891. doi: 10.1038/s41419-022-05336-0

131. DeNardo DG, Ruffell B. Macrophages as regulators of tumour immunity and immunotherapy. *Nat Rev Immunol* (2019) 19:369–82. doi: 10.1038/s41577-019-0127-6

132. Viola A, Bronte V. Metabolic mechanisms of cancer-induced inhibition of immune responses. *Semin Cancer Biol* (2007) 17:309–16. doi: 10.1016/j.semcancer.2007.06.005

133. Viola A, Munari F, Sánchez-Rodríguez R, Scolaro T, Castegna A. The metabolic signature of macrophage responses. *Front Immunol* (2019) 10:1462. doi: 10.3389/fimmu.2019.01462

134. Mojsilovic SS, Mojsilovic S, Villar VH, Santibanez JF. The metabolic features of tumor-associated macrophages: opportunities for immunotherapy? *Anal Cell Pathol (Amst)* (2021) 2021:5523055. doi: 10.1155/2021/5523055

135. Wu L, Zhang X, Zheng L, Zhao H, Yan G, Zhang Q, et al. RIPK3 orchestrates fatty acid metabolism in tumor-associated macrophages and hepatocarcinogenesis. *Cancer Immunol Res* (2020) 8:710–21. doi: 10.1158/2326-6066.CIR-19-0261

136. Jha AK, Huang SC-C, Sergushichev A, Lampropoulou V, Ivanova Y, Loginicheva E, et al. Network integration of parallel metabolic and transcriptional data reveals metabolic modules that regulate macrophage polarization. *Immunity* (2015) 42:419–30. doi: 10.1016/j.immuni.2015.02.005

137. Van den Bossche J, Lamers WH, Koehler ES, Geuns JM, Alhonen L, Uimari A, et al. Pivotal advance: arginase-1-independent polyamine production stimulates the expression of IL-4-induced alternatively activated macrophage markers while inhibiting LPS-induced expression of inflammatory genes. *J Leukoc Biol* (2012) 91:685–99. doi: 10.1189/jlb.0911453

138. Oh MH, Sun IH, Zhao L, Leone RD, Sun IM, Xu W, et al. Targeting glutamine metabolism enhances tumor-specific immunity by modulating suppressive myeloid cells. *J Clin Invest* (2020) 130:3865–84. doi: 10.1172/JCI131859

139. Meireson A, Devos M, Brochez L. IDO expression in cancer: different compartment, different functionality? *Front Immunol* (2020) 11. doi: 10.3389/fimmu.2020.531491

140. Zhao Q, Kuang DM, Wu Y, Xiao X, Li XF, Li TJ, et al. Activated CD69+ T cells foster immune privilege by regulating IDO expression in tumor-associated macrophages. *J Immunol* (2012) 188:1117–24. doi: 10.4049/jimmunol.1100164

141. Boussiotis VA, Patsoukis N. Effects of PD-1 signaling on immunometabolic reprogramming. *Immunometabolism* (2022) 4:e220007. doi: 10.20900/immunometab20220007

142. Patsoukis N, Bardhan K, Chatterjee P, Sari D, Liu B, Bell LN, et al. PD-1 alters T-cell metabolic reprogramming by inhibiting glycolysis and promoting lipolysis and fatty acid oxidation. *Nat Commun* (2015) 6:6692. doi: 10.1038/ncomms7692

143. Petty AJ, Yang Y. Tumor-associated macrophages: implications in cancer immunotherapy. *Immunotherapy* (2017) 9:289–302. doi: 10.2217/imt-2016-0135

144. Cassetta L, Kitamura T. Targeting tumor-associated macrophages as a potential strategy to enhance the response to immune checkpoint inhibitors. *Front Cell Dev Biol* (2018) 6:38. doi: 10.3389/fcell.2018.00038

145. Mantovani A, Marchesi F, Malesci A, Laghi L, Allavena P. Tumour-associated macrophages as treatment targets in oncology. *Nat Rev Clin Oncol* (2017) 14:399–416. doi: 10.1038/nrclinonc.2016.217

146. SenGupta S, Hein LE, Parent CA. The recruitment of neutrophils to the tumor microenvironment is regulated by multiple mediators. *Front Immunol* (2021) 12. doi: 10.3389/fimmu.2021.734188

147. Coffelt SB, Wellenstein MD, de Visser KE. Neutrophils in cancer: neutral no more. *Nat Rev Cancer* (2016) 16:431–46. doi: 10.1038/nrc.2016.52

148. Kolaczkowska E, Kubes P. Neutrophil recruitment and function in health and inflammation. *Nat Rev Immunol* (2013) 13:159–75. doi: 10.1038/nri3399

149. Powell DR, Huttenlocher A. Neutrophils in the tumor microenvironment. *Trends Immunol* (2016) 37:41–52. doi: 10.1016/j.it.2015.11.008

150. Nicolás-Ávila JÁ., Adrover JM, Hidalgo A. Neutrophils in homeostasis, immunity, and cancer. *Immunity* (2017) 46:15–28. doi: 10.1016/j.immuni.2016.12.012

151. Geh D, Leslie J, Rumney R, Reeves HL, Bird TG, Mann DA. Neutrophils as potential therapeutic targets in hepatocellular carcinoma. *Nat Rev Gastroenterol Hepatol* (2022) 19:257–73. doi: 10.1038/s41575-021-00568-5

152. Patel S, Fu S, Mastio J, Dominguez GA, Purohit A, Kossenkov A, et al. Unique pattern of neutrophil migration and function during tumor progression. *Nat Immunol* (2018) 19:1236–47. doi: 10.1038/s41590-018-0229-5

153. Walmsley SR, Print C, Farahi N, Peyssonnaux C, Johnson RS, Cramer T, et al. Hypoxia-induced neutrophil survival is mediated by HIF-1alpha-dependent NF-kappaB activity. *J Exp Med* (2005) 201:105–15. doi: 10.1084/jem.20040624

154. Thompson AA, Elks PM, Marriott HM, Eamsamarng S, Higgins KR, Lewis A, et al. Hypoxia-inducible factor 2α regulates key neutrophil functions in humans, mice, and zebrafish. *Blood* (2014) 123:366–76. doi: 10.1182/blood-2013-05-500207

155. Kumar S, Dikshit M. Metabolic insight of neutrophils in health and disease. *Front Immunol* (2019) 10. doi: 10.3389/fimmu.2019.02099

156. Britt EC, Lika J, Giese MA, Schoen TJ, Seim GL, Huang Z, et al. Switching to the cyclic pentose phosphate pathway powers the oxidative burst in activated neutrophils. *Nat Metab* (2022) 4:389–403. doi: 10.1038/s42255-022-00550-8

157. Azevedo EP, Rochael NC, Guimarães-Costa AB, de Souza-Vieira TS, Ganilho J, Saraiva EM, et al. A metabolic shift toward pentose phosphate pathway is necessary for amyloid fibril- and phorbol 12-myristate 13-acetate-induced neutrophil extracellular trap (NET) formation. *J Biol Chem* (2015) 290:22174–83. doi: 10.1074/jbc.M115.640094

158. Fridlender ZG, Sun J, Kim S, Kapoor V, Cheng G, Ling L, et al. Polarization of tumor-associated neutrophil phenotype by TGF-beta: "N1" versus "N2" TAN. *Cancer Cell* (2009) 16:183–94. doi: 10.1016/j.ccr.2009.06.017

159. Flavell RA, Sanjabi S, Wrzesinski SH, Licona-Limón P. The polarization of immune cells in the tumour environment by TGFβ. *Nat Rev Immunol* (2010) 10:554–67. doi: 10.1038/nri2808

160. Shaul ME, Levy L, Sun J, Mishalian I, Singhal S, Kapoor V, et al. Tumor-associated neutrophils display a distinct N1 profile following TGFβ modulation: a transcriptomics analysis of pro- vs. *antitumor TANs. Oncoimmunology* (2016) 5:e1232221. doi: 10.1080/2162402X.2016.1232221

161. Hsu BE, Tabariès S, Johnson RM, Andrzejewski S, Senecal J, Lehuédé C, et al. Immature low-density neutrophils exhibit metabolic flexibility that facilitates breast cancer liver metastasis. *Cell Rep* (2019) 27:3902–3915.e6. doi: 10.1016/j.celrep.2019.05.091

162. Rayes RF, Mouhanna JG, Nicolau I, Bourdeau F, Giannias B, Rousseau S, et al. Primary tumors induce neutrophil extracellular traps with targetable metastasis-promoting effects. *JCI Insight* (2019) 4:e128008. doi: 10.1172/jci.insight.128008

163. Cristinziano L, Modestino L, Antonelli A, Marone G, Simon H-U, Varricchi G, et al. Neutrophil extracellular traps in cancer. *Semin Cancer Biol* (2022) 79:91–104. doi: 10.1016/j.semcancer.2021.07.011

164. Veglia F, Perego M, Gabrilovich D. Myeloid-derived suppressor cells coming of age. *Nat Immunol* (2018) 19:108–19. doi: 10.1038/s41590-017-0022-x

165. Gabrilovich DI, Nagaraj S. Myeloid-derived suppressor cells as regulators of the immune system. *Nat Rev Immunol* (2009) 9:162–74. doi: 10.1038/nri2506

166. Veglia F, Sanseviero E, Gabrilovich DI. Myeloid-derived suppressor cells in the era of increasing myeloid cell diversity. *Nat Rev Immunol* (2021) 21:485–98. doi: 10.1038/s41577-020-00490-y

167. Tcyganov E, Mastio J, Chen E, Gabrilovich DI. Plasticity of myeloid-derived suppressor cells in cancer. *Curr Opin Immunol* (2018) 51:76–82. doi: 10.1016/j.coi.2018.03.009

168. Veglia F, Hashimoto A, Dweep H, Sanseviero E, De Leo A, Tcyganov E, et al. Analysis of classical neutrophils and polymorphonuclear myeloid-derived suppressor cells in cancer patients and tumor-bearing mice. *J Exp Med* (2021) 218:e20201803. doi: 10.1084/jem.20201803

169. Li B-H, Garstka MA, Li Z-F. Chemokines and their receptors promoting the recruitment of myeloid-derived suppressor cells into the tumor. *Mol Immunol* (2020) 117:201–15. doi: 10.1016/j.molimm.2019.11.014

170. Kumar V, Patel S, Tcyganov E, Gabrilovich DI. The nature of myeloid-derived suppressor cells in the tumor microenvironment. *Trends Immunol* (2016) 37:208–20. doi: 10.1016/j.it.2016.01.004

171. Liu Y, Lai L, Chen Q, Song Y, Xu S, Ma F, et al. MicroRNA-494 is required for the accumulation and functions of tumor-expanded myeloid-derived suppressor cells via targeting of PTEN. *J Immunol* (2012) 188:5500–10. doi: 10.4049/jimmunol.1103505

172. Ya G, Ren W, Qin R, He J, Zhao S. Role of myeloid-derived suppressor cells in the formation of pre-metastatic niche. *Front Oncol* (2022) 12:975261. doi: 10.3389/fonc.2022.975261

173. Shojaei F, Singh M, Thompson JD, Ferrara N. Role of Bv8 in neutrophil-dependent angiogenesis in a transgenic model of cancer progression. *Proc Natl Acad Sci* (2008) 105:2640–5. doi: 10.1073/pnas.0712185105

174. Trovato R, Canè S, Petrova V, Sartoris S, Ugel S, De Sanctis F. The engagement between MDSCs and metastases: partners in crime. *Front Oncol* (2020) 10. doi: 10.3389/fonc.2020.00165

175. Al-Khami AA, Rodriguez PC, Ochoa AC. Metabolic reprogramming of myeloid-derived suppressor cells (MDSC) in cancer. *Oncoimmunology* (2016) 5: e1200771. doi: 10.1080/2162402X.2016.1200771

176. Hossain F, Al-Khami AA, Wyczechowska D, Hernandez C, Zheng L, Reiss K, et al. Inhibition of fatty acid oxidation modulates immunosuppressive functions of myeloid-derived suppressor cells and enhances cancer therapies. *Cancer Immunol Res* (2015) 3:1236–47. doi: 10.1158/2326-6066.CIR-15-0036

177. Hammami I, Chen J, Murschel F, Bronte V, De Crescenzo G, Jolicoeur M. Immunosuppressive activity enhances central carbon metabolism and bioenergetics in myeloid-derived suppressor cells *in vitro* models. *BMC Cell Biol* (2012) 13:18. doi: 10.1186/1471-2121-13-18

178. Mehta K, Fok J, Miller FR, Koul D, Sahin AA. Prognostic significance of tissue transglutaminase in drug resistant and metastatic breast cancer. *Clin Cancer Res* (2004) 10:8068–76. doi: 10.1158/1078-0432.CCR-04-1107

179. Hammami I, Chen J, Bronte V, DeCrescenzo G, Jolicoeur M. L-glutamine is a key parameter in the immunosuppression phenomenon. *Biochem Biophys Res Commun* (2012) 425:724–9. doi: 10.1016/j.bbrc.2012.07.139

180. Al-Khami AA, Zheng L, Del Valle L, Hossain F, Wyczechowska D, Zabaleta J, et al. Exogenous lipid uptake induces metabolic and functional reprogramming of tumor-associated myeloid-derived suppressor cells. *Oncoimmunology* (2017) 6: e1344804. doi: 10.1080/2162402X.2017.1344804

181. Yan D, Adeshakin AO, Xu M, Afolabi LO, Zhang G, Chen YH, et al. Lipid metabolic pathways confer the immunosuppressive function of myeloid-derived suppressor cells in tumor. *Front Immunol* (2019) 10:1399. doi: 10.3389/fimmu.2019.01399

182. Veglia F, Tyurin VA, Blasi M, De Leo A, Kossenkov AV, Donthireddy L, et al. Fatty acid transport protein 2 reprograms neutrophils in cancer. *Nature* (2019) 569:73–8. doi: 10.1038/s41586-019-1118-2

183. Wellenstein MD, de Visser KE. Fatty acids corrupt neutrophils in cancer. *Cancer Cell* (2019) 35:827–9. doi: 10.1016/j.ccell.2019.05.007

184. Shi X, Pang S, Zhou J, Yan G, Sun J, Tan W. Feedback loop between fatty acid transport protein 2 and receptor interacting protein 3 pathways promotes polymorphonuclear neutrophil myeloid-derived suppressor cells-potentiated suppressive immunity in bladder cancer. *Mol Biol Rep* (2022) 49(12):11643–52. doi: 10.1007/s11033-022-07924-x

185. Yan G, Zhao H, Zhang Q, Zhou Y, Wu L, Lei J, et al. A RIPK3-PGE(2) circuit mediates myeloid-derived suppressor cell-potentiated colorectal carcinogenesis. *Cancer Res* (2018) 78:5586–99. doi: 10.1158/0008-5472.CAN-17-3962

186. Corzo CA, Condamine T, Lu L, Cotter MJ, Youn JI, Cheng P, et al. HIF-1α regulates function and differentiation of myeloid-derived suppressor cells in the tumor microenvironment. *J Exp Med* (2010) 207:2439–53. doi: 10.1084/jem.20100587

187. Chang WH, Lai AG. The hypoxic tumour microenvironment: a safe haven for immunosuppressive cells and a therapeutic barrier to overcome. *Cancer Lett* (2020) 487:34–44. doi: 10.1016/j.canlet.2020.05.011

188. Noman MZ, Desantis G, Janji B, Hasmim M, Karray S, Dessen P, et al. PD-L1 is a novel direct target of HIF-1α, and its blockade under hypoxia enhanced MDSC-mediated T cell activation. *J Exp Med* (2014) 211:781–90. doi: 10.1084/jem.20131916

189. Husain Z, Seth P, Sukhatme VP. Tumor-derived lactate and myeloid-derived suppressor cells: linking metabolism to cancer immunology. *Oncoimmunology* (2013) 2:e26383. doi: 10.4161/onci.26383

190. Husain Z, Huang Y, Seth P, Sukhatme VP. Tumor-derived lactate modifies antitumor immune response: effect on myeloid-derived suppressor cells and NK cells. *J Immunol* (2013) 191:1486–95. doi: 10.4049/jimmunol.1202702

191. Yang X, Lu Y, Hang J, Zhang J, Zhang T, Huo Y, et al. Lactate-modulated immunosuppression of myeloid-derived suppressor cells contributes to the radioresistance of pancreatic cancer. *Cancer Immunol Res* (2020) 8:1440–51. doi: 10.1158/2326-6066.CIR-20-0111

192. Kumar V. Dendritic cells in sepsis: potential immunoregulatory cells with therapeutic potential. *Mol Immunol* (2018) 101:615–26. doi: 10.1016/j.molimm.2018.07.007

193. Steinman RM. Decisions about dendritic cells: past, present, and future. *Annu Rev Immunol* (2012) 30:1–22. doi: 10.1146/annurev-immunol-100311-102839

194. Broz ML, Binnewies M, Boldajipour B, Nelson AE, Pollack JL, Erle DJ, et al. Dissecting the tumor myeloid compartment reveals rare activating antigen-presenting cells critical for T cell immunity. *Cancer Cell* (2014) 26:638–52. doi: 10.1016/j.ccell.2014.09.007

195. Gardner A, Ruffell B. Dendritic cells and cancer immunity. *Trends Immunol* (2016) 37:855–65. doi: 10.1016/j.it.2016.09.006

196. Bonaccorsi I, Campana S, Morandi B, Ferlazzo G. Acquisition and presentation of tumor antigens by dendritic cells. *Crit Rev Immunol* (2015) 35:349–64. doi: 10.1615/CritRevImmunol.v35.i5.10

197. Murphy TL, Grajales-Reyes GE, Wu X, Tussiwand R, Briseño CG, Iwata A, et al. Transcriptional control of dendritic cell development. *Annu Rev Immunol* (2016) 34:93–119. doi: 10.1146/annurev-immunol-032713-120204

198. Böttcher JP, Reis e Sousa C. The role of type 1 conventional dendritic cells in cancer immunity. *Trends Cancer* (2018) 4:784–92. doi: 10.1016/j.trecan.2018.09.001

199. Balan S, Radford KJ, Bhardwaj N. Chapter two - unexplored horizons of cDC1 in immunity and tolerance. In: Alt FW, editor. *Advances in immunology*, vol. 148 . Academic Press (2020). p. 49–91. doi: 10.1016/bs.ai.2020.10.002

200. Böttcher JP, Bonavita E, Chakravarty P, Blees H, Cabeza-Cabrerizo M, Sammicheli S, et al. NK cells stimulate recruitment of cDC1 into the tumor microenvironment promoting cancer immune control. *Cell* (2018) 172:1022–1037.e14. doi: 10.1016/j.cell.2018.01.004

201. Bordon Y. Tumour immunology: NK cells bring in the troops. *Nat Rev Immunol* (2018) 18:151. doi: 10.1038/nri.2018.14

202. Brown CC, Wolchok JD. PD-L1 blockade therapy: location, location, location. *Cancer Cell* (2020) 38:615–7. doi: 10.1016/j.ccell.2020.10.017

203. Dammeijer F, van Gulijk M, Mulder EE, Lukkes M, Klaase L, van den Bosch T, et al. The PD-1/PD-L1-Checkpoint restrains T cell immunity in tumor-draining lymph nodes. *Cancer Cell* (2020) 38:685–700.e8. doi: 10.1016/j.ccell.2020.09.001

204. Sharma MD, Baban B, Chandler P, Hou DY, Singh N, Yagita H, et al. Plasmacytoid dendritic cells from mouse tumor-draining lymph nodes directly activate mature tregs via indoleamine 2,3-dioxygenase. *J Clin Invest* (2007) 117:2570–82. doi: 10.1172/JCI31911

205. Wculek SK, Cueto FJ, Mujal AM, Melero I, Krummel MF, Sancho D. Dendritic cells in cancer immunology and immunotherapy. *Nat Rev Immunol* (2020) 20:7–24. doi: 10.1038/s41577-019-0210-z

206. Kvedaraite E, Ginhoux F. Human dendritic cells in cancer. *Sci Immunol* (2022) 7:eabm9409. doi: 10.1126/sciimmunol.abm9409

207. Gerhard GM, Bill R, Messemaker M, Klein AM, Pittet MJ. Tumor-infiltrating dendritic cell states are conserved across solid human cancers. *J Exp Med* (2020) 218: e2020026. doi: 10.1084/jem.20200264

208. Tel J, Anguille S, Waterborg CEJ, Smits EL, Figdor CG, de Vries IJM. Tumoricidal activity of human dendritic cells. *Trends Immunol* (2014) 35:38–46. doi: 10.1016/j.it.2013.10.007

209. Krawczyk CM, Holowka T, Sun J, Blagih J, Amiel E, DeBerardinis RJ, et al. Toll-like receptor–induced changes in glycolytic metabolism regulate dendritic cell activation. *Blood* (2010) 115:4742–9. doi: 10.1182/blood-2009-10-249540

210. O'Neill LAJ, Pearce EJ. Immunometabolism governs dendritic cell and macrophage function. *J Exp Med* (2015) 213:15–23. doi: 10.1084/jem.20151570

211. Everts B, Amiel E, Huang SC, Smith AM, Chang CH, Lam WY, et al. TLR-driven early glycolytic reprogramming via the kinases TBK1-IKKε supports the anabolic demands of dendritic cell activation. *Nat Immunol* (2014) 15:323–32. doi: 10.1038/ni.2833

212. Guak H, Al Habyan S, Ma EH, Aldossary H, Al-Masri M, Won SY, et al. Glycolytic metabolism is essential for CCR7 oligomerization and dendritic cell migration. *Nat Commun* (2018) 9:2463. doi: 10.1038/s41467-018-04804-6

213. Gotoh K, Morisaki T, Setoyama D, Sasaki K, Yagi M, Igami K, et al. Mitochondrial p32/C1qbp is a critical regulator of dendritic cell metabolism and maturation. *Cell Rep* (2018) 25:1800–1815.e4. doi: 10.1016/j.celrep.2018.10.057

214. Thwe PM, Pelgrom LR, Cooper R, Beauchamp S, Reisz JA, D'Alessandro A, et al. Cell-intrinsic glycogen metabolism supports early glycolytic reprogramming required for dendritic cell immune responses. *Cell Metab* (2017) 26:558–567.e5. doi: 10.1016/j.cmet.2017.08.012

215. Murray PJ. Understanding and exploiting the endogenous interleukin-10/STAT3-mediated anti-inflammatory response. *Curr Opin Pharmacol* (2006) 6:379–86. doi: 10.1016/j.coph.2006.01.010

216. Rehman A, Hemmert KC, Ochi A, Jamal M, Henning JR, Barilla R, et al. Role of fatty-acid synthesis in dendritic cell generation and function. *J Immunol* (2013) 190:4640–9. doi: 10.4049/jimmunol.1202312

217. Basit F, de Vries IJM. Dendritic cells require PINK1-mediated phosphorylation of BCKDE1α to promote fatty acid oxidation for immune function. *Front Immunol* (2019) 10:2386. doi: 10.3389/fimmu.2019.02386

218. Garcia D, Shaw RJ. AMPK: mechanisms of cellular energy sensing and restoration of metabolic balance. *Mol Cell* (2017) 66:789–800. doi: 10.1016/j.molcel.2017.05.032

219. Kelly B, O'Neill LA. Metabolic reprogramming in macrophages and dendritic cells in innate immunity. *Cell Res* (2015) 25:771–84. doi: 10.1038/cr.2015.68

220. Giovanelli P, Sandoval TA, Cubillos-Ruiz JR. Dendritic cell metabolism and function in tumors. *Trends Immunol* (2019) 40:699–718. doi: 10.1016/j.it.2019.06.004

221. Kumar V. Adenosine as an endogenous immunoregulator in cancer pathogenesis: where to go? *Purinergic Signal* (2013) 9:145–65. doi: 10.1007/s11302-012-9349-9

222. Kumar V, Sharma A. Adenosine: an endogenous modulator of innate immune system with therapeutic potential. *Eur J Pharmacol* (2009) 616:7–15. doi: 10.1016/j.ejphar.2009.05.005

223. Novitskiy SV, Ryzhov S, Zaynagetdinov R, Goldstein AE, Huang Y, Tikhomirov OY, et al. Adenosine receptors in regulation of dendritic cell differentiation and function. *Blood* (2008) 112:1822–31. doi: 10.1182/blood-2008-02-136325

224. Munn DH, Mellor AL. IDO in the tumor microenvironment: inflammation, counter-regulation, and tolerance. *Trends Immunol* (2016) 37:193–207. doi: 10.1016/j.it.2016.01.002

225. Munn DH, Sharma MD, Baban B, Harding HP, Zhang Y, Ron D, et al. GCN2 kinase in T cells mediates proliferative arrest and anergy induction in response to indoleamine 2,3-dioxygenase. *Immunity* (2005) 22:633–42. doi: 10.1016/j.immuni.2005.03.013

226. Fallarino F, Grohmann U, You S, McGrath BC, Cavener DR, Vacca C, et al. The combined effects of tryptophan starvation and tryptophan catabolites down-regulate T cell receptor ζ-chain and induce a regulatory phenotype in naive T cells. *J Immunol* (2006) 176:6752–61. doi: 10.4049/jimmunol.176.11.6752

227. Fallarino F, Grohmann U, You S, McGrath BC, Cavener DR, Vacca C, et al. Tryptophan catabolism generates autoimmune-preventive regulatory T cells. *Transplant Immunol* (2006) 17:58–60. doi: 10.1016/j.trim.2006.09.017

228. Mezrich JD, Fechner JH, Zhang X, Johnson BP, Burlingham WJ, Bradfield CA. An interaction between kynurenine and the aryl hydrocarbon receptor can generate regulatory T cells. *J Immunol* (2010) 185:3190–8. doi: 10.4049/jimmunol.0903670

229. Manlapat AK, Kahler DJ, Chandler PR, Munn DH, Mellor AL. Cell-autonomous control of interferon type I expression by indoleamine 2,3-dioxygenase in regulatory CD19+ dendritic cells. *Eur J Immunol* (2007) 37:1064–71. doi: 10.1002/eji.200636690

230. Campesato LF, Budhu S, Tchaicha J, Weng CH, Gigoux M, Cohen IJ, et al. Blockade of the AHR restricts a treg-macrophage suppressive axis induced by l-kynurenine. *Nat Commun* (2020) 11:4011. doi: 10.1038/s41467-020-17750-z

231. Heikenwalder M, Polymenidou M, Junt T, Sigurdson C, Wagner H, Akira S, et al. Lymphoid follicle destruction and immunosuppression after repeated CpG oligodeoxynucleotide administration. *Nat Med* (2004) 10:187–92. doi: 10.1038/nm987

232. Wingender G, Garbi N, Schumak B, Jüngerkes F, Endl E, von Bubnoff D, et al. Systemic application of CpG-rich DNA suppresses adaptive T cell immunity via induction of IDO. *Eur J Immunol* (2006) 36:12–20. doi: 10.1002/eji.200535602

233. Kumar S, Calianese D, Birge RB. Efferocytosis of dying cells differentially modulate immunological outcomes in tumor microenvironment. *Immunol Rev* (2017) 280:149–64. doi: 10.1111/imr.12587

234. Papagno L, Kuse N, Lissina A, Gostick E, Price DA, Appay V, et al. The TLR9 ligand CpG ODN 2006 is a poor adjuvant for the induction of *de novo* CD8+ T-cell responses *in vitro*. *Sci Rep* (2020) 10:11620. doi: 10.1038/s41598-020-67704-0

235. Malinarich F, Duan K, Hamid RA, Bijin A, Lin WX, Poidinger M, et al. High mitochondrial respiration and glycolytic capacity represent a metabolic phenotype of human tolerogenic dendritic cells. *J Immunol* (2015) 194:5174–86. doi: 10.4049/jimmunol.1303316

236. Herber DL, Cao W, Nefedova Y, Novitskiy SV, Nagaraj S, Tyurin VA, et al. Lipid accumulation and dendritic cell dysfunction in cancer. *Nat Med* (2010) 16:880–6. doi: 10.1038/nm.2172

237. Zitvogel L, Kroemer G. Targeting dendritic cell metabolism in cancer. *Nat Med* (2010) 16:858–9. doi: 10.1038/nm0810-858

238. Zhao F, Xiao C, Evans KS, Theivanthiran T, DeVito N, Holtzhausen A, et al. Paracrine Wnt5a-β-Catenin signaling triggers a metabolic program that drives dendritic cell tolerization. *Immunity* (2018) 48:147–160.e7. doi: 10.1016/j.immuni.2017.12.004

239. Holtzhausen A, Zhao F, Evans KS, Tsutsui M, Orabona C, Tyler DS, et al. Melanoma-derived Wnt5a promotes local dendritic-cell expression of IDO and immunotolerance: opportunities for pharmacologic enhancement of immunotherapy. *Cancer Immunol Res* (2015) 3:1082–95. doi: 10.1158/2326-6066.CIR-14-0167

240. Hong Y, Manoharan I, Suryawanshi A, Majumdar T, Angus-Hill ML, Koni PA, et al. β-catenin promotes regulatory T-cell responses in tumors by inducing vitamin a metabolism in dendritic cells. *Cancer Res* (2015) 75:656–65. doi: 10.1158/0008-5472.CAN-14-2377

241. Kumar V. Chapter 8 - innate lymphoid cells in autoimmune diseases. In: Rezaei N, editor. *Translational autoimmunity*, vol. 1 . Academic Press (2022). p. 143–75. doi: 10.1016/B978-0-12-822564-6.00007-0

242. Kumar V. Innate lymphoid cells: new paradigm in immunology of inflammation. *Immunol Lett* (2014) 157:23–37. doi: 10.1016/j.imlet.2013.11.003

243. Kumar V. Innate lymphoid cells: immunoregulatory cells of mucosal inflammation. *Eur J Inflammation* (2014) 12:11–20. doi: 10.1177/1721727X1401200102

244. Kumar V. Innate lymphoid cell and adaptive immune cell cross-talk: a talk meant not to forget. *J Leukocyte Biol* (2020) 108:397–417. doi: 10.1002/JLB.4MIR0420-500RRR

245. Kumar V. Innate lymphoid cells and adaptive immune cells cross-talk: a secret talk revealed in immune homeostasis and different inflammatory conditions. *Int Rev Immunol* (2021) 40:217–51. doi: 10.1080/08830185.2021.1895145

246. Simoni Y, Fehlings M, Kløverpris HN, McGovern N, Koo S-L, Loh CY, et al. Human innate lymphoid cell subsets possess tissue-type based heterogeneity in phenotype and frequency. *Immunity* (2017) 46:148–61. doi: 10.1016/j.immuni.2016.11.005

247. Jacquelot N, Seillet C, Vivier E, Belz GT. Innate lymphoid cells and cancer. *Nat Immunol* (2022) 23:371–9. doi: 10.1038/s41590-022-01127-z

248. Loyon R, Jary M, Salomé B, Gomez-Cadena A, Galaine J, Kroemer M, et al. Peripheral innate lymphoid cells are increased in first line metastatic colorectal carcinoma patients: a negative correlation with Th1 immune responses. *Front Immunol* (2019) 10:2121. doi: 10.3389/fimmu.2019.02121

249. Bie Q, Zhang P, Su Z, Zheng D, Ying X, Wu Y, et al. Polarization of ILC2s in peripheral blood might contribute to immunosuppressive microenvironment in patients with gastric cancer. *J Immunol Res* (2014) 2014:923135. doi: 10.1155/2014/923135

250. de Weerdt I, van Hoeven V, Munneke JM, Endstra S, Hofland T, Hazenberg MD, et al. Innate lymphoid cells are expanded and functionally altered in chronic lymphocytic leukemia. *Haematologica* (2016) 101:e461–4. doi: 10.3324/haematol.2016.144725

251. Cristiani CM, Capone M, Garofalo C, Madonna G, Mallardo D, Tuffanelli M, et al. Altered frequencies and functions of innate lymphoid cells in melanoma patients are modulated by immune checkpoints inhibitors. *Front Immunol* (2022) 13:811131. doi: 10.3389/fimmu.2022.811131

252. Imai K, Matsuyama S, Miyake S, Suga K, Nakachi K. Natural cytotoxic activity of peripheral-blood lymphocytes and cancer incidence: an 11-year follow-up study of a general population. *Lancet* (2000) 356:1795–9. doi: 10.1016/S0140-6736(00)03231-1

253. Hersey P, Edwards A, Honeyman M, McCarthy WH. Low natural-killer-cell activity in familial melanoma patients and their relatives. *Br J Cancer* (1979) 40:113–22. doi: 10.1038/bjc.1979.147

254. Jović V, Konjević G, Radulović S, Jelić S, Spuzić I. Impaired perforin-dependent NK cell cytotoxicity and proliferative activity of peripheral blood T cells is associated with metastatic melanoma. *Tumori* (2001) 87:324–9. doi: 10.1177/030089160108700509

255. Nussbaum JC, Van Dyken SJ, von Moltke J, Cheng LE, Mohapatra A, Molofsky AB, et al. Type 2 innate lymphoid cells control eosinophil homeostasis. *Nature* (2013) 502:245–8. doi: 10.1038/nature12526

256. Jacquelot N, Seillet C, Wang M, Pizzolla A, Liao Y, Hediyeh-Zadeh S, et al. Blockade of the co-inhibitory molecule PD-1 unleashes ILC2-dependent antitumor immunity in melanoma. *Nat Immunol* (2021) 22:851–64. doi: 10.1038/s41590-021-00943-z

257. Grisaru-Tal S, Dulberg S, Beck L, Zhang C, Itan M, Hediyeh-Zadeh S, et al. Metastasis-entrained eosinophils enhance lymphocyte-mediated antitumor immunity. *Cancer Res* (2021) 81:5555–71. doi: 10.1158/0008-5472.CAN-21-0839

258. Simson L, Ellyard JI, Dent LA, Matthaei KI, Rothenberg ME, Foster PS, et al. Regulation of carcinogenesis by IL-5 and CCL11: a potential role for eosinophils in tumor immune surveillance. *J Immunol* (2007) 178:4222–9. doi: 10.4049/jimmunol.178.7.4222

259. Goc J, Lv M, Bessman NJ, Flamar AL, Sahota S, Suzuki H, et al. Dysregulation of ILC3s unleashes progression and immunotherapy resistance in colon cancer. *Cell* (2021) 184:5015–5030.e16. doi: 10.1016/j.cell.2021.07.029

260. Warner K, Ghaedi M, Chung DC, Jacquelot N, Ohashi PS. Innate lymphoid cells in early tumor development. *Front Immunol* (2022) 13:948358. doi: 10.3389/fimmu.2022.948358

261. Wolf NK, Kissiov DU, Raulet DH. Roles of natural killer cells in immunity to cancer, and applications to immunotherapy. *Nat Rev Immunol* (2022) 23:90–105. doi: 10.1038/s41577-022-00732-1

262. Gao Y, Souza-Fonseca-Guimaraes F, Bald T, Ng SS, Young A, Ngiow SF, et al. Tumor immunoevasion by the conversion of effector NK cells into type 1 innate lymphoid cells. *Nat Immunol* (2017) 18:1004–15. doi: 10.1038/ni.3800

263. Silver JS, Humbles AA. NK cells join the plasticity party. *Nat Immunol* (2017) 18:959–60. doi: 10.1038/ni.3817

264. Cuff AO, Sillito F, Dertschnig S, Hall A, Luong TV, Chakraverty R, et al. The obese liver environment mediates conversion of NK cells to a less cytotoxic ILC1-like phenotype. *Front Immunol* (2019) 10:2180. doi: 10.3389/fimmu.2019.02180

265. Simonetta F, Pradier A, Roosnek E. T-Bet and eomesodermin in NK cell development, maturation, and function. *Front Immunol* (2016) 7:241. doi: 10.3389/fimmu.2016.00241

266. Gordon SM, Chaix J, Rupp LJ, Wu J, Madera S, Sun JC, et al. The transcription factors T-bet and eomes control key checkpoints of natural killer cell maturation. *Immunity* (2012) 36:55–67. doi: 10.1016/j.immuni.2011.11.016

267. Daussy C, Faure F, Mayol K, Viel S, Gasteiger G, Charrier E, et al. T-Bet and eomes instruct the development of two distinct natural killer cell lineages in the liver and in the bone marrow. *J Exp Med* (2014) 211:563–77. doi: 10.1084/jem.20131560

268. Shimizu K, Sato Y, Kawamura M, Nakazato H, Watanabe T, Ohara O. Eomes transcription factor is required for the development and differentiation of invariant NKT cells. *Commun Biol* (2019) 2:150. doi: 10.1038/s42003-019-0389-3

269. Qin Y, Oh S, Lim S, Shin JH, Yoon MS, Park S-H. Invariant NKT cells facilitate cytotoxic T-cell activation via direct recognition of CD1d on T cells. *Exp Mol Med* (2019) 51:1–9. doi: 10.1038/s12276-019-0329-9

270. McEwen-Smith RM, Salio M, Cerundolo V. The regulatory role of invariant NKT cells in tumor immunity. *Cancer Immunol Res* (2015) 3:425–35. doi: 10.1158/2326-6066.CIR-15-0062

271. Wang S, Qu Y, Xia P, Chen Y, Zhu X, Zhang J, et al. Transdifferentiation of tumor infiltrating innate lymphoid cells during progression of colorectal cancer. *Cell Res* (2020) 30:610–22. doi: 10.1038/s41422-020-0312-y

272. Huang Y, Guo L, Qiu J, Chen X, Hu-Li J, Siebenlist U, et al. IL-25-responsive, lineage-negative KLRG1(hi) cells are multipotential 'inflammatory' type 2 innate lymphoid cells. *Nat Immunol* (2015) 16:161–9. doi: 10.1038/ni.3078

273. Jou E, Rodriguez-Rodriguez N, Ferreira A-CF, Jolin HE, Clark PA, Sawmynaden K, et al. An innate IL-25–ILC2–MDSC axis creates a cancer-permissive microenvironment for apc mutation–driven intestinal tumorigenesis. *Sci Immunol* (2022) 7:eabn0175. doi: 10.1126/sciimmunol.abn0175

274. Koyasu S. Inflammatory ILC2 cells: disguising themselves as progenitors? *Nat Immunol* (2015) 16:133–4. doi: 10.1038/ni.3080

275. Gowhari Shabgah A, Amir A, Gardanova ZR, Olegovna Zekiy A, Thangavelu L, Ebrahimi Nik M, et al. Interleukin-25: new perspective and state-of-the-art in cancer prognosis and treatment approaches. *Cancer Med* (2021) 10:5191–202. doi: 10.1002/cam4.4060

276. Chevalier MF, Trabanelli S, Racle J, Salomé B, Cesson V, Gharbi D, et al. ILC2-modulated T cell-to-MDSC balance is associated with bladder cancer recurrence. *J Clin Invest* (2017) 127:2916–29. doi: 10.1172/JCI89717

277. Trabanelli S, Chevalier MF, Martinez-Usatorre A, Gomez-Cadena A, Salomé B, Lecciso M, et al. Tumour-derived PGD2 and NKp30-B7H6 engagement drives an immunosuppressive ILC2-MDSC axis. *Nat Commun* (2017) 8:593. doi: 10.1038/s41467-017-00678-2

278. Zhao N, Zhu W, Wang J, Liu W, Kang L, Yu R, et al. Group 2 innate lymphoid cells promote TNBC lung metastasis via the IL-13-MDSC axis in a murine tumor model. *Int Immunopharmacol* (2021) 99:107924. doi: 10.1016/j.intimp.2021.107924

279. O'Keefe RN, Carli AL, Baloyan D, Afshar-Sterle S, Eissmann MF, Poh AR, et al. Inhibition of the tuft cell/ILC2 axis reduces gastric tumor development in mice. *bioRxiv* (2022) 2022.02.16.480779. doi: 10.1101/2022.02.16.480779

280. Hatzioannou A, Banos A, Sakelaropoulos T, Fedonidis C, Vidali M-S, Köhne M, et al. An intrinsic role of IL-33 in treg cell–mediated tumor immunoevasion. *Nat Immunol* (2020) 21:75–85. doi: 10.1038/s41590-019-0555-2

281. Fournié JJ, Poupot M. The pro-tumorigenic IL-33 involved in antitumor immunity: a yin and yang cytokine. *Front Immunol* (2018) 9:2506. doi: 10.3389/fimmu.2018.02506

282. Ercolano G, Gomez-Cadena A, Dumauthioz N, Vanoni G, Kreutzfeldt M, Wyss T, et al. PPARγ drives IL-33-dependent ILC2 pro-tumoral functions. *Nat Commun* (2021) 12:2538. doi: 10.1038/s41467-021-22764-2

283. Gardiner CM, Finlay DK. What fuels natural killers? metabolism and NK cell responses. *Front Immunol* (2017) 8. doi: 10.3389/fimmu.2017.00367

284. Poznanski SM, Barra NG, Ashkar AA, Schertzer JD. Immunometabolism of T cells and NK cells: metabolic control of effector and regulatory function. *Inflammation Res* (2018) 67:813–28. doi: 10.1007/s00011-018-1174-3

285. Marçais A, Cherfils-Vicini J, Viant C, Degouve S, Viel S, Fenis A, et al. The metabolic checkpoint kinase mTOR is essential for IL-15 signaling during the development and activation of NK cells. *Nat Immunol* (2014) 15:749–57. doi: 10.1038/ni.2936

286. Keppel MP, Saucier N, Mah AY, Vogel TP, Cooper MA. Activation-specific metabolic requirements for NK cell IFN-γ production. *J Immunol* (2015) 194:1954–62. doi: 10.4049/jimmunol.1402099

287. Donnelly RP, Loftus RM, Keating SE, Liou KT, Biron CA, Gardiner CM, et al. mTORC1-dependent metabolic reprogramming is a prerequisite for NK cell effector function. *J Immunol* (2014) 193:4477–84. doi: 10.4049/jimmunol.1401558

288. Zaiatz-Bittencourt V, Finlay DK, Gardiner CM. Canonical TGF-β signaling pathway represses human NK cell metabolism. *J Immunol* (2018) 200:3934–41. doi: 10.4049/jimmunol.1701461

289. Viel S, Marçais A, Guimaraes FS-F, Loftus R, Rabilloud J, Grau M, et al. TGF-b inhibits the activation and functions of NK cells by repressing the mTOR pathway. . *Sci Signaling* (2016) 9:ra19–9. doi: 10.1126/scisignal.aad1884

290. Besson L, Mery B, Morelle M, Rocca Y, Heudel PE, You B, et al. Cutting edge: mTORC1 inhibition in metastatic breast cancer patients negatively affects peripheral NK cell maturation and number. *J Immunol* (2021) 206:2265–70. doi: 10.4049/jimmunol.2001215

291. Harmon C, Robinson MW, Hand F, Almuaili D, Mentor K, Houlihan DD, et al. Lactate-mediated acidification of tumor microenvironment induces apoptosis of liver-resident NK cells in colorectal liver metastasis. *Cancer Immunol Res* (2019) 7:335–46. doi: 10.1158/2326-6066.CIR-18-0481

292. Park YJ, Song B, Kim YS, Kim EK, Lee JM, Lee GE, et al. Tumor microenvironmental conversion of natural killer cells into myeloid-derived suppressor cells. *Cancer Res* (2013) 73:5669–81. doi: 10.1158/0008-5472.CAN-13-0545

293. Surace L, Di Santo JP. Local and systemic features of ILC immunometabolism. *Curr Opin Hematol* (2022) 29:209–17. doi: 10.1097/MOH.0000000000000722

294. Li Q, Li D, Zhang X, Wan Q, Zhang W, Zheng M, et al. E3 ligase VHL promotes group 2 innate lymphoid cell maturation and function *via* glycolysis inhibition and induction of interleukin-33 receptor. *Immunity* (2018) 48:258–270.e5. doi: 10.1016/j.immuni.2017.12.013

295. Wilhelm C, Harrison OJ, Schmitt V, Pelletier M, Spencer SP, Urban JFJr., et al. Critical role of fatty acid metabolism in ILC2-mediated barrier protection during malnutrition and helminth infection. *J Exp Med* (2016) 213:1409–18. doi: 10.1084/jem.20151448

296. Surace L, Doisne JM, Croft CA, Thaller A, Escoll P, Marie S, et al. Dichotomous metabolic networks govern human ILC2 proliferation and function. *Nat Immunol* (2021) 22:1367–74. doi: 10.1038/s41590-021-01043-8

297. Michla M, Wilhelm C. Food for thought - ILC metabolism in the context of helminth infections. *Mucosal Immunol* (2022) 15:1234–42. doi: 10.1038/s41385-022-00559-y

298. Karagiannis F, Masouleh SK, Wunderling K, Surendar J, Schmitt V, Kazakov A, et al. Lipid-droplet formation drives pathogenic group 2 innate lymphoid cells in airway inflammation. *Immunity* (2020) 52:620–634.e6. doi: 10.1016/j.immuni.2020.03.003

299. Zheng C, Wu H, Lu Z, Bi J, Wan X. IL-33-induced reactive oxygen species are required for optimal metabolic programming in group 2 innate lymphoid cells. *Cell Mol Immunol* (2020) 17:1266–8. doi: 10.1038/s41423-020-0393-z

300. Michalek RD, Gerriets VA, Jacobs SR, Macintyre AN, MacIver NJ, Mason EF, et al. Cutting edge: distinct glycolytic and lipid oxidative metabolic programs are essential for effector and regulatory CD4+ T cell subsets. *J Immunol* (2011) 186:3299–303. doi: 10.4049/jimmunol.1003613

301. Shi LZ, Wang R, Huang G, Vogel P, Neale G, Green DR, et al. HIF1α–dependent glycolytic pathway orchestrates a metabolic checkpoint for the differentiation of TH17 and treg cells. *J Exp Med* (2011) 208:1367–76. doi: 10.1084/jem.20110278

302. Chang CH, Curtis JD, Maggi LBJr., Faubert B, Villarino AV, O'Sullivan D, et al. Posttranscriptional control of T cell effector function by aerobic glycolysis. *Cell* (2013) 153:1239–51. doi: 10.1016/j.cell.2013.05.016

303. Peng M, Yin N, Chhangawala S, Xu K, Leslie CS, Li MO. Aerobic glycolysis promotes T helper 1 cell differentiation through an epigenetic mechanism. *Science* (2016) 354:481–4. doi: 10.1126/science.aaf6284

304. Quinn WJ, Jiao J, TeSlaa T, Stadanlick J, Wang Z, Wang L, et al. Lactate limits T cell proliferation via the NAD(H) redox state. *Cell Rep* (2020) 33:108500. doi: 10.1016/j.celrep.2020.108500

305. Angelin A, Gil-de-Gómez L, Dahiya S, Jiao J, Guo L, Levine MH, et al. Foxp3 reprograms T cell metabolism to function in low-glucose, high-lactate environments. *Cell Metab* (2017) 25:1282–1293.e7. doi: 10.1016/j.cmet.2016.12.018

306. Grzes KM, Field CS, Pearce EJ. Treg cells survive and thrive in inhospitable environments. *Cell Metab* (2017) 25:1213–5. doi: 10.1016/j.cmet.2017.05.012

307. Watson MJ, Vignali PDA, Mullett SJ, Overacre-Delgoffe AE, Peralta RM, Grebinoski S, et al. Metabolic support of tumour-infiltrating regulatory T cells by lactic acid. *Nature* (2021) 591:645–51. doi: 10.1038/s41586-020-03045-2

308. Kumagai S, Koyama S, Itahashi K, Tanegashima T, Lin YT, Togashi Y, et al. Lactic acid promotes PD-1 expression in regulatory T cells in highly glycolytic tumor microenvironments. *Cancer Cell* (2022) 40:201–218.e9. doi: 10.1016/j.ccell.2022.01.001

309. Johnson S, Haigis MC, Dougan SK. Dangerous dynamic duo: lactic acid and PD-1 blockade. *Cancer Cell* (2022) 40:127–30. doi: 10.1016/j.ccell.2022.01.008

310. Gu J, Zhou J, Chen Q, Xu X, Gao J, Li X, et al. Tumor metabolite lactate promotes tumorigenesis by modulating MOESIN lactylation and enhancing TGF-β signaling in regulatory T cells. *Cell Rep* (2022) 39:110986. doi: 10.1016/j.celrep.2022.110986

311. Itahashi K, Irie T, Yuda J, Kumagai S, Tanegashima T, Lin Y-T, et al. BATF epigenetically and transcriptionally controls the activation program of regulatory T cells in human tumors. *Sci Immunol* (2022) 7:eabk0957. doi: 10.1126/sciimmunol.abk0957

312. Field CS, Baixauli F, Kyle RL, Puleston DJ, Cameron AM, Sanin DE, et al. Mitochondrial integrity regulated by lipid metabolism is a cell-intrinsic checkpoint for treg suppressive function. *Cell Metab* (2020) 31:422–437.e5. doi: 10.1016/j.cmet.2019.11.021

313. Kobayashi S, Wannakul T, Sekino K, Takahashi Y, Kagawa Y, Miyazaki H, et al. Fatty acid-binding protein 5 limits the generation of Foxp3(+) regulatory T cells through regulating plasmacytoid dendritic cell function in the tumor microenvironment. *Int J Cancer* (2022) 150:152–63. doi: 10.1002/ijc.33777

314. Delgoffe GM, Kole TP, Zheng Y, Zarek PE, Matthews KL, Xiao B, et al. The mTOR kinase differentially regulates effector and regulatory T cell lineage commitment. *Immunity* (2009) 30:832–44. doi: 10.1016/j.immuni.2009.04.014

315. Wang H, Franco F, Tsui YC, Xie X, Trefny MP, Zappasodi R, et al. CD36-mediated metabolic adaptation supports regulatory T cell survival and function in tumors. *Nat Immunol* (2020) 21:298–308. doi: 10.1038/s41590-019-0589-5

316. Chen Y, Zhang J, Cui W, Silverstein RL. CD36, a signaling receptor and fatty acid transporter that regulates immune cell metabolism and fate. *J Exp Med* (2022) 219:e20211314. doi: 10.1084/jem.20211314

317. Xu S, Chaudhary O, Rodríguez-Morales P, Sun X, Chen D, Zappasodi R, et al. Uptake of oxidized lipids by the scavenger receptor CD36 promotes lipid peroxidation and dysfunction in CD8(+) T cells in tumors. *Immunity* (2021) 54:1561–1577.e7. doi: 10.1016/j.immuni.2021.05.003

318. Henson SM, Lanna A, Riddell NE, Franzese O, Macaulay R, Griffiths SJ, et al. p38 signaling inhibits mTORC1-independent autophagy in senescent human CD8$^+$ T cells. *J Clin Invest* (2014) 124:4004–16. doi: 10.1172/JCI75051

319. Ma X, Xiao L, Liu L, Ye L, Su P, Bi E, et al. CD36-mediated ferroptosis dampens intratumoral CD8+ T cell effector function and impairs their antitumor ability. *Cell Metab* (2021) 33:1001–1012.e5. doi: 10.1016/j.cmet.2021.02.015

320. Gerriets VA, Kishton RJ, Johnson MO, Cohen S, Siska PJ, Nichols AG, et al. Foxp3 and toll-like receptor signaling balance t(reg) cell anabolic metabolism for suppression. *Nat Immunol* (2016) 17:1459–66. doi: 10.1038/ni.3577

321. Jang G-Y, Lee J, Kim YS, Lee SE, Han HD, Hong K-J, et al. Interactions between tumor-derived proteins and toll-like receptors. *Exp Mol Med* (2020) 52:1926–35. doi: 10.1038/s12276-020-00540-4

322. Downs-Canner S, Berkey S, Delgoffe GM, Edwards RP, Curiel T, Odunsi K, et al. Suppressive IL-17A+Foxp3+ and ex-Th17 IL-17AnegFoxp3+ treg cells are a source of tumour-associated treg cells. *Nat Commun* (2017) 8:14649. doi: 10.1038/ncomms14649

323. Clever D, Roychoudhuri R, Constantinides MG, Askenase MH, Sukumar M, Klebanoff CA, et al. Oxygen sensing by T cells establishes an immunologically tolerant metastatic niche. *Cell* (2016) 166:1117–1131.e14. doi: 10.1016/j.cell.2016.07.032

324. Haas R, Smith J, Rocher-Ros V, Nadkarni S, Montero-Melendez T, D'Acquisto F, et al. Lactate regulates metabolic and pro-inflammatory circuits in control of T cell migration and effector functions. *PlLS Biol* (2015) 13:e1002202. doi: 10.1371/journal.pbio.1002202

325. Brand A, Singer K, Koehl GE, Kolitzus M, Schoenhammer G, Thiel A, et al. LDHA-associated lactic acid production blunts tumor immunosurveillance by T and NK cells. *Cell Metab* (2016) 24:657–71. doi: 10.1016/j.cmet.2016.08.011

326. Scott KEN, Cleveland JL. Lactate wreaks havoc on tumor-infiltrating T and NK cells. *Cell Metab* (2016) 24:649–50. doi: 10.1016/j.cmet.2016.10.015

327. Yu YR, Imrichova H, Wang H, Chao T, Xiao Z, Gao M, et al. Disturbed mitochondrial dynamics in CD8(+) TILs reinforce T cell exhaustion. *Nat Immunol* (2020) 21:1540–51. doi: 10.1038/s41590-020-0793-3

328. Li W, Cheng H, Li G, Zhang L. Mitochondrial damage and the road to exhaustion. *Cell Metab* (2020) 32:905–7. doi: 10.1016/j.cmet.2020.11.004

329. Vardhana SA, Hwee MA, Berisa M, Wells DK, Yost KE, King B, et al. Impaired mitochondrial oxidative phosphorylation limits the self-renewal of T cells exposed to persistent antigen. *Nat Immunol* (2020) 21:1022–33. doi: 10.1038/s41590-020-0725-2

330. Schurich A, Pallett LJ, Jajbhay D, Wijngaarden J, Otano I, Gill US, et al. Distinct metabolic requirements of exhausted and functional virus-specific CD8 T cells in the same host. *Cell Rep* (2016) 16:1243–52. doi: 10.1016/j.celrep.2016.06.078

331. Lim TS, Chew V, Sieow JL, Goh S, Yeong JP, Soon AL, et al. PD-1 expression on dendritic cells suppresses CD8(+) T cell function and antitumor immunity. *Oncoimmunology* (2016) 5:e1085146. doi: 10.1080/2162402X.2015.1085146

332. Oh SA, Wu D-C, Cheung J, Navarro A, Xiong H, Cubas R, et al. PD-L1 expression by dendritic cells is a key regulator of T-cell immunity in cancer. *Nat Cancer* (2020) 1:681–91. doi: 10.1038/s43018-020-0075-x

333. Siska PJ, Rathmell JC. T Cell metabolic fitness in antitumor immunity. *Trends Immunol* (2015) 36:257–64. doi: 10.1016/j.it.2015.02.007

334. Nakaya M, Xiao Y, Zhou X, Chang JH, Chang M, Cheng X, et al. Inflammatory T cell responses rely on amino acid transporter ASCT2 facilitation of glutamine uptake and mTORC1 kinase activation. *Immunity* (2014) 40:692–705. doi: 10.1016/j.immuni.2014.04.007

335. Cham CM, Driessens G, O'Keefe JP, Gajewski TF. Glucose deprivation inhibits multiple key gene expression events and effector functions in CD8+ T cells. *Eur J Immunol* (2008) 38:2438–50. doi: 10.1002/eji.200838289

336. Sinclair LV, Rolf J, Emslie E, Shi YB, Taylor PM, Cantrell DA. Control of amino-acid transport by antigen receptors coordinates the metabolic reprogramming essential for T cell differentiation. *Nat Immunol* (2013) 14:500–8. doi: 10.1038/ni.2556

337. MacIver NJ, Michalek RD, Rathmell JC. Metabolic regulation of T lymphocytes. *Annu Rev Immunol* (2013) 31:259–83. doi: 10.1146/annurev-immunol-032712-095956

338. Alves NL, Derks IAM, Berk E, Spijker R, van Lier RAW, Eldering E. The Noxa/Mcl-1 axis regulates susceptibility to apoptosis under glucose limitation in dividing T cells. *Immunity* (2006) 24:703–16. doi: 10.1016/j.immuni.2006.03.018

339. Ecker C, Guo L, Voicu S, Gil-de-Gómez L, Medvec A, Cortina L, et al. Differential reliance on lipid metabolism as a salvage pathway underlies functional differences of T cell subsets in poor nutrient environments. *Cell Rep* (2018) 23:741–55. doi: 10.1016/j.celrep.2018.03.084

340. Zhang Y, Kurupati R, Liu L, Zhou XY, Zhang G, Hudaihed A, et al. Enhancing CD8+ T cell fatty acid catabolism within a metabolically challenging tumor microenvironment increases the efficacy of melanoma immunotherapy. *Cancer Cell* (2017) 32:377–391.e9. doi: 10.1016/j.ccell.2017.08.004

341. Bailis W, Shyer JA, Chiorazzi M, Flavell RA. No oxygen? no glucose? no problem: fatty acid catabolism enhances effector CD8+ TILs. *Cancer Cell* (2017) 32:280–1. doi: 10.1016/j.ccell.2017.08.013

342. Gaggero S, Martinez-Fabregas J, Cozzani A, Fyfe PK, Leprohon M, Yang J, et al. IL-2 is inactivated by the acidic pH environment of tumors enabling engineering of a pH-selective mutein. *Sci Immunol* (2022) 7:eade5686. doi: 10.1126/sciimmunol.ade5686

343. Gerriets VA, Kishton RJ, Nichols AG, Macintyre AN, Inoue M, Ilkayeva O, et al. Metabolic programming and PDHK1 control CD4+ T cell subsets and inflammation. *J Clin Invest* (2015) 125:194–207. doi: 10.1172/JCI76012

344. Wang R, Dillon CP, Shi LZ, Milasta S, Carter R, Finkelstein D, et al. The transcription factor myc controls metabolic reprogramming upon T lymphocyte activation. *Immunity* (2011) 35:871–82. doi: 10.1016/j.immuni.2011.09.021

345. Klysz D, Tai X, Robert PA, Craveiro M, Cretenet G, Oburoglu L, et al. Glutamine-dependent α-ketoglutarate production regulates the balance between T helper 1 cell and regulatory T cell generation. *Sci Signal* (2015) 8:ra97. doi: 10.1126/scisignal.aab2610

346. Leone RD, Zhao L, Englert JM, Sun IM, Oh MH, Sun IH, et al. Glutamine blockade induces divergent metabolic programs to overcome tumor immune evasion. *Science* (2019) 366:1013–21. doi: 10.1126/science.aav2588

347. Gnanaprakasam JNR, Sherman JW, Wang R. MYC and HIF in shaping immune response and immune metabolism. *Cytokine Growth Factor Rev* (2017) 35:63–70. doi: 10.1016/j.cytogfr.2017.03.004

348. Scharping NE, Menk AV, Moreci RS, Whetstone RD, Dadey RE, Watkins SC, et al. The tumor microenvironment represses T cell mitochondrial biogenesis to drive intratumoral T cell metabolic insufficiency and dysfunction. *Immunity* (2016) 45:374–88. doi: 10.1016/j.immuni.2016.07.009

349. Scharping NE, Rivadeneira DB, Menk AV, Vignali PDA, Ford BR, Rittenhouse NL, et al. Mitochondrial stress induced by continuous stimulation under hypoxia rapidly drives T cell exhaustion. *Nat Immunol* (2021) 22:205–15. doi: 10.1038/s41590-020-00834-9

350. Soto-Heredero G, Desdín-Micó G, Mittelbrunn M. Mitochondrial dysfunction defines T cell exhaustion. *Cell Metab* (2021) 33:470–2. doi: 10.1016/j.cmet.2021.02.010

351. Liu X, Peng G. Mitochondria orchestrate T cell fate and function. *Nat Immunol* (2021) 22:276–8. doi: 10.1038/s41590-020-00861-6

352. Priyadharshini B, Loschi M, Newton RH, Zhang JW, Finn KK, Gerriets VA, et al. Cutting edge: TGF-β and phosphatidylinositol 3-kinase signals modulate distinct metabolism of regulatory T cell subsets. *J Immunol* (2018) 201:2215–9. doi: 10.4049/jimmunol.1800311

353. Francisco LM, Salinas VH, Brown KE, Vanguri VK, Freeman GJ, Kuchroo VK, et al. PD-L1 regulates the development, maintenance, and function of induced regulatory T cells. *J Exp Med* (2009) 206:3015–29. doi: 10.1084/jem.20090847

354. Tu E, Chia CPZ, Chen W, Zhang D, Park SA, Jin W, et al. T Cell receptor-regulated TGF-β type I receptor expression determines T cell quiescence and activation. *Immunity* (2018) 48:745–759.e6. doi: 10.1016/j.immuni.2018.03.025

355. de Visser KE, Korets LV, Coussens LM. *De novo* carcinogenesis promoted by chronic inflammation is b lymphocyte dependent. *Cancer Cell* (2005) 7:411–23. doi: 10.1016/j.ccr.2005.04.014

356. Houghton AN, Uchi H, Wolchok JD. The role of the immune system in early epithelial carcinogenesis: b-ware the double-edged sword. *Cancer Cell* (2005) 7:403–5. doi: 10.1016/j.ccr.2005.04.026

357. DiLillo DJ, Yanaba K, Tedder TF. B cells are required for optimal CD4+ and CD8+ T cell tumor immunity: therapeutic b cell depletion enhances B16 melanoma growth in mice. *J Immunol* (2010) 184:4006–16. doi: 10.4049/jimmunol.0903009

358. Singh S, Roszik J, Saini N, Singh VK, Bavisi K, Wang Z, et al. B cells are required to generate optimal anti-melanoma immunity in response to checkpoint blockade. *Front Immunol* (2022) 13:794684. doi: 10.3389/fimmu.2022.794684

359. Sagiv-Barfi I, Czerwinski DK, Shree T, Lohmeyer JJK, Levy R. Intratumoral immunotherapy relies on b and T cell collaboration. *Sci Immunol* (2022) 7:eabn5859. doi: 10.1126/sciimmunol.abn5859

360. Cabrita R, Lauss M, Sanna A, Donia M, Skaarup Larsen M, Mitra S, et al. Tertiary lymphoid structures improve immunotherapy and survival in melanoma. *Nature* (2020) 577:561–5. doi: 10.1038/s41586-019-1914-8

361. Fridman WH, Petitprez F, Meylan M, Chen TW-W, Sun C-M, Roumenina LT, et al. B cells and cancer: to b or not to b? *J Exp Med* (2020) 218. doi: 10.1084/jem.20200851

362. Iglesia MD, Vincent BG, Parker JS, Hoadley KA, Carey LA, Perou CM, et al. Prognostic b-cell signatures using mRNA-seq in patients with subtype-specific breast and ovarian cancer. *Clin Cancer Res* (2014) 20:3818–29. doi: 10.1158/1078-0432.CCR-13-3368

363. Iglesia MD, Parker JS, Hoadley KA, Serody JS, Perou CM, Vincent BG. Genomic analysis of immune cell infiltrates across 11 tumor types. *JNCI: J Natl Cancer Institute* (2016) 108:djw144. doi: 10.1093/jnci/djw144

364. Selitsky SR, Mose LE, Smith CC, Chai S, Hoadley KA, Dittmer DP, et al. Prognostic value of b cells in cutaneous melanoma. *Genome Med* (2019) 11:36. doi: 10.1186/s13073-019-0647-5

365. Petitprez F, de Reyniès A, Keung EZ, Chen TW, Sun CM, Calderaro J, et al. B cells are associated with survival and immunotherapy response in sarcoma. *Nature* (2020) 577:556–60. doi: 10.1038/s41586-019-1906-8

366. Helmink BA, Reddy SM, Gao J, Zhang S, Basar R, Thakur R, et al. B cells and tertiary lymphoid structures promote immunotherapy response. *Nature* (2020) 577:549–55. doi: 10.1038/s41586-019-1922-8

367. Germain C, Gnjatic S, Tamzalit F, Knockaert S, Remark R, Goc J, et al. Presence of b cells in tertiary lymphoid structures is associated with a protective immunity in patients with lung cancer. *Am J Respir Crit Care Med* (2014) 189:832–44. doi: 10.1164/rccm.201309-1611OC

368. Wang Z, Wu X. Study and analysis of antitumor resistance mechanism of PD1/PD-L1 immune checkpoint blocker. *Cancer Med* (2020) 9:8086–121. doi: 10.1002/cam4.3410

369. Yuen GJ, Demissie E, Pillai S. B lymphocytes and cancer: a love-hate relationship. *Trends Cancer* (2016) 2:747–57. doi: 10.1016/j.trecan.2016.10.010

370. Laumont CM, Banville AC, Gilardi M, Hollern DP, Nelson BH. Tumour-infiltrating b cells: immunological mechanisms, clinical impact and therapeutic opportunities. *Nat Rev Cancer* (2022) 22:414–30. doi: 10.1038/s41568-022-00466-1

371. Fridman WH, Meylan M, Petitprez F, Sun C-M, Italiano A, Sautès-Fridman C. B cells and tertiary lymphoid structures as determinants of tumour immune contexture and clinical outcome. *Nat Rev Clin Oncol* (2022) 19:441–57. doi: 10.1038/s41571-022-00619-z

372. Chiaranunt P, Burrows K, Ngai L, Cao EY, Tai SL, Liang H, et al. Microbial energy metabolism fuels a CSF2-dependent intestinal macrophage niche within tertiary lymphoid organs. *bioRxiv* (2022), 2022.03.23.485563. doi: 10.1101/2022.03.23.485563

373. Carrega P, Loiacono F, Di Carlo E, Scaramuccia A, Mora M, Conte R, et al. NCR(+)ILC3 concentrate in human lung cancer and associate with intratumoral lymphoid structures. *Nat Commun* (2015) 6:8280. doi: 10.1038/ncomms9280

374. Lu Y, Yuan X, Wang M, He Z, Li H, Wang J, et al. Gut microbiota influence immunotherapy responses: mechanisms and therapeutic strategies. *J Hematol Oncol* (2022) 15:47. doi: 10.1186/s13045-022-01273-9

375. Cerutti A, Cols M, Puga I. Marginal zone b cells: virtues of innate-like antibody-producing lymphocytes. *Nat Rev Immunol* (2013) 13:118–32. doi: 10.1038/nri3383

376. LeBien TW, Tedder TF. B lymphocytes: how they develop and function. *Blood* (2008) 112:1570–80. doi: 10.1182/blood-2008-02-078071

377. Akkaya M, Pierce SK. From zero to sixty and back to zero again: the metabolic life of b cells. *Curr Opin Immunol* (2019) 57:1–7. doi: 10.1016/j.coi.2018.09.019

378. Montecino-Rodriguez E, Fice M, Casero D, Berent-Maoz B, Barber CL, Dorshkind K. Distinct genetic networks orchestrate the emergence of specific waves of fetal and adult b-1 and b-2 development. *Immunity* (2016) 45:527–39. doi: 10.1016/j.immuni.2016.07.012

379. Clarke AJ, Riffelmacher T, Braas D, Cornall RJ, Simon AK. B1a b cells require autophagy for metabolic homeostasis and self-renewal. *J Exp Med* (2018) 215:399–413. doi: 10.1084/jem.20170771

380. Jellusova J, Cato MH, Apgar JR, Ramezani-Rad P, Leung CR, Chen C, et al. Gsk3 is a metabolic checkpoint regulator in b cells. *Nat Immunol* (2017) 18:303–12. doi: 10.1038/ni.3664

381. De Silva NS, Klein U. Dynamics of b cells in germinal centres. *Nat Rev Immunol* (2015) 15:137–48. doi: 10.1038/nri3804

382. Mesin L, Ersching J, Victora GD. Germinal center b cell dynamics. *Immunity* (2016) 45:471–82. doi: 10.1016/j.immuni.2016.09.001

383. Victora GD, Nussenzweig MC. Germinal centers. *Annu Rev Immunol* (2022) 40:413–42. doi: 10.1146/annurev-immunol-120419-022408

384. Dominguez-Sola D, Victora GD, Ying CY, Phan RT, Saito M, Nussenzweig MC, et al. The proto-oncogene MYC is required for selection in the germinal center and cyclic reentry. *Nat Immunol* (2012) 13:1083–91. doi: 10.1038/ni.2428

385. Luo W, Weisel F, Shlomchik MJ. B cell receptor and CD40 signaling are rewired for synergistic induction of the c-myc transcription factor in germinal center b cells. *Immunity* (2018) 48:313–326.e5. doi: 10.1016/j.immuni.2018.01.008

386. Li F, Wang Y, Zeller KI, Potter JJ, Wonsey DR, O'Donnell KA, et al. Myc stimulates nuclearly encoded mitochondrial genes and mitochondrial biogenesis. *Mol Cell Biol* (2005) 25:6225–34. doi: 10.1128/MCB.25.14.6225-6234.2005

387. Li L, Feng C, Qin J, Li D, Liu M, Han S, et al. Regulation of humoral immune response by HIF-1α-dependent metabolic reprogramming of the germinal center reaction. *Cell Immunol* (2021) 367:104409. doi: 10.1016/j.cellimm.2021.104409

388. Lam WY, Becker AM, Kennerly KM, Wong R, Curtis JD, Llufrio EM, et al. Mitochondrial pyruvate import promotes long-term survival of antibody-secreting plasma cells. *Immunity* (2016) 45:60–73. doi: 10.1016/j.immuni.2016.06.011

389. Lam WY, Bhattacharya D. Metabolic links between plasma cell survival, secretion, and stress. *Trends Immunol* (2018) 39:19–27. doi: 10.1016/j.it.2017.08.007

390. Waters LR, Ahsan FM, Wolf DM, Shirihai O, Teitell MA. Initial b cell activation induces metabolic reprogramming and mitochondrial remodeling. *iScience* (2018) 5:99–109. doi: 10.1016/j.isci.2018.07.005

391. Lam WY, Jash A, Yao CH, D'Souza L, Wong R, Nunley RM, et al. Metabolic and transcriptional modules independently diversify plasma cell lifespan and function. *Cell Rep* (2018) 24:2479–2492.e6. doi: 10.1016/j.celrep.2018.07.084

392. Sandoval H, Kodali S, Wang J. Regulation of b cell fate, survival, and function by mitochondria and autophagy. *Mitochondrion* (2018) 41:58–65. doi: 10.1016/j.mito.2017.11.005

393. Kunisawa J, Sugiura Y, Wake T, Nagatake T, Suzuki H, Nagasawa R, et al. Mode of bioenergetic metabolism during b cell differentiation in the intestine determines the distinct requirement for vitamin B1. *Cell Rep* (2015) 13:122–31. doi: 10.1016/j.celrep.2015.08.063

394. Hu Q, Hong Y, Qi P, Lu G, Mai X, Xu S, et al. Atlas of breast cancer infiltrated b-lymphocytes revealed by paired single-cell RNA-sequencing and antigen receptor profiling. *Nat Commun* (2021) 12:2186. doi: 10.1038/s41467-021-22300-2

395. Meylan M, Petitprez F, Becht E, Bougoüin A, Pupier G, Calvez A, et al. Tertiary lymphoid structures generate and propagate anti-tumor antibody-producing plasma cells in renal cell cancer. *Immunity* (2022) 55:527–541.e5. doi: 10.1016/j.immuni.2022.02.001

396. Ruffin AT, Cillo AR, Tabib T, Liu A, Onkar S, Kunning SR, et al. B cell signatures and tertiary lymphoid structures contribute to outcome in head and neck squamous cell carcinoma. *Nat Commun* (2021) 12:3349. doi: 10.1038/s41467-021-23355-x

397. Weiner AB, Vidotto T, Liu Y, Mendes AA, Salles DC, Faisal FA, et al. Plasma cells are enriched in localized prostate cancer in black men and are associated with improved outcomes. *Nat Commun* (2021) 12:935. doi: 10.1038/s41467-021-21245-w

398. Rosser EC, Oleinika K, Tonon S, Doyle R, Bosma A, Carter NA, et al. Regulatory b cells are induced by gut microbiota-driven interleukin-1β and interleukin-6 production. *Nat Med* (2014) 20:1334–9. doi: 10.1038/nm.3680

399. Wang RX, Yu CR, Dambuza IM, Mahdi RM, Dolinska MB, Sergeev YV, et al. Interleukin-35 induces regulatory b cells that suppress autoimmune disease. *Nat Med* (2014) 20:633–41. doi: 10.1038/nm.3554

400. Dambuza IM, He C, Choi JK, Yu CR, Wang R, Mattapallil MJ, et al. IL-12p35 induces expansion of IL-10 and IL-35-expressing regulatory b cells and ameliorates autoimmune disease. *Nat Commun* (2017) 8:719. doi: 10.1038/s41467-017-00838-4

401. Rosser EC, Mauri C. Regulatory b cells: origin, phenotype, and function. *Immunity* (2015) 42:607–12. doi: 10.1016/j.immuni.2015.04.005

402. Balkwill F, Montfort A, Capasso M. B regulatory cells in cancer. *Trends Immunol* (2013) 34:169–73. doi: 10.1016/j.it.2012.10.007

403. Mirlekar B, Wang Y, Li S, Zhou M, Entwistle S, De Buysscher T, et al. Balance between immunoregulatory b cells and plasma cells drives pancreatic tumor immunity. *Cell Rep Med* (2022) 3:100744. doi: 10.1016/j.xcrm.2022.100744

404. Sharma A, Liaw K, Sharma R, Thomas AG, Slusher BS, Kannan S, et al. Targeting mitochondria in tumor-associated macrophages using a dendrimer-conjugated TSPO ligand that stimulates antitumor signaling in glioblastoma. *Biomacromolecules* (2020) 21:3909–22. doi: 10.1021/acs.biomac.0c01033

405. Sharma R, Liaw K, Sharma A, Jimenez A, Chang M, Salazar S, et al. Glycosylation of PAMAM dendrimers significantly improves tumor macrophage targeting and specificity in glioblastoma. *J Control Release* (2021) 337:179–92. doi: 10.1016/j.jconrel.2021.07.018

406. Halbrook CJ, Pontious C, Kovalenko I, Lapienyte L, Dreyer S, Lee H-J, et al. Macrophage-released pyrimidines inhibit gemcitabine therapy in pancreatic cancer. *Cell Metab* (2019) 29:1390–1399.e6. doi: 10.1016/j.cmet.2019.02.001

407. Shan X, Hu P, Ni L, Shen L, Zhang Y, Ji Z, et al. Serine metabolism orchestrates macrophage polarization by regulating the IGF1–p38 axis. *Cell Mol Immunol* (2022) 19:1263–78. doi: 10.1038/s41423-022-00925-7

408. Wang W, Guo MN, Li N, Pang DQ, Wu JH. Glutamine deprivation impairs function of infiltrating CD8(+) T cells in hepatocellular carcinoma by inducing mitochondrial damage and apoptosis. *World J Gastrointest Oncol* (2022) 14:1124–40. doi: 10.4251/wjgo.v14.i6.1124

409. Feng Q, Liu Z, Yu X, Huang T, Chen J, Wang J, et al. Lactate increases stemness of CD8 + T cells to augment anti-tumor immunity. *Nat Commun* (2022) 13:4981. doi: 10.1038/s41467-022-32521-8

410. Beckermann KE, Hongo R, Ye X, Young K, Carbonell K, Healey DCC, et al. CD28 costimulation drives tumor-infiltrating T cell glycolysis to promote inflammation. *JCI Insight* (2020) 5(16):e138729. doi: 10.1172/jci.insight.138729

411. Cribioli E, Giordano Attianese GMP, Ginefra P, Signorino-Gelo A, Vuillefroy de Silly R, Vannini N, et al. Enforcing GLUT3 expression in CD8(+) T cells improves fitness and tumor control by promoting glucose uptake and energy storage. *Front Immunol* (2022) 13:976628. doi: 10.3389/fimmu.2022.976628

412. Sukumar M, Liu J, Ji Y, Subramanian M, Crompton JG, Yu Z, et al. Inhibiting glycolytic metabolism enhances CD8+ T cell memory and antitumor function. *J Clin Invest* (2013) 123:4479–88. doi: 10.1172/JCI69589

413. Nath PR, Pal-Nath D, Kaur S, Gangaplara A, Meyer TJ, Cam MC, et al. Loss of CD47 alters CD8+ T cell activation *in vitro* and immunodynamics in mice. *Oncoimmunology* (2022) 11:2111909. doi: 10.1080/2162402X.2022.2111909

414. Liu X, Pu Y, Cron K, Deng L, Kline J, Frazier WA, et al. CD47 blockade triggers T cell-mediated destruction of immunogenic tumors. *Nat Med* (2015) 21:1209–15. doi: 10.1038/nm.3931

415. Vonderheide RH. CD47 blockade as another immune checkpoint therapy for cancer. *Nat Med* (2015) 21:1122–3. doi: 10.1038/nm.3965

416. Wang Z, Li B, Li S, Lin W, Wang Z, Wang S, et al. Metabolic control of CD47 expression through LAT2-mediated amino acid uptake promotes tumor immune evasion. *Nat Commun* (2022) 13:6308. doi: 10.1038/s41467-022-34064-4

417. Minogue E, Cunha PP, Quaranta A, Zurita J, Teli SS, Wadsworth BJ, et al. Glutarate regulates T cell function and metabolism. *bioRxiv* (2022), 2022.10.20.513065. doi: 10.1101/2022.10.20.513065

418. Lötscher J, Martí i Líndez A-A, Kirchhammer N, Cribioli E, Giordano Attianese GMP, Trefny MP, et al. Magnesium sensing via LFA-1 regulates CD8+ T cell effector function. *Cell* (2022) 185:585–602.e29. doi: 10.1016/j.cell.2021.12.039

419. Vardhana S, Dustin ML. Magnesium for T cells: strong to the finish! *Trends Immunol* (2022) 43:277–9. doi: 10.1016/j.it.2022.02.004

420. Geiger R, Rieckmann JC, Wolf T, Basso C, Feng Y, Fuhrer T, et al. L-arginine modulates T cell metabolism and enhances survival and anti-tumor activity. *Cell* (2016) 167:829–842.e13. doi: 10.1016/j.cell.2016.09.031

421. Martí i Líndez AA, Dunand-Sauthier I, Conti M, Gobet F, Núñez N, Hannich JT, et al. Mitochondrial arginase-2 is a cell–autonomous regulator of CD8+ T cell function and antitumor efficacy. *JCI Insight* (2019) 4(24):e132975. doi: 10.1172/jci.insight.132975

422. Bronte V, Zanovello P. Regulation of immune responses by l-arginine metabolism. *Nat Rev Immunol* (2005) 5:641–54. doi: 10.1038/nri1668

423. Canale FP, Basso C, Antonini G, Perotti M, Li N, Sokolovska A, et al. Metabolic modulation of tumours with engineered bacteria for immunotherapy. *Nature* (2021) 598:662–6. doi: 10.1038/s41586-021-04003-2

424. Griffin ME, Hang HC. Improving immunotherapy response through the use of designer bacteria. *Cancer Cell* (2021) 39:1576–7. doi: 10.1016/j.ccell.2021.11.009

425. Van Wilpe S, Koornstra R, Den Brok M, De Groot JW, Blank C, De Vries J, et al. Lactate dehydrogenase: a marker of diminished antitumor immunity. *Oncoimmunology* (2020) 9:1731942. doi: 10.1080/2162402X.2020.1731942

426. Cascone T, McKenzie JA, Mbofung RM, Punt S, Wang Z, Xu C, et al. Increased tumor glycolysis characterizes immune resistance to adoptive T cell therapy. *Cell Metab* (2018) 27:977–987.e4. doi: 10.1016/j.cmet.2018.02.024

427. Halford SER, Jones P, Wedge S, Hirschberg S, Katugampola S, Veal G, et al. A first-in-human first-in-class (FIC) trial of the monocarboxylate transporter 1 (MCT1) inhibitor AZD3965 in patients with advanced solid tumours. *J Clin Oncol* (2017) 35:2516–6. doi: 10.1200/JCO.2017.35.15_suppl.2516

428. Polański R, Hodgkinson CL, Fusi A, Nonaka D, Priest L, Kelly P, et al. Activity of the monocarboxylate transporter 1 inhibitor AZD3965 in small cell lung cancer. *Clin Cancer Res* (2014) 20:926–37. doi: 10.1158/1078-0432.CCR-13-2270

429. Silva A, Antunes B, Batista A, Pinto-Ribeiro F, Baltazar F, Afonso J. *In vivo* anticancer activity of AZD3965: a systematic review. *Molecules* (2021) 27. doi: 10.3390/molecules27010181

430. Morris A. Inhibiting glycolysis in tumour cells. *Nat Rev Endocrinol* (2018) 14:323. doi: 10.1038/s41574-018-0017-1

431. Tang H, Fu YX. Immune evasion in tumor's own sweet way. *Cell Metab* (2018) 27:945–6. doi: 10.1016/j.cmet.2018.03.013

432. Gill KS, Fernandes P, O'Donovan TR, McKenna SL, Doddakula KK, Power DG, et al. Glycolysis inhibition as a cancer treatment and its role in an anti-tumour immune response. *Biochim Biophys Acta* (2016) 1866:87–105. doi: 10.1016/j.bbcan.2016.06.005

433. Mei Y, Zhao L, Jiang M, Yang F, Zhang X, Jia Y, et al. Characterization of glucose metabolism in breast cancer to guide clinical therapy. *Front Surg* (2022) 9:973410. doi: 10.3389/fsurg.2022.973410

434. Cheng J, Liu Y, Yan J, Zhao L, Zhou Y, Shen X, et al. Fumarate suppresses b-cell activation and function through direct inactivation of LYN. *Nat Chem Biol* (2022) 18:954–62. doi: 10.1038/s41589-022-01052-0

435. Baryła M, Semeniuk-Wojtaś A, Róg L, Kraj L, Małyszko M, Stec R. Oncometabolites-a link between cancer cells and tumor microenvironment. *Biol (Basel)* (2022) 11(2):270. doi: 10.3390/biology11020270

436. Wang C, Dong Z, Hao Y, Zhu Y, Ni J, Li Q, et al. Coordination polymer-coated CaCO3 reinforces radiotherapy by reprogramming the immunosuppressive metabolic microenvironment. *Advanced Materials* (2022) 34:2106520. doi: 10.1002/adma.202106520

437. Wang Y, Gao D, Jin L, Ren X, Ouyang Y, Zhou Y, et al. NADPH selective depletion nanomedicine-mediated radio-immunometabolism regulation for strengthening anti-PDL1 therapy against TNBC. *Advanced Sci* (2023) 10:2203788. doi: 10.1002/advs.202203788

438. Yang Z, Gao D, Zhao J, Yang G, Guo M, Wang Y, et al. Thermal immuno-nanomedicine in cancer. *Nat Rev Clin Oncol* (2023) 20:116–34. doi: 10.1038/s41571-022-00717-y

439. Martin JD, Cabral H, Stylianopoulos T, Jain RK. Improving cancer immunotherapy using nanomedicines: progress, opportunities and challenges. *Nat Rev Clin Oncol* (2020) 17:251–66. doi: 10.1038/s41571-019-0308-z

440. Irvine DJ, Dane EL. Enhancing cancer immunotherapy with nanomedicine. *Nat Rev Immunol* (2020) 20:321–34. doi: 10.1038/s41577-019-0269-6

441. van Gisbergen MW, Zwilling E, Dubois LJ. Metabolic rewiring in radiation oncology toward improving the therapeutic ratio. *Front Oncol* (2021) 11. doi: 10.3389/fonc.2021.653621

442. Nian Y, Minami K, Maenesono R, Iske J, Yang J, Azuma H, et al. Changes of T-cell immunity over a lifetime. *Transplantation* (2019) 103:2227–33. doi: 10.1097/TP.0000000000002786

443. Martin DE, Torrance BL, Haynes L, Bartley JM. Targeting aging: lessons learned from immunometabolism and cellular senescence. *Front Immunol* (2021) 12. doi: 10.3389/fimmu.2021.714742

444. Kurupati RK, Haut LH, Schmader KE, Ertl HC. Age-related changes in b cell metabolism. *Aging (Albany NY)* (2019) 11:4367–81. doi: 10.18632/aging.102058

445. Wang H JD, Liu L, Zhang Y, Qin M, Qu Y, Wang L, et al. Spermidine promotes Nb CAR-T mediated cytotoxicity to lymphoma cells through elevating proliferation and memory. *Onco Targets Ther* (2022) 5:1229–43. doi: 10.2147/OTT.S382540

446. Chon HJ, Lee WS, Yang H, Kong SJ, Lee NK, Moon ES, et al. Tumor microenvironment remodeling by intratumoral oncolytic vaccinia virus enhances the efficacy of immune-checkpoint blockade. *Clin Cancer Res* (2019) 25:1612–23. doi: 10.1158/1078-0432.CCR-18-1932

447. Zuo S, Wei M, He B, Chen A, Wang S, Kong L, et al. Enhanced antitumor efficacy of a novel oncolytic vaccinia virus encoding a fully monoclonal antibody against T-cell immunoglobulin and ITIM domain (TIGIT). *EBioMedicine* (2021) 64:103240. doi: 10.1016/j.ebiom.2021.103240

448. Ribas A, Dummer R, Puzanov I, VanderWalde A, Andtbacka RHI, Michielin O, et al. Oncolytic virotherapy promotes intratumoral T cell infiltration and improves anti-PD-1 immunotherapy. *Cell* (2017) 170:1109–1119.e10. doi: 10.1016/j.cell.2017.08.027

449. Haanen JBAG. Converting cold into hot tumors by combining immunotherapies. *Cell* (2017) 170:1055–6. doi: 10.1016/j.cell.2017.08.031

frontiers | Frontiers in Immunology

TYPE Mini Review
PUBLISHED 12 July 2023
DOI 10.3389/fimmu.2023.1193235

OPEN ACCESS

EDITED BY
Soumya R. Mohapatra,
KIIT University, India

REVIEWED BY
Remya Raja,
Mayo Clinic Arizona, United States

*CORRESPONDENCE
Laura Brunelli
laura.brunelli@marionegri.it
Matteo Donadon
matteo.donadon@uniupo.it

†These authors have contributed equally to this work and share senior authorship

RECEIVED 24 March 2023
ACCEPTED 22 June 2023
PUBLISHED 12 July 2023

CITATION
De Simone G, Soldani C, Morabito A, Franceschini B, Ferlan F, Costa G, Pastorelli R, Donadon M and Brunelli L (2023) Implication of metabolism in the polarization of tumor-associated-macrophages: the mass spectrometry-based point of view.
Front. Immunol. 14:1193235.
doi: 10.3389/fimmu.2023.1193235

Implication of metabolism in the polarization of tumor-associated-macrophages: the mass spectrometry-based point of view

Giulia De Simone[1,2], Cristiana Soldani[3], Aurelia Morabito[1,4], Barbara Franceschini[3], Fabrizio Ferlan[3], Guido Costa[3,5,6], Roberta Pastorelli[1], Matteo Donadon[3,6,7,8*†] and Laura Brunelli[1*†]

[1]Laboratory of Metabolites and Proteins in Translational Research, Istituto di Ricerche Farmacologiche Mario Negri IRCCS, Milan, Italy, [2]Department of Biotechnologies and Biosciences, Università degli Studi Milano Bicocca, Milan, Italy, [3]Hepatobiliary Immunopathology Laboratory, IRCCS Humanitas Research Hospital, Milan, Italy, [4]Department of Electronics, Information and Bioengineering, Politecnico di Milano, Milan, Italy, [5]Department of Biomedical Sciences, Humanitas University, Milan, Italy, [6]Department of Hepatobiliary and General Surgery, IRCCS Humanitas Research Hospital, Milan, Italy, [7]Department of Health Sciences, Università del Piemonte Orientale, Novara, Italy, [8]Department of General Surgery, University Maggiore Hospital, Novara, Italy

Tumor-associated macrophages (TAMs) represent one of the main tumor-infiltrating immune cell types and are generally categorized into either of two functionally contrasting subtypes, namely classical activated M1 macrophages and alternatively activated M2 macrophages. TAMs showed different activation states that can be represent by the two extremes of the complex profile of macrophages biology, the M1-like phenotype (pro-inflammatory activity) and the M2-like phenotype (anti-inflammatory activity). Based on the tumor type, and grades, TAMs can acquire different functions and properties; usually, the M1-like phenotype is typical of early tumor stages and is associated to an anti-tumor activity, while M2-like phenotype has a pro-inflammatory activity and is related to a poor patients' prognosis. The classification of macrophages into M1/M2 groups based on well-defined stimuli does not model the infinitely more complex tissue milieu where macrophages (potentially of different origin) would be exposed to multiple signals in different sequential order. This review aims to summarize the recent mass spectrometry-based (MS-based) metabolomics findings about the modifications of metabolism in TAMs polarization in different tumors. The published data shows that MS-based metabolomics is a promising tool to help better understanding TAMs metabolic phenotypes, although it is still poorly applied for TAMs metabolism. The knowledge of key metabolic alterations in TAMs is an essential step for discovering TAMs polarization novel biomarkers and developing novel therapeutic approaches targeting TAM metabolism to repolarize TAMs towards their anti-tumor phenotype.

KEYWORDS

tumor associated macrophages (TAMs), prognostic markers, metabolism, mass spectrometry, TAM polarization

10.3389/fimmu.2023.1193235

Introduction

Macrophages are immune cells essential component of the innate immune system, with a wide distribution in lymphoid and non-lymphoid tissues throughout the body that play a pivotal role in innate immunity, tissue homeostasis, and response to adverse signals, such as pathogenic infections or inflammatory stimuli (1–3).

Macrophages principally originate from monocyte precursors mainly generated from hematopoietic stem cells placed in the bone marrow; then, monocytes migrate to several tissues and differentiate into tissue-specific macrophages (3, 4). Instead, tissue-resident macrophages such as Kupffer cells (liver), microglia (central nervous system), and Langerhans cells (skin) originate from the yolk sac and fetal liver during primitive and definitive hematopoiesis and they are responsible for the innate immunity (5, 6).

Circulating monocytes are recruited by chemotactic signals generated upon injury, infection etc. and migrate to the target tissues where they differentiate and polarize into mature macrophages depending on the microenvironment (5, 7, 8). It is possible to identify two main activation states that represent the two extremes of the complex profile of macrophage biology (9). The current classification into M1-type (classically activated macrophage) and M2-type (alternatively activated macrophage) is based upon macrophage polarization and describe macrophages different behaviors (10). One phenotype, the pro-inflammatory or classically activated M1 phenotype, allows the host to fight infections and pathogens and exhibits anti-tumoral activity. The second phenotype, the anti-inflammatory or alternatively activated M2 phenotype, displays the capability to repair damaged tissues but also presents a pro-tumoral functions (Figure 1A) (11–15).

The M1 phenotype is induced by microbial products like lipopolysaccharide and cytokines secreted by Th1 lymphocytes, such as Interferon-γ (IFN-γ) and tumor necrosis factor-alpha (TNF-α). On the other hand, anti-inflammatory molecules, such

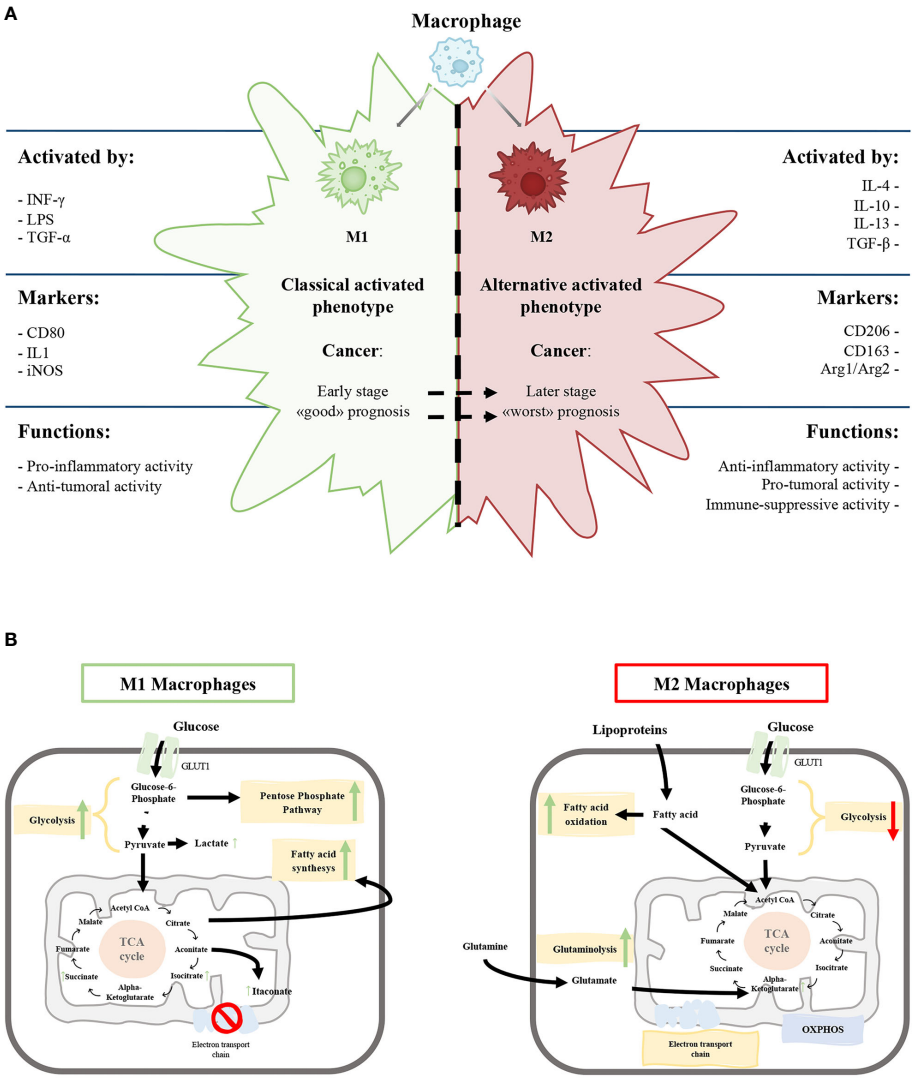

FIGURE 1
(A) Schematic representation of the characteristics of M1 and M2 macrophages phenotypes. **(B)** Schematic view of M1 and M2 macrophages metabolism. Green and red arrows indicate an up-regulation and down-regulation of a specific pathway respectively.

as glucocorticoid hormones and interleukin (IL)-4, IL-10, IL-13, secreted by Th2 lymphocytes, induce the M2 phenotype (Figure 1A) (5, 16, 17).

M1 macrophages express high levels of inducible nitric oxide synthetase (iNOS) that promote the release of nitric oxide, reactive oxygen species and pro-inflammatory cytokines (IL-1β, IL-6, IL-12) promoting Th1 response (2, 13). The high production of anti-microbial and anti-tumoral molecules gives to M1 macrophages the capability to kill intracellular pathogens (5, 18). Classically activated macrophages express specific surface proteins, such as CD68, CD80, and CD86 (Figure 1A).

In contrast, M2 macrophages produce a high amount of anti-inflammatory cytokines (IL-10, TGF-β), low levels of pro-inflammatory cytokines (IL-12) and diminished expression of the NOS enzyme. M2 macrophages have a strong phagocytosis capacity and induce angiogenesis and lymphangiogenesis (2, 19, 20). Furthermore, the arginase pathway induces increased production of ornithine, collagen, and polyamines with an elevated expression of arginase-1 (Arg1) (Figure 1A).

From a biochemical point of view, the metabolism of M1 and M2 activated macrophages were extensively characterized. M1 macrophages metabolism is based on anaerobic glycolysis, truncated tricarboxylic acid cycle (itaconate production), fatty acid synthesis and pentose phosphate pathway (Figure 1B) with, a consequent decrease in oxidative phosphorylation (OXPHOS) and fatty acid oxidation (5, 21–23)

M2 macrophages have a poorly glycolytic profile with higher arginine metabolism and preferential fatty acid oxidation (oxidative glucose metabolism), glutamine metabolism and OXPHOS (Figure 1B) (5, 18, 19, 24). Glycolysis is not essential for M2 phenotype, and glucose is mainly employed to sustain OXPHOS (25–27).

In tumors, monocytes from bone marrow and circulating monocytes are recruited through the release of cytokines and macrophages were functionally polarized in tumor-associated macrophages (TAMs) (9, 28). Within the tumor microenvironment (TME), TAMs exhibit high plasticity and undergo specific functional metabolic alterations according to the availability of tumor tissue oxygen and nutrients, thus further contributing to tumorigenesis and cancer progression.

In this review, we describe the relationship between TAMs metabolic profile and activation states and their involvement in cancer pathologies. We focus on mass spectrometry (MS)-based metabolomics analysis that is able to detect, quantify and map a huge number of molecules for recapitulate the different TAMs metabolic phenotypes (29).

TAMs density and polarization as prognostic marker in cancer pathologies: state of the art

TAMs are one of the most abundant immune myeloid populations in the TME (30). Meta-Analyses indicates that high density of TAM (CD68+) could be associated with worse prognosis in almost all cancers (31–35), contradictory in gastric cancer (32, 36) or should be linked to a favorable prognosis in colorectal cancer (37, 38).

TAMs could exhibit pro-tumoral or anti-tumoral roles depending on the stimuli generated by the TME and can acquire different functions and properties depending on cancer type, grade, and during tumor progression (39). Several studies are committed to quantify and characterize the M1 and M2 TAM phenotype to better refine the prognostic significance of TAMs.

M1-like TAMs as prognostic marker

TAMs can show a M1-like phenotype, in particular during the early stages of tumor development (2, 20, 39, 40), promoting antineoplastic and phagocytose activity. During the tumor progression, the TME produce a large amount of growth factors and anti-inflammatory mediators that induce a shift in TAMs phenotype.

In ovarian cancer, two prospective observational studies (140 Italian and 112 Chinese patients) showed that intratumoral M1/M2 TAM ratio decreased as the cancer stage increased (41) with a significant association between higher M1/M2 TAMs ratio and the longer overall survival and progression-free survival (42),

Similar findings were obtained in Non-Small Cell Lung Cancer (NSCLC) studies, where high infiltration of M1 like TAMs (41 UK and 80 Lithuanian subjects) were associated with a better survival outcomes (43, 44). Consistently with these studies, a high density of iNOS+ M1-like macrophages predicted the improved survival rate in a cohort (40 Finland patients) of HER2+ breast cancer subjects (45). Also considering TAMs morphologies, M1-like macrophages more frequently appear round and flattened, as opposed to M2-like cells that present an elongated morphology. A higher percentage of TAMs with small dimensions and regular shape were associated with a better prognosis in colorectal liver metastasis patients (101 Italian patients) (46).

Overall, these data point out that M1-like TAMs infiltrate may be associated with a favorable survival rate in several cancer pathologies.

M2-like TAMs as prognostic marker

The alternative activated M2-like phenotype promote cancer cells growth through the secretion of pro-angiogenic factors, like vascular endothelial growth factors, and immunosuppressive factors, as IL-10 and TGF-β (47). This M2-like phenotype is considered as pro-tumoral increasing neovascularization, angiogenesis, infiltration and consequently metastatization; has therefore an immune-suppressive activity and antitumor adaptive immune response (14, 16, 26, 48).

High number of M2-like TAMs were observed associated with tumor growth and poor patient prognosis in breast (562 Finland, 144 Sweden patients), NSCLC (349 Korean patients) and melanoma (184 Finland, 94 Italian patients) cancers (49–52).

Overall, these studies highlight that M1 and M2 TAMs may be useful markers of patient prognosis (M1-like better and M2-like

worst) regardless of tumor type and patient ethnicity. However, meta-analyses considering prospective studies employing standardized methodology and larger sample sizes are still needed to validate the prognostic significance of M1 and M2 TAMs infiltration.

Metabolism as modulator of macrophage functionality driving the balance between M1-like and M2-like TAMs might lead to different strategies for chemotherapeutic and/or immunotherapeutic approaches.

Mass spectrometry-based metabolomics approaches in cancer research

Metabolomics is the large-scale study of endogenous small molecules of low molecular weight molecules (<1000 Da), commonly known as metabolites, within cells, biofluids, tissues, or organisms. Metabolomics together with genomics, transcriptomics, and proteomics, drive the connection between the genotype and the phenotype in both physiological and pathological processes in order to be a powerful tool in biomarker discovery, developing drugs, and personalized medicine (53–55). Metabolomics is an essential tool for the simultaneous measurement and quantification of thousands of small metabolites from biological matrices, with the possibility to be hypothesis-generating, without *a priori* knowledge, or hypothesis-driven, with *a priori* knowledge about the metabolites present in the sample. The applicability of metabolomics in identifying metabolic dysregulation has been demonstrated in a wide range of human diseases, including cardiovascular diseases, diabetes, obesity, and cognitive disorders, but also cancers (54). For this reason, metabolomics could be considered a promising approach for the identification of metabolites acting as biomarkers to allow early diagnosis, to follow pathological processes and progression or response to treatments.

The two main analytical techniques employed for metabolomics profiling are Nuclear Magnetic Resonance (NMR) and Mass Spectrometry (MS), which allow the achievement of both qualitative and quantitative information. We will focus on the role of MS as a powerful tool for the identification of a large set of ionized analytes based on their mass-to-charge ratio (*m/z*) (53, 56).

Analytical methods for MS-based metabolomics

MS is usually coupled with a chromatographic separation system (hyphenated techniques), such as gas chromatography (GC)-MS, liquid chromatography (LC)-MS [both high-performance LC (HPLC) and ultra-performance LC (UPLC)], and capillary electrophoresis (CE)-MS, but a sample could be also directly injected into the MS (flow-injection analysis-MS) (56, 57). GC-MS is employed for the identification of volatile compounds, like fatty acids and organic acids, requiring a derivatization step before the analysis (58). Electron impact (EI) and chemical ionization (CI) sources are commonly used with a GC separation system (59). However, LC-MS does not require any derivatization and allows the detection of more analytes (60), and it is usually combined with an electrospray (ESI) and CI sources.

CE-MS allows the separation of polar and charged metabolites based on their electrophoretic mobility, an intrinsic property that depends on the size and charge of the molecule (61). To date, MS-based metabolomics strategies are widely employed in the tumor research area to identify biomarkers for prediction, diagnosis, and prognosis (62, 63).

Metabolomics approaches

Untargeted and targeted MS are the two methods used for the identification of endogenous small molecules (58). The untargeted strategy allows the identification of a huge number of metabolites with high accuracy using high-resolution MS, without knowing basic information about the metabolome of the sample.

Orbitrap and Time-of-flight (ToF) are the preferred mass analyzers for high-resolution untargeted metabolomics analysis. Ionized molecules in the orbitrap analyzer are forced to move in complex spiral patterns by the electrostatic field, combining axial oscillations with rotation around the central axis (56). Different frequencies of oscillation are then associated with different *m/z*. In the ToF analyzer, ions with initial kinetic energy enter a field-free drift region of known length and are dispersed in time based on their different *m/z*. Ions with the larger *m/z* arrive at the end of the drift length after ions with a smaller *m/z* (64).

Then, after the final ion detection, the use of database is required for metabolites identification and annotation [HMDB (65), METLIN (66)]. This annotation is performed by comparing the experimental mass to libraries within a mass tolerance frame, depending on the mass spectrometer used for the analysis (58, 60, 67). On the other hand, the information should be incomplete cause of employed solvents, pH, chromatographic separation, ionization techniques; and the detection of chemical unknowns with no annotation in database. MS/MS fragmentation experiments are then required to confirm the metabolites' structure, especially to distinguish co-eluting isobaric species (67).

Targeted metabolomics is a hypothesis-driven strategy that allows the identification of a specific set of metabolites from a panel of interest with high accuracy, selectivity and sensitivity (59).

Triple quadrupole (QQQ) and quadrupole ion trap are useful mass analyzers for targeted metabolomics (56, 58). QQQ is the most common type of tandem MS, the first and the third quadrupole are used as mass filters, while the second quadrupole is used as a collision cell to generate fragment ions. Into the Q, ions with a particular range of *m/z* values have stable periodic trajectories imposed by the direct current and the radio frequency potential of the four rod electrodes composing the Q that periodically changes in time (56, 68). The voltage polarity between two adjacent rods is opposite (64). The quadrupole is often combined with other mass analyzers to filter ions to remove matrix ions such as in Q-Trap.

The ion trap analyzer is a modification of the Q with improved sensibility. The operating principle of Q and ion trap is the same: ions of different *m/z* are selectively ejected from the analyzer by varying the radio frequency potential (68).

Targeted metabolomics allows the quantification and semi-quantification using internal standards (69) and the Multiple Reaction Monitoring (MRM) approach, performed on QQQ or Q-ion trap, is used for the exact identification of the molecules of interest, selecting specific precursor and product ions.

The number of publications in PubMed related to cancer metabolomics shows that the MS-based approach has been largely preferred over NMR with more than 4000 results obtained for the search query "*cancer metabolomics AND mass spectrometry*" and less than 1500 results obtained for the search "*cancer metabolomics AND NMR*", supporting the higher impact of MS-based techniques on cancer research.

MS-based metabolomics limitations and future perspective

Mass spectrometry (MS) techniques, because of their sensitivity and selectivity, have become methods of choice to characterize the human metabolome, being able to detect and quantify many thousands of metabolite features simultaneously. Because the metabolite composition is central to every living organism the in-depth biological insides, metabolomics can advance research across a variety of scientific areas. However many challenges still exist for a successful metabolomics study. Much has been discussed on this issue elsewhere (67, 70, 71), here we address few of the unique challenges for metabolomics. The first one is analytical, due to the chemical diversity of the metabolites, their wide dynamic range and the confidence for their unambiguous identification. To this purpose, implementation of analytical and bioinformatic tools for the accurate and standardized metabolites identification is a current goal to be achieve for a large-scale coverage of metabolites and to facilitate data processing. Although there is no single analytical platform strategy that provides the complete coverage for the whole metabolome, there are common experimental criteria to all strategies that need to be addressed. Robust metabolomics results hinge on further key elements such as a proper study design (e.g. number of observations, power size, and sampling storage), method optimization, data processing and final validation. The application of this virtuous workflow will help not only in assigning biological meaning to metabolites but also to move towards finding robust mechanism of diseases. Metabolomics as for the other omics, is not a separate discipline, and the implementation of bioinformatic algorithms and computational strategies for multi-omics integration is fundamental to place metabolites in a biological context and to associate metabolites with phenotype causality. This promotes the understanding of metabolome in a system-wide level in order to develop personalized treatments and help in early diagnosis of disease. It is believed that the continuous progress in technologies together with bioinformatics and computational tools will feed metabolomics research to guide not only biomarkers discovery but also to delve and discover mechanisms of disease development and progression.

The MS-based metabolomics profile of TAMs in cancer pathologies

Exploring the biochemical mechanisms underlying TAMs polarization during tumor development and progression could contribute to the development of new therapeutic approaches. In the last few years, metabolism of M1 and M2-like macrophages was mainly studied in *in-vitro* polarized TAMs (72, 73). Nevertheless, the *in-vivo* metabolic phenotypes of resident TAMs directly isolated from fresh tumor specimens are not largely explored. Considering the heterogeneity of activation stimuli from TME, deciphering the TAMs metabolism in the tissue has a vital importance in cancer research.

We summarized the scientific analysis of TAMs metabolism obtained by MS-based metabolomics studies in different cancer pathologies. MS-based studies on TAMs metabolism could determinate the metabolic alterations in different metabolic pathways such as glycolysis, mitochondrial machinery, amino acids, and lipid metabolism. These information are critical for identifying new biochemical pathways underlying tumor resident TAMs polarization useful to influence overall patient survival.

Central cellular biochemical pathways in TAMs

Untargeted metabolomics by using CE-ToF-MS of *in-vivo* sorted murine TAMs from a colon adenocarcinoma xenograft model in both early (14 days after tumor implantation) and late tumor stage (28 days after tumor implantation) showed an increasing of different cellular metabolic pathways (glycolysis, methionine metabolism, TCA cycle, and glutamine and glutamate metabolism) in the tumor resident TAMs relative to myeloid-derived suppressor cells (74). This metabolic asset [increase in oxidative phosphorylation (OXPHOS) and glycolysis] of TAMs was confirmed in peritoneal Mϕ macrophages isolated from naive and ID8 tumor-bearing mice (75). The untargeted metabolomics (GC-TOF) identified itaconic acid, the product of the catabolism of mitochondrial cis-aconitate, the most highly upregulated metabolites in Mϕ macrophages of tumor-bearing mice (75). The high glycolytic activity of TAMs was also observed by untargeted metabolomics (by means of UHPLC-Orbitrap) on *in-vitro* generated human pancreatic ductal adenocarcinoma (PDAC) TAMs. The mixed M1/M2 TAMs generated from monocytes exposed to PDAC conditioned medium were characterized by elevated glycolysis, increased lactate production and reduced OXPHOS compared to normal macrophages (76).

The reliance on glycolysis of pancreatic cancer derived TAMs was confirmed by untargeted metabolomics (using both LC-ToF-MS and CE-ToF-MS) on TAMs deleted for the Glucose Transporter 1 (GLUT1). Tumor resident GLUT1 deleted TAMs showed the

decrement of glycolytic intermediates such as glucose-6-phosphate and fructose 1,6-biphosphate with no substantial difference of the TCA cycle relative to control (77).

For the characterization of metabolic pattern characteristic of M1 and M2-like TAMs, a metabolic flux analysis (13C-labeling experiments coupled with GC-MS) on *in-vivo* sorted NSCLC resident TAMs (3LL-R Lewis lung murine model) was used. In this model M1-like TAMs (major histocompatibility complex (MHC)-IIhi) display a hampered tricarboxylic acid (TCA) cycle, while M2-like TAMs (MHC-IIlo) show higher OXPHOS and glycolytic metabolism (78). Another metabolic profiling (through UPLC QQQ tandem MS) of *in-vitro* conditioned PDAC TAMs indicated that nucleoside metabolism is the principal biochemical pathway able to distinguish TAM and M2 macrophages from the M1 (72).

Metabolism of M1 was also studied in *ex vivo* NSCLC tumor slices. Slices were treated with the macrophage activator β-glucan, and metabolic changes were monitored by metabolic flux analysis ($13C_6$-glucose LC–MS). MS highlighted a higher synthesis of itaconate and higher levels of NADPH in M1-like generated TAMs relative to the general TAMs population (79).

Lipid metabolism in TAMs

Lipidomics is focused on the identification of lipid species present within a cell, organ, or biological system. The lipidome compartment in the cells is composed of several lipid categories (e.g., fatty acids, glycerolipids, sphingolipids, and sterol lipids). Among the metabolic alterations observed in TAMs, lipid metabolism seems to directly affected TAMs polarization and function (80).

Eicosanoids quantification (Target lipodomics by using LC-QQQ tandem MS) on *in-vivo* sorted tumor resident TAMs populations (resident alveolar macrophages MacA and M2-like TAMs MacB) in orthotropic lung cancer model, showed that M2-like TAMs had low level of eicosanoids production relative to resident alveolar macrophages (81).

Global lipidomics analysis (by using LC-HRMS with Orbitrap) on *in-vitro* generated TAMs (monocytes exposure to gastric cancer conditioned medium) showed almost 10-fold higher triacylglycerol levels relative to control macrophages (73). This data was also supported by the high amount of total lipid found in *in-vivo* TAM sorted from both murine and human gastric cancer specimens. The lipid accumulation seems to occur by uptakes of lipids released by cancer cells, that drives TAMs polarization toward an M2-like profile (73). Finally, target lipidomics (by QTrap analyzer) on conditioned medium from *in-vivo* sorted TAMs reveal that M2-like TAMs (CD163+CD206+) actively released of PLA2G7 and autotaxin that play an essential role in ovarian cancer invasiveness and metastatic spread (82).

Overall, mass spectrometry-based metabolic profiling of TAMs converges to define the increased glycolytic and OXPHOS activity of TAMs relative to control macrophages also considering the *in-vivo* sorted and *in vitro* conditioned TAMs (Table 1). Considering the heterogeneity of the TAMs populations in the cancer microenvironment and the different experimental settings for determining TAMs subpopulation, it is difficult to speculate the attribution of the augmented metabolism at a particular TAMs populations. It is possible to speculate that M2-like TAMs identified as CD11b+Ly6G–Ly6ClowMHC-IIhigh (78) rely on glycolysis, mitochondrial machinery, and lipid metabolism to sustain their functionality (Table 1). On the contrary, M1-like TAMs, when compared to the general control macrophages cells, seem be less metabolic active with a hampered OXPHOS capacity (Table 1). These data only partially agree with the metabolic characteristics of M1, and M2 polarized macrophages. Indeed, the M2 phenotype is mainly defined by a poor glycolytic profile with higher arginine metabolism and preferential fatty acid oxidation (oxidative glucose metabolism) and OXPHOS (5, 19) (Figure 1).

Discussion

TAMs are one of the most common immune cells in the TME and they are characterized by a great plasticity and adaptability to the environment they infiltrate by re-programming their activation state towards a pro- (M1) or an anti- (M2) inflammatory phenotype (26). Macrophages polarization in various malignancies appears to be complex, and the M1 to M2 phenotype switching can occur during cancer progression. M1-like and M2-like TAMs can be co-expressed inside the tumor environment and their ratio can change during cancer progression. A high amount of M1-like TAMs is typical of the early stages of tumors development and it is associated with good prognosis in several malignancies, while M2-like TAMs have a strong correlation with worst prognosis and advanced tumor stage. Understanding and deciphering the complexity of metabolic mechanisms involved in TAMs polarization could be a useful strategy to target cancer. Mass spectrometry-based metabolomics/lipidomics provide the capability to profile and detail the metabolic alterations in TAMs providing new mechanistic hypothesis for find more effective TAMs-targeted therapy. The collected results point to the fact that there are few articles dissecting the metabolic characteristics of the *in-vivo* derived human TAMs populations and up to now it is only possible to state that *in-vivo* patient derived TAMs populations (mixed M1- M2-like phenotypes) had an augmented metabolic activity that not completely recapitulate the M1, M2 macrophages metabolic peculiarity. Of note, current evidence based on MS-metabolomics studies are still limited and mostly focused in comparing TAMs metabolism relative to non-tumor

TABLE 1 List of papers employing mass spectrometry based metabolomics approaches to describe the metabolic state of TAMs populations.

Study	Specimens	TAMs populations	Metabolic pathways	Trend of metabolic alterations
(74)	Subcutaneous colon adenocarcinoma mouse model	General macrophages (CD11b+ sorted cells)	Glycolysis TCA cycle Glutamine Methionine metabolism	Increased in CD11b+ resident tumor cells relative to the spleen resident cells)
(75)	Orthotropic mouse model of ovarian cancer	General macrophages (F4/80+ sorted cells).	Glycolysis Polyamines TCA cycle	Increased in resident peritoneal macrophages Mϕ of bearing tumor mice relative to peritoneal resident naive Mϕ
(76)	Human pancreatic ductal adenocarcinoma (PDAC) cell lines	Mixed M1, M2 phenotype (*in-vitro* conditioned monocytes CD68+, CD163+, M-CSFR, and CD206+)	Glycolysis	Increased in conditioned TAMs relative to control monocytes
(77)	Orthotropic mouse model of PDAC	General macrophages (CD45+ sorted cells)	Glycolysis	Increased in resident tumor CD45+ TAMs relative to the non-tumor bearing controls cells
(78)	Subcutaneous Lewis Lung carcinoma mouse model	M1-like and M2-like TAMs (CD11b+Ly6G −Ly6ClowMHC-IIlow and CD11b+Ly6G −Ly6ClowMHC-IIhigh sorted cells)	TCA cycle Glutamine metabolism	Increased in tumor resident MHC-IIhi TAMs relative to the Ly6ClowMHC-IIlow
(72)	Human PDAC cell lines	M2 macrophages (*in-vitro* conditioned murine bone-marrow-monocytes)	Pyrimidines	Increased in conditioned murine M2 like TAMs relative to control macrophages
(79)	Non-small cell lung cancer tumor slices	M1-like TAMs (iNOS and CD68+ stained cells)	Glycolysis TCA cycle	Increased in iNOS and CD68+ TAMs
(81)	Orthotropic Lewis lung mouse model	Mixed macrophages populations (SigF+/CD11c +/F480+/CD11b (MacA), F480+/CD11b+/Ly6G-/ SigF-, (MacB) sorted cells)	Eicosanoids	Increased in MacA relative to MacB populations
(73)	Gastric cancer cell line	M2-like TAMs (*in-vitro* conditioned CD206, CD163, TGFβ, Arg-1 murine bone-marrow cells)	Triacylglycerol	Increased in conditioned TAMs relative to control
(82)	High-grade serous adenocarcinoma	General macrophages (EpCAM+ CD14+ CD163+ CD206+ sorted cells)	Lysophosphatidic acid	Increased in TAMs populations

For each paper, the reference, the specimens, the TAMs populations selected in the study, the altered metabolic pathway and the trend of deregulation.

counterparts, thus not allowing an in-depth metabolic characterization of TAMs subset. So far, metabolic profiling is mainly related to the general description of metabolic pathways and does not go deeply into the definition of the enzyme activity to discover new fragile metabolic points that might be pharmacologically targeted. Considering the technological advances in the field of cytofluorimetry and mass spectrometry, it is urgent and feasible to investigate the metabolic structure of TAMs sorted directly from patients, without having to analyze orthotropic mouse models or *in vitro* conditioned monocytes.

Therefore, more effort is needed to implement bulk metabolic analyses such as targeted metabolomics, 13C-label-tracing, and extracellular flux analysis to provide the complete metabolic picture and address the therapeutic implications of TAMs metabolism.

Author contributions

Conceptualization, all authors. Project administration, MD. Resources, MD. Supervision, LB. Writing original draft, GD and LB. Review and editing, all authors. All authors contributed to the article and approved the submitted version.

Funding

This study was supported by Italian Ministry of Health grant number RF-2018-12367150.

Conflict of interest

The authors declare that the research was conducted in the absence of any commercial or financial relationships that could be construed as a potential conflict of interest.

Publisher's note

References

1. Castegna A, Gissi R, Menga A, Montopoli M, Favia M, Viola A, et al. Pharmacological targets of metabolism in disease: opportunities from macrophages. *Pharmacol Ther* (2020) 210:107521. doi: 10.1016/j.pharmthera.2020.107521

2. Petty AJ, Yang Y. Tumor-associated macrophages: implications in cancer immunotherapy. *Immunotherapy* (2017) 9(3):289–302. doi: 10.2217/imt-2016-0135

3. Chanmee T, Ontong P, Konno K, Itano N. Tumor-associated macrophages as major players in the tumor microenvironment. *Cancers* (2014) 6(3):1670–90. doi: 10.3390/cancers6031670

4. Murray PJ, Wynn TA. Protective and pathogenic functions of macrophage subsets. *Nat Rev Immunol* (2011) 11(11):723–37. doi: 10.1038/nri3073

5. Viola A, Munari F, Sánchez-Rodríguez R, Scolaro T, Castegna A. The metabolic signature of macrophage responses. *Front Immunol* (2019) 10:1462. doi: 10.3389/fimmu.2019.01462

6. Dey A, Allen J, Hankey-Giblin PA. Ontogeny and polarization of macrophages in inflammation: blood monocytes versus tissue macrophages. *Front Immunol* (2015) 5:683/abstract. doi: 10.3389/fimmu.2014.00683/abstract

7. Cassetta L, Pollard JW. Tumor-associated macrophages. *Curr Biol* (2020) 30(6): R246–8. doi: 10.1016/j.cub.2020.01.031

8. Cassetta L, Fragkogianni S, Sims AH, Swierczak A, Forrester LM, Zhang H, et al. Human tumor-associated macrophage and monocyte transcriptional landscapes reveal cancer-specific reprogramming, biomarkers, and therapeutic targets. *Cancer Cell* (2019) 35(4):588–602.e10. doi: 10.1016/j.ccell.2019.02.009

9. Joyce JA, Fearon DT. T Cell exclusion, immune privilege, and the tumor microenvironment. *Science* (2015) 348(6230):74–80. doi: 10.1126/science.aaa6204

10. Biswas SK, Mantovani A. Macrophage plasticity and interaction with lymphocyte subsets: cancer as a paradigm. *Nat Immunol* (2010) 11(10):889–96. doi: 10.1038/ni.1937

11. Cortese N, Donadon M, Rigamonti A, Marchesi F. Macrophages at the crossroads of anticancer strategies. *Front Biosci Landmark Ed* (2019) 24(7):1271–83. doi: 10.2741/4779

12. Murray PJ. Macrophage polarization. *Annu Rev Physiol* (2017) 79(1):541–66. doi: 10.1146/annurev-physiol-022516-034339

13. Mosser DM, Edwards JP. Exploring the full spectrum of macrophage activation. *Nat Rev Immunol* (2008) 8(12):958–69. doi: 10.1038/nri2448

14. Mantovani A, Sozzani S, Locati M, Allavena P, Sica A. Macrophage polarization: tumor-associated macrophages as a paradigm for polarized M2 mononuclear phagocytes. *Trends Immunol* (2002) 23(11):549–55. doi: 10.1016/S1471-4906(02)02302-5

15. Kodelja V, Müller C, Tenorio S, Schebesch C, Orfanos CE, Goerdt S. Differences in angiogenic potential of classically vs alternatively activated macrophages. *Immunobiology* (1997) 197(5):478–93. doi: 10.1016/S0171-2985(97)80080-0

16. Mojsilovic SS, Mojsilovic S, Villar VH, Santibanez JF. The metabolic features of tumor-associated macrophages: opportunities for immunotherapy? *Anal Cell Pathol* (2021) 2021:1–12. doi: 10.1155/2021/5523055

17. Mantovani A, Sica A, Sozzani S, Allavena P, Vecchi A, Locati M. The chemokine system in diverse forms of macrophage activation and polarization. *Trends Immunol* (2004) 25(12):677–86. doi: 10.1016/j.it.2004.09.015

18. Anders CB, Lawton TMW, Smith HL, Garret J, Doucette MM, Ammons MCB. Use of integrated metabolomics, transcriptomics, and signal protein profile to characterize the effector function and associated metabotype of polarized macrophage phenotypes. *J Leukoc Biol* (2021), 6A1120–744R. doi: 10.1101/2020.03.10.985788

19. Shapouri-Moghaddam A, Mohammadian S, Vazini H, Taghadosi M, Esmaeili S, Mardani F, et al. Macrophage plasticity, polarization, and function in health and disease. *J Cell Physiol* (2018) 233(9):6425–40. doi: 10.1002/jcp.26429

20. Sica A, Mantovani A. Macrophage plasticity and polarization: *in vivo* veritas. *J Clin Invest* (2012) 122(3):787–95. doi: 10.1172/JCI59643

21. Xia Y, Brown ZJ, Huang H, Tsung A. Metabolic reprogramming of immune cells: shaping the tumor microenvironment in hepatocellular carcinoma. *Cancer Med* (2021) 10(18):6374–83. doi: 10.1002/cam4.4177

22. Zhu L, Zhao Q, Yang T, Ding W, Zhao Y. Cellular metabolism and macrophage functional polarization. *Int Rev Immunol* (2015) 34(1):82–100. doi: 10.3109/08830185.2014.969421

23. Van den Bossche J, O'Neill LA, Menon D. Macrophage immunometabolism: where are we (Going)? *Trends Immunol* (2017) 38(6):395–406. doi: 10.1016/j.it.2017.03.001

24. Noe JT, Rendon BE, Geller AE, Conroy LR, Morrissey SM, Young LEA, et al. Lactate supports a metabolic-epigenetic link in macrophage polarization. *Sci Adv* (2021) 7(46):eabi8602. doi: 10.1126/sciadv.abi8602

25. Zhang Q, Wang J, Yadav DK, Bai X, Liang T. Glucose metabolism: the metabolic signature of tumor associated macrophage. *Front Immunol* (2021) 12:702580. doi: 10.3389/fimmu.2021.702580

26. Vitale I, Manic G, Coussens LM, Kroemer G, Galluzzi L. Macrophages and metabolism in the tumor microenvironment. *Cell Metab* (2019) 30(1):36–50. doi: 10.1016/j.cmet.2019.06.001

27. Locati M, Curtale G, Mantovani A. Diversity, mechanisms, and significance of macrophage plasticity. *Annu Rev Pathol Mech Dis* (2020) 15(1):123–47. doi: 10.1146/annurev-pathmechdis-012418-012718

28. Zhou J, Tang Z, Gao S, Li C, Feng Y, Zhou X. Tumor-associated macrophages: recent insights and therapies. *Front Oncol* (2020) 10:188. doi: 10.3389/fonc.2020.00188

29. Cui L, Lu H, Lee YH. Challenges and emergent solutions for LC-MS/MS based untargeted metabolomics in diseases. *Mass Spectrom Rev* (2018) 37(6):772–92. doi: 10.1002/mas.21562

30. Rabold K, Aschenbrenner A, Thiele C, Boahen CK, Schiltmans A, Smit JWA, et al. Enhanced lipid biosynthesis in human tumor-induced macrophages contributes to their protumoral characteristics. *J Immunother Cancer* (2020) 8(2):e000638. doi: 10.1136/jitc-2020-000638

31. Chen YL. Prognostic significance of tumor-associated macrophages in patients with nasopharyngeal carcinoma: a meta-analysis. *Med (Baltimore)* (2020) 99(39): e21999. doi: 10.1097/MD.0000000000021999

32. Wang XL, Jiang JT, Wu CP. Prognostic significance of tumor-associated macrophage infiltration in gastric cancer: a meta-analysis. *Genet Mol Res* (2016) 15 (4). doi: 10.4238/gmr15049040

33. Guo B, Cen H, Tan X, Ke Q. Meta-analysis of the prognostic and clinical value of tumor-associated macrophages in adult classical Hodgkin lymphoma. *BMC Med* (2016) 14(1):159. doi: 10.1186/s12916-016-0711-6

34. Wu P, Wu D, Zhao L, Huang L, Chen G, Shen G, et al. Inverse role of distinct subsets and distribution of macrophage in lung cancer prognosis: a meta-analysis. *Oncotarget* (2016) 7(26):40451–60. doi: 10.18632/oncotarget.9625

35. Zhang Qw, Liu L, Gong Cy, Shi Hs, Zeng Yh, Wang X, et al. Prognostic significance of tumor-associated macrophages in solid tumor: a meta-analysis of the literature. hoque MO. *PloS One* (2012) 7(12):e50946. doi: 10.1371/journal.pone.0050946

36. Liu JY, Yang XJ, Geng XF, Huang CQ, Yu Y, Li Y. Prognostic significance of tumor-associated macrophages density in gastric cancer: a systemic review and meta-analysis. *Minerva Med* (2016) 107(5):314–21.

37. Li J, Li L, Li Y, Long Y, Zhao Q, Ouyang Y, et al. Tumor-associated macrophage infiltration and prognosis in colorectal cancer: systematic review and meta-analysis. *Int J Colorectal Dis* (2020) 35(7):1203–10. doi: 10.1007/s00384-020-03593-z

38. Cortese N, Soldani C, Franceschini B, Barbagallo M, Marchesi F, Torzilli G, et al. Macrophages in colorectal cancer liver metastases. *Cancers* (2019) 11(5):633. doi: 10.3390/cancers11050633

39. Sica A, Erreni M, Allavena P, Porta C. Macrophage polarization in pathology. *Cell Mol Life Sci* (2015) 72(21):4111–26. doi: 10.1007/s00018-015-1995-y

40. Movahedi K, Laoui D, Gysemans C, Baeten M, Stangé G, Van den Bossche J, et al. Different tumor microenvironments contain functionally distinct subsets of macrophages derived from Ly6C(high) monocytes. *Cancer Res* (2010) 70(14):5728–39. doi: 10.1158/0008-5472.CAN-09-4672

41. Zhang M, He Y, Sun X, Li Q, Wang W, Zhao A, et al. A high M1/M2 ratio of tumor-associated macrophages is associated with extended survival in ovarian cancer patients. *J Ovarian Res* (2014) 7(1):19. doi: 10.1186/1757-2215-7-19

42. Macciò A, Gramignano G, Cherchi MC, Tanca L, Melis L, Madeddu C. Role of M1-polarized tumor-associated macrophages in the prognosis of advanced ovarian cancer patients. *Sci Rep* (2020) 10(1):6096. doi: 10.1038/s41598-020-63276-1

43. Garrido-Martin EM, Mellows TWP, Clarke J, Ganesan AP, Wood O, Cazaly A, et al. M1 ^{hot} tumor-associated macrophages boost tissue-resident memory T cells infiltration and survival in human lung cancer. *J Immunother Cancer* (2020) 8(2): e000778. doi: 10.1136/jitc-2020-000778

44. Jackute J, Zemaitis M, Pranys D, Sitkauskiene B, Miliauskas S, Vaitkiene S, et al. Distribution of M1 and M2 macrophages in tumor islets and stroma in relation to prognosis of non-small cell lung cancer. *BMC Immunol* (2018) 19(1):3. doi: 10.1186/s12865-018-0241-4

45. Honkanen TJ, Tikkanen A, Karihtala P, Mäkinen M, Väyrynen JP, Koivunen JP. Prognostic and predictive role of tumour-associated macrophages in HER2 positive breast cancer. *Sci Rep* (2019) 9(1):10961. doi: 10.1038/s41598-019-47375-2

46. Donadon M, Torzilli G, Cortese N, Soldani C, Di Tommaso L, Franceschini B, et al. Macrophage morphology correlates with single-cell diversity and prognosis in colorectal liver metastasis. *J Exp Med* (2020) 217(11):e20191847. doi: 10.1084/jem.20191847

47. Ostuni R, Kratochvill F, Murray PJ, Natoli G. Macrophages and cancer: from mechanisms to therapeutic implications. *Trends Immunol* (2015) 36(4):229–39. doi: 10.1016/j.it.2015.02.004

48. Shu Y, Cheng P. Targeting tumor-associated macrophages for cancer immunotherapy. *Biochim Biophys Acta BBA - Rev Cancer* (2020) 1874(2):188434. doi: 10.1016/j.bbcan.2020.188434

49. Sousa S, Brion R, Lintunen M, Kronqvist P, Sandholm J, Mönkkönen J, et al. Human breast cancer cells educate macrophages toward the M2 activation status. *Breast Cancer Res* (2015) 17(1):101. doi: 10.1186/s13058-015-0621-0

50. Medrek C, Pontén F, Jirström K, Leandersson K. The presence of tumor associated macrophages in tumor stroma as a prognostic marker for breast cancer patients. *BMC Cancer* (2012) 12(1):306. doi: 10.1186/1471-2407-12-306

51. Salmi S, Siiskonen H, Sironen R, Tyynelä-Korhonen K, Hirschovits-Gerz B, Valkonen M, et al. The number and localization of CD68+ and CD163+ macrophages in different stages of cutaneous melanoma. *Melanoma Res* (2019) 29(3):237–47. doi: 10.1097/CMR.0000000000000522

52. Falleni M, Savi F, Tosi D, Agape E, Cerri A, Moneghini L, et al. M1 and M2 macrophages' clinicopathological significance in cutaneous melanoma. *Melanoma Res* (2017) 27(3):200–10. doi: 10.1097/CMR.0000000000000352

53. Ciocan-Cartita CA, Jurj A, Buse M, Gulei D, Braicu C, Raduly L, et al. The relevance of mass spectrometry analysis for personalized medicine through its successful application in cancer "Omics". *Int J Mol Sci* (2019) 20(10):2576. doi: 10.3390/ijms20102576

54. Hu R, Li Y, Yang Y, Liu M. Mass spectrometry-based strategies for single-cell metabolomics. *Mass Spectrom Rev* (2021) 42(1):67–94. doi: 10.1002/mas.21704

55. Griffiths WJ, Koal T, Wang Y, Kohl M, Enot DP, Deigner HP. Targeted metabolomics for biomarker discovery. *Angew Chem Int Ed* (2010) 49(32):5426–45. doi: 10.1002/anie.200905579

56. Gross JH. *Mass spectrometry: a textbook*. Berlin; New York: Springer (2004). p. 518.

57. Chen JH, Singer S. Chromatographic and electrophoretic separations combined with mass spectrometry for metabonomics. In: *The handbook of metabonomics and metabolomics*. Elsevier (2007). p. 149–69. Available at: https://www.sciencedirect.com/book/9780444528414/the-handbook-of-metabonomics-and-metabolomics.

58. Johnson CH, Ivanisevic J, Siuzdak G. Metabolomics: beyond biomarkers and towards mechanisms. *Nat Rev Mol Cell Biol* (2016) 17(7):451–9. doi: 10.1038/nrm.2016.25

59. Dudley E, Yousef M, Wang Y, Griffiths WJ. Targeted metabolomics and mass spectrometry. In: *Advances in protein chemistry and structural biology*. Elsevier (2010). p. 45–83. Available at: https://linkinghub.elsevier.com/retrieve/pii/B9780123812643000023.

60. Cheung PK, Ma MH, Tse HF, Yeung KF, Tsang HF, Chu MKM, et al. The applications of metabolomics in the molecular diagnostics of cancer. *Expert Rev Mol Diagn* (2019) 19(9):785–93. doi: 10.1080/14737159.2019.1656530

61. Zhang W, Hankemeier T, Ramautar R. Next-generation capillary electrophoresis–mass spectrometry approaches in metabolomics. *Curr Opin Biotechnol* (2017) 43:1–7. doi: 10.1016/j.copbio.2016.07.002

62. Gao P, Huang X, Fang XY, Zheng H, Cai SL, Sun AJ, et al. Application of metabolomics in clinical and laboratory gastrointestinal oncology. *World J Gastrointest Oncol* (2021) 13(6):536–49. doi: 10.4251/wjgo.v13.i6.536

63. Gonzalez-Covarrubias V, Martínez-Martínez E, del Bosque-Plata L. The potential of metabolomics in biomedical applications. *Metabolites* (2022) 12(2):194. doi: 10.3390/metabo12020194

64. Li C, Chu S, Tan S, Yin X, Jiang Y, Dai X, et al. Towards higher sensitivity of mass spectrometry: a perspective from the mass analyzers. *Front Chem* (2021) 9:813359. doi: 10.3389/fchem.2021.813359

65. Wishart DS, Guo A, Oler E, Wang F, Anjum A, Peters H, et al. HMDB 5.0: the human metabolome database for 2022. *Nucleic Acids Res* (2022) 50(D1):D622–31. doi: 10.1093/nar/gkab1062

66. Guijas C, Montenegro-Burke JR, Domingo-Almenara X, Palermo A, Warth B, Hermann G, et al. METLIN: a technology platform for identifying knowns and unknowns. *Anal Chem* (2018) 90(5):3156–64. doi: 10.1021/acs.analchem.7b04424

67. Schrimpe-Rutledge AC, Codreanu SG, Sherrod SD, McLean JA. Untargeted metabolomics strategies–challenges and emerging directions. *J Am Soc Mass Spectrom* (2016) 27(12):1897–905. doi: 10.1007/s13361-016-1469-y

68. Mirzaei H, Carrasco M. Modern proteomics – sample preparation, analysis and practical applications. In: *Advances in experimental medicine and biology* (2016). vol. 919. Cham: Springer International Publishing. doi: 10.1007/978-3-319-41448-5

69. Roberts LD, Souza AL, Gerszten RE, Clish CB. Targeted metabolomics. *Curr Protoc Mol Biol* (2012) 98(1):1–24. doi: 10.1002/0471142727.mb3002s98

70. Zhou J, Zhong L. Applications of liquid chromatography-mass spectrometry based metabolomics in predictive and personalized medicine. *Front Mol Biosci* (2022) 9:1049016. doi: 10.3389/fmolb.2022.1049016

71. Rampler E, Abiead YE, Schoeny H, Rusz M, Hildebrand F, Fitz V, et al. Recurrent topics in mass spectrometry-based metabolomics and lipidomics-standardization, coverage, and throughput. *Anal Chem* (2021) 93(1):519–45. doi: 10.1021/acs.analchem.0c04698

72. Halbrook CJ, Pontious C, Kovalenko I, Lapienyte L, Dreyer S, Lee HJ, et al. Macrophage-released pyrimidines inhibit gemcitabine therapy in pancreatic cancer. *Cell Metab* (2019) 29(6):1390–1399.e6. doi: 10.1016/j.cmet.2019.02.001

73. Luo Q, Zheng N, Jiang L, Wang T, Zhang P, Liu Y, et al. Lipid accumulation in macrophages confers protumorigenic polarization and immunity in gastric cancer. *Cancer Sci* (2020) 111(11):4000–11. doi: 10.1111/cas.14616

74. Umemura N, Sugimoto M, Kitoh Y, Saio M, Sakagami H. Metabolomic profiling of tumor-infiltrating macrophages during tumor growth. *Cancer Immunol Immunother* (2020) 69(11):2357–69. doi: 10.1007/s00262-020-02622-8

75. Weiss JM, Davies LC, Karwan M, Ileva L, Ozaki MK, Cheng RY, et al. Itaconic acid mediates crosstalk between macrophage metabolism and peritoneal tumors. *J Clin Invest* (2018) 128(9):3794–805. doi: 10.1172/JCI99169

76. Penny HL, Sieow JL, Adriani G, Yeap WH, See Chi Ee P, San Luis B, et al. Warburg metabolism in tumor-conditioned macrophages promotes metastasis in human pancreatic ductal adenocarcinoma. *OncoImmunology* (2016) 5(8):e1191731. doi: 10.1080/2162402X.2016.1191731

77. Penny HL, Sieow JL, Gun SY, Lau MC, Lee B, Tan J, et al. Targeting glycolysis in macrophages confers protection against pancreatic ductal adenocarcinoma. *Int J Mol Sci* (2021) 22(12):6350. doi: 10.3390/ijms22126350

78. Geeraerts X, Fernández-Garcia J, Hartmann FJ, de Goede KE, Martens L, Elkrim Y, et al. Macrophages are metabolically heterogeneous within the tumor microenvironment. *Cell Rep* (2021) 37(13):110171. doi: 10.1016/j.celrep.2021.110171

79. Fan TWM, Warmoes MO, Sun Q, Song H, Turchan-Cholewo J, Martin JT, et al. Distinctly perturbed metabolic networks underlie differential tumor tissue damages induced by immune modulator β-glucan in a two-case ex vivo non-small-cell lung cancer study. *Mol Case Stud* (2016) 2(4):a000893. doi: 10.1101/mcs.a000893

80. Li Y. Lipid metabolism in tumor immunity. In: *Advances in experimental medicine and biology*, vol. 1316. . Singapore: Springer Singapore (2021). doi: 10.1007/978-981-33-6785-2

81. Poczobutt JM, Gijon M, Amin J, Hanson D, Li H, Walker D, et al. Eicosanoid profiling in an orthotopic model of lung cancer progression by mass spectrometry demonstrates selective production of leukotrienes by inflammatory cells of the microenvironment. *PloS One* (2013) 8(11):e79633. doi: 10.1371/journal.pone.0079633

82. Reinartz S, Lieber S, Pesek J, Brandt DT, Asafova A, Finkernagel F, et al. Cell type-selective pathways and clinical associations of lysophosphatidic acid biosynthesis and signaling in the ovarian cancer microenvironment. *Mol Oncol* (2019) 13(2):185–201. doi: 10.1002/1878-0261.12396

Frontiers in Immunology

Explores novel approaches and diagnoses to treat immune disorders.

The official journal of the International Union of Immunological Societies (IUIS) and the most cited in its field, leading the way for research across basic, translational and clinical immunology.

Discover the latest Research Topics

See more →

Frontiers

Avenue du Tribunal-Fédéral 34
1005 Lausanne, Switzerland
frontiersin.org

Contact us

+41 (0)21 510 17 00
frontiersin.org/about/contact